frontiers | Research Topics

Biological contaminants of concern in water and wastewater: an environmental health perspective

Edited by
Visva Bharati Barua, Vivek Francis Pulikkal, Roshan Prabhakar, Divya Pal and Isaac Dennis Amoah

Published in
Frontiers in Environmental Science
Frontiers in Public Health

FRONTIERS EBOOK COPYRIGHT STATEMENT

The copyright in the text of individual articles in this ebook is the property of their respective authors or their respective institutions or funders. The copyright in graphics and images within each article may be subject to copyright of other parties. In both cases this is subject to a license granted to Frontiers.

The compilation of articles constituting this ebook is the property of Frontiers.

Each article within this ebook, and the ebook itself, are published under the most recent version of the Creative Commons CC-BY licence. The version current at the date of publication of this ebook is CC-BY 4.0. If the CC-BY licence is updated, the licence granted by Frontiers is automatically updated to the new version.

When exercising any right under the CC-BY licence, Frontiers must be attributed as the original publisher of the article or ebook, as applicable.

Authors have the responsibility of ensuring that any graphics or other materials which are the property of others may be included in the CC-BY licence, but this should be checked before relying on the CC-BY licence to reproduce those materials. Any copyright notices relating to those materials must be complied with.

Copyright and source acknowledgement notices may not be removed and must be displayed in any copy, derivative work or partial copy which includes the elements in question.

All copyright, and all rights therein, are protected by national and international copyright laws. The above represents a summary only. For further information please read Frontiers' Conditions for Website Use and Copyright Statement, and the applicable CC-BY licence.

ISSN 1664-8714
ISBN 978-2-8325-6385-4
DOI 10.3389/978-2-8325-6385-4

About Frontiers

Frontiers is more than just an open access publisher of scholarly articles: it is a pioneering approach to the world of academia, radically improving the way scholarly research is managed. The grand vision of Frontiers is a world where all people have an equal opportunity to seek, share and generate knowledge. Frontiers provides immediate and permanent online open access to all its publications, but this alone is not enough to realize our grand goals.

Frontiers journal series

The Frontiers journal series is a multi-tier and interdisciplinary set of open-access, online journals, promising a paradigm shift from the current review, selection and dissemination processes in academic publishing. All Frontiers journals are driven by researchers for researchers; therefore, they constitute a service to the scholarly community. At the same time, the *Frontiers journal series* operates on a revolutionary invention, the tiered publishing system, initially addressing specific communities of scholars, and gradually climbing up to broader public understanding, thus serving the interests of the lay society, too.

Dedication to quality

Each Frontiers article is a landmark of the highest quality, thanks to genuinely collaborative interactions between authors and review editors, who include some of the world's best academicians. Research must be certified by peers before entering a stream of knowledge that may eventually reach the public - and shape society; therefore, Frontiers only applies the most rigorous and unbiased reviews. Frontiers revolutionizes research publishing by freely delivering the most outstanding research, evaluated with no bias from both the academic and social point of view. By applying the most advanced information technologies, Frontiers is catapulting scholarly publishing into a new generation.

What are Frontiers Research Topics?

Frontiers Research Topics are very popular trademarks of the *Frontiers journals series*: they are collections of at least ten articles, all centered on a particular subject. With their unique mix of varied contributions from Original Research to Review Articles, Frontiers Research Topics unify the most influential researchers, the latest key findings and historical advances in a hot research area.

Find out more on how to host your own Frontiers Research Topic or contribute to one as an author by contacting the Frontiers editorial office: frontiersin.org/about/contact

Biological contaminants of concern in water and wastewater: an environmental health perspective

Topic editors

Visva Bharati Barua — University of North Carolina at Charlotte, United States
Vivek Francis Pulikkal — Civil & Environmental Consultants, Inc., United States
Roshan Prabhakar — Indian Institute of Technology Dhanbad, India
Divya Pal — Stockholm University, Sweden
Isaac Dennis Amoah — University of Arizona, United States

Citation

Barua, V. B., Pulikkal, V. F., Prabhakar, R., Pal, D., Amoah, I. D., eds. (2025). *Biological contaminants of concern in water and wastewater: an environmental health perspective*. Lausanne: Frontiers Media SA. doi: 10.3389/978-2-8325-6385-4

Topic editor Dr Vivek Pulikkal is employed by Civil & Environmental Consultants, Inc., Charlotte, USA. All other topic editors declare no competing interests concerning the Research Topic subject.

Table of contents

frontiers | Frontiers in Genetics

TYPE Original Research
PUBLISHED 11 January 2024
DOI 10.3389/fgene.2023.1334646

Check for updates

OPEN ACCESS

EDITED BY
Muhammad Yasir,
King Abdulaziz University, Saudi Arabia

REVIEWED BY
Bin Hu,
Los Alamos National Laboratory (DOE), United States
Meng Zhang,
Inner Mongolia Agricultural University, China

*CORRESPONDENCE
Adrian Gorecki,
adrian_gorecki@sggw.edu.pl

RECEIVED 08 November 2023
ACCEPTED 26 December 2023
PUBLISHED 11 January 2024

CITATION
Gorecki A, Ostapczuk P and Dziewit L (2024), Diversity of antibiotic resistance gene variants at subsequent stages of the wastewater treatment process revealed by a metagenomic analysis of PCR amplicons.
Front. Genet. 14:1334646.
doi: 10.3389/fgene.2023.1334646

COPYRIGHT
© 2024 Gorecki, Ostapczuk and Dziewit. This is an open-access article distributed under the terms of the Creative Commons Attribution License (CC BY). The use, distribution or reproduction in other forums is permitted, provided the original author(s) and the copyright owner(s) are credited and that the original publication in this journal is cited, in accordance with accepted academic practice. No use, distribution or reproduction is permitted which does not comply with these terms.

Diversity of antibiotic resistance gene variants at subsequent stages of the wastewater treatment process revealed by a metagenomic analysis of PCR amplicons

Adrian Gorecki[1]*, Piotr Ostapczuk[2] and Lukasz Dziewit[2]

[1]Department of Biochemistry and Microbiology, Institute of Biology, Warsaw University of Life Sciences (SGGW), Warsaw, Poland, [2]Department of Environmental Microbiology and Biotechnology, Institute of Microbiology, Faculty of Biology, University of Warsaw, Warsaw, Poland

Wastewater treatment plants have been recognised as point sources of various antibiotic-resistant bacteria (ARB) and antibiotic resistance genes (ARG) which are considered recently emerging biological contaminants. So far, culture-based and molecular-based methods have been successfully applied to monitor antimicrobial resistance (AMR) in WWTPs. However, the methods applied do not permit the comprehensive identification of the true diversity of ARGs. In this study we applied next-generation sequencing for a metagenomic analysis of PCR amplicons of ARGs from the subsequent stages of the analysed WWTP. The presence of 14 genes conferring resistance to different antibiotic families was screened by PCR. In the next step, three genes were selected for detailed analysis of changes of the profile of ARG variants along the process. A relative abundance of 79 variants was analysed. The highest diversity was revealed in the *ermF* gene, with 52 variants. The relative abundance of some variants changed along the purification process, and some ARG variants might be present in novel hosts for which they were currently unassigned. Additionally, we identified a pool of novel ARG variants present in the studied WWTP. Overall, the results obtained indicated that the applied method is sufficient for analysing ARG variant diversity.

KEYWORDS

antibiotic resistance gene, antibiotic resistance gene amplicon, antibiotic resistant bacteria, wastewater treatment plant, PCR diversification power

1 Introduction

Antimicrobial resistance (AMR) is considered to be one of the most serious threats to public health and has become a major concern for national governments and international organisations (O'Neil, 2014). This is mainly due to constantly increasing market demands coupled with poorly-controlled utilisation and usage of antibiotics (Alanis, 2005). Since their initial introduction 60 years ago, millions of metric tons of antibiotics have been used in a variety of applications (Davies and Davies, 2010). Additionally, there is plenty of evidence of the overuse and inappropriate prescription of antibiotics in the fields of medicine and veterinary medicine. Studies have shown that between 30% and 60% of antibiotics prescribed are incorrect in choice, indication or duration of treatment (Luyt

et al., 2014). Such circumstances provoke the selection of opportunistic multi-resistant bacteria and novel antibiotic resistance genes (ARGs). Wastewater treatment plants (WWTPs) are considered a point source of significantly accumulated diverse contaminants, including: i) mobile genetic elements (MGEs) as potential vectors of genes (e.g., ARGs) impacting bacterial fitness under various environmental conditions, ii) heavy metals and iii) emerging pollutants (e.g., antibiotics, microplastics, nanomaterials, pharmaceuticals and personal care products and quorum sensing inhibitors), that can impact the proliferation of ARGs and antibiotic resistant bacteria (ARB). WWTPs are also one of the most important interfaces between the human population and the environment (Gao et al., 2022).

There are multiple techniques available to monitor ARB and ARGs in WWTPs (Wengenroth et al., 2021). These include culture-based and molecular-based (culture-independent) approaches. Culture-dependent methods are usually used to identify phenotypes of specific bacterial taxa, including coliform bacteria and enterococci. The most commonly used cultured-based methods are dilution tests, disk diffusion tests, E-tests and automated systems, such as VITEK2. However, since less than 10% of known bacterial species can be cultivated (Dziurzynski et al., 2023), culture-based methods are strongly biased and leave considerable amounts of information concerning the environmental dimension of AMR unexplored. In the second approach, molecular-based techniques allow detailed insight into a non-cultivable fraction of microbiota, with a special focus on diversity and prevalence of particular genes, e.g., ARGs. Commonly used molecular monitoring methods include: PCR, multiplex PCR, quantitative PCR, shotgun sequencing or microarrays (Miłobedzka et al., 2021). In those approaches there are also some limitations of which the uncertainty about the functionality and completeness of identified genes and bias towards the most abundant variants of searched ARG are the most important issues.

In this study, next-generation sequencing (NGS) was applied for the generation of ARG-amplicon metagenomic data. They were produced for three selected genes (i.e., *ermF*, *sul2* and *tetX*) conferring resistance to macrolides, sulfonamides and tetracyclines, respectively. These genes were detected at all stages of the purification process in the studied WWTP. Subsequent bioinformatic analysis showed the internal heterogeneity of generated PCR amplicons and revealed a high diversity of ARG variants. To the best of our knowledge, this is the first study showing the diversity of ARG variants at subsequent stages of a WWTP.

2 Materials and methods

2.1 Characterisation of samples and sampling location

All samples were collected from the municipal and industrial WWTP located in Oswiecim (Poland) in October 2016. The criteria for the selection of this WWTP were as follows: i) relatively large capacity (of about 195 m^3 of wastewater per day); ii) mixed wastes (including communal and industrial wastes); iii) dividing of the treatment process into three main stages, i.e., primary treatment (PS), secondary treatment (AS) and anaerobic digestion (ADS). The sludge samples (5 L from each above-mentioned stage) were collected into sterile glass bottles and transferred directly to the laboratory. In the laboratory, the samples were distributed into sterile 50 mL Falcon™ tubes and centrifuged for 10 min at 5,900 g. After the supernatant was removed, the samples were procced for DNA extraction.

2.2 DNA extraction

Total DNA was extracted from 500 mg of pellet obtained from raw sludge using a Fast DNA Spin Kit for Feces (MP Biomedicals, Illkirch, France) in accordance with the manufacturer's instructions. The DNA concentration was determined using the Qubit™ 2.0 Fluorometer (Invitrogen, Carlsbad, CA, United States).

2.3 Screening of ARGs in samples from the WWTP

The occurrence of ARGs in the analysed samples was investigated using PCR assays. The PCRs were performed in triplicates with 10 pmol of each primer (Table 1), DreamTaq PCR Master Mix (Thermo Fisher Scientific, Waltham, MA, United States) and 10 ng of the DNA template. The PCR conditions changed as per the recommended annealing temperature for each primer pair (Table 1). The amplification of all genes began with denaturation at 95°C for 3 min. Denaturation was followed by 30 cycles of 30 s at 98°C, 30 s at the annealing temperature (Table 1), and 30 s of extension at 72°C. A final extension of 72°C for 10 min was used for all samples. The PCR products were resolved by electrophoresis in 1.50% agarose gel. PCR products of the correct size were excised from the gel after electrophoresis, purified using an Agarose-Out DNA purification Kit (EURx, Gdansk, Poland) and then ligated to vector pNZY28-A (Nzytech, Lisbon, Portugal) and introduced into *Escherichia coli* DH5α (Hanahan, 1983) via chemical transformation (Kushner, 1978). The DNA of recombinant plasmids carrying the cloned PCR products was purified using a Plasmid Miniprep DNA Purification Kit (EURx, Gdansk, Poland) and the inserts of three clones were sequenced using universal primers (M13/pUC) with an ABI-PRISM 377 capillary DNA analyser (Applied Biosystem, Foster City, CA, United States) at the Genomed company (Poland).

2.4 Taxonomic classification of 16S rDNA amplicons

The bacterial 16S rRNA genes were amplified using extracted total DNAs in the year 2016 as matrixes with the primers Bac341F (Muyzer et al., 1993) and Bac805R (Herlemann et al., 2011) at a final concentration of 300 nM each (Table 1). For each reaction, KAPA HiFi HotStart DNA polymerase (Kapa Biosystems, Inc., Wilmington, MA, United States) at a concentration of 0.5 U was used. The matrix DNAs at a concentration of 10 ng and in a total amount of 25 μL of reaction volume were used. PCR conditions comprised an initial denaturation at 95°C for 3 min, followed by 24 cycles of denaturation (98°C for 20 s), annealing (58°C for 15 s),

TABLE 1 Primer pairs used in this study.

Target gene	Forward primer (5′ to 3′)	Reverse primer (5′ to 3′)	PCR product size (bp)	Annealing temperature (°C)	References
aadB	ANT2-FW: ATCTGCCGCTCTGGAT	ANT2-RV: CGAGCCTGTAGGACT	405	44.70	This study
ermB	ERMB-FW: GGTTGCTCTTGC ACACTCAAG	ERMB-RV: CAGTTGACGATA TTCTCGATTG	191	51.10	Koike et al. (2010)
ermF	ERMF-FW: TCTGGGAGGTTC CATTGTCC	ERMF-RV: TTCAGGGACAAC TTCCAGC	424	51.10	Koike et al. (2010)
qrnB	QNRB-FW: GATCGTGAAAGC CAGAAAGG	QNRB-RV: ACGATGCCTGGT AGTTGTCC	469	51.80	Robicsek et al. (2006)
sul1	SUL1-FW: CGGCGTGGGCTA CCTGAACG	SUL1-RV: GCCGATCGCGTG AAGTTCCG	432	57.90	Arabi et al. (2015)
sul2	SUL2-FW: GCGCTCAAGGCA GATGGCATT	SUL2-RV: GCGTTTGATACCGGC ACCCGT	293	56.30	Arabi et al. (2015)
tetA	TETA-FW: GTAATTCTGAGC ACTGTCGC	TETA-RV: CTGCCTGGACAA CATTGCTT	957	51.80	Guardabassi et al. (2000)
tetB	TETB-FW: ACACTCAGTATT CCAAGCCTTTG	TETB-RV: GATAGACATCAC TCCCTGTAATGC	205	53.50	Peak et al. (2007)
tetC	TETC-FW: CTTGAGAGCCTT CAACCCAG	TETC-RV: ATGGTCGTCATC TACCTGCC	418	53.80	Ng et al. (2001)
tetG	TETG-FW: TTATCGCCGCCG CCCTTCT	TETG-RV: TCATCCAGCCGT AACAGAAC	133	51.80	Song et al. (2021)
tetM	TETM-FW: GTGGACAAAGGT ACAACGAG	TETM-RV: CGGTAAAGTTCG TCACACAC	406	51.80	Ng et al. (2001)
tetO	TETO-FW: GATGGCATACAG GCACAGACC	TETM-RV: GCCCAACCTTTT GCTTCACTA	172	52.40	Luo et al. (2010)
tetT	TETT-FW: AACGGATTCGAT GGAACTTG	TETT-RV: GGACTTGAATTCCTT CTTTTGC	199	49.70	Szczepanowski et al. (2009)
tetX	TETX-FW: CAATAATTGGTG GTGGACCC	TETX-RV: TTCTTACCTTGGACA TCCCG	468	51.80	Ng et al. (2001)

elongation (72°C for 30 s), and a final extension step of 72 °C for 1 min. Each reaction was performed in six repetitions that were then pooled and purified using the PCR/DNA Clean-Up Purification Kit (EURx, Gdansk, Poland). An amplicon library was sequenced on an Illumina MiSeq instrument in the DNA Sequencing and Oligonucleotide Synthesis Labolatory (oligo.pl) IBB PAS using the v3 chemistry kit in a paired-end mode.

Initial raw data quality control along with adapter trimming was performed using the fastp tool (version 0.21.0) (Chen et al., 2018). Trimmed sequences were imported into the Qiime2 software package (release 2020.11) for subsequent analysis (Bolyen et al., 2019). Read sequences were truncated (271/209 forward/reverse). The quality filtering, denoising, paired-end read merging and *de novo* chimera removal was performed using a DADA2 plugin (Callahan et al., 2016) in order to obtain Amplicon Sequence Variants (ASVs) using specified parameters (--p-min-fold-parent-over-abundance 4.00; --p-max-ee-f 2.80; --p-max-ee-r 2.80). Bacterial taxonomy was assigned for each of the ASVs using a pre-trained Naive Bayes classifier, based on the Silva 138.1 SSU database (Quast et al., 2013), which was trimmed to include only the V3–V4 region of the 16S rRNA gene, bound by Bakt_341F/Bakt_805R primer pairs. Raw sequencing data are available at the European Nucleotide Archive (ENA) under BioProject accession number PRJNA986332 and sample accession number SAMN35826646 to SAMN35826648.

2.5 Antibiotic resistance genes amplicons generation and sequencing

Fragments of three ARGs (namely,: *ermF*, *sul2* and *tetX*, which were identified in all stages of the purification process) were amplified from the extracted total DNAs in the year 2019 using primers ERMF-FW and ERMF-RV (Koike et al., 2010), SUL2-FW and SUL2-RW (Arabi et al., 2015) and TETX-FW and TETX-RV (Ng et al., 2001) listed in Table 1 with an attached Illumina Nextera XT adapter sequence on 3' ends (forward adapter: TCGTCGGCA GCGTCAGATGTGTATAAGAGACAG and reverse adapter: GTC TCGTGGGCTCGGAGATGTGTATAAGAGACAG). Each reaction contained primers at a final concentration of 300 nM each, and KAPA HiFi HotStart DNA polymerase (Kapa Biosystems) at a concentration of 0.5 U. A DNA matrix at a concentration of 10 ng was used, totalling 25 µL in reaction volume. The following conditions were applied for the reactions: i) for *ermF*–95°C for 3 min (1 cycle), 98°C for 20 s, 58°C for 15 s and 72 °C for 30 s (30 cycles); ii) for *sul2*–95°C for 3 min (1 cycle), 98°C

for 20 s, 68.6°C for 15 s and 72°C for 30 s (29 cycles) and for iii) *tetX*–95°C for 3 min (1 cycle), 98°C for 20 s, 68°C for 15 s and 72°C for 30 s (30 cycles). Each reaction was performed in three repetitions, which then were pooled and purified using the PCR/DNA Clean-Up Purification Kit (EURx). An amplicon library was sequenced on an Illumina MiSeq instrument at the Genomed company (Poland) using the v3 chemistry kit in a paired-end mode.

2.6 Bioinformatic processing of raw antibiotic resistance gene amplicon data

Raw reads were subjected to quality filtering using the QIIME 2 package (release 2021.11) (Bolyen et al., 2019) prior to analysis with the same tool. During filtering, reads shorter than 100 bp were excluded from further analysis. Read sequences were truncated (290/220 forward/reverse). The quality filtering, denoising, paired-end read merging and *de novo* chimera removal was performed using DADA2 using specified parameters (-p-min-fold-parent-over-abundance 1.00; --p-max-ee-f 2.00; --p-max-ee-r 2.00). In the next step, obtained sequences and the frequency of sequences were exported from qimme artifacts to a csv table and subjected to further bioinformatic analysis. To remove artificial reads from the amplicon datasets, a BLASTN was performed against the reference sequence from the CARD database (*ermF* - ARO: 3000498, *sul2* - ARO: 3000412 and *tetX* - ARO: 3000205). Amplicon sequences for which the query coverage was below 100.00% was rejected from analysis. Raw sequencing data is available at the European Nucleotide Archive (ENA) under BioProject accession number PRJNA986332 and sample accession number SAMN35826649 to SAMN35826657.

2.7 Building the reference datasets of antibiotic resistance gene variants

We built the reference datasets by extracting nucleotide sequences from the NCBI NT database using specific thresholds for sequence identity and query coverage as they relate to the reference sequences. These thresholds varied. For gene *sul2* we applied 98.00% sequence identity and 98.00% query coverage. In case of gene *ermF* we used 86.00% identity and 98.00% query coverage as this was the lowest identity identified in amplicon sequences for that gene. In the case of *tetX* we applied 96.00% percent identity and 98.00% query coverage. That threshold was predicted by additional analysis which aimed to analyse the clusterisation of *tetX* variants present in the CARD database (Supplementary Table S3). The primers used were able to only amplify the *tetX* gene (ARO: 3000205). For the extension of datasets we used three reference sequences, for *ermF*–ARO: 3000498, for *sul2*–ARO: 3000412 and for *tetX*–ARO: 3000205. To each sequence, additional information about taxonomic assignment was extracted by adding a -sscinames flag in the BLASTN output format. Extracted sequences in .fas format are available at the following address: http://ddlemb.com/bioinformatic-tools-and-databases/.

2.8 Reference sequences diversity analysis—conservation genetics

To analyse the diversity of the reference sequence of ARGs, we applied the ClustalW (Chenna et al., 2003) algorithm for the multi-sequence alignment using the default option (gap open penalty: 15.00 and gap extension penalty: 6.66) in MEGA11 software (Tamura et al., 2021). In the next step, aligned sequences were applied to create the logo consensus frequency plot using an online tool (weblogo.berkeley.edu). Aligned sequences were also used to build phylogenetic trees using the Maximum Likelihood method and Tamura-Nei model (Tamura and Nei, 1993). Initial tree(s) for the heuristic search were obtained automatically by applying the Neighbor-Join and BioNJ algorithms to a matrix of pairwise distances estimated using the Tamura-Nei model, and then selecting the topology with a superior log likelihood value. Trees were developed using MEGA11 (Tamura et al., 2021).

2.9 *In silico* primer pairs validation

Primer pairs used for the PCR amplicon generation were subjected to *in silico* validation using the UniPriVal software (Gorecki et al., 2019). Initial validation was aimed to assign previously described parameters, i.e., specificity (showing if the primer pair is specific to the target gene), efficacy (showing if the primer pair cover all gene variants), taxonomic efficacy (showing if the primer pair cover all putative bacterial hosts). Parameters are expressed in values from 0.00 to 1.00.

2.10 Calculating the diversification power of primer pairs

Based on data obtained from *in silico* validation, we applied a new calculation model which aims to estimate the diversification power of the primer pairs (DP). The DP value indicates the proportion of amplicons obtained by the particular primer pair which can be assigned to a unique reference sequence representing a given variant of the analysed gene. The DP of primer pair *i* for the amplification of ARG *j* is calculated as the ratio of the number of correct *in silico* PCR products obtained for the particular ARG using NT database as a matrix with the perfect match to only one reference sequence ($CPRSPM_{i,j}NT$) and the number of all reference sequences within the reference datasets (*RS*) of the particular ARG *j*. (1)

$$DP_{i,j} = \frac{CPRSPM_{i,j}NT}{RS_j} \quad (1)$$

The DP parameter is expressed in values from 0.00 (none of the correct *in silico* PCR products matched the given reference sequence) to 1.00 (all of the correct *in silico* PCR products matched the specific gene variants). It should be mentioned that the formula is not working when RS_j value equals 1 (as in that case no variability of the reference sequences is observed).

3 Results and discussion

3.1 Occurrence of antibiotic resistance genes in wastewater samples from Oswiecim (Poland)

A qualitative PCR screening of 14 ARGs conferring resistance to aminoglycosides (one gene), MLS group (two genes), quinolones (one gene), sulfonamides (two genes) and tetracyclines (eight genes) at subsequent stages of the purification process at the WWTP in Oswiecim (Poland) was performed. The results showed that all analysed genes were found in at least one of analysed samples. The highest number of different genes (13, namely: *ermB*, *ermF*, *qrnB*, *sul1*, *sul2*, *tetA*, *tetB*, *tetC*, *tetG*, *tetM*, *tetO*, *tetT*, *tetX*) were found in primary sludge (PS). In the activated sludge (AS) seven genes (*ANT(2″)-Ia/aadB*, *ermF*, *sul1*, *sul2*, *tetC*, *tetM*, *tetX*) and in the anaerobic digestion sludge (ADS) eight (*ANT(2″)-Ia/aadB*, *ermB*, *ermF*, *sul2*, *tetC*, *tetM*, *tetT*, *tetX*) were identified. It was observed that the *qnrB*, *tetA*, *tetB* and *tetG* genes were exclusively identified in PS, while the *ermF*, *tetC*, *tetM*, *tetX* and *sul2* genes were prevalent in all samples from the WWTP (Supplementary Table S2).

The results clearly show a high prevalence of ARGs in the analysed WWTP, which stays in good agreement with previous reports (Laht et al., 2014; Karkman et al., 2016). Genes conferring resistance to aminoglycosides, macrolides, quinolones, sulfonamides and tetracyclines (including glycylcyclines) were present in at least one stage of the waste purification process. Interestingly, a retrospective analysis revealed that in 2017 (around the time of sampling) amongst the antibiotics most frequently prescribed in Poland were azithromycin (macrolide), ciprofloxacin (quinolone), sulfamethoxazole (sulfonamide) and doxycycline (glycylcycline). There was no information about the usage of aminoglycosides during antibiotic treatment (Olczak-Pieńkowska and Hryniewicz, 2021).

It is also worth mentioning that a high prevalence of the *tetX* gene was observed (identified along all stages of the tested WWTP). That gene, which confers resistance to tigecycline, is classified by the WHO as a critically important antimicrobial. Tigecycline is used for patients with serious infections in healthcare settings, who are affected by diseases for which there are very limited antimicrobial choices (WHO, 2019). Interestingly, doxycycline, which was first-line therapy around 2017, might be also modified by flavin-dependent monooxygenase encoded by *tetX* genes (Yang et al., 2004).

Results showed that the *tetX* gene and some four other genes (*ermF*, *tetC*, *sul2*, *tetM*) were prevalent along all stages of the tested WWTP. For further analyses, three of them, i.e., *ermF*, *sul2* and *tetX*, conferring resistances to various antibiotic groups, were selected.

3.2 Variability of ARG reference sequences

The main aim of this study was to analyse the diversity of three selected ARGs (*ermF*, *sul2* and *tetX*) applying a novel approach utilising the metagenomic analysis of PCR gene amplicons. To analyse generated ARG amplicon data, the databases of the reference sequences which gathered all variants of the analysed genes were prepared. This included 45 different variants of *ermF* gene, five variants of *sul2* gene and 37 variants of *tetX* gene, which were extracted from public repositories (Figure 2). All variants were assigned to the bacterial hosts in which they were identified. Variants of the *ermF* gene were found in 19 bacterial genera, *sul2* in 28 and *tetX* in 13. It was shown that *Acinetobacter* spp., *Bacteroides* spp., *Eschericha* spp., *Klebsiella* spp., *Rimerella* spp. and *Salmonella* spp. are the most common genera in which the analysed ARG variants were identified. It was observed that in the case of *ermF* and *tetX* genes, with a high number of variants, 37.50% and 53.80% respectively, were identified in uncultured bacteria (Supplementary Figure S1).

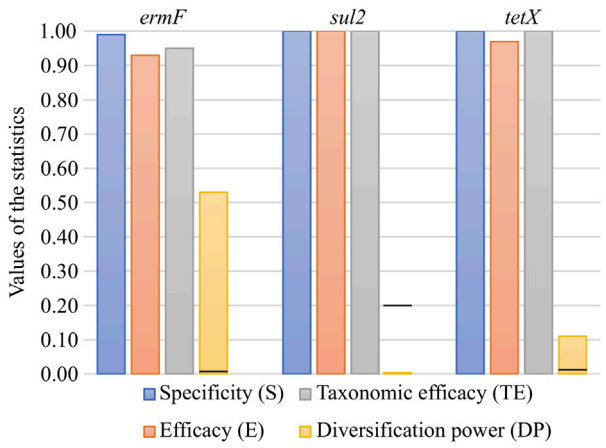

FIGURE 1
In silico validation of the specificity, efficacy, taxonomic efficacy and diversification power of the primer pairs used for ARG amplicon generation. The black lines on the DP bars correspond to the first value greater than 0 for the given set.

The nucleotide sequence diversity of the analysed reference ARG variants differed significantly. The highest identity level was observed for the *sul2* gene, with 99.14% positions conserved. Conserved sequences cover 78.18% of the *ermF* gene variants and 87.94% of the *tetX* gene variants. It was observed that the *ermF* and *tetX* genes exhibited nucleotide polymorphism in 175 and 141 different loci, respectively. Differences are distributed unequally along the whole sequence (Supplementary Figures S3, S5). The *sul2* gene exhibited nucleotide polymorphism in only 7 loci, which are located at the beginning and the end of the sequence (Supplementary Figure S4).

3.3 Statistics of primer pairs used for generation of ARG amplicon data

In silico validation revealed that all three primer pairs used for PCR amplicon generation were specific to the analysed ARGs. The primer pairs exhibited very high parameters, ranging from 0.93 to 1.00 for efficacy (E) and from 0.95 to 1.00 for taxonomic efficacy (TE). These results indicated that the primer pairs used were sufficient in the general screening of ARGs in the environmental samples (Figure 1). The primer pairs varied significantly when calculating the novel parameter, developed in this study, i.e., the diversification power (DP) value. It was shown that the primer pair

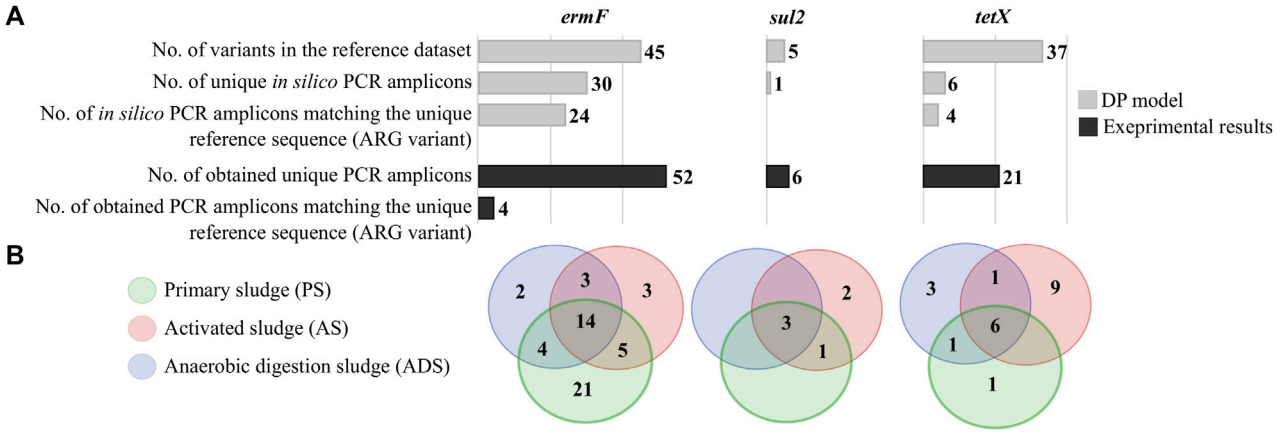

FIGURE 2
Occurrence and distribution of the *ermF*, *sul2* and *tetX* gene variants in the Oswiecim WWTP. **(A)**, Number of different variants calculated by the diversification power (DP) model and obtained from the laboratory experiments. **(B)**, Distribution of the unique variants obtained from the laboratory experiments along subsequent stages of the purification process in the WWTP.

for the *ermF* gene was distinguishing only slightly over half of all variants (DP = 0.53). It was the highest DP value obtained for the analysed set of primer pairs. The DP value equal to 0.11 was observed for the primer pair for the *tetX* gene. Analysis showed that none of variants can be distinguished by primer pairs used for the *sul2* gene, since the primer pair amplifies a highly conserved (identical in all variants) DNA fragment (DP = 0.00) (Figure 1). The analysis performed indicated that high divergence between DP values was the result of the region which was amplified by the primer pairs used. It was shown that in the case of the *sul2* and *tetX* genes, the majority of single nucleotide polymorphisms (SNPs, distinguishing between variants) were present outside of the amplified region (Supplementary Figures S4, S5). To maximise the DP value of the primer pair, it should be designed within the region showing high variability but shared between the highest possible number of variants.

It should be remembered that increasing the value of DP has limitations. The currently used preparation kits for the construction of the Illumina library make it possible to generate pair-end amplicon reads of maximal length, reaching 600 base pairs (bp). Therefore, in the case of large genes, it might be unfeasible to cover the whole variability by using only one primer pair.

3.4 Antibiotic resistance gene variants drift along subsequent stages of the WWTP

The model used for calculations indicated the actual number of various amplicons that might be theoretically obtained by a particular primer pair. According to calculations, a maximum of 30 unique PCR amplicons, characteristic for 24 reference sequences (gene variants) could be obtained for the *ermF* gene. Six out of 30 unique PCR amplicons were identical with two or more reference sequences. In total, 45 variants of the *ermF* gene were distinguished so far, as revealed by an analysis of public databases. In the case of the *sul2* gene, only one unique PCR amplicon should be observed. This amplicon cannot be assigned to a particular variant as the region amplified by the primer pairs is identical in all (six) variants. For the *tetX* gene, in total 37 variants were identified in the NT database. According to the DP model, the PCR primer pair used for *tetX* amplicon generation should amplify a maximum of six unique amplicons, from which only four could be assigned to a unique reference sequence (Figure 2A).

The primer pairs described have been utilized for the PCR amplicon generation using total DNA matrices isolated from three WWTP samples from subsequent stages of the waste purification process. The total of 385,809 paired-end reads was obtained from the DNA sequencing run. Average reads count per sample was 128,603 reads (min. 109,845, max. 149,021). In the course of the quality control, which removed low quality and unspecific reads, the average number of reads per sample dropped to 140,870 (min. 49,229, max. 183,069). It resulted in obtaining 52 unique *ermF* amplicons, six amplicons of the *sul2* gene and 21 different amplicons of the *tetX* gene. An analysis of the results obtained showed that only four out of 79 generated amplicons can be assigned to a unique reference sequence. Other PCR amplicons obtained showed identity with more than one variant collected in the reference dataset. In all cases, the number of unique amplicons obtained is greater than the number of unique PCR products predicted by *in silico* calculations (Figure 2A). Assuming the sequencing was performed correctly to the highest degree possible, it may be stated that the novel variants of the analysed ARGs have been identified. However, here one has to be critical as it was described that next-generation sequencing (NGS) may generate errors. The substitution error rate by conventional NGS techniques is reported to be around >0.10% (Goodwin et al., 2016; Salk et al., 2018; Ma et al., 2019). In the case of the Illumina MiSeq platform which has been applied in this study, the median error rate is 0.47% (Stoler and Nekrutenko, 2021).

Around 28.00% ± 0.01% of identified variants were identified in samples originating from all stages of the analysed WWTP. It was observed that the highest variability of the *ermF* variants (84.60% of all identified variants) occurred in the primary sludge

10.3389/fgene.2023.1334646

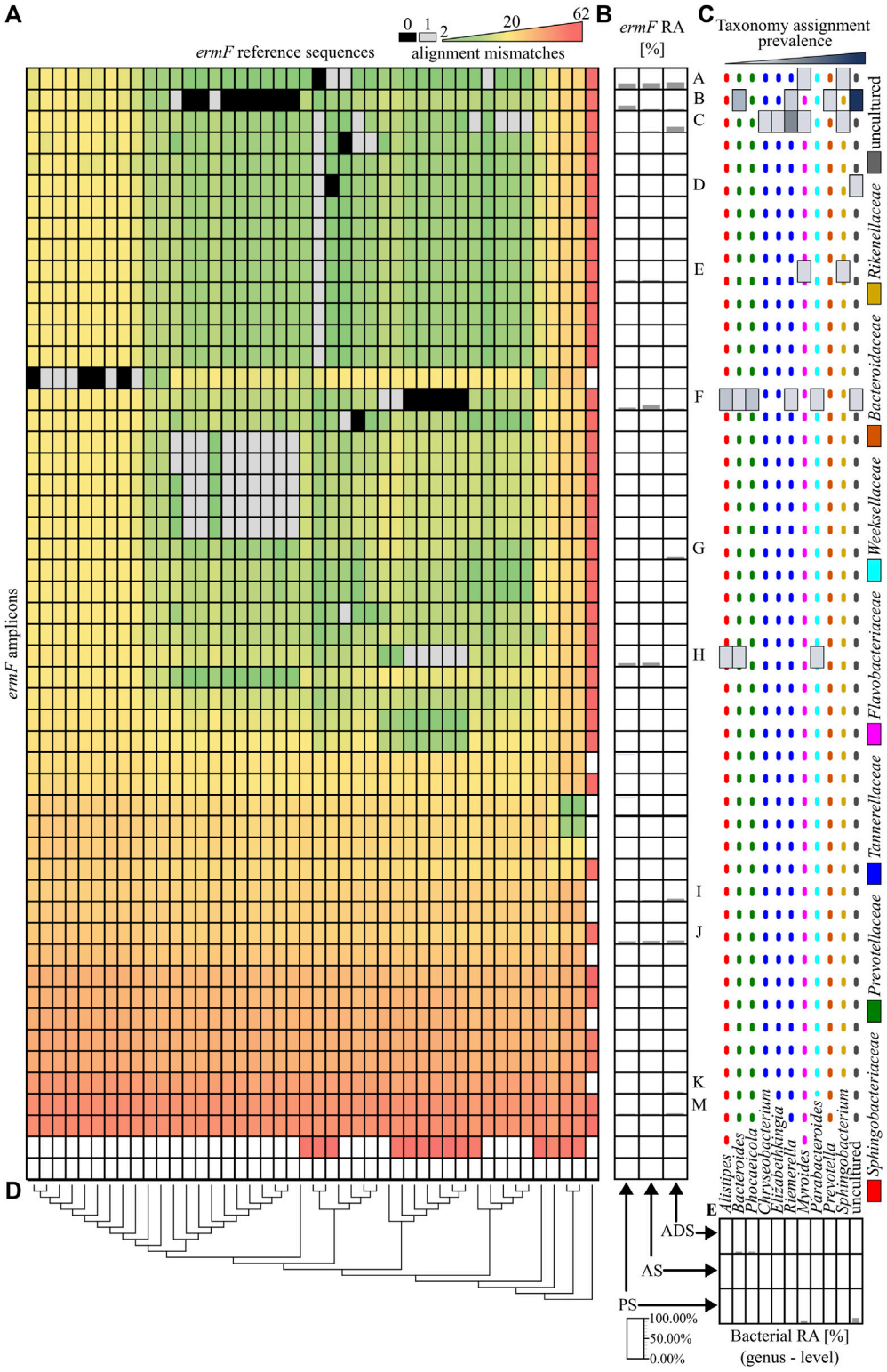

FIGURE 3
Analysis of the *ermF* amplicons. **(A)**, A heat map showing the similarity of obtained PCR amplicons to the reference sequences, based on the mismatch value from the BLASTN output. The black colour indicates 0 mismatches and the grey colour, 1 mismatch. **(B)**, The relative abundance of the *ermF* amplicons in the different stages of the purification process. The *ermF* amplicons with an abundance higher than 1.00% in any of the samples have been marked with a unique capital letter (from A to M). **(C)**, The hosts of the *ermF* gene for which the given amplicon has a perfect match (0 mismatches or 1 mismatch) according to NCBI NT database. The dotted, coloured lines indicate different families of the hosts. **(D)**, The phylogenetic tree, representing the homology of the reference sequences. **(E)**, The relative abundance of the bacterial community in the analysed samples. Abbreviations: RA–relative abundance, PS–primary sludge, AS–activated sludge, ADS–anaerobic digestion sludge.

10.3389/fgene.2023.1334646

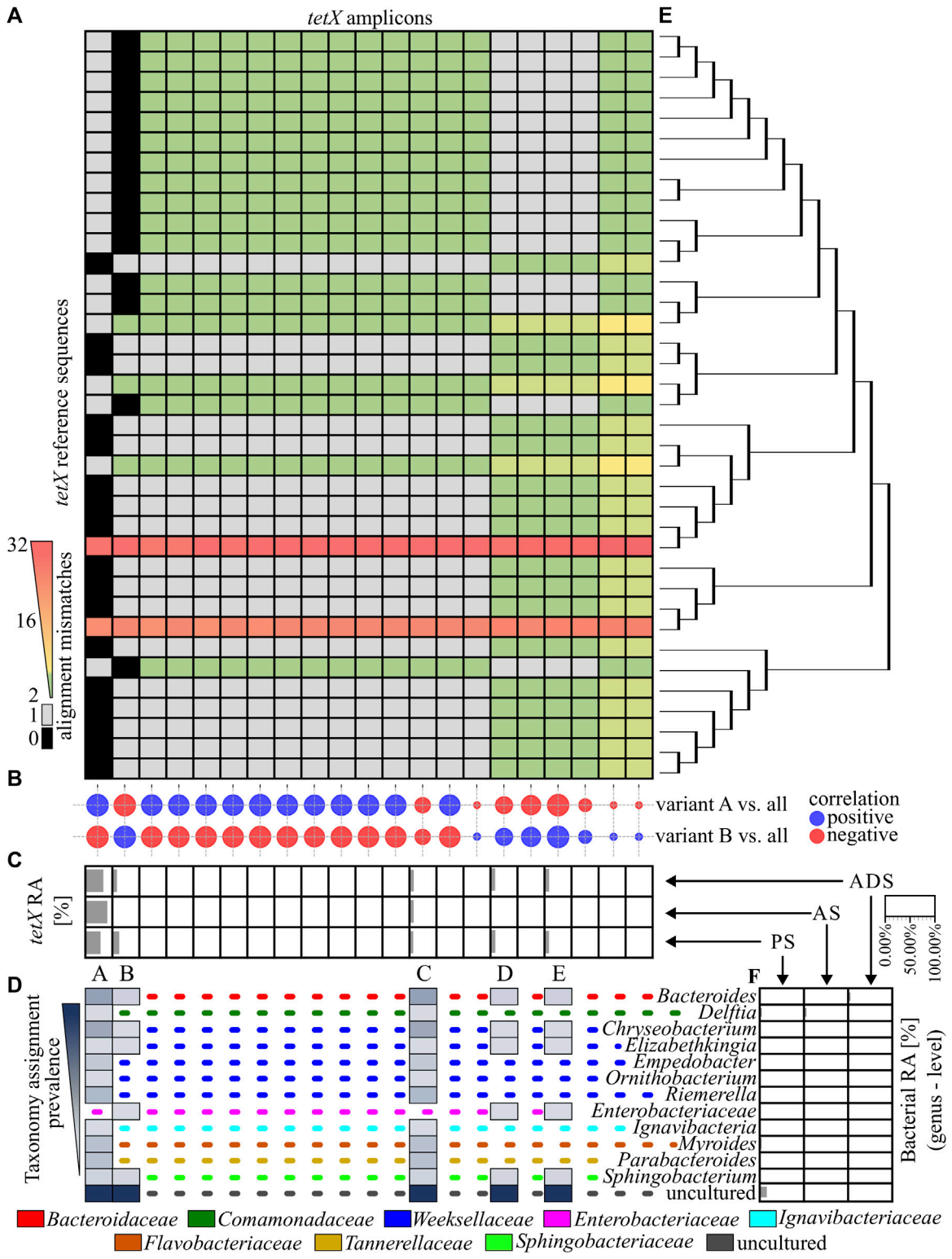

FIGURE 4
Analysis of the *tetX* amplicons. **(A)**, A heat map showing the similarity of the PCR amplicons obtained to the reference sequences, based on the mismatch value from the BLASTN output. The black colour indicate 0 mismatches and the grey colour, 1 mismatch. **(B)**, The correlation plot, showing the similarity of the relative abundance pattern for a particular *tetX* amplicon between the analysed samples. The size of the bubbles correspond to R^2 values; the red colour is a negative correlation and the blue colour is a positive correlation. **(C)**, The relative abundance of the *ermF* amplicons in the different stages of the purification process. The *tetX* amplicon with an abundance higher than 1.00% in any of the samples have been marked with a unique capital letter (from A to E). **(D)**, The host of the *tetX* gene for which the given amplicon has a perfect match (0 mismatches or 1 mismatch) according to NCBI NT database. The dotted, coloured lines indicate different families of the listed hosts. **(E)**, The phylogenetic tree representing the homology of the reference sequences. **(F)**, The relative abundance of the bacterial community in the analysed samples. Abbreviations: RA–relative abundance, PS–primary sludge, AS–activated sludge, ADS–anaerobic digestion sludge.

sample (PS), whereas in the case of the *sul2* and *tetX* amplicons, the highest variability was observed in the activated sludge samples (AS). The results showed that anaerobic digestion sludge (ADS) reduces the number of unique variants of the *ermF* and *sul2* genes (Figure 2B).

3.5 Matching antibiotic resistance gene amplicons to reference variants

In the next step, the similarity of obtained ARG amplicons to reference sequences of variants was analysed. It was revealed that 11 out of 79 identified amplicons perfectly matched one or more reference sequences. From those, only four amplicons of the *ermF* gene could be assigned to the unique reference sequence (variant). It was observed that the vast majority of *ermF* amplicons and two of the *tetX* amplicons had at least two mismatches with known reference sequences. The maximum dissimilarity between the amplicons obtained and the reference sequences reached up to 50 mismatches (Figure 3A and Figure 4A).

The relative abundance of obtained amplicons in subsequent stages of the WWTP has been analysed. It was shown that the relative abundance of 12 *ermF* amplicons, five *tetX* amplicons and one *sul2* amplicon was higher than 1.00% in at least one of the analysed samples, and these dominant variants constituted on average 97.97% ± 1.61% of all obtained amplicons in the analysed sample (Figure 3B and Figure 4C).

Within the highly abundant PCR amplicons of the *ermF* gene, only two (A and D) can be assigned to a unique reference sequence. Variant A maintains high abundance along subsequent stages of the analysed WWTP (35.49% ± 3.00%). It was shown that these amplicons are identical to the homologous region of the reference sequences which previously were identified in *Myroides* spp., *Sphingobacterium* spp. and numerous undefined non-cultivable bacteria. The highest relative abundance was observed for amplicon F of the *ermF* gene. The amplicon reached 44.22% in the AS sample. It was shown that the amplicon is identical to the homologous region of five different reference sequences which were previously identified in *Alistipes* spp., *Bacteroides* spp. *Parabacteroides* spp., *Phocaeicola* spp. and *Rimieralla* spp. and some uncultured bacteria. However, it is important to mention that the high relative abundance of some amplicons might be the result of a multiplication signal from different variants of a given ARG that could not be distinguished by the primer pairs used. The largest shift of the abundance of a specific *ermF* amplicon was observed for amplicon C, for which a significant change between aerobic samples (PS and AS) and anaerobic sample (ADS) was observed. Here, the relative abundance increased from 5.30% ± 1.33% (PS and AS) to 29.52% (ADS). Amplicon C did not show a perfect match to any of the reference sequences. Eventually, it was shown that there are some completely novel variants present in the analysed WWTP. The relative abundance of the amplicons marked as I, J, K, M fluctuate from 0.42% to 11.84%. Those amplicons exhibited at least 13 mismatches to the closest reference variant of the *ermF* gene. This indicates that there is a pool of unexplored variants of ARGs present in the WWTP (Figures 3A–C).

Amplicons of the *tetX* gene were equally similar to many reference sequences. It was shown that only two out of the 21 amplicons obtained perfectly matched to the reference sequences. The amplicon marked A matched to 16 reference sequences which were identified in 12 genera belonging to eight bacterial families. Amplicon B matched to 14 another reference sequences. These *tetX* gene variants were previously identified in six different genera belonging to five bacterial families. The relative abundance of amplicon A was dominating and reached 63.45% in PS, 93.91% in AS and 75.65% in ADS (Figures 4A, B, D).

In the case of the *sul2*, one out of six obtained amplicons matched to all reference sequences. Other PCR amplicons exhibited a single mismatch to the reference sequences. Additionally, it was observed that the amplicon with the perfect match significantly dominated in the analysed WWTP. The relative abundance of this amplicon reached 99.52% ± 0.26% (Supplementary Figures S2A, B). It is worth mentioning that the DP value of the primer pair used for amplification of the *sul2* gene was 0.00, which means that only one sequence should be observed. It is highly probable that other observed amplicons of the *sul2* gene were generated via sequencing errors or these are truly novel variants. However, the contribution of these amplicons in the samples are scarce (less than 0.20%), and the dissimilarity to reference sequences (1 mismatch) is located in random loci. A similar conclusion might be derived from the results obtained for the *tetX* analysis. That primer pair also exhibited a very low value of DP (0.11), showing that only four unique sequences should be observed (Figure 2).

Overall result indicates that the tested WWTP (and other WWTPs by default) are reservoirs of many different alleles of the genes encoding the same mechanism of resistance to antibiotics. It was shown that some of identified variants may persist along the whole purification process at the significant abundance. It was observed for variants A, C, K, M of the *ermF* gene or variants A and C of the *tetX* gene. Results showed that some of these variants are present in more than one host assigned to different bacterial families (Figures 3B–D). It suggest that those particular variants might be present on mobile genetic elements and can be easily spread between different type of bacteria (Che et al., 2019). We also observed that some of the identified variants change their abundance along the process, e.g., variant B or C of the *ermF* gene. It indicated that some of gene variants might be highly strain specific (Van Meervenne et al., 2012; Rosconi et al., 2022). The changes of the conditions at subsequent stages of the purification process impacted the community structure which might results in the reduction or enrichment of the particular ARGs variants. It might be a possible explanation for the enrichment of the variant C in ADS stage where level of oxygen is relevantly reduced (Guo et al., 2015). Lastly, we observed the situation where variant was present at high abundance on the first stage of the process and then declined (variant B of the *ermF* gene).

3.6 Prediction bacterial hosts of the generated antibiotic resistance gene amplicons

To predict the potential host of identified ARG amplicon variants, a taxonomic analysis of the WWTP samples was

performed. The total of 2,069,058 paired-end reads was obtained from the DNA sequencing run. Average reads count per sample was 229,895 reads (min. 162,918, max. 302,738). In the course of the quality control, which removed low quality and unspecific reads, the average number of reads per sample dropped to 22,899 (min. 17,985, max. 29,466).

Previously, it was shown that some of the obtained amplicons might be assigned to a specific gene variant, perfectly matching one or more reference sequences. However, the taxonomic analysis performed showed that the majority of genera in which these variants were previously identified were not present in the Oswiecim WWTP. Only five out of 42 genera previously assigned to the analysed ARGs were identified in the WWTP samples that were analysed. Those include representatives of *Acinetobacter* spp., *Aeromonas* spp., *Bacteroidestes* spp., *Ignavibacteria* spp., and *Prevotella* spp. However, even though the above-mentioned ARG amplicons are prevalent in the WWTP samples, the relative abundance of the listed strains were very low (form 0.05%–1.12%), and these genera were detected in a maximum of two out of three stages of the purification process (Figure 3E and Figure 4F). This suggested that some of the ARG variants already described in reference databases might be present in novel hosts to which they were currently unassigned.

Finally, an attempt was made to assign the hosts by analysing the correlation of relative abundance changes along the process between obtained ARGs amplicons and the present taxa. It is worth mentioning that the analysis could produce reliable results only in the case of amplicons to which only one reference sequence was assigned. In other cases, the relative abundance might be factitiously enhanced by multiplication of abundance by different variants which were not distinguished by the primer pair used. Therefore, for this analysis, only primer pairs with the highest possibly DP should be utilised. Only four amplicons generated for the *ermF* gene from which two exhibited substantial relative abundance fulfilled the rule. It was shown that amplicon A exhibited strong correlation ($R^2 = 0.93 \pm 0.07$) with six undefined genera, and amplicon D exhibited a positive correlation with an unspecified taxon belonging to the *Anaerolineae* class.

4 Conclusion

- The analysis of ARGs amplicons is sufficient method for ARG variant diversity and dynamics analyses. However, it needs the usage of primer pairs with possibly the highest diversification power value, which enhance the chance to identify all present variants and assign identified amplicons to potential hosts. In this study we proposed an approach which shown to be effective in selection of the most suitable primer pairs for such analyses.
- Further development of the method should focus on: i) the removal of the subclonal variants generated by sequencing errors, to be sure that identified variants are not the sequencing artifacts; ii) further extension of the reference datasets with special attention to the assignment of bacterial hosts. A better taxonomic assignment of ARG variants may be a crucial point for better removal of AMR via host eradication by setting harmful conditions for the specific groups of bacteria.
- The diversity of the genes encoding the same mechanism of resistance to antibiotics in much more complex than expected. There are still a large pool of ARG variants which are not identified and described in details.
- The wastewater treatment processes have a strong impact on the diversity of the ARG variants. The basis of that phenomenon is not well understood and needs further considerations.

Data availability statement

The datasets presented in this study can be found in online repositories. The names of the repository/repositories and accession number(s) can be found in the article/Supplementary Material.

Author contributions

AG: Conceptualization, Data curation, Formal Analysis, Investigation, Methodology, Software, Validation, Visualization, Writing–original draft, Writing–review and editing. PO: Investigation. LD: Conceptualization, Formal Analysis, Funding acquisition, Methodology, Project administration, Resources, Supervision, Validation, Writing–review and editing.

Funding

The author(s) declare financial support was received for the research, authorship, and/or publication of this article. This work was supported by the National Science Centre (Poland) (grant number 2021/41/B/NZ9/01552).

Conflict of interest

The authors declare that the research was conducted in the absence of any commercial or financial relationships that could be construed as a potential conflict of interest.

Publisher's note

All claims expressed in this article are solely those of the authors and do not necessarily represent those of their affiliated organizations, or those of the publisher, the editors and the reviewers. Any product that may be evaluated in this article, or claim that may be made by its manufacturer, is not guaranteed or endorsed by the publisher.

Supplementary material

The Supplementary Material for this article can be found online at: https://www.frontiersin.org/articles/10.3389/fgene.2023.1334646/full#supplementary-material

References

Alanis, A. J. (2005). Resistance to antibiotics: are we in the post-antibiotic era? *Archives Med. Res.* 36 (6), 697–705. doi:10.1016/j.arcmed.2005.06.009

Arabi, H., Pakzad, I., Nasrollahi, A., Hosainzadegan, H., Azizi Jalilian, F., Taherikalani, M., et al. (2015). Sulfonamide resistance genes (sul) M in extended spectrum beta lactamase (ESBL) and non-ESBL producing *Escherichia coli* isolated from Iranian hospitals. *Jundishapur J. Microbiol.* 8 (7), e19961. doi:10.5812/jjm.19961v2

Bolyen, E., Rideout, J. R., Dillon, M. R., Bokulich, N. A., Abnet, C. C., Al-Ghalith, G. A., et al. (2019). Reproducible, interactive, scalable and extensible microbiome data science using QIIME 2. *Nat. Biotechnol.* 37 (8), 852–857. doi:10.1038/s41587-019-0209-9

Callahan, B. J., Mcmurdie, P. J., Rosen, M. J., Han, A. W., Johnson, A. J., and Holmes, S. P. (2016). DADA2: high resolution sample inference from Illumina amplicon data. *Nat. Methods* 13 (7), 581–583. doi:10.1038/nmeth.3869

Che, Y., Xia, Y., Liu, L., Li, A. D., Yang, Y., and Zhang, T. (2019). Mobile antibiotic resistome in wastewater treatment plants revealed by Nanopore metagenomic sequencing. *Microbiome* 7 (1), 44. doi:10.1186/s40168-019-0663-0

Chen, S., Zhou, Y., Chen, Y., and Gu, J. (2018). Fastp: an ultra-fast all-in-one FASTQ preprocessor. *Bioinformatics* 34 (17), i884–i890. doi:10.1093/bioinformatics/bty560

Chenna, R., Sugawara, H., Koike, T., Lopez, R., Gibson, T. J., Higgins, D. G., et al. (2003). Multiple sequence alignment with the Clustal series of programs. *Nucleic Acids Res.* 31 (13), 3497–3500. doi:10.1093/nar/gkg500

Davies, J., and Davies, D. (2010). Origins and evolution of antibiotic resistance. *Mol. Biol. Rev. Microbiol. Mol. Biol. Rev.* 74 (3), 417–433. doi:10.1128/MMBR.00016-10

Dziurzynski, M., Gorecki, A., Pawlowska, J., Istel, L., Decewicz, P., Golec, P., et al. (2023). Revealing the diversity of bacteria and fungi in the active layer of permafrost at Spitsbergen island (Arctic) - combining classical microbiology and metabarcoding for ecological and bioprospecting exploration. *Sci. Total Environ.* 856 (2), 159072. doi:10.1016/j.scitotenv.2022.159072

Gao, Y.-X., Li, X., Fan, X.-Y., Zhao, J.-R., and Zhang, Z.-X. (2022). Wastewater treatment plants as reservoirs and sources for antibiotic resistance genes: a review on occurrence, transmission and removal. *J. Water Process Eng.* 46, 102539. doi:10.1016/j.jwpe.2021.102539

Goodwin, S., McPherson, J. D., and McCombie, W. R. (2016). Coming of age: ten years of next-generation sequencing technologies. *Nat. Rev. Genet.* 17 (6), 333–351. doi:10.1038/nrg.2016.49

Gorecki, A., Decewicz, P., Dziurzynski, M., Janeczko, A., Drewniak, L., and Dziewit, L. (2019). Literature-based, manually-curated database of PCR primers for the detection of antibiotic resistance genes in various environments. *Water Res.* 161, 211–221. doi:10.1016/j.watres.2019.06.009

Guardabassi, L., Dijkshoorn, L., Collard, J.-M., Olsen, J. E., and Dalsgaard, A. (2000). Distribution and *in-vitro* transfer of tetracycline resistance determinants in clinical and aquatic Acinetobacter strains. *J. Med. Microbiol.* 49 (10), 929–936. doi:10.1099/0022-1317-49-10-929

Guo, J., Peng, Y., Ni, B. J., Han, X., Fan, L., Yuan, Z., et al. (2015). Dissecting microbial community structure and methane-producing pathways of a full-scale anaerobic reactor digesting activated sludge from wastewater treatment by metagenomic sequencing. *Microb Cell Fact.* 14. doi:10.1186/s12934-015-0218-4

Hanahan, D. (1983). Studies on transformation of *Escherichia coli* with plasmids. *J. Mol. Biol.* 166 (4), 557–580. doi:10.1016/S0022-2836(83)80284-8

Herlemann, D. P. R., Labrenz, M., Jürgens, K., Bertilsson, S., Waniek, J. J., and Andersson, A. F. (2011). Transitions in bacterial communities along the 2000 km salinity gradient of the Baltic Sea. *ISME J.* 5 (10), 1571–1579. doi:10.1038/ismej.2011.41

Karkman, A., Johnson, T. A., Lyra, C., Stedtfeld, R. D., Tamminen, M., Tiedje, J. M., et al. (2016). High-throughput quantification of antibiotic resistance genes from an urban wastewater treatment plant. *FEMS Microbiol. Ecol.* 92 (3), fiw014–7. doi:10.1093/femsec/fiw014

Koike, S., Aminov, R. I., Yannarell, A. C., Gans, H. D., Krapac, I. G., Chee-Sanford, J. C., et al. (2010). Molecular ecology of macrolide-lincosamide-streptogramin B methylases in waste lagoons and subsurface waters associated with swine production. *Microb. Ecol.* 59 (3), 487–498. doi:10.1007/s00248-009-9610-0

Kushner, S. R. (1978). "An improved method for transformation of *E. coli* with ColE1 derived plasmids," in *Genetic engineering*. Editors H. B. Boyer and S. Nicosia (Elsevier/North Holland), 17–23.

Laht, M., Karkman, A., Voolaid, V., Ritz, C., Tenson, T., Virta, M., et al. (2014). Abundances of tetracycline, sulphonamide and beta-lactam antibiotic resistance genes in conventional wastewater treatment plants (WWTPs) with different waste load. *PloS One* 9 (8), e103705. doi:10.1371/journal.pone.0103705

Luo, Y., Mao, D., Rysz, M., Zhou, Q., Zhang, H., Xu, L., et al. (2010). Trends in antibiotic resistance genes occurrence in the Haihe River, China. *Environ. Sci. Technol.* 44 (19), 7220–7225. doi:10.1021/es100233w

Luyt, C.-E., Bréchot, N., Trouillet, J.-L., and Chastre, J. (2014). Antibiotic stewardship in the intensive care unit. *Crit. Care (London, Engl.* 18 (5), 480. doi:10.1186/s13054-014-0480-6

Ma, X., Shao, Y., Tian, L., Flasch, D. A., Mulder, H. L., Edmonson, M. N., et al. (2019). Analysis of error profiles in deep next-generation sequencing data. *Genome Biol.* 20 (1), 50. doi:10.1186/s13059-019-1659-6

Miłobedzka, A., Ferreira, C., Vaz-Moreira, I., Calderón-Franco, D., Gorecki, A., Purkrtova, S., et al. (2021). Monitoring antibiotic resistance genes in wastewater environments: the challenges of filling a gap in the One-Health cycle. *J. Hazard. Mater.* 424, 127407. doi:10.1016/j.jhazmat.2021.127407

Muyzer, G., De Waal, E. C., and Uitterlinden, A. G. (1993). Profiling of complex microbial populations by denaturing gradient gel electrophoresis analysis of polymerase chain reaction-amplified genes coding for 16S rRNA. *Appl. Environ. Microbiol.* 59 (3), 695–700. doi:10.1128/aem.59.3.695-700.1993

Ng, L. K., Martin, I., Alfa, M., and Mulvey, M. (2001). Multiplex PCR for the detection of tetracycline resistant genes. *Mol. Cell. Probes* 15 (4), 209–215. doi:10.1006/mcpr.2001.0363

Olczak-Pieńkowska, A., and Hryniewicz, W. (2021). Impact of social, economic, and healthcare factors on the regional structure of antibiotic consumption in primary care in Poland (2013-2017). *Front. Public Health* 9, 680975. doi:10.3389/fpubh.2021.680975

O' Neil, J. (2014). Review on Antibiotic resistance. Antimicrobial Resistance: tackling a crisis for the health and wealth of nations. *Health Wealth Nations*, 1–16. https://amr-review.org/sites/default/files/AMRReviewPaper-Tacklingacrisisforthehealthandwealthofnations_1.pdf.

Peak, N., Knapp, C. W., Yang, R. K., Hanfelt, M. M., Smith, M. S., Aga, D. S., et al. (2007). Abundance of six tetracycline resistance genes in wastewater lagoons at cattle feedlots with different antibiotic use strategies. *Environ. Microbiol.* 9 (1), 143–151. doi:10.1111/j.1462-2920.2006.01123.x

Quast, C., Pruesse, E., Yilmaz, P., Gerken, J., Schweer, T., Yarza, P., et al. (2013). The SILVA ribosomal RNA gene database project: improved data processing and web-based tools. *Nucleic Acids Res.* 41, D590–D596. doi:10.1093/nar/gks1219

Robicsek, A., Strahilevitz, J., Sahm, D. F., Jacoby, G. A., and Hooper, D. C. (2006). Qnr prevalence in ceftazidime-resistant Enterobacteriaceae isolates from the United States. *Antimicrob. Agents Chemother.* 50 (8), 2872–2874. doi:10.1128/AAC.01647-05

Rosconi, F., Rudmann, E., Li, J., Surujon, D., Anthony, J., Frank, M., et al. (2022). A bacterial pan-genome makes gene essentiality strain-dependent and evolvable. *Nat. Microbiol.* 7 (10), 1580–1592. doi:10.1038/s41564-022-01208-7

Salk, J. J., Schmitt, M. W., and Loeb, L. A. (2018). Enhancing the accuracy of next-generation sequencing for detecting rare and subclonal mutations. *Nat. Rev. Genet.* 19 (5), 269–285. doi:10.1038/nrg.2017.117

Song, T., Li, H., Li, B., Yang, J., Sardar, M. F., Yan, M., et al. (2021). Distribution of antibiotic-resistant bacteria in aerobic composting of swine manure with different antibiotics. *Environ. Sci. Eur.* 33 (1), 91. doi:10.1186/s12302-021-00535-6

Stoler, N., and Nekrutenko, A. (2021). Sequencing error profiles of Illumina sequencing instruments. *NAR Genomics Bioinforma.* 3 (1), lqab019. doi:10.1093/nargab/lqab019

Szczepanowski, R., Linke, B., Krahn, I., Gartemann, K.-H., Gützkow, T., Eichler, W., et al. (2009). Detection of 140 clinically relevant antibiotic-resistance genes in the plasmid metagenome of wastewater treatment plant bacteria showing reduced susceptibility to selected antibiotics. *Microbiol. Read. Engl.* 155 (7), 2306–2319. doi:10.1099/mic.0.028233-0

Tamura, K., and Nei, M. (1993). Estimation of the number of nucleotide substitutions in the control region of mitochondrial DNA in humans and chimpanzees. *Mol. Biol. Evol.* 10 (3), 512–526. doi:10.1093/oxfordjournals.molbev.a040023

Tamura, K., Stecher, G., and Kumar, S. (2021). MEGA11: molecular evolutionary genetics analysis version 11. *Mol. Biol. Evol.* 38 (7), 3022–3027. doi:10.1093/molbev/msab120

Van Meervenne, E., Van Coillie, E., Kerckhof, F.-M., Devlieghere, F., Herman, L., De Gelder, L. S. P., et al. (2012). Strain-specific transfer of antibiotic resistance from an environmental plasmid to foodborne pathogens. *J. Biomed. Biotechnol.* 2012, 834598. doi:10.1155/2012/834598

Wengenroth, L., Berglund, F., Blaak, H., Chifiriuc, M. C., Flach, C.-F., Pircalabioru, G. G., et al. (2021). Antibiotic resistance in wastewater treatment plants and transmission risks for employees and residents: the concept of the AWARE study. *Antibiot. (Basel, Switz.* 10 (5), 478. doi:10.3390/antibiotics10050478

WHO (2019). *WHO list of critically important antimicrobials (WHO CIA list).*

Yang, W., Moore, I. F., Koteva, K. P., Bareich, D. C., Hughes, D. W., and Wright, G. D. (2004). TetX is a flavin-dependent monooxygenase conferring resistance to tetracycline antibiotics. *J. Biol. Chem.* 279 (50), 52346–52352. doi:10.1074/jbc.M409573200

frontiers | Frontiers in Environmental Science

TYPE Original Research
PUBLISHED 29 January 2024
DOI 10.3389/fenvs.2024.1340875

Check for updates

OPEN ACCESS

EDITED BY
Visva Bharati Barua,
University of North Carolina at Charlotte, United States

REVIEWED BY
Krishna Yadav,
Iowa State University, United States
Priyanka Uddandarao,
National Institute of Technology, India

*CORRESPONDENCE
Raju Sekar,
Sekar.Raju@xjtlu.edu.cn

RECEIVED 19 November 2023
ACCEPTED 08 January 2024
PUBLISHED 29 January 2024

CITATION
Liu S, Lu J, Adriaenssens EM, Wang J, McCarthy AJ and Sekar R (2024), Industrial and agricultural land uses affected the water quality and shaped the bacterial communities in the inflow rivers of Taihu Lake.
Front. Environ. Sci. 12:1340875.
doi: 10.3389/fenvs.2024.1340875

COPYRIGHT
© 2024 Liu, Lu, Adriaenssens, Wang, McCarthy and Sekar. This is an open-access article distributed under the terms of the Creative Commons Attribution License (CC BY). The use, distribution or reproduction in other forums is permitted, provided the original author(s) and the copyright owner(s) are credited and that the original publication in this journal is cited, in accordance with accepted academic practice. No use, distribution or reproduction is permitted which does not comply with these terms.

Industrial and agricultural land uses affected the water quality and shaped the bacterial communities in the inflow rivers of Taihu Lake

Shuang Liu[1], Jing Lu[2], Evelien M. Adriaenssens[3], Jianjun Wang[4], Alan J. McCarthy[5] and Raju Sekar[1]*

[1]Department of Biological Sciences, School of Science, Xi'an Jiaotong-Liverpool University, Suzhou, China, [2]Department of Forestry and Environmental Management, Universidad Politécnica de Madrid (UPM), Madrid, Spain, [3]Quadram Institute Bioscience, Norwich, United Kingdom, [4]State Key Laboratory of Lake Science and Environment, Nanjing Institute of Geography and Limnology, Chinese Academy of Sciences, Nanjing, China, [5]Institute of Infection, Veterinary and Ecological Sciences, University of Liverpool, Liverpool, United Kingdom

Taihu Lake is the third-largest freshwater lake in China and is vital as a drinking water source, as well as for irrigation water, flood control, and other functions. Taihu Lake is connected to many inflow rivers, which contribute to the water resource but also to its pollution. Investigating the correlation between water quality, bacterial community structure, and land-use types is essential for pollution control. Yet, few studies have been conducted on all the major inflow rivers of Taihu Lake. This study aimed to assess the bacterial community composition of major inflow rivers of the lake and determine the relationship between the bacterial community, water quality, and land-use. Water samples were collected from ten inflow rivers across four seasons in 2019–2020. DNA extracted from the samples was used for 16S rRNA gene-targeted next-generation sequencing to determine the bacterial community structures. Thirteen physicochemical and microbiological parameters were used to assess the water quality, and the land-use pattern surrounding each sampling location was also profiled. The bacterial community composition demonstrated significant seasonal variation. In summer, the community variation was correlated with chlorophyll *a*, pH, and phosphate-P, and electric conductivity, nitrate-N, and ammonium-N in winter. Rivers in the northwest were more nutrient-rich than those in the southwest. The industrial, residential, and agricultural land-use categories correlated strongly with the bacterial community composition and water nutrient parameters. Accordingly, farmland drainage, untreated domestic wastewater, and industrial pollution were identified as the major objectives for more effective water quality management in the region.

KEYWORDS

pollution, land-use patterns, molecular microbial ecology, 16S rRNA gene sequencing, freshwater microbiology, bacterial community structure, water quality

1 Introduction

Freshwater is an essential source of life on earth, as it provides water for human consumption, functions in agriculture, aquaculture, industries, flood control, and power generation, while also contributing positively to ecology and biodiversity (Nyingi et al., 2013; Biddanda, 2017; Guo et al., 2020). However, deterioration of surface water quality has become a significant worldwide problem (UNESCO, 2019; Yi et al., 2019). Freshwater systems are being polluted by excessive levels of inorganic nutrients, pharmaceutical compounds, heavy metals, and pathogenic microbes (Okada et al., 2018; Koch et al., 2019; Yi et al., 2019).

Water quality in China has declined in recent decades due to rapid urbanization and industrialization (Liu and Raven, 2010; Ma et al., 2022). Although measures have been continuously taken to control pollution, the problems of eutrophication, antibiotics, heavy metals, microbial pathogens, and other pollutants persist (Xu et al., 2014; Mekonnen and Hoekstra, 2015; Zhang et al., 2015; Zhao et al., 2018; Yang et al., 2020). Deaths and illnesses including diarrhoea and liver and gastric cancers caused by the consumption of contaminated water have been reported in some areas of China over the past decade (Tao and Xin, 2014; Chen et al., 2019). Eutrophication, the major concern for freshwater ecology in China, has been reported in lakes and rivers nationwide (Wang et al., 2019a; Wang et al., 2019b; Lin et al., 2021) and algal blooms remain a common unresolved issue in some water bodies (Paerl et al., 2011; Yu et al., 2020; Ma et al., 2022). As a consequence, it is important that pollution sources are identified and efficiently tracked, and management strategies properly developed.

Pollution is introduced into surface water systems through various natural and anthropogenic point and non-point sources (Vega et al., 1998; Yotova et al., 2021). Point sources are single identifiable entities such as wastewater treatment plant effluents (faecal pollution) and factory outlets (chemical pollution) (Islam et al., 2018). Non-point source pollution usually involves large land areas, with transportation of pollutants occurring overland, underground, or even through the atmosphere (USEPA, 2021). Examples include land runoff, precipitation, rainfall, melting snow, seepage and drainage (Liu et al., 2020). Excessive manure, chemical fertilizer or pesticides from agricultural land, toxic chemicals and oil from urban-domestic lands, and soil erosion from forestry or farmlands are the common sources of these pollutions (Bu et al., 2014; Rissman and Carpenter, 2015; USEPA, 2021). Correlating land-use types with sources of pollution will be helpful in the management and control of water quality. Previous studies conducted worldwide showed that the hotspots of water pollution lies around urban, agricultural, industrial and forest land uses (Wijesiri et al., 2018; Xu et al., 2019; Camara et al., 2019; Githinji et al., 2019). Some also concluded that human activity and land-use could have more influence on freshwater ecosystems than seasonal changes (Yu et al., 2018).

In addition to the chemical environment, the microbiological communities need to be considered as they play essential roles in biochemical cycles, food webs and ecosystem functioning (Liu et al., 2018). Next-generation sequencing (NGS) of environmental DNA has been used more recently to describe microbial community structures in freshwater habitats (Zheng et al., 2017; Tang et al., 2018; Ren et al., 2019; Shang et al., 2022). It has been reported that community structures varied in response to temperature, pH, salinity, geographical region, anthropogenic activities, and pollution (Sunagawa et al., 2015; Yang et al., 2016a; Yang et al., 2016b; Chi et al., 2021). Therefore, community structures can be a good indicator of perturbation in ecosystems. Microbial community profiling also provides information on the occurrence, or potential presence, of pathogenic bacteria, which should be monitored in relation to public health protection (Tan et al., 2015; Pereira et al., 2018). NGS has also been successfully used to identify faecal contamination in freshwater (Ashbolt, 2015; Unno et al., 2018; Vadde et al., 2019a). Studying the microbial community structure also provides data for the development of pollution tracking methods, such as microbial source tracking markers for faecal contamination (Vadde et al., 2019b; Mathai et al., 2020).

Taihu Lake is the third largest freshwater lake in China, and is essential for water supply, flood control, recreational activities, fisheries, tourism, transportation, and a drinking water source for approximately 30 million residents (Hu et al., 2017). The greater Taihu watershed is also essential for aquaculture and as a wildlife ecology resource (Cai et al., 2013; Cheng et al., 2014). However, the watershed is now facing environmental issues including deterioration of water quality and eutrophication, which lead to cyanobacterial blooms and cyanotoxin occurrence (Wu et al., 2018; Wang et al., 2021; Xu et al., 2021). These are believed to be the consequences of human and animal waste discharges, farmland runoff, as well as urban domestic, industrial, agriculture and wastewater treatment plant effluents (Ti et al., 2011; Huang et al., 2013; Xu et al., 2019; Zhang et al., 2019). Both small-scale (Guo et al., 2004; Tang et al., 2018) and macroscopic (Zhao et al., 2014; Sunagawa et al., 2015) land-use analyses were conducted in cities and rural towns around Taihu Lake. It was concluded that agricultural land, low- and mid-density residential areas, industrial and poultry factories were the main land-use types that could introduce pollution into the Lake. However, the pollution into Taihu Lake is not always discharged into the lake directly, especially under the strict control of the government in the recent decade. The inflow rivers, as reported previously, are the major contributors to eutrophication and algal blooming in Taihu Lake (Wang et al., 2011a; Du et al., 2017; Wu et al., 2018). Our previous study also reported heavy contamination including faecal pollution in Tiaoxi River, the major inflow river contributing 60% of water into Taihu Lake (Vadde et al., 2018).

The general ecological status and associated environmental parameters of the inflow rivers of Taihu Lake are of paramount importance, but there have been no comprehensive and systematic studies of their water quality and microbiology and also on the impacts of land-use on bacterial communities in the Taihu watershed. Here, the aim was to determine and correlate water quality parameters, bacterial community compositions, and land-use patterns for ten major inflow rivers of Taihu Lake to provide a much more complete environmental profile that will inform pollution and management practices. The results will help our understanding of how pollution sources affect freshwater ecology,

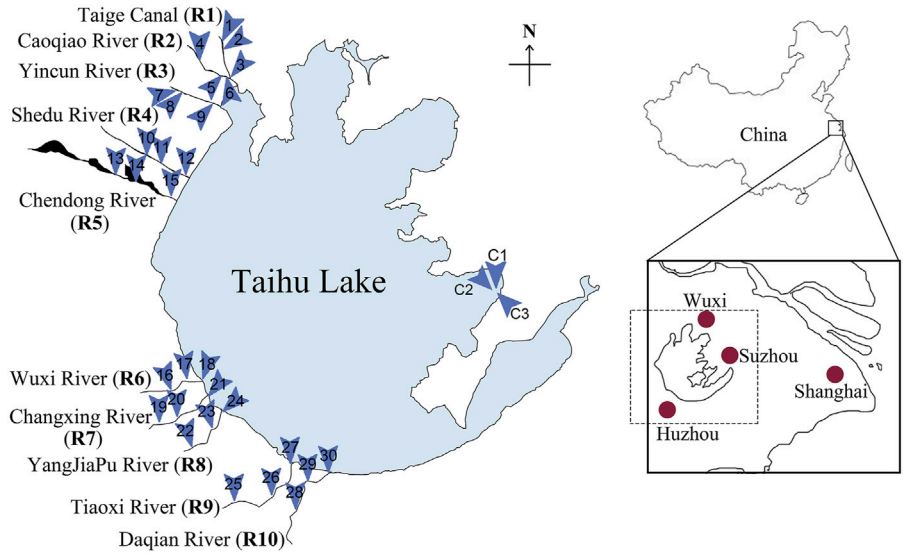

FIGURE 1
The locations of Taihu Lake, the inflow rivers and the selected sampling locations. The ten major inflow rivers (R1-R10) are located on the west side of Taihu Lake. Three sampling locations were selected for each inflow river; thirteen locations were selected in total (1-30). The control locations (C1-C3) in the Taihu Source Water Protection area can be found on the east side of Taihu Lake.

enabling the prediction of pollution risks, the development of water quality management regimes, and urban planning.

2 Materials and methods

2.1 Study area and sampling locations

This study was conducted in the Taihu watershed, particularly targeting the inflow rivers located on the west side of the Taihu Lake (Figure 1). Among the 200 rivers connected to the lake, thirteen are considered as the main inflow rivers. Here, ten of these main inflow rivers selected for the study were Taige Canal (R1), Caoqiao River (R2), Yincun River (R3), Shedu River (R4), Chendong River (R5), Yang Jia Pu River (R6), Wuxi River (R7), Changxing River (R8), Tiaoxi River (R9) and Daqian River (R10). These rivers were selected largely because they contribute the highest volume of water (Wang et al., 2011a) and are the primary contributors of pollution including eutrophication-related nutrients (Qin et al., 2007; Wang et al., 2011a; Du et al., 2017; Vadde et al., 2018). In each river, three points (upstream, middle-stream and downstream) were selected as sampling locations. Three points in the Taihu Source Water Protection Area in Wuzhong district, Suzhou were selected as the control locations (Figure 1). At least two group members participated in all the sampling trips to avoid biases introduced during sampling and sample processing.

2.2 Collection of water samples

Water sampling was conducted once per season in spring 2019, summer 2019, summer 2020 and winter 2020. The surface water samples were collected from the 33 sampling locations including the controls. In total, 132 samples were collected. For each location, 5 L of surface water was directly collected using sterile polyethylene containers and kept at ambient temperature until brought to the laboratory for filtration and DNA extraction. Five hundred mL of water was directly collected in sterile polyethylene bottles and kept on ice during transport to the laboratory, where they were transferred to −20°C until processed for nutrient analyses. Fifty mL of water was also collected using sterile polypropylene centrifuge tubes. This sample was kept on ice until used for microbiological analyses. The air temperature (AT) and water temperature (WT), pH and electrical conductivity (EC) were measured on-site and recorded.

2.3 DNA extraction

Water samples (250 mL each) were filtered through an isopore™ 0.22 μm polycarbonate membrane filter (Merck, Germany) to collect the cellular fraction, with at least six filters prepared for each location. The filters were kept at −20°C until they were used for DNA extraction using the PowerSoil DNA Isolation Kit (MoBio Inc., Carlsbad, CA) according to the manufacturer's instructions. This kit and procedure were used in our previous studies (Vadde et al., 2019b; Fernanda et al., 2022). At least three DNA extracts were prepared for each location and season. The concentrations and the quality of the DNA were measured using a NanoDrop 2000/2000c spectrophotometer (Thermo Fisher Scientific Inc., United States). Replicates were prepared until all the DNA samples achieved 1.8 < A260/A280 < 2.0 and A260/A230 > 1.5. The samples were stored at −80°C until required for further processing.

2.4 Bacterial community analysis by next-generation sequencing

Composite DNA samples from each inflow river were prepared by mixing DNA extracts from three locations. DNA extracts from each location with good quality and quantity (determined by Nanodrop measurement) were selected, and forty-four composite samples in total were prepared. The bacterial community composition of the pooled inflow river surface water DNA extracts was analysed by next-generation sequencing (NGS) of 16S rRNA gene amplicons. Sequencing was carried out at GENEWIZ Suzhou, China on an Illumina MiSeq (Illumina, San Diego, CA, United States) platform. Specially designed primers (Forward: 3′-CCTACGGRRBGCASCAGKVRVGAAT-5'; Reverse: 3′-GGACTACNVGGGTWTCTAATCC-5′) were used in the 16S MetaVx™ method, targeting V3 and V4 hypervariable regions of the 16S rRNA genes. Indexed adapters were added to the ends of the amplicons by limited cycle PCR. The PCR products were then purified with magnetic beads. The concentration of the PCR products was determined using a microplate reader. The fragment sizes were examined by agarose gel electrophoresis. The library was then quantified to 10nM, and PE250/FE300 paired-end sequencing was performed as outlined in the Illumina MiSeq (Illumina, San Diego, CA, United States) manual. The MiSeq Control Software (MCS) was used to read the sequence information.

The sequences obtained in this study were submitted to the NCBI Short Read Archive (SRA) database under the accession numbers 29255681 to 29255724.

2.5 Processing of sequencing data and further analysis

Raw sequence data was processed in QIIME (1.9.1) and VSEARCH (1.9.6). Poor quality reads, chimaeras or short sequences (<200bp) were filtered out. Adaptor, primers, and barcode sequences were trimmed off to get the non-chimera effective reads. Sequences that appeared only once were removed, and the remaining reads were used for clustering of Operational Taxonomic Units (OTU) with a 97% similarity, using VSEARCH (version 1.9.6). The OTU sequences were aligned with the SILVA 138 16S rRNA reference database (Quast et al., 2012; Yilmaz et al., 2014), and the RDP (Ribosomal Database Program) Classifier (Wang et al., 2007a) was used to make taxonomic assignments. Consequently, community structure was analyzed at different phylogenetic levels.

2.6 Water physicochemical analysis

In addition to the parameters measured on-site, total nitrogen (TN), Total phosphorus (TP), nitrate nitrogen (NO_3-N), nitrite nitrogen (NO_2-N), ammonium nitrogen (NH_4-N), phosphate (PO_4-P), total organic carbon (TOC) and chlorophyll *a* (Chl *a*) were measured in the lab. TN and TP were determined by peroxodisulphate oxidation and spectrophotometric methods (Ebina et al., 1983). NO_3-N, NO_2-N, NH_4-N, and PO_4-P were determined as described by Wang et al. (2011b). TOC was analysed by high-temperature oxidation using a Shimadzu analyser (model 5,000; Tokyo, Japan). Chl *a* values were quantified by acetone extraction and spectrophotometry methods as described by American Public Health Association (APHA, 2005).

2.7 Microbiological analyses

Total coliform (TC) and faecal coliform (FC, or thermotolerant coliforms) were quantified as described previously (Vadde et al., 2018) within 24 h of sample collection. For TC quantification, 100 µL of each sample was plated on Harlequin™ *Escherichia coli*/coliform medium (LabM, Heywood, UK) and the plates were incubated at 37°C for 24 h. The blue colonies (*E. coli*) and pink-purple colonies (coliforms) were counted, and the TC expressed in cfu/mL. FC values were determined by filtering 2 mL of water samples through isopore™ 0.45 µm gridded mixed cellulose ester (MCE) membrane filters (Merck, Germany). The membranes were placed with gridded side up on mFC agar plates (HopeBio, Qingdao) and incubated at 45.5°C for 24 h. Colonies with blue shades were counted and the FC values were expressed in cfu/100 mL.

2.8 Land-use pattern analysis

The land-use maps were prepared using the geographical information system software ArcGIS 10.3 and ArcGIS Pro. Based on the Google Earth China Service Map of cities around Taihu Lake, a layer of buffer zones with a radius of 1 km around each sample point was created. The 1 km catchment radius was selected based on the 15-min pedestrian-scale neighbourhood with a complete provision of required basic services and facilities in accordance with the Chinese national standard for urban residential area planning and design (GB 50180-2018) (MOHURD, 2018). This could fully represent the diversity of land-use types around one particular point in a typical Chinese city, with avoidance of biases due to selection of the location (Yang, 2008). By referencing the official land-use maps of Changzhou, Wuxi, and Huzhou, as well as Google Earth and Baidu maps covering the sample areas, the detailed land-use classifications were digitized within these buffer zones per the national *Code for classification of urban land-use and planning standards of development land* (GB50137-200) (MOHURD, 2011) and the recently released national *Guidance of Territorial Spatial Investigation, Plan, Land use control Classification* (MOHURD, 2020). The Tier-2 classification percentages were averaged for three sampling locations in each river to represent the land-use status, and this was used in the clustering analysis.

2.9 Statistical analyses

Microsoft Excel was used for data entry and basic processing of raw data. R (version 4.0.3) and R studio (version 1.4.1717) were used for further data analyses. Spatial and seasonal variations of physicochemical and microbiological parameters were analysed by one-way analysis of variance (ANOVA) in R. Principal

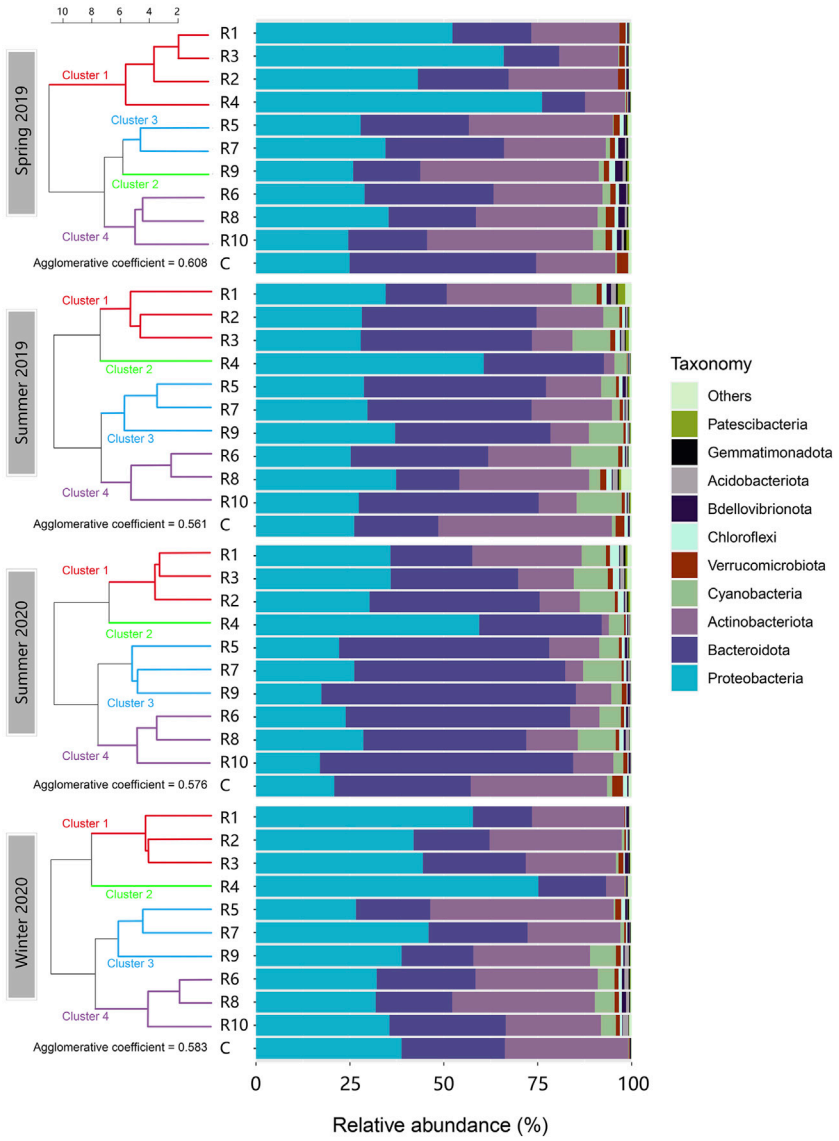

FIGURE 2
Phylum-level composition of the microbial communities in the inflow rivers in the four seasons aligned with clustering. (R1, Taige Canal; R2, Caoqiao River; R3, Yincun River; R4, Shedu River; R5, Chendong River; R6, Yang Jia Pu River; R7, Wuxi River; R8, Changxing River; R9, Tiaoxi River; R10, Daqian River.) The top ten abundant phyla found in the surface water samples are shown in this figure. Proteobacteria, Bacteroidota, Actinobacteria, and Cyanobacteria were the predominant phyla which accounted for more than 90% of the bacterial community. The clusters in different colours are shown on the left.

Component Analysis (PCA) of water quality was done using the R code "princomp" after confirmation with Kaiser-Meyer-Olkin (KMO) and Bartlett's tests. WT was not included in the PCA to avoid its impact on the seasonal distribution pattern.

The rivers were clustered for each season based on both water quality (EC, pH, TN, TP, NO_3-N, NO_2-N, PO_4-P, NH_4-N, TOC, *Chl a*) and Tier-2 land-use status (municipal and services, logistics and transportation, industrial, residential, green spaces, semi-artificial landscape, semi-natural landscape and others). Hierarchical clustering was performed using normalized data with a target of four clusters for each season.

For the microbial community analyses, alpha diversity calculations, including Shannon diversity index, Simpson diversity index, abundance-based coverage estimator (ACE), Chao1 richness estimator and good's coverage were calculated using QIMME (1.9.1). Permutational Multivariate Analysis of Variance (PERMANOVA, performed in R using "adonis2" in the "vegan" package) was used to identify the differences in the microbial community between four seasons and between rivers in different locations.

3 Results

3.1 Alpha-diversity of the bacterial community

Forty-four composite DNA samples extracted from inflow rivers and control locations were profiled by sequencing the 16S rRNA

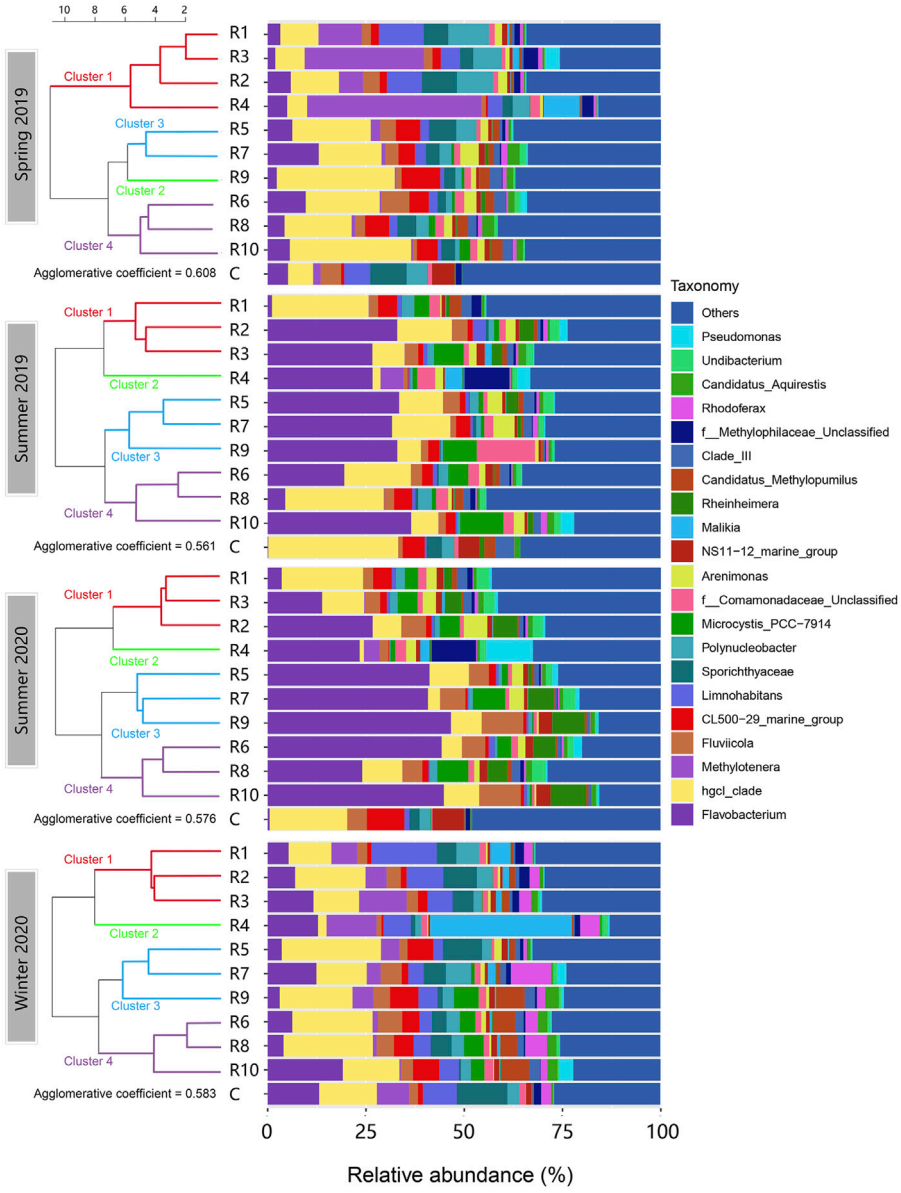

FIGURE 3
Genus-level composition of the microbial communities in the inflow rivers in the four seasons aligned with clustering. (R1, Taige Canal; R2, Caoqiao River; R3, Yincun River; R4, Shedu River; R5, Chendong River; R6, Yang Jia Pu River; R7, Wuxi River; R8, Changxing River; R9, Tiaoxi River; R10, Daqian River.) The top twenty-one abundant genus-level OTUs found in the surface water samples are shown in this figure. *Flavobacterium, hgcI_clade, Methylotenera* and *Fluviicola* were the OTUs with the highest average abundance. The clusters in different colours are shown on the left.

gene amplicons and the diversity and community compositions were analysed. A total of 2,423,270 non-chimera effective reads were generated, and the number of reads in the individual samples ranged from 35,202 to 86,820. The read number was normalized to 21,268 after removing the sequences that appeared only once. In total, 868 OTUs were generated (similarity <97%). The rarefaction curves based on these data are shown in Supplementary Figure S1. The read and OTU numbers, Good's coverage, alpha diversity indices including ACE and Chao1 for community richness and Shannon and Simpson for community diversity for individual samples are shown in Supplementary Table S1.

The results showed similar average diversity and richness for summer and spring-winter samples, with no significant changes between seasons ($p > 0.05$), although detailed analysis does show that the structures were quite distinct. This could also be related to the high variance introduced by the spatial changes. Samples collected from R3 in summer 2020 (SU20-R3) had the most OTUs (600) among all samples, as well as the highest diversity (Shannon = 7.445, Simpson = 0.987). The highest richness was observed in the samples from R5, summer 2019 (ACE = 663, Chao1 = 679). On the contrary, R10 samples collected in the summer 2020 had the fewest OTU number (394) and the lowest richness (ACE = 474. Chao1 = 487). R4 in winter 2020 showed the lowest level of diversity (Shannon = 4.799, Simpson = 0.851).

The OTUs were classified from phylum to genus levels. In total, 30 different bacterial phyla were identified, with the predominant

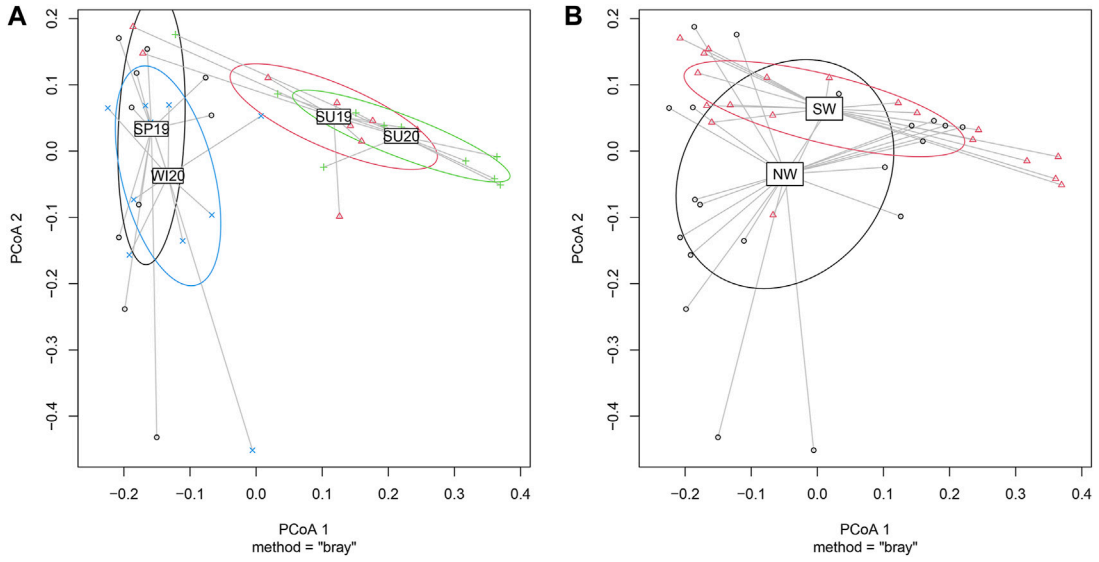

FIGURE 4
Clustered PCoA showing differences in microbial community structures between **(A)** seasons and **(B)** geographical locations. (SP19, spring of 2019; SU19, summer of 2019; SU20, summer of 2020; WI20, winter of 2020). The PcoA figures were plotted based on the genus-level microbial community structures. PCoA 1 explained 32.17% of the variation, while PCoA 2 explained 15.50%. **(A)** Samples collected in cold seasons (spring 2019 and winter 2020) mostly overlapped, while the samples collected in warm seasons (summer 2019 and summer 2020) overlapped. Significant differences were observed between cold seasons and warm seasons ($p < 0.001$). **(B)** Samples collected in the NW also differed significantly from samples collected in SW ($p < 0.05$).

phyla Proteobacteria, Bacteroidota, Actinobacteria and Cyanobacteria accounting for over 90% of the relative abundance in all samples (Figure 2). No significant differences were observed in the bacterial community profile between the control locations and the inflow rivers at the phylum level. The control locations were not included in further analyses but used as a reference. The composition of phyla varied both seasonally and spatially. Bacteroidota and Cyanobacteria were more abundant in summer seasons than spring and winter, and the opposite pattern was observed for Proteobacteria and Actinobacteria. Proteobacteria was the most abundant phylum observed in winter 2020 (26.6%–75.2% with a mean of 43.0%), followed by spring 2019 (24.6%–76.2% with a mean of 41.5%). Proteobacteria was significantly less abundant in the warm seasons (summers 2019 and 2020) than cold seasons (spring 2019 and winter 2020) ($p < 0.05$). However, high relative abundance of Proteobacteria (59.4%–76.2%) was also observed in R4 in all four seasons. Bacteroidota was the second most abundant phylum observed. There was a clear pattern that Bacteroidota was significantly higher in summer than in spring and winter (43.0% vs 22.6%; $p < 0.001$). The highest proportion of Bacteroidota was found in Tiaoxi River (R9) in summer 2020, accounting for 67.7% of the total community. Actinobacteria, similar to Proteobacteria, was also significantly more abundant in spring and winter (4.9%–48.8%) than in summer (1.9%–34.5%) ($p < 0.001$). On the contrary, Cyanobacteria occupied 2.1%–12.5% of the communities with an average of 6.6% in summer and 0.01%–6.9% with an average of 1.7% in cold seasons, showing a significant increase in warm seasons ($p < 0.001$).

Of 125 identified order-level OTUs, *Burkholderiales*, *Flavobacteriales*, *Frankiales* and *Chitinophagales* were the predominant orders and accounted for over 50% of the community in all samples (Supplementary Figure S2). At the genus level, a total of 298 different genera were identified across all the samples. The relative abundances of the top twenty-one genus-level OTUs are shown in Figure 3. These OTUs in sum accounted for at least 50% of the relative abundance in each microbial community. *Flavobacterium* (Bacteroidota), *hgcI_clade* (Actinobacteria) and *Methylotenera* (Proteobacteria) were the predominant genus-level OTUs observed. *Flavobacterium* was the major genus that contributed to Bacteroidota abundance in this study. It was most abundant in the summer seasons. *HgcI_clade* was more abundant in spring 2019 and winter 2020, but it also showed high spatial variations. R4 had the lowest relative abundance of *HgcI_clade* (1.08%–5.07%) in all seasons, while the other rivers had varying abundance across seasons. *Methylotenera* was clearly more abundant in spring and winter than in summer. They were also found more abundant in the rivers located in the northwest (R1-R4) of Taihu Lake, especially in R4. Spatial and seasonal changes were also observed in other genus-level OTUs.

3.2 Beta-diversity of bacteria and community composition

The bacterial community data were analysed using multivariate statistics to assess the beta-diversity. The analyses showed the differences in the bacterial community structures between seasons or between rivers. PCoA (principal co-ordinate analysis) results showed that two main co-ordinates contributed to the variation among samples (Figure 4). PCoA 1 and 2 together explained 47.67% of the variations. PCoA 1 explained 32.17% of the variation, while PCoA 2 explained 15.50%. Permutational

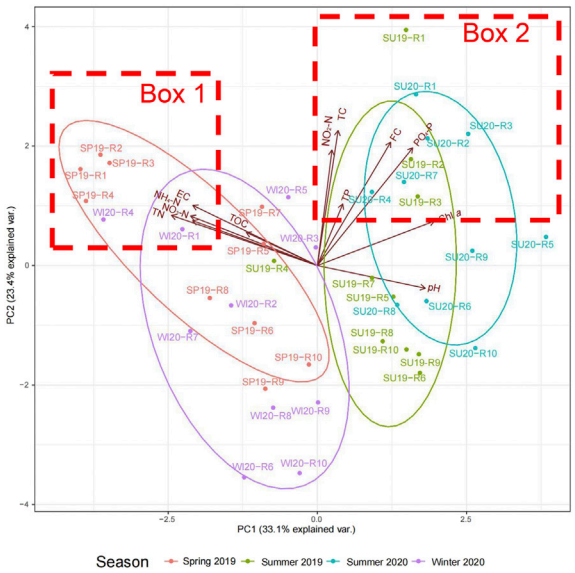

FIGURE 5
PCA of inflow river water quality distribution in different seasons. (SP19, spring of 2019; SU19, summer of 2019; SU20, summer of 2020; WI20, winter of 2020. R1, Taige Canal; R2, Caoqiao River; R3, Yincun River; R4, Shedu River; R5, Chendong River; R6, Yang Jia Pu River; R7, Wuxi River; R8, Changxing River; R9, Tiaoxi River; R10, Daqian River. Box 1: Samples most affected by TN, EC, NH_4-N, NO_3-N, and TOC. Box 2: Samples most affected by FC and PO_4-P). The PCA was plotted based on the water physicochemical and microbiological characteristics of the inflow river water samples in four sampling seasons. Samples collected in different seasons are shown in different colours. PC 1 explains 33.1% of the variations. PC2 explains 23.4% of the variations.

Multivariate Analysis of Variance (PERMANOVA) allowed comparisons of multiple variables between grouped multiple samples (Figure 4). The bacterial community structure significantly varied across seasons according to the overall PERMANOVA test ($p < 0.001$) (Figure 4A). Pairwise PERMANOVA showed significant differences between spring 2019 and summer 2019 ($p < 0.01$), spring 2019 and summer 2020 ($p < 0.001$), summer 2019 and winter 2020 ($p < 0.001$), and summer 2020 and winter 2020 ($p < 0.001$). There were no significant differences in the bacterial community compositions between the two cold seasons (spring and winter) or between the two summers. For location comparisons, the clustering is shown in Figure 4B. A significant difference was observed between rivers located in the northwest side of Taihu Lake (Jiangsu Province) and those located in the southwest (Zhejiang Province) ($p < 0.05$).

3.3 Water quality analyses

Water physicochemical and microbiological characteristics at the selected sampling locations in the summer and winter of 2020 are shown in Supplementary Figure S3. Results for the spring and summer of 2019 have been reported previously (Fernanda et al., 2022). Two-way ANOVA showed that all parameters except water temperature (WT) showed spatial differences between rivers, while all parameters except chlorophyll *a* showed significant seasonal variation (Supplementary Table S2). WT, EC, pH, TP, NO_2-N, NH_4-N, PO_4-P and Chl *a* significantly varied with the combined effects of spatial and seasonal impacts.

The PCA results showed the distribution of water physico-chemical and microbiological parameters (Figure 5). PC1 explained 33.1% of the total variation, which was mainly composed of negative loadings of TN, NH_4-N, NO_3-N, EC and TOC and positive loadings of Chl *a*, higher pH, PO_4-P and FC. PC2, which explained 23.4% of the total variation, mainly comprised positive loadings of most of the parameters, especially TC, FC, PO_4-P, NO_2-N. pH had a weak negative loading of PC2. The samples were clearly separated by seasons. Samples collected in spring 2019 and winter 2020 were clustered towards negative PC1, showing that TN, NH_4-N, NO_3-N, EC and TOC were the major factors that influenced the samples in cold seasons. Samples collected in summer 2019 and summer 2020 were distributed towards positive PC1, indicating that increased Chl *a*, pH, PO_4-P and FC were the main factors that affected the water quality in summer seasons. With respect to location, the rivers located on the northwest side of Taihu Lake, especially R1-R4, were more distributed towards positive PC2 in all seasons (Box 1 and Box 2 in Figure 5). This indicated that these rivers were subject to higher nutrients especially PO_4-P and NO_2-N, lower pH, and higher TC and FC counts, compared to the other rivers.

3.4 Land-use analyses

Land-use in a radius of 1 km around each sampling location was analysed and categorized into 38 different second-tier and third-tier classifications, according to the national standard (MOHURD, 2011; MOHURD, 2020). The percentages of the land-use types around the sampling location are shown in Supplementary Figure S4, and Supplementary Table S3 explains the land-use categories. The most dominant land-use type was cultivated land, which occupied an average of 35% of the land around the sampling locations. This indicates that agriculture is the main activity occupying most of the inflow rivers' land. The average percentage of cultivated land was highest near R4 (56.2%), R1 (51.8%), and R3 (48.0%), which are all located northwest of Taihu Lake.

The sum of low and mid-density residential land occupied on average 15.6% of the area near the sampling locations. R5 (23.3%) and R7 (22.6%) had the most residential land coverage. The residential areas were most evenly distributed near R1 (12.8%) and R2 (15.1%). With respect to industrial lands, Class A, B, and C industrial land added up to 10.37% of the area near sampling locations. The highest industrial land percentages were found around the R2 sampling locations (24.7%) and R1 locations (15.6%). Although the most densely distributed industrial lands were located near some of the R7 and R8 sampling locations in the southwest, Class C industrial lands were found only along R1, R2, and R3. Industrial lands were also evenly distributed along these three rivers in the northwest, unlike other rivers where industries appeared in only one or two locations. Semi-natural landscapes, including rivers, lakes, and forests, which are indicators of less anthropogenic footprints, were more abundant near R8 and R10, and least near the rivers in the northwest (R1-R4).

The land-use analyses showed the highest anthropogenic activities northwest of Taihu Lake. R1-R4 are located across

TABLE 1 The Hierarchical clustering results of the ten inflow rivers based on the physicochemical features and land-use patterns. In spring 2019, cluster 1 = R1, R2, R3, R4; cluster 2 = R9; cluster 3 = R5, R7; cluster 4 = R6, R8, R10. In summer 2019, summer 2020, and winter 2020, cluster 1 = R1, R2, R3; cluster 2 = R4; cluster 3 = R5, R7, R9; cluster 4 = R6. R8, R10. (R1, Taige Canal; R2, Caoqiao River; R3, Yincun River; R4, Shedu River; R5, Chendong River; R6, Yang Jia Pu River; R7, Wuxi River; R8, Changxing River; R9, Tiaoxi River; R10, Daqian River).

Rivers	Spring 2019	Summer 2019	Summer 2020	Winter 2020
R1	1	1	1	1
R2	1	1	1	1
R3	1	1	1	1
R4	1	2	2	2
R5	3	3	3	3
R6	4	4	4	4
R7	3	3	3	3
R8	4	4	4	4
R9	2	3	3	3
R10	4	4	4	4

industrialised towns. The sampling locations are mostly surrounded by agricultural land (52.3%, 34.7%, 49.1%, and 57.9%, respectively), industries (15.6%, 24.7%, 10.0%, and 10.6%), and some mid- or low-density residences (12.8%, 15.1%, 17.6%, and 11.9%, respectively). Areas near R6 and R8 locations most resemble traditional Chinese rural areas, as they are most affected by the vast cultivated land around them (44.8% and 39.5%). In comparison, the residential land is mainly low-density (9.3% and 10.4%). Locations around R5, R7, and R9 are more like small towns, where the road (6.5%, 10.2% and 11.4%) and mid-density residential land (21.1%, 15.8%, and 18.1%) occupy relatively higher proportions than other places. R10, however, showed the least impact of human activities and the most considerable abundance of semi-natural landscapes (21.2%). Overall, this profile aligns well with the nutrient levels of the inflow rivers, i.e., higher nutrient levels were observed where anthropogenic activities were abundant (Figure 5).

3.5 Clustering of water physicochemical and land-use patterns

The average water physicochemical parameter levels and the average land-use patterns of each river were combined to classify the ten rivers into four clusters (Table 1), and the contribution values are present in Supplementary Table S4. The clustering pattern was identical in summer 2019, summer 2020, and winter 2020. Cluster 1 (R1, R2, R3) featured high percentages of industrial land but lower percentages of semi-natural land. A higher industrial footprint were found around rivers in this cluster. Increased EC, TN, TP, NO_3-N, NO_2-N, and PO_4-P were observed in these rivers. Cluster 2 had only R4, surrounded by semi-artificial lands indicating high agricultural activities. Municipal and services, residential land, green spaces, and semi-natural land were relatively lower around R4. Although this cluster showed soft TP, NO_3-N, and PO_4-P levels in the water, high EC, NH_4-N, TOC, and low pH were found. High TN and *Chl a* levels were also observed in summer. Cluster 3 (R5, R7, R9) was not abundant in any of the nutrients. Logistic and transportation land, residential land, and others (mostly reserved land) were the predominant land-use types around this cluster. Cluster 4 (R6, R8, R10) featured the most abundant semi-natural lands and the lowest residential land percentages, representing the lowest anthropogenic activities. The rivers in this cluster also showed the most oligotrophic water of all the clusters.

The clustering results for spring 2019 were slightly different from the other seasons. Instead of a separate cluster, R4 was clustered with R1, R2, and R3 in cluster 1, possibly due to their similar nutrient levels observed in this season. This cluster represented high levels of industrial land, semi-artificial land, and low levels of semi-natural land. Elevated nutrient levels and a lower pH were also found in this cluster compared to the others. In addition, cluster 2 consisted only of R9, close to logistic and transportation lands, green spaces, and others. Water nutrient levels were lower in R9 as compared to the others. Cluster 3 (R5, R7) also showed low levels of most nutrients, but increased PO_4-P. Municipal services lands and residential lands were the major land-use types here. Cluster 4 (R6, R8, R10) in spring 2019 still represents the least anthropogenic activities and the most oligotrophic water as in other seasons.

3.6 Relationship between environmental features and bacterial community structure

To investigate the relationships between rivers with more similar patterns of bacterial community structure, the phylum-level communities were clustered (Figure 2). In spring 2019, Cluster 1 (R1-R4) showed overall higher levels of Proteobacteria as compared to the other clusters. Bacteroidota and Actinobacteria occupied fewer percentages of the communities in cluster 1 than in the other clusters. Similarly in winter 2020, cluster 1 (R1, R2, R3) and cluster 2 (R4) were richer in Proteobacteria but less abundant in Bacteroidota and Actinobacteria. Cluster 1 (R1, R2, R3) in the summer seasons did not show a higher abundance of Proteobacteria than clusters 3 and 4, but cluster 2 still showed this pattern. Notably, R4 always showed the highest Proteobacteria and lowest Actinobacteria abundances among all rivers across the four seasons. Moreover, low Cyanobacteria abundance was observed in the spring and winter seasons, but rivers with less anthropogenic

activities (R9, R6, R8, R10) clearly showed more cyanobacterial abundance than the others. Nonetheless, Cyanobacteria populations in summer did not show clear spatial change patterns.

Investigating the genus-level community structure and river clustering (Figure 3), *Flavobacterium* (*Flavobacteriales*) was the most abundant genus-level OTU in summer samples. It was lowest in the control and R1, and most abundant in R5, R7, R9 and R10. In spring and winter, the levels of *Flavobacterium* were significantly lower than in summer, and the spatial variation pattern was not aligned with the clustering. *HgcI_clade* was the most abundant genus-level OTU in spring and winter. R1-R4 in spring 2019 and winter 2020 showed relatively lower *HgcI_clade* abundance than the other rivers. In summer, R4 showed the lowest abundance of *HgcI_clade* compared to the other rivers. Moreover, some genus-level OTUs appeared in significantly higher abundance in eutrophic rivers like R1-R4 in spring and winter and R4 in summer than in other rivers. Examples include *Methylotenera*, *Limnohabitans*, *Malikia* and the unclassified Methylophilaceae group. *Pseudomonas* also had a high abundance in R4 in the summer seasons. In contrast, *Fluviicola*, *CL500-29_marine* group and the Candidatus *Methylopumilus* group were more abundant in clusters 3 and 4 where nutrient levels were lower.

4 Discussion

4.1 Physicochemical and microbiological features indicate water quality

The Ministry of Environmental Protection (MEP, renamed as Ministry of Ecology and Environment) of People's Republic of China issued a surface water quality guideline in which all surface waters were classified at five levels (GB 3838-2002), class I (source water, national nature reservoir) being the highest quality and class V (agricultural water, common landscape water) being the lowest quality (MEP, 2002). Class III water was defined as "domestic and drinking water source second class reservoir, aquatic life wintering area, migration channels, aquaculture areas, fishery waters and swimming areas", which is a healthy level for both water-related human activities and water ecosystems. In this study, at least one water sample across four seasons exceeded the acceptable limit for pH, TN, TP, NO_2-N, NH_4-N, PO_4-P and FC for class III water, showing the need for stricter water quality monitoring and management.

For the microbiological features, TC has been used as a faecal contamination indicator in the US (USEPA, 2013). Earlier studies demonstrated that coliform groups could exist naturally in the environment, for example, in fresh and marine waters (Pisciotta et al., 2002; Baudart et al., 2009). Thus, this parameter is no longer used as an indicator for faecal contamination but still an indicator for drinking water quality and health risk assessments (e.g. (Zhang et al., 2018)). Faecal coliform is still used as a traditional indicator for faecal contamination in China, and the MEP guideline value for it is less than 1,000 per 100 mL (MEP, 2002). Exceeding levels of FC undoubtedly showed evidence of faecal pollution in the inflow rivers. Untreated domestic wastewater, runoff from poultry farms, application of human, and animal faeces as fertilizers can be the possible causes of this pollution. Tracking the sources of these faecal pollutions can contribute to management of water quality and public health.

The water physicochemical and microbiological parameters in the inflow rivers changed significantly both seasonally and spatially. The samples were clearly grouped by season and distributed on the positive (summer 2019 and 2020) and negative sides (spring 2019 and winter 2020) of PC1. This was consistent with the significant seasonal differences as presented in the ANOVA results shown in Supplementary Table S1. The PCA also showed that EC, TN, NH_4-N, NO_3-N, PO_4-P, TC and FC are the major factors that contributed to the water quality variations. Similar spatial and seasonal variations were found in Tiaoxi River (R9) during 2014–2015, as one of our previous studies reported (Vadde et al., 2018). TN, NH_4-N, NO_3-N, PO_4-P were observed as major influencing factors in other studies based on Taihu Lake (Paerl et al., 2011; Zheng et al., 2017; Wang et al., 2019a) and other water bodies around the world (Bai et al., 2020; Naranjo et al., 2019). These inputs were easily introduced to surface water by anthropogenic activities, especially through applications of fertilizers. Over the past decades, effective monitoring and control measures have been taken to reduce the pollution in the Taihu Lake (Sunagawa et al., 2015). However, excess nutrients still existed in the inflow rivers of Taihu Lake. This demonstrates that further management and maintenance of inflow river water quality is essential for the improvement of Taihu water quality and ecology. Tracking the sources of the pollution and implementation of appropriate policies could help to reduce these inputs.

As the PCA showed the major contributors to changes in water quality, the hierarchical clustering results showed that the water quality was well aligned with the land-use patterns. For example, cluster 1 in summer 2019, summer 2020, and winter 2020 included the most industrial lands (R1, R2, R3) and was highly consistent with the appearance of high TN, TP, NO_3-N, NO_2-N, and PO_4-P. R4, which was notable among the rivers, showed the highest agricultural activities as well as high NH_4-N, TOC, and EC. Cluster 3 (R5, R7, R9) categorised as municipal, transportation, and residential areas, was characterised by moderate water nutrient levels, while the least anthropogenically affected cluster 4 (R6, R8, R10) showed the most oligotrophic, but alkaline, water.

TN exceeding the acceptable limit of MEP (≤10 mg/L) showed the overall eutrophic status of the inflow rivers of Taihu Lake and especially cluster 1. NO_3-N and NO_2-N were the major TN contributors in this cluster, with NH_4-N less so. NO_3-N is a significant cause of water eutrophication. Chemical fertilizers, animal manure, industrial discharges, and effluent from wastewater treatment plants are the primary sources of NO_3-N (Bakhsh et al., 2005; USEPA, 2009; USEPA, 2012). NO_2-N was beyond the MEP limit in R1, R2, R3, and R8 in at least one season. Human and animal faecal contaminations, fertilizers, and natural deposit erosion are regarded as the main sources of NO_2-N in surface water (Lucassen et al., 2004). In cluster 1, the combination of industrial and agricultural activities was probably the major explanation for the nutrient-rich status of these rivers. TP and PO_4-P showed similar trends, and as Yan et al. (2015) stated, the causes of elevated phosphate content in water could be domestic wastewater, farmland runoff, and the use of animal manure in agriculture. Combining the potential sources and the land-use profile, the agricultural lands were probably the primary source of phosphates in this area. There is no MEP guideline value for PO_4-P, but Shock et al. (2003) reported that PO_4-P levels higher than 20 μg/L will lead to elevated algal growth. There was no significant correlation

between PO_4-P and *Chl a* in this study, which was unexpected. However, Chl *a* showed a significant difference between samples under combined spatial and seasonal effects. This observation was possibly due to high variation between locations increasing the standard deviation of the Chl *a* value for each season.

Cluster 2 (R4) results indicated that agricultural manure and fertilizer runoff was probably a major source of NH_4-N and TOC. Fu et al. (2012) also reported high NH_4-N and TOC from agricultural sources. In addition, lower NO_3-N levels compared to R1-R3 were observed in R4. Slow nitrification might be another reason for the high NH_4-N in this area (Vaishali and Punita, 2013). On the other hand, EC evaluates conductive ions and dissolved solids in freshwater and is usually related to soil runoff into water (Chapman, 2021). USEPA (USEPA, 2022) suggested an EC within the range of 150–500 μS/cm was necessary for certain fish or macroinvertebrates species to be sustained. In this study, R1, R2, R3, R4, and R8 showed EC values higher than this limit in at least one location. Among them, R4 showed the highest average EC among all inflow rivers in all four seasons, indicating that agricultural land has higher risks of soil runoff.

Cluster 3 (R5, R7, R9) was more residential than the other clusters. Water in these rivers had relatively lower nutrient levels than in clusters 1 and 2. Still, it was more nutrient-rich than cluster 4 (R6, R8, R10), which was the least affected by human activities being surrounded by the most semi-natural lands. The water nutrient levels were the lowest across the seasons. However, relatively higher pH values were observed in these rivers, compared to the others. For sustainable biodiversity of aquatic life, a pH range of 6.5 to 8 is preferred (Pearce et al., 1998). The MEP guideline suggested a pH range of 6 to 9 for all water classes (MEP, 2002), and R10 exceeded this limit. According to Bhuyan et al. (1990), high pH is usually related to high levels of photosynthesis or extensive usage of alkaline chemicals in farmlands. More frequent use of fertilizers in the summer could explain the seasonal variation in the pH observed in this study. Nevertheless, considering that R4 (agricultural) did not show any increased pH, the algal content and photosynthesis level may be the main reason for the spatial variation of pH.

4.2 Bacterial community structures under the effects of water quality and land-use

Aligning the clustering results with the bacterial community structures showed difference in bacterial communities between different types of rivers. The predominating phyla Proteobacteria and Bacteroidota in the inflow river samples were commonly found abundant in past research conducted both in the Taihu watershed (Vadde et al., 2019b; Zhu et al., 2019; Zhang et al., 2022) and in other surface freshwater samples (Kirchman, 2002; Allgaier and Grossart, 2006). These phyla have essential functions in multiple nutrient cycling processes, such as nitrification, carbon, and sulphur cycling (Evans et al., 2008; Han et al., 2018). In this study, most of the Proteobacteria found in our samples were Gammaproteobacteria (Supplementary Figure S3). Higher levels of TOC in clusters 1 and 2 (cluster 1 in spring 2019) could be one reason for increased Proteobacteria in R1-R4, as both Beta- and Gamma-proteobacteria are major degraders of organic carbon in water ecosystems (Lin et al., 2021). High levels of NO_2-N and NO_3-N could also be related to them, as some genera of Proteobacteria are good nitrite-oxidizers (Han et al., 2018). As for the seasonal differences, the average level of Proteobacteria was higher in spring and winter than in summer, and the changes in each river were also similar. A higher level of Proteobacteria in winter than in summer was also reported previously on the west side of Taihu Lake (Zhu et al., 2019). However, high spatial variations made it difficult to correlate the abundance of this phylum with seasons (Brummer et al., 2003). Most of the Proteobacteria found in our samples were Gammaproteobacteria (Supplementary Figure S3), which correlated well with gut microbiome and municipal wastewater (Mlejnková and Sovová, 2010). This suggested possible pollution from farmland and residential lands in R1-R4.

Bacteroidota was more abundant in warm seasons than cold seasons. Summer in the Taihu watershed is rainier compared to spring and winter. Thus, the seasonal changes could be related to rainfall in this study. Kavamura et al. (2013) reported a strong correlation between rainfall and *Bacteroidetes* possibly because of high abundance of these bacteria in the rhizosphere, leading to surface water infiltration resulting from storm activity. The spatial changes in Bacteroidota were insignificant, but they could be related to soil runoff or the use of manure fertilisers. *Flavobacterium* (Bacteroidota) is a genus widely found in freshwater samples and has been isolated from various samples such as diseased fish and domestic sewer lines (Jo et al., 2016). They can form biofilms and utilize various organic compounds, which may help explain their predominance in summer when resource availability is high (Liu and Raven, 2010; Zhao et al., 2014). Flavobacteria are usually in higher abundance at lower inorganic nutrient levels. In this study, the higher abundances in cluster 3 (R5, R7, R9) and R10 were consistent with this pattern.

Significant changes in nutrient levels between seasons and locations were also a possible cause for changes in the relative abundances of bacteria. For example, in this study Actinobacteria was more abundant in clusters 3 and 4, where nutrient levels were relatively lower. Increases in the abundance of Actinobacteria were also reported to correlate with reduced nutrients in freshwater in past studies (Meng et al., 2021; Ruprecht et al., 2021). The *hgcI_clade,* a group of Actinobacteria showed strong negative correlations with nutrients in cold weather (spring of 2019 and winter of 2020) but did not show good correlations with nutrient parameters in the summer seasons. Due to their ability to assimilate nutrients present at low concentrations, *hgcI_clade* were previously found to be negatively correlated with nutrient levels, making them good indicators of oligotrophic water (Liu et al., 2020; Ruprecht et al., 2021; Wang et al., 2021).

Cyanobacteria occupied a significantly higher proportion of the bacterial communities in the summer than in winter ($p < 0.01$). Increased temperature and nutrient levels enriched Cyanobacteria in summer, especially PO_4-P, which promotes algal growth (Shock et al., 2003). Notably, in spring and winter, Cyanobacteria were more abundant in clusters 3 and 4 than in 1 and 2. This was opposite to the nutrient levels, including PO_4-P. In the summer samples, however, the variation in Cyanobacteria was more random and not directly related to nutrient richness. Cyanobacterial growth in the inflow rivers may have been affected by a number of other factors which was not tested in this study, such as sunlight or trace elements.

4.3 Water ecosystems and anthropogenic activities

Geographical variations, land uses, and different local policies for water protection could all be the reasons for the changes observed in water quality and microbial communities. R1-R4 were located on the northwest side of Taihu Lake in Yixing, which is a heavily industrialised city in Wuxi. More anthropogenic activities could have impacted these rivers. Significantly different bacterial communities, higher nutrient levels, higher TC and FC counts, lower pH and relatively more algal contents were observed in these rivers, compared to the other inflow rivers. The Taihu watershed's nutrient status has been studied for decades, and the north part of the Taihu watershed has been frequently reported for its more eutrophic status compared to the other parts (Wang et al., 2007b; Zhang et al., 2011; Yu et al., 2020). The eutrophic status of these rivers could have already altered the healthy communities if they were compared with cluster 4, the more semi-natural areas. Notably, R4 and its particular land-use composition could well have caused a significant change in the bacterial community compared to the other rivers, especially R5-R10. The community's relatively low richness and diversity are probably consistent with reduced activity of nitrifying bacteria, slow nitrification and, therefore, high NH_4-N and low NO_3-N. Considering the land-use patterns, this river could have been severely affected by agricultural pollution.

Interestingly, older studies in the Taihu watershed tend to conclude that the residential lands and the industrial lands were the major contributors to contamination (Yuan et al., 2011; Zhao et al., 2013). More recent studies, however, started to report more influences from the industrial and agricultural lands (Sunagawa et al., 2015). This might be the result of urbanization and improvement of domestic wastewater treatment systems in this area. The local government could thus pay more attention to hidden illegal discharges of industrial wastewater to minimize point-source pollution. Standardising agricultural activities and animal farming around the river is the best way to reduce non-point source pollution. Providing guidance to the farmers for more environmentally friendly choices of fertilizers and reducing excessive use of fertilizer could be helpful in maintaining healthy water ecosystems.

5 Conclusion

Overall, this study focused on the relationship between bacterial community structure, water physicochemical properties, and land-use patterns around ten major inflow rivers of Taihu Lake. The bacterial communities were profiled by 16S rRNA gene sequencing, and the alpha and beta diversities of the communities were analysed. Significant spatial and seasonal variations were observed in bacterial communities in the studied rivers. For the water quality, statistical analyses were conducted, and evident seasonal and spatial variations were found. EC, TN, NH_4-N, NO_3-N, PO_4-P, TC, and FC were identified as the major contributors to the changes in water quality in the inflow rivers. The land-use pattern and clustering analyses showed the land-use composition and its potential relationships to water quality and bacterial communities. The rivers located in the northwest, especially R1-R4, were more eutrophic than those in the southwest. The high percentages of industrial land and semi-artificial (agricultural) land were identified as the probable causes of high nutrient levels and altered microbial community structures in these rivers. Industrial waste and agricultural land runoff are undoubtedly the major pollution sources in this area. For other lakes around the world with multiple main estuaries, management of the inflow river water quality could also be essential. It would be beneficial for local management departments to understand the impacts of land-use patterns on water quality and microbial ecology. The methods used in this study could be widely and routinely applied as part of water quality evaluation and management strategies. Similar investigations could also target other sample types such as underground water, soil, and sediment.

Data availability statement

The datasets presented in this study can be found in online repositories. The names of the repository/repositories and accession number(s) can be found below: NCBI Short Read Archive (SRA) database under the accession numbers 29255681 to 29255724.

Author contributions

SL: Conceptualization, Data curation, Formal Analysis, Investigation, Methodology, Writing–original draft. JL: Formal Analysis, Methodology, Writing–review and editing. EA: Conceptualization, Methodology, Supervision, Validation, Writing–review and editing. JW: Formal Analysis, Methodology, Resources, Writing–review and editing. AM: Conceptualization, Methodology, Supervision, Validation, Writing–review and editing. RS: Conceptualization, Data curation, Funding acquisition, Investigation, Methodology, Project administration, Supervision, Writing–review and editing.

Funding

The author(s) declare financial support was received for the research, authorship, and/or publication of this article. We acknowledge the Key Program Special Fund in Xi'an Jiaotong-Liverpool University (XJTLU; Grant No. KSF-E-20); Continuous Support Fund (RDF-SP-88); and Research Enhancement Fund (REF-22-02-007) for funding support. SL was supported by the Postgraduate Research Scholarship (PGRS1906018) awarded to RS by the XJTLU. EA is supported by the Biotechnology and Biological Sciences Research Council (BBSRC); under the BBSRC Institute Strategic Program Gut Microbes and Health BB/R012490/1 and its constituent projects BBS/E/F/000PR10353 and BBS/E/F/000PR10356.

Acknowledgments

We would like to thank Prilli Fernanda, Tianma Yuan, and Li Sun for their support for this project and the Department of Biological Sciences, Xi'an Jiaotong-Liverpool University for the laboratory facilities.

Conflict of interest

The authors declare that the research was conducted in the absence of any commercial or financial relationships that could be construed as a potential conflict of interest.

The author(s) declared that they were an editorial board member of Frontiers, at the time of submission. This had no impact on the peer review process and the final decision.

Publisher's note

All claims expressed in this article are solely those of the authors and do not necessarily represent those of their affiliated organizations, or those of the publisher, the editors and the reviewers. Any product that may be evaluated in this article, or claim that may be made by its manufacturer, is not guaranteed or endorsed by the publisher.

Supplementary material

The Supplementary Material for this article can be found online at: https://www.frontiersin.org/articles/10.3389/fenvs.2024.1340875/full#supplementary-material

References

Allgaier, M., and Grossart, H.-P. (2006). Diversity and seasonal dynamics of Actinobacteria populations in four lakes in northeastern Germany. *Appl. Environ. Microbiol.* 72, 3489–3497. doi:10.1128/aem.72.5.3489-3497.2006

APHA (2005). *Standard methods for the examination of water and wastewater*. America: American Public Health Association.

Ashbolt, N. J. (2015). Microbial contamination of drinking water and human health from community water systems. *Curr. Environ. health Rep.* 2, 95–106. doi:10.1007/s40572-014-0037-5

Bai, G., Zhang, Y., Yan, P., Yan, W., Kong, L., Wang, L., et al. (2020). Spatial and seasonal variation of water parameters, sediment properties, and submerged macrophytes after ecological restoration in a long-term (6 year) study in Hangzhou west lake in China: Submerged macrophyte distribution influenced by environmental variables. *Water Research* 186, 116379. doi:10.1016/j.watres.2020.116379

Bakhsh, A., Kanwar, R. S., and Karlen, D. (2005). Effects of liquid swine manure applications on NO3–N leaching losses to subsurface drainage water from loamy soils in Iowa. *Agric. Ecosyst. Environ.* 109, 118–128. doi:10.1016/j.agee.2005.01.018

Baudart, J., Servais, P., de Paoli, H., Henry, A., and Lebaron, P. (2009). Rapid enumeration of *Escherichia coli* in marine bathing waters: potential interference of nontarget bacteria. *J. Appl. Microbiol.* 107, 2054–2062. doi:10.1111/j.1365-2672.2009.04392.x

Bhuyan, D., Lake, L. W., and Pope, G. A. (1990). Mathematical modeling of high-pH chemical flooding. *SPE Reserv. Eng.* 5, 213–220. doi:10.2118/17398-pa

Biddanda, B. (2017). *Global significance of the changing freshwater carbon cycle*. USA: Eos.

Brummer, I., Felske, A., and Wagner-Dobler, I. (2003). Diversity and seasonal variability of β-proteobacteria in biofilms of polluted rivers: analysis by temperature gradient gel electrophoresis and cloning. *Appl. Environ. Microbiol.* 69, 4463–4473. doi:10.1128/aem.69.8.4463-4473.2003

Bu, H., Meng, W., and Zhang, Y. (2014). Spatial and seasonal characteristics of river water chemistry in the Taizi River in Northeast China. *Environ. Monit. Assess.* 186, 3619–3632. doi:10.1007/s10661-014-3644-6

Cai, C., Gu, X., Ye, Y., Yang, C., Dai, X., Chen, D., et al. (2013). Assessment of pollutant loads discharged from aquaculture ponds around Taihu Lake, China. *Aquac. Res.* 44, 795–806. doi:10.1111/j.1365-2109.2011.03088.x

Camara, M., Jamil, N. R., and Abdullah, A. F. B. (2019). Impact of land uses on water quality in Malaysia: a review. *Ecol. Process.* 8, 10. doi:10.1186/s13717-019-0164-x

Chapman, D. (2021). *Water quality assessments: a guide to the use of biota, sediments and water in environmental monitoring*. Germany: CRC Press.

Chen, B., Wang, M., Duan, M., Ma, X., Hong, J., Xie, F., et al. (2019). In search of key: protecting human health and the ecosystem from water pollution in China. *J. Clean. Prod.* 228, 101–111. doi:10.1016/j.jclepro.2019.04.228

Cheng, J., Deng, C., and Lu, C. (2014). Bird communities in artificial and native reed wetland, Taihu lake bank, Suzhou. *Chin. J. Zoology* 49, 347–356. doi:10.13859/j.cjz.201403006

Chi, Z., Zhu, Y., Li, H., Wu, H., and Yan, B. (2021). Unraveling bacterial community structure and function and their links with natural salinity gradient in the Yellow River Delta. *Sci. Total Environ.* 773, 145673. doi:10.1016/j.scitotenv.2021.145673

Du, C., Li, Y., Wang, Q., Liu, G., Zheng, Z., Mu, M., et al. (2017). Tempo-spatial dynamics of water quality and its response to river flow in estuary of Taihu Lake based on GOCI imagery. *Environ. Sci. Pollut. Res.* 24, 28079–28101. doi:10.1007/s11356-017-0305-7

Ebina, J., Tsutsui, T., and Shirai, T. (1983). Simultaneous determination of total nitrogen and total phosphorus in water using peroxodisulfate oxidation. *Water Res.* 17, 1721–1726. doi:10.1016/0043-1354(83)90192-6

Evans, F. F., Egan, S., and Kjelleberg, S. (2008). Ecology of type II secretion in marine gammaproteobacteria. *Environ. Microbiol.* 10, 1101–1107. doi:10.1111/j.1462-2920.2007.01545.x

Fernanda, P., Liu, S., Yuan, T., Ramalingam, B., Lu, J., and Sekar, R. (2022). Diversity and abundance of antibiotic resistance genes and their relationship with nutrients and land use of the inflow rivers of Taihu Lake. *Front. Microbiol.* 13, 1009297. doi:10.3389/fmicb.2022.1009297

Fu, Q., Zheng, B., Zhao, X., Wang, L., and Liu, C. (2012). Ammonia pollution characteristics of centralized drinking water sources in China. *J. Environ. Sci.* 24, 1739–1743. doi:10.1016/s1001-0742(11)61011-5

Githinji, M. W., Mwaura, F., and Wamalwa, J. (2019). Land use and water pollution along the altitudinal gradient of the Likii River, Laikipia County, Kenya. *J. Environ. Pollut. Hum. Health* 7, 39–52. doi:10.12691/jephh-7-1-6

Guo, H. Y., Wang, X. R., and Zhu, J. G. (2004). Quantification and Index of Non-Point Source Pollution in Taihu Lake Region with GIS. *Environmental Geochemistry and Health* 26 (2), 147–156. doi:10.1023/B:EGAH.0000039577.67508.76

Guo, J., Zheng, Y., Teng, J., Song, J., Wang, X., and Zhao, Q. (2020). The seasonal variation of microbial communities in drinking water sources in Shanghai. *Journal of Cleaner Production* 265, 121604. doi:10.1016/j.jclepro.2020.121604

Han, S., Li, X., Luo, X., Wen, S., Chen, W., and Huang, Q. (2018). Nitrite-oxidizing bacteria community composition and diversity are influenced by fertilizer regimes, but are independent of the soil aggregate in acidic subtropical red soil. *Front. Microbiol.* 9, 885. doi:10.3389/fmicb.2018.00885

Hu, X.-L., Bao, Y.-F., Hu, J.-J., Liu, Y.-Y., and Yin, D.-Q. (2017). Occurrence of 25 pharmaceuticals in Taihu Lake and their removal from two urban drinking water treatment plants and a constructed wetland. *Environ. Sci. Pollut. Res.* 24, 14889–14902. doi:10.1007/s11356-017-8830-y

Huang, T.-Y., Wu, W., and Li, W.-W. (2013). Identifying the major pollution sources and pollution loading status of Qiputang River in Taihu Lake basin of China. *Desalination Water Treat.* 51, 4736–4743. doi:10.1080/19443994.2012.752764

Islam, F., Lian, Q., Ahmad, Z. U., Zappi, M. E., Yao, L., and Gang, D. D. (2018). Nonpoint source pollution. *Water Environment Research* 90 (10), 1872–1898. doi:10.2175/106143017X15131012188033

Jo, S. J., Kwon, H., Jeong, S.-Y., Lee, C.-H., and Kim, T. G. (2016). Comparison of microbial communities of activated sludge and membrane biofilm in 10 full-scale membrane bioreactors. *Water Res.* 101, 214–225. doi:10.1016/j.watres.2016.05.042

Kavamura, V. N., Taketani, R. G., Lançoni, M. D., Andreote, F. D., Mendes, R., and Soares de Melo, I. (2013). Water regime influences bulk soil and rhizosphere of Cereus jamacaru bacterial communities in the Brazilian Caatinga biome. *PloS one* 8 (9), e73606. doi:10.1371/journal.pone.0073606

Kirchman, D. L. (2002). The ecology of Cytophaga–Flavobacteria in aquatic environments. *FEMS Microbiol. Ecol.* 39, 91–100. doi:10.1016/s0168-6496(01)00206-9

Koch, A., Kärrman, A., Yeung, L. W., Jonsson, M., Ahrens, L., and Wang, T. (2019). Point source characterization of per-and polyfluoroalkyl substances (PFASs) and extractable organofluorine (EOF) in freshwater and aquatic invertebrates. *Environ. Sci. Process. Impacts* 21, 1887–1898. doi:10.1039/c9em00281b

Kutvonen, H., Rajala, P., Carpén, L., and Bomberg, M. (2015). Nitrate and ammonia as nitrogen sources for deep subsurface microorganisms. *Front. Microbiol.* 6, 1079. doi:10.3389/fmicb.2015.01079

Lauber, C. L., Ramirez, K. S., Aanderud, Z., Lennon, J., and Fierer, N. (2013). Temporal variability in soil microbial communities across land-use types. *ISME J.* 7, 1641–1650. doi:10.1038/ismej.2013.50

Lin, S.-S., Shen, S.-L., Zhou, A., and Lyu, H.-M. (2021). Assessment and management of lake eutrophication: a case study in Lake Erhai, China. *Sci. Total Environ.* 751, 141618. doi:10.1016/j.scitotenv.2020.141618

Liu, J., Chen, X., Shu, H.-Y., Lin, X.-R., Zhou, Q.-X., Bramryd, T., et al. (2018). Microbial community structure and function in sediments from e-waste contaminated

rivers at Guiyu area of China. *Environ. Pollut.* 235, 171–179. doi:10.1016/j.envpol.2017.12.008

Liu, J., and Raven, P. H. (2010). China's environmental challenges and implications for the world. *Crit. Rev. Environ. Sci. Technol.* 40, 823–851. doi:10.1080/10643389.2010.502645

Liu, Y., Li, H., Cui, G., and Cao, Y. (2020). Water quality attribution and simulation of non-point source pollution load flux in the Hulan River basin. *Sci. Rep.* 10, 3012–3015. doi:10.1038/s41598-020-59980-7

Lucassen, E., Smolders, A. J., van der Salm, A. L., and Roelofs, J. (2004). High groundwater nitrate concentrations inhibit eutrophication of sulphate-rich freshwater wetlands. *Biogeochemistry* 67, 249–267. doi:10.1023/b:biog.0000015342.40992.cb

Mathai, P. P., Staley, C., and Sadowsky, M. J. (2020). Sequence-enabled community-based microbial source tracking in surface waters using machine learning classification: a review. *J. Microbiol. Methods* 177, 106050. doi:10.1016/j.mimet.2020.106050

Ma, X., Deng, Z., Blair, D., Bi, Y., Hu, W., and Yin, M. (2022). Cyanobacterial bloom associated with a complete turnover of a Daphnia population in a warm-temperate eutrophic lake in Eastern China. *Freshw. Biol.* 67, 508–517. doi:10.1111/fwb.13858

Mekonnen, M. M., and Hoekstra, A. Y. (2015). Global gray water footprint and water pollution levels related to anthropogenic nitrogen loads to fresh water. *Environ. Sci. Technol.* 49, 12860–12868. doi:10.1021/acs.est.5b03191

Meng, L.-J., Zhang, Y., Li, X.-X., Liu, J.-H., Wen, B., Gao, J.-Z., et al. (2021). Comparative analysis of bacterial communities of water and intestines of silver carp (*Hypophthalmichthys molitrix*) and bighead carp (H. nobilis) reared in aquaculture pond systems. *Aquaculture* 534, 736334. doi:10.1016/j.aquaculture.2020.736334

MEP, (2002). *Ministry of environmental protection of the People's Republic of China)*. Beijing, China: Environmental Quality Standards for Surface Water. GB 3838-2002).

Mlejnková, H., and Sovová, K. (2010). Impact of pollution and seasonal changes on microbial community structure in surface water. *Water Sci. Technol.* 61, 2787–2795. doi:10.2166/wst.2010.080

MOHURD (2011). *Ministry of housing urban–rural development of the People's Republic of China, code for classification of urban land use and planning standards of development land (GB 50137–2011)*. China: China Architecture and Building Press Beijing.

MOHURD (2018). Ministry of Housing Urban–rural Development of the People's Republic of China, Chinese national standard for urban residential area planning and design (GB 50180-2018). China: China Architecture and Building Press Beijing.

MOHURD (2020). *Ministry of housing urban–rural development of the People's Republic of China, guidance of territorial spatial investigation, plan, land use control classification*. China: China Architecture and Building Press Beijing.

Naranjo, R. C., Niswonger, R. G., Smith, D., Rosenberry, D., and Chandra, S. (2019). Linkages between hydrology and seasonal variations of nutrients and periphyton in a large oligotrophic subalpine lake. *Journal of Hydrology* 568, 877–890. doi:10.1016/j.jhydrol.2018.11.033

Nyingi, D. W., Gichuki, N., and Ogada, M. O. (2013). *Kenya: a natural outlook: chapter 16. Freshwater ecology of Kenyan highlands and lowlands*. Germany: Elsevier Inc. Chapters.

Okada, E., Pérez, D., de Gerónimo, E., Aparicio, V., Massone, H., and Costa, J. L. (2018). Non-point source pollution of glyphosate and AMPA in a rural basin from the southeast Pampas, Argentina. *Environ. Sci. Pollut. Res.* 25, 15120–15132. doi:10.1007/s11356-018-1734-7

Paerl, H. W., Xu, H., Mccarthy, M. J., Zhu, G., Qin, B., Li, Y., et al. (2011). Controlling harmful cyanobacterial blooms in a hyper-eutrophic lake (Lake Taihu, China): the need for a dual nutrient (N and P) management strategy. *Water Res.* 45, 1973–1983. doi:10.1016/j.watres.2010.09.018

Pearce, G., Ramzan Chaudhry, M., and Ghulam, S. (1998). *A simple methodology for water quality monitoring*.

Pereira, R., Peplies, J., Mushi, D., Brettar, I., and Höfle, M. G. (2018). Pseudomonas-specific NGS assay provides insight into abundance and dynamics of Pseudomonas species including *P. aeruginosa* in a cooling tower. *Front. Microbiol.* 9, 1958. doi:10.3389/fmicb.2018.01958

Pisciotta, J. M., Rath, D. F., Stanek, P. A., Flanery, D. M., and Harwood, V. J. (2002). Marine bacteria cause false-positive results in the Colilert-18 rapid identification test for *Escherichia coli* in Florida waters. *Appl. Environ. Microbiol.* 68, 539–544. doi:10.1128/aem.68.2.539-544.2002

Qin, B., Xu, P., Wu, Q., Luo, L., and Zhang, Y. (2007). Environmental issues of lake Taihu, China. *Eutrophication of shallow lakes with special reference to Lake Taihu*. Editors B. Qin, Z. Liu, and K. Havens Dordrecht: Springer 194. doi:10.1007/978-1-4020-6158-5_2

Quast, C., Pruesse, E., Yilmaz, P., Gerken, J., Schweer, T., Yarza, P., et al. (2012). The SILVA ribosomal RNA gene database project: improved data processing and web-based tools. *Nucleic acids Res.* 41, D590–D596. doi:10.1093/nar/gks1219

Ren, Z., Qu, X., Zhang, M., Yu, Y., and Peng, W. (2019). Distinct bacterial communities in wet and dry seasons during a seasonal water level fluctuation in the largest freshwater lake (Poyang Lake) in China. *Front. Microbiol.* 1167, 1167. doi:10.3389/fmicb.2019.01167

Rissman, A. R., and Carpenter, S. R. (2015). Progress on nonpoint pollution: barriers and opportunities. *Daedalus* 144, 35–47. doi:10.1162/daed_a_00340

Ruprecht, J., Birrer, S., Dafforn, K., Mitrovic, S., Crane, S., Johnston, E., et al. (2021). Wastewater effluents cause microbial community shifts and change trophic status. *Water Res.* 200, 117206. doi:10.1016/j.watres.2021.117206

Shang, Y., Wu, X., Wang, X., Wei, Q., Ma, S., Sun, G., et al. (2022). Factors affecting seasonal variation of microbial community structure in Hulun Lake, China. *Sci. Total Environ.* 805, 150294. doi:10.1016/j.scitotenv.2021.150294

Shock, C. C., Pratt, K., and Station, M. (2003). Phosphorus effects on surface water quality and phosphorus TMDL development. *West. Nutr. Manag. Conf.* 5 (21), 1.

Sunagawa, S., Coelho, L. P., Chaffron, S., Kultima, J. R., Labadie, K., Salazar, G., et al. (2015). Ocean plankton. Structure and function of the global ocean microbiome. *Science* 348, 1261359. doi:10.1126/science.1261359

Tan, B., Ng, C. M., Nshimyimana, J. P., Loh, L.-L., Gin, K. Y.-H., and Thompson, J. R. (2015). Next-generation sequencing (NGS) for assessment of microbial water quality: current progress, challenges, and future opportunities. *Front. Microbiol.* 6, 1027. doi:10.3389/fmicb.2015.01027

Tang, Y., Li, M., Zou, Y., Lv, M., and Sun, J. (2018). Mechanism of aerobic denitrifiers and calcium nitrate on urban river sediment remediation. *Int. Biodeterior. Biodegrad.* 126, 119–130. doi:10.1016/j.ibiod.2017.10.002

Tao, T., and Xin, K. (2014). Public health: a sustainable plan for China's drinking water. *Nature* 511, 527–528. doi:10.1038/511527a

Ti, C., Xia, Y., Pan, J., Gu, G., and Yan, X. (2011). Nitrogen budget and surface water nitrogen load in Changshu: a case study in the Taihu Lake region of China. *Nutrient Cycl. Agroecosyst.* 91, 55–66. doi:10.1007/s10705-011-9443-3

UNESCO (2019). *International initiative on water quality (IIWQ)*.

Unno, T., Staley, C., Brown, C. M., Han, D., Sadowsky, M. J., and Hur, H. G. (2018). Fecal pollution: new trends and challenges in microbial source tracking using next-generation sequencing. *Environ. Microbiol.* 20, 3132–3140. doi:10.1111/1462-2920.14281

USEPA (2009). Total nitrogen. Available at: https://nepis.epa.gov/Exe/ZyPURL.cgi?Dockey=P10070OQ.txt (Accessed September 24, 2022).

USEPA (2012). 5.7 nitrates. Available at: https://archive.epa.gov/water/archive/web/html/vms57.html (Accessed November 10, 2020).

USEPA (2013). Coliforms, fecal coliforms, and E. Coli. Available at: https://www.waterfilteradvisor.com/glossary/coliform/(Accessed September 24, 2022).

USEPA (2021). *Basic information about nonpoint source (NPS) pollution*.

USEPA (2022). Indicators: conductivity. Available at: https://www.epa.gov/national-aquatic-resource-surveys/indicators-conductivity (Accessed September 24, 2022).

Vadde, K. K., Feng, Q., Wang, J., Mccarthy, A. J., and Sekar, R. (2019a). Next-generation sequencing reveals fecal contamination and potentially pathogenic bacteria in a major inflow river of Taihu Lake. *Environ. Pollut.* 254, 113108. doi:10.1016/j.envpol.2019.113108

Vadde, K. K., Mccarthy, A. J., Rong, R., and Sekar, R. (2019b). Quantification of microbial source tracking and pathogenic bacterial markers in water and sediments of Tiaoxi River (Taihu Watershed). *Front. Microbiol.* 10, 699. doi:10.3389/fmicb.2019.00699

Vadde, K. K., Wang, J., Cao, L., Yuan, T., Mccarthy, A. J., and Sekar, R. (2018). Assessment of water quality and identification of pollution risk locations in Tiaoxi River (Taihu Watershed), China. *Water* 10, 183. doi:10.3390/w10020183

Vaishali, P., and Punita, P. (2013). Assessment of seasonal variation in water quality of river mini, at sindhrot, vadodara. *Int. J. Environ. Sci.* 3, 1424–1436. doi:10.6088/ijes.2013030500013

Vega, M., Pardo, R., Barrado, E., and Debán, L. (1998). Assessment of seasonal and polluting effects on the quality of river water by exploratory data analysis. *Water Res.* 32, 3581–3592. doi:10.1016/s0043-1354(98)00138-9

Wang, Q., Garrity, G. M., Tiedje, J. M., and Cole, J. R. (2007a). Naive Bayesian classifier for rapid assignment of rRNA sequences into the new bacterial taxonomy. *Appl. Environ. Microbiol.* 73, 5261–5267. doi:10.1128/aem.00062-07

Wang, X.-L., Lu, Y.-L., Han, J.-Y., He, G.-Z., and Wang, T.-Y. (2007b). Identification of anthropogenic influences on water quality of rivers in Taihu watershed. *J. Environ. Sci.* 19, 475–481. doi:10.1016/s1001-0742(07)60080-1

Wang, F.-E., Tian, P., Yu, J., Lao, G.-M., and Shi, T.-C. (2011a). Variations in pollutant fluxes of rivers surrounding Taihu Lake in zhejiang Province in 2008. *Phys. Chem. Earth, Parts A/b/c* 36, 366–371. doi:10.1016/j.pce.2010.04.019

Wang, J., Soininen, J., Zhang, Y., Wang, B., Yang, X., and Shen, J. (2011b). Contrasting patterns in elevational diversity between microorganisms and macroorganisms. *J. Biogeogr.* 38, 595–603. doi:10.1111/j.1365-2699.2010.02423.x

Wang, E., Li, Q., Hu, H., Peng, F., Zhang, P., and Li, J. (2019a). Spatial characteristics and influencing factors of river pollution in China. *Water Environ. Res.* 91, 351–363. doi:10.1002/wer.1044

Wang, J., Fu, Z., Qiao, H., and Liu, F. (2019b). Assessment of eutrophication and water quality in the estuarine area of Lake Wuli, Lake Taihu, China. *Sci. Total Environ.* 650, 1392–1402. doi:10.1016/j.scitotenv.2018.09.137

Wang, M., Zhang, H., du, C., Zhang, W., Shen, J., Yang, S., et al. (2021). Spatiotemporal differences in phosphorus release potential of bloom-forming cyanobacteria in Lake Taihu. *Environ. Pollut.* 271, 116294. doi:10.1016/j.envpol.2020.116294

Wijesiri, B., Deilami, K., and Goonetilleke, A. (2018). Evaluating the relationship between temporal changes in land use and resulting water quality. *Environ. Pollut.* 234, 480–486. doi:10.1016/j.envpol.2017.11.096

Wu, Z., Wang, X., Chen, Y., Cai, Y., and Deng, J. (2018). Assessing river water quality using water quality index in Lake Taihu Basin, China. *Sci. Total Environ.* 612, 914–922. doi:10.1016/j.scitotenv.2017.08.293

Xu, H., Mccarthy, M. J., Paerl, H. W., Brookes, J. D., Zhu, G., Hall, N. S., et al. (2021). Contributions of external nutrient loading and internal cycling to cyanobacterial bloom dynamics in Lake Taihu, China: implications for nutrient management. *Limnol. Oceanogr.* 66, 1492–1509. doi:10.1002/lno.11700

Xu, J., Jin, G., Tang, H., Mo, Y., Wang, Y.-G., and Li, L. (2019). Response of water quality to land use and sewage outfalls in different seasons. *Sci. Total Environ.* 696, 134014. doi:10.1016/j.scitotenv.2019.134014

Xu, J., Zhang, Y., Zhou, C., Guo, C., Wang, D., du, P., et al. (2014). Distribution, sources and composition of antibiotics in sediment, overlying water and pore water from Taihu Lake, China. *Sci. Total Environ.* 497, 267–273. doi:10.1016/j.scitotenv.2014.07.114

Yan, C.-A., Zhang, W., Zhang, Z., Liu, Y., Deng, C., and Nie, N. (2015). Assessment of water quality and identification of polluted risky regions based on field observations and GIS in the honghe river watershed, China. *PloS one* 10, e0119130. doi:10.1371/journal.pone.0119130

Yang, J., Jiang, H., Wu, G., Liu, W., and Zhang, G. (2016a). Distinct factors shape aquatic and sedimentary microbial community structures in the lakes of western China. *Front. Microbiol.* 7, 1782. doi:10.3389/fmicb.2016.01782

Yang, J., Ma, L. A., Jiang, H., Wu, G., and Dong, H. (2016b). Salinity shapes microbial diversity and community structure in surface sediments of the Qinghai-Tibetan Lakes. *Sci. Rep.* 6, 25078–25086. doi:10.1038/srep25078

Yang, K. (2008). *Urban land use/cover and spatial pattern analysis*. China: Central South University.

Yang, W., Zhao, Y., Wang, D., Wu, H., Lin, A., and He, L. (2020). Using principal components analysis and IDW interpolation to determine spatial and temporal changes of surface water quality of Xin'anjiang river in Huangshan, China. *Int. J. Environ. Res. public health* 17, 2942. doi:10.3390/ijerph17082942

Yilmaz, P., Parfrey, L. W., Yarza, P., Gerken, J., Pruesse, E., Quast, C., et al. (2014). The SILVA and "all-species living tree project (LTP)" taxonomic frameworks. *Nucleic acids Res.* 42, D643–D648. doi:10.1093/nar/gkt1209

Yi, X., Lin, C., Ong, E. J. L., Wang, M., and Zhou, Z. (2019). Occurrence and distribution of trace levels of antibiotics in surface waters and soils driven by non-point source pollution and anthropogenic pressure. *Chemosphere* 216, 213–223. doi:10.1016/j.chemosphere.2018.10.087

Yotova, G., Varbanov, M., Tcherkezova, E., and Tsakovski, S. (2021). Water quality assessment of a river catchment by the composite water quality index and self-organizing maps. *Ecol. Indic.* 120, 106872. doi:10.1016/j.ecolind.2020.106872

Yu, R.-C., Lu, S.-H., Qi, Y.-Z., and Zhou, M.-J. (2020). Progress and perspectives of harmful algal bloom studies in China. *Oceanol. Limnologia Sinica* 51, 768–788. doi:10.11693/hyhz20200400127

Yu, Z., Liu, J., Li, Y., Jin, J., Liu, X., and Wang, G. (2018). Impact of land use, fertilization and seasonal variation on the abundance and diversity of nirS-type denitrifying bacterial communities in a Mollisol in Northeast China. *Eur. J. Soil Biol.* 85, 4–11. doi:10.1016/j.ejsobi.2017.12.001

Yuan, H., Shen, J., Liu, E., Wang, J., and Meng, X.-h. (2011). Assessment of Nutrients and Heavy Metals Enrichment in Surface Sediments from Taihu Lake, a Eutrophic Shallow Lake in China. *Environmental geochemistry and health* 33, 67–81. doi:10.1007/s10653-010-9323-9

Zhang, G., Chen, Y., Hu, L., Melka, D., Wang, H., Laasri, A., et al. (2018). Survey of foodborne pathogens, aerobic plate counts, total coliform counts, and *Escherichia coli* counts in leafy greens, sprouts, and melons marketed in the United States. *J. Food Prot.* 81, 400–411. doi:10.4315/0362-028x.jfp-17-253

Zhang, S., Yu, J., Wang, S., Singh, R. P., and Fu, D. (2019). Nitrogen fertilization altered arbuscular mycorrhizal fungi abundance and soil erosion of paddy fields in the Taihu Lake region of China. *Environ. Sci. Pollut. Res.* 26, 27987–27998. doi:10.1007/s11356-019-06005-0

Zhang, S. H., Lv, X., Han, B., Gu, X., Wang, P. F., Wang, C., et al. (2015). Prevalence of antibiotic resistance genes in antibiotic-resistant *Escherichia coli* isolates in surface water of Taihu Lake Basin, China. *Environ. Sci. Pollut. Res.* 22, 11412–11421. doi:10.1007/s11356-015-4371-4

Zhang, Y., Zhang, Y., Gao, Y., Zhang, H., Cao, J., Cai, J., et al. (2011). Water pollution control technology and strategy for river–lake systems: a case study in Gehu Lake and Taige Canal. *Ecotoxicology* 20, 1154–1159. doi:10.1007/s10646-011-0676-3

Zhang, Y., Zhang, Y., Wei, L., Li, M., Zhu, W., and Zhu, L. (2022). Spatiotemporal correlations between water quality and microbial community of typical inflow river into Taihu Lake, China. *Environ. Sci. Pollut. Res.* 29, 63722–63734. doi:10.1007/s11356-022-19023-2

Zhao, H., You, B., Duan, X., Becky, S., and Jiang, X. (2013). Industrial and agricultural effects on water environment and its optimization in heavily polluted area in Taihu Lake Basin, China. *Chinese Geographical Science* 23 (2), 203–215. doi:10.1007/s11769-013-0593-x

Zhao, D., Huang, R., Zeng, J., Yu, Z., Liu, P., Cheng, S., et al. (2014). Pyrosequencing analysis of bacterial community and assembly in activated sludge samples from different geographic regions in China. *Appl. Microbiol. Biotechnol.* 98, 9119–9128. doi:10.1007/s00253-014-5920-3

Zhao, Y., Xu, M., Liu, Q., Wang, Z., Zhao, L., and Chen, Y. (2018). Study of heavy metal pollution, ecological risk and source apportionment in the surface water and sediments of the Jiangsu coastal region, China: a case study of the Sheyang Estuary. *Mar. Pollut. Bull.* 137, 601–609. doi:10.1016/j.marpolbul.2018.10.044

Zheng, J., Gao, R., Wei, Y., Chen, T., Fan, J., Zhou, Z., et al. (2017). High-throughput profiling and analysis of antibiotic resistance genes in East Tiaoxi River, China. *Environ. Pollut.* 230, 648–654. doi:10.1016/j.envpol.2017.07.025

Zhu, C., Zhang, J., Nawaz, M. Z., Mahboob, S., al-Ghanim, K. A., Khan, I. A., et al. (2019). Seasonal succession and spatial distribution of bacterial community structure in a eutrophic freshwater Lake, Lake Taihu. *Sci. Total Environ.* 669, 29–40. doi:10.1016/j.scitotenv.2019.03.087

frontiers | Frontiers in Environmental Science

TYPE Original Research
PUBLISHED 01 March 2024
DOI 10.3389/fenvs.2024.1336318

Check for updates

OPEN ACCESS

EDITED BY
Maria Elisa Magri,
Federal University of Santa Catarina, Brazil

REVIEWED BY
Niti B Jadeja,
University of Virginia, United States
Arnaud Dechesne,
Technical University of Denmark, Denmark
Guilherme Sgobbi Zagui,
University of Ribeirão Preto, Brazil

*CORRESPONDENCE
Anni Djurhuus,
anni.djurhuus@gmail.com

†These authors have contributed equally to this work

RECEIVED 10 November 2023
ACCEPTED 15 February 2024
PUBLISHED 01 March 2024

CITATION
Mortensen AMS, Poulsen SJ, Berbisá MáF and Djurhuus A (2024), Distribution of antibiotic resistant bacteria and genes in sewage and surrounding environment of Tórshavn, Faroe Islands.
Front. Environ. Sci. 12:1336318.
doi: 10.3389/fenvs.2024.1336318

COPYRIGHT
© 2024 Mortensen, Poulsen, Berbisá and Djurhuus. This is an open-access article distributed under the terms of the Creative Commons Attribution License (CC BY). The use, distribution or reproduction in other forums is permitted, provided the original author(s) and the copyright owner(s) are credited and that the original publication in this journal is cited, in accordance with accepted academic practice. No use, distribution or reproduction is permitted which does not comply with these terms.

Distribution of antibiotic resistant bacteria and genes in sewage and surrounding environment of Tórshavn, Faroe Islands

Anna Maria Steintún Mortensen†, Sissal Jóhanna Poulsen†, Marjun á Fríðriksmørk Berbisá and Anni Djurhuus*

Faculty of Science and Technology, University of the Faroe Islands, Tórshavn, Faroe Islands

Several studies have investigated the effects of swimming in sewage-polluted recreational beach water, highlighting the associated health hazards. To mitigate potential pathogen transmission, it is imperative that the polluted water is released away from recreational waters and foreshores, where children tend to play. At present, domestic sewage in the Faroe Islands solely undergoes primary wastewater treatment within primary settling tanks before being discharged into the ocean. Effluents are a major anthropogenic source of antibiotic resistance genes and antibiotic resistant bacteria, which are released into the environment. The aim of this study was to investigate antibiotic resistant Gram-negative bacteria and antibiotic resistance genes in influents and effluents of wastewater subjected solely to primary treatment, along with their release into the environment during both summer and winter. Water samples were collected from influents and effluents as well as with increasing distance away from the wastewater outlet and from nearby tidepools. Samples were cultured on MacConkey agar with four different antibiotics for detection of antibiotic-resistant bacteria and antibiotic resistance genes were quantified by droplet digital PCR. All multi-drug resistant bacteria were identified using the API 20E kit. We observed an overall decrease of the abundance of Gram-negative bacteria from the effluents compared to influents, however, we observed the opposite trend in the antibiotic resistance genes. Antibiotic resistant bacteria and antibiotic resistance genes in addition to multi-drug resistant bacteria were found in the surrounding oceanic and several terrestrial tidepool samples. Of the multi-drug resistant bacteria, we found, e.g., *Escherichia coli*, *P. aeruginosa*, and *A. hydrophila* species, which can be pathogenic, potentially causing an infection if encountering a host. These results indicate a relatively wide pollution range of the effluents from the septic tank and treated sewage released into the environment, posing a potential hazard for both humans and wildlife.

KEYWORDS

sewage, gram-negative bacteria, multi-drug resistance, *enterobacteriaceae*, antibiotic resistance genes, wastewater

Introduction

Recent research has unveiled new insight into the composition of wastewater and its environmental implications globally (J. Li and Zhang, 2019; Pendergraft et al., 2023). Of particular concern is the presence of antibiotic resistant bacteria (ARB) and antibiotic resistance genes (ARGs) in wastewater and its release into the environment (Da Silva et al., 2006; Munk et al., 2022). This concern stems in part from the fact that antibiotic resistance represents a significant and pressing threat to global health (WHO, 2020) and was estimated to directly cause 1.27 million deaths and associated with~5 million deaths globally in 2019 (Global burden of bacterial antimicrobial resistance in 2019: a systematic analysis, 2022).

Municipal wastewater systems have been identified as significant reservoirs and hotspots for ARB and ARGs (Da Silva et al., 2006; Berendonk et al., 2015; Cesare et al., 2016; Fouz et al., 2020). These systems receive wastewater from various sources, including households, hospitals, and industries, which can contain a wide range of antibiotics and human gut bacteria. While bacterial concentrations typically diminish throughout wastewater treatment plants, a significant load can persist, ultimately being discharged into the environment and posing potential exposure to nearby animals and humans (Akiyama and Savin, 2010). Studies have also illustrated the mobilization of ARGs in wastewater, even spreading to divergent bacterial phyla and potentially undergoing further evolution (Berendonk et al., 2015; Shi et al., 2023; Ochman et al., 2024). A recent study demonstrated that reduction in tetracycline resistance genes after primary treatment seemed to be insignificant but reduced after secondary treatment (Ochman et al., 2024), highlighting the importance of properly treating wastewater before its release into the environment.

One consequence of the spread of ARGs and ARB into the environment is that pathogenic bacteria that previously were thought to be controlled, are resurfacing in new, more resistant forms, rendering traditional antibiotic therapies ineffective (Levy and Marshall, 2004). Unlike many chemical contaminants that tend to decrease in concentration through processes like degradation, dilution or sorption, ARB and mobile genetic elements containing ARGs can persist and even spread in the environment (Berendonk et al., 2015).

This investigation focused on specific ARGs deliberately chosen to typify genes commonly present in wastewater, demonstrating resistance across multiple antibiotic classes, β-lactams (bla_{OXA}-like genes), sulfonamides (*sul*2) and tetracyclines (*tet*A) (Auerbach et al., 2007; Du et al., 2007; Zieliński et al., 2019; Munk et al., 2022).

Several studies have investigated the effects of swimming in sewage polluted recreational beach water, demonstrating a health hazard and increased cases of GI (gastrointestinal) illnesses such as vomiting and diarrhoea (Dwight et al., 2004; J; Li and Zhang, 2019; Wade et al., 2010). Thus, it is imperative that the polluted water is released away from recreational waters and foreshores, where children tend to play. However, pollution from wastewater is not only limited to the coastal waters where it is discharged, bacteria has also been found to transfer from the polluted ocean to the atmosphere in sea spray aerosol, affecting more individuals than previously anticipated (Pendergraft et al., 2023).

For densely populated areas, large wastewater treatment plants (WWTPs) use treatments such as biological treatment, chemical treatment, and radiation to eliminate most contaminants (Lira et al., 2020). Currently, household sewage in the Faroe Islands exclusively undergoes primary wastewater treatment through individual or communal septic tanks (Umhvørvisstovan, 2023). Substances denser and lighter than water remain in the primary settling tanks and the wastewater is subsequently discharged through outlets into the ocean; in certain locations discharge is only 3 m from the shoreline (The municipality of Tórshavn, 2021; Kunngerð um spillivatn, 2009). As the Faroe Islands are surrounded by turbid waters, the general idea is that the ocean dilutes wastewater to such a degree that it poses little to no risk to the environment or humans. However, more recent reports show that in some areas the concentrations of faecal indicators are higher than the recommended threshold for recreational purposes (The municipality of Tórshavn, 2023).

Antibiotics can enter the sewage system by inappropriate disposal or in urine and excrements as parent compounds or metabolites (Kümmerer, 2009; Leung et al., 2012). Sub-inhibitory concentrations of antibiotics present in sewage serve as an optimal environment for development of antibiotic resistance, partly due to selection pressure (Da Silva et al., 2006; Auerbach et al., 2007). The effect of antibiotics in wastewater is not fully understood but it can cause alterations in bacteria, such as changes in the expression of virulence genes, in the transfer of antibiotic resistance and affect cell functions (Ohlsen et al., 1998; Goh et al., 2002; Scornec et al., 2017) potentially causing great environmental damage of unknown proportions.

No studies have investigated whether bacteria from wastewater can be detected on land and in the ocean surrounding the wastewater outlets in the Faroe Islands and its possible effect on wildlife as well as humans on land. The aim of this study is to evaluate presence and abundance of ARB and ARGs at three locations within Tórshavn municipality. In particular, we want to investigate if there is an increase in the concentration of antibiotic resistant Gram-negative bacteria and of specific ARGs in the effluents compared to the influents to provide insight into the effect of the primary treatment processes on ARB and ARG concentrations. Additionally, we seek to assess the extent of dissemination into the marine ecosystem and identify multi-drug resistant bacteria present.

Methods

Combined, there are 20 outlets releasing wastewater in Tórshavn, Argir, and Hoyvík. Three of these outlets Skansin (Station S), Argir (Station A), and Havnará (Station H) are subjected to primary treatment and subsequently discharged into the ocean. Station S and Station A have smaller and larger primary settling tanks, where sewage from multiple households and businesses are combined and undergo primary treatment. The Skansin (Station S) outlet is situated in the North-eastern part of Tórshavn and releases wastewater from >550 citizens~3 m from land (Figure 1A). In Argir, the South-eastern part of Tórshavn, wastewater is collected from ~3,100 individuals and is discharged ~50 m away from the shore, within the pier (Figure 1B).

FIGURE 1
Sampling locations at Station S and H **(A)**, and at Station A **(B)**. Circles are oceanic samples, rectangles are tidepools on land, clouds are samplings from the well. The star is where the effluents are released into the ocean. **(A)** S-1N = influents, S-OUT = effluents, H0 = effluents. **(B)** A-OUT = effluents, no influent samples were accessible for this location.

On the shore right next to Skansin there is an outlet that originates from the main river that flows, mostly under the streets, through the centre of Tórshavn (Supplementary Figure S1). This river (Havnará, Station H) carries waste from some relatively large corporations, institutions, and approximately 6,000–7,000 citizens (Supplementary Table S1). The wastewater from these three outlets (Station S, A and H) and its distribution in the surrounding areas will be the focus of this study.

Sample collection

Thirty-three samples were collected on 17 August 2022 and 31 samples on 7 February 2023 from all stations (S, A, and H, Figure 1). In addition, samples were collected from Gomlurætt Station G at the same dates as a negative control site, situated relatively far away from any settlements approx. 15 min drive from Tórshavn. We filtered 250–300 mL of water from all samples collected with increasing distances away from the wastewater outlets (source).

At Station S (Figure 1A), we collected influents and effluents from the primary settling tank (S-IN and S-OUT) as well as eight marine water samples (S1-S8) from the ocean close to the shore. In addition, samples were collected from four different tidepools (SP1-SP4). In the same area, effluents from Havnará (H0) and four marine water samples (H1-H4), with increasing distance from H0, were collected (Figure 1A).

At Argir (Figure 1B), effluents (A-OUT) and ten marine water samples (A1-A10) were collected from the shore with increasing distance from the wastewater outlet, as well as samples from five different tidepools (AP1-AP5) on the foreshore. All samples from effluents and influents were tested in triplicates.

All samples were transported back to the laboratory and kept cold until further processing done on the same day of collection. All samples were cultivated and tested for gene copy numbers of bla_{OXA}-like genes, *tet*A, and *sul*2. Multi-drug resistant (MDR) colony forming units (CFUs) were species identified. Samples for cultivation were preserved in glycerol by adding 7–8 mL of each water sample in 15 mL tubes with autoclaved glycerol, with the ratio of water sample to glycerol being approx. 1:4. The tubes were frozen at 80°C prior to further processing (Islam, n.d, 2023). Samples to be analyzed for ARGs were immediately filtered using 0.22 µm Sterivex™ (Millipore). Approx. 300 mL of each water sample was filtered by forcing the liquid through each filter, using a sterile syringe. With some highly concentrated samples, less than 100 mL could be filtered. The sterivex filters were frozen at −80°C until further analysis.

Cultivation of bacteria

Frozen samples were thawed prior to cultivation. An amount corresponding to 100 µL of water sample was pipetted onto Petri dishes containing *just* MacConkey agar (MacConkey agar No. 2, Oxoid) and Petri dishes containing MacConkey agar *and* ampicillin. Concentrated samples of influents and effluents were diluted through a serial dilution to 10^{-2} and 10^{-3}, before being added onto agar plates.

To spread the sample on the agar plates, a spread plate technique called "Copacabana" was performed, using sterile glass beads (Dahal, 2022). Beads were added to the Petri dish before putting the lid back on the plate. The agar plate was then slid back and forth to distribute the sample on the plate. The beads were removed, and agar plates incubated for 48–72 h at 37 °C. Colony forming units (CFUs) were counted after 24 h, 48 h and 72 h because colonies from the thawed samples required a longer time to develop.

Antibiotics preparations

Antibiotics in powder form were dissolved in autoclaved, distilled water and diluted to achieve minimum inhibitory concentration (MIC) for the respective antibiotics in agar (Supplementary Table S2). The Minimum Inhibitory Concentrations (MICs) were derived from antibiotic susceptibility testing performed on enteric bacteria by the National Antimicrobial Resistance Monitoring System for Enteric Bacteria (NARMS). The concentrations considered were specifically those relevant to *Shigella*, *Salmonella*, and *E. coli* (*Escherichia coli*). These bacteria, being opportunistic pathogens, are commonly employed for the assessment of microbial quality in water.

A few drops of HCl were added to the ciprofloxacin solution to make it dissolve completely. The antibiotic solutions were filtered through 0.22 µm Sterivex™ filters (Millipore). Antibiotic solutions were then added to liquid MacConkey agar that had cooled to 50°C and poured into Petri dishes.

MDR testing and bacteria identification

Colonies resistant to ampicillin were subsequently tested for multi-drug resistance. They were subjected to tetracycline, ciprofloxacin, kanamycin, and ampicillin in agar at concentrations corresponding to their respective MIC (Supplementary Table S2). Ampicillin agar plates were a positive control.

Triplicate samples were inoculated, however due to the high number of CFUs on each agar plate, the one with the highest amount of CFUs was selected for MDR testing using the API 20E system. In the assessment of MDR, the CFUs that were resistant were further tested for identification (Supplementary Figure S2). To identify the MDR bacteria, API 20 E kit (bioMérieux) was used as described by the manufacturer. API 20E kit is used to identify bacteria belonging to the Enterobacteriaceae family and other non-fastidious Gram-negative bacteria. Before the identification using the API 20 E kit, the individual MDR colonies were re-streaked 4 times on MacConkey agar and incubated at 37°C to get pure colonies that were no older than 24 h.

Freshly isolated colonies were also subjected to an oxidase test. A drop of oxidase reagent (bioMérieux) was added onto clean filter paper placed in a Petri dish and a sterile inoculation loop was used to transfer bacteria onto the filter paper. A positive reaction turned the colony purple within approximately 10 seconds and a negative reaction left the colour unchanged (UK Standards, 2009).

DNA extraction and ddPCR

DNA was extracted from the sterivex filters using DNeasy® PowerWater® Sterivex™ Kit (Qiagen) as described by the manufacturer. The concentration of the DNA was measured using Qubit (Invitrogen) as described by the manufacturer.

Absolute quantification of the genes bla_{OXA}, *tet*A, and *sul*2 (Table 1) was performed using ddPCR and EvaGreen Supermix (BioRad) according to the manufacturer's protocol. Threshold was set based on the number of positive droplets in the negatives for each of the genes (Supplementary Figure S5).

Statistical analysis

T-tests, means, and variance was calculated to assess statistical differences between: Summer and winter samples, influents (S-IN) and effluents (S-OUT), bla_{OXA}-like genes, *tet*A, and *sul*2. When comparing temporal data, only samples with data from all relevant dates were used. When cultivating bacteria on agar, marine water samples and tidepools were not made into triplicates and were for that reason not used to make statistical tests. All other samples were done in triplicates and could be used for statistical analyses. A few of these samples had CFU counts fewer than ten, but the triplicates had little variation in CFUs, indicating consistency in pipetting technique.

Results

Culturable bacteria and antibiotic resistance gene concentrations

Culturable bacterial concentrations (grown on MacConkey agar) in source samples (S-IN, S-OUT, A-OUT and H0) ranged from ~5×10^4–1.6×10^5 bacteria/mL bacteria/mL in summer and ~1.2×10^4–9.9×10^4 bacteria/mL in winter (Figure 2; Supplementary Table S3), with a significant difference between the seasons for all source locations at stations S, A and H ($p = 0.019$).

The ARG concentrations in source samples from stations S, A and H showed similar trends to the culturable bacteria with higher concentrations in summer than winter. In the summer *tet*A, bla_{OXA}-like genes, and *sul*2 had concentrations of ~2.2×10^4–1×10^5, ~1.8×10^4–6.4×10^4, and ~1.2×10^4–6×10^4 gene copies/mL, respectively, and winter concentrations of ~5×10^3–1.1×10^4, ~3×10^3–6×10^3, and ~5×10^3–1.5×10^4 gene copies/mL, respectively (*tet*A $p = 0.032$, bla_{OXA}–like genes $p = 0.033$, and *sul*2 $p = 0.037$).

In addition, both culturable bacteria and ARGs, showed opposite trends between influent and effluent concentrations (S-IN and S-OUT), for summer especially. There were significantly fewer culturable bacteria released into the environment (*t*-test, $p = 0.028$) but relatively higher concentrations of ARGs. This was especially pronounced during the summer while ARG concentrations were approximately the same for S-OUT and S-IN in the winter samples for *tet*A and *sul*2.

Compared to the source samples, relatively low concentrations of both culturable bacteria and ARGs were found in the environment (Figure 2; Figure 3). Concentrations of bacteria

TABLE 1 *Primers used for quantification of bla*$_{OXA}$-like genes, *tet*A gene *and sul2 gene in the samples.*

Gene	Antibiotic resistance to	Type	Primer sequence (5′-3′)	Amplicon size (bp)	Annealing temperature (°C)
bla$_{OXA}$	Beta-lactams (Zieliński et al., 2021)	Forward	ATTATCTACAGCAGCGCC AGTG	296	61
		Reverse	TGCATCCACGTCTTTGGTG		
tetA	Tetracyclines (Nawaz et al., 2006)	Forward	GCTACATCCTGCTTGCCTTC	211	53
		Reverse	GCATAGATCGCCGTGAAGAG		
sul2	Sulfonamides (Pei et al., 2006)	Forward	TCCGGTGGAGGCCGGTAT CTGG	191	60
		Reverse	CGGGAATGCCATCTGCCT TGAG		

ranged from ~0 to 400 bacteria/mL in the summer and ~0–500 bacteria/mL in the winter (Figure 1; Supplementary Table S3). All ARGs also showed this same trend with ~0–1.5×10^3 gene copies/mL in the summer and ~0–3.8×10^3 in the winter. Station A generally had lower bacterial and ARG concentrations in the environment (A1-A10) and tidepools (AP1-AP5), compared to the environmental samples (S1-S8) and tidepools (SP1-SP4) from Station S (Supplementary Table S3). Environmental samples from Station H (H2-H4), had higher bacterial and gene concentrations, where winter had the highest concentrations measured in any environmental sample at 530 bacteria/mL, ~2×10^3 *bla*$_{OXA}$-like gene copies/mL, ~3.8×10^3 *tet*A gene copies/mL, and ~3.2×10^3 *sul*2 gene copies/mL (Figure 2D; Figure 3B).

The highest concentrations of culturable bacteria found in the tidepools were in Station S in SP1 at 140 bacteria/mL. Highest number of gene copies were in AP4 and SP3. AP4 had 500 *tet*A gene copies/mL, ~220 *bla*$_{OXA}$-like gene copies/mL. SP3 had ~460 *sul*2 gene copies/mL (Figure 3; Supplementary Table S3). Several of the tidepools had higher ARG concentrations than the marine water samples close to the effluent outlets (Supplementary Table S3).

Gomlurætt (Station G) was used as background sample and had zero culturable bacteria, and gene copies ranged from 0–11 copies/mL (Supplementary Table S3). Of all the samples collected for gene copy numbers, 18 samples of *bla*$_{OXA}$-like genes, 9 samples of *tet*A and 12 samples of *sul*2 contained a greater amount of gene copies/mL in summer compared to winter, however the difference was only statistically significant for *sul*2 (*bla*$_{OXA}$like genes $p = 0.059$, *tet*A $p = 0.067$, *sul*2 $p = 0.048$).

Dilution of culturable bacteria and antibiotic resistance genes

At both Station S and Station A, *the highest environmental* bacterial and gene concentrations were found in the locations nearest the effluent outlets in *both* summer and winter, around S5 and S6 (Station S) and at A5 and A6 (Station A), compared to the other marine samples (Supplementary Table S3). The concentrations of bacteria/mL and *bla*$_{OXA}$-like genes, *tet*A and *sul*2 gene copies/mL decreased drastically *within the first* 40 m *from the effluent outlet* (Figure 4).

The highest ARG concentrations were measured at Station H and Station S (Supplementary Table S3). The samples closest to the effluent outlet at Station S and H were within 20 m from the effluent outlet in contrast to the closest sample at Station A, which was located 36 m from the effluent outlet.

Sampling locations furthest from the effluent outlet still contain bacteria and ARGs exceeding the background concentration. S8, which is the sampling location furthest from the effluent outlet at Station S (59 m), had 20 culturable bacteria/mL in winter and zero in summer and ARG concentrations all exceeding the background concentration ranging from 21 to 116 gene copies. A10 at Station A is 162 m from the effluent outlet and had zero culturable bacteria but all ARG concentrations, except *sul*2 in summer, exceeded the background concentrations.

Multi-drug resistance and species identification

In all source samples (S-IN, S-OUT, A-OUT and H0), there were fewer CFUs growing on MacConkey agar *with* ampicillin compared to CFUs growing on MacConkey agar *without* ampicillin (Figure 5). Concentrations of culturable bacteria on McConkey agar *with* ampicillin from the source ranged from ~4.3 × 10^4–9×10^4 ampicillin-resistant bacteria/mL in the summer, and ~5 × 10^3–1.3×10^3 ampicillin-resistant bacteria/mL in the winter ($p = 0.013$). The collective samples exhibit an average resistance of 61% to ampicillin. The highest (90%) and lowest (45%) percentage of ampicillin resistant bacteria were found in H0 in summer and winter, respectively (Figure 5). A higher number of ampicillin resistant bacteria was found in most tidepools from Stations S compared to Station A.

Of all 565 ampicillin-resistant bacteria tested for multi-drug resistance, summer, and winter, 39% of them were resistant to tetracycline, 33% to kanamycin and the least resistance was to ciprofloxacin at 19% (Figure 6B). Similar pattern of resistance was observed at Station A and S, but not for Station H, where resistance to kanamycin rather than tetracycline was highest (Figure 6B). Only bacteria from the replicate with the highest number of colonies were identified, resulting in 87 bacteria in total from winter and summer. Of 87 only 67 bacteria could be identified, 54 of which belonged to the Enterobacteriaceae family, while 13 belonged to other bacterial families (Figure 6A). Specific

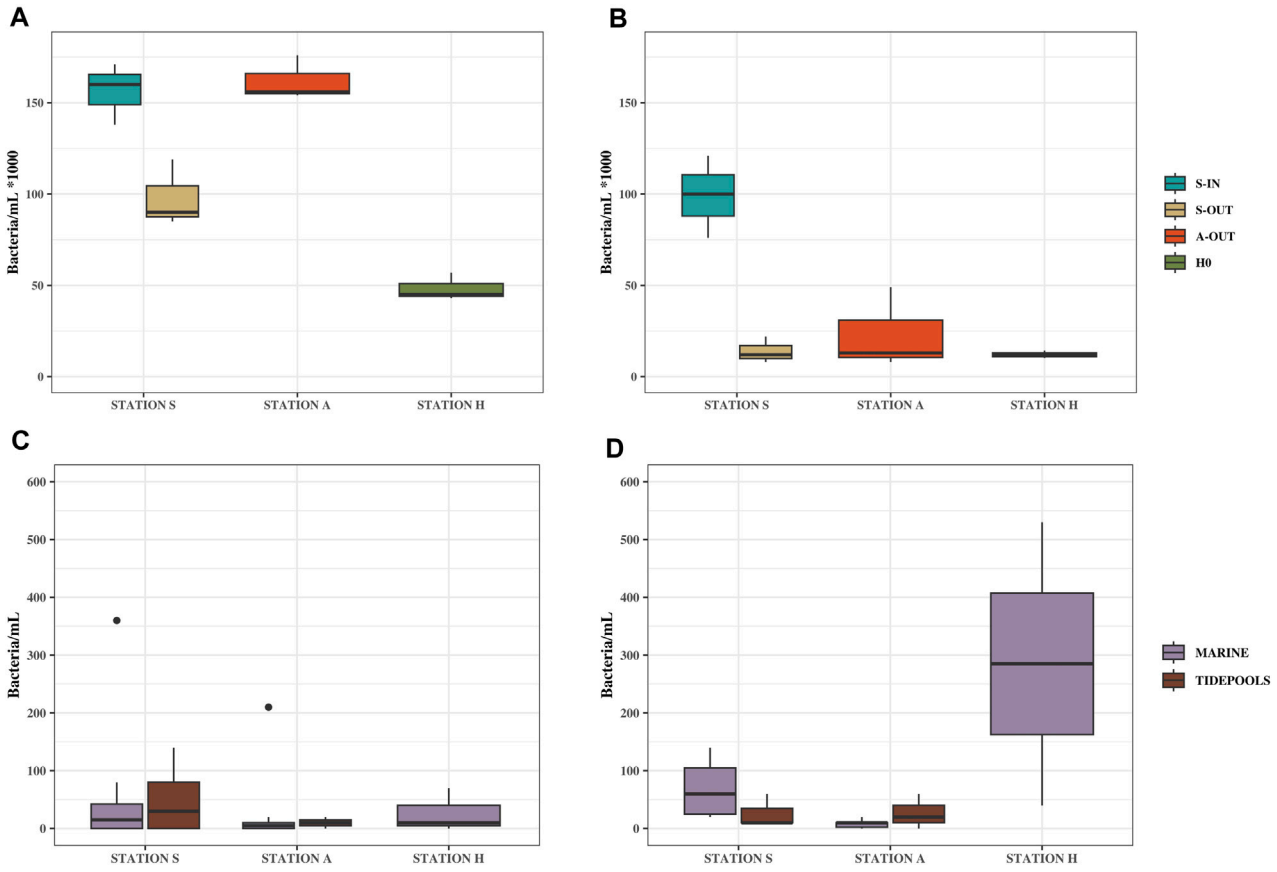

FIGURE 2
Culturable bacteria/mL from source, tidepools and marine water samples. Samples from Station S, A and H, summer (August 17, 2022) and winter (February 7, 2023). **(A)** Bacterial concentrations from source samples in summer **(B)** Bacterial concentrations from source samples in winter. **(C)** Bacterial concentrations from tidepools and marine water samples in summer. **(D)** Bacterial concentrations from tidepools and marine water samples in winter.

locations of the identified bacteria are listed in the Supplementary Table S4. 41 out of 87 were identified as *Klebsiella* (47%). 20 of these were *Klebsiella pneumoniae* spp. *1* and *2*, while 20 were *K. oxytoca,* and one was only identified as *Klebsiella.* 15 out of 87 (17%) tested MDR bacteria tested positive for oxidase. Ten of these were not identified, while the other five were: *Pseudomonas* species and *Aeromonas* and *Elizabethkingia* belonging to the classes Gammaproteobacteria and Flavobacteria, respectively.

Discussion

Bacteria and antibiotic resistance genes

When comparing influents and effluents from Station S (S-IN and S-OUT respectively), S-IN contained a significantly higher concentration of bacteria, when cultivated on agar, compared to S-OUT, demonstrating that the primary treatment is reducing the number of culturable bacteria being released into the environment. Bacteria transferred from their niche to an environment with different temperatures and conditions, such as gut bacteria transferred to sewage, can also enter the viable but non-culturable (VBNC) state due to the stressful conditions, which could also affect the bacterial count on agar (Du et al., 2007; Li et al., 2014). This could presumably account for a small decrease seen from S-IN to S-OUT, while much of the decrease in bacterial concentration could be due to bacteria dying in the well or being withheld in the well along with the solids.

In contrast to the tendency of culturable bacterial concentration, bla_{OXA}-like genes, *tet*A and *sul*2 concentrations were generally higher in S-OUT compared to S-IN, especially in summer. This could indicate that horizontal gene transfer occurs in the well at Station S. This is in accordance with other studies, demonstrating that wastewater treatment plants could function as horizontal gene transfer hotspots (Berendonk et al., 2015). Instead of reducing the number of antibiotic resistance genes released into the environment, in this instance, the concentrations are increased.

Horizontal gene transfer most likely happens through conjugation, as the resistant bacteria are in close contact with other non-resistant bacteria in the wells (Norman et al., 2009; Wintersdorff et al., 2016). Wastewater treatment in the Faroe Islands does not consist of the removal of chemicals, which means that antibiotics also end up in the effluents. Broadly speaking, antibiotic concentrations in untreated sewage are typically around 1 ug/L, which can cause selection pressure for antibiotic resistance (Larsson and Flach, 2022).

10.3389/fenvs.2024.1336318

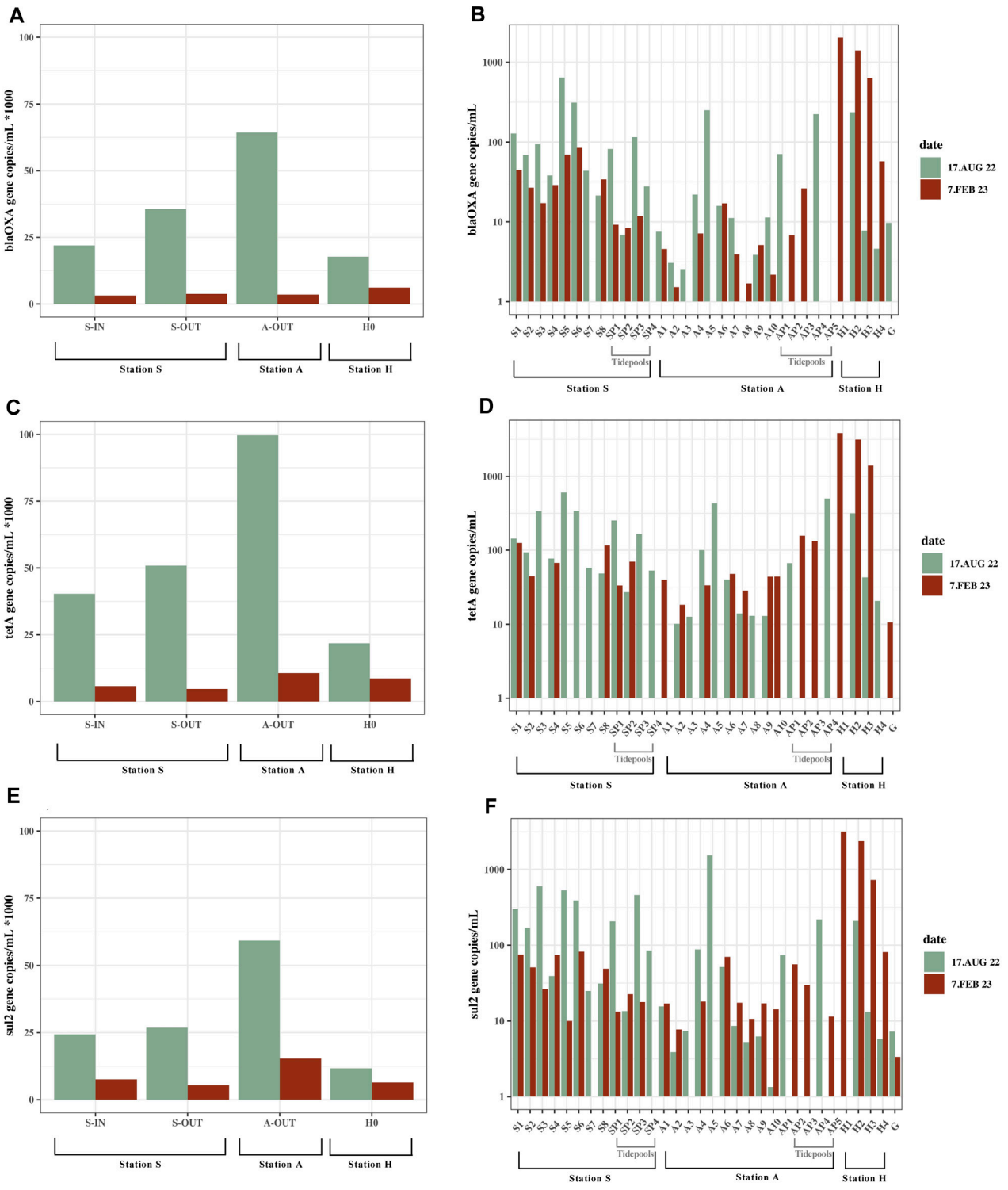

FIGURE 3
Gene copies/mL from all locations; seawater, tidepools and source. Samples from Station S, A and H, summer (August 17, 2022) and winter (February 7, 2023). Data does not exist for all locations on both dates (Supplementary Table S3). **(A)** bla_{OxA}—like gene concentrations in source samples. Shown as 1/1,000 of the actual concentrations. **(B)** bla_{OxA}—like gene concentrations in marine water samples and tidepools. Values are on a logarithmic scale. **(C)** *tetA* concentrations in source samples. Shown as 1/1000 of the actual concentrations. **(D)** *tetA* concentrations in marine water samples and tidepools. Values are on a logarithmic scale. **(E)** *sul2* concentrations in source samples. Shown as 1/1000 of the actual concentrations. **(F)** *sul2* concentrations in marine water samples and tidepools. Values are on a logarithmic scale.

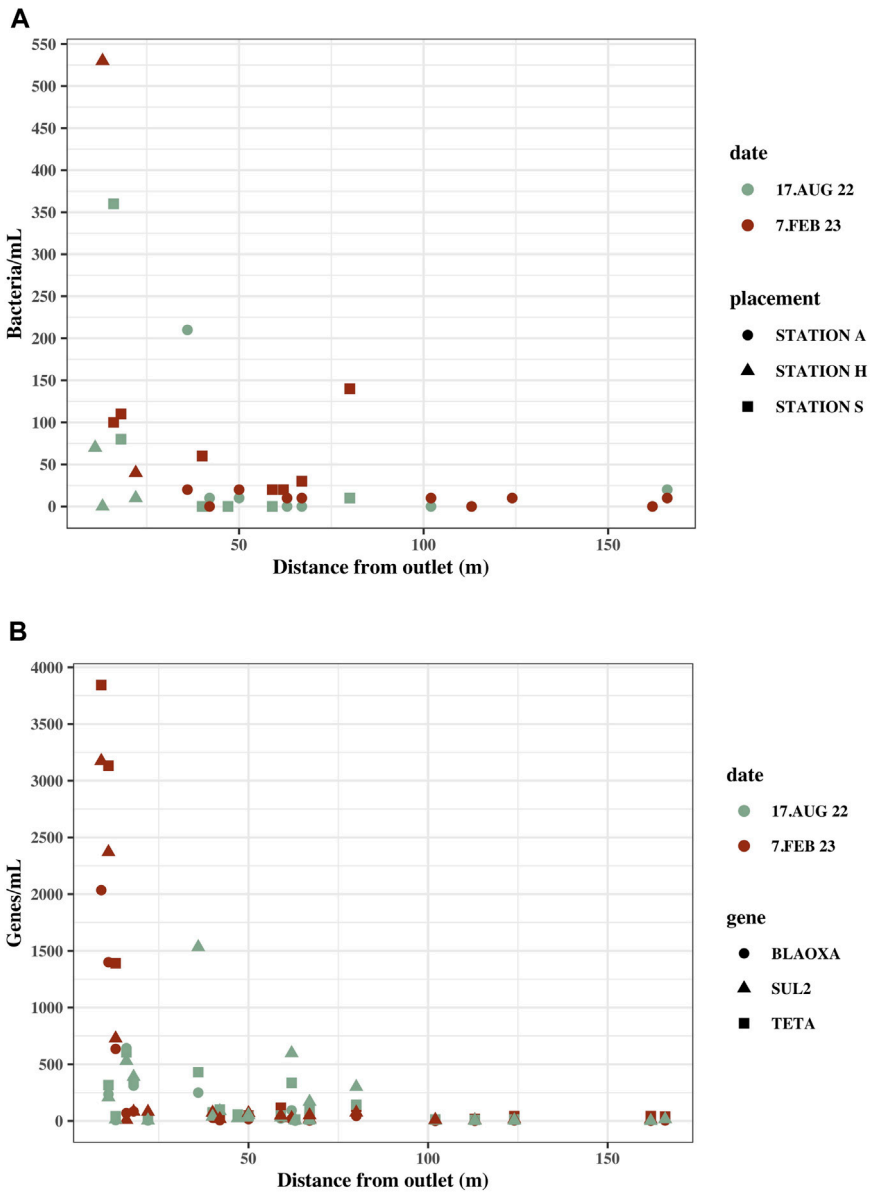

FIGURE 4
Concentrations in marine water samples with distance from the effluent outlet in the ocean. Distance from sample location to effluent outlet was measured on kortal.fo. **(A)** Culturable bacteria/mL in marine water samples at their distance from the effluent outlet. Samples are from Station S, A and H. **(B)** *bla*$_{OxA}$—like genes, *tetA* and *sul2* gene copies/mL in marine water samples at their distance from effluent outlet. Samples are from Station S, A and H.

The presence of antibiotics has also been shown to induce competence in several species of bacteria, competence being a physiological state that is necessary for most bacteria to take up free DNA (Thomas and Nielsen, 2005; Huddleston, 2014). The HGT could therefore also happen through transformation. Antibiotics are then not only selecting for resistance but also act as a catalyst for transformation of antibiotic resistant genes.

Multiple ARGs are often located on the same resistance plasmids, giving resistance to multiple classes of antibiotics at once during HGT. The copy number of plasmids in each bacterium can vary, depending on the type of plasmid (Rozwandowicz et al., 2018). The generally higher *tet*A concentrations compared to *bla*$_{OXA}$-like genes and *sul*2 does not necessarily indicate more tetracycline-resistant bacteria, but rather serve as an indication of ARG pollution, potentially leading to increased resistance in the surrounding environment. High levels of ARGs in the environment can also be an indicator of large amounts of wastewater reaching the specific location, which is the case in this study.

Both the ARG concentration and the ratio of ampicillin-resistant bacteria increased in S-OUT compared to S-IN in summer, indicate selection pressure on the culturable bacteria (Figure 3; Figure 5). However, more samples are required to give more insight into the seasonal and daily fluctuation of ampicillin resistance, due to the large variation between sampling events. Looking at bacterial counts from cultivation on agar, a significant difference was seen in the mean bacterial concentration of source samples between summer (17 August 2022) and winter (7 February 2023), with over threefold as many bacteria in summer.

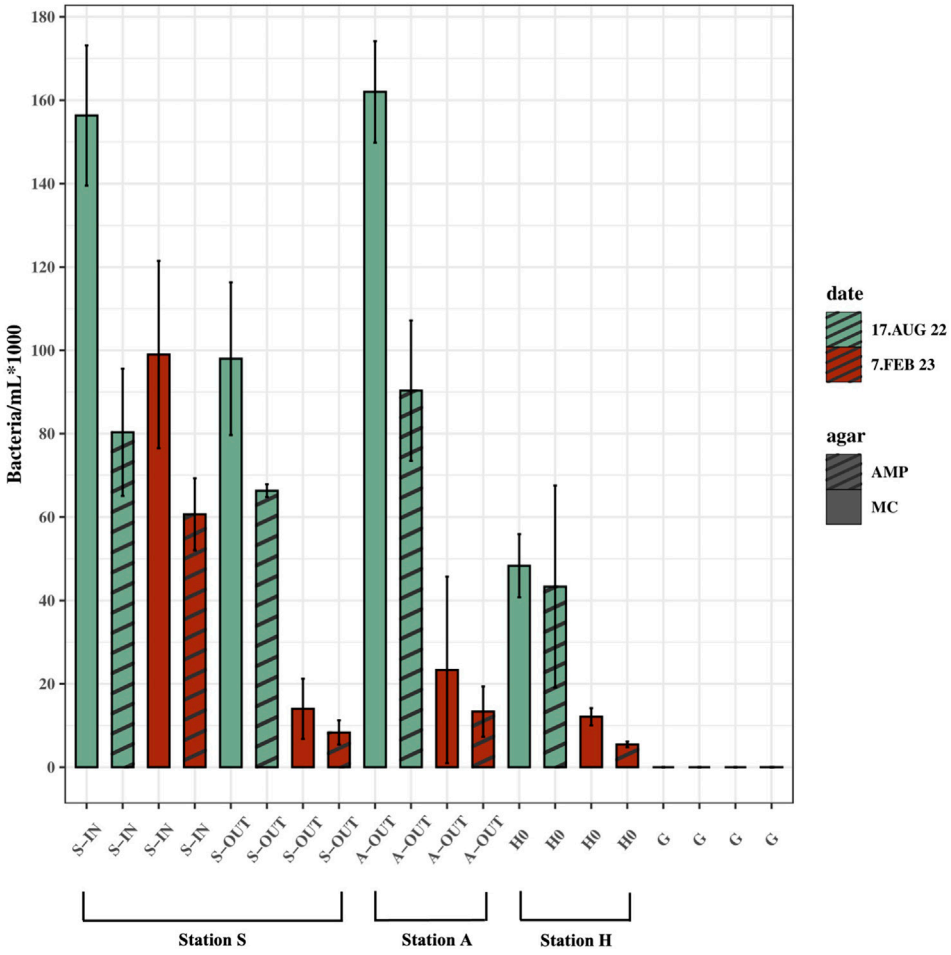

FIGURE 5
Ampicillin-resistant culturable bacteria/mL (AMP) vs. culturable bacteria/mL grown on agar without ampicillin (MC). Samples from source (S-IN, S-OUT, A-OUT and H0) and background sample from Gomlurætt (G) grown on agar with ampicillin (AMP) and without ampicillin (MC), situated side by side in the figure. Samples are from summer (August 17, 2022) and winter (February 7, 2023). Concentrations are based on the mean of triplicates.

Weather conditions might have influenced these results. As storm sewers are connected to the sewage pipes, precipitation might dilute the wastewater, leading to lower bacterial concentrations/mL. In February, it had rained the previous day, compared to August, when it had been sunny and dry for days prior to the sampling event (Supplementary Figure S3; Figure 4). Temperature could also be a factor influencing the viability of the bacteria as well as the ARGs (Gutiérrez-Cacciabue et al., 2016; Yang et al., 2020). A study has demonstrated a strong correlation between temperature and the abundance of ARGs, where abundance was lower in winter, when temperatures were low (Yang et al., 2020). This is in accordance with our findings from the gene quantification of *tet*A, bla_{OXA}-like genes and *sul*2, where there also was a statistically significant decrease in the concentration of gene copies/mL in winter compared to summer in the source samples.

Dilution of bacteria and antibiotic resistance genes

Through cultivation of samples on MacConkey agar and quantification of bla_{OXA}-like and *tet*A genes, there was a general tendency of lower concentrations in the marine water samples from Station A (Supplementary Table S3), where the wastewater outlet is situated farther away from land (50 m), than the wastewater outlets at Station S (3 m) and Station H (0 m). The concentration of bacteria and bla_{OXA}-like genes, *tet*A and *sul*2 in the effluents from Station A were approximately the same as in the effluents from Station H and Station S, or higher, and does therefore not account for the low bacterial and ARG concentrations in the environment at Station A. In some instances, the concentrations in effluents from Station A were, in fact, the highest of the effluents measured on certain dates. This gives an indication, that the distance from wastewater release to land affects the dilution of wastewater and contamination reaching the foreshore, which is important to consider for city planning and potentially hazardous recreational areas. The relatively high concentrations in marine water samples closest to the wastewater outlets, both at Station A and Station S, further support the tendency of decreasing concentrations with distance from the effluent discharge.

At Station S, S1 had a higher bacterial concentration in winter than S2 and S3, which are situated closer to the wastewater outlet (Figure 1A). This tendency was also seen for bla_{OXA}-like genes, *tet*A

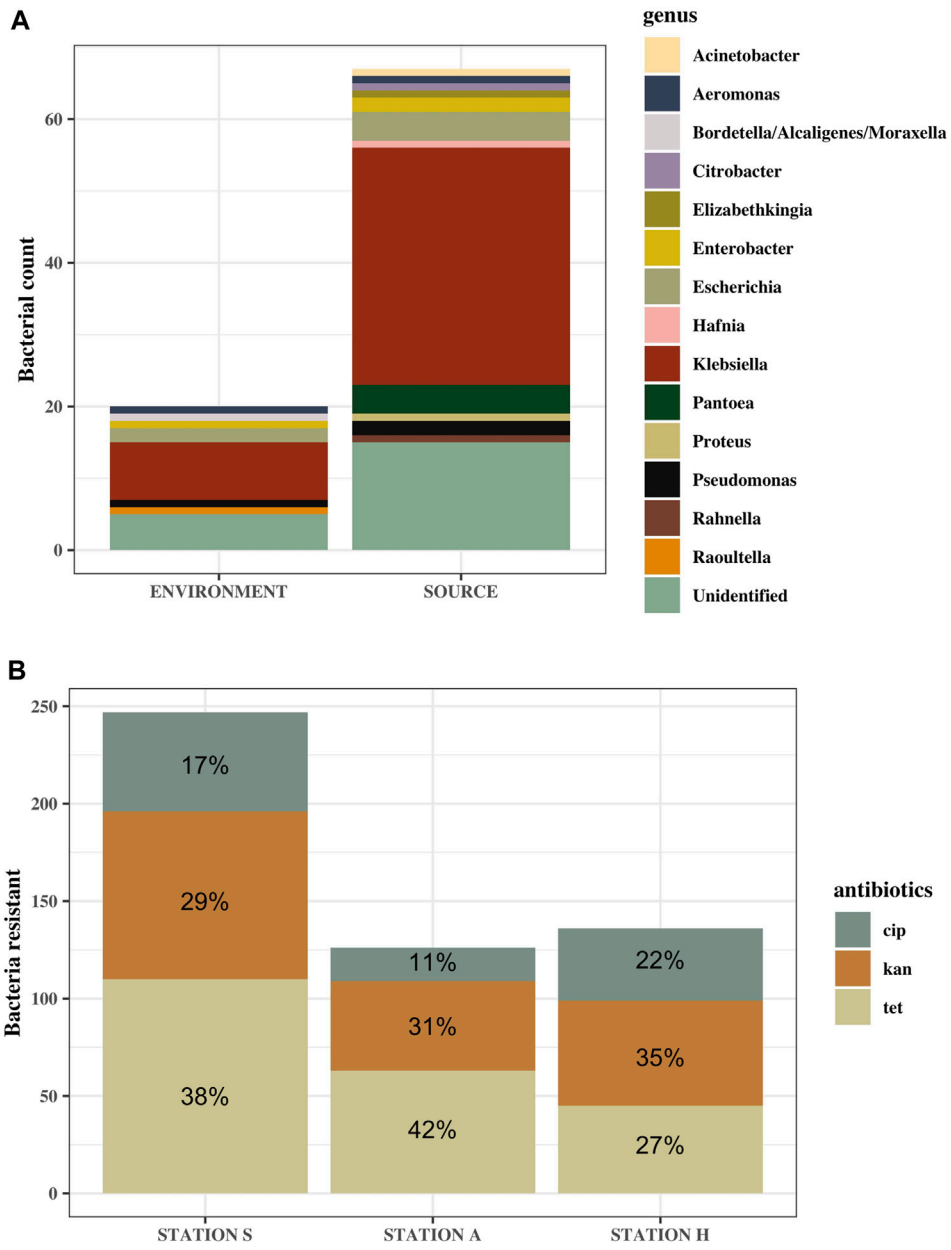

FIGURE 6
Identified genus of MDR bacteria **(A)** and the ratio of antibiotic resistance to the different antibiotics transferred from agar containing ampicillin **(B)**. **(A)** Genus of identified bacteria from source samples (S-IN, S-OUT, A-OUT and H0) and the environmental samples, including tidepools and seawater. "Unidentified" are MDR bacteria that could not be identified using the API 20 E kit. More bacteria from source were subjected to MDR testing, hence the larger difference in number of bacteria in this category. **(B)** n = 564. Ratio is based on the mean of how many of the ampicillin-resistant bacteria were resistant to ciprofloxacin (cip), kanamycin (kan) and tetracycline (tet).

and *sul*2 concentrations in these locations (Figure 3). On the collection date, the ocean current was flowing towards the sampling locations and was predominately directed towards S1 (Supplementary Figure S4). This could indicate that not only distance is of importance, but that currents could also affect the spread of wastewater contamination.

Most tidepools had ARG concentrations exceeding the background concentration. In addition, at Station S, culturable bacteria were detected in three tidepools, indicating that treated sewage reaches the tidepools through sea spray aerosols or by surf, which would be in accordance with research regarding the transfer of wastewater in aerosols (Pendergraft et al., 2023). Two tidepools at Station A and one at Station S only contained ARGs and no culturable bacteria. ARGs can persist longer in the environment (especially those carried on plasmids) than bacteria and could have been transferred either as free ARGs or with bacteria by surf during turbulent weather or aerosols, persisting after the bacteria died (Zhang et al., 2018). However, the bacteria and ARGs could also have been transferred from wildlife, such as rats, in the nearby environment. The normally nocturnal rat species (*Rattus Norwegicus*) present in the Faroe Islands,

was spotted multiple times while sampling in the daytime, indicating an abundant rat population on the foreshore (Puckett et al., 2020). Rats were observed at Station A, although more frequently at Station S. The rats are in close contact with wastewater from the well, being situated only 3 m from land and with wastewater from Station H, which is an open cave, both serving as an abundant and easily accessible food source. Rats can contaminate the surrounding area with their own urine and faeces and are also plausible vectors and reservoirs of contaminants from sewage such as pathogenic and multi-drug resistant bacteria, spreading them to tidepools and terrestrial ground (Byers et al., 2021).

Station H is the location, where the effluent outlet is closest to land. The reason for the high concentrations of bacteria and ARGs at this location compared to the other locations is presumably also because the area is relatively isolated, decelerating the dispersion of wastewater (Supplementary Figure S1). Without specific metrics in the guidelines, stating that there should be no accumulation of wastewater in the environment (Kunngerð um spillivatn, 2009), the meaning of accumulation becomes a subjective assessment. However, with constant flow of wastewater and bacteria, there is no need for accumulation to maintain high bacterial concentrations.

To ensure statistical accuracy of bacterial numbers, it is common practice to plate the samples in triplicates and count the CFUs from plates that contain a visible colony amount ranging from ~20 to 200. However, in several of the environmental samples in our study, this criterion was not fulfilled, resulting in the low bacterial abundances, and the exclusion of the environmental samples from statistical tests. Nevertheless, despite their unquantifiable nature, they still provide valuable information by indicating the presence of bacteria and have therefore been included in Supplementary Table S3, as well as in Figure 2D. Similar tendencies were generally seen in the concentrations of bla_{OXA}-like genes, *tet*A and *sul*2 in the marine water samples as in the cultivated samples. ddPCR allows for absolute quantification of samples containing low concentrations of ARGs (Taylor et al., 2017), adding to the reliability of the concentrations in the cultivated samples. To increase the reliability of the results from statistical tests, biological triplicates of all samples and more frequent sampling could further strengthen the tendencies observed in our study. However, the background sampling from Station G was made into triplicates and indirectly served as a control for contamination, as the background samples did not have any CFUs (apart from 1 single CFU on one plate out of several, Supplementary Table S3), we still deem our data reliable. The low concentration in the background sample from Station G gives an indication of the bacteria found at Stations S, A and H being a result of wastewater contamination. If this were not the case, the background samples would likely have had a higher bacterial concentration or a concentration in the same range as those seen at Station S, A and H. This gives further confidence to the CFUs from environmental samples not being due to contamination or due to ubiquitous bacteria.

Wastewater contamination in Tórshavn has been investigated previously, but little is known about how winds and currents affect the advection, diffusion, and dispersion of effluents in the ocean (The Municipality of Tórshavn, 2021). Attempts have been made abroad to predict and simulate effluent release and spread and could determine, that wastewater released many meters under the ocean surface tends to spread upwards in all directions, without contaminating the deeper layers due to the lower density of the treated sewage water compared to the surrounding ocean (Thupaki et al., 2010; Dumasdelage and Delestre, 2020). So even though the wastewater outlet at Station A is situated around 5 m below the surface, the wastewater is not necessarily dispersed at that depth predominately.

Seabirds were observed to cluster around the plume where wastewater is released in the ocean, presumably feeding off the effluents. Small birds were also seen in the cave, where effluents from Station H are led into the ocean. Birds that have been in contact with sewage or sewage contaminated waters have been shown to contain a higher amount of resistance genes than other birds, serving as vectors and reservoirs of ARGs (Marcelino et al., 2019). Northern fulmars (*Fulmaris glacialis*) are frequently hunted for food by Faroese people and these birds were in particular seen gathering around the wastewater. The close contact during hunting could possibly cause pathogenic and multi-drug resistant bacteria to be transmitted to humans. The birds can travel long distances, possibly spreading the contaminants even further. Our study gives an indication of the bacterial and ARG concentrations that humans and wildlife can be exposed to at the foreshore near wastewater outlets in Tórshavn.

Multi-drug resistance

Out of all the multi-drug resistant (MDR) bacteria tested using API 20 E, ~62% belonged to the Enterobacteriaceae family, which are common inhabitants of the human GI tract. In fact, *E. coli,* which belongs to this family, is an indicator of faecal contamination (Holcomb and Stewart, 2020).

Escherichia coli and *Klebsiella*, which belong to Enterobacteriaceae, are opportunistic pathogens known to cause disease in humans (Brinas et al., 2002; Paterson, 2006). These were found in several sample locations, also far away from the wastewater outlets such as S1 and A9, meaning, that they can survive 90 m and 120 m from the wastewater outlets. *P. aeruginosa*, and *A. hydrophila* were also detected in oceanic samples and are known to cause disease in humans, such as necrotizing fasciitis (Tsai et al., 2012). It is not clear, how the bacteria natural to the GI tract, can survive the extreme changes from gut to wastewater to oceanic waters (Cohen et al., 2020). However, it has been speculated that the spatial and temporal heterogeneity in osmolarity within the human gut has led to an adaption, enabling the gut bacteria to cope with varying salinity levels, which might improve their chances of survival in the marine environment (Cohen et al., 2020).

Several of the cultivated environmental samples from our study contained few CFUs, it is however noteworthy, that from these few, MDR bacteria were found that are associated with disease in humans (Brinas et al., 2002; Paterson, 2006; Aiello et al., 2008; Kim et al., 2009; Rizzo et al., 2013; Akbari et al., 2016; Prokesch et al., 2016; DavinRegli et al., 2019; CDC, 2023).

Data availability statement

The original contributions presented in the study are included in the article/Supplementary Material, further inquiries can be directed to the corresponding author.

Author contributions

AM: Writing–original draft, Investigation, Conceptualization, Data curation, Formal Analysis, Methodology, Visualization. SP: Writing–original draft, Investigation, Conceptualization, Data curation, Formal Analysis, Methodology, Visualization. MB: Writing–review and editing, Data curation, Methodology, Resources, Validation. AD: Supervision, Writing–review and editing, Conceptualization, Data curation, Funding acquisition, Investigation, Methodology, Project administration.

Funding

The author(s) declare financial support was received for the research, authorship, and/or publication of this article. The municipality of Tórshavn.

Acknowledgments

Special thanks to the Municipality of Tórshavn for financially supporting this project and in particular the Technical Department, for general interest and assistance. Thanks also to The University of Faroe Islands for use of facilities as well as financial support. We are also grateful to Marjun í Túni Mortensen for great assistance, advice in the laboratory and moral support. Lastly, we would like to thank Jóhanna Jørgensen for good advice.

Conflict of interest

The authors declare that the research was conducted in the absence of any commercial or financial relationships that could be construed as a potential conflict of interest.

Publisher's note

All claims expressed in this article are solely those of the authors and do not necessarily represent those of their affiliated organizations, or those of the publisher, the editors and the reviewers. Any product that may be evaluated in this article, or claim that may be made by its manufacturer, is not guaranteed or endorsed by the publisher.

Supplementary material

The Supplementary Material for this article can be found online at: https://www.frontiersin.org/articles/10.3389/fenvs.2024.1336318/full#supplementary-material

References

Aiello, A. E., Larson, E., and Sedlak, R. (2008). Hidden heroes of the health revolution Sanitation and personal hygiene. *Am. J. Infect. Control* 36 (10), S128–S151. doi:10.1016/j.ajic.2008.09.008

Akbari, M., Bakhshi, B., and Peerayeh, S. N. (2016). Particular distribution of *Enterobacter cloacae* strains isolated from urinary tract infection within clonal complexes. *PubMed* 20 (1), 49–55. doi:10.7508/ibj.2016.01.007

Akiyama, T., and Savin, M. C. (2010). Populations of antibiotic-resistant coliform bacteria change rapidly in a wastewater effluent dominated stream. *Sci. Total Environ.* 408 (24), 6192–6201. doi:10.1016/j.scitotenv.2010.08.055

Antimicrobial Resistance Collaborators (2022). Global burden of bacterial antimicrobial resistance in 2019: a systematic analysis. *Lancet* 399 (10325), 629–655. doi:10.1016/S0140-6736(21)02724-0

Auerbach, E., Seyfried, E. E., and McMahon, K. D. (2007). Tetracycline resistance genes in activated sludge wastewater treatment plants. *Water Res.* 41 (5), 1143–1151. doi:10.1016/j.watres.2006.11.045

Berendonk, T. U., Manaia, C. M., Merlin, C., Fatta-Kassinos, D., Cytryn, E., Walsh, F., et al. (2015). Tackling antibiotic resistance: the environmental framework. *Nat. Rev. Microbiol.* 13 (5), 310–317. doi:10.1038/nrmicro3439

Briñas, L., Zarazaga, M., Saenz, Y., Ruiz-Larrea, F., and Torres, C. (2002). β-Lactamases in ampicillin-resistant *Escherichia coli*isolates from foods, humans, and healthy animals. *Antimicrob. Agents Chemother.* 46 (10), 3156–3163. doi:10.1128/aac.46.10.31563163.2002

Byers, K. A., Booker, T. R., Combs, M., Himsworth, C. G., Munshi-South, J., Patrick, D. M., et al. (2020). Using genetic relatedness to understand heterogeneous distributions of urban rat-associated pathogens. *Evol. Appl.* 14 (1), 198–209. doi:10.1111/eva.13049

CDC (2023). CDC (no date) Antibiotics Tested by NARMS. Available at: https://www.cdc.gov/narms/antibioticstested.html (Accessed May 20, 2023).

Cohen, R., Paikin, S., Rokney, A., Rubin-Blum, M., and Astrahan, P. (2020). Multidrug-resistant enterobacteriaceae in coastal water: an emerging threat. *Antimicrob. Resist. Infect. Control* 9 (1), 169. doi:10.1186/s13756-020-00826-2

Dahal, P. (2023). Spread Plate method- definition, principle, procedure, uses. Available at: https://microbenotes.com/spread-plate-technique/.

Da Silva, M. F., Tiago, I., Veríssimo, A., Boaventura, R. A. R., Nunes, O. C., and Manaia, C. M. (2006). Antibiotic resistance of enterococci and related bacteria in an urban wastewater treatment plant. *FEMS Microbiol. Ecol.* 55 (2), 322–329. doi:10.1111/j.1574-6941.2005.00032.x

Davin-Régli, A., Lavigne, J. P., and Pagès, J. (2019). *Enterobacter* spp.: update on taxonomy, clinical aspects, and emerging antimicrobial resistance. *Clin. Microbiol. Rev.* 32 (4), e00002-19. doi:10.1128/cmr.00002-19

Di Cesare, A., Eckert, E. M., D'Urso, S., Bertoni, R., Gillan, D. C., Wattiez, R., et al. (2016). Co-occurrence of integrase 1, antibiotic and heavy metal resistance genes in municipal wastewater treatment plants. *Water Res.* 94, 208–214. doi:10.1016/j.watres.2016.02.049

Du, M., Chen, J., Zhang, X., Li, Y., and Wang, Y. (2007). Retention of virulence in a viable but nonculturable *Edwardsiella tarda* isolate. *Appl. Environ. Microbiol.* 73 (4), 1349–1354. doi:10.1128/aem.02243-06

Dumasdelage, R., and Delestre, O. (2020). Simulating coliform transport and decay from 3D hydrodynamics model and *in situ* observation in Nice area. *SN Appl. Sci.* 2 (8), 1348. doi:10.1007/s42452-020-3122-4

Dwight, R. H., Baker, D. B., Semenza, J. C., and Olson, B. H. (2004). Health effects associated with recreational coastal water use: urban versus Rural California. *Am. J. Public Health* 94 (4), 565–567. doi:10.2105/ajph.94.4.565

Fouz, N., Pangesti, K. N. A., Yasir, M., Al-Malki, A. L., Azhar, E. I., Hill-Cawthorne, G. A., et al. (2020). The contribution of wastewater to the transmission of antimicrobial resistance in the environment: implications of mass gathering settings. *Trop. Med. Infect. Dis.* 5 (1), 33. doi:10.3390/tropicalmed5010033

Goh, E.-B., Yim, G., Tsui, W., McClure, J., Surette, M. G., and Davies, J. (2002). Transcriptional modulation of bacterial gene expression by subinhibitory concentrations of antibiotics. *Proc. Natl. Acad. Sci. U. S. A.* 99 (26), 17025–17030. doi:10.1073/pnas.252607699

Gutiérrez-Cacciabue, D., Cid, A. G., and Rajal, V. B. (2016). How long can culturable bacteria and total DNA persist in environmental waters? The role of sunlight and solid particles. *Sci. Total Environ.* 539, 494–502. doi:10.1016/j.scitotenv.2015.07.138

Holcomb, D., and Stewart, J. R. (2020). Microbial Indicators of fecal pollution: recent progress and challenges in assessing water quality. *Curr. Environ. Health Rep.* 7 (3), 311–324. doi:10.1007/s40572-020-00278-1

Huddleston, J. R. (2014). Horizontal gene transfer in the human gastrointestinal tract: potential spread of antibiotic resistance genes. *Infect. Drug Resist.* 167, 167–176. doi:10.2147/idr.s48820

Islam, P. (2023). Creating bacterial glycerol stocks for long-term storage. Available at: https://www.protocols.io/view/creating-bacterial-glycerol-stocks-for-long-terms-bf5qjq5w.pdf (Accessed May 21, 2023).

Kim, J., Jeon, S., Rhie, H., Lee, B., Park, M., Lee, H., et al. (2009). Rapid detection of extended spectrum β-lactamase (ESBL) for enterobacteriaceae by use of a multiplex PCR-based method. *Infect. Chemother.* 41 (3), 181. doi:10.3947/ic.2009.41.3.181

Kümmerer, K. (2009). Antibiotics in the aquatic environment – a review – Part I. *Chemosphere* 75 (4), 417–434. doi:10.1016/j.chemosphere.2008.11.086

Kunngerð um spillivatn (2009). Kunngerð nr. 111 frá 7. september 2009 um spillivatn (no date). Available at: https://logir.fo/Kunngerd/111-fra-07-09-2009-um-spillivatn.

Larsson, D. G. J., and Flach, C.-F. (2021). Antibiotic resistance in the environment. *Nat. Rev. Microbiol.* 20 (5), 257–269. doi:10.1038/s41579-021-00649-x

Leung, H. W., Minh, T., Murphy, M., Lam, J. C., So, M., Martin, M., et al. (2012). Distribution, fate and risk assessment of antibiotics in sewage treatment plants in Hong Kong, South China. *South China Environ. Int.* 42, 1–9. doi:10.1016/j.envint.2011.03.004

Levy, S. B., and Marshall, B. (2004). Antibacterial resistance worldwide: causes, challenges and responses. *Nat. Med.* 10 (S12), S122–S129. doi:10.1038/nm1145

Li, J., and Zhang, X. (2019). Beach pollution effects on health and productivity in California. *Int. J. Environ. Res. Public Health* 16 (11), 1987. doi:10.3390/ijerph16111987

Li, L., Mendis, N., Trigui, H., Oliver, J. D., and Faucher, S. P. (2014). The importance of the viable but non-culturable state in human bacterial pathogens. *Front. Microbiol.* 5, 258. doi:10.3389/fmicb.2014.00258

Lira, F., Vaz-Moreira, I., Tamames, J., Manaia, C. M., and Martínez, J. L. (2020). Metagenomic analysis of an urban resistome before and after wastewater treatment. *Sci. Rep.* 10 (1), 8174. doi:10.1038/s41598020-65031-y

Marcelino, V. R., Wille, M., Hurt, A. C., González-Acuña, D., Klaassen, M., Schlub, T. E., et al. (2019). Meta-transcriptomics reveals a diverse antibiotic resistance gene pool in avian microbiomes. *BMC Biol.* 17 (1), 31. doi:10.1186/s12915-019-0649-1

Munk, P., Brinch, C., Møller, F. D., Petersen, T. N., Hendriksen, R. S., Seyfarth, A. M., et al. (2022). Genomic analysis of sewage from 101 countries reveals global landscape of antimicrobial resistance. *Nat. Commun.* 13 (1), 7251. doi:10.1038/s41467-022-34312-7

Nawaz, M. S., Sung, K., Khan, S. A., Khan, A. A., and Steele, R. (2006). Biochemical and molecular characterization of tetracycline-resistant *Aeromonas veronii* isolates from catfish. *Appl. Environ. Microbiol.* 72 (10), 6461–6466. doi:10.1128/aem.00271-06

Norman, A., Hansen, L. H., and Sørensen, S. J. (2009). Conjugative plasmids: vessels of the communal gene pool. *Philosophical Trans. R. Soc. B* 364 (1527), 2275–2289. doi:10.1098/rstb.2009.0037

Ochman, H., Quandt, E. M., Gottell, N., and Gilbert, J. A. (2024). Examining the taxonomic distribution of tetracycline resistance in a wastewater plant. *Sustain. Microbiol.* 1, qvad003. doi:10.1093/sumbio/qvad003

Ohlsen, K., Ziebuhr, W., Koller, K. P., Hell, W., Wichelhaus, T. A., and Hacker, J. (1998). Effects of subinhibitory concentrations of antibiotics on alpha-toxin (*hla*) gene expression of methicillin-sensitive and methicillin-resistant *Staphylococcus aureus* isolates. *Antimicrob. Agents Chemother.* 42 (11), 2817–2823. doi:10.1128/aac.42.11.2817

Paterson, D. L. (2006). Resistance in gram-negative bacteria: enterobacteriaceae. *Am. J. Infect. Control* 34 (5), S20–S28. doi:10.1016/j.ajic.2006.05.238

Pei, R., Kim, S. C., Carlson, K. H., and Pruden, A. (2006). Effect of River Landscape on the sediment concentrations of antibiotics and corresponding antibiotic resistance genes (ARG). *Water Res.* 40 (12), 2427–2435. doi:10.1016/j.watres.2006.04.017

Pendergraft, M. A., Belda-Ferre, P., Petras, D., Morris, C. K., Mitts, B. A., Aron, A. T., et al. (2023). Bacterial and chemical evidence of coastal water pollution from the tijuana river in sea spray aerosol. *Environ. Sci. Technol.* 57 (10), 4071–4081. doi:10.1021/acs.est.2c02312

Prokesch, B. C., TeKippe, M., Kim, J., Raj, P., TeKippe, E. M., and Greenberg, D. E. (2016). Primary osteomyelitis caused by hypervirulent *Klebsiella pneumoniae*. *Lancet Infect. Dis.* 16 (9), e190–e195. doi:10.1016/s1473-3099(16)30021-4

Puckett, E. E., Magnussen, E., Khlyap, L. A., Strand, T. M., Lundkvist, Å., and Munshi-South, J. (2019). Genomic analyses reveal three independent introductions of the invasive brown rat (*Rattus norvegicus*) to the Faroe Islands. *Heredity* 124 (1), 15–27. doi:10.1038/s41437-019-0255-6

Rizzo, L., Manaia, C., Merlin, C., Schwartz, T., Dagot, C., Ploy, M., et al. (2013). 'Urban wastewater treatment plants as hotspots for antibiotic resistant bacteria and genes spread into the environment: a review. *Sci. Total Environ.* 447, 345–360. doi:10.1016/j.scitotenv.2013.01.032

Rozwandowicz, M., Brouwer, M. S. M., Fischer, J., Wagenaar, J. A., Gonzalez-Zorn, B., Guerra, B., et al. (2018). Plasmids carrying antimicrobial resistance genes in Enterobacteriaceae. *J. Antimicrob. Chemother.* 73 (5), 1121–1137. doi:10.1093/jac/dkx488

Scornec, H., Bellanger, X., Guilloteau, H., Groshenry, G., and Merlin, C. (2017). Inducibility of Tn916 conjugative transfer in *Enterococcus faecalis* by subinhibitory concentrations of ribosome-targeting antibiotics. *J. Antimicrob. Chemother.* 72 (10), 2722–2728. doi:10.1093/jac/dkx202

Shi, B., Zhao, R., Su, G., Liu, B., Liu, W., Xu, J., et al. (2023). Metagenomic surveillance of antibiotic resistome in influent and effluent of wastewater treatment plants located on the Qinghai-Tibetan Plateau. *Sci. Total Environ.* 870, 162031. doi:10.1016/j.scitotenv.2023.162031

Taylor, S. C., Laperriere, G., and Germain, H. (2017). Droplet Digital PCR versus qPCR for gene expression analysis with low abundant targets: from variable nonsense to publication quality data. *Sci. Rep.* 7 (1), 2409. doi:10.1038/s41598-017-02217-x

The municipality of Tórshavn (2023). Soleiðis er vatngóðskan til útisvimjing í løtuni. Available at: https://www.torshavn.fo/nattura-fritid-og-mentan/upplivingar-inatturuni/soleidis-er-vatngodskan-til-utisvimjing-i-loetuni (Accessed September 15, 2023).

Thomas, C. M., and Nielsen, K. M. (2005). Mechanisms of, and barriers to, horizontal gene transfer between bacteria. *Nat. Rev. Microbiol.* 3 (9), 711–721. doi:10.1038/nrmicro1234

Thupaki, P., Phanikumar, M. S., Beletsky, D., Schwab, D. J., Nevers, M. B., and Whitman, R. L. (2009). Budget analysis of *Escherichia coli* at a southern lake Michigan beach. *Environ. Sci. Technol.* 44 (3), 1010–1016. doi:10.1021/es902232a

The Municipality of Tórshavn (2021). Umhvørviskanning av Havnarvág. Available at: https://www.torshavn.fo/media/hmekw0qm/vatng%C3%B3%C3%B0skukanning-havnarv%C3%A1g-2021.pdf (Accessed March 4, 2023).

Tsai, Y.-H., Huang, K. C., Shen, S. H., Hsu, W. H., Peng, K. T., and Huang, T. J. (2012). Microbiology and surgical indicators of necrotizing fasciitis in a tertiary hospital of southwest Taiwan. *Int. J. Infect. Dis.* 16 (3), e159–e165. doi:10.1016/j.ijid.2011.11.001

UK Standards (2009). UK Standards for microbiology investigations. Available at: https://assets.publishing.service.gov.uk/government/uploads/system/uploads/attachment_data/file/771781/TP_26i4.pdf (Accessed February 5, 2023).

Umhvørvisstovan (2023). Rottangar og reinsiverk. Available at: https://www.us.fo/Umhvørvisstovan/Umhvørvisstovan%20og%20dalking/A%20sjonum/Spillivatn/Rottangar%20og%20reinsiverk (Accessed May 28, 2023).

Von Wintersdorff, C. J. H., Penders, J., van Niekerk, J. M., Mills, N. D., Majumder, S., van Alphen, L. B., et al. (2016). Dissemination of antimicrobial resistance in microbial ecosystems through horizontal gene transfer. *Front. Microbiol.* 7, 173. doi:10.3389/fmicb.2016.00173

Wade, T. J., Sams, E., Brenner, K. P., Haugland, R., Chern, E., Beach, M., et al. (2010). Rapidly measured indicators of recreational water quality and swimming-associated illness at marine beaches: a prospective cohort study. *Environ. Health* 9 (1), 66. doi:10.1186/1476-069x-9-66

World Health Organization (2020). Antibiotic resistance. Available at: https://www.who.int/news-room/fact-sheets/detail/antibiotic-resistance.

Yang, J., Wang, H., Roberts, D. J., Du, H. N., Yu, X. F., Zhu, N. Z., et al. (2020). Persistence of antibiotic resistance genes from river water to tap water in the Yangtze River Delta. *Sci. Total Environ.* 742, 140592. doi:10.1016/j.scitotenv.2020.140592

Zhang, Y., Li, A., Dai, T., Li, F., Xie, H., Chen, L., et al. (2017). Cell-free DNA: a neglected source for antibiotic resistance genes spreading from WWTPs. *Environ. Sci. Technol.* 52 (1), 248–257. doi:10.1021/acs.est.7b04283

Zieliński, W., Buta, M., Hubeny, J., Korzeniewska, E., Harnisz, M., Nowrotek, M., et al. (2019). Prevalence of beta lactamases genes in sewage and sludge treated in Mechanical-Biological Wastewater treatment plants. *J. Ecol. Eng.* 20 (9), 80–86. doi:10.12911/22998993/112506

Zieliński, W., Korzeniewska, E., Harnisz, M., Drzymała, J., Felis, E., and Bajkacz, S. (2021). Wastewater treatment plants as a reservoir of integrase and antibiotic resistance genes – an epidemiological threat to workers and environment. *Environ. Int.* 156, 106641. doi:10.1016/j.envint.2021.106641

frontiers | Frontiers in Environmental Science

TYPE Review
PUBLISHED 08 April 2024
DOI 10.3389/fenvs.2024.1390510

Check for updates

OPEN ACCESS

EDITED BY
Divya Pal,
Stockholm University, Sweden

REVIEWED BY
Isha Burman,
Indian Institute of Technology Dhanbad, India
Andrey E. Krauklis,
University of Latvia, Latvia

*CORRESPONDENCE
Qudrat Ullah,
qudrat.ullah@uad.edu.pk
Pavel Horky,
pavel.horky@mendelu.cz

RECEIVED 23 February 2024
ACCEPTED 19 March 2024
PUBLISHED 08 April 2024

CITATION
Naz S, Chatha AMM, Khan NA, Ullah Q, Zaman F, Qadeer A, Khan IM, Danabas D, Kiran A, Skalickova S, Bernatova S, Khan MZ and Horky P (2024), Unraveling the ecotoxicological effects of micro and nano-plastics on aquatic organisms and human health.
Front. Environ. Sci. 12:1390510.
doi: 10.3389/fenvs.2024.1390510

COPYRIGHT
© 2024 Naz, Chatha, Khan, Ullah, Zaman, Qadeer, Khan, Danabas, Kiran, Skalickova, Bernatova, Khan and Horky. This is an open-access article distributed under the terms of the Creative Commons Attribution License (CC BY). The use, distribution or reproduction in other forums is permitted, provided the original author(s) and the copyright owner(s) are credited and that the original publication in this journal is cited, in accordance with accepted academic practice. No use, distribution or reproduction is permitted which does not comply with these terms.

Unraveling the ecotoxicological effects of micro and nano-plastics on aquatic organisms and human health

Saima Naz[1], Ahmad Manan Mustafa Chatha[2], Nisar Ahmed Khan[3], Qudrat Ullah[4]*, Faisal Zaman[5], Abdul Qadeer[6], Ibrar Muhammad Khan[7], Durali Danabas[8], Azka Kiran[1], Sylvie Skalickova[9], Silvie Bernatova[10], Muhammad Zahoor Khan[11] and Pavel Horky[9]*

[1]Department of Zoology, Government Sadiq College Women University, Bahawalpur, Punjab, Pakistan, [2]Department of Entomology, Faculty of Agriculture and Environment, The Islamia University of Bahawalpur, Bahawalpur, Punjab, Pakistan, [3]School of Economics and Management, Beijing University of Technology, Beijing, China, [4]Department of Theriogenology, Faculty of Veterinary and Animal Sciences, Cholistan University of Veterinary and Animal Sciences, Bahawalpur, Punjab, Pakistan, [5]Key Laboratory of Plant-Soil Interactions of MOE, College of Resources and Environmental Sciences, National Academy of Agriculture Green Development, China Agricultural University, Beijing, China, [6]Department of Cell Biology, School of Life Sciences, Central South University, Changsha, China, [7]College of Life Science, Anhui Agricultural University, Hefei, Anhui, China, [8]Fisheries Faculty, Munzur University, Tunceli, Türkiye, [9]Department of Animal Nutrition and Forage Production, Faculty of AgriSciences, Mendel University in Brno, Brno, Czechia, [10]Institute of Scientific Instruments of the Czech Academy of Sciences, Brno, Czechia, [11]College of Agricultural Science and Engineering, Liaocheng University, Shangdong, China

Plastic pollution ranks among the most severe environmental disasters caused by humans, generating millions of tonnes of waste annually. The extensive and unregulated use of plastics has led to ecotoxicity and environmental imbalance. Microplastics (MPs) are prevalent in aquatic environments, and these MPs further degrade into even smaller particles known as nano-plastics (NPs). Both MPs and NPs impact the environment by readily absorbing organic pollutants and pathogens from their surroundings, owing to their bigger surface area to volume ratio. This review focuses on the source of origin, bioaccumulation, and potential impact of MPs and NPs on aquatic organisms and human health. Additionally, the review explores various methods employed for identification and quantification of these particles in aquatic ecosystems. Sufficient information is available on their characteristics, distributions, and effects on marine ecosystems compared with freshwater ecosystems. For plastic particles <10 μm, more toxicological effects were observed compared with larger size particles, in aquatic life. Understanding the mechanism of action and ecotoxicological effects of micro/nano-plastics on the health of aquatic life across various trophic levels, as well as human health, is of utmost importance. We address knowledge gaps and provide insights into future research approaches for a better understanding of the interactive mechanisms between binary pollutants.

KEYWORDS

plastics, marine ecosystems, pollution, aquatic organism, public health, toxicity

1 Introduction

Plastic debris has emerged as a global environmental issue, and the improper handling of plastic waste has led to a rapid escalation of its presence in ecosystems (Oliveira et al., 2019; Yu et al., 2019) especially aquatic ecosystems (Han et al., 2024). The worldwide annual production of plastic materials now exceeds 320 million tonnes, with 40% dedicated to single-use packaging (Food and Agriculture Organization, 2013). A staggering 70% of plastic material, amounting to 5,800 million tonnes, has transformed

TABLE 1 Toxicological effects of various microplastics and nanoplastics on aquatic organisms.

Test organism	Size (nm)	Concentration (mg/L)	Contaminant type	Exposure duration	Observations	References
Ctenopharyngdon idella	470	0.034	Polystyrene	20 days	DNA damage, erythrocytes mutagenic and cytotoxic effect	Guimarães et al. (2021)
Daphnia pulex	60	76.69	Polystyrene	96 h	Nanoplastics induce immune defence and oxidative stress	Liu et al. (2021)
Macrobrachium nipponense	75	40	Polystyrene	28 days	Effects on reproduction	Li et al. (2021)
Hydra viridissima	40	40	Polymethyl Methacrylate	96 h	Morphological alteration like partial or complete loss of tentacles	Venancio et al. (2021)
Daphnia pulex	75	.001	Polystyrene	21 days	Effects on growth rate and reproduction	Liu et al. (2020)
Danio rerio	1,000	50	Polystyrene NPs	12 h	Nanoplastics induce immune response in test organism	Brandts et al. (2020)
Phaedactylum tricornutum	60	100	Carboxylated polystyrene	72 h	Reduction of intracellular generation rate of ROS	Grassi et al. (2020)
Chlorella vulgaris	500	250	Polystyrene	12 h	Deformation of cell wall, cellular stress	Gomes et al. (2020), Hazeem et al. (2020)
Rhodomonas baltica	50	0.5–100	Polymethyl Methacrylate	72 h	Pigment overproduction, membrane integrity lost, and mitochondrial membrane hyperpolarization	
Artemia franciscana	100	500	Polystyrene	24 h	Greater bioaccumulation of PS in stomach and gut	Qiao et al. (2019b), Sendra et al. (2020)
Danio rerio	5,000	0.5	Polystyrene	3 weeks	Inflammation and thinning of intestinal wall, intestinal damage 86%	
Danio rerio	20,000–100000	0.01	Nano-plastics	21 days	An increase in mast cells based on intestinal epithelium, Defects in the intestinal mucosa	Qiao et al. (2019a)
Chaetoceros neogracile	50	5	Polystyrene amino modified	4 days	Chlorophyll rate decrease due to microplastic exposure	González-Fernández et al. (2019), Sallam et al. (2020)
Mytilus galloprovincialis	2–4,000 µm	5×10^5 particles/L	Polystyrene, polypropylene, polyethylene terephthalate	3 days	Sex and gametogenesis cycle could influence contaminant uptake and elimination or biomarkers levels in molluscs	Pizzurro et al. (2024)
Isochrysis galbana	40	83.7	Polymethyl Methacrylate	96 h	Effects on growth rate	Venâncio et al. (2019)
Phaeodactylum tricornutum	50	50	Polystrene	72 h	Population growth inhibition and decrease in chlorophyll content	Sendra et al. (2019)
Carassius auratus	700,000–5000000	100	Polystyrene	6 weeks	Intestinal inflammation, liver inflammation and infiltration	Jabeen et al. (2018)
Caenorhabditis elegans	5,000	0.01–10	Polystyrene	10 days	Reproduction inhibition and swollen abdomen in dead fish	Lei et al. (2018)

*ROS (Reactive oxygen species), PS (Polystyrene).

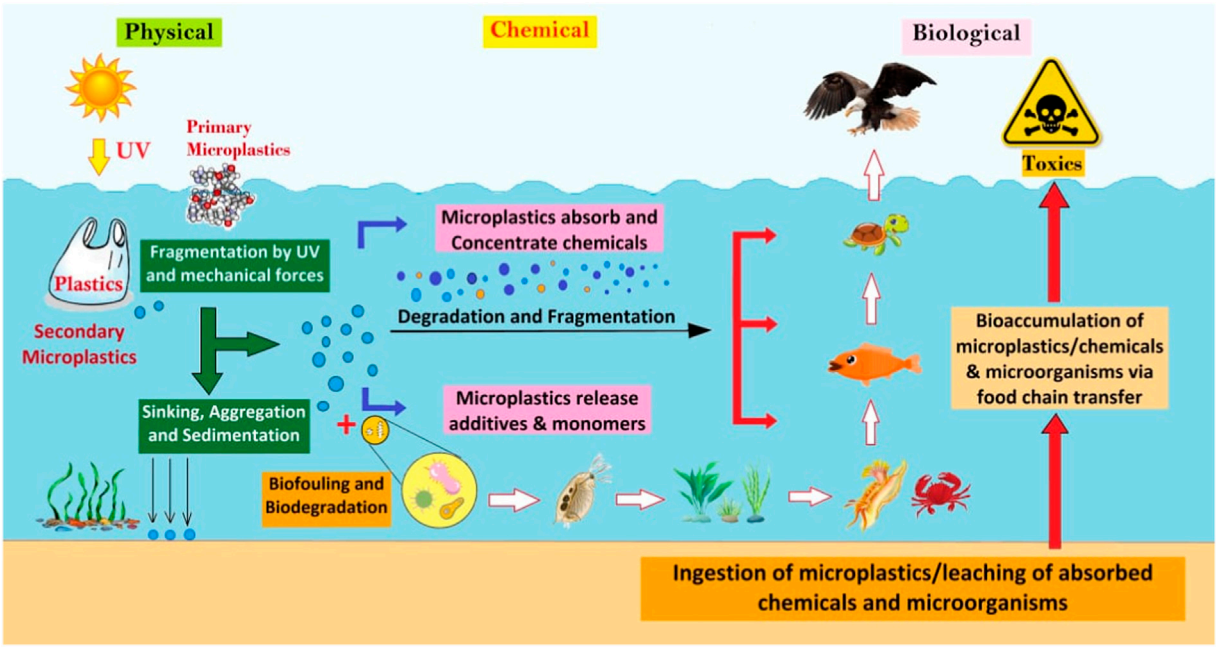

FIGURE 1
Different processes affecting microplastics in aquatic systems.

into debris, and approximately 79% (4,900 million tonnes) has amassed in ecosystems or landfills as of 2015 (Geyer et al., 2017). The widespread use of plastics in various applications persists due to their cost-effective manufacturing, utility, and durability (Barría et al., 2020). Plastics have been the preferred material for many years owing to their versatility, ubiquity, lightness, durability, and adaptability (Nielsen et al., 2020). The use of plastics is also increasing every day in agriculture benefitting agricultural production. However, the misuse of plastics after agricultural operations can lead to plastic waste and consequent environmental contamination by plastic debris (Mongil-Manso et al., 2023; Kudzin et al., 2024). Unfortunately, due to careless and excessive use, improper management, and inadvertent disposal, a significant volume of plastics has amassed in aquatic systems (Peng et al., 2020). Thus, they can accumulate at higher trophic levels, infiltrate the food chain, and pose a potential risk to ecosystems, native and non-native species, and human health (Neves et al., 2024).

Plastics of various types are globally produced, with polyethylene, polyvinyl chloride, polystyrene, polypropylene, polyethylene terephthalate, and polyurethane identified as the most prevalent plastic varieties (Al-Thawadi, 2020). Through processes like mechanical abrasion and biological deterioration, plastics can undergo fragmentation, resulting in the formation of secondary microplastics (MPs) and nano-plastics (NPs), (Alimi et al., 2018; Oliveira et al., 2019). Micro/nano-plastics (MNPs), owing to their capacity to absorb and accumulate co-contaminants, exert a physical and chemical impact on the environment. The attachment of metallic/organic toxins to MNPs and their subsequent transport into animal bodies depend on sorption mechanisms primarily influenced by the physico-chemical characteristics of MNPs and the type of pollutants (Thiagarajan et al., 2021). Nanoplastics and MPs are categorized based on their size, with NPs measuring less than 1000 nm and MPs being less than 5 mm (Frias and Nash, 2019). Although there is currently no formal definition for NPs, they are generally considered to share the same origin and composition as MPs but with a size of less than 1,000 nm (Gigault et al., 2018; Ferreira et al., 2019; Barría et al., 2020). Generally, MNPs are classified into primary and secondary MNPs. Examples of primary MNPs include synthetic fibers, cosmetics, pharmaceuticals, and raw materials (Li et al., 2018; Wang et al., 2018; Wang et al., 2020). Primary MNPs, being smaller in size, have a larger surface area, facilitating the adsorption of hydrophobic constituents from marine systems, such as polycyclic aromatic hydrocarbons (PAHs), perfluorooctanoic acid (PFOA), dichlorodiphenyltrichloroethane (DDT), polybrominated diphenyl ethers (PBDEs), polychlorinated biphenyls (PCBs), and metals (Li et al., 2018; Ferreira et al., 2019).

Micro and nano plastics have caused significant pollution in water bodies including drinking water (Li et al., 2023; Brancaleone et al., 2023). Moreover, aquatic organisms are regularly being exposed to pharmaceuticals nanomaterials (PC/NM prevalent in industrial and urban areas (Naz et al., 2021; Fernandes et al., 2023). Wastewater treatment plants appear to be a major source of contamination in the aquatic ecosystem (Vaid et al., 2021; Gagné et al., 2023). Consequently, investigations into the interactions between MNPs and PC/NM, along with their ecotoxicological effects on aquatic biota, have been conducted. Fish easily ingest microplastic particles, both unintentionally due to their small size and deliberately, due to resemblance to food sources (Zubair et al., 2020; Naz et al., 2022). A study by Wang et al. (Wang et al., 2020) revealed the presence of microplastics in over 150 fish species in aquatic environments. In the Gorgan Bay of the Caspian Sea, various types of microplastics, including polypropylene, polyester, nylon,

TABLE 2 Toxicological effects of various microplastics and nanoplastics on mammals.

Animal strain	Plastic type	Particle size (μm)	Route of administration	Dose	Exposure duration	Changes	References
BALB/c mice	Polystyrene	5.0–5.9	Oral	0.01–1 mg/day	6 weeks	Decrease in sperm no., motility, and serum testosterone; increase in sperm deformity rate; oxidative stress	Xie et al. (2020)
ICR male mice	Polystyrene	20 nm	injected via tail vein	50 μg/kg·d	48 h	Inhibited StAR mRNA and protein expression in mice testis and TM3 cells. and induced mTOR/4E-BP1 phosphorylation by ERK1/2 MAPK and AKT pathways.	Sui et al. (2023)
C57BL/6 mice	Polyethylene	10–150	Oral	6, 60, and 600 μg/day	5 weeks	Intestinal inflammation, alterations in gut microbiome at 600 μg/day, changes in innate immunity at all doses	Li et al. (2020a)
BALB/c mice	Polystyrene	0.5, 4, and 10	Oral	10 mg/mL	24 h and 28 days	Spermatogenic disorder, testicular inflammation, decreased testosterone levels	Jin et al. (2021)
C57BL/6NTac mice	Polystyrene	1, 4, and 10	Oral	1.49–4.55 3,107 particles	4 weeks	No intestinal inflammation or changes in body or organ wt	Stock et al. (2019)
ICR mice	Polystyrene	5	Oral	500 μg/mL	28 days	Aggravation of dextran sodium sulfate– based acute colitis and increased intestinal permeability	Zheng et al. (2021)
Mice	Polystyrene	20 nm	TM3 cells culture	50–150 μg/mL	24 h	Mitochondrial impairment and apoptosis in TM3 cells. Compromised energy metabolism and testosterone synthesis in TM3 cells. plasma membrane integrity of TM3 cells was Destructed	Sun et al. (2023)
CD-1 mice	Polyethylene and Polystyrene	0.5–1	Oral	2 mg/L	90 days	Increased toxicity to flame retardants	Deng et al. (2018)
ICR mice	Polyethylene	~16.9	Oral	0.125–2.0 mg/kg	90 days	Changes in lymphocyte subpopulation in spleen, decrease in IgA in females, alterations in live births per dam and pup body wt	Park et al. (2020)
ICR mice	Polystyrene	5	Oral	0.6–70 μg/day	35 days	Sperm cell apoptosis and expression of proinflammatory cytokines	Hou et al. (2021)
Sprague-Dawley rats	Polystyrene	~24	Intrajugular	1.3–1.95 million beads/100 g body wt	One-time administration	Pulmonary embolism, hypoxemia, increase in alveolar neutrophil chemotaxis and decrease in survival	Zagorski et al. (2003)
Sprague-Dawley rats	Polystyrene	0.02	Intratracheal instillation	2.64 3 1014 particles	24 h	Particles present in maternal lungs, heart, spleen, placenta and fetal lungs, heart, liver, kidney, and brain	Fournier et al. (2020)

(Continued on following page)

TABLE 2 (*Continued*) Toxicological effects of various microplastics and nanoplastics on mammals.

Animal strain	Plastic type	Particle size (μm)	Route of administration	Dose	Exposure duration	Changes	References
Sprague-Dawley rats	Polystyrene	0.01	Inhalation	0.75–3 3,105 particles/cm	14 days	Male rats: decrease in inspiratory time. Female rats: decrease in inspiratory, expiratory times and respiratory frequency in some groups; elevated markers of lung fibrosis and inflammation	Lim et al. (2021)
Mice	Polystyrene	50 nm	Oral	100 mg/mL	24 h	weight loss, increased death rate, alternated biomarkers, and histological damage of the kidney	Meng et al. (2022)
Wistar rat	Polystyrene	25, 50	Oral	1–10 mg/kg	5 weeks	Subtle changes in neurobehavior	Rafiee et al. (2018)
Wistar rat	Polystyrene	0.5	Oral	0.015–1.5 mg/kg/day	90 days	Ovarian fibrosis, decrease in ovarian follicle and reserve capacity	An et al. (2021)
Mice	Polystyrene MPs	-	Oral	0.5, 4, 10 μm	28 days	Decreased sperm quality and testosterone level, and testicular inflammation	Jin et al. (2021)
Rats	Polystyrene NPs	-	Oral	1, 3, 6 and 10 mg kg−1 day−1	5 Weeks	thyroid endocrine disruption, metabolic deficit, decreased serum levels	Amereh et al. (2019)
C57BL/6 mice	Polyethylene MPs	-	Oral	6, 60, and 600 μg/day	5 weeks	Intestinal dysbacteriosis and inflammation	Li et al. (2020b)
Mice	Polystyrene MPs	0.5, 50	Oral	1,000 μg/L	5 weeks	Hepatic triglyceride (TG) and total cholesterol (TCH) levels decreased, modified the gut microbiota composition and induce hepatic lipid disorder	Lu et al. (2018)
ICR mice	Polystyrene	0.5, 5	Oral	0.024 and 0.24 mg/kg/day	3 weeks	Disorders of fatty acid metabolism were observed in the offspring of mice that consumed MPs	Luo et al. (2019)
ICR mice	Polystyrene	5	Oral	0.024 and 0.24 mg/kg/day	6 weeks	MP accumulates in the intestine, causes a disturbance of the intestinal barrier, changes in the intestinal microflora, disturbances in the metabolism of bile acids	Jin et al. (2019)
C57BL/6 mice	Polystyrene	1–10 μm and 50–100	Oral	2.4 mg/kg/days	8 weeks	MP consumption led to overproduction of ROS, the development of oxidative stress, and impaired skeletal muscle regeneration. MP suppressed myogenic and stimulated adipogenic differentiation of myosatellite cells. Muscle regeneration was negatively correlated with MP particle size	Shengchen et al. (2021), Li et al. (2023b)

and polystyrene, were detected in sediment, fishes, and benthic organisms, ranging from 80 to 105 MP/kg (Bagheri et al., 2020). Given that fish is a significant protein source for humans, the existence of microplastics in fish and their ecotoxicological effects could have adverse consequences for both aquatic food sources and human health (Barboza et al., 2018). There is an urgent need to find or develop various methods like the use of microorganisms (Herrera et al., 2023) or the use of non-toxic, novel agglomerate (Peller et al.,

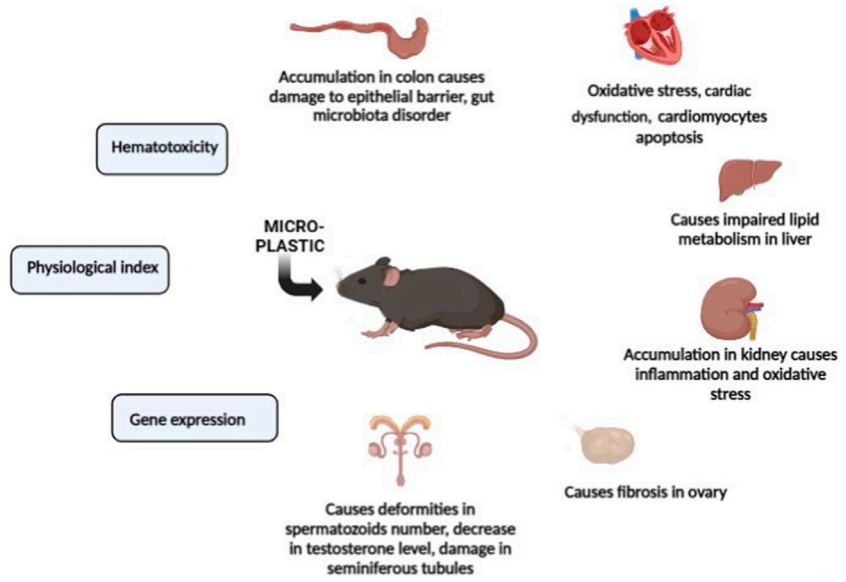

FIGURE 2
Effects of microplastics on mammals.

2024) for degradation of micro and nano plastics for sustainable plastic waste management. Furthermore, social responsibility and a shift in consumer behaviours and habits in adopting low-risk products should also be encouraged (Rashed et al., 2023). Despite an abundance of research on the ingestion and consequences of MNPs, there has been a scarcity of review publications on this topic until recently. Therefore, this review specifically focuses on a multidisciplinary approach, drawing upon insights from environmental science, ecology, toxicology, and public health. It covers various types of micro and nano-plastics, including microbeads, microfibers, and nanoplastics, and their interactions with different aquatic organisms ranging from plankton to fish. Furthermore, the review considers diverse aquatic environments such as oceans, rivers, lakes, and estuaries, acknowledging the variability in plastic pollution levels and ecological dynamics across these habitats. Additionally, the review highlights uncertainties and information gaps in understanding the fate, distribution, and harmful mechanisms of MNPs and PC/NM to aquatic organisms.

2 Toxic effects of MNPs on aquatic organisms

Microplastics (MPs) may have detrimental effects on aquatic ecosystems, impacting various organisms such as phytoplankton, invertebrates, mollusks, and fish, as they enter freshwater networks in substantial quantities (0.12–387 items/m^3) (Brandts et al., 2018; Triebskorn et al., 2019). Numerous studies have been conducted to investigate the toxic effects of MNPs on water-dwelling organisms. A study conducted by Chae et al. (Chae et al., 2018) observed the trophic transfer and effects of 51 nm polystyrene nano-plastics (PS-NPs) on four freshwater species, including the alga *Chlamydomonas reinhardtii*. Despite exposure to concentrations as high as 100 mg/L resulting in little to no mortality, confocal laser microscopy revealed the attachment of NPs to the zoospores' surface and outer layer penetration during cell division. Nano-plastics also led to reduced locomotor activity and induced histological abnormalities in the livers of fish directly exposed to them. Furthermore, the study observed that NPs could pass through embryonic walls and persist in hatched larvae yolk. In another investigation (Sökmen et al., 2020), the effects of short-term (24 h) exposure to negatively charged fluorescent PS-NPs (50 nm), aggregated with gold nanoparticles (Au ions), were explored in *Danio rerio*. Comparing the impacts of individual exposure to PS-NPs and Au ions, the study found increased mortality and deformation rates in the exposed organisms. Additionally, there was a stimulated immunological response, indicated by elevated expression of IL-6 and IL-1 β. Exposure to PS NPs or Au ions individually resulted in higher levels of reactive oxygen species (ROS), formation of intracellular vacuoles, and mitochondrial damage (Lee et al., 2019).

Exposure to 45 nm polymethyl methacrylate nanoparticles (PMMA-NPs) at concentrations of ≤20 mg/L was found to affect the immune system of fish, with an observed increase in mRNA transcripts associated with lipid metabolism (Brandts et al., 2018). In *Sebastes schlegelii* samples exposed to 0.5 and 15 μm PS-NPs (190 μg/L) exhibited clustering, reduced swimming speed, increased oxygen consumption, and ammonia excretion, as well as lower protein and lipid contents (Yin et al., 2019; Jiang et al., 2023a). Despite ingesting more than 90% of microalgae containing polystyrene nanoparticles (PS-NPs), brine shrimp (*Artemia franciscana*) did not show any significant effects (Sendra et al., 2020). Zebrafish exposed to secondary nanoparticles showed a 54% increase in cell death through skin diffusion compared to microplastics (Enfrin et al., 2020; Jiang et al., 2023b). Sökmen et al. (Sökmen et al., 2020) explored the impacts of NPs on zebrafish (*D. rerio*), revealing that 20 nm diameter PS-NPs reached and accumulated in the zebrafish brain, causing

TABLE 3 Effect of microplastics and nanoplastics on human health.

Plastic type	Size	Effect	Target cell line	References
Polypropylene MNPs	1–2 μm and 400–500 nm	Caused the death of 76.70% and 77.18% of human embryonic kidney cells after exposure of 48 and 72 h, respectively	HEK293T human embryonic kidney cell line	Hussain et al. (2023)
Polystyrene NPs	100 nm and 500 nm	500 nm PS-NPs bound to the surface of cell membranes causing cell membrane damage. 100 nm PS-NPs aggregated in the cytoplasm and blocked the autophagic flux in HUVECs	Human umbilical vein endothelial cells (HUVECs)	Lu et al. (2022)
Polystyrene MPs	1 and 10 μm	Caused a significant reduction in cell proliferation and changed the morphology of cells exposed	Cultured human alveolar A549 cells	Goodman et al. (2021)
Polystyrene MPs	50 nm	Caused genotoxicity through different mechanisms of DNA damage	Three human leukocytic cell lines: Raji-B (B-lymphocytes), TK6 (lymphoblasts) and THP-1 (monocytes)	Rubio et al. (2020)
Polystyrene MPs	5 and 20 μm	Induced inflammation Induced adverse effects on neurotransmission	Liver cells	Deng et al. (2017)
Polystyrene NPs	60 nm	Strong interaction and aggregation with mucin. Induced apoptosis	Intestinal epithelial cells	Inkielewicz-Stepniak et al. (2018)
Polystyrene NPs	60 nm	Induced ROS generation and ER stress Induced autophagic cell death	Lung epithelial cells	Xia et al. (2008)
Polystyrene MPs	5 μm	Changes in amino acid and bile acid metabolism. Induced gut microbiota dysbiosis and intestinal barrier dysfunction	Intestine	Jin et al. (2019)
Microplastics	0.5 and 5 μm	Metabolic disorder associated with gut microbiota dysbiosis and gut barrier dysfunction	Gut cells	Luo et al. (2019)
Polystyrene	44 nm	induced strong upregulation of IL-6 and IL-8 genes	Human gastric adenocarcinoma cells (AGS)	Forte et al. (2016)
Polystyrene	50, 100 nm	Size dependency regarding particle translocation	Human colon carcinoma cells (Caco-2)	Walczak et al. (2015)
Polystyrene	57 nm	Binding of mucin and induction of adoptosis	Human colon carcinoma cells	Inkielewicz-Stepniak et al. (2018)
Polystyrene	20,40, 100 nm	40 nm particles internalized faster than 20 or 100 nm particles in both cell line	human lung carcinoma cells (A549), human astrocytoma 132	Varela et al. (2012)
Polystyrene	116 nm	Cellular uptake	Human lung carcinoma cells	Deville et al. (2015)
Polystyrene	40, 50 nm	Cellular uptake irreversible, intracellular concentration increased linearly	Human lung carcinoma cells	Salvati et al. (2011)
Polystyrene	60 nm	Amino-functionalized polystyrene particles induce autophagic cell death through the induction of endoplasmic reticulum stress	Human bronchial epithelium	Chiu et al. (2015)

oxidative DNA damage. Other organs were also reported to be affected by NPs, establishing zebrafish as a valuable model for studying NP toxicity (Bhagat et al., 2020a; Sarasamma et al., 2020). The hydrophobicity of tetracycline-incubated NPs contributed to variations in toxic effects observed in the marine microalgae *Skeletonema costatum* (Feng et al., 2020a). Nano-plastics adsorption on microalgae has been documented in several studies, with some cases showing a reduction in algal growth while others did not (Bergami et al., 2017; Heinlaan et al., 2020).

The aggregation behaviour of globular PS-NPs is influenced by the chemical conditions of the solution, which may be enhanced by increasing ionic strength and electrolyte valence (Cai et al., 2021). In freshwater biofilms, PS-NPs (positively charged amide-modified) are more hazardous to photosynthesis and extracellular enzymatic activity than negatively charged particles (Miao et al., 2019). Eutrophication may be aggravated by freshwater NPs and marine rotifer *Brachionus koreanus* showed elevated stress effects from NPs, and the related oxidative stress caused damage to the lipid membranes (Jeong et al., 2018; Feng et al., 2020b). Since their ingestion has been seen in numerous aquatic species (marine mammals, turtles, and fish) as well as invertebrates (zooplankton, bivalves, and crustaceans), plastic particles have raised some serious environmental concerns (Botterell et al., 2019; Wang et al., 2019; Huang et al., 2020; Zitouni et al., 2020; Naz et al., 2023a). Aside from particle features, the environment also has an impact on how NP pollution affects aquatic species. Exopolymeric substances (EPS) are the aggregation agents produced by microorganisms; nevertheless, when synthesized by diatoms and algae, they have been proven to inhibit NP harmful effects (Grassi et al., 2020; Mao et al., 2020). Apart from that various toxicological effects of MNPs are also reported in different species (Table 1).

TABLE 4 Identification and quantification of microplastics and nanoplastics.

Technique	Advantages	Disadvantages	References
FTIR	• Simple and reliable	• High concentration for NPs	Wang et al. (2018), Strungaru et al. (2019), Granek et al. (2020), Cai et al. (2021)
	• Particle quantification	• Water interference	
	• Identifying polymeric microplastics (>10–20 μm size)	• Unable to adequately characterize very small particles or fibers (<20 μm)	
	• Non-destructive	• A time-consuming work	
	• Aliphatic compounds and polyesters are well detectable	• Limited size (~25 μm) and thickness (<100 μm)	
	• Operative for thin film NPs	• Contaminants may overlap polymeric bands	
Roman Spectroscopy	• Higher resolution	• Fluorescent interference	Wang et al. (2018), Prata et al. (2019), Strungaru et al. (2019), Alprol et al. (2021), Cai et al. (2021), Zhou et al. (2021)
	• Identify trace PS-NPs	• Trade-off between measurement time as well as representativeness	
	• Non-destructive chemical characterization of microplastics	• Lacks a high lateral resolution	
	• Lower water interference	• Low signal intensity	
	• Effective for polymer chemical composition, organic and inorganic fillers	• Are unable to adequately characterize very small particles or fibers <1 μm	
	• Aliphatic and aromatic compounds, are well detectable	• Time needed for characterization is highly limiting for environmental samples	
	• Characterization of microplastics <20 μm	• Polymer heating as well as degradation	
	• Not reserved for sample thickness or shape	• Affected by colour, additives, fluorescence, and contaminants adsorbed on microplastics	
	• Good for spatial resolution	• Long time measurement	
	• More sensitive to non-polar groups		
Mass spectrometry	• Less mass sample	• Preconcentration of sample needed	Fu et al. (2020), Cai et al. (2021), Vega-Herrera et al. (2022)
	• Numerous polymers for a single run	• Lack morphological information	
	• Purification and vaporization of polymers	• Not popular owing to severe extraction and purification	
	• Determine Mass/number concentration		
Pyrolysis GC/MS	• Analysis of polymers and additives at a time	• Expensive	Prata et al. (2019), Alprol et al. (2021)
	• Chemical characterization of microplastics (single or bulk sample)	• Need pre-selection	
		• Not effective for large quantity of sample	
		• Lack information of number, size or shape	
		• Time consuming	
TED–GC/MS	• Effective for complex matrices	• Identify few polymers as PE and PET	Prata et al. (2019), Alprol et al. (2021)
	• Use high sample masses and measure complex heterogeneous matrices for polymer identification and quantification	• Costly	
		• Need more time	
XPS	• Surface characterization	• No polymer type information	Cai et al. (2021)
		• Expensive	
SEM/TEM	• Size and number of particles	• Polymer identification required	Wang et al. (2018), Strungaru et al. (2019), Fu et al. (2020), Cai et al. (2021)
	• Provide high resolution topography images and enable microplastics differentiation from other plastics	• Costly	

(Continued on following page)

TABLE 4 (*Continued*) Identification and quantification of microplastics and nanoplastics.

Technique	Advantages	Disadvantages	References
	• Examine surface characteristics of microplastics	• Not valid for bulk samples	
	• High-resolution image require laborious preparation steps	• Representativeness issue	
		• For NPs, sample preparation needed	
MALS	• Online connection with AF4/CF3	• Nano-plastics separation needs perfectness	Cai et al. (2021)
	• Particles size distribution	• Polymer identification required	
DLS	• Simple, easy and reliable	• Not appropriate for polydisperse particles	Fu et al. (2020), Cai et al. (2021)
	• Effective for nano-sized particles and size distribution	• Need polymer identification	
	• Facile sample preparation, high throughput and reproducibility	• Cause significant bias on determination of size	
		• Merely for spherical particles	
Nanoparticle Tracking Analysis	• Simple, reliable and easy to use	• Complex in operation	Fu et al. (2020), Cai et al. (2021)
	• Size resolution	• Only for spherical particles	
	• Size distribution and particles concentration	• Data analysis affected by analysis factors	
	• More sensitive		
	• Effective for nano-sized particles		
	• Operative for single particle counts		
Impedance Spectroscopy	• Fast measurement of size and concentration of microplastics	• Need to expand this method to cover a greater (1–1,000 μm) size range	Colson and Michel (2021)
	• Characterize electrical properties of individual particles		
	• No visual sorting or filtration required		
Fluorescence Spectroscopy	• Little detection limit	• Sample preparation need fluorescent dyes or labels	Fu et al. (2020)
	• Provide single absorption or emission line, and a linear standard curve	• Less elemental sensitivity	
	• More sensitive		
Visual Sorting	• Cheap	• Unable to characterize to molecule <500 μm	Alprol et al. (2021)
	• Suitable for pre-sorting of samples	• Underestimation of small or transparent elements	
	• Classify particles by shape, size, and colour	• Non-chemical composition	
		• Less the particle size more will be the error	
		• Over-estimation owing to mis-identification	

*FTIR (Fourier transform infrared spectroscopy), TED–GC/MS (Thermoextraction and desorption coupled with gas chromatography-mass spectroscopy), XPS (X-ray photoelectron spectroscopy), SEM/TEM (Scanning electron microscopy or Transmission electron microscopy), MALS (Multi-angle light scattering), DLS (Dynamic light scattering).

3 Ecological toxicity and human health risk

3.1 Effect on organisms

In addition to their small size, physical and chemical properties of M NPs, can have a significant impact on aquatic species and human health. Adsorption of harmful chemicals on the MNPs raises concerns about how various lethal chemicals may interact with these particles, desorbing into animal tissues and causing harmful effects (Yu et al., 2019; Zhang et al., 2020). Nano-plastics have a greater surface area than MPs, allowing them to adsorb contaminants such as hazardous compounds or heavy metals at higher concentrations (Al-Thawadi, 2020; Naz et al., 2023b). These can be ingested by

organisms and then transported and accumulated in their different organs. Aquatic life at all trophic levels, including bacteria, bivalves, algae, echinoderms, rotifers, arthropods, and fish, can be affected by NPs in terms of reproduction, mortality, multiple molting, growth, feeding, immunological responses, and antioxidation (Liu et al., 2019; Bibi et al., 2023). Once NPs enter the aquatic environment, they are easily transported down the food chain, posing a major threat to the ecological environment's long-term growth, as well as food safety and human health (Zhang F. et al., 2020; Shi et al., 2020).

The interaction of NPs with heavy metals, polycyclic aromatic hydrocarbons, medicines, organic halogens, and pesticides, has become a major concern of environmental risks (Jacob et al., 2020). Extensive research has been conducted on the ecological toxicity of NPs, but few have been conducted on the combined toxicity induced by compound pollution (Bhagat et al., 2020b; Zhu et al., 2020). Interactions with co-pollutants can modify the uptake and accumulation of plastics and/or contaminants in exposed organisms, causing significant changes in the surface characteristics of plastics (Ghaffar et al., 2018; Zhang et al., 2020). The toxicity of MPs to organisms is determined by their aggregate size (Zhang et al., 2019). Because particle toxicity was inversely related to size in general, the aggregated MPs could be less bioavailable to aquatic organisms (Wang et al., 2020; Choi et al., 2020). Outside the organisms, MPs aggregates may have a harmful effect. MPs aggregates, for example, impeded photosynthesis and limited the transfer of nutrients and energy by microalgae in marine ecosystems. Furthermore, MP-biota hetero-aggregates may cause physical harm to organisms, such as splits and oxidative stress (Wu et al., 2019; Zhu et al., 2019; Choi et al., 2020).

There is still a lack of knowledge about the hazardous contaminants, additives, and infections found in fish and shellfish, as well as their potential consequences on human health. According to the Food and Agriculture Organization (FAO) essential food risk evaluations are lacking, with no information on metabolism and nothing on the excretion of MPs and NPs after intake (Al-Thawadi, 2020). Accumulation and biomagnification of hazardous compounds connected with MPs in marine trophic webs is another harmful impact (Figure 1). When top predators and humans consume species polluted with MPs or chemicals released from these particles after ingestion, this magnification raises the danger of harmful effects of these chemicals (Gallo et al., 2018; Vedolin et al., 2018). As a result, it is been suggested that plastic debris raises the global risk of human and animal diseases by creating new contamination/infection pathways, introducing pathogens through the environmental spread of MPs, or migrating organisms contaminated with MPs linked to pathogens (Bhagat et al., 2020a; Al-Thawadi, 2020; Haroon et al., 2022).

3.1.1 Effects on mammals

One of the most prominent classes of non-natural products made by humans that have pervaded earth's surface environment is plastics, so much so that these durable synthetic organic polymers are heralded as a defining stratigraphic marker for the Anthropocene (Zalasiewicz et al., 2016). Geyer and colleagues (Geyer et al., 2017) recently estimated that 8.3 billion metric tons of virgin plastics have been produced up to the year 2017, and with the continuation of current production and waste management practices, about 12 billion tons of plastic waste would be found in landfills and the natural environment by 2050. Plastic wastes are persistent environmental pollutants. Larger pieces of plastic waste present well-publicized ecological problems in terms of physical entanglement and entrapment (Gündoğdu et al., 2019). In the past 3 years, a good number of studies have examined the effect of pristine MNPs in mammalian models (largely mice). These studies are summarized in Table 2 and are broadly recapped below. In mice, ingested MNPs could be found in the gut (Deng et al., 2017), liver and kidney (Yang et al., 2019). Pathological changes to the gut include a reduction in mucus secretion, gut barrier dysfunction (Jin et al., 2019), intestinal inflammation, and gut microbiota dysbiosis (Lu et al., 2018; Li B. et al., 2020). Figure 2 shows the effects of microplastic on mammalian model species (mouse).

3.2 Effects on human health

Studies on the toxic effects of M NPs on human health are mainly focused on gastrointestinal and pulmonary toxicity, which includes oxidative stress, metabolic problems, and inflammatory reactions. Furthermore, it is crucial to know whether MPs can be destroyed further after ingestion in the gut's acidic environment or inside cells' lysosomes. As a result, greater research into the long-term fate of ingested MPs and NPs in the human body is required (Yee et al., 2021).

Micro-plastics have been found in a variety of seafood species, including bivalves, fish, and shrimp as well as in sea salt and food packaging (Peixoto et al., 2019; Li et al., 2020; Jacob et al., 2020). These are thought to be bio-persistent, causing unfavourable biological responses in humans such as oxidative stress, inflammation, cell apoptosis, genotoxicity, and tissue necrosis, as well as localized cell and tissue damage, fibrosis, and even carcinogenesis (Peixoto et al., 2019). Ingestion, oral inhalation, or skin contact with NPs may occur as a result of the usage of plastic items or through unintended methods (Lehner et al., 2019). As a result, human exposure to NPs has been attributed to the ingestion of NP particles, which can be easily ingested through the consumption of contaminated seafood or water. If NPs enter the gastrointestinal tract, they can cause tissue inflammation or enter the circulatory system via the mesenteric lymph, where they can build up in the liver. Furthermore, oxidative stress, the gut microbiome, and lipid metabolism have all shown significant modifications. As a result, NPs may affect the central nervous system in humans (Mattsson et al., 2017). Most of the reported studies used polystyrene due to its ease of synthesis and processing into nanoparticles, whereas polyurethanes, polyolefins (e.g., polyethylene and polypropylene), polyesters, and are the most often used commercial plastics (Gunasekaran et al., 2020). The hazardous effects of different forms of MNPs on human health are mainly unknown due to variations in the shape, particle size, and chemical composition of plastics (Leslie and Depledge, 2020; Khan et al., 2023). Table 3 shows various studies related to the effect of micro and nano-plastics on human beings. Recent studies showed that various types of MNPs can affect the survival of human foetus during early embryonic development (Hussain et al., 2023). Likewise, the MNPs can cause severe damage to cell membrane (Lu et al., 2022), alter the morphology of the exposed human alveolar cells (Goodman et al., 2021) and cause genotoxicity in human blood cells (Rubio et al., 2020).

As a result, we recommend that future research needs focus on determining the potential risks associated with chronic exposure to various M NPs at appropriate concentrations. Unfortunately, the assessment of human exposure to NPs is still a scientific challenge owing to inappropriate methods, practiced reference materials, and standard analytical techniques (Brachner et al., 2020; Paul et al., 2020). Some common techniques used for the identification of M NPs are listed in table (Table 4).

4 Conclusion

Micro and nano-plastics are significant sources of plastic contamination in marine ecosystems and the production of M NPs has increased due to biodegradation, thermo-oxidative degradation, thermal and hydrolysis processes, and also photodegradation. The effects of MPs on marine life are well explored. However, their effects on freshwater species have very little literature as data on freshwater species is insufficient. So, freshwater systems are suffering from severe contamination compared with marine systems and the ecotoxicological effects of M NPs on freshwater species need more research efforts. The development of analytical methods for M NPs, as well as their standardization, is becoming more important to allow the detection, identification, and quantification of polymers in environmental matrices. While research on micro and nano-plastics is advancing rapidly, several significant limitations and gaps like lack of standardized methods for detection and characterization, limited understanding of fate and behavior of MNPs, ecological effects of MNPs on different trophic levels, long-term effects of MNPs, and ingestion and trophic transfer of MNPs still exist. Addressing these limitations and filling these knowledge gaps is essential for developing effective mitigation strategies, informing policy decisions, and safeguarding both aquatic ecosystems and human health from the impacts of micro and nano-plastic pollution. Furthermore, New ways to study the impacts of MNPs on the biota and humans (*in vitro*) are also required.

Author contributions

SN: Conceptualization, Data curation, Investigation, Methodology, Resources, Software, Validation, Writing–original draft, Writing–review and editing. AC: Conceptualization, Data curation, Investigation, Methodology, Writing–original draft, Writing–review and editing. NK: Conceptualization, Data curation, Investigation, Writing–review and editing. QU: Conceptualization, Project administration, Supervision, Validation, Visualization, Writing–original draft, Writing–review and editing. FZ: Conceptualization, Data curation, Investigation, Writing–review and editing. AQ: Data curation, Methodology, Writing–review and editing. IM: Conceptualization, Data curation, Writing–review and editing. AK: Data curation, Investigation, Methodology, Writing–review and editing. SS: Writing–review and editing. SB: Writing–review and editing. MK: Conceptualization, Data curation, Visualization, Writing–review and editing. PH: Funding acquisition, Investigation, Project administration, Resources, Software, Supervision, Validation, Visualization, Writing–original draft, Writing–review and editing.

Funding

The author(s) declare that financial support was received for the research, authorship, and/or publication of this article. This study was funded under project TAČR SS06020224 Development of an analytical platform for monitoring microplastic circulation in agricultural production.

Conflict of interest

The authors declare that the research was conducted in the absence of any commercial or financial relationships that could be construed as a potential conflict of interest.

Publisher's note

All claims expressed in this article are solely those of the authors and do not necessarily represent those of their affiliated organizations, or those of the publisher, the editors and the reviewers. Any product that may be evaluated in this article, or claim that may be made by its manufacturer, is not guaranteed or endorsed by the publisher.

References

Alimi, O. S., Farner Budarz, J., Hernandez, L. M., and Tufenkji, N. (2018). Microplastics and nanoplastics in aquatic environments: aggregation, deposition, and enhanced contaminant transport. *Environ. Sci. Technol.* 52 (4), 1704–1724. doi:10.1021/acs.est.7b05559

Alprol, A. E., Gaballah, M. S., and Hassaan, M. A. (2021). Micro and nanoplastics analysis: focus on their classification, sources, and impacts in marine environment. *Reg. Stud. Mar. Sci.* 42, 101625. doi:10.1016/j.rsma.2021.101625

Al-Thawadi, S. (2020). Microplastics and nanoplastics in aquatic environments: challenges and threats to aquatic organisms. *Arab. J. Sci. Eng.* 45 (6), 4419–4440. doi:10.1007/s13369-020-04402-z

Amereh, F., Eslami, A., Fazelipour, S., Rafiee, M., Zibaii, M. I., and Babaei, M. (2019). Thyroid endocrine status and biochemical stress responses in adult male Wistar rats chronically exposed to pristine polystyrene nanoplastics. *Toxicol. Res.* 8, 953–963. doi:10.1039/c9tx00147f

An, R., Wang, X., Yang, L., Zhang, J., Wang, N., Xu, F., et al. (2021). Polystyrene microplastics cause granulosa cells apoptosis and fibrosis in ovary through oxidative stress in rats. *Toxicology* 449, 152665. doi:10.1016/j.tox.2020.152665

Bagheri, T., Gholizadeh, M., Zakeri, M., Hedayati, A., Rabaniha, M., Aghaeimoghadam, A., et al. (2020). Microplastics distribution, abundance and composition in sediment, fishes and benthic organisms of the gorgan Bay, Caspian Sea. *Chemosphere* 257, 127201. doi:10.1016/j.chemosphere.2020.127201

Barboza, L. G. A., Vethaak, A. D., Lavorante, B. R., Lundebye, A. K., and Guilhermino, L. (2018). Marine microplastic debris: an emerging issue for food security, food safety and human health. *Mar. Pollut. Bull.* 133, 336–348. doi:10.1016/j.marpolbul.2018.05.047

Barría, C., Brandts, I., Tort, L., Oliveira, M., and Teles, M. (2020). Effect of nanoplastics on fish health and performance: a review. *Mar. Pollut. Bull.* 151, 110791. doi:10.1016/j.marpolbul.2019.110791

Bergami, E., Pugnalini, S., Vannuccini, M. L., Manfra, L., Faleri, C., Savorelli, F., et al. (2017). Long-term toxicity of surface-charged polystyrene nanoplastics to marine planktonic species Dunaliella tertiolecta and Artemia franciscana. *Aquat. Toxicol.* 189, 159–169. doi:10.1016/j.aquatox.2017.06.008

Bhagat, J., Nishimura, N., and Shimada, Y. (2020a). Toxicological interactions of microplastics/nanoplastics and environmental contaminants: current knowledge and future perspectives. *J. Hazard. Mat.* 405, 123913. doi:10.1016/j.jhazmat.2020.123913

Bhagat, J., Zang, L., Nishimura, N., and Shimada, Y. (2020b). Zebrafish: an emerging model to study microplastic and nanoplastic toxicity. *Sci. Total Environ.* 728, 138707. doi:10.1016/j.scitotenv.2020.138707

Bibi, S., Abbas, G., Khan, M. Z., Nawaz, T., Ullah, Q., Uddin, A., et al. (2023). The mutational analysis of mitochondrial DNA in maternal inheritance of polycystic ovarian syndrome. *Front. Endocrinol.* 14, 1093353. doi:10.3389/fendo.2023.1093353

Botterell, Z. L., Beaumont, N., Dorrington, T., Steinke, M., Thompson, R. C., and Lindeque, P. K. (2019). Bioavailability and effects of microplastics on marine zooplankton: a review. *Environ. Pollut.* 245, 98–110. doi:10.1016/j.envpol.2018.10.065

Brachner, A., Fragouli, D., Duarte, I. F., Farias, P., Dembski, S., Ghosh, M., et al. (2020). Assessment of human health risks posed by nano-and microplastics is currently not feasible. *Int. J. Environ. Res. Public Health* 17 (23), 8832. doi:10.3390/ijerph17238832

Brancaleone, E., Mattei, D., Fuscoletti, V., Lucentini, L., Favero, G., Frugis, A., et al. (2023). "Microplastic in drinking water: a pilot study," in *Proceedings of the 3rd international conference on microplastic pollution in the mediterranean sea* (Cham: Springer International Publishing), 165–172.

Brandts, I., Garcia-Ordoñez, M., Tort, L., Teles, M., and Roher, N. (2020). Polystyrene nanoplastics accumulate in ZFL cell lysosomes and in zebrafish larvae after acute exposure, inducing a synergistic immune response *in vitro* without affecting larval survival *in vivo*. *Environ. Sci. Nano* 7 (8), 2410–2422. doi:10.1039/d0en00553c

Brandts, I., Teles, M., Tvarijonaviciute, A., Pereira, M. L., Martins, M. A., Tort, L., et al. (2018). Effects of polymethylmethacrylate nanoplastics on *Dicentrarchus labrax*. *Genom* 110 (6), 435–441. doi:10.1016/j.ygeno.2018.10.006

Cai, H., Xu, E. G., Du, F., Li, R., Liu, J., and Shi, H. (2021). Analysis of environmental nanoplastics: progress and challenges. *Chem. Eng. J.* 410, 128208. doi:10.1016/j.cej.2020.128208

Chae, Y., Kim, D., Kim, S. W., and An, Y. J. (2018). Trophic transfer and individual impact of nano-sized polystyrene in a four-species freshwater food chain. *Sci. Rep.* 8 (1), 284–311. doi:10.1038/s41598-017-18849-y

Chiu, H. W., Xia, T., Lee, Y. H., Chen, C. W., Tsai, J. C., and Wang, Y. J. (2015). Cationic polystyrene nanospheres induce autophagic cell death through the induction of endoplasmic reticulum stress. *J. Nanobiotechnology* 13, 76. doi:10.1039/c4nr05509h

Choi, J. S., Hong, S. H., and Park, J. W. (2020). Evaluation of microplastic toxicity in accordance with different sizes and exposure times in the marine copepod Tigriopus japonicus. *Mar. Environ. Res.* 153, 104838. doi:10.1016/j.marenvres.2019.104838

Colson, B. C., and Michel, A. P. (2021). Flow-through quantification of microplastics using impedance spectroscopy. *ACS Sens.* 6 (1), 238–244. doi:10.1021/acssensors.0c02223

Deng, Y., Zhang, Y., Lemos, B., and Ren, H. (2017). Tissue accumulation of microplastics in mice and biomarker responses suggest widespread health risks of exposure. *Sci. Rep.* 7, 46687. doi:10.1038/srep46687

Deng, Y., Zhang, Y., Lemos, B., Ren, H., Yang, X., et al. (2018). Evidence that microplastics aggravate the toxicity of organophosphorus flame retardants in mice (*Mus musculus*). *J. Hazard Mater* 357, 348–354. doi:10.1016/j.jhazmat.2018.06.017

Deville, S., Penjweini, R., Smisdom, N., Notelaers, K., Nelissen, I., Hooyberghs, J., et al. (2015). Intracellular dynamics and fate of polystyrene nanoparticles in A549 lung epithelial cells monitored by image (cross-)correlation spectroscopy and single particle tracking. *Biochim. Biophys. Acta Mol. Cell Res.* 1853, 2411–2419. doi:10.1016/j.bbamcr.2015.07.004

Enfrin, M., Lee, J., Gibert, Y., Basheer, F., Kong, L., and Dumée, L. F. (2020). Release of hazardous nanoplastic contaminants due to microplastics fragmentation under shear stress forces. *J. Hazard. Mat.* 384, 121393. doi:10.1016/j.jhazmat.2019.121393

Feng, L. J., Shi, Y., Li, X. Y., Sun, X. D., Xiao, F., Sun, J. W., et al. (2020b). Nanoplastics promote microcystin synthesis and release from cyanobacterial Microcystis aeruginosa. *Environ. Sci. Technol.* 54 (6), 3386–3394. doi:10.1021/acs.est.9b06085

Feng, L. J., Sun, X. D., Zhu, F. P., Feng, Y., Duan, J. L., Xiao, F., et al. (2020a). Behavior of tetracycline and polystyrene nanoparticles in estuaries and their joint toxicity on marine microalgae Skeletonema costatum. *Environ. Pollut.* 263, 114453. doi:10.1016/j.envpol.2020.114453

Fernandes, V. C., Boesmans, D., Domingues, V. F., and Delerue-Matos, C. (2023). Evaluating contaminants in fish: plastic additives and pesticides in the context of food safety. *Biol. Life Sci. Forum.* doi:10.3390/Foods2023-15052

Ferreira, I., Venâncio, C., Lopes, I., and Oliveira, M. (2019). Nanoplastics and marine organisms: what has been studied? *Environ. Toxicol. Pharmacol.* 67, 1–7. doi:10.1016/j.etap.2019.01.006

Food and Agriculture Organization. *The state of food insecurity in the world 2013: the multiple dimensions of food security*. Rome: FAO; 2013. Available at: https://www.fao.org/news/archive/news-by-date/2013/en/(accessed on (accessed on 23 February 2024).

Forte, M., Iachetta, G., Tussellino, M., Carotenuto, R., Prisco, M., De Falco, M., et al. (2016). Polystyrene nanoparticles internalization in human gastric adenocarcinoma cells. *Toxicol Vitro* 31, 126–136. doi:10.1016/j.tiv.2015.11.006

Fournier, S. B., D'Errico, J. N., Adler, D. S., Kollontzi, S., Goedken, M. J., Fabris, L., et al. (2020). Nanopolystyrene translocation and fetal deposition after acute lung exposure during late-stage pregnancy. *Part Fibre Toxicol.* 17, 55. doi:10.1186/s12989-020-00385-9

Frias, JPGL, and Nash, R. (2019). Microplastics: finding a consensus on the definition. *Mar. Pollut. Bull.* 138, 145–147. doi:10.1016/j.marpolbul.2018.11.022

Fu, W., Min, J., Jiang, W., Li, Y., and Zhang, W. (2020). Separation, characterization and identification of microplastics and nanoplastics in the environment. *Sci. Total Environ.* 721, 137561. doi:10.1016/j.scitotenv.2020.137561

Gagné, F., Roubeau-Dumont, E., André, C., and Auclair, J. (2023). Micro and nanoplastic contamination and its effects on freshwater mussels caged in an urban area. *J. Xenobiotics* 13, 761–774. doi:10.3390/jox13040048

Gallo, F., Fossi, C., Weber, R., Santillo, D., Sousa, J., Ingram, I., et al. (2018). Marine litter plastics and microplastics and their toxic chemicals components: the need for urgent preventive measures. *Environ. Sci. Eur.* 30 (1), 13–14. doi:10.1186/s12302-018-0139-z

Geyer, R., Jambeck, J. R., and Law, K. L. (2017). Production, use, and fate of all plastics ever made. *Sci. Adv.* 3, e1700782. doi:10.1126/sciadv.1700782

Ghaffar, A., Jamil, H., Zubair, M., Farooq, M., Murtaza, A., and Ullah, Q. (2018). Effect of dietary supplementation with propylene glycol on blood metabolites and hormones of nili-ravi Buffalo heifers: effect of dietary supplementation on blood metabolites. *Proc. Pak. Acad. Sci. B Life Environ. Sci.* 55 (3), 55–59. Available at: https://ppaspk.org/index.php/PPAS-B/article/view/164

Gigault, J., Ter Halle, A., Baudrimont, M., Pascal, P. Y., Gauffre, F., Phi, T. L., et al. (2018). Current opinion: what is a nanoplastic? *Environ. Pollut.* 235, 1030–1034. doi:10.1016/j.envpol.2018.01.024

Gomes, T., Almeida, A. C., and Georgantzopoulou, A. (2020). Characterization of cell responses in Rhodomonas baltica exposed to PMMA nanoplastics. *Sci. Total Environ.* 726, 138547. doi:10.1016/j.scitotenv.2020.138547

González-Fernández, C., Toullec, J., Lambert, C., Le Goïc, N., Seoane, M., Moriceau, B., et al. (2019). Do transparent exopolymeric particles (TEP) affect the toxicity of nanoplastics on Chaetoceros neogracile? *Environ. Pollut.* 250, 873–882. doi:10.1016/j.envpol.2019.04.093

Goodman, K. E., Hare, J. T., Khamis, Z. I., Hua, T., and Sang, Q. X. A. (2021). Exposure of human lung cells to polystyrene microplastics significantly retards cell proliferation and triggers morphological changes. *Chem. Res. Toxicol.* 34, 1069–1081. doi:10.1021/acs.chemrestox.0c00486

Granek, E. F., Brander, S., and Holland, E. B. (2020). Microplastics in aquatic organisms: improving understanding and identifying research directions for the next decade. *Limnol. Oceanogr. Lett.* 5, 1–4. doi:10.1002/lol2.10145

Grassi, G., Gabellieri, E., Cioni, P., Paccagnini, E., Faleri, C., Lupetti, P., et al. (2020). Interplay between extracellular polymeric substances (EPS) from a marine diatom and model nanoplastic through eco-corona formation. *Sci. Total Environ.* 725, 138457. doi:10.1016/j.scitotenv.2020.138457

Guimarães, A. T. B., Estrela, F. N., Pereira, P. S., Vieira, J. E. A., Rodrigues, A. S. L., Silva, F. G., et al. (2021). Toxicity of polystyrene nanoplastics in Ctenopharyngodon idella juveniles: a genotoxic, mutagenic and cytotoxic perspective. *Sci. Total Environ.* 752, 141937. doi:10.1016/j.scitotenv.2020.141937

Gunasekaran, D., Chandrasekaran, N., Jenkins, D., and Mukherjee, A. (2020). Plain polystyrene microplastics reduce the toxic effects of ZnO particles on marine microalgae Dunaliella salina. *J. Environ. Chem. Eng.* 8 (5), 104250. doi:10.1016/j.jece.2020.104250

Gündoğdu, S., Yeşilyurt, İ. N., and Erbaş, C. (2019). Potential interaction between plastic litter and green turtle *Chelonia mydas* during nesting in an extremely polluted beach. *Mar. Pollut. Bull.* 140, 138–145. doi:10.1016/j.marpolbul.2019.01.032

Han, B., Yacoub, M., Li, A., Nicholson, K., Gruver, J., Neumann, K., et al. (2024). Human activities increased microplastics contamination in the himalaya mountains. *Hydrology* 11, 4. doi:10.3390/hydrology11010004

Haroon, M., Jamil, H., Ullah, Q., Farooq, Q., and Inamullah, M. (2022). Cholesterol and serum minerals profile in the pregnancy and peurperium period of Beetal Goats. *Biosci. Res.* 19 (1), 381–385.

Hazeem, L. J., Yesilay, G., Bououdina, M., Perna, S., Cetin, D., Suludere, Z., et al. (2020). Investigation of the toxic effects of different polystyrene micro-and nanoplastics on microalgae Chlorella vulgaris by analysis of cell viability, pigment content, oxidative stress and ultrastructural changes. *Mar. Pollut. Bull.* 156, 111278. doi:10.1016/j.marpolbul.2020.111278

Heinlaan, M., Kasemets, K., Aruoja, V., Blinova, I., Bondarenko, O., Lukjanova, A., et al. (2020). Hazard evaluation of polystyrene nanoplastic with nine bioassays did not show particle-specific acute toxicity. *Sci. Total Environ.* 707, 136073. doi:10.1016/j.scitotenv.2019.136073

Herrera, D. A. G., Mojicevic, M., Pantelic, B., Joshi, A., Collins, C., Batista, M., et al. (2023). Exploring microorganisms from plastic-polluted sites: unveiling plastic degradation and PHA production potential. *Microorganisms* 11, 2914. doi:10.3390/microorganisms11122914

Hou, B., Wang, F., Liu, T., and Wang, Z. (2021). Reproductive toxicity of polystyrene microplastics: *in vivo* experimental study on testicular toxicity in mice. *J. Hazard Mater* 405, 124028. doi:10.1016/j.jhazmat.2020.124028

Huang, D., Tao, J., Cheng, M., Deng, R., Chen, S., Yin, L., et al. (2020). Microplastics and nanoplastics in the environment: macroscopic transport and effects on creatures. *J. Hazard. Mat.* 407, 124399. doi:10.1016/j.jhazmat.2020.124399

Hussain, K. A., Romanova, S., Okur, I., Zhang, D., Kuebler, J., Huang, X., et al. (2023). Assessing the release of microplastics and nanoplastics from plastic containers and reusable food pouches: implications for human health. *Environ. Sci. Technol.* 57, 9782–9792. doi:10.1021/acs.est.3c01942

Inkielewicz-Stepniak, I., Tajber, L., Behan, G., Zhang, H., Radomski, M. W., Medina, C., et al. (2018). The role of mucin in the toxicological impact of polystyrene nanoparticles. *Materials* 11, 724. doi:10.3390/ma11050724

Jabeen, K., Li, B., Chen, Q., Su, L., Wu, C., Hollert, H., et al. (2018). Effects of virgin microplastics on goldfish (*Carassius auratus*). *Chemosphere* 213, 323–332. doi:10.1016/j.chemosphere.2018.09.031

Jacob, H., Besson, M., Swarzenski, P. W., Lecchini, D., and Metian, M. (2020). Effects of virgin micro-and nanoplastics on fish: trends, meta-analysis, and perspectives. *Environ. Sci. Technol.* 54 (8), 4733–4745. doi:10.1021/acs.est.9b05995

Jeong, C. B., Kang, H. M., Lee, Y. H., Kim, M. S., Lee, J. S., Seo, J. S., et al. (2018). Nanoplastic ingestion enhances toxicity of persistent organic pollutants (POPs) in the monogonont rotifer Brachionus koreanus via multixenobiotic resistance (MXR) disruption. *Environ. Sci. Technol.* 52 (19), 11411–11418. doi:10.1021/acs.est.8b03211

Jiang, N., Luo, C., Shao, M., Zheng, Z., Ullah, Q., Khan, M. Z., et al. (2023a). Uncovering the role of ribosomal protein L8 in milk fat synthesis mechanisms in yak mammary epithelial cells. *Pak. J. Zool.*, 1–16. doi:10.17582/journal.pjz/20230415100435

Jiang, N., Naz, S., Ma, Y., Ullah, Q., Khan, M. Z., Wang, J., et al. (2023b). An overview of comet assay application for detecting DNA damage in aquatic animals. *Agriculture* 13 (3), 623. doi:10.3390/agriculture13030623

Jin, H., Ma, T., Sha, X., Liu, Z., Zhou, Y., Meng, X., et al. (2021). Polystyrene microplastics induced male reproductive toxicity in mice. *J. Hazard Mater* 401, 123430. doi:10.1016/j.jhazmat.2020.123430

Jin, Y., Lu, L., Tu, W., Luo, T., and Fu, Z. (2019). Impacts of polystyrene microplastic on the gut barrier, microbiota, and metabolism of mice. *Sci. Total Environ.* 649, 308–317. doi:10.1016/j.scitotenv.2018.08.353

Khan, R. U., Khan, M., Ullah, Q., Khan, M. Z., Sohail, A., Islam, R., et al. (2023). *In vitro* and *in vivo* effects of conventional and chitosan nanoparticle-encapsulated miltefosine drug for treatment of cutaneous leishmaniasis. *Med. Sci. Forum* 21 (1), 19. doi:10.3390/ECB2023-14334

Kudzin, M. H., Piwowarska, D., Festinger, N., and Chruściel, J. J. (2024). Risks associated with the presence of polyvinyl chloride in the environment and methods for its disposal and utilization. *Materials* 17, 173. [Online]. doi:10.3390/ma17010173

Lee, W. S., Cho, H. J., Kim, E., Huh, Y. H., Kim, H. J., Kim, B., et al. (2019). Bioaccumulation of polystyrene nanoplastics and their effect on the toxicity of Au ions in zebrafish embryos. *Nanoscale* 11 (7), 3173–3185. doi:10.1039/c8nr09321k

Lehner, R., Weder, C., Petri-Fink, A., and Rothen-Rutishauser, B. (2019). Emergence of nanoplastic in the environment and possible impact on human health. *Environ. Sci. Technol.* 53 (4), 1748–1765. doi:10.1021/acs.est.8b05512

Lei, L., Wu, S., Lu, S., Liu, M., Song, Y., Fu, Z., et al. (2018). Microplastic particles cause intestinal damage and other adverse effects in zebrafish *Danio rerio* and nematode *Caenorhabditis elegans*. *Sci. Total Environ.* 619-620, 1–8. doi:10.1016/j.scitotenv.2017.11.103

Leslie, H. A., and Depledge, M. H. (2020). Where is the evidence that human exposure to microplastics is safe? *Environ. Int.* 142, 105807. doi:10.1016/j.envint.2020.105807

Li, B., Ding, Y., Cheng, X., Sheng, D., Xu, Z., Rong, Q., et al. (2020a). Polyethylene microplastics affect the distribution of gut microbiota and inflammation development in mice. *Chemosphere* 244, 125492. doi:10.1016/j.chemosphere.2019.125492

Li, B., Khan, M. Z., Khan, I. M., Ullah, Q., Cisang, Z. M., Zhang, N., et al. (2023a). Genetics, environmental stress, and amino acid supplementation affect lactational performance via mTOR signaling pathway in bovine mammary epithelial cells. *Front. Genet.* 14, 1195774. doi:10.3389/fgene.2023.1195774

Li, S., Liu, H., Gao, R., Abdurahman, A., Dai, J., and Zeng, F. (2018). Aggregation kinetics of microplastics in aquatic environment: complex roles of electrolytes, pH, and natural organic matter. *Environ. Pollut.* 237, 126–132. doi:10.1016/j.envpol.2018.02.042

Li, Y., Du, X., Liu, Z., Zhang, M., Huang, Y., Tian, J., et al. (2021). Two genes related to reproductive development in the juvenile prawn, Macrobrachium nipponense: molecular characterization and transcriptional response to nanoplastic exposure. *Chemosphere* 281, 130827. doi:10.1016/j.chemosphere.2021.130827

Li, Y., Meng, Y., Qin, L., Shen, M., Qin, T., Chen, X., et al. (2023b). Occurrence and removal efficiency of microplastics in four drinking water treatment plants in zhengzhou, China. *China. Water* 16, 131. doi:10.3390/w16010131

Li, Z., Feng, C., Wu, Y., and Guo, X. (2020b). Impacts of nanoplastics on bivalve: fluorescence tracing of organ accumulation, oxidative stress and damage. *J. Hazard Mater* 392, 122418. doi:10.1016/j.jhazmat.2020.122418

Lim, D., Jeong, J., Song, K. S., Sung, J. H., Oh, S. M., and Choi, J. (2021). Inhalation toxicity of polystyrene micro(nano)plastics using modified OECD TG 412. *Chemosphere* 262, 128330. doi:10.1016/j.chemosphere.2020.128330

Liu, Z., Cai, M., Wu, D., Yu, P., Jiao, Y., Jiang, Q., et al. (2020). Effects of nanoplastics at predicted environmental concentration on *Daphnia pulex* after exposure through multiple generations. *Environ. Pollut.* 256, 113506. doi:10.1016/j.envpol.2019.113506

Liu, Z., Li, Y., Pérez, E., Jiang, Q., Chen, Q., Jiao, Y., et al. (2021). Polystyrene nanoplastic induces oxidative stress, immune defense, and glycometabolism change in *Daphnia pulex*: application of transcriptome profiling in risk assessment of nanoplastics. *J. Hazard Mat.* 402, 123778. doi:10.1016/j.jhazmat.2020.123778

Liu, Z., Yu, P., Cai, M., Wu, D., Zhang, M., Huang, Y., et al. (2019). Polystyrene nanoplastic exposure induces immobilization, reproduction, and stress defense in the freshwater cladoceran *Daphnia pulex*. *Chemosphere* 215, 74–81. doi:10.1016/j.chemosphere.2018.09.176

Lu, L., Wan, Z., Luo, T., Fu, Z., and Jin, Y. (2018). Polystyrene microplastics induce gut microbiota dysbiosis and hepatic lipid metabolism disorder in mice. *Sci. Total Environ.* 631-632, 449–458. doi:10.1016/j.scitotenv.2018.03.051

Lu, Y. Y., Li, H., Ren, H., Zhang, X., Huang, F., Zhang, D., et al. (2022). Size-dependent effects of polystyrene nanoplastics on autophagy response in human umbilical vein endothelial cells. *J. Hazard Mater* 421, 126770. doi:10.1016/j.jhazmat.2021.126770

Luo, T., Zhang, Y., Wang, C., Wang, X., Zhou, J., Shen, M., et al. (2019). Maternal exposure to different sizes of polystyrene microplastics during gestation causes metabolic disorders in their offspring. *Environ. Pollut.* 255, 113122. doi:10.1016/j.envpol.2019.113122

Mao, Y., Li, H., Huangfu, X., Liu, Y., and He, Q. (2020). Nanoplastics display strong stability in aqueous environments: insights from aggregation behaviour and theoretical calculations. *Environ. Pollut.* 258, 113760. doi:10.1016/j.envpol.2019.113760

Mattsson, K., Johnson, E. V., Malmendal, A., Linse, S., Hansson, L. A., and Cedervall, T. (2017). Brain damage and behavioural disorders in fish induced by plastic nanoparticles delivered through the food chain. *Sci. Rep.* 7 (1), 11452–11457. doi:10.1038/s41598-017-10813-0

Meng, X., Zhang, J., Wang, W., Gonzalez-Gil, G., Vrouwenvelder, J. S., and Li, Z. (2022). Effects of nano- and microplastics on kidney: physicochemical properties, bioaccumulation, oxidative stress and immunoreaction. *Chemosphere* 288, 132631. doi:10.1016/j.chemosphere.2021.132631

Miao, L., Hou, J., You, G., Liu, Z., Liu, S., Li, T., et al. (2019). Acute effects of nanoplastics and microplastics on periphytic biofilms depending on particle size, concentration and surface modification. *Environ. Pollut.* 255, 113300. doi:10.1016/j.envpol.2019.113300

Mongil-Manso, J., Jiménez-Ballesta, R., Trujillo-González, J. M., San José Wery, A., and Díez Méndez, A. (2023). A comprehensive review of plastics in agricultural soils: a case study of castilla y león (Spain) farmlands. *Land* 12, 1888. doi:10.3390/land12101888

Naz, S., Chatha, A., Ullah, Q., Maqbool, B., Iqbal, S., Khan, A., et al. (2023a). Impact of chronic exposure to heavy metal mixtures on selected biological parameters of freshwater fish species. *J. Anim. Plant Sci.* 33, 2023. doi:10.36899/JAPS.2023.6.0677

Naz, S., Chatha, A. M. M., Téllez-Isaías, G., Ullah, S., Ullah, Q., Khan, M. Z., et al. (2023b). A comprehensive review on metallic trace elements toxicity in fishes and potential remedial measures. *Water* 15 (16), 3017. doi:10.3390/w15163017

Naz, S., Hussain, R., Ullah, Q., Chatha, A. M. M., Shaheen, A., and Khan, R. U. (2021). Toxic effect of some heavy metals on hematology and histopathology of major carp (catla catla). *Environ. Sci. Pollut. Res.* 28, 6533–6539. doi:10.1007/s11356-020-10980-0

Naz, S., Mansouri, B., Chatha, A. M. M., Ullah, Q., Abadeen, Z. U., Khan, M. Z., et al. (2022). Water quality and health risk assessment of trace elements in surface water at punjnad headworks, Punjab, Pakistan. *Environ. Sci. Pollut. Res.* 29 (40), 61457–61469. doi:10.1007/s11356-022-20210-4

Neves, R. A. F., Guimarães, T. B., and Santos, L. N. (2024). First record of microplastic contamination in the non-native dark false mussel mytilopsis leucophaeata (Bivalvia: Dreissenidae) in a coastal urban lagoon. *Int. J. Environ. Res. Public Health* 21, 44. doi:10.3390/ijerph21010044

Nielsen, T. D., Hasselbalch, J., Holmberg, K., and Stripple, J. (2020). Politics and the plastic crisis: a review throughout the plastic life cycle. *Wiley Interdiscip. Rev. Energy Environ.* 9 (1), e360. doi:10.1002/wene.360

Oliveira, M., Almeida, M., and Miguel, I. A. (2019). A micro (nano) plastic boomerang tale: a never ending story? *Trac. Trends Anal. Chem.* 112, 196–200. doi:10.1016/j.trac.2019.01.005

Park, E. J., Han, J. S., Park, E. J., Seong, E., Lee, G. H., Kim, D. W., et al. (2020). Repeated-oral dose toxicity of polyethylene microplastics and the possible implications on reproduction and development of the next generation. *Toxicol. Lett.* 324, 75–85. doi:10.1016/j.toxlet.2020.01.008

Paul, M. B., Stock, V., Cara-Carmona, J., Lisicki, E., Shopova, S., Fessard, V., et al. (2020). Micro-and nanoplastics–current state of knowledge with the focus on oral uptake and toxicity. *Nanoscale Adv.* 2 (10), 4350–4367. doi:10.1039/d0na00539h

Peixoto, D., Pinheiro, C., Amorim, J., Oliva-Teles, L., Guilhermino, L., and Vieira, M. N. (2019). Microplastic pollution in commercial salt for human consumption: a review. *Estuar. Coast Shelf Sci.* 219, 161–168. doi:10.1016/j.ecss.2019.02.018

Peller, J. R., Tabor, G., Davis, C., Iceman, C., Nwachukwu, O., Doudrick, K., et al. (2024). Distribution and fate of polyethylene microplastics released by a portable toilet manufacturer into a freshwater wetland and lake. *Water* 16, 11. doi:10.3390/w16010011

Peng, L., Fu, D., Qi, H., Lan, C. Q., Yu, H., and Ge, C. (2020). Micro- and nano-plastics in marine environment: source, distribution and threats- A review. *Sci. Total Environ.* 698, 134254. doi:10.1016/j.scitotenv.2019.134254

Pizzurro, F., Nerone, E., Ancora, M., Di Domenico, M., Mincarelli, L. F., Cammà, C., et al. (2024). Exposure of *Mytilus galloprovincialis* to microplastics: accumulation, depuration and evaluation of the expression levels of a selection of molecular biomarkers. *Animals* 14, 4. doi:10.3390/ani14010004

Prata, J. C., da Costa, J. P., Duarte, A. C., and Rocha-Santos, T. (2019). Methods for sampling and detection of microplastics in water and sediment: a critical review. *Trac. Trends Anal. Chem.* 110, 150–159. doi:10.1016/j.trac.2018.10.029

Qiao, R., Deng, Y., Zhang, S., Wolosker, M. B., Zhu, Q., Ren, H., et al. (2019a). Accumulation of different shapes of microplastics initiates intestinal injury and gut microbiota dysbiosis in the gut of zebrafish. *Chemosphere* 236, 124334. doi:10.1016/j.chemosphere.2019.07.065

Qiao, R., Sheng, C., Lu, Y., Zhang, Y., Ren, H., and Lemos, B. (2019b). Microplastics induce intestinal inflammation, oxidative stress, and disorders of metabolome and microbiome in zebrafish. *Sci. Total Environ.* 662, 246–253. doi:10.1016/j.scitotenv.2019.01.245

Rafiee, M., Dargahi, L., Eslami, A., Beirami, E., Jahangiri-Rad, M., Sabour, S., et al. (2018). Neurobehavioral assessment of rats exposed to pristine polystyrene nanoplastics upon oral exposure. *Chemosphere* 193, 745–753. doi:10.1016/j.chemosphere.2017.11.076

Rashed, A. H., Yesilay, G., Hazeem, L., Rashdan, S., Almealla, R., Kilinc, Z., et al. (2023). Micro- and nano-plastics contaminants in the environment: sources, fate, toxicity, detection, remediation, and sustainable perspectives. *Water* 15, 3535. doi:10.3390/w15203535

Rubio, L., Barguilla, I., Domenech, J., Marcos, R., and Hernández, A. (2020). Biological effects, including oxidative stress and genotoxic damage, of polystyrene nanoparticles in different human hematopoietic cell lines. *J. Hazard Mater* 398, 122900. doi:10.1016/j.jhazmat.2020.122900

Sallam, M. A., Zubair, M., Gul, S. T., Ullah, Q., and Idrees, M. (2020). Evaluating the protective effects of vitamin E and selenium on hematology and liver, lung and uterus histopathology of rabbits with cypermethrin toxicity. *Toxin Rev.* 39 (3), 236–241. doi:10.1080/15569543.2018.1518335

Salvati, A., Åberg, C., Dos Santos, T., Varela, J., Pinto, P., Lynch, I., et al. (2011). Experimental and theoretical comparison of intracellular import of polymeric nanoparticles and small molecules: toward models of uptake kinetics. *Nanomedicine* 7, 818–826. doi:10.1016/j.nano.2011.03.005

Sarasamma, S., Audira, G., Siregar, P., Malhotra, N., Lai, Y. H., Liang, S. T., et al. (2020). Nanoplastics cause neurobehavioral impairments, reproductive and oxidative damages, and biomarker responses in zebrafish: throwing up alarms of wide spread health risk of exposure. *Int. J. Mol. Sci.* 21 (4), 1410. doi:10.3390/ijms21041410

Sendra, M., Sparaventi, E., Blasco, J., Moreno-Garrido, I., and Araujo, C. V. (2020). Ingestion and bioaccumulation of polystyrene nanoplastics and their effects on the microalgal feeding of Artemia franciscana. *Ecotoxicol. Environ. Saf.* 188, 109853. doi:10.1016/j.ecoenv.2019.109853

Sendra, M., Staffieri, E., Yeste, M. P., Moreno-Garrido, I., Gatica, J. M., Corsi, I., et al. (2019). Are the primary characteristics of polystyrene nanoplastics responsible for toxicity and ad/absorption in the marine diatom Phaeodactylum tricornutum? *Environ. Pollut.* 249, 610–619. doi:10.1016/j.envpol.2019.03.047

Shengchen, W., Jing, L., Yujie, Y., Yue, W., and Shiwon, X. (2021). Polystyrene microplastics-induced ROS overproduction disrupts the skeletal muscle regeneration by converting myoblasts into adipocytes. *J. Hazard Mater* 417, 125962. doi:10.1016/j.jhazmat.2021.125962

Shi, W., Han, Y., Sun, S., Tang, Y., Zhou, W., Du, X., et al. (2020). Immunotoxicities of microplastics and sertraline, alone and in combination, to a bivalve species: size-dependent interaction and potential toxication mechanism. *J. Hazard Mat.* 396, 122603. doi:10.1016/j.jhazmat.2020.122603

Sökmen, T. Ö., Sulukan, E., Türkoğlu, M., Baran, A., Özkaraca, M., and Ceyhun, S. B. (2020). Polystyrene nanoplastics (20 nm) are able to bioaccumulate and cause oxidative DNA damages in the brain tissue of zebrafish embryo (*Danio rerio*). *NeuroToxicology* 77, 51–59. doi:10.1016/j.neuro.2019.12.010

Stock, V., Böhmert, L., Lisicki, E., Block, R., Cara-Carmona, J., Pack, L. K., et al. (2019). Uptake and effects of orally ingested polystyrene microplastic particles *in vitro* and *in vivo*. *Arch. Toxicol.* 93 (7), 1817–1833. doi:10.1007/s00204-019-02478-7

Strungaru, S. A., Jijie, R., Nicoara, M., Plavan, G., and Faggio, C. (2019). Micro-(nano) plastics in freshwater ecosystems: abundance, toxicological impact and quantification methodology. *Trac. Trends Anal. Chem.* 110, 116–128. doi:10.1016/j.trac.2018.10.025

Sui, A., Yao, C., Chen, Y., Li, Y., Yu, S., Qu, J., et al. (2023). Polystyrene nanoplastics inhibit StAR expression by activating HIF-1α via ERK1/2 MAPK and AKT pathways in TM3 Leydig cells and testicular tissues of mice. *Food Chem. Toxicol.* 173, 113634. doi:10.1016/j.fct.2023.113634

Sun, Z., Wen, Y., Zhang, F., Fu, Z., Yuan, Y., Kuang, H., et al. (2023). Exposure to nanoplastics induces mitochondrial impairment and cytomembrane destruction in Leydig cells. *Ecotoxicol. Environ. Saf.* 255, 114796. doi:10.1016/j.ecoenv.2023.114796

Thiagarajan, V., Alex, S. A., Seenivasan, R., Chandrasekaran, N., and Mukherjee, A. (2021). Interactive effects of micro/nanoplastics and nanomaterials/pharmaceuticals: their ecotoxicological consequences in the aquatic systems. *Aquat. Toxicol.* 232, 105747. doi:10.1016/j.aquatox.2021.105747

Triebskorn, R., Braunbeck, T., Grummt, T., Hanslik, L., Huppertsberg, S., Jekel, M., et al. (2019). Relevance of nano- and microplastics for freshwater ecosystems: a critical review. *Trac. Trends Anal. Chem.* 110, 375–392. doi:10.1016/j.trac.2018.11.023

Vaid, M., Sarma, K., and Gupta, A. (2021). Microplastic pollution in aquatic environments with special emphasis on riverine systems: current understanding and way forward. *J. Environ. Manage.* 293, 112860. doi:10.1016/j.jenvman.2021.112860

Varela, J. A., Bexiga, M. G., Åberg, C., Simpson, J. C., and Dawson, K. A. (2012). Quantifying size-dependent interactions between fluorescently labeled polystyrene nanoparticles and mammalian cells. *J. Nanobiotechnol* 10, 39. doi:10.1186/1477-3155-10-39

Vedolin, M. C., Teophilo, C. Y. S., Turra, A., and Figueira, R. C. L. (2018). Spatial variability in the concentrations of metals in beached microplastics. *Mar. Pollut. Bull.* 129 (2), 487–493. doi:10.1016/j.marpolbul.2017.10.019

Vega-Herrera, A., Llorca, M., Borrell-Diaz, X., Redondo-Hasselerharm, P. E., Abad, E., Villanueva, C. M., et al. (2022). Polymers of micro(nano) plastic in household tap water of the Barcelona Metropolitan Area. *Water Res.* 220, 118645. doi:10.1016/j.watres.2022.118645

Venâncio, C., Ferreira, I., Martins, M. A., Soares, A. M., Lopes, I., and Oliveira, M. (2019). The effects of nanoplastics on marine plankton: a case study with polymethylmethacrylate. *Ecotoxicol. Environ. Saf.* 184, 109632. doi:10.1016/j.ecoenv.2019.109632

Venancio, C., Savuca, A., Oliveira, M., Martins, M. A., and Lopes, I. (2021). Polymethylmethacrylate nanoplastics effects on the freshwater cnidarian *Hydra viridissima*. *J. Hazard Mat.* 402, 123773. doi:10.1016/j.jhazmat.2020.123773

Walczak, A. P., Kramer, E., Hendriksen, P. J. M., Tromp, P., Helsper, J. P. F., van der Zande, M., et al. (2015). Translocation of differently sized and charged polystyrene nanoparticles in *in vitro* intestinal cell models of increasing complexity. *Nanotoxicology* 9, 453–461. doi:10.3109/17435390.2014.944599

Wang, F., Wang, B., Qu, H., Zhao, W., Duan, L., Zhang, Y., et al. (2020a). The influence of nanoplastics on the toxic effects, bioaccumulation, biodegradation and enantioselectivity of ibuprofen in freshwater algae chlorella pyrenoidosa. *Environ. Pollut.* 263, 114593. doi:10.1016/j.envpol.2020.114593

Wang, T., Zou, X., Li, B., Yao, Y., Li, J., Hui, H., et al. (2018). Microplastics in a wind farm area: a case study at the rudong offshore wind farm, yellow sea, China. *Mar. Pollut. Bull.* 128, 466–474. doi:10.1016/j.marpolbul.2018.01.050

Wang, W., Ge, J., and Yu, X. (2020b). Bioavailability and toxicity of microplastics to fish species: a review. *Ecotoxicol. Environ. Saf.* 189, 109913. doi:10.1016/j.ecoenv.2019.109913

Wang, Y., Mao, Z., Zhang, M., Ding, G., Sun, J., Du, M., et al. (2019). The uptake and elimination of polystyrene microplastics by the brine shrimp, Artemia parthenogenetica, and its impact on its feeding behavior and intestinal histology. *Chemosphere* 234, 123–131. doi:10.1016/j.chemosphere.2019.05.267

Wu, J., Jiang, R., Lin, W., and Ouyang, G. (2019). Effect of salinity and humic acid on the aggregation and toxicity of polystyrene nanoplastics with different functional groups and charges. *Environ. Pollut.* 245, 836–843. doi:10.1016/j.envpol.2018.11.055

Xia, T., Kovochich, M., Liong, M., Zink, J. I., and Nel, A. E. (2008). Cationic polystyrene nanosphere toxicity depends on cell-specific endocytic and mitochondrial injury pathways. *ACS Nano* 2, 85–96. doi:10.1021/nn700256c

Xie, X., Deng, T., Duan, J., Xie, J., Yuan, J., and Chen, M. (2020). Exposure to polystyrene microplastics causes reproductive toxicity through oxidative stress and activation of the p38 MAPK signaling pathway. *Ecotoxicol. Environ. Saf.* 190, 110133. doi:10.1016/j.ecoenv.2019.110133

Yang, Y. F., Chen, C. Y., Lu, T. H., and Liao, C. M. (2019). Toxicity-based toxicokinetic/toxicodynamic assessment for bioaccumulation of polystyrene microplastics in mice. *J. Hazard Mater* 366, 703–713. doi:10.1016/j.jhazmat.2018.12.048

Yee, M. S. L., Hii, L. W., Looi, C. K., Lim, W. M., Wong, S. F., Kok, Y. Y., et al. (2021). Impact of microplastics and nanoplastics on human health. *Nanomaterials* 11 (2), 496. doi:10.3390/nano11020496

Yin, L., Liu, H., Cui, H., Chen, B., Li, L., and Wu, F. (2019). Impacts of polystyrene microplastics on the behavior and metabolism in a marine demersal teleost, black rockfish (Sebastes schlegelii). *J. Hazard. Mat.* 380, 120861. doi:10.1016/j.jhazmat.2019.120861

Yu, F., Yang, C., Zhu, Z., Bai, X., and Ma, J. (2019). Adsorption behavior of organic pollutants and metals on micro/nanoplastics in the aquatic environment. *Sci. Total Environ.* 694, 133643. doi:10.1016/j.scitotenv.2019.133643

Zagorski, J., Debelak, J., Gellar, M., Watts, J. A., and Kline, J. A. (2003). Chemokines accumulate in the lungs of rats with severe pulmonary embolism induced by polystyrene microspheres. *J. Immunol.* 171 (10), 5529–5536. doi:10.4049/jimmunol.171.10.5529

Zalasiewicz, J., Waters, C. N., Ivar do Sul, J. A., Corcoran, P. L., Barnosky, A. D., Cearreta, A., et al. (2016). The geological cycle of plastics and their use as a stratigraphic indicator of the Anthropocene. *Anthropocene* 13, 4–17. doi:10.1016/j.ancene.2016.01.002

Zhang, F., Wang, Z., Song, L., Fang, H., and Wang, D. G. (2020a). Aquatic toxicity of iron-oxide-doped microplastics to Chlorella pyrenoidosa and Daphnia magna. *Environ. Pollut.* 257, 113451. doi:10.1016/j.envpol.2019.113451

Zhang, F., Wang, Z., Wang, S., Fang, H., and Wang, D. (2019). Aquatic behavior and toxicity of polystyrene nanoplastic particles with different functional groups: complex roles of pH, dissolved organic carbon and divalent cations. *Chemosphere* 228, 195–203. doi:10.1016/j.chemosphere.2019.04.115

Zhang, Y., Pu, S., Lv, X., Gao, Y., and Ge, L. (2020). Global trends and prospects in microplastics research: a bibliometric analysis. *J. Hazard. Mat.* 400, 123110. doi:10.1016/j.jhazmat.2020.123110

Zheng, H., Wang, J., Wei, X., Chang, L., and Liu, S. (2021). Proinflammatory properties and lipid disturbance of polystyrene microplastics in the livers of mice with acute colitis. *Sci. Total Environ.* 750, 143085. doi:10.1016/j.scitotenv.2020.143085

Zhou, X. X., Liu, R., Hao, L. T., and Liu, J. F. (2021). Identification of polystyrene nanoplastics using surface enhanced Raman spectroscopy. *Talanta* 221, 121552. doi:10.1016/j.talanta.2020.121552

Zhu, X., Zhao, W., Chen, X., Zhao, T., Tan, L., and Wang, J. (2020). Growth inhibition of the microalgae Skeletonema costatum under copper nanoparticles with microplastic exposure. *Mar. Environ. Res.* 158, 105005. doi:10.1016/j.marenvres.2020.105005

Zhu, Z. L., Wang, S. C., Zhao, F. F., Wang, S. G., Liu, F. F., and Liu, G. Z. (2019). Joint toxicity of microplastics with triclosan to marine microalgae Skeletonema costatum. *Environ. Pollut.* 246, 509–517. doi:10.1016/j.envpol.2018.12.044

Zitouni, N., Bousserrhine, N., Belbekhouche, S., Missawi, O., Alphonse, V., Boughatass, I., et al. (2020). First report on the presence of small microplastics (≤3 μm) in tissue of the commercial fish Serranus scriba (Linnaeus, 1758) from Tunisian Coasts and associated cellular alterations. *Environ. Pollut.* 263, 114576. doi:10.1016/j.envpol.2020.114576

Zubair, M., Ahmad, M., Saleemi, M. K., Gul, S. T., Ahmad, M., Martyniuk, C. J., et al. (2020). Sodium arsenite toxicity on hematology indices and reproductive parameters in teddy goat bucks and their amelioration with vitamin C. *Environ. Sci. Pollut. Res.* 27, 15223–15232. doi:10.1007/s11356-020-08049-z

frontiers | Frontiers in Environmental Science

TYPE Data Report
PUBLISHED 28 May 2024
DOI 10.3389/fenvs.2024.1390323

Check for updates

OPEN ACCESS

EDITED BY
Visva Bharati Barua,
University of North Carolina at Charlotte, United States

REVIEWED BY
Yabing Li,
Michigan State University, United States
Ranjith Kumar Rajendran,
University of New South Wales, Australia

*CORRESPONDENCE
Mary Ann Cielo V. Relucio-San Diego,
mrsandiego@up.edu.ph

RECEIVED 23 February 2024
ACCEPTED 13 May 2024
PUBLISHED 28 May 2024

CITATION
Relucio-San Diego MACV, Gloria PCT and Obusan MCM (2024), 16S metabarcoding of the bacterial community of a poultry wastewater treatment plant in the Philippines.
Front. Environ. Sci. 12:1390323.
doi: 10.3389/fenvs.2024.1390323

COPYRIGHT
© 2024 Relucio-San Diego, Gloria and Obusan. This is an open-access article distributed under the terms of the Creative Commons Attribution License (CC BY). The use, distribution or reproduction in other forums is permitted, provided the original author(s) and the copyright owner(s) are credited and that the original publication in this journal is cited, in accordance with accepted academic practice. No use, distribution or reproduction is permitted which does not comply with these terms.

16S metabarcoding of the bacterial community of a poultry wastewater treatment plant in the Philippines

Mary Ann Cielo V. Relucio-San Diego[1,2]*, Paul Christian T. Gloria[1] and Marie Christine M. Obusan[2]

[1]Microbiological Research and Services Laboratory, Natural Sciences Research Institute, College of Science, University of the Philippines, Quezon City, Philippines, [2]Microbial Ecology of Terrestrial and Aquatic Systems Laboratory, Institute of Biology, College of Science, University of the Philippines, Quezon City, Philippines

KEYWORDS

metabarcoding, bacteria, wastewater, poultry, treatment

Introduction

Wastewaters are loaded with many types of microorganisms but are predominantly composed of bacteria with different roles in the water treatment system (Kumar et al., 2022). Some belong to functional genera, which are mainly responsible for the removal of pollutants in wastewater while others are potentially pathogenic bacteria, which can pose threats to public health and the environment (Fan et al., 2018). The functional bacterial groups reported to be found in wastewater treatment plants (WWTPs) include ammonia-oxidizing bacteria (AOB), nitrite-oxidizing bacteria (NOB), polyphosphate-accumulating organisms (PAOs), glycogen-accumulating organisms (GAOs), acetogens, methanogens, and sulfur-reducing bacteria (Gallert and Winter, 2005; López-Vazquez et al., 2007; Dueholm et al., 2022). These types of bacteria are very favorable for plant operations because of their high pollutant removal rates, hence, ensuring their maintenance and sustainability in the systems is critical for the continuous efficacy of wastewater treatment operations (Gude, 2015). WWTPs are also known reservoirs of pathogenic microorganisms (Azli et al., 2022). Current microbial monitoring for contamination is limited to a few indicators such as coliforms, *Salmonella* sp., *Shigella* sp., *Vibrio* sp., *Legionella* sp., and fecal streptococci and enterococci (Naidoo and Olaniran, 2014; Garrido-Cardenas et al., 2017). However, the microbial indicators may mask the concentration of pathogens due to their lower concentration than the microbial indicators, hence a more sensitive approach is needed for pathogen detection (Zhang et al., 2021). Understanding the composition of bacterial communities is thus crucial in providing the basis for optimizing treatment conditions favoring the functional bacteria and detecting the presence of pathogenic bacteria. With the advent of new sequencing technologies, 16S metabarcoding may be utilized to explore and characterize wastewater microbiomes without the need for conventional culture methods. For these reasons, we sought to profile the bacterial communities in a poultry WWTP to serve as reference and baseline information on potentially functional and pathogenic bacteria present in wastewater, and to infer possible implications to wastewater treatment and management.

Here, we report data on the taxonomic composition of four treatment stages, i.e., Influent Tank, two aeration tanks where activated sludges were used (Aeration Tank 3 and Aeration Tank 1), and the Effluent flow, in a poultry wastewater treatment plant. The metabarcoding data offer insights into the bacterial diversity through ecological

indices and may be used for further analyses relevant to the role of bacteria in wastewater treatment.

Methods

Sample collection, processing, and sequencing

The samples were collected from a poultry dressing plant with a wastewater treatment facility in Cavite, Region IV-A, Philippines on 1 August 2022. Short interviews were conducted with the plant engineers to determine the operation protocols of the plant. The following consequent sampling points were chosen: (1) Influent Tank, where raw wastewater from the dressing plant was kept before entering the treatment system, (2) Aeration Tank 3, where the raw wastewater entered the system and where activated sludge was used, (3) Aeration Tank 1, where activated sludge was also used after treatment in the anaerobic digester, and the (4) Effluent, where it was free-flowing towards the nearest creek.

Triplicate 1L samples were collected using properly labeled sterile bottles at four sampling areas: Influent Tank, Aeration Tank 3, Aeration Tank 1, and Effluent flow. For the Influent Tank, only the top portion of the tank was collected due to the limitations of the sampler and the small opening of the tank. For the Aeration Tanks, the sampling protocol of the Global Water Microbiome Consortium (GWMC) was followed with modifications (Wu et al., 2019), wherein the sampling points depended only on the accessible areas of the tanks instead of having three different positions per zone. Hence, only one sampling point at a time was accessed with a time interval of 10 min per sampling. For the Effluent, since this was free-flowing, the samples were collected directly from the effluent water.

The twelve samples collected were immediately processed for sub-sampling. Approximately 300 mg of sludge/precipitate was collected from each sampling container and transferred into 1.5 mL cryovials. Triplicate samples from each treatment stage were processed. DNA was extracted following the manufacturer's protocol using Qiagen DNeasy PowerSoil Pro (QIAGEN, United States). DNA concentration was measured using a Denovix DS-11 fluorometer (Denovix, United States) and samples that met sequencing standards were sent to Macrogen, South Korea for 16S V1-V3 metabarcoding employing 27F (5′-AGAGTTTGATCCTGGCTCAG-3′) and 534R (5′-ATTACCGCGGCTGCTGG-3′) primers (Dueholm et al., 2022). The sequencing platform used was an Illumina MiSeq platform, 2 × 300 bp, 100,000 reads per sample, using Nextera XT-prepared libraries. Raw reads were deposited in the National Center for Biotechnology Information (NCBI) Short Read Archive (SRA) (Supplementary Table S1).

Bioinformatics analysis

An end-to-end workflow for 16S metabarcoding was employed using QIIME2-2022.8 (Hall and Beiko, 2018). Raw reads were quality-checked, primer trimmed at 0% error rate, and merged using 70 as the optimal --p-minovlen parameter. All merged reads were quality-filtered at Phred 30, dereplicated, and clustered at 97% using an open reference OTU picking technique through VSEARCH (Rognes et al., 2016). Subsequently, singletons and chimeras were removed before taxonomy assignment using a Naive-Bayes trained classifier from SILVA 138-99 (Quast et al., 2012). The resulting taxonomy assignments were filtered to retain only bacterial sequences. Samples were rarefied to a depth of 8,900 features and subsequently, ecological indices along with statistical comparisons were done through the QIIME2 --diversity plugin. The taxonomy bar plot showing relative frequency was generated in R (R Core Team, 2021) using the package ggplot2 (Wickham, 2016) while other figures were directly lifted from QIIME2-generated tools.

Results and discussion

Resulting raw reads for all samples yielded a total of 1029761 sequences which was reduced to 806085 after primer trimming. Merging at a minimum overlap length of 70bp yielded 513586 merged reads and subsequent quality trimming at Q30, dereplication, and open-reference-based OTU clustering at 97% using SILVA 138-99 produced 306092 features. Filtering of features to include only bacterial sequences yielded 180324 features. Figure 1 shows the taxonomy bar plots of bacterial sequences present in each sample and treatment stage.

Effluent samples are dominated by *Delftia* sp. which comprises approximately 40% of each replicate. This genus has displayed remarkable biotechnological potential in wastewater applications. *Delftia tsuruhatensis* SDU2 showed excellent ammonium removal in high-strength nitrogen wastewater (Chen et al., 2023). Other studies demonstrated the ability of *Delftia* to metabolize organic pollutants (Custodio et al., 2022), inhibit biofilm formation in sludge through quorum quenching (Xu et al., 2023), and assimilate terephthalate from sludge (Shigematsu et al., 2003). *Flavobacterium* sp. is the next dominant member, with a relative frequency of 4.093%–7.283%. Other bacterial community members with a relative frequency of more than 1% are as follows: unclassified and uncultured bacteria (3.224%–4.497%), a bacterium under family *Comamonadaceae* (2.735%–5.153%), a bacterium under family *Rhodocyclaceae* (1.186%–1.938%), a bacterium under order Burkholderiales (1.832%–2.655%), a bacterium under order Rhizobiales (1.195%–1.389%), a bacterium under order Campylobacterales (2.126%–9.594%), a bacterium under family *Arcobacteraceae* (1.730%–3.234%), and an uncultured *Tepidibacter* sp. (1.616%–2.050%).

Influent samples show a high frequency of family *Comamonadaceae*, family *Arcobacteriaceae* members, and *Aquaspirillum* uncultured bacterium with relative frequency ranges of 7.247%–19.041%, 6.547%–7.799%, and 4.777%–10.197%, respectively. Family *Comamonadaceae* members were previously reported in influent raw wastewater samples collected from Canadian Arctic ponds (Huang et al., 2021). However, their role in other stages such as in activated sludge is more documented (Sadaie et al., 2007; Ge et al., 2015). Ge et al. (2015) have reported a novel PAO clade *Comamonadaceae* as integral in the removal of biological phosphorus from abattoir wastewater while its domination in sludge microbiome was seen as a result of sludge reduction due to reduced oxygen supply in a food-processing

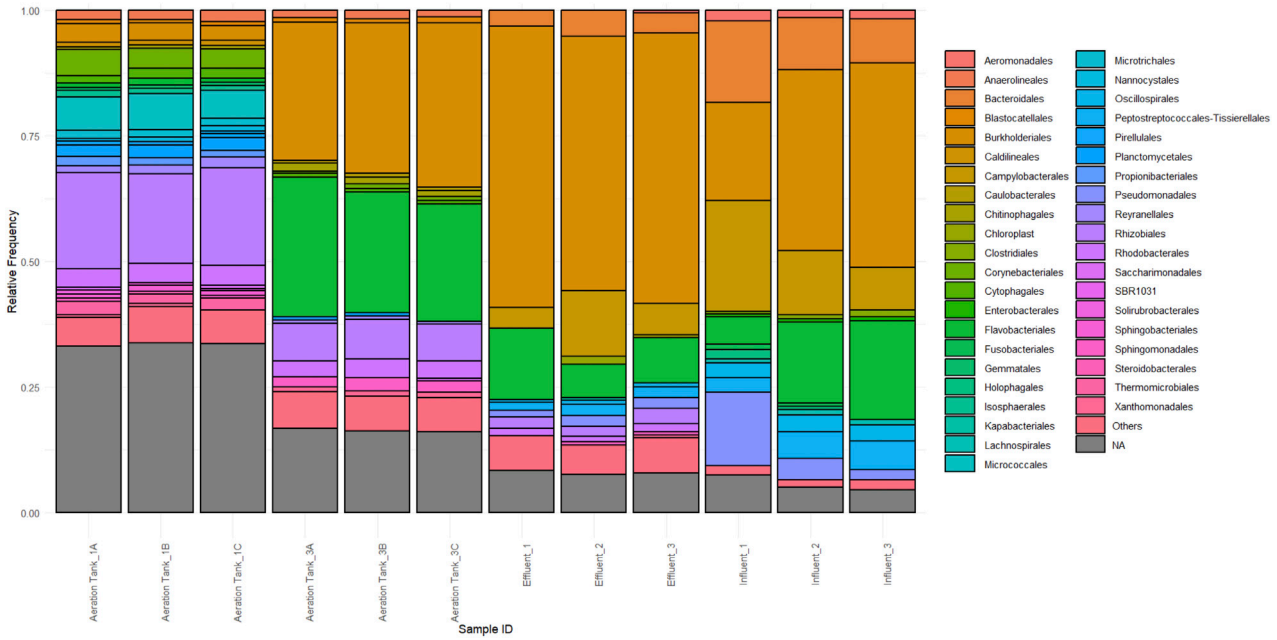

FIGURE 1
Taxonomy bar plot at the order level of triplicated wastewater samples at various treatment stages.

wastewater treatment plant (Sadaie et al., 2007). Family *Arcobacteriaceae* was found to be the dominant influent and "clean" effluent microbiome member in 14 Danish wastewater treatment plants (Kristensen et al., 2020). In addition, *Arcobacter* species have been isolated and characterized to harbor various multi-antibiotic resistance genes and phenotypes from poultry in Ghana and Tunisia (Jribi et al., 2020; Zautner et al., 2023). Thus, it is not surprising that this was also dominant in our Influent samples. Lastly, *Aquaspirilum* has been consistently found to be a major denitrifier in various reactors in WWTPs in Korea (Lee et al., 2008).

Some highly abundant members in the Effluent were also found in the Influent, namely, *Flavobacterium* sp. (1.956%–4.881%), a family *Rhodocyclaceae* member (1.179%–1.392%), an order Burkholderiales member (2.553%–3.306%), and an order Campylobacterales member (1.498%–14.929%). Other detected bacteria with high relative frequnecy are a class Bacteroidia member at 1.784%–3.634%, a family *Prevotellaceae* member at 2.200%–2.668%, a family *Weeksellaceae* member at 1.328%–2.842%, *Bacteroides luti* at 1.324%–1.616%, and *Aeromonas* E1-54 at 1.403%–1.997%.

Aeration Tank 3 samples are dominated by *Flavobacterium* sp. at 18.578%–19.575%, followed by the family *Rhodocyclaceae* at 12.960%–19.813%, and order Burkholderiales members at 7.266%–10.564%. *Flavobacterium* has been previously reported as an abundant member in wastewater effluent in springtime from a site in Korea (Chen et al., 2019); *Flavobacterium* has also been extensively documented in wastewater (Ryu et al., 2007; Fujii et al., 2014; Liu et al., 2017). *Rhodocyclaceae* is also a dominant member of wastewater microbiomes such as in poultry, cattle, and pigs WWTPs (Boukerb et al., 2021). In addition, they were pointed out as important denitrifiers in treatment plants as indicated by metagenomic and phylogenomic analyses (Wang et al., 2020). Order Burkholderiales, another dominant Aeration Tank 3 taxon, has been well documented in wastewater samples such as in the fermentation tank of a piggery WWTP (Shi et al., 2021), in a microbial fuel cell-treated wastewater input with high antibiotic load (Chen et al., 2022), and effluent input into riverine systems (Ruprecht et al., 2021). The following bacteria are detected in this treatment stage with their relative frequency ranges: the same unclassified and uncultured bacteria detected on the Effluent at 8.883%–9.320%, a family *Comamonadaceae* member at 2.961%–3.319%, a class Actinobacteria member at 1.459%–1.788%, an order Rhizobiales member at 4.394%–4.606%, a family *Rhizobiaceae* member at 1.235%–1.569%, *Flavobacterium cucumis* at 3.295%–7.102%, a family *Rhodobacteraceae* member at 1.981%–2.442%, a class Gammaproteobacteria member at 1.412%–1.774%, a class Alphaproteobacteria member at 1.119%–1.409%, and a family *Sphingomonadaceae* member at 1.995%–2.635%.

Lastly, Aeration Tank 1 samples show a high frequency of class Actinobacteria (12.824%–14.199%), the same uncultured bacteria seen on the Effluent and Aeration Tank 3 (8.835%–10.582%), an order Rhizobiales member (8.285%–8.680%), a family *Rhizobiaceae* member (5.472%–6.126%), and *Lapilicoccus* sp. (5.260%–6.918%). A family *Comamonadaceae* member (1.384%–1.892%), a class Bacteroidia member (1.286%–1.663%), a family *Rhodobacteraceae* member (1.648%–1.857%), a class Gammaproteobacteria member (2.081%–2.140%), a class Planctomycetes member (3.068%–3.358%), a class Alphaproteobacteria member (1.491%–1.589%), *Mycobacterium* sp. (2.215%–3.132%), *Gemmobacter* sp. (1.157%–1.715%), *Reyranella* sp. (1.350%–2.197%), an order Thermomicrobiales member (1.851%–2.691%), a family Rhizobiales *incertae sedis* member (1.468%–1.857%), and an order Corynebacteriales member (1.301%–1.791%) were also present in this treatment stage. A class Actinobacteria member showed high predominance in Aeration Tank 1 microbiomes. Such

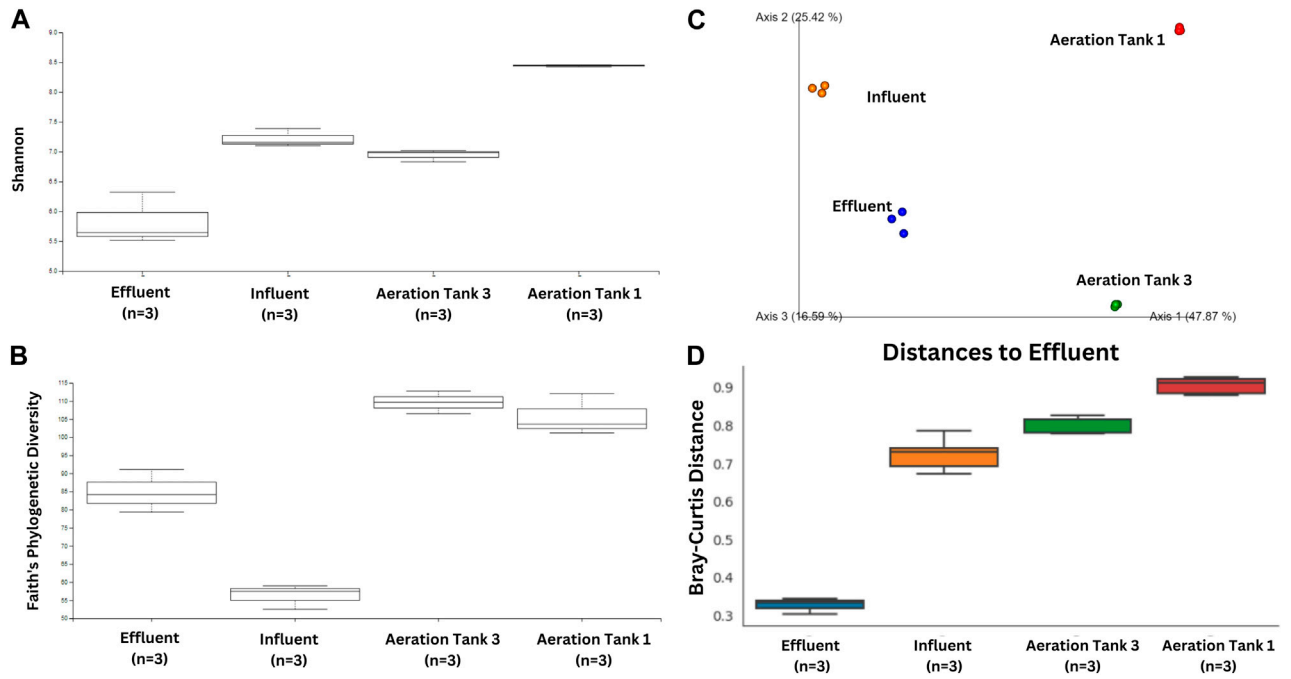

FIGURE 2
Ecological indices and microbiome composition comparisons. Box-and-whisker plots showing the alpha diversity indices of each wastewater treatment stage according to **(A)** Shannon's and **(B)** Faith's Phylogenetic Diversity **(C)** Principal Coordinates Analysis plot of the microbiome for each wastewater treatment stage. **(D)** PERMANOVA-subjected Box-and-whisker plot for Bray Curtis distances showing the beta diversity index of each treatment stage relative to the effluent bacterial community.

has been reported of high predominance in effluent microbiomes in a full-scale plant (Kaevska et al., 2016). Other studies show the potential of Actinobacterial members as bioflocculants that aid the treatment process (Agunbiade et al., 2016). Meanwhile, order Rhizobiales and class Rhizobiaceae members have increased in frequency in Aeration Tank 1 which is recapitulative of what is reported by Bia et al. (2021) where a switch of anoxic to oxic conditions permitted its sudden increase. Another group has also reported increased counts of Rhizobiales in activated sludge (Fredriksson et al., 2013). *Lapilicoccus* also showed high counts in this treatment stage. Interestingly, to our knowledge, there is no report of this genus in other wastewater microbiomes. To date, only two published studies are available: one which discusses its isolation from a botanical garden in Indonesia (Ratnakomala et al., 2016) and another that showed its presence in zinc-contaminated soil microbiome (Zaborowska et al., 2022).

In the case of the functional bacteria in WWTPs, their frequency in the wastewater treatment plant is quite low. *Nirosomonas* sp., a common NOB, is only present in Aeration Tank 3, with an average of 0.001%. Another bacterium, *Thauera* sp., which was reported to have denitrification and phosphorus removal capabilities (Ren et al., 2021), is more abundant in Aeration Tank 3, with an average relative frequency of 0.468%, than Aeration Tank 1 with an average relative frequency of 0.086%. A sulfate-reducing bacterium, *Ochrobactrum* sp. (Yang et al., 2021) was also detected in both Aeration Tanks 3 and 1 with mean relative frequencies of 0.260% and 0.215%, respectively. Two *Nitrospira* spp., which are AOB, were also detected on both Aeration Tanks with mean relative frequencies of 0.238% and 0.064% in Aeration Tank 3 and 0.051% and 0.115% in Aeration Tank 1. These may not reflect the true frequency of functional bacteria as there are many unidentified bacteria from the samples.

The use of metabarcoding for microbial monitoring revealed some pathogenic bacteria present in the poultry wastewater. Here, we report some of the potential pathogens found in the poultry wastewater treatment plant. *Mycobacterium* sp., a possible pathogen, has been detected in all treatment stages, with averages of 0.020%, 0.676%, 2.640%, and 0.157% in Influent, Aeration Tank 3, Aeration Tank 1, and Effluent, respectively. Another pathogen, *Aeromonas* sp., was also detected on the influent, with a relative frequency range of 1.403%–1.997%, in Aeration Tank 3 at 0.014%–0.034%, and in the Effluent at 0.151%–0.520%. *Bacteroides* spp. are clinically important pathogens where three different species, aside from *B. luti*, were detected in the Influent and Effluent with a total mean relative frequency of approximately 1.00% per sample. *Pseudomonas* sp., a ubiquitous and opportunistic pathogen, was present in all sites with the highest frequency in the Influent and the lowest at Aeration Tank 1. *Leptospira* sp. Was also detected with mean relative frequency of 0.040% in the Effluent and 0.094% in Aeration Tank 3.

The water flow in the treatment plant was as follows: Influent→ Aeration Tank 3 → Aeration Tank 1 → Effluent (Supplementary Figure S1). Aeration Tank 1 had the highest Shannon entropy values ranging from 8.42 to 8.45, which suggests the highest species diversity among all samples, while effluent had the lowest (Figure 2A). Also, Faith's Phylogenetic Diversity of bacterial composition increased along the treatment stage except for the Effluent where there was a decline in bacterial diversity relative to Aeration Tank 1 (Figure 2B).

As for bacterial composition, distinct bacterial communities across treatment stages suggested significant alterations in communities as they passed through different tanks (Figure 2C). This observation was corroborated by Bray-Curtis distances relative to Effluent's bacterial composition where a significant difference in beta diversity was observed. Shifts in each treatment stage's bacterial community were observed (Figure 2D). In a microbial ecosystem, stochastic and deterministic processes determine community assembly (Dottorini et al., 2021). In the case of WWTPs, bacterial communities are affected by the plant's capacity, which are composed of equipment capacity, volume of reactors, characteristics of the influent, sludge retention time, and hydraulic retention time (Kim et al., 2019). Hence, these processes may have contributed to the bacterial community shifts in the poultry WWTP system.

Conclusion

The bacterial community profiles of a poultry farm wastewater treatment plant in the Philippines showed that different bacteria dominated the different phases. In the Influent, the most prominent are members of the family *Comamonadaceae* and of family *Arcobacteriaceae*, and an uncultured *Aquaspirillum* bacterium while *Delftia* sp. and *Flavobacterium* sp. were dominant in the Effluent. Despite both having activated sludges, the bacterial composition of Aeration Tanks 3 and 1 were also different. For Aeration Tank 3, members of the family *Rhodocyclaceae* and order Burkholderiales, and *Flavobacterium* sp. had the highest frequencies while members of class Actinobacteria, order Rhizobiales, family *Rhizobiaceae,* and *Lapilicoccus* sp. were the highest for Aeration Tank 1. Common nitrifiers such as *Nitrosomonas* and *Nitrospira* were found at a low frequency. *Mycobacterium* sp., *Aeromonas* sp., *Bacteroides* spp., *Pseudomonas* sp., and *Leptospira* sp. were the potential pathogens detected in the system that may be disseminated in the environment. This will serve as baseline information on the microbial dimensions in poultry wastewater treatment plants and will allow other researchers to use it as a reference. The bacterial taxonomic information can guide the development of wastewater-related policies and guidelines for improved treatment processes and biotechnological explorations in the future.

Data availability statement

The datasets presented in this study can be found in online repositories. The names of the repository/repositories and accession number(s) can be found in the article/Supplementary Material.

Author contributions

MR-S: Conceptualization, Data curation, Formal Analysis, Funding acquisition, Investigation, Methodology, Project administration, Resources, Supervision, Writing–original draft, Writing–review and editing. PG: Data curation, Formal Analysis, Investigation, Methodology, Validation, Visualization, Writing–original draft, Writing–review and editing. MO: Conceptualization, Funding acquisition, Methodology, Resources, Supervision, Writing–review and editing.

Funding

The author(s) declare that financial support was received for the research, authorship, and/or publication of this article. This work was funded by the University of the Philippines System Enhanced Creative Work and Research Grant (ECRWG-2021-2-13R). The study also received partial funding from the Department of Science and Technology through "Project 2. Microbial Community Composition and Function for the Removal of Excess Nitrogen and Endocrine Disruptors in Wastewater Treatment," which is monitored by the Philippine Council for Industry, Energy and Emerging Technology Research and Development (PCIEERD).

Conflict of interest

The authors declare that the research was conducted in the absence of any commercial or financial relationships that could be construed as a potential conflict of interest.

Publisher's note

All claims expressed in this article are solely those of the authors and do not necessarily represent those of their affiliated organizations, or those of the publisher, the editors and the reviewers. Any product that may be evaluated in this article, or claim that may be made by its manufacturer, is not guaranteed or endorsed by the publisher.

Supplementary material

The Supplementary Material for this article can be found online at: https://www.frontiersin.org/articles/10.3389/fenvs.2024.1390323/full#supplementary-material

References

Agunbiade, M. O., Pohl, C. H., and Ashafa, A. O. (2016). A review of the application of biofloccualnts in wastewater treatment. *Pol. J. Environ. Stud.* 25 (4), 1381–1389. doi:10.15244/pjoes/61063

Azli, B., Razak, M. N., Omar, A. R., Mohd Zain, N. A., Abdul Razak, F., and Nurulfiza, I. (2022). Metagenomics insights into the microbial diversity and microbiome network analysis on the heterogeneity of influent to effluent water. *Front. Microbiol.* 13, 779196. doi:10.3389/fmicb.2022.779196

Bia, Y., Hanb, Z., Fengb, S., Wangb, X., Xud, Z., Zhange, Y., et al. (2021). Microbial community changes in a full-scale wastewater treatment system with a rotating biological contactor integrated into anaerobic-anoxic-oxic-oxic processes. *Desalination Water Treat.* 228, 165–175. doi:10.5004/dwt.2021.27346

Boukerb, A. M., Noël, C., Quenot, E., Cadiou, B., Chevé, J., Quintric, L., et al. (2021). Comparative analysis of fecal microbiomes from wild waterbirds to poultry, cattle, pigs, and wastewater treatment plants for a microbial source tracking approach. *Front. Microbiol.* 12, 697553. doi:10.3389/fmicb.2021.697553

Chen, J., Guo, J., Zhang, K., Wang, T., Luo, H., Chen, W., et al. (2022). Reduction and control of antibiotic-resistance genes and mobile genetic elements in tetracycline

livestock wastewater treated by microbial fuel cell. *J. Environ. Eng.* 148 (8), 04022039. doi:10.1061/(asce)ee.1943-7870.0002028

Chen, L. F., Chen, L. X., Pan, D., Ren, Y. L., Zhang, J., Zhou, B., et al. (2023). Ammonium removal characteristics of *Delftia tsuruhatensis* SDU2 with potential application in ammonium-rich wastewater treatment. *Int. J. Environ. Sci. Technol.* 20 (4), 3911–3926. doi:10.1007/s13762-022-04219-3

Chen, X., Lang, X. L., Xu, A. L., Song, Z. W., Yang, J., and Guo, M. Y. (2019). Seasonal variability in the microbial community and pathogens in wastewater final effluents. *Water* 11 (12), 2586. doi:10.3390/w11122586

Custodio, M., Peñaloza, R., Espinoza, C., Espinoza, W., and Mezarina, J. (2022). Treatment of dairy industry wastewater using bacterial biomass isolated from eutrophic lake sediments for the production of agricultural water. *Bioresour. Technol. Rep.* 17, 100891. doi:10.1016/j.biteb.2021.100891

Dottorini, G., Michaelsen, T. Y., Kucheryavskiy, S., Andersen, K. S., Kristensen, J. M., Peces, M., et al. (2021). Mass-immigration determines the assembly of activated sludge microbial communities. *Proc. Natl. Acad. Sci.* 118 (27), e2021589118. doi:10.1073/pnas.2021589118

Dueholm, M. K. D., Nierychlo, M., Andersen, K. S., Rudkjøbing, V., Knutsson, S., Albertsen, M., et al. (2022). MiDAS 4: a global catalogue of full-length 16S rRNA gene sequences and taxonomy for studies of bacterial communities in wastewater treatment plants. *Nat. Commun.* 13 (1), 1908. doi:10.1038/s41467-022-29438-7

Fan, X. Y., Gao, J. F., Pan, K. L., Li, D. C., Dai, H. H., and Li, X. (2018). Functional genera, potential pathogens and predicted antibiotic resistance genes in 16 full-scale wastewater treatment plants treating different types of wastewater. *Bioresour. Technol.* 268, 97–106. doi:10.1016/j.biortech.2018.07.118

Fredriksson, N. J., Hermansson, M., and Wilén, B. M. (2013). The choice of PCR primers has great impact on assessments of bacterial community diversity and dynamics in a wastewater treatment plant. *PloS one* 8 (10), e76431. doi:10.1371/journal.pone.0076431

Fujii, D., Nagai, F., Watanabe, Y., and Shirasawa, Y. (2014). *Flavobacterium longum* sp. nov. and *Flavobacterium urocaniciphilum* sp. nov., isolated from a wastewater treatment plant, and emended descriptions of *Flavobacterium caeni* and *Flavobacterium terrigena*. *Int. J. Syst. Evol. Microbiol.* 64 (Pt_5), 1488–1494. doi:10.1099/ijs.0.054312-0

Gallert, C., and Winter, J. (2005). "Bacterial metabolism in wastewater treatment systems," in *Environmental Biotechnology. Concepts and applications* (Hoboken, New Jersey, United States: Wiley).

Garrido-Cardenas, J. A., Polo-López, M. I., and Oller-Alberola, I. (2017). Advanced microbial analysis for wastewater quality monitoring: metagenomics trend. *Appl. Microbiol. Biotechnol.* 101, 7445–7458. doi:10.1007/s00253-017-8490-3

Ge, H., Batstone, D. J., and Keller, J. (2015). Biological phosphorus removal from abattoir wastewater at very short sludge ages mediated by novel PAO clade Comamonadaceae. *Water Res.* 69, 173–182. doi:10.1016/j.watres.2014.11.026

Gude, V. G. (2015). A new perspective on microbiome and resource management in wastewater systems. *J. Biotechnol. Biomater.* 5 (184), 2. doi:10.4172/2155-952x.1000184

Hall, M., and Beiko, R. G. (2018). 16S rRNA gene analysis with QIIME2. *Microbiome analysis methods Protoc.* 1849, 113–129. doi:10.1007/978-1-4939-8728-3_8

Huang, Y., Ragush, C. M., Johnston, L. H., Hall, M. W., Beiko, R. G., Jamieson, R. C., et al. (2021). Changes in bacterial communities during treatment of municipal wastewater in arctic wastewater stabilization ponds. *Front. Water* 3, 710853. doi:10.3389/frwa.2021.710853

Jribi, H., Sellami, H., Amor, S. B., Ducournau, A., Sifre, E., Benejat, L., et al. (2020). Occurrence and antibiotic resistance of arcobacter species isolates from poultry in Tunisia. *J. Food Prot.* 83 (12), 2080–2086. doi:10.4315/jfp-20-056

Kaevska, M., Videnska, P., and Vasickova, P. (2016). Changes in microbial composition of wastewater during treatment in a full-scale plant. *Curr. Microbiol.* 72, 128–132. doi:10.1007/s00284-015-0924-5

Kim, Y. K., Yoo, K., Kim, M. S., Han, I., Lee, M., Kang, B. R., et al. (2019). The capacity of wastewater treatment plants drives bacterial community structure and its assembly. *Sci. Rep.* 9 (1), 14809. doi:10.1038/s41598-019-50952-0

Kristensen, J. M., Nierychlo, M., Albertsen, M., and Nielsen, P. H. (2020). Bacteria from the genus Arcobacter are abundant in effluent from wastewater treatment plants. *Appl. Environ. Microbiol.* 86 (9), 030444-19–e3119. doi:10.1128/aem.03044-19

Kumar, A., Chalotra, T., Pathak, A. K., and Raina, N. (2022). Role of microbes in wastewater treatment and Energy generation potentials: a sustainable approach. *Microb. Biotechnol. Role Ecol. Sustain. Res.* 265–311. doi:10.1002/9781119834489.ch15

Lee, H. W., Park, Y. K., Choi, E. S., and Lee, J. W. (2008). Bacterial community and biological nitrate removal: comparisons of autotrophic and heterotrophic reactors for denitrification with raw sewage. *J. Microbiol. Biotechnol.* 18 (11), 1826–1835. doi:10.4014/jmb.0800.276

Liu, H., Lu, P., and Zhu, G. (2017). *Flavobacterium cloacae* sp. nov., isolated from waste water. *Int. J. Syst. Evol. Microbiol.* 67 (3), 659–663. doi:10.1099/ijsem.0.001684

López-Vasquez, C. M., Hooijmans, C. M., Brdjanovic, D., Gijzen, H. J., and van Loosdrecht, M. C. (2007). "A practical method for quantification of PAO and GAO populations in activated sludge systems," in *Nutrient removal and recovery symposium 2007* (St, Alexandria, VA, United States: Water Environment Federation), 39–63.

Naidoo, S., and Olaniran, A. O. (2014). Treated wastewater effluent as a source of microbial pollution of surface water resources. *Int. J. Environ. Res. Public Health* 11 (1), 249–270. doi:10.3390/ijerph110100249

Quast, C., Pruesse, E., Yilmaz, P., Gerken, J., Schweer, T., Yarza, P., et al. (2012). The SILVA ribosomal RNA gene database project: improved data processing and web-based tools. *Nucleic acids Res.* 41 (D1), D590–D596. doi:10.1093/nar/gks1219

Ratnakomala, S., Lisdiyanti, P., Prayitno, N. R., Triana, E., Lestari, Y., Hastuti, R. D., et al. (2016). Diversity of actinomycetes Eka Karya Botanical Garden, Bali. *BIOTROPIA-The Southeast Asian J. Trop. Biol.* 23 (1), 42–51. doi:10.11598/btb.2016.23.1.504

R Core Team (2021) *R: a language and environment for statistical computing*. Vienna, Austria: R Foundation for Statistical Computing.

Ren, T., Chi, Y., Wang, Y., Shi, X., Jin, X., and Jin, P. (2021). Diversified metabolism makes novel *Thauera* strain highly competitive in low carbon wastewater treatment. *Water Res.* 206, 117742.

Rognes, T., Flouri, T., Nichols, B., Quince, C., and Mahé, F. (2016). VSEARCH: a versatile open source tool for metagenomics. *PeerJ* 4, e2584. doi:10.7717/peerj.2584

Ruprecht, J. E., Birrer, S. C., Dafforn, K. A., Mitrovic, S. M., Crane, S. L., Johnston, E. L., et al. (2021). Wastewater effluents cause microbial community shifts and change trophic status. *Water Res.* 200, 117206.

Ryu, S. H., Park, M., Jeon, Y., Lee, J. R., Park, W., and Jeon, C. O. (2007). *Flavobacterium filum* sp. nov., isolated from a wastewater treatment plant in Korea. *Int. J. Syst. Evol. Microbiol.* 57 (9), 2026–2030. doi:10.1099/ijs.0.65138-0

Sadaie, T., Sadaie, A., Takada, M., Hamano, K., Ohnishi, J., Ohta, N., et al. (2007). Reducing sludge production and the domination of *Comamonadaceae* by reducing the oxygen supply in the wastewater treatment procedure of a food-processing factory. *Biosci. Biotechnol. Biochem.* 71 (3), 791–799. doi:10.1271/bbb.60632

Shi, L., Liu, N., Liu, G., and Fang, J. (2021). Bacterial community structure and dynamic changes in different functional areas of a piggery wastewater treatment system. *Microorganisms* 9 (10), 2134. doi:10.3390/microorganisms9102134

Shigematsu, T., Yumihara, K., Ueda, Y., Numaguchi, M., Morimura, S., and Kida, K. (2003). *Delftia tsuruhatensis* sp. nov., a terephthalate-assimilating bacterium isolated from activated sludge. *Int. J. Syst. Evol. Microbiol.* 53 (5), 1479–1483.

Wickham, H. (2016) *ggplot2: elegant graphics for data Analysis*. New York: Springer-Verlag.

Wu, L., Ning, D., Zhang, B., Li, Y., Zhang, P., Shan, X., et al. (2019). Global diversity and biogeography of bacterial communities in wastewater treatment plants. *Nat. Microbiol.* 4 (7), 1183–1195.

Xu, F., Liao, J., Hu, J., Feng, Y., Huang, Y., Feng, X., et al. (2023). Biofouling mitigation and microbial community dynamics in the membrane bioreactor by the indigenous quorum quenching bacterium *Delftia* sp. JL5. *Bioresour. Technol.* 388, 129753.

Yang, Z., Liu, Z., Dabrowska, M., Debiec-Andrzejewska, K., Stasiuk, R., Yin, H., et al. (2021). Biostimulation of sulfate-reducing bacteria used for treatment of hydrometallurgical waste by secondary metabolites of urea decomposition by *Ochrobactrum* sp. POC9: from genome to microbiome analysis. *Chemosphere* 282, 131064.

Zaborowska, M., Wyszkowska, J., Borowik, A., and Kucharski, J. (2022). Effect of separate and combined toxicity of bisphenol A and zinc on the soil microbiome. *Int. J. Mol. Sci.* 23 (11), 5937. doi:10.3390/ijms23115937

Zautner, A. E., Riedel, T., Bunk, B., Spröer, C., Boahen, K. G., Akenten, C. W., et al. (2023). Molecular characterization of *Arcobacter butzleri* isolates from poultry in rural Ghana. *Front. Cell. Infect. Microbiol.* 13, 1094067. doi:10.3389/fcimb.2023.1094067

Zhang, S., Li, X., Wu, J., Coin, L., O'brien, J., Hai, F., et al. (2021). Molecular methods for pathogenic bacteria detection and recent advances in wastewater analysis. *Water* 13 (24), 3551. doi:10.3390/w13243551

frontiers | Frontiers in Environmental Science

TYPE Original Research
PUBLISHED 17 July 2024
DOI 10.3389/fenvs.2024.1396772

Check for updates

OPEN ACCESS

EDITED BY
Visva Bharati Barua,
University of North Carolina at Charlotte, United States

REVIEWED BY
Arnab Ghosh,
Dong-A University, Republic of Korea
Divya Pal,
Stockholm University, Sweden

*CORRESPONDENCE
Sun Wen,
511058758@qq.com,
imsunwen@gmail.com

RECEIVED 07 March 2024
ACCEPTED 17 May 2024
PUBLISHED 17 July 2024

CITATION
Wen S, Yang Z, Biao P and Jing W (2024), Effect mechanism of nutrients on pathogenic bacteria at the sediment-water interface in eutrophic water.
Front. Environ. Sci. 12:1396772.
doi: 10.3389/fenvs.2024.1396772

COPYRIGHT
© 2024 Wen, Yang, Biao and Jing. This is an open-access article distributed under the terms of the Creative Commons Attribution License (CC BY). The use, distribution or reproduction in other forums is permitted, provided the original author(s) and the copyright owner(s) are credited and that the original publication in this journal is cited, in accordance with accepted academic practice. No use, distribution or reproduction is permitted which does not comply with these terms.

Effect mechanism of nutrients on pathogenic bacteria at the sediment-water interface in eutrophic water

Sun Wen[1,2,3]*, Zhang Yang[2,3], Peng Biao[2,3] and Wang Jing[2,3]

[1]Technology Innovation Center for Land Engineering and Human Settlements, Shaanxi Land Engineering Construction Group Co., Ltd., and Xi'an Jiaotong University, Xi'an, China, [2]Key Laboratory of Degraded and Unused Land Consolidation Engineering, Ministry of Natural and Resources of China, Xi'an, China, [3]Shaanxi Provincial Land Engineering Construction Group, Land Engineering Technology Innovation Center, Ministry of Natural Resources, Xi'an, China

This research analyzed the structure of microbial groups in the sediment–water interface (SWI) and the relationship between the gene expression levels of two typical pathogenic bacteria *Escherichia coli* and *Enterococcus*, and nutrient levels using modern biological techniques. The nutrient distribution at the SWI revealed significantly higher nutrient content in the sediment compared to the overlying water. According to Fick's first law, the release flux indicated that PO_4^{3-}-P in the upper reaches of the reservoir was deposited from the overlying water, while the release rate of NH_4^+-N, in addition to sedimentation, was significantly greater than that of PO_4^{3-}P. The microbial community structure was primarily dominated by the genera *Methyloparacoccus*, *Methylomonas*, and *Arenimonas*. The abundances of *E. coli* and *Enterococcus* were higher in the surface sediment than in the overlying water. Pearson correlation analysis demonstrated that *E. coli* had a significant positive correlation with total nitrogen (TN) ($p < 0.05$) and total phosphorus (TP) ($p < 0.05$), whereas *Enterococcus* had a very significant positive correlation with TN and TP ($p < 0.01$).

KEYWORDS

sediment-water interface, nutrients, pathogenic bacteria, correlation, eutrophic water

1 Introduction

Eutrophication in closed water bodies, such as lakes and reservoirs, has become a pollution problem encountered in water environments worldwide. Statistics show (Zhao et al., 2010) that more than 75% of the world's closed water bodies have eutrophication problems. Of the 132 major lakes in China, 61 or 46.21% are eutrophic. The northeast and eastern plain lake areas are more severely eutrophic than other areas, with their eutrophication ratios reaching 66.70% and 53.90%, respectively. Sediment has attracted attention as a main endogenous polluter of lakes and reservoirs. Nitrogen and phosphorus tend to accumulate in sediments (Liu et al., 2012) and can diffuse into the water column through changes in environmental factors, such as hydrodynamic disturbances, temperature fluctuations, and dissolved oxygen (Portielje and Lijklema, 1999), causing secondary pollution. When the nitrogen and phosphorus content in the water column increases to a certain level, algae overgrow, leading to the eutrophication of the water column and posing a severe threat to the ecological environment (Chen et al., 2022). This study

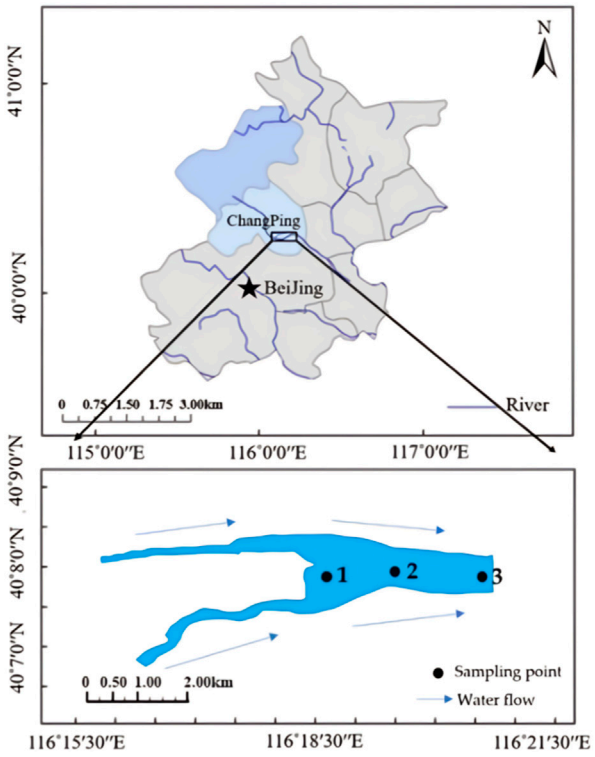

FIGURE 1
Arrangement and zoning map of sampling points in Shahe Reservoir. (The figure wascreated by S.W (Sun et al., 2021), and modifed using ArcGIS sofware 10.2; Source: WGS 1984).

selected the Shahe Reservoir located in Changping District, Beijing, which belongs to the Shahe River Basin. It is mainly recharged by the return water from urban sewage treatment plants, which increases the content of organic matter and nutrients in the reservoir water.

The sediment–water interface (SWI), as one of the most important interfaces in water ecosystems, is a crucial site for controlling material cycling in lakes and reservoirs (Fan, 2019). Nutrient production, cycling, and transfer are exceptionally active at the SWI zone, and most of these processes exert physical, chemical and biological effects on the microscale (millimeter and submillimeter) environment (Fielding et al., 2020). Given that many metabolic processes in reservoirs occur at the SWI and the transport and transformation of contaminants at the SWI is complex. While existing research extensively examines the distribution and release patterns of pollutants at the sediment-water interface, scant attention has been devoted to the presence of pathogenic bacteria. Therefore, this study is dedicated to elucidating the distribution characteristics and release dynamics of nutrients at the sediment-water interface, with a specific focus on their correlation with pathogenic bacteria. By exploring the underlying laws governing these phenomena, this research bears significant theoretical and practical implications for understanding the environmental behavior of pathogenic bacteria (Xu et al., 2013; Lei et al., 2018; Wen et al., 2018).

2 Materials and methods

2.1 Brief mapping of the studied area

The North Canal water system originates from the Southern foot of Yanshan Mountain in Changping District, Beijing, and flows through Beijing, Langfang, Hebei Province and Tianjin, successively (Yang et al., 2012). Shahe Reservoir is an important node located in the source area of the NorthCanal (Figure 1). The drainage area of Shahe Reservoir is about 1,125 km^2, of which the mountain area accountsfor about 75%. Shahe Reservoir is a typical channel-type reservoir in the upper reaches of the North Canal. The water in the Shahe Reservoir area has a long residence time and is a stagnant water body (Yu et al., 2012). The issue of eutrophication in reservoirs has garnered significant attention. Nutrients stored within reservoir sediments posed potential risks of release, thereby serving as a source of endogenous pollution within the reservoir. (Sun et al., 2021).

2.2 Sample collection and processing

Based on their topographical characteristics, three sediment sampling points were set up within the Shahe Reservoir study area (Figure 1). In September 2018, Three columnar sediment samples were collected at sampling points S1,S2, and S3 using a mud core sampler to analyze the vertical distribution characteristics of nutrients and pathogens. (r = 50 mm, h = 60 cm).

The sediment columns were layered at 2 cm intervals, and the layered samples were freeze-dried (Model FD-1A-50 freeze dryer, Beijing Boyikang Experimental Instrument Co., Ltd.), crushed with a glass rod to remove impurities such as gravel, shells, and animal and plant residues, ground with a mortar, and passed through a 100-mesh sieve before analysis. Meanwhile, the samples obtained by the Peterson mud harvester were mixed and put into a 50 mL centrifuge tube, centrifuged at 4,000 rpm for 20 min to obtain interstitial water, and stored at −4 °C. The overlying water was sucked from the gravity column mud extractor by siphon method, put into a 50 mL centrifuge tube, and stored at −4°C (Sun et al., 2022).

Determination of nutrient indicators in interstitial water includes ammonia nitrogen (NH_4^+-N), total nitrogen (TN), orthophosphate (PO_4^{3-}-P) and total phosphorus (TP) (Sun et al., 2021): where TN: interstitial water is diluted to below 4 mg L^{-1}, and after potassium sulfate digestion (Alfa Aesar,United Kingdom), UV spectrophotometer colorimetry is used; TP:The interstitial water is diluted with raw water to below 1.2 mg L^{-1} and after potassium sulfate digestion, molybdenum antimony anti-spectrophotometry is used. NH_4^+-N: After the interstitial water was filtered through a 0.45 μm filter membrane and diluted to diluted to below 2 mg L^{-1}, the Nessler reagent spectrophotometry was used; PO_4^{3-}-P: After the interstitial water was filtered through a 0.45 μm filter membrane and diluted to below 1.2 mg L^{-1}, the molybdenum antimony was used to Anti-spectrophotometry; the instruments used for the measurement are UV-Vis spectrophotometers (TU-1901, Beijing Puxi General Instrument Co., Ltd.)

TABLE 1 Primers and their mechanisms used in this study.

Target genes	Primer	Sequences	Amplico Size (bp)	Annealing Temp (°C)
16 s rRNA	1369F	CGG TGA ATA CGT TCY CGG	128	55
	1492R	GGW TAC CTT GTT ACG ACT T		
Enterococci	ECST784F	AGA AAT TCC AAA CGA ACT TG	93	55
	ENC854R	CAG TGC TCT ACC TCC ATC ATT		
E.coli	23 s rRNA-F	GGT AGA GCA CTG TTT TGG CA	87	60
	23 s rRNA-R	TGT CTC CCG TGA TAA CTT TCTC		

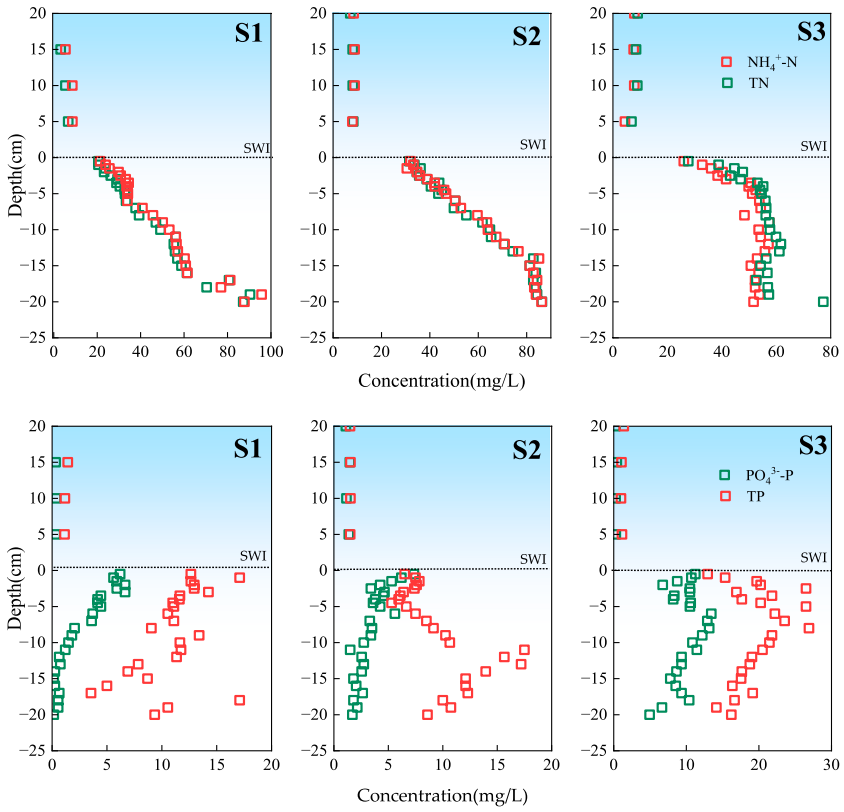

FIGURE 2
Spatial distribution characteristics of NH_4^+-N, TN, $PO4^{3-}$-P and TP at SWI.

2.2.1 DNA extraction

The DNA extraction process involved several steps: Soil samples were crushed into fine particles to aid DNA release. Following the instructions of the FastDNA Spin Kit for Soil (MP Bio, USA), soil samples were added to extraction reagents containing cell lysis agents and proteinase. The samples were thoroughly mixed and briefly centrifuged to pelletize soil particles. The supernatant, containing released DNA, was transferred to a new centrifuge tube. DNA precipitation was achieved by adding an appropriate solution, followed by centrifugation to pelletize DNA. The DNA pellet was washed with 70% ethanol to remove contaminants. After dissolution in provided buffer, DNA concentration and purity were measured using a spectrophotometer. The extracted DNA was then stored at −20°C or −80°Cfor subsequent molecular biology experiments.

2.2.2 Microbial community structure analysis

The gene sequences of the 16S rRNA V4 region PCR products were determined based on high-throughput sequencing, and the microbial community structure in each sample was analyzed. The PCR primer used was 515F/806R, and the barcode sequence was added before the forward primer to distinguish the PCR products from different samples. PCR was repeated three times for each sample and mixed, and then PCR products were recovered from

TABLE 2 Fluxes of NH_4^+-N and PO_4^{3-}P.

Nutrients	Sampling point	Curve fitting	R	$D_s \times 10^{-6}\,(cm^2 \cdot s^{-1})$	$\partial_c / \partial_x mg\,(L \cdot cm)^{-1}$	$Fmg\,(m^2 \cdot d)^{-1}$
NH_4^+-N	S1	y = 17.57e-0.093x	0.97	11.3	−1.63	12.72
	S2	y = 29.578e-0.069x	0.95	11.3	−0.93	7.26
	S3	y = 25.622e-0.06x	0.82	11.3	−1.54	11.97
PO_4^{3-}-P	S1	y = 1.9464e0.0502x	0.33	3.92	0.1	−0.26
	S2	y = 2.7313e-0.005x	0.10	3.92	−0.01	0.03
	S3	y = 3.4611e-0.091x	0.72	3.92	−0.31	0.85

different samples. PCR products were mixed in equal amounts, and libraries were built and sequenced; library building and sequencing were done by Sankyo Bioengineering (Shanghai) Co. The Illumina MiSeq™ platform was employed for sequencing. Primer-linked sequences (TGG AAT TTC TCT GGG TGC CCA AGG AACTC) were initially removed from the MiSeq paired-end sequencing data. Following this, paired reads were merged into single sequences based on their overlap. Samples were then distinguished according to their individual sequences. Finally, the quality of each sample data was controlled and filtered to ensure the validity of the data obtained. (Sun et al., 2021; Wei et al., 2021).

2.2.3 Quantitative PCR (qPCR) analysis

The main reagents used for quantitative PCR (qPCR) analysis in this study were SYBR® Premix Ex Taq™ (Tli RNaseH Plus) (TAKARA) and RNase-free Water (Ambion). The qPCR analysis was carried out on a micro ultraviolet spectrophotometer (Nanodrop 2000) and a fluorescent quantitative PCR instrument (StepOne Plus). The amplification efficiencies of the target gene fragments of *Enterococcus* and *E. coli* were 99.54% and 97.82%, respectively. The specific primer sequences and PCR conditions are shown in Table 1 (Sun et al., 2021).

2.2.4 Calculation of release flux

The presence of nutrients in sediments, acting as endogenous pollution, exerted a significant influence on water bodies and was closely intertwined with nutrient exchange at the SWI (Serruya et al., 1974). The concentration gradient of nutrients between the overlying water and the interstitial water of the sediment facilitated molecular diffusion, resulting in the release of nutrient salts from the interstitial water into the overlying water or their diffusion from the overlying water into the interstitial water. Consequently, investigating the release flux of interfacial nutrients at the SWI was of paramount importance (Huang et al., 2006). According to the concentration gradient of different nutrient concentrations at the SWI of the Shahe Reservoir, and using the one-dimensional pore water diffusion model (Selig et al., 2007) (Fick's law) and related literature (Ullman and Aller, 1982; Mccomb et al., 1998), the endogenous nutrient diffusion flux of the Shahe Reservoir can be estimated, and its improved formula is as follows:

$$F = \varphi \times D_s \times \frac{\partial c}{\partial x} \quad (1)$$

where F indicates diffusion flux at the SWI($mg \cdot m^{-2}\,d^{-1}$);

φ indicates the surface sediment porosity(%);

D_s indicates the actual molecular diffusion coefficient considering the bending effect of the sediment($m^2 \cdot s^{-1}$);

∂_c/∂_x indicates the interface substance concentration gradient($mg \cdot L^{-1}\,cm^{-1}$);

The empirical relationship between D_s and porosity is: $\varphi < 0.7$, $D_s = \varphi \times D_0$; when $\varphi > 0.7$, $D_s = \varphi^2 \times D_0$; D_0 indicates the ideal diffusion coefficient of infinitely diluted solution($cm^2 \cdot s^{-1}$).

2.3 Analysis of microbial community structure and typical, pathogens

Based on metagenomic classification and sequencing, the PCR products of 16S rRNA V4 regions were determined, and the microbial community structure in each sample was analyzed. The PCR for each sample was repeated three times before they were mixed. For this, the PCR products were recovered using gel, and the PCR products from different samples were mixed in equal amounts for library construction and sequencing; library construction and sequencing were completed by related sequencing companies, and the sequencing platform was Illumina Miseq × 250. For Miseq paired-end sequencing data, the primer adapter sequence (TGG AAT TCT CGG GTG CCA AGG AAC TC) needed to be removed first, and then the paired reads were merged into a sequence according to the overlap relationship between paired-end reads. Samples were then identified and distinguished according to the barcode tag sequence. Finally, quality control filtering was performed on the samples to ensure valid data for each sample (Pawlowski et al., 2022).

Following guidance on relevant standards for pathogens in surface waters from the United States Environmental Protection Agency, the European Union, and the World Health Organization, this study selected the typical pathogens *Escherichia coli* and *ENT* for analysis, using their gene copy numbers (DNA copies·g^{-1}) to represent their corresponding content in the sediment, and their proportion (%) in 16S rRNA to represent their abundance.

2.4 Data processing and analysis methods

SPSS 25.0 software was used to analyze the correlation between the pathogens and Nutrients in interstitial water. The vertical spatial distribution of nutrients in the interstitial waterand the absolute content of pathogens(copies·g^{-1}) were analyzed by Origin 2017. The heat map of the microbial community structure in the sediment was

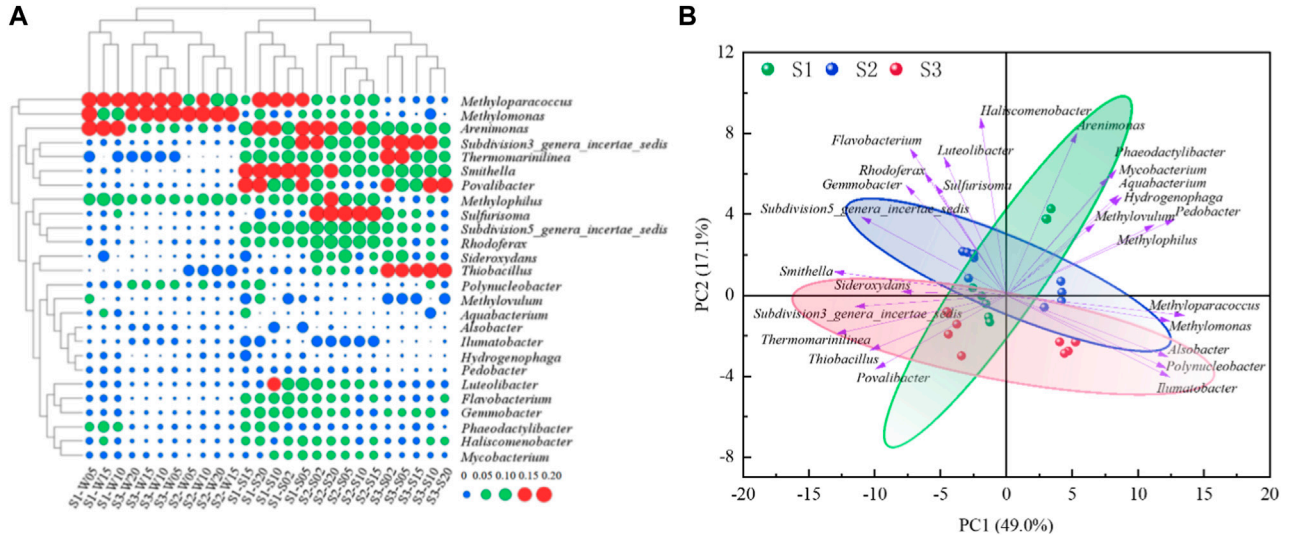

FIGURE 3
(A) SWI community structure diagram(log2 transformed) **(B)** SWI community structure principal component analysis diagram.

constructed using Heml 1.0 (http://hemi.biocuckoo.org/down.php). The R language ade4 package (https://www.R-project.org/.12c) was used to perform noise reduction analysis on operational taxonomic units (OTUs) in the community structure. The average abundance of OTUs in all samples were required to be higher than 0.01%. The OTUs after noise reduction analysis were used for subsequent analysis.

3 Results

3.1 Vertical distribution characteristics of nitrogen nutrients at the SWI

The spatial distribution characteristics of NH_4^+-N and TN at the SWI are shown in Figure 2. At the upstream of the reservoir (S1), the central area of the reservoir (S2), and the downstream of the reservoir (S3) in the overlying water, NH_4^+-N had the same vertical change trend as TN, and its concentration did not change. The concentrations of NH_4^+-N and TN in S1 were 3.20–90.35 and 5.85–95.75 mg·L^{-1}, respectively, with average values of 41.77 ± 23.21 and 44.60 ± 22.86 mg·L^{-1}, respectively. The concentrations of NH_4^+-N and TN in S2 were 9.11–86.35 and 9.32–86.40 mg·L^{-1}, respectively, with average values of 53.18 ± 25.22 and 54.02 ± 25.19 mg·L^{-1}, respectively. The concentrations of NH_4^+-N and TN in S3 were 4.45–57.45 and 6.83–77.30 mg·L^{-1}, respectively, with mean values of 43.09 ± 16.25 and 47.49 ± 17.71 mg·L^{-1}, respectively. With the increase in depth from the SWI downward, the oxygen content in the sediment decreased, the anaerobic environment became conducive to the ammonification of organic nitrogen, and ammonia consumption weakened, resulting in the accumulation of NH_4^+-N in sediments (Shen et al., 2020), These results showed that the concentration of NH_4^+-N increases with depth.

The spatial distribution characteristics of PO_4^{3-}-P and TP at the SWI are shown in Figure 2. In the water overlying S1, S2, and S3, PO_4^{3-}-P and TP exhibited the same vertical change trend and their concentration did not change. However, the concentration of PO_4^{3-}-P and TP in the interstitial water of the sedimentary column at each sampling point gradually increased with the increase in depth. The concentrations of PO_4^{3-}-P and TP in S1 were 0.15–6.65 and 1.31–17.10 mg·L^{-1}, respectively, with the average values of 2.60 ± 2.33 and 10.27 ± 4.42 mg·L^{-1}, respectively. The concentrations of PO_4^{3-}-P and TP in S2 were between 1.10–7.35 and 1.48–17.50 mg·L^{-1}, respectively, with the average values of 3.19 ± 1.57 8.60 ± 4.26 mg·L^{-1}, respectively. The PO_4^{3-}-P and TP concentrations in S3 were 0.26–13.45 and 1.00–26.90 mg·L^{-1}, respectively, with the mean values of 8.50 ± 3.79 and 17.05 ± 7.19 mg·L^{-1}, respectively. Related research (Gong et al., 2017) found that with the strengthening of the reducing environment inside the sediment, Fe^{3+} is continuously reduced into Fe^{2+}, and iron-bound phosphorus is also released such that the release of phosphorus at the SWI increases. Under reducing conditions within sediment, Fe3+ is converted to Fe2+ through reductive dissolution. This process is driven by microbial activity and anaerobic conditions. As Fe3+ is reduced to Fe2+, iron-bound phosphorus is released into the surrounding water. (Ding et al., 2016). At the same time, related works discovered that the secretion of nitrate bacteria (like *Nitrosomonas* and *Nitrobacter)* can accelerate the dissolution of Fe^{3+}, releasing the phosphorus adsorbed by $Fe(OH)_3$ (Jansson, 1986). Therefore, the orthophosphate content at 0–3 cm in the SWI environment showed a gradually decreasing distribution.

The release flux (F) of NH_4^+-N at the SWI is shown in Table 2. Its correlation coefficient in S1, S2, and S3 exceeded 0.80. The exponential fitting curve was ideal. As can be concluded from the value of F, NH_4^+-N at the SWI is released from the sediment in the interstitial water to the overlying water body and sediment is the source of NH_4^+-N. The F of NH_4^+-N ranged from 7.26 mg·m^2·day^{-1} to 12.72 mg·m^2·day^{-1}. NH_4^+-N in the sediment interstitial water enters the overlying water body with the concentration gradient under the action of molecular diffusion; therefore, NH_4^+-N is

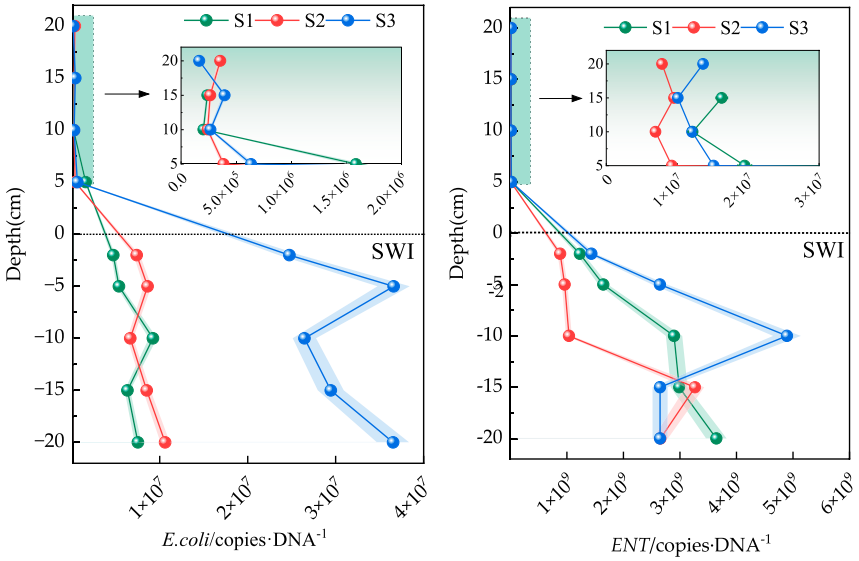

FIGURE 4
Distribution characteristics of *E. coli* and *ENT* in the SWI.

potentially released from the sediment in the interstitial water to the overlying water (Nicholls and Trimmer, 2009). NH_4^+-N had high F in the upper reaches because aquatic plants and phytoplankton utilize NH_4^+-N first when using nitrogen nutrients (Melzer and Melzer, 2004). Most of the NH_4^+-N in interstitial water originates from organic matter decomposition, which regenerates NH_4^+-N (Meng et al., 2020). Moreover, human activities and industrial production in the upper reaches contribute abundant nitrogen nutrients to the upper reaches.

The F value (−0.26 mg m^{-2}·day^{-1}) of PO_4^{3-}-P at the SWI was different from that of NH_4^+-N. PO_4^{3-}-P at the SWI in the upper reaches (S1) is absorbed by sediments. As can be concluded from the F values in S2 and S3, PO_4^{3-}-P at the SWI is released from the sediment in the interstitial water to the overlying water body. The F values in S2 and S3 were 0.03 and 0.85 mg m^{-2}·day^{-1}, respectively. The migration and release of PO_4^{3-}-P at the SWI is affected by many factors (Liu et al., 2018). Li found that under aerobic conditions, the millimeter-scale aerobic layer on the sediment surface and the diffusion boundary layer below the SWI prevent the release of phosphorus in the interstitial water to the overlying water (Li et al., 2016), Moreover, when the dissolved oxygen content in the overlying water decreases, the diffusion boundary layer or aerobic layer becomes thin or disappears, and phosphorus in the interstitial water is released to the overlying water body along the concentration gradient under the action of molecular diffusion (Wang et al., 2010).

The distribution of nutrient content at the SWI mainly shows that the nutrient content in the sediment was significantly greater than that in the overlying water body. The calculation of F in accordance with Fick's first law revealed that only the F value of PO_4^{3-}-P in S1 was negative (−0.26 mg/m^2·day), that is, PO_4^{3-}-P is deposited from the overlying water to the sediment. The release rates of NH_4^+-N in S1, S2, and S3 (12.72, 7.26, and 11.97 mg/m^2·day) were significantly greater than those of PO_4^{3-}-P in S2 and S3 (0.03 and 0.85 mg/m^2·day) because when aquatic plants and phytoplankton use nitrogen nutrients, they first use NH_4^+-N. Moreover, most of the NH_4^+-N in interstitial water originates from the decomposition of organic matter, which regenerates NH_4^+-N. Meanwhile, for PO_4^{3-}-P, the diffusion boundary and aerobic layer in the lower layer of the interface prevent the release of phosphorus in the interstitial water. Moreover, overlying water or the peak concentration of PO_4^{3-}-P in the sediment surface inhibits the migration and release of PO_4^{3-}-P in the lower layer to the upper layer. The F of PO_4^{3-}-P was significantly lower than that of NH_4^+-N.

3.2 Structural characteristics of microbial communities at the SWI

The distribution characteristics of the microbial community structure at the SWI are shown in Figure 3A, the results of principal component analysis are shown in Figure 3B, which shows that the similarities and differences of the microbial community structure at the SWI are reflected in the overlying water bodies and sediments, respectively. *Methyloparacoccus* is a strictly respiratory Gram-negative aerobic genus that uses oxygen as the terminal electron acceptor, and its average relative abundance in the SWI of each sampling point was the highest (13.88% ± 6.30%). Its relative abundance was the highest (23.42%) at the 20 cm layer of the overlying water downstream of the reservoir (3# sedimentation column), and its relative abundance was the lowest (1.58%) at the −2 cm layer of the sediment. The genus *Methylomonas* has a wide distribution and is a chemoorganotrophic bacterium without strict requirements for inorganic nutrients. It may grow on natural substrates containing methane (Tikhonova et al., 2023). Most of its members are symbiotic or associated with heterotrophic bacteria that cannot oxidize methane, and isolating, purifying, and maintaining pure species of this genus are extremely difficult. Trace amounts of organic substances, such as amino acids and polypeptides, can inhibit their growth, and even some methane-oxidizing bacteria are inhibited by very small amounts of methanol.

10.3389/fenvs.2024.1396772

TABLE 3 The Pearson correlation analysis between pathogenic bacteria and TN, TP in the SWI.

Types of pathogens	Pearson correlation	S1 sedimentary column		S2 sedimentary column		S3 sedimentary column	
		TN	TP	TN	TP	TN	TP
E. coli	Correlation coefficient	0.862*	0.830*	0.993*	0.990*	0.972**	0.969**
	Significance	0.027	0.041	0.045	0.045	0.001	0.001
ENT	Correlation coefficient	0.996**	0.999**	0.981	0.977	0.981**	0.983**
	Significance	0.00003	0.000	0.123	0.136	0.001	0.0004

Some bacteria are strictly aerobic, using oxygen molecules as electron acceptors to oxidize methane gradually into alcohols, aldehydes, acids, and finally into carbon dioxide, and obtain energy through the monophosphate ribose or serine pathway (Khalifa et al., 2015). The average relative abundance of *Methylomonas* at the SWI was 13.60% ± 8.55% and was second only to that of *Methyloparacoccus*. It was highest (28.24%) at the 5 cm layer of the overlying water in S2 and lowest (2.12%) at the −2 cm layer of S1. The average abundances of *Arenimonas* and *Methylophilus* at the SWI at each sampling point were also relatively high, reaching 9.57% ± 3.46% and 7.94% ± 2.26%, respectively. The maximum values appeared at 10 (14.54%) and 15 cm (9.66%) of S1, and the smallest values were distributed at 5 cm of the upper water in S2 (5.79%) and the −2 cm layer of sediment in S3 (1.96%). The average abundances of *Polynucleobacter, Phaeodactylibacter, Sulfurisoma*, and *Subdivision3_genera_incertae_sedis* at the SWI at each sampling point exceeded 3.00%. The maximum abundances of *Phaeodactylibacter* and *Sulfurisoma* were 7.20% and 8.84%, respectively, and appeared at 20 cm above S1. The maximum abundance of *Subdivision3_genera_incertae_sedis* was 9.44% and was found at the −2 cm sediment layer in S3. The minimum abundances of *Polynucleobacter* and *Phaeodactylibacter* were 0.55% and 1.32%, respectively, and appeared at the −2 cm layer in S3. The minimum abundance of *Sulfurisoma* was 0.64% and appeared at the 10 cm layer of the overlying water of S3. The minimum value of *Subdivision3_genera_incertae_sedis* was 1.69% and was found at the 25 cm layer of the overlying water of S3.

3.3 Relative abundance of pathogenic bacteria in the SWI

The absolute abundance distribution of *E. coli* and *Enterococcus* at the SWI is shown in Figure 4. Given that the sediment layer in S3 was relatively high, the overlying water body was only sampled to 10 cm above the surface sediment. The figure shows that the absolute abundance ranges of *E. coli* in S1, S2, and S3 were 2.03×10^5–4.72×10^6, 2.41×10^5–7.39×10^6 and 2.20×10^5–2.47×10^7 copies·g^{-1}, respectively. The absolute abundance of *E. coli* at the SWI negligibly differed. Notably, the absolute abundance of *E. coli* in the surface layer of the SWI at the −2 cm sediment layer in the three sedimentary columns was one order of magnitude higher than that in the overlying water body. Although the absolute abundance of *E. coli* at the SWI in the overlying water showed little difference, that at 20 cm above the SWI in S1 and S3 was slightly higher than that at other depths of overlying water.

The distribution characteristics of the absolute abundances of *Enterococcus* and *E. coli* at the SWI were not considerably different and were both higher in sediment than in the overlying water body. However, the absolute abundance of *Enterococcus* at the SWI was approximately two orders of magnitude higher than that of *E. coli*. *Enterococcus* species are known for their resilience and ability to survive in harsh environmental conditions, including low nutrient environments and fluctuating temperatures. They can form biofilms and persist in sediments for extended periods, enhancing their abundance at the SWI compared to *E. coli*, which

may be less adapted to such conditions. The absolute abundance ranges of *Enterococcus* in S1, S2, and S3 were 6.30×10^6–1.23×10^9, 6.94×10^6–8.81×10^8 and 8.28×10^6–1.43×10^9, respectively. The abundance of *Enterococcus* in S3 was approximately 1.60 and 1.37 times that in the sedimentation columns in S2 and S1, respectively. The absolute abundance of *Enterococcus* at the SWI was not significantly different. Similar to that of *E. coli*, the absolute abundance of *Enterococcus* in the three sediment columns was approximately one order of magnitude higher than that in the surface −2 cm sediment in the SWI than in the overlying water.

Table 3 shows that *E. coli*, *ENT*, TN, and TP in the SWI in S1 and S3 had extremely significant positive correlations ($p < 0.01$) or significant positive correlations ($p < 0\ .05$). Specifically, *E. coli* had a positive correlation with TN and TP ($p < 0.05$) at the SWI in S1, whereas *ENT* at the SWI in S1 had extremely significant positive correlations with TN and TP ($p < 0.01$). However, the correlation of *Enterococcus* with TN and TP in the SWI in S2 was not significant ($p > 0.05$). *Enterococcus* had extremely significant positive correlations with TN and TP ($p < 0.01$) at the SWI in S3. Relevant studies (Xiang et al., 2023) have found that nitrite can effectively improve denitrification efficiency and enrich bacteria during the nitrification and denitrification processes. Therefore, ammonia can be regarded as one of the pathogenic bacteria pollution source parameters.

4 Conclusion

The distribution of nutrient content at the SWI of the Shahe Reservoir mainly revealed that nutrient content in the sediment was significantly greater than that in the overlying water body. The F values calculated in accordance with Fick's first law showed that the F value of PO_4^{3-}-P was negative only in S1, that is, sediment is deposited from the overlying water. The release rate of NH_4^+-N in S1, S2 and S3 was significantly greater than that of PO_4^{3-}-P in S2 and S3.

The horizontal community structure of pathogenic bacteria at the SWI of Shahe Reservoir was mainly dominated by three genera, namely, *Methyloparacoccus*(13.88%), *Methylomonas*(13.60%), *Arenimonas* (9.57%), *Sulfurisoma*(8.84%) and *Methylophilus*(7.94%).

Pearson correlation analysis showed that at the SWI, *E. coli* had a significant positive correlation with TP and TN ($p < 0.05$), where as *Enterococcus* had a very significant positive correlation with TP and TN ($p < 0.01$).

In conclusion, this study illuminates nutrient dynamics and microbial communities at the sediment–water interface (SWI) of Shahe Reservoir. It underscores sediment's role as a nutrient reservoir, impacting water quality and ecosystem health. Identification of dominant pathogenic bacteria highlights potential public health risks. Future research should explore mechanisms driving nutrient release and microbial dynamics at SWI, considering seasonal variations and anthropogenic influences. Integrated approaches combining metagenomics, geochemistry, and hydrology are crucial for comprehensive understanding and informing sustainable management strategies. This work is vital amid increasing pressures from urbanization, agriculture, and climate change, offering insights for effective water quality preservation and public health safeguarding.

Data availability statement

The original contributions presented in the study are included inthe article/Supplementary Material, further inquiries can be directedto the corresponding authors.

Author contributions

SW: Conceptualization, Writing–original draft, Writing–review and editing. ZY: Investigation, Writing–original draft, Writing–review and editing. PB: Investigation, Resources. WJ: Validation, Software. All authors contributed to the article and approved the submitted version.

Funding

The author(s) declare that financial support was received for the research, authorship, and/or publication of this article. This work was supported by (Shaanxi Key Laboratory of Land Consolidation Open Fund) [Grant number (300102353506)] and (The project of Shaanxi Province Land Engineering Construction Group) [Grant number (DJTD 2023-02) and (DJTD 2022-04)].

Conflict of interest

Author SW was employed by Shaanxi Land Engineering Construction Group Co., Ltd.

The remaining authors declare that the research was conducted in the absence of any commercial or financial relationships that could be construed as a potential conflict of interest.

Publisher's note

All claims expressed in this article are solely those of the authors and do not necessarily represent those of their affiliated organizations, or those of the publisher, the editors and the reviewers. Any product that may be evaluated in this article, or claim that may be made by its manufacturer, is not guaranteed or endorsed by the publisher.

References

Chen, T., Liu, C. Q., Shi, X. L., Li, Y., Fan, Z. W., Jia, B. Y., et al. (2022). Ten-year trend analysis of eutrophication status and the related causes in lake hongze. *Environ. Sci.* 43 (7), 3523–3531. doi:10.13227/j.hjkx.202110006

Ding, S., Wang, Y., Wang, D., Li, Y. Y., Gong, M., and Zhang, C. (2016). *In situ*, high-resolution evidence for iron-coupled mobilization of phosphorus in sediments. *Sci. Rep.* 6 (1), 24341. doi:10.1038/srep24341

Fan, C. (2019). Advances and prospect in sediment-water interface of lakes: a review. *J. Lake Sci.* 31 (5), 1191–1218. doi:10.18307/2019.0514

Fielding, J. J., Croudace, I. W., Kemp, A. E., Pearce, R. B., Cotterill, C. J., Langdon, P., et al. (2020). Tracing lake pollution, eutrophication and partial recovery from the sediments of Windermere, UK, using geochemistry and sediment microfabrics. *Sci. total Environ.* 722, 137745. doi:10.1016/j.scitotenv.2020.137745

Gong, M., Zengfeng, J., Yan, W., Juan, L., and Shiming, D. (2017). Coupling between iron and phosphorus in sediments of shallow lakes in the middle and lower reaches of Yangtze River using diffusive gradients in thin films (DGT). *J. Lake Sci.* 29, 1103–1111. doi:10.18307/2017.0508

Huang, X., Guo, F., and Yue, W. (2006). Studies on nutrients in sediment interstitial water in northern South China Sea. *J. Trop. Oceanogr.* 25 (5), 43–48. doi:10.3969/j.issn.1009-5470.2006.05.008

Jansson, M. (1986) *Nitrate as a catalyst for phosphorus mobilization in sediments*. New York: Springer.

Khalifa, A., Lee, C. G., Ogiso, T., Ueno, C., Dianou, D., Demachi, T., et al. (2015). Methylomagnum ishizawai gen. nov., sp. nov., a mesophilic type I methanotroph isolated from rice rhizosphere. *Int. J. Syst. Evol. Microbiol.* 65 (10), 3527–3534. doi:10.1099/ijsem.0.000451

Lei, P., Hong, Z., Chao, W., and Ke, P. (2018). Migration and diffusion for pollutants across the sediment - water interface in lakes, a review. *Environ. Res.* 30 (6), 1489–1508. doi:10.18307/2018.0602

Li, H., Song, C. L., Cao, X. Y., and Zhou, Y. Y. (2016). The phosphorus release pathways and their mechanisms driven by organic carbon and nitrogen in sediments of eutrophic shallow lakes. *Sci. Total Environ.* 572, 280–288. doi:10.1016/j.scitotenv.2016.07.221

Liu, C., Gu, X., Chen, K., Fan, C., Zhang, L., and Huang, W. (2018). Nitrogen and phosphorus exchanges across the sediment–water interface in a bay of lake chaohu. *Water Environ. Res.* 90 (11), 1956–1963. doi:10.2175/106143017x15131012188079

Liu, J., Zheng, X., Chen, L., Wu, C., et al. (2012). Study on flux and release law of nitrogen and phosphorus of sediment in reservoir. *J. Hydraulic Eng.* 43 (3), 339–343.

Mccomb, A. J., Qiu, S., Lukatelich, R., and McAuliffe, T. (1998). Spatial and temporal heterogeneity of sediment phosphorus in the peel-harvey estuarine system. *Estuar. Coast. Shelf Sci.* 47 (5), 561–577. doi:10.1006/ecss.1998.0389

Melzer, S. A., and Melzer, A. (2004). Sediment and water nutrient characteristics in patches of submerged macrophytes in running waters. *Hydrobiologia* 527, 195–207. doi:10.1023/b:hydr.0000043301.50788.36

Meng, X., Zhang, W., and Shan, B. (2020). Distribution of nitrogen and phosphorus and estimation of nutrient fluxes in the water and sediments of Liangzi Lake, China. *Environ. Sci. Pollut. Res. Int.* 27 (7), 7096–7104. doi:10.1007/s11356-019-07398-8

Nicholls, J. C., and Trimmer, M. (2009). Widespread occurrence of the anammox reaction in estuarine sediments. *Aquat. Microb. Ecol.* 55, 105–113. doi:10.3354/ame01285

Pawlowski, J., Bruce, K., Panksep, K., Aguirre, F., Amalfitano, S., Apothéloz-Perret-Gentil, L., et al. (2022). Environmental DNA metabarcoding for benthic monitoring: a review of sediment sampling and DNA extraction methods. *Sci. Total Environ.* 818, 151783. doi:10.1016/j.scitotenv.2021.151783

Portielje, R., and Lijklema, L. (1999). Estimation of sediment–water exchange of solutes in Lake Veluwe, The Netherlands. *Water Res.* 33 (1), 279–285. doi:10.1016/s0043-1354(98)00202-4

Selig, U., Berghoff, S., and Schubert, H. (2007). Transformation of particulate phosphorus at the sediment-water interface in a shallow coastal water on the Baltic Sea. *Int. Assoc. Theor. Appl. limnoloy* 30 (2), 235–238. doi:10.1080/03680770.2008.11902116

Serruya, C., Edelstein, M., Pollingher, U., and Serruya, S. (1974). Lake Kinneret sediments: nutrient composition of the pore water and mud water exchanges 1. *Limnol. Oceanogr.* 19 (3), 489–508. doi:10.4319/lo.1974.19.3.0489

Shen, L. Q., Amatulli, G., Sethi, T., Raymond, P., and Domisch, S. (2020). Estimating nitrogen and phosphorus concentrations in streams and rivers, within a machine learning framework. *Sci. Data* 7 (1), 161. doi:10.1038/s41597-020-0478-7

Sun, W., Yang, K., Li, R., Chen, T., Xia, L., Sun, X., et al. (2022). Distribution characteristics and ecological risk assessment of heavy metals in sediments of Shahe reservoir. *Sci. Rep.* 12 (1), 16239. doi:10.1038/s41598-022-20540-w

Sun, W., Yang, K., Li, R., Chen, T., Xia, L., Wang, Z., et al. (2021). The spatial distribution characteristics of typical pathogens and nitrogen and phosphorus in the sediments of Shahe reservoir and their relationships. *Sci. Rep.* 11 (1), 21745. doi:10.1038/s41598-021-01252-z

Tikhonova, E. N., Suleimanov, R. Z., Miroshnikov, K. K., Oshkin, I. Y., Belova, S. E., Danilova, O. V., et al. (2023). Methylomonas rapida sp. nov., a novel species of fast-growing, carotenoid-producing obligate methanotrophs with high biotechnological potential. *Syst. Appl. Microbiol.* 46 (2), 126398. doi:10.1016/j.syapm.2023.126398

Ullman, W. J., and Aller, R. C. (1982). Diffusion coefficients in nearshore marine sediments. *Limnol. Oceanogr.* 27 (3), 552–556. doi:10.4319/lo.1982.27.3.0552

Wang, J., Shen, J., Zhang, L., Fan, C., Li, W., Pan, J., et al. (2010). Sediment-water nutrient fluxes and the effects of oxygen in lake dianchi and lake Fuxian,Yunnan Province. *J. Lake Sci.* 22 (5), 640–648. doi:10.18307/2010.0503

Wei, Y., Chang, G., Wu, J., Lin, J., Jiang, H., Wang, P., et al. (2021). Preface: special issue on water quality improvement and ecological restoration for river replenished with reclaimed water based on "Source-Flow-Sink" concept. *Acta Sci. Circumstantiae* 41 (1), 1–6.

Wen, S., Gong, W. Q., Wu, T., Zheng, X. L., Jiang, X., Li, X., et al. (2018). Distribution characteristics and fluxes of nitrogen and phosphorus at the sediment-water interface of yuqiao reservoir. *Environ. Sci.* 39 (5), 2154–2164. doi:10.13227/j.hjkx.201709081

Xiang, Y., Zhou, T., Deng, S., Shao, Z., Liu, Y., He, Q., et al. (2023). Nitrite improved nitrification efficiency and enriched ammonia-oxidizing archaea and bacteria in the simultaneous nitrification and denitrification process. *Statements Declar. Water Res. X* 21, 100204. doi:10.1016/j.wroa.2023.100204

Xu, D., Chen, Y., Ding, S., Sun, Q., Wang, Y., and Zhang, C. (2013). Diffusive gradients in thin films technique equipped with a mixed binding gel for simultaneous measurements of dissolved reactive phosphorus and dissolved iron. *Environ. Sci. Technol.* 47 (18), 10477–10484. doi:10.1021/es401822x

Yang, Y., Wei, Y., Zheng, X., Wang, Y., Yu, M., Xiao, Q., et al. (2012). Investigation of microbial contamination in wenyu river of beijing. *Acta Sci. Circumstantiae* 32 (1), 9–18.

Yu, D., Yu, M., Wei, Y., Wang, Y., Zheng, X., Yang, Y., et al. (2012). Spatio-temporal evolution of water environment quality in Wenyu River during 1980—2010. *Acta Sci. Circumstantiae* 32 (11), 2803–2813.

Zhao, Y., Deng, X., Zhan, J., Xi, B., and Li, Q. (2010). Progress on preventing and controlling strategies of lake eutrophication in China. *Environ. Sci. Technol.* 33, 92–98.

frontiers | Frontiers in Environmental Science

TYPE Original Research
PUBLISHED 25 July 2024
DOI 10.3389/fenvs.2024.1423339

Check for updates

OPEN ACCESS

EDITED BY
Visva Bharati Barua,
University of North Carolina at Charlotte, United States

REVIEWED BY
Sayanti Ghosh,
University of Hawaii at Manoa, United States
Yabing Li,
Michigan State University, United States
Poulami Datta,
West Virginia University, United States

*CORRESPONDENCE
Mulalo I. Mutoti,
mutotimi@tut.ac.za

RECEIVED 25 April 2024
ACCEPTED 08 July 2024
PUBLISHED 25 July 2024

CITATION
Mutoti MI, Gumbo JR, Khwathisi A and Jideani AIO (2024), Newly isolated strains of potentially microcystin-producing cyanobacteria in potable water: case study of Mawoni village, South Africa.
Front. Environ. Sci. 12:1423339.
doi: 10.3389/fenvs.2024.1423339

COPYRIGHT
© 2024 Mutoti, Gumbo, Khwathisi and Jideani. This is an open-access article distributed under the terms of the Creative Commons Attribution License (CC BY). The use, distribution or reproduction in other forums is permitted, provided the original author(s) and the copyright owner(s) are credited and that the original publication in this journal is cited, in accordance with accepted academic practice. No use, distribution or reproduction is permitted which does not comply with these terms.

Newly isolated strains of potentially microcystin-producing cyanobacteria in potable water: case study of Mawoni village, South Africa

Mulalo I. Mutoti[1]*, Jabulani R. Gumbo[2], Adivhaho Khwathisi[3] and Afam I. O. Jideani[4]

[1]Department of Environmental, Water and Earth Sciences, Faculty of Science, Tshwane University of Technology, Pretoria, South Africa, [2]Department of Earth Sciences, Faculty of Science, Engineering and Agriculture, University of Venda, Thohoyandou, South Africa, [3]Department of Biochemistry and Microbiology, Faculty of Science, Engineering and Agriculture, University of Venda, Thohoyandou, South Africa, [4]Department of Food Science and Technology, Faculty of Science, Engineering and Agriculture, University of Venda, Thohoyandou, South Africa

Toxic cyanobacterial species occur in aquatic ecosystems when favourable environmental conditions prevail. These bacteria can produce natural hepatotoxic metabolites called microcystins that can affect the quality of water. Human exposure to microcystins results from ingesting contaminated drinking water and therefore cyanobacterial species producing these toxins should be monitored in these waters. The present study aimed to trace and identify cyanobacterial strains that potentially produce microcystins in drinking water. To achieve this objective, advanced digital flow cytometry and polymerized chain reaction were used for the detection and identification of cyanobacterial strains in water samples collected from water storage containers in Mawoni village. Full-length 16S rRNA genes from cultured cyanobacteria were amplified and sequenced using the 16S primers. Three novel strains of *Chroococcus* sp. (m64187e-7881, m64187e-2143, and m64187e-0930) and two strains of *Microcystis aeruginosa* (m64187e-6729 and m64187e-1069) were detected and identified in drinking water samples. The presence of these strains could indicate the potential of microcystins occurrence in drinking water, which therefore, could present potential human health risk due to exposure to such cyanotoxins.

KEYWORDS

cyanotoxins, drinking water, human health, molecular identification, microcystins

1 Introduction

The cyanobacteria phylum of the photosynthetic prokaryotes has been in existence for over 3.5 billion years and can be found in various habitats including freshwater bodies (Chia et al., 2022; Wang et al., 2024). They are considered the oldest organisms in the evolutionary process which are capable of performing oxygenic photosynthesis and are known to oxygenate the atmosphere of the earth (Balasooriya, 2019). Favourable physicochemical

conditions support the growth of these phyla (Chia et al., 2022). According to Chia et al. (2022); Melaram et al. (2022), factors influenced by global warming, such as eutrophication, high temperatures and increased solar irradiation can influence the excessive growth of harmful cyanobacteria in aquatic systems. Amongst the cyanobacteria species are those that produce and release a copious number of metabolites called cyanotoxin-microcystin. Currently, cyanobacteria have more than 60 species that are known as microcystin producers worldwide (Usman et al., 2022), and some of these species include *Microcystis* and *Chroococcus* sp. (Magonono et al., 2018; Chen et al., 2021; Mirasbekoc et al., 2021; Valadez-Cano et al., 2022; Thawabteh et al., 2023). Apart from being the water quality problem such as affecting the aquatic ecosystem and aquatic animals, the occurrence of cyanobacterial species and their toxins can also pose severe health threats to humans and animals (Chen et al., 2021; Jia et al., 2024). These toxins have been reported to comprise potent neurotoxic, hepatotoxic, dermatoxic and cytotoxic agents that they produce (Nowruzi et al., 2023) as well as causing gastro-intestinal toxicity (Li et al., 2024). Many studies have been focused on microcystins globally, due to their extensive occurrence, steadiness and resilience to chemical and biological breakdown, as well as their ability to reach high concentrations in scums and blooms (Dai et al., 2016; Welten et al., 2020).

According to Carmichael et al. (2013), microcystins are clyclic heptapeptides tha consist five common amino acids and pairs of L-amino acids as variants; with the most known acids being methyl aspartic acid, N-methyldehydroalanine, alanine, glutamic acid, and Adda (3-amino-9-methoxy-2,6,8-trimethyl-10- phenyldeca-4,6 dienoic acid) (Pearson et al., 2010). It was further reported that microcystins fall within a group of small molecular weight causing human and animal poisoning that involves acute hepatotoxicosis (Sarma, 2013). Previous studies have reported that most human health problems are linked with continuous low microcystin concentrations exposure (Drobac et al., 2013), of which one of the common exposure routes is through drinking microcystins-contaminated water (Mutoti et al., 2022; Melaram et al., 2022). The health threats caused by microcystins have led the World Health Organization (WHO) to set the standards for drinking water quality for these toxins; for example, a guideline value for total MCs is 1 μg/L in drinking water (Farrer et al., 2015; WHO, 2017). A liver is one of the variety of organs that can be targeted by microcystins. Acute exposure to these toxins can result in headaches, eye pain, blurred vision, nausea, and vomiting (Lad et al., 2022; Lim et al., 2023). With many studies focused on the cyanotoxins impact on animal health, there is limited information on the human health impact of cyanotoxins. Therefore, the human health effects of microcystins are still not well understood in some cases, mostly chronic health impacts (O'Keeffe, 2019). Potential associations have been identified by various studies between liver disease and microcystin exposure. The tissue of dialysis patients in Brazil dialysis centre were found to be accumulated by microcystins, causing death to many patients due to liver failure (O'Keeffe, 2019). Similarly, correlation was observed between freshwater microcystins-producing cyanobacteria with incident of liver cancer and mortalities in central Serbia (Melaran et al., 2022).

Most drinking water authorities have been facing the challenges of treating water contaminated with cyanobacteria. Although a guideline document to assist portable water producers in dealing with toxic cyanobacteria in water sources has been developed (WHO, 2017), Mutoti et al. (2022) reported that there is still a lack of personnel who are skilled enough to develop protocols and programmes to monitor cyanobacteria toxins, consequently becoming the key challenge faced by water treatment works (DWTW) in Southern Africa.

Currently, numerous analytical methods have been used for the assessment of microbiological characteristics of the water samples globally. A polyphasic approach has been utilized as a system of cyanobacterial species description that combines 16S rRNA, morphology, phycology, and ecology in trying to acknowledge the need to incorporate phylogenetics into cyanobacterial taxonomy (Willis and Woodhouse, 2020). This approach has been supported by taxonomists such as Komárek et al. (2014) and Komárek (2020) who pointed out that the polyphasic approach provides the best means of conducting taxonomic practice. Reviews have been conducted on DNA sequencing that is used for the phylogenetic and taxonomic analysis of cyanobacterial isolates (Mutoti et al., 2022). Many studies have utilized these approaches for the classification and identification of cyanobacteria species in drinking water (Mutoti et al., 2022; Valade-Cano et al., 2022). Moreover, FlowCAM has been used that capture images of cyanobacteria that are then identified based on their morphological parameters (area, length, width, equivalent spherical diameter, and area-based diameter) and shape; whereas, the PCR uses 16S rRNA gene sequencing to identify cyanobacterial to their species level (Wilson et al., 2000). Both FlowCAM and PCR techniques are taxonomic methods that enable the identification of cyanobacterial species in natural habitats (Lee et al., 2017) based on morphological characteristics and genomic information (Willis and Woodhouse, 2020). Komárek et al. (2014) reported that there is very limited data for most genera such as *Chroococcus* within the Chroococcaceae family; whereas, the well-known genus *Microcystis* is constantly monophyletic, but the species level classification within the genus can be controversial. This therefore triggers studies of this nature to try and fill up this vital data gap.

Containers (20–25 L) are used in rural areas such as Mawoni for collection and storing water for future use. The presence of pathogenic bacteria, including cyanobacteria in this water has been assumed. There has been some observation of cyanobacteria development inside these containers forming biofilm, which potentially pose threats to the households that use such water. Studies on the occurrence of cyanobacteria blooms have been seldom conducted in African aquatic resources (Chia et al., 2022). In Mawoni village and the surrounding areas located in the North part of South Africa in Limpopo, nothing or limited information has been reported regarding the underlying genetic characterization, morphology, and geographical origin among the strains of cyanobacteria. This gap in knowledge limits our understanding of cyanobacteria diversity, distribution, toxin production, and the nature of their congeners, highlighting the risks of exposure through potable water resource contamination. Therefore, to fill-up this gap, the present study is the first of its kind to assess the presence of cyanobacteria strains that potentially produce and release microcystins in drinking water collected from water storage containers in Mawoni village. This

information is fundamental to the water supply authorities that require critical control and management approaches to prevent health problems that are associated with these bioactive metabolites.

2 Materials and methods

2.1 Cyanobacteria culture and strains and microscopic analysis

In the present study, sixteen water samples (four batch of four samples: n = 16) were collected using Latex Free, Polypropylene Medline Basic Specimen containers with screw lids (manufactured by Medline, US). Samples were collected from water containers that contain green seeded biomass on their side walls and are used to store drinking water in Mawoni village. Sampling was conducted ones during summer season. During samples collection, physicochemical parameters were measured *insitu* using the Accsen PC 70 multimeter (manufactured by Accsen Instrumental in Italy) and the Turbicheck WL portable turbidity meter (TB 250 WL) (manufactured by Lovibond Water Testing, Germany) was used for turbidity measurements. Instruments were calibrated before use and all the physicochemical parameters were measured in triplicates from all the samples collected. Cyanobacterial strains from the collected water samples were cultured and grown in sterile shake flasks containing liquid medium (BG11). Before the examination, these cultures were incubated for 4 weeks at room temperature (25°C) and elevated temperature (40°C) under 24 h of white fluorescent lamp light (at 27 μmol m^{-2} s^{-1}) as described by Magonono et al. (2018); Mutoti et al. (2022). Since the taxonomic system of cyanobacteria according to Komárek et al. (2014) has radically changed due to the introduction of electron microscopy; and molecular and genetic methods for the characterization of cyanobacterial taxa; this study further utilizes a Leica DM3000 semi-automated laboratory microscope (Leica, Germany) to observe morphological characteristics of filaments and cells. Furthermore, the bench-top FlowCAM (8100-C, Fluid Imaging Technologies Inc., Scarborough., ME, United States) was used to generate images of cyanobacterial strains. Microscope and bench-top FlowCAM were adopted for preliminary analysis of water samples. The FlowCAM captures cyanobacterial cells as the water sample flows past the filter tube inside the FlowCAM device. The instrument was equipped with software (VisualSpreadsheet V3.2.2) used to view and select images of interest. During analysis, the instrument was on auto-image mode (capture rate of 20 frame/sec) and auto-focused for ×10 objective with the flow rate of 0.4 mL/min. Although the primary morphological characteristics that are diagnostic of the families were first given in Anagnostidis and Komárek (1990) and updated in Komárek (2013), the morphology of captured cyanobacterial strains in the present study was further identified according to van Vuuren et al. (2006); Balsooriya (2019) descriptions.

Furthermore, cyanobacterial cells harvested from cultures of four samples (each sample from each batch) by filtering were further used for molecular characterization and identification using PCR. The included analytical procedures were DNA extraction, amplification using PCR, sequencing, and phylogenetic analysis, and these procedures are described below.

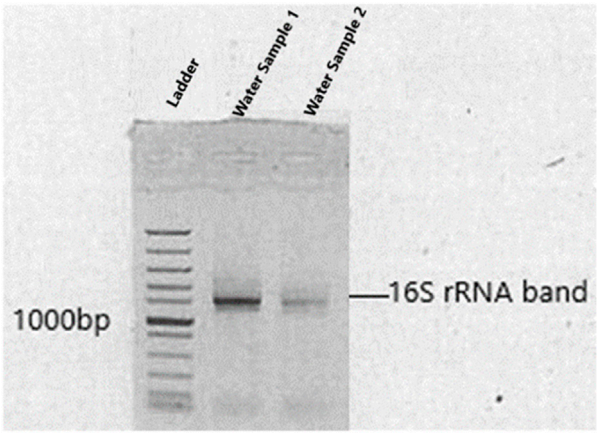

FIGURE 1
Amplified 16S rRNA of bacterial isolates shown on agarose gel electrophoresis. Levels of gene migration are expressed by lanes (water samples 1 and 2).

2.2 Extraction of genomic DNA

Standard procedures for extraction of total gDNA were performed according to the instructions supplied by the manufacturer. Quick-DNA/RNA™ Miniprep Plus Kit (supplied by Inqaba Biotech Laboratories, South Africa) was used for the isolation of DNA. The first step of extraction began with cyanobacteria cell lysis, where an equal mixture of 400 μL of 2X concentrate with 400 μL of nuclease-free water was homogenized in a Lysis Tubes to get 1X DNA/RNA Shield™, followed by 10 min of centrifugation at 1600 × g and transfer of supernatant into an RNase-free tube. An equal volume of DNA/RNA Lysis Buffer was added, mixed well and then transferred into a Spin-Away™ Filter in collection tubes and centrifuged for 1 min. The Spin-Away™ Filter was again transferred into a new collection tube, 400 μL DNA/RNA Prep Buffer was added to the column and centrifuged for 30 s and the flow-through was discarded. 700 μL of DNA/RNA Wash Buffer was then added and centrifuged for 30 s and again the flow-through was discarded. 400 μL of DNA/RNA Wash Buffer was added and centrifuged for 2 min to ensure complete removal of wash buffer then the column was carefully transferred into clean microcentrifuge tubes. A volume of 100 μL of DNase/RNase-Free Water was directly added to the column matrix, let stand for 5 min, and then centrifuged to elute DNA from the respective column. The eluted DNA was stored at −70°C and then sent to Inqaba Biotech Laboratories for further analysis.

2.3 Molecular characterization of strains

The basic molecular characterization of strains were performed after 16S rRNA gene fragments amplification with PCR using the primers: 27F (/5AmMC6/gcagtcgaacatgtagctgactcaggtcac-AGAGTTTGATCCTGGCTCAG) and 1492R (/5AmMC6/tggatcacttgtgcaagcatcacatcgtag-TACGGYTACCTTGTTACGACTT), which were adopted from Meirkhanova et al. (2023). The methods for the multi-gene analysis and sequencing were carried out as per Mutoti

TABLE 1 Physicochemical parameters (mean and STDEV) status of water determined during the collection of water sample (n = 16).

TDS (mg/L)	EC (mS/m)	Turbidity (NTU)	DO (mg/L)	pH	Salinity (ppm)	Temp (°C)
37.8 ± 1.1	52.6 ± 0.4	2.2 ± 0.2	7.7 ± 0.2	7.8 ± 0.4	23.8 ± 0.4	20.1 ± 0.2
38.2 ± 0.7	52.8 ± 0.6	1.2 ± 0.2	7.8 ± 0.2	7.3 ± 0.2	25.1 ± 0.2	21.1 ± 0.1
38.4 ± 0.2	56.3 ± 0.4	22.3 ± 0.4	7.5 ± 0.2	6.8 ± 0.4	25.5 ± 1.4	19.5 ± 0.7
36.6 ± 1.1	50.8 ± 2.2	17.9 ± 0.7	13.0 ± 0.5	6.9 ± 0.2	27.3 ± 0.4	21.6 ± 0.7
37.3 ± 1.3	52.6 ± 0.4	2.2 ± 0.1	7.5 ± 0.2	7.5 ± 0.3	24.5 ± 0.5	18.8 ± 0.3
37.7 ± 0.5	53.2 ± 1.4	1.2 ± 0.1	7.5 ± 0.2	7.5 ± 0.1	25.1 ± 0.2	20.6 ± 0.4
38.4 ± 0.2	55.4 ± 0.4	24.2 ± 0.9	7.3 ± 0.2	6.5 ± 0.3	24.2 ± 0.2	19.9 ± 0.6
36.2 ± 1.2	50.0 ± 2.3	17.4 ± 0.6	12.7 ± 0.4	6.7 ± 0.2	28.0 ± 0.2	21.3 ± 0.9
38.0 ± 0.4	55.4 ± 0.1	3.1 ± 0.2	8.7 ± 0.3	7.2 ± 0.0	25.3 ± 0.3	19.4 ± 0.1
36.6 ± 0.4	56.5 ± 0.4	2.5 ± 0.1	8.7 ± 0.3	7.2 ± 0.1	24.7 ± 0.3	20.1 ± 0.2
36.1 ± 0.7	48.9 ± 0.3	38.7 ± 0.3	8.6 ± 0.3	6.3 ± 0.2	25.2 ± 0.3	20.1 ± 0.4
38.1 ± 0.2	48.7 ± 0.4	18.7 ± 0.3	11.4 ± 0.3	6.4 ± 0.0	27.7 ± 0.4	22.6 ± 0.4
37.1 ± 0.1	49.5 ± 0.4	2.5 ± 0.2	9.3 ± 0.1	7.1 ± 0.0	26.2 ± 0.2	20.2 ± 0.2
36.9 ± 0.5	58.5 ± 1.1	1.7 ± 1.0	7.8 ± 0.0	7.4 ± 0.1	26.0 ± 0.2	20.9 ± 0.2
37.7 ± 0.8	49.0 ± 0.2	38.9 ± 0.1	8.5 ± 0.0	6.8 ± 0.2	24.7 ± 0.1	21.7 ± 0.3
36.0 ± 0.4	49.1 ± 0.2	19.0 ± 0.3	12.2 ± 0.1	6.4 ± 0.1	27.2 ± 0.4	22.3 ± 0.6

Abbreviations: TDS: total dissolves solids, EC: electrical conductivity, DO: dissolved oxygen, Temp: temperature.

et al. (2022). The Barcoded Universal Primer approach was used for multiplexing 16S amplicons using two rounds of PCR workflow (Supplementary Table S1). The first round used the universal primer-tailed 16S primers (targeting the bacterial 16S rRNA genes) and the PacBio Barcoded Universal Primers were used in the second round (Gueidan et al., 2019). DNA bands of amplified PCR products were clearly shown on agarose gel sizing at base pairs of ≥1100 (Figure 1). A PacBio (www.pacb.com) sequel system was used for sample sequencing. Version 9.0 Single Molecular Real Time (SMRT) link was used for processing raw subreads to produce highly accurate reads. The V-search (https://github.com/torognes/vsearch) was then used to process these highly accurate reads and based on QIMME2 the taxonomic information was determined.

2.4 Accession numbers of nucleotide sequence and phylogenetic sequence analysis

GenBank was used to deposit sequences of novel strains found in this study under accession numbers OP323090, OP323094, and OP323097 for *Chroococcus* sp. and accession numbers OP323093 and OP323094 for *Microcystis aeruginosa*. The alignment of sequences obtained was performed using a program (BioEdit software) for DNA sequencing and a ClustalW (MEGA-X Version 4.0). To validate the origin of cyanobacteria of sequenced samples, NCBI/BLAST (obtainable from http://www.ncbi.nlm.nih.gov/BLAST/) was used for comparison of 16S rRNA gene sequences compiled from available databases with sequences obtained in this study; therefore, these sequences were used to construct phylogenetic trees. The p-distance method (Nei and Kumar, 2000) and the neighbour-joining method (Saitou and Nei, 1987) were used to calculate and construct evolutionary distances and phylogenetic trees, respectively, using 1000 replicates for bootstrap analysis and only bootstrap above 50%. *Bacillus subtilis* strain was used as an out-group taxon when contracting the phylogenetic tree.

2.5 Data analysis

Pearson's correlation coefficient analysis was utilized in the present study to determine the aspects of a linear relationship between various physical and chemical parameters observed during water sample collection.

3 Results

3.1 Physicochemical parameters

The physicochemical parameters that were determined in this study indicated values that met World Health Organization recommended standards for domestic requirements (WHO, 2022). The mean and standard deviation (STDEV) for seven important physicochemical parameters were determined and shown in Table 1. Furthermore, Pearson's correlation analysis was conducted in the present study (Table 2); and this analysis revealed a strong correlation between parameters with values highlighted in blue and further indicated moderate positive

TABLE 2 Relationship between physicochemical parameters determined by the Pearson's correlation analysis (n = 16).

	TDS	EC	Turbidity	DO	pH	Salinity	Temp
TDS	1						
EC	0.339*	1					
Turbidity	−0.134	−0.470	1				
DO	−0.572	−0.571	0.225	1			
pH	0.242	0.481*	−0.794	−0.517	1		
Salinity	−0.452	−0.445	0.137	0.886**	−0.517	1	
Temp	−0.260	−0.550	0.303*	0.678**	−0.470	0.662**	1

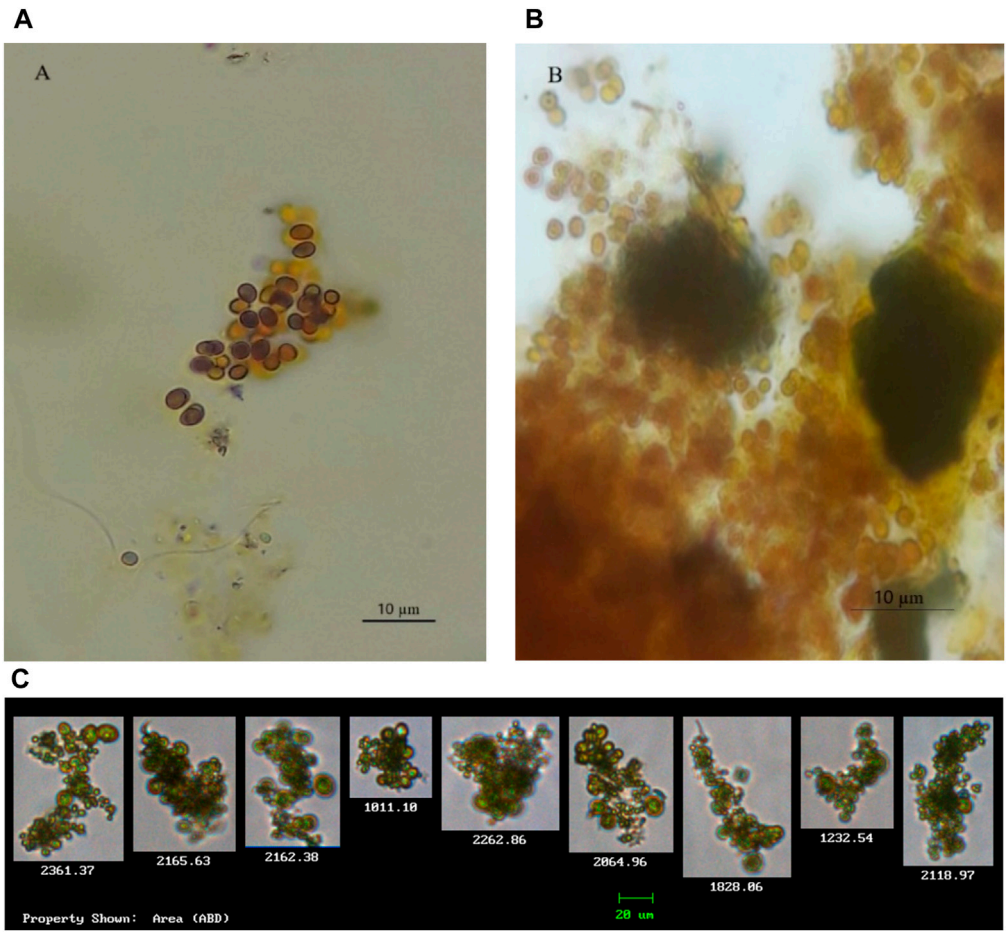

FIGURE 2
Isolated cyanobacterial species and their morphological features. **(A,B)** *Chroococcus* strains (observed with a microscope); **(C)** *Chroococcus* sp. (observed and captured with FlowCAM).

correlations between parameters with values highlighted in orange at a 0.01 level of significance.

3.2 Morphological characterization

Morphological characteristics were used for the identification of two cyanobacteria species *Microcystis* and *Chroococcus*. The isolated *Chroococcus* sp. (Figure 2) was observed as a group of two and/or four cells enclosed with clear and an amorphous mucilage sheath, with each cell having an individual envelope. *Chroococcus* sp. are prokaryotic organisms that have chlorophyll pigment, are unicellular, have a coccus cell shape, and form a mucous membrane (Goshtasbi et al., 2022; Fendiyanto et al., 2023). *Chroococcus* are egg to rod-shaped unicellular algae with a diameter of 0.4–50 µm. It is an autotrophic organism capable of

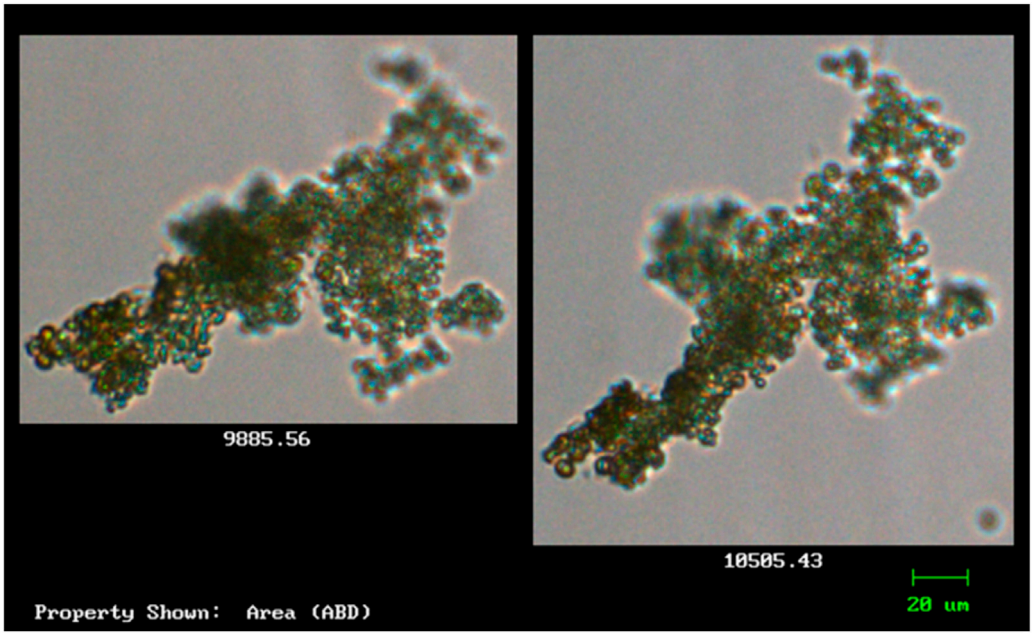

FIGURE 3
The morphological features of the isolated cyanobacteria species *Microcystis* (observed and captured with FlowCAM).

surviving without oxygen. The mucus layers of different colonies stick together so that they can form a biofilm visible to the naked eye. *Chroococcus* sp. is classified as division cyanophyta, class cyanophyceae, order chroococcales, and genus *Chroococcus*. In the new classification system, this species, based on microalgae phylogeny studies by Shayler and Siver (2006), is classified closer to bacteria than other eukaryotic algae organisms (Fendiyanto et al., 2023).

Species with cells that are green in colour and spherical were observed and captured using the FlowCAM. Characteristics of such species resemble that of *Microcystis* (Figure 3). According to Balsooriya (2019), Mutoti et al. (2022), and Thawabteh et al. (2023), cells of this species are spherical and green in colour and strains are classified as large since their diameter varies from 0.5 to 9 µm. They further reported that the cells of *Microcystis* are densely or sparsely, and irregularly arranged with fine and colourless mucilage that sometimes forms a wide margin around the cells. Cells of *Microcystis* are pale-blue–green and are spherical or hemispherical after division, but they appear brownish due to aerotopes that mask the blue–green colour of the protoplast. Due to vacuoles that are found within the cells, when they are viewed through a light microscope, they often have a black appearance (Mutoti et al., 2022).

3.3 Molecular identification of cyanobacteria strains

Sequences of cyanobacteria were targeted by primers set that were adopted in this study to target the 16S rDNA genes. Amongst these, were the sequences that resemble that of *M. aeruginosa* and *Chroococcus* sp. from the order chroococcales with sequences of *Chroococcus* sp. dominating the water samples. Table 3 shows strains of cyanobacteria that could not be identified using morphological characters, instead, were identified using molecular characters performed after culturing and isolation of samples. Sequence homology search performed by use of the BLAST program shows strains of cyanobacteria (Table 3) aligning most confidently to their closest related sequences from the NCBI database. Table 3 shows that strains m64187e-7881, m64187e-2143, and m64187e-0930 were closely related to *Chroococcus* sp. JJCM with percentage similarities of 95%, 96%, and 94%, respectively. On the other hand, cyanobacterial species *M. aeruginosa* NIES-1062 and strain m64187e-6729 had a similarity of 93%. Strain m64187e-1069 and species *M. aeruginosa* NIES-933 were found with a similarity of 93%.

3.4 Phylogenetic analysis

In Figures 4, 5, the neighbour-joining method (Saitou and Nei, 1986) was used to construct the topology of sequences isolated from the present study and their closely related sequences from the NCBI database. The percentage of replicates for the bootstrap test (1000 replicates) is shown next to the branches (Felsenstein, 1985). Five base substitutions for nucleotide positions are represented by the scale bar. An outgroup taxon is shown by red dot.

4 Discussion

This study aimed at detecting and identifying the presence of cyanobacteria strains producing microcystin in drinking water.

TABLE 3 Cyanobacterial strains and their closest species from blast search.

Strain	Closest species	Accession number	Similarity (%)
m64187e-7881	*Chroococcus* sp. JJCM	AM710384.1	95
m64187e-2143	*Chroococcus* sp. JJCM	AM710384.1	96
m64187e-0930	*Chroococcus* sp. JJCM	AM710384.1	94
m64187e-6729	*Microcystis aeruginosa* NIES-1062	KX014841.1	93
m64187e-1069	*Microcystis aeruginosa* NIES-933	LC557455.1	93

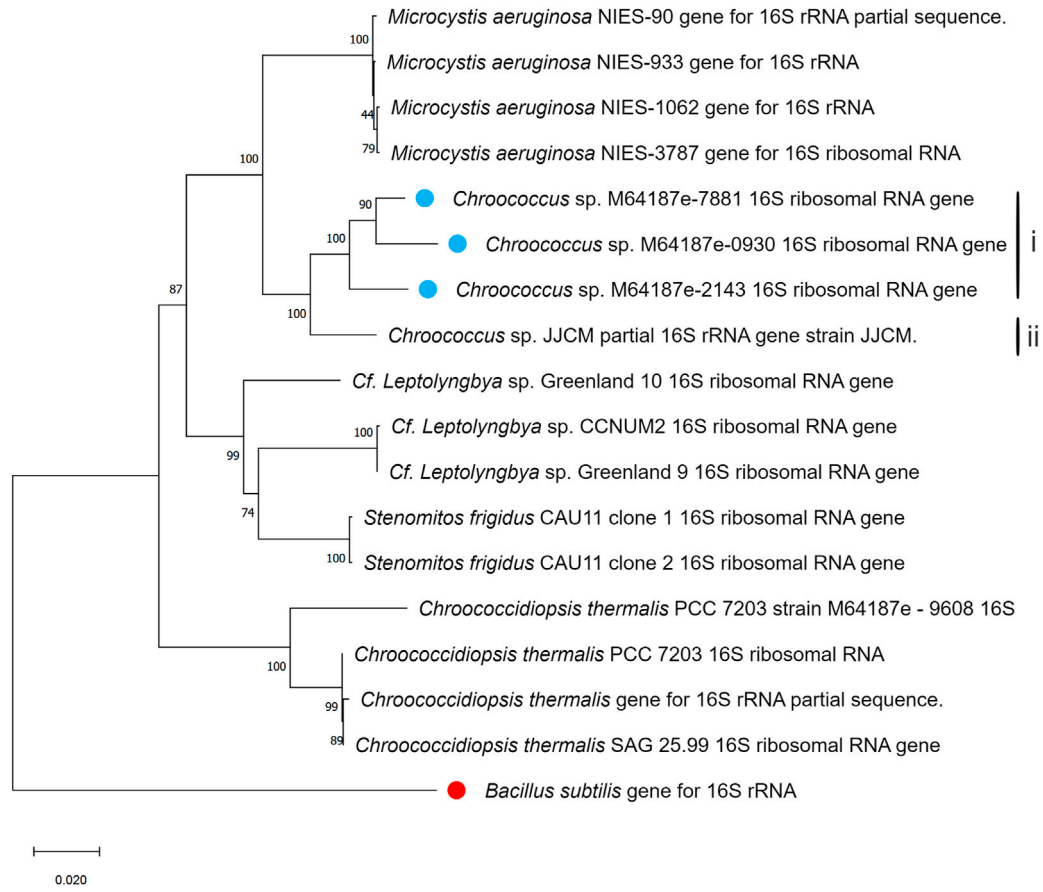

FIGURE 4
Phylogenetic tree of isolated *Chroococcus* sp. based on sequences isolated from the present study and sequences of its neighbouring species from the NCBI database. The tree was calculated using a maximum-likelihood algorithm with the bootstrap values given at the nodes. The cyanobacterial strains from the current study are indicated by a blue dot.

Leica DM3000 Semi-Automated Laboratory Microscope and FlowCAM were used for morphological characterization of cyanobacteria species detected in the present study. Captured images of cyanobacterial species were identified through comparison based on available literature. Cyanobacteria species (*Microcystis* and *Chroococcus*) from order Chroococcales were detected and identified, showing diverse morphological characteristics and phylogenetic relationships. Their morphological characteristics resemble that of Balsooriya (2019); Wang et al. (2021); Fendiyanto et al. (2023). Moreover, further morphological description of *Chroococcus* sp. in the present study was also consistent with previous descriptions by Balasooriya (2019); Goshtasbi et al. (2022). In a study conducted by Fendiyanto et al. (2023) in Dramaga Bogor, water samples were collected from freshwater found in high and low light-intensity environments. In their study, they aimed to identify the morphological diversity level of microalgae-based on their environment (high light and low light environment). Their results indicated that cyanobacterial species *Chroococcus* and *Microcystis* from order chroococcales were found among the most dominating species in freshwater samples collected from high-light intensity environment. They concluded that light was the main environmental factor influencing the growth and production

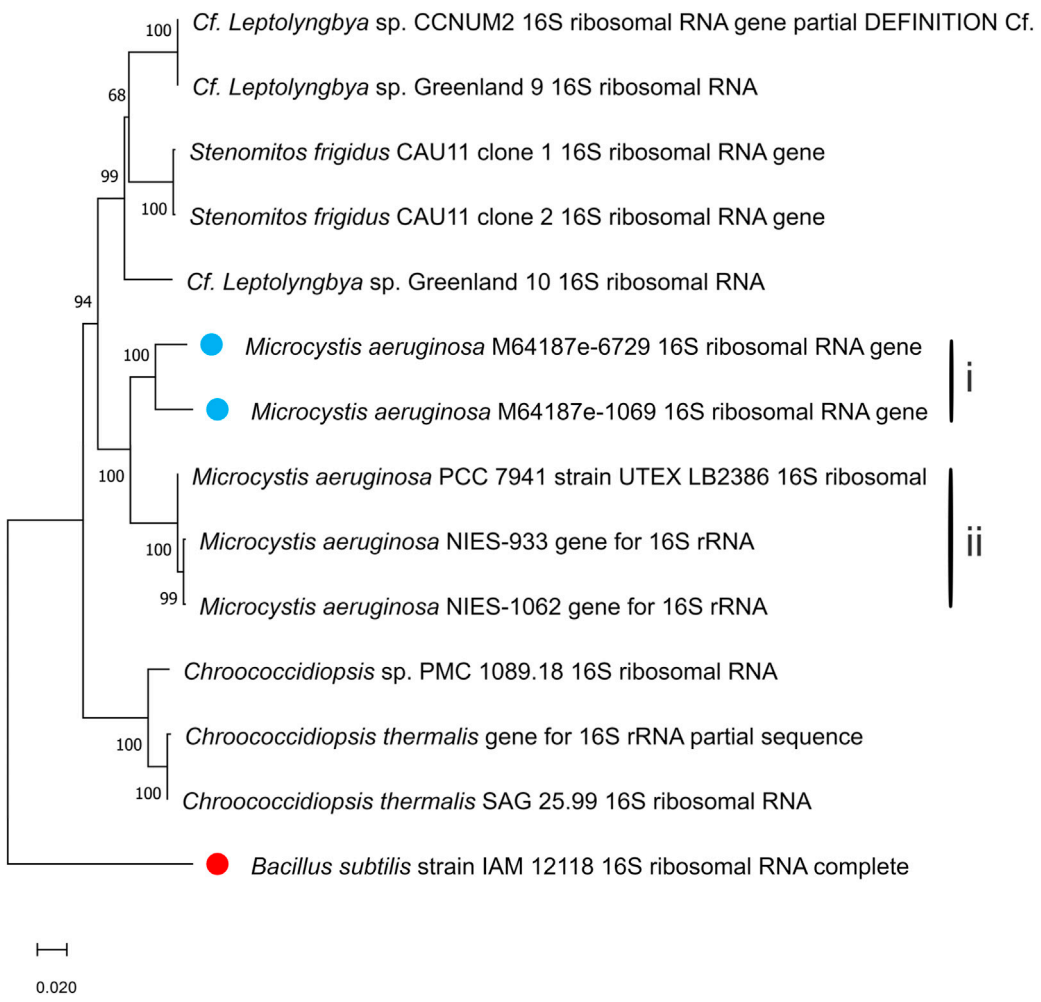

FIGURE 5
Phylogenetic tree of isolated *Microcystis aeruginosa* based on sequences isolated from the present study and sequences of its neighbouring species from the NCBI database. The tree was calculated using a maximum-likelihood algorithm with the bootstrap values given at the nodes. The cyanobacterial strains from the current study are indicated by a blue dot.

of these microalgae in freshwater, posing a threat to humans and the aquatic environment.

In addition, the BLAST program (NCBI) was further utilized in the present study to search for strains of cyanobacteria, which are closely related to the strains of cyanobacteria found in this study. The BLAST search confirmed that the stains of cyanobacteria found in this study were closely related to species of cyanobacteria that have the potential to produce microcystins, such as *Microcystis* and *Chroococcus* (Mirazbekov et al., 2021). Borowitzka (2018) reported that the genus *Microcystis* contains several toxins-producing species, with *M. aeruginosa* being the best-known and globally distributed. They further highlighted that microcystins produced by *Microcystis* are a family of monocyclic heptapeptides with a characteristic feature, the unusual β-amino acid, Adda (3-amino-9-methoxy-2,6,8-trimethyl-10-phenyldeca-4E,6E-dienoic acid). Numerous research studies that have been conducted previously have reported on microcystins released by *Microcystis* and *Chroococcus* species in freshwater bodies. A review study by Chia et al. (2022) reports on the presence of potentially toxic *Microcystis* strains in natural lakes found in the Middle Atlas Mountains in Morocco. In their study, they detected microcystin synthetase *mcy* genes using PCR. They further reported a study that characterized 27 potentially toxic cyanobacterial strains including *Microcystis* from seven reservoirs in Tunisia, which also detected microcystin synthetase *mcy* cluster (*mcy*A, -B, -C, -D, -E, and -G). Apart from these findings, there are numerous studies that have been conducted previously across the world and have reported on microcystins-producing cyanobacteria in drinking water (Table 4).

In humans, exposure to low doses of microcystin may lead to liver and kidney failure (Mutoti et al., 2022; Chia et al., 2022); on the other hand, exposure to high doses may lead to immediate liver necrosis and intrahepatic hemorrhage (Chia et al., 2022). Therefore, understanding the potential health effects of microcystins exposure underscore the importance of implementing comprehensive measures to prevent and minimize the presence of these toxins in drinking water. Hence, standards that serve as benchmarks for water quality management have been established by regulatory agencies and health organizations such as WHO and DWS

TABLE 4 Cyanobacterial species responsible for the production of microcystins in water.

Microcystin-producing species	References
Eucapsis sp.	Mioni et al. (2011)
Oscillatoria sp.	Christoffersen and Kaas (2010); Mohamed (2016)
Leptolyngbya sp.	Frazão et al. (2010); Somdee et al. (2013)
Pseudanabaena sp.	Borges et al. (2015); Wiltsie et al. (2018); Graham et al. (2020)
Nostoc sp.	Graham et al. (2020); Ivanov et al. (2021)
Phormidium sp.	Graham et al. (2020); Wood et al. (2017)

(Mutoti et al., 2022; Mutoti et al., 2022). Maximum permissible levels of microcystins in portable water have been established to protect consumers from the potential health risks associated with these toxins (WHO, 2017). They safe guide public health and ensure the quality of water supplies. Moreover, these standards guide the implementation of monitoring and treatment measures to mitigate microcystin contamination.

Furthermore, sequences of different nucleotides together with those observed in the present study were utilized for the construction of the phylogenetic trees, where *B. subtilis* strain was included as an external group. The phylogenetic trees generated based on 16S rDNA displayed the phylogenetic position of the strains among their closely related cyanobacteria (Figures 4, 5). According to the phylogenetic tree in Figure 4, the maximum likelihood tree of the 16S rDNA sequences showed a tight cluster of *Chroococcus* sp. strains separated from all the other strains of the order chroococcales included in the present study. The whole cluster was supported by a bootstrap value of 100%. Two separate sub-clusters within the *Chroococcus* sp. cluster could be distinguished in the phylogenetic tree (Figure 4). The first cluster (I) comprised the strains m64187e-7881, m64187e-2143, and m64187e-0930, and the second cluster (II), which was separated from cluster I comprised *Chroococcus* sp. JJCM. Cluster I was supported by a bootstrap value of 100%. All the strains within cluster I, that is, m64187e-7881 (now referred to as *Chroococcus* sp. M64187e-7881 16S ribosomal RNA gene), m64187e-2143 (now referred to as *Chroococcus* sp. M64187e-2143 16S ribosomal RNA gene), and m64187e-0930 (now referred to as *Chroococcus* sp. M64187e-0930 16S ribosomal RNA gene) showed identical 16S rDNA sequences similarities of 94%–95% with strain *Chroococcus* sp. JJCM (with accession number AM710384) in cluster II isolated from the freshwater reservoir in South Bohemia (Jezberova, 2006).

Another tight cluster of *M. aeruginosa* is shown by the maximum likelihood three of the 16S rDNA sequences in Figure 5, supported by a bootstrap of 100%. Figure 5 also distinguished two separated clusters within the *Microcystis* cluster, with cluster I comprising strains m64187e-6729 and m64187e-1069, and cluster II comprising three different strains of *M. aeruginosa*; that is, *M. aeruginosa* PCC 7941, *M. aeruginosa* NIES-933, and *M. aeruginosa* NIES-1062. Both cluster I and II were supported by 100% bootstrap. Strain m64187e-6729 (thereafter called *M. aeruginosa* M64187e-6729 16S ribosomal RNA gene) had identical 16S rDNA sequences similarities of 93% with strain *M. aeruginosa* NIES-1062 gene (KX014841) isolated from farm ponds in USA by Yuan et al. (2020). Moreover, another identical 16S rDNA sequence similarity of 93% was observed between strain m64187e-1069 (thereafter called *M. aeruginosa* M64187e-1069 16S ribosomal RNA gene) and strain *M. aeruginosa* NIES-933 gene (LC557455) isolated from Japan by Suzuki et al. (2022).

5 Conclusion

In conclusion, this study has successfully identified and characterized two microcystin-producing cyanobacteria, *M. aeruginosa* and *Chroococcus* sp., isolated from drinking water samples in Mawoni village, South Africa. Utilizing a polyphasic approach combining morphological and molecular techniques, we employed FlowCAM imaging and PCR analysis to confirm the presence of these cyanobacteria species, which gave positive results for the identification and classification of members of the genus from the order Chroococcales, supported by BLAST analysis and phylogenetic tree construction. Notably, this study reports for the first time the presence of these biofilm-producing strains in drinking water, highlighting potential health risks associated with stored water. The findings of this study suggest that the potential for treated water stored in storage containers to support a range of toxic cyanobacteria may currently be underestimated, and therefore, isolation and screening of more cultured strains from treated water is required to further investigate the diversity of toxin-producing cyanobacteria. As such, future research should prioritize the analysis of microcystin synthetase genes and quantification of microcystins in potable water to assess health risks accurately. This approach could lead to improved monitoring and management strategies for cyanobacterial toxins in drinking water supplies. By focusing on these advancements, researchers and public health authorities can better safeguard water quality and protect community health. Furthermore, future research should also be focused on conducting cytotoxicity studies in these microcystin-producing species and more experimental studies to understand the detailed change in microbial diversity considering the variation in temperature and pH range in freshwater.

Data availability statement

The datasets presented in this study can be found in online repositories. The names of the repository/repositories and accession number(s) can be found below: https://www.ncbi.nlm.nih.gov/, OP323090, OP323093, OP323097, OP323100, and OP323094.

Author contributions

MM: Conceptualization, Data curation, Formal Analysis, Funding acquisition, Methodology, Validation, Writing–original draft, Writing–review and editing. JG: Conceptualization,

Methodology, Project administration, Resources, Supervision, Validation, Writing–review and editing. AK: Data curation, Formal Analysis, Methodology, Validation, Writing–review and editing. AJ: Conceptualization, Formal Analysis, Supervision, Validation, Writing–review and editing.

Funding

The author(s) declare that financial support was received for the research, authorship, and/or publication of this article. This research was funded by the National Research Foundation (South Africa) through a Doctoral scholarship, grant number UID 102072.

Acknowledgments

The authors thank the National Research Foundation for funding this project through Doctoral Scholarship (UID 102072) for MM.

Conflict of interest

The authors declare that the research was conducted in the absence of any commercial or financial relationships that could be construed as a potential conflict of interest.

Publisher's note

All claims expressed in this article are solely those of the authors and do not necessarily represent those of their affiliated organizations, or those of the publisher, the editors and the reviewers. Any product that may be evaluated in this article, or claim that may be made by its manufacturer, is not guaranteed or endorsed by the publisher.

Supplementary material

The Supplementary Material for this article can be found online at: https://www.frontiersin.org/articles/10.3389/fenvs.2024.1423339/full#supplementary-material

References

Anagnostidis, K., and Komárek, J. (1990). Modern approach to the classification system of the cyanophytes: stigonematales. *Algol. Stud.* 86, 1–74.

Balasooriya, B. L. W. K. (2019). *Culture collection of cyanobacteria and microalgae at department of biotechnology wayamba university of Sri Lanka*. Sri Lanka: Nethwin Printers Kandy. 978-624-5327-00-3.

Borges, H. L., Branco, L. H., Martins, M. D., Lima, C. S., Barbosa, P. T., Lira, G. A., et al. (2015). Cyanotoxin production and phylogeny of benthic cyanobacterial strains isolated from the northeast of Brazil. *Harmful Algae* 43, 46–57. doi:10.1016/j.hal.2015.01.003

Borowitzka, M. A., Schembri, M. A., Baker, P. D., and Saint, C. P. (2018). Molecular characterization of the toxic cyanobacterium Cylindrospermopsis raciborskii and design of a species-specific PCR. *Appl. Environ. Microbiol.* 66, 332–338. doi:10.1128/aem.66.1.332-338.2000

Carmichael, W. W., Billing, L. M., Blais, S., Hyde, J. B., Masonbrink, L. M., Palmer, M., et al. (2013). *Human health effects from harmful algal blooms: a synthesis submitted by the HPAB to the International Joint Commission*. Ottawa, Canada: International Joint Commission.

Chen, L., Giesy, J. P., Adamovsky, O., Svirčev, Z., Meriluoto, J., Codd, G. A., et al. (2021). Challenges of using blooms of Microcystis spp. in animal feeds: a comprehensive review of nutritional, toxicological and microbial health evaluation. *Sci. Total Environ.* 764, 142319. doi:10.1016/j.scitotenv.2020.142319

Chia, M. A., Ameh, I., George, K. C., Balogun, E. O., Akinyemi, S. A., and Lorenzi, A. S. (2022). Genetic diversity of microcystin producers (cyanobacteria) and microcystin congeners in aquatic resources across africa: a review paper. *Toxics* 10, 772. doi:10.3390/toxics10120772

Christoffersen, K., and Kaas, H. (2010). Toxic cyanobacteria in water. A guide to their public health consequences, monitoring and management. *Limnol. Oceanogr.* 45, 1212. doi:10.4319/lo.2000.45.5.1212

Dai, R., Wang, P., Jia, P., Zhang, Y., Chu, X., and Wang, Y. (2016). A review on factors affecting microcystins production by algae in aquatic environments. *World J. Microbiol. Biotechnol.* 32, 51–57. doi:10.1007/s11274-015-2003-2

Drobac, D., Tokodi, N., Simeunović, J., Baltić, V., Stanić, D., and Svirčev, Z. (2013). Human exposure to cyanotoxins and their effects on health. *Arh. za Hig. rada i Toksikol.* 64, 305–316. doi:10.2478/10004-1254-64-2013-2320

Farrer, D., Counter, M., Hillwig, R., and Cude, C. (2015). Health-based cyanotoxin guideline values allow for cyanotoxin-based monitoring and efficient public health response to cyanobacterial blooms. *Toxins* 7 (2), 457–477. doi:10.3390/toxins7020457

Felsenstein, J. (1985). Confidence limits on phylogenies: an approach using the bootstrap. *evolution* 39, 783–791. doi:10.2307/2408678

Fendiyanto, M. H., Pratami, M. P., Satrio, R. D., Nikmah, I. A., Sari, P., Intan, N., et al. (2023). Species diversity of freshwater microalgae in Dramaga, bogor based on morpho-ecological identification between low and high light intensity environment. *Jordan J. Biol. Sci.* 16.

Frazão, B., Martins, R., and Vasconcelos, V. (2010). Are known cyanotoxins involved in the toxicity of picoplanktonic and filamentous North Atlantic marine cyanobacteria? *Mar. Drugs* 8 (6), 1908–1919. doi:10.3390/md8061908

Goshtasbi, H., Atazadeh, E., and Movafeghi, A. (2022). Polyphasic study of three cyanobacteria species from Kani Barazan international wetland in the northwest of Iran using morphological, molecular, biochemical, and bioinformatics approaches. *Biologia.* 77, 503–516. doi:10.1007/s11756-021-00940-5

Graham, J. L., Dubrovsky, N. M., Foster, G. M., King, L. R., Loftin, K. A., Rosen, B. H., et al. (2020). Cyanotoxin occurrence in large rivers of the United States. *Inland Waters* 10 (1), 109–117. doi:10.1080/20442041.2019.1700749

Gueidan, C., Elix, J. A., McCarthy, P. M., Roux, C., Mallen-Cooper, M., and Kantvilas, G. (2019). PacBio amplicon sequencing for metabarcoding of mixed DNA samples from lichen herbarium specimens. *MycoKeys* 53, 73–91. doi:10.3897/mycokeys.53.34761

Ivanov, D., Yaneva, G., Potoroko, I., and Ivanova, D. G. (2021). Contribution of cyanotoxins to the ecotoxicological role of lichens. *Toxins* 13 (5), 321. doi:10.3390/toxins13050321

Jezberová, J. (2006). *Phenotypic diversity and phylogeny of picocyanobacteria in mesotrophic and eutrophic freshwater reservoirs investigated by a cultivation-dependent polyphasic approach*. Czechia: University of Bohemia.

Jia, Y., Huang, Y., Ma, J., Zhang, S., Liu, J., Li, T., et al. (2024). Toxicity of the disinfectant benzalkonium chloride (C14) towards cyanobacterium Microcystis results from its impact on the photosynthetic apparatus and cell metabolism. *J. Environ. Sci.* 135, 198–209. doi:10.1016/j.jes.2022.11.007

Komárek, J. (2013). "Cyanoprokaryota and heterocytous genera," in *Freshwater flora of central europe*. Editors B. Büdel, G. Gärtner, L. Krienitz, and M. Schagerl (Berlin, Heidelberg: Springer Spektrum).

Komárek, J. (2020). *Quo vadis*, taxonomy of cyanobacteria. *Fottea* 20, 104–110. doi:10.5507/fot.2019.020

Komárek, J., Kaštovský, J., Mareš, J., and Johansen, J. R. (2014). Taxonomic classification of cyanoprokaryotes (cyanobacterial genera) 2014, using a polyphasic approach. *Preslia* 86, 295–335.

Lad, A., Breidenbach, J. D., Su, R. C., Murray, J., Kuang, R., Mascarenhas, A., et al. (2022). As we drink and breathe: adverse health effects of microcystins and other harmful algal bloom toxins in the liver, gut, lungs and beyond. *Life* 12 (3), 418. doi:10.3390/life12030418

Lee, E., Khurana, M. S., Whiteley, A. S., Monis, P. T., Bath, A., Gordon, C., et al. (2017). Novel primer sets for next generation sequencing-based analyses of water quality. *PLoS One* 12, e0170008. doi:10.1371/journal.pone.0170008

Li, S. C., Gu, L. H., Wang, Y. F., Wang, L. M., Chen, L., Giesy, J. P., et al. (2024). A proteomic study on gastric impairment in rats caused by microcystin-LR. *Sci. Total Environ.* 917, 169306. doi:10.1016/j.scitotenv.2023.169306

Lim, C. C., Yoon, J., Reynolds, K., Gerald, L. B., Ault, A. P., Heo, S., et al. (2023). Harmful algal bloom aerosols and human health. *EBioMedicine* 93, 104604. doi:10.1016/j.ebiom.2023.104604

Magonono, M., Oberholster, P. J., Shonhai, A., Makumire, S., and Gumbo, J. R. (2018). The presence of toxic and non-toxic cyanobacteria in the sediments of the Limpopo River Basin: implications for human health. *Toxins* 10, 269. doi:10.3390/toxins10070269

Meirkhanova, A., Zhumakhanova, A., Len, P., Schoenbach, C., Levi, E. E., Jeppesen, E., et al. (2023). Dynamics of associated microbiomes during algal bloom development: to see and to be seeing. *bioRxiv*, 2023–2109.

Melaram, R., Newton, A. R., and Chafin, J. (2022). Microcystin contamination and toxicity: implications for agriculture and public health. *Toxins* 14, 350. doi:10.3390/toxins14050350

Mioni, C., Kudela, R., Baxa, D., Sullivan, M., Hayashi, K., Smythe, U. T., et al. (2011). Harmful cyanobacteria blooms and their toxins in clear lake and the sacramento-san joaquin delta (California). *Delta (California)* 10, 058–150.

Mirasbekov, Y., Abdimanova, A., Sarkytbayev, K., Samarkhanov, K., Abilkas, A., Potashnikova, D., et al. (2021). Combining imaging flow cytometry and molecular biological methods to reveal presence of potentially toxic algae at the Ural River in Kazakhstan. *Front. Mar. Sci.* 8, 680482. doi:10.3389/fmars.2021.680482

Mohamed, Z. A. (2016). Breakthrough of Oscillatoria limnetica and microcystin toxins into drinking water treatment plants-examples from the Nile River, Egypt. *Water sa.* 42 (1), 161–165. doi:10.4314/wsa.v42i1.16

Mutoti, M., Gumbo, J., and Jideani, A. I. (2022a). Occurrence of cyanobacteria in water used for food production: a review. *Phys. Chem. Earth* 125, 103101. doi:10.1016/j.pce.2021.103101

Mutoti, M. I., Jideani, A. I., and Gumbo, J. R. (2022b). Using FlowCam and molecular techniques to assess the diversity of Cyanobacteria species in water used for food production. *Sci. Rep.* 12, 18995. doi:10.1038/s41598-022-23818-1

Nei, M., and Kumar, S. (2000). *Molecular evolution and phylogenetics*. Oxford University Press.

Nowruzi, B., Becerra-Absalón, I., and Metcalf, J. S. (2023). A novel microcystin-producing cyanobacterial species from the genus desmonostoc, desmonostoc alborizicum sp. nov., isolated from a water supply system of Iran. *Curr. Microbiol.* 80, 49. doi:10.1007/s00284-022-03144-5

O'Keeffe, J. (2019). *Cyanobacteria and drinking water: occurrence, risks, management and knowledge gaps for public health*. Vancouver, BC, Canada: National Collaborating Centre for Environmental Health.

Pearson, L., Mihali, T., Moffitt, M., Kellmann, R., and Neilan, B. (2010). On the chemistry, toxicology and genetics of the cyanobacterial toxins, microcystin, nodularin, saxitoxin and cylindrospermopsin. *Mar. Drugs.* 8, 1650–1680.

Saitou, N., and Nei, M. (1987). The neighbor-joining method: a new method for reconstructing phylogenetic trees. *Mol. Biol. Evol.* 4, 406–425. doi:10.1093/oxfordjournals.molbev.a040454

Sarma, T. A. (2013). *Cyanobacterial toxins. In: Handbook of Cyanobacteria*. Boca Raton, FL: CRC Press, Taylor and Francis Group, 487–606.

Shayler, H. A., and Siver, P. A. (2006). Key to Freshwater Algae: a web-based tool to enhance understanding of microscopic biodiversity. *J. Sci. Educ. Technol.* 15, 298–303. doi:10.1007/s10956-006-9016-4

Somdee, T., Kaewsan, T., and Somdee, A. (2013). Monitoring toxic cyanobacteria and cyanotoxins (microcystins and cylindrospermopsins) in four recreational reservoirs (Khon Kaen, Thailand). *Environ. Monit. Assess.* 185, 9521–9529. doi:10.1007/s10661-013-3270-8

Suzuki, S., Yamaguchi, H., and Kawachi, M. (2022) Potential genetic diversity of synechococcus-related strains maintained in the microbial culture collection of the national institute for environmental studies, Japan. Microbial resources and systematics, 38, 63–74.

Thawabteh, A. M., Naseef, H. A., Karaman, D., Bufo, S. A., Scrano, L., and Karaman, R. (2023). Understanding the risks of diffusion of cyanobacteria toxins in rivers, lakes, and potable water. *Toxins* 15, 582. doi:10.3390/toxins15090582

Usman, A. S., Merican, F., Zaki, S., Broady, P., Convey, P., and Muangmai, N. (2022). Microcystin production by oscillatorialean cyanobacteria isolated from cryopreserved Antarctic mats. *Harmful algae*. 120, 102336. doi:10.1016/j.hal.2022.102336

Valadez-Cano, C., Hawkes, K., Calvaruso, R., Reyes-Prieto, A., and Lawrence, J. (2022). Amplicon-based and metagenomic approaches provide insights into toxigenic potential in understudied Atlantic Canadian lakes. *Facets* 7, 194–214. doi:10.1139/facets-2021-0109

van Vuuren, S. J., Taylor, J., Gerber, A., and van Ginkel, C. (2006) "Easy identification of the most common freshwater algae. A guide for the identification of microscopic algae in South African freshwater," in *Brendan hohls: resource quality services*.

Wang, X., Luo, Y., Zhang, S., and Zhou, L. (2024). Acetylacetone effectively controlled the secondary metabolites of Microcystis aeruginosa under simulated sunlight irradiation. *J. Environ. Sci.* 135, 285–295. doi:10.1016/j.jes.2022.12.004

Wang, Y., Jia, N., Geng, R., Yu, G., and Li, R. (2021). Phylogenetic insights into chroococcus-like taxa (Chroococcales, Cyanobacteria), describing Cryptochroococcus tibeticus gen. nov. sp. nov. and Limnococcus fonticola sp. nov. from Qinghai-Tibet plateau. *J. Phycol.* 57, 1739–1748. doi:10.1111/jpy.13205

Welten, R. D., Meneely, J. P., and Elliott, C. T. (2020). A comparative review of the effect of microcystin-LR on the proteome. *Expo. Health* 12, 111–129. doi:10.1007/s12403-019-00303-1

Willis, A., and Woodhouse, J. N. (2020). Defining cyanobacterial species: diversity and description through genomics. *Crit. Rev. Plant Sci.* 39, 101–124. doi:10.1080/07352689.2020.1763541

Wilson, K. M., Schembri, M. A., Baker, P. D., and Saint, C. P. (2000). Molecular characterization of the toxic cyanobacterium Cylindrospermopsis raciborskii and design of a species-specific PCR. *Appl. Environ. Microbiol.* 66, 332–338. doi:10.1128/aem.66.1.332-338.2000

Wiltsie, D., Schnetzer, A., Green, J., Borgh, M. V., and Fensin, E. (2018). Algal blooms and cyanotoxins in Jordan Lake, North Carolina. *Toxins* 10, 92. doi:10.3390/toxins10020092

Wood, S. A., Puddick, J., Fleming, R., and Heussner, A. H. (2017). Detection of anatoxin-producing Phormidium in a New Zealand farm pond and an associated dog death. *N. Z. J. Bot.* 55 (1), 36–46. doi:10.1080/0028825x.2016.1231122

World Health Organization (WHO) (2017). *Guidelines for drinking-water quality: fourth edition incorporating the first addendum*. Geneva: World Health Organization.

World Health Organization (WHO) (2022). *Guidelines for drinking-water quality: fourth edition incorporating the first and second addenda*. Geneva: CC BY-NC-SA 3.0 IGO. License.

Yuan, J., Kim, H. J., Filstrup, C. T., Guo, B., Imerman, P., Ensley, S., et al. (2020). Utility of a PCR-based method for rapid and specific detection of toxigenic Microcystis spp. in farm ponds. *J. Veterinary Diagnostic Investigation* 32, 369–381. doi:10.1177/1040638720916156

frontiers | Frontiers in Environmental Science

TYPE Original Research
PUBLISHED 06 August 2024
DOI 10.3389/fenvs.2024.1404230

Check for updates

OPEN ACCESS

EDITED BY
Visva Bharati Barua,
University of North Carolina at Charlotte,
United States

REVIEWED BY
Sol Park,
FAMU-FSU College of Engineering,
United States
Kiran Kumar Vadde,
University of Texas at San Antonio, United States

*CORRESPONDENCE
Rommel Thiago Juca Ramos,
rommelramos@ufpa.br

†These authors have contributed equally to this work and share first authorship

RECEIVED 20 March 2024
ACCEPTED 15 July 2024
PUBLISHED 06 August 2024

CITATION
Cardenas-Alegria OV, Ferreira VBC, Noguera WG, Martins DT, Martins Neto AP, Monteiro Pontes PR, Lopes Cavalcante RB, Aguiar Alves SI, Luiz da Costa da Silva A, Gomes Costa R, Franco de Los Santos EF, Azevedo VAdC and Ramos RTJ (2024), Microbiome analyses of the Uraim River in the Amazon and georeferencing analyses to establish correlation with anthropogenic impacts of land use.
Front. Environ. Sci. 12:1404230.
doi: 10.3389/fenvs.2024.1404230

COPYRIGHT
© 2024 Cardenas-Alegria, Ferreira, Noguera, Martins, Martins Neto, Monteiro Pontes, Lopes Cavalcante, Aguiar Alves, Luiz da Costa da Silva, Gomes Costa, Franco de Los Santos, Azevedo and Ramos. This is an open-access article distributed under the terms of the Creative Commons Attribution License (CC BY). The use, distribution or reproduction in other forums is permitted, provided the original author(s) and the copyright owner(s) are credited and that the original publication in this journal is cited, in accordance with accepted academic practice. No use, distribution or reproduction is permitted which does not comply with these terms.

Microbiome analyses of the Uraim River in the Amazon and georeferencing analyses to establish correlation with anthropogenic impacts of land use

Oscar Victor Cardenas-Alegria[1,2†], Victor Benedito Costa Ferreira[1,2†], Wylerson Guimarães Noguera[3], David Tavares Martins[1,2], Artur Pedro Martins Neto[1], Paulo Rógenes Monteiro Pontes[4], Rosane Barbosa Lopes Cavalcante[4], Sandy Ingrid Aguiar Alves[1,2], Artur Luiz da Costa da Silva[5], Rosilene Gomes Costa[6,7], Edian Franklin Franco de Los Santos[8], Vasco Ariston de Carvalho Azevedo[3,9] and Rommel Thiago Juca Ramos[1,2,3]*

[1]Laboratory of Bioinformatics and Genetic of Microorganisms, Institute of Biological Sciences, Federal University of Pará, Belem, Brazil, [2]Postgraduate Program in Bioinformatics, Institute of Biological Sciences, Federal University of Minas Gerais, Belo Horizonte, Brazil, [3]Vale Institute of Technology - Sustainable Development, Belem, Brazil, [4]Vale Institute of Technology, Sustainable Development, Belém, Brazil, [5]Institute of Biological Sciences, Federal University of Pará, Belém, Brazil, [6]Paragominas Sanitation Agency, Paragominas, Brazil, [7]Natural Products Engineering Laboratory, Federal University of Pará, Belém, Brazil, [8]Technological University of Santiago, Santo Domingo, Dominican Republic, [9]Bacterial Disease Laboratory, Postgraduate Program in Animal Science in Tropics, Federal University of Bahia, Salvador, Brazil

One of the primary challenges in the spread of infectious diseases is the consumption of poorly or untreated water, which is increasingly being used due to the growth of different human activities and the effect of urbanization on freshwater sources, which are often used for consumption purposes. The determination of pathogenic bacteria in freshwater rivers influenced by anthropogenic activities allows for the assessment of the impact these factors have on water quality. Thus, the purpose of this study was to identify the diversity of pathogenic bacteria and virulence genes in the Uraim River in the northern region of Brazil. For this purpose, surface water was collected from five points with varying degrees of anthropogenic impact along the Uraim River. *In situ* measurements of physicochemical components were conducted, and metagenomic analysis was used for the identification of pathogenic bacteria and virulence genes. Regarding the physicochemical parameters, variability was observed among the different analysis points, as well as diversity among bacteria and virulence genes. Notably, enterobacteria and the ESKAPE group were highlighted among the bacteria, with significant negative associations found between dissolved oxygen and the diversity of virulence genes and between deforestation and population density with the presence of ESKAPE group bacteria.

KEYWORDS

anthropogenic activity, microbial diversity, bacterial pathogens, virulence genes, Uraim River

1 Introduction

Global estimates suggest that 80% of industrial and municipal wastewater is discharged into the environment without prior treatment, leading to adverse effects on human health and ecosystems. This is particularly prevalent in less developed countries due to deficiencies in sanitation and wastewater treatment facilities (Lin et al., 2022).

However, water pollution primarily occurs due to industrialization, agricultural activities, natural factors, inadequate water supply, and inadequate sewage treatment facilities. According to the UNESCO World Water Development Report 2021, approximately 829,000 people die each year from diarrhea caused by the consumption of unsafe water due to lack of basic sanitation, including nearly 300,000 children under the age of five, accounting for 5.3% of all deaths in this age group (Lin et al., 2022).

On the other hand, urbanization worldwide is rapidly progressing. From 1950 to 2020, the global population living in cities increased from 0.8 billion (29.6%) to 4.4 billion (56.2%), and it is projected to reach 6.7 billion (68.4%) by 2050. A key issue is water scarcity, a critical aspect of water security that directly impacts the health and wellbeing of urban residents, urban environmental quality, and socioeconomic development (He et al., 2021; Strokal et al., 2021).

Freshwater is a finite natural resource essential for life on Earth. It is crucial for urban, agricultural, and industrial activities, as well as providing a habitat for a rich diversity of macro and microorganisms. However, anthropogenic activities, climate change, and a growing global population pose threats to its quality and availability worldwide (Pandey et al., 2014; Chopyk et al., 2020).

While the monitoring of bacterial indicator organisms (e.g., *Escherichia coli*) is widely standardized, waterborne viral and protozoan pathogens remain poorly characterized (Ko et al., 2022). A better understanding of the transport of pathogens from agricultural or urban areas to rivers is a major challenge. Many environmental changes caused by anthropogenic activities have a direct impact on water resource development, climate warming, and interactions between humans and animals, both domestic and wild. These factors promote the dissemination and diversification of pathogenic microorganisms (Pandey et al., 2014). Additionally, the use of various chemicals to ensure production serves as selective components for microbial adaptation, potentially altering ecosystem composition (Schwarzenbach et al., 2010).

In the northern region of Brazil, specifically in the Amazon part, there is significant macro-diversity, and it is made up of various bodies of water. In the state of Pará, the municipality of Paragominas is characterized by two main rivers: the Paragominas River and the Uraim River, the latter belonging to the Northeast Atlantic Western hydrographic region and the Gurupi hydrographic sub-region (Agência Nacional de Águas, 2020), the hydrographic basin is mixed, covering the urban and rural areas of the municipality, has a drainage area of 4,873 km^2, a length of the main river of 129.5613 km and a circular shape (Correa, 2017).

Over the past 20 years, these areas have been utilized for diverse agricultural activities, as seen in the municipality of Paragominas. The latter drains the city center towards the northwest and serves as the primary water source for distribution to the population through water acquisition stations (Pereira Júnior et al., 2023a). However, studies carried out in this region are scarce; the few accessible works were on the characterization of physical and chemical characteristics, diatom studies, and geoprocessing analyses (Santos and Picanço, 2008; De Araujo, 2010; Giuliatti et al., 2017; Da Silva et al., 2020), no studies are using metagenomic analysis in the region. In this context, this study aims to identify the diversity of pathogenic bacteria and virulence genotypes in the Uraim River and their relationship with anthropogenic activities.

2 Materials and methods

2.1 Samples

The samples were obtained from the Uraim River in September 2022, which flows through Paragominas. Five sampling points were selected based on varying levels of anthropogenic impact: P1 (P1A, P1B, P1C), P2 (P2A, P2B, P2C), P3 (P3A, P3B, P3C), P4 (P4A, P4B, P4C), and P5 (P5A, P5B, P5C), were collected 1 m away from the banks and in the center of the river for each point. Three biological replicates were collected at each point, and fifteen samples were obtained from all points.

The point P1 was located in an untouched, pristine site, while the final point (P5) was located downstream after passing through the city. The remaining points were intermediate between these two extremes. The samples were collected at a depth of 20 cm, with a volume of 5L taken at each point in triplicate, with help from a Van Dorn bottle. They were preserved on ice and immediately transported to the laboratory. Upon arrival, the water samples were filtered using a negative pressure filtration system with the assistance of a vacuum pump and 47 mm membranes with a porosity of 0.22 µm. These membranes were preserved in 50 mL falcon tubes containing TSE buffer (Tris HCl 10 mM pH = 8, Sodium Chloride 100 mM, EDTA 1 mM pH = 8) and stored at −20°C.

Physical-chemical component measurements were conducted *in situ* using a multi-parameter water analyzer (HI 9829, HANNA), considering the parameters of pH, electrical conductivity (EC), dissolved oxygen (DO), and total dissolved solids (TDS).

2.2 Georeferencing analysis

The methodology for mapping the anthropic signature of land use and land cover in rivers employs the concept of a hydrographic basin and geoprocessing techniques. The deforestation level and population density were evaluated following the methodology of Cavalcante et al. (2023). The deforested area was calculated as the sum of all areas with non-natural land use and land cover based on the classification of the Mapbiomas Brasil project (https://brasil.mapbiomas.org/en/) version six for the year 2020.

The sampling points were chosen following a bioprospecting approach, with consideration given to the gradient of anthropogenic impact and accessibility for sample collection. These points were situated at the outset of the pristine site, specifically at coordinates 3°

3′28.512″S, 47° 25′2.172″W. Following the initial point, the subsequent sampling locations were designated as P2 (3° 0′24.737″S, 47° 22′52.941″W), P3 (2° 59′56.264″S, 47° 22′17.735″W), P4 (2° 58′56.895″S, 47° 21′37.938″W) and extending to the river outlet from the city of Paragominas at P5 (2° 57′54.169″S, 47° 20′15.140″W).

2.3 Genetic material and sequencing

In the laboratory, the membranes containing the samples were first shaken at 250 RPM at room temperature. Subsequently, the liquid containing the suspended particles retained in the membrane was centrifuged at 13200 RPM for 10 min in Eppendorf tubes. Genetic material was then extracted following the manufacturer's instructions of the Pro-DNeasy PowerSoil kit (Qiagen). The integrity of the obtained genetic material was assessed through horizontal electrophoresis. DNA quantification was conducted using Qubit (Thermo Fisher Scientific), and purity indices were obtained via Nanodrop (Thermo Fisher Scientific).

For the construction of DNA libraries, the samples were processed according to the manufacturer's protocol for the Nextera XT DNA Library kit (Illumina). Sequencing was performed using the NextSeq 550 System High-Output kit, generating paired-end reads of 150 bp, using the Illumina NovaSeq 500/550 High-Output platform.

2.4 Sequence analysis

The quality of the sequencing reads was initially analyzed using the software FASTQC–Version 0.11.9 (Wingett and Andrew, 2018). Subsequently, the reads were trimmed and filtered with a minimum Phred quality score of 20 using the software Trimmomatic (Bolger et al., 2014). The obtained sequences were submitted to the National Center for Biotechnology Information NCBI database (https://www.ncbi.nlm.nih.gov/), with Submission ID SUB14513086 and BioProject ID PRJNA1122411, accessible with the following link https://www.ncbi.nlm.nih.gov/sra/PRJNA1122411.

2.5 Pathogen identification

The pathogenic species in the collections were identified by comparing the output from Kraken2 with a local database of pathogenic bacteria from various isolates associated with pathogenicity in food, water, and clinical hosts. Analyses were conducted at both the species and genus levels. The local database was created using complete genome records labelled as pathogenic by the NCBI Pathogen Detection Project (https://www.ncbi.nlm.nih.gov/pathogens/). Records were extracted using the NCBI FTP protocol and manipulated using the Python programming language. For information extraction from HTML pages and for the grouping, filtering, and sorting of records, the beautifulSoup and pandas packages were utilized, respectively. The records were saved in the MongoDB database, employing the NoSQL format, hosted in a Docker container https://github.com/labgm/pathogen-detection.git.

2.6 Determination of microbial diversity

For the identification of different taxonomic groups, the previously trimmed reads were used. These reads were then evaluated using the Plants, Fungi, and Protists (PFP) database within the Kraken2 program (Wood et al., 2019). The output format of Kraken2 was converted to be recognized by the MicrobiomeAnalyst program (Chong et al., 2020) for the transformation of abundances using Trimmed Mean of M-values (TMM), then, relative abundances were processed to determine alpha and beta diversity indices and associations between taxa.

2.7 Analysis of virulence genes

For the identification of bacterial virulence factors, the Virulence Factor Database (VFDB) (Liu et al., 2022) was used. This database contains 32 genera of bacterial pathogens, classified into 14 basal categories. The database was indexed using the Bowtie2 software (Langmead and Salzberg, 2012), and then the reads obtained from the sequencing were aligned against the database to capture the presence and abundance of virulence factors in each sample. The alignment result was processed using the Pileup software to identify and quantify the aligned reads at each position of the reference database. The information obtained from Pileup, including the columns of identification and abundance, served as the basis for the subsequent step where they were organized into a tabular structure file containing the identified virulence factors and their respective abundance values for each sample. This facilitated the comparison and interpretation of the data.

2.8 Statistical analysis

The data obtained from the different analyses were evaluated for normality using the Shapiro-Wilk test. Subsequently, they were analyzed using ANOVA or Kruskal–Wallis tests, multiple regression, and principal component analysis (PCA) using the PAST 4.05 software (Hammer et al., 2001). For the preparation of the graphs, the Orange Data Mining program (Demsar et al., 2013), as well as the Seaborn and Vegan-Altair libraries of Python, were used.

3 Results and discussion

3.1 Characterization of physicochemical components and microbial diversity

The points where samples were collected in the Uraim River are highlighted in yellow in Figure 1, observed through satellite images. In Figure 1A, the population density in inhabitants per square kilometer along the river is emphasized, allowing for the observation of human settlement and agricultural areas near certain areas of the river. In Figure 1B, the percentage of deforestation in the areas along the river is further observed. It is

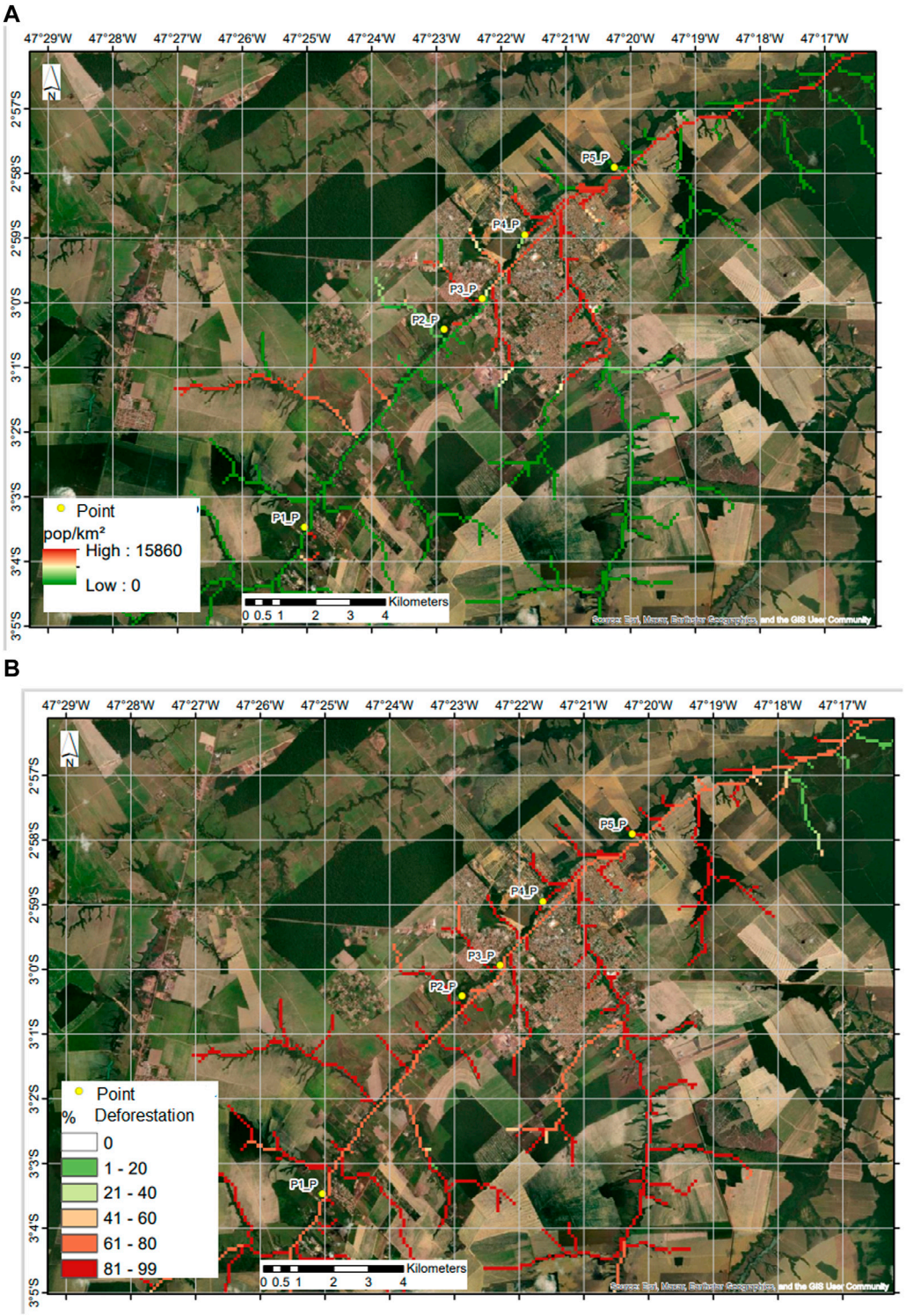

FIGURE 1
Satellite images of the municipality of Paragominas-PA delineating the path of the Uraim River as it crosses the municipality. **(A)** Population density in inhabitants per square kilometer along the river. **(B)** Percentage of deforestation in the areas along the river.

noted that the collection sites showed a deforestation percentage ranging from 70% to 73%, with population densities ranging from 1 to 184 inhabitants per square kilometer.

The Uraim River basin exhibits considerable deforestation of its native vegetation, resulting in a 25% reduction in average precipitation during the deforested period compared to years with forest presence, consequently leading to a 22% reduction in channel flow (Sardinha and Ventura, 2022). Different anthropogenic activities have repercussions on various water resources (Pereira Júnior et al., 2023a).

TABLE 1 Physical-chemical characteristics and total microbial diversity at different sampling points in the Uraim River, Paragominas-PA.

Point	pH	Ec (uS/cm)	DO (ppm)	TDS (ppm)	Shannon	Simpson
P1	4.433 ± 0.215	27.333 ± 1.154	5.7 ± 0.269	19.333 ± 1.155	7.413 ± 0.356	0.997 ± 0.002
P2	3.547 ± 0.236	24 ± 3	5.53 ± 0.387	17 ± 2	7.184 ± 0.293	0.996 ± 0.001
P3	4.173 ± 0.19	29 ± 1	5.59 ± 0.225	23.667 ± 6.423	7.323 ± 0.127	0.996 ± 0.001
P4	3.693 ± 0.029	27 ± 2	5.89 ± 0.507	18.667 ± 1.527	7.406 ± 0.218	0.997 ± 0.001
P5	4.627 ± 0.121	32 ± 0	4.413 ± 0.051	22.333 ± 0.577	7.488 ± 0.077	0.997 ± 0.001

EC, electrical conductivity; DO, dissolved oxygen; TDS, total dissolved solids.

In the municipality of Paragominas-PA, the forest area was 3420.27 km^2 in 2000 and decreased to 2784.23 km^2 in 2021, representing a forest area loss of 18.6%. Regarding the expansion of the urban area, the development began in 2000 (133156 km^2) and 2021 (20.2687 km^2), which is linked to population growth: in 2000, the population of Paragominas was 76450 inhabitants, and it increased to 115538 inhabitants in 2021. This implies changes in ecosystems, such as the reduction of the precipitation rate that affects the water recharge of rivers, streams, and creeks, among others (Pereira Júnior et al., 2023a). These characteristics are evident in the images obtained for this study and also in the alterations in chemical and microbiological components.

In the physicochemical analyses, acidic pH was found, ranging between 3.547 and 4.627, with significant differences between the points (ANOVA; F = 23.47; *p*-value = 0.0001). notably, these differences occurred in the comparison between: points P1 and P2 (Tukey's test; Q = 9.235; *p*-value = 0.001); P2 and P3 (Tukey's test; Q = 6.527; *p*-value = 0.011); P1 and P4 (Tukey's test; Q = 7.707; *p*-value = 0.004); P3 and P4 (Tukey's test; Q = 4.999; *p*-value = 0.048); P2 and P5 (Tukey's test; Q = 2.014; *p*-value = 0.0003), and P4 between P5 (Tukey's test; Q = 9.721; *p*-value = 0.001) (Supplementary Figure S1).

The values of electrical conductivity varied across all points but were not significant. In the case of dissolved oxygen, a decrease was evidenced at P5, with average values of 4.413, showing significant differences (ANOVA; F = 8.148; *p*-value = 0.006) for this point compared to the others. For total dissolved solids (TDS), despite the variation in values at the collection points, the differences were not significant (Table 1).

These findings underscore a potential public health concern should the population consume untreated water, including water from the river, typically used for domestic, agricultural, and livestock purposes. Anthropogenic activities stand out as primary factors influencing the quality of surface waters (Tornevi et al., 2014; Vinueza et al., 2021). In the Uram River area, agricultural practices have been observed to increase the concentrations of various chemical compounds in the river. As it flows through urban areas, the river's natural pH, nitrogen and oxygen concentrations, turbidity, and other parameters can be altered, affecting the standards of freshwater quality intended for human consumption (Pereira Júnior et al., 2023b).

In the sequencing, an average of 35468174.13 reads were obtained from the different sample collection points, of which about 33% were used for taxonomic classification. Bacteria accounted for 30% of the reads, while opportunistic pathogenic bacteria for humans represented 0.34%, Table 1.

Regarding total diversity in these ecosystems, up to 7.190 different species were identified, with Shannon index values above 7.184 and Simpson index values close to 1, indicating no dominance of a single species (Table 1). In the Tama River in Tokyo, Japan, it was observed that bacterial communities exhibited significant differences along the river's course, showcasing variations in diversity (Mizusawa et al., 2021). This phenomenon was also noted in the Uraim River in Paragominas, Brazil, highlighting the dynamic nature of microbial communities in urban river systems. Interestingly, the Amazon region, home to the Amazon River, lacks comprehensive studies on microbial diversity. Despite being the world's largest river in terms of discharge, the Amazon River remains relatively understudied, with existing research exhibiting considerable heterogeneity (Li et al., 2021).

In our study of the Uraim River, the most abundant phyla were Pseudomonadota and Actinomycetota, the taxonomic class of Betaproteobacteria was noteworthy, followed by Alphaproteobacteria, Actinomycetes and Gammaproteobacteria. However, in freshwater studies, the dominant classes are usually Alphaproteobacteria, Betaproteobacteria, and Actinobacteria, which complex changes in nutrient composition can alter (Santos-Júnior et al., 2020; Mizusawa et al., 2021).

3.2 Pathogenic bacterial evaluation

A higher abundance of pathogenic species was detected at point P5, averaging 226.7 (Figure 2A). The Shannon index showed lower values on average at point P2, with a value of 3.955 ± 0.592, and the highest average value of 4.312 ± 0.102 was found at point P3 (Figure 2B). The Simpson index presented average values between 0.914 and 0.971 at the same aforementioned points (Figure 2C).

Beta diversity analysis of biological replicates revealed a clustering trend in the bacterial composition corresponding to P5, with R^2 values of 0.576 (PERMANOVA F-value = 3.3961; *p*-value = 0.001), indicating a cumulative variation of 70.6% for the PCoA analysis (Supplementary Figure S2).

Regarding the phylum composition of pathogenic microorganisms identified across all sampling points, Pseudomonadota, Bacillota, and Campylobacterota are highlighted, respectively. Among the eight microorganisms identified, Gammaproteobacteria were predominant, followed by

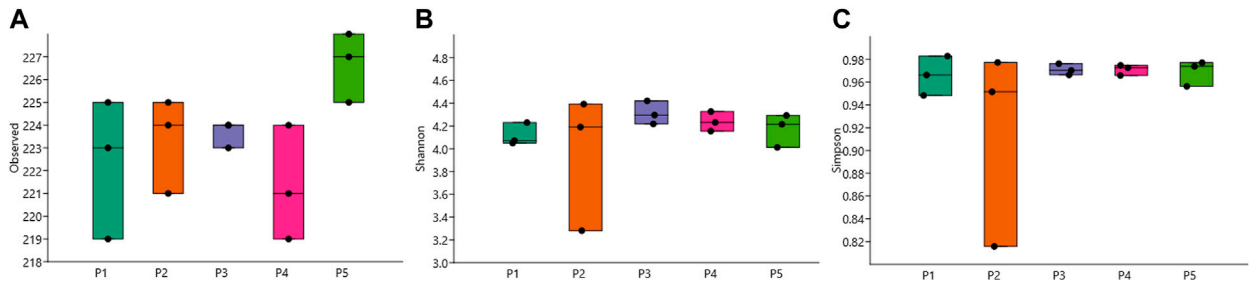

FIGURE 2
Box plot of alpha diversity values of opportunistic pathogenic bacteria for humans, showing **(A)** Observed, **(B)** Shannon, and **(C)** Simpson indices.

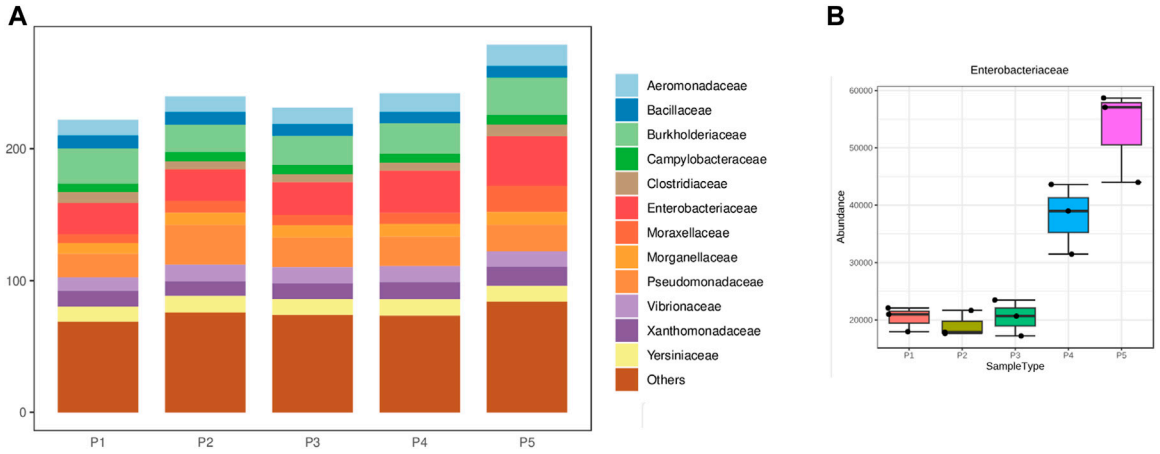

FIGURE 3
(A) Distribution of the main taxonomic family groupings, **(B)** Proportion of Enterobacteriaceae at different sampling points.

Betaproteobacteria and Bacilli, with the remaining classes taxonomic in smaller proportions (refer to Supplementary Figure S3). Among the 27 identified families, Enterobacteriaceae, Burkholderiaceae, *and* Pseudomonadaceae exhibited the highest abundance (see Figure 3A). Particularly for Enterobacteriaceae, a substantial increase was observed in points 4 and 5, with statistically significant differences noted between these points (ANOVA; F = 78.96; p-value = 1.59×10^{-7}) (see Figure 3B).

Metagenomic analysis allows for the simultaneous screening of various potential pathogens and fecal indicators. The river's microbiome serves as a significant indicator of urban pollution alteration, demonstrating a prevalence of human intestinal bacteria, predominantly pathogenic (Acharya et al., 2022). Among the most abundant genera identified at all detecting points were *Burkholderia and Pseudomonas*, with a notable presence of *Acinetobacter, Escherichia, Klebsiella*, and *Enterobacter* at point 5 (Figure 4A). The most abundant pathogenic species belong to the ESKAPE group. Less frequently detected species include *Burkholderia cepacia* complex (Bcc), *E. coli,* and *Stenotrophomonas maltophila* (Figure 4B). Regarding ESKAPE group species, *Enterobacter* spp. Exhibited a distribution with minor variations across sampling points (R^2 = 0.768; p-value = 1.825×10^{-5}), consistent with the observations for *Acinetobacter baumanii* and *Klebsiella pneumoniae*, which displayed higher abundance at point 5. Notably, *Pseudomonas aeruginosa* demonstrated an inverse trend compared to the species above (Figure 4C), which could influence changes environmental characteristics and microbial communities (Philippot et al., 2021), but we could not identify specific facts against these microorganisms due to the complexity of the variables that make up the ecosystems.

In the correlation analysis with the relative abundances of pathogenic bacterial species, *Enterobacter cloacae* stands out as significantly associated with the presence of *Klebsiella variicola, Citrobacter freundii, Aeromonas veronii* and *Enterobacter kobei*. The latter is correlated with the presence of *E. coli* and is involved with the occurrence of *Acinetobacter nosocomiais, Streptococcus susis, Enterococcus hirae* and *Enterococcus faecium,* which are associated with *Streptococcus pyogenes* and *Streptococcus equi,* as indicated by the interaction network presented in Figure 5.

The substantial presence of human pathogens is notable, constituting approximately 7% of all taxonomically described bacterial species. These pathogenic entities span 24 distinct taxonomic classes, with prominent contributions from Gammaproteobacteria and Actinomycetia in terms of genus and species diversity. The identified pathogen pool encompasses 1513 species categorized into 327 genera, of which 267 genera encompass at least one established pathogenic species (Bartlett

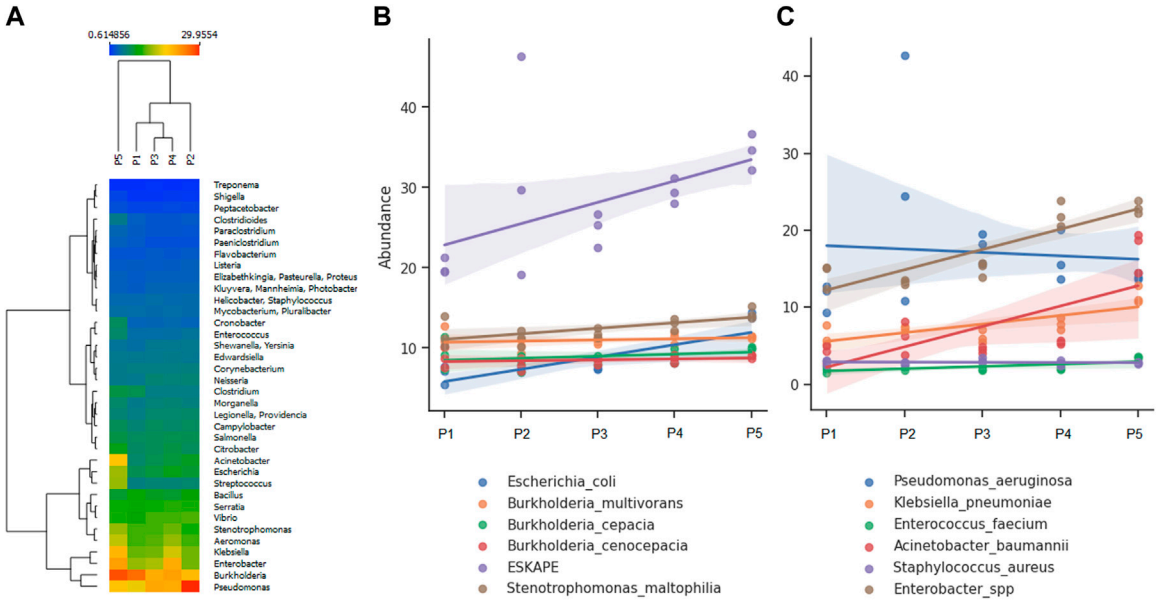

FIGURE 4
Analysis of abundance according to the identified bacterial genera and species: **(A)** Most abundant genera, **(B)** Most abundant species, **(C)** Species composing the ESKAPE group.

FIGURE 5
Interaction network revealing associations of presence among pathogenic bacteria. Generated through correlation analysis with Pearson coefficient algorithm. Significant index values are highlighted in red lines.

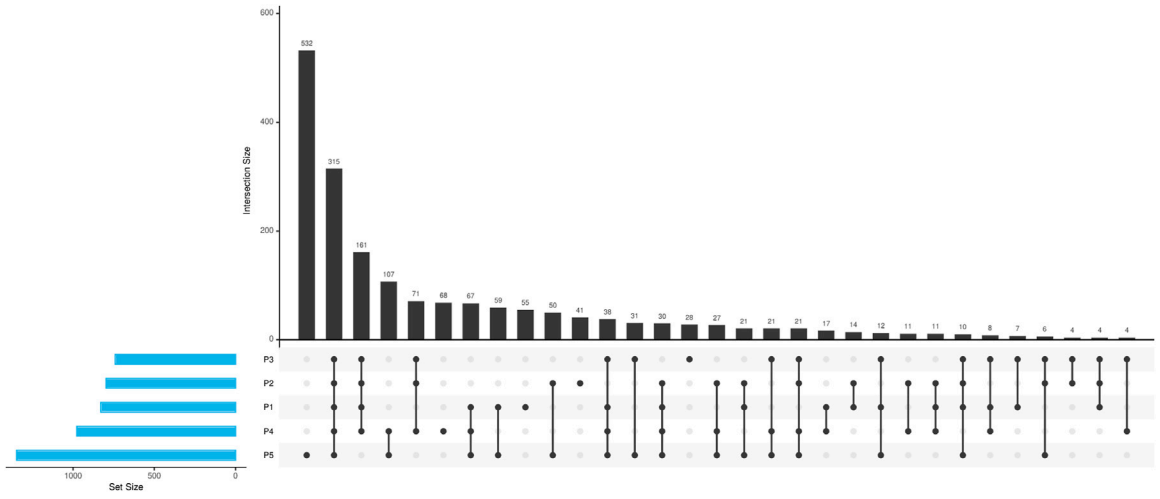

FIGURE 6
Characterization of virulence genes identified in different points of the Uraim River.

et al., 2022). Waterborne illnesses persist as a significant global health concern, prompting numerous regulatory bodies to utilize coliform assessments in water quality testing as an indicator of fecal contamination levels and associated disease risks (Hamner et al., 2019).

The findings presented in this study align with the expected bacterial populations that thrive in sewage-contaminated environments, characterized by a dominance of Proteobacteria and Bacteroidetes (Godoy et al., 2020). Additionally, the prevalence of Actinobacteria in freshwater environments is consistent with previous studies (Mizusawa et al., 2021).

The presence of pathogenic microorganisms allows us to assess the quality of these aquatic systems in terms of environmental impact and anthropogenic activities. In this study, the presence of the ESKAPE group is notable, given its ability to possess and transfer antibiotic resistance genes (Denissen et al., 2022; Aguilar-Salazar et al., 2023). The results highlight a higher abundance, on the bodies of water, of *K. pneumoniae*, *E. cloacae, E. faecium,* and *E. faecalis*. Additionally, the metagenomic analysis reveals the presence of bacteria that serve as bioindicators for chronic diseases in humans, such as *Fusobacterium nucleatum* associated with colorectal cancer (VanEvery et al., 2023).

3.3 Characterization of virulence genes

Upon examination of the virulence genes identified across the various sampling points, as illustrated in Figure 6, it was noted that point P5 exhibited a greater prevalence of unique genes, not identified in other points. This observation aligns with expectations, given that P5 is situated downstream from the urbanized area of Paragominas, experiencing a range of anthropogenic influences and cumulative pressures from upstream points. Additionally, a total of 315 genes were found to be common among all five sampling locations, indicating a potential presence of native core microbiota unaffected by anthropogenic activities.

Virulence factors (VFs) can affect a wide range of cellular processes, such as cell-cell signaling, ion secretion, protein synthesis, mitosis, cytoskeleton structure, and mitochondrial function, although their role in natural environments is not yet well understood (Vinueza et al., 2021). Our analyses identified numerous genes related to virulence factors, especially in sites with higher anthropogenic activity (Figure 6), particularly in P5 where there is a greater abundance and diversity of VFs. This site also showed a higher quantity of pathogenic bacteria (Supplementary Figures S4A, B).

The diversity of virulence genes calculated was highest at point P5 with a value of 105.6 for the Fisher alpha diversity index, followed by 77.96 at point P4, values close to 60 at points P1 and P2, and the lowest value of 58 at P3 (Figure 7A). The most relevant virulence mechanism is adhesion, present in all points; points P2 and P5 highlight the effector delivery system mechanism, and in P1, the nutritional/metabolic factor and invasion mechanisms are present (Figure 7B).

In studies conducted on rivers traversing urban areas, it has been revealed that urbanization increases environmental risk and the occurrence of resistance and virulence genes compared to those in rural regions. Among the main virulence factors (VFs) are offensive, nonspecific, defensive, and regulatory VFs, which were found in all samples. The dominant subtypes include iron acquisition systems, adhesion, secretion systems, regulation mechanisms, toxins, and antiphagocytosis (Mizusawa et al., 2021; Li et al., 2022). In our samples, secretion systems and adhesion were the most relevant factors.

In all sampling points, a high abundance of the gene *fbpC*, which is involved in the Secreted fibronectin-binding protein C (VF0311), was observed. These adherence proteins can ensure the adhesion of these pathogens to hosts, with many of these molecules being diverse and not fully described (Aono et al., 2023).

At sampling point P5, there is a notable abundance of genes involved in secretion systems, with the most prominent being the gene *vgrG/tssI*, which is associated with the synthesis of type VI secretion system tip protein VgrG (VF1337). At P2,

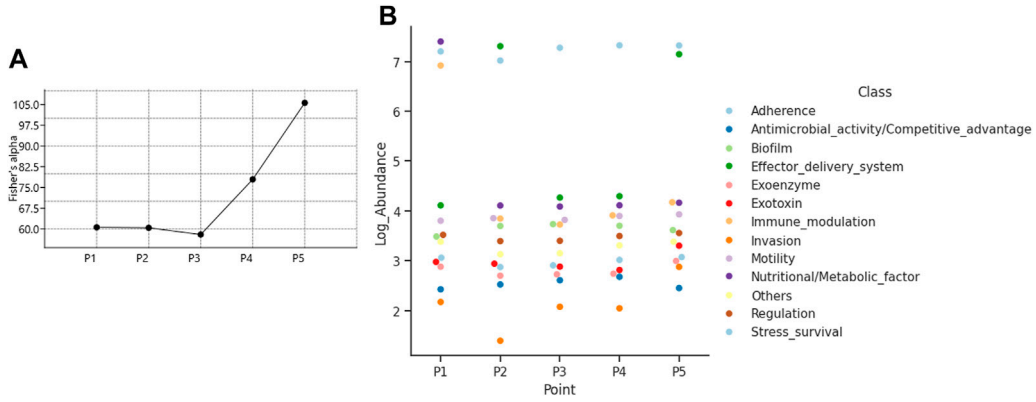

FIGURE 7
Characterization of virulence genes **(A)** Fisher alpha diversity index, and **(B)** Composition of virulence mechanisms.

the gene *vgrG1a*, which synthesizes the type VI secretion system substrate VgrG1 (VF0334), stands out (Supplementary Figure S4A).

The identification of genes related to Type III and Type IV secretion systems is essential in bacterial pathogenesis, facilitating direct interactions with host cells. The presence of these genes may reflect regional variations in the bacteria-host dynamics or environmental factors that favor certain pathogenic strategies (Rout et al., 2023). Metagenomic analysis of the Ganges River (India) revealed the widespread distribution of genes associated with flagella, which are related to Type III and Type IV secretion systems, the latter being the most abundant marker identified in different sites. This study highlights the complexity of bacterial virulence and its dependence on environmental context. The detection of flagella-associated genes in various locations implies a widespread reliance on motility and adhesion as critical virulence factors. This suggests a common strategy employed by bacteria to establish infection and colonization across different geographic areas (Godoy et al., 2020; Rout et al., 2023).

In point 1, the gene *lic2A* synthesizes glycosyltransferase (VF0044), and *glnA1* is involved in the production of Probable glutamine synthetase, type I (VF0816) (Supplementary Figure S4A). The *glnA1* gene is involved in nitrogen metabolism and is necessary for the development of *Mycobacterium tuberculosis* and *E. coli* in the environment (Xu et al., 2023).

The secretion systems identified in this study are characteristic of a variety of Gram-negative bacteria, contributing to the virulence of Type I and Type VI secretion systems, which are commonly described in the genome of *P. aeruginosa* (Green and Mecsas, 2016), and in members of the genus *Pseudomonas*, *Acinetobacter*, *Klebsiella*, and *Enterobacter*, which are part of the ESKAPE group and they are the most abundant among the identified pathogenic bacteria identified in our results, which could contribute to the high abundance of this gene.

Another mechanism of adaptation and resistance is the production of biofilms, whose production is induced by the presence of N-acyl-homoserine lactone (Alio et al., 2023), providing significant advantages to bacteria such as resistance to antibiotics and protection against host immune responses. In the environment, biofilms allow bacteria to resist unfavorable conditions (Gomes et al., 2020; Rout et al., 2023), and are present across different sites studied (P1, P2, P3, P4 e P5) in Paragominas.

3.4 Association of variables

In the PCA analysis, an accumulated percentage of 88.04% of variation in the variables was found, with 58.8% variation in principal component 1 (PC1), highlighting the following associations: between the physicochemical components of pH, Ec, and TDS with the alpha diversity indices of Shannon, although these were not evident in one analyzed point. In the case of P5, a strong correlation was observed with population occupancy, and Fisher's alpha diversity of virulence genes (Pearson; $\rho = 0.972$; p-value = 0.006). Furthermore, a high correlation was identified between the relative abundance of the ESKAPE group and the percentage of deforestation (Pearson; $\rho = 0.86$; p-value = 0.061); a significant inverse association between dissolved oxygen variables and deforestation percentage (Pearson; $\rho = -0.912$; p-value = 0.03); and a significant association between virulence gene diversity and the percentage of inhabitants per surface area (Pearson; $\rho = 0.972$; p-value = 0.005) and with deforestation (Pearson; $\rho = 0.907$; p-value = 0.033) (Figure 8).

The significant associations found between urban and rural population growth and the functioning and biodiversity of the ecosystem by microorganisms responsible for the purification and removal of nutrients in rivers, as well as the nutrient cycle and interactions between plants in the soil (Gomes et al., 2020), are reflected in different analytes. Similarly, biochemical and chemical oxygen demands are influenced by the urbanization process, temperature, dissolved oxygen, ammonia, and phosphorus (Giuliatti et al., 2017).

In this study, the assessed physicochemical properties underwent significant alterations, acting as crucial factors that modify bacterial community structures within these ecosystems and facilitate the acquisition of genetic components associated with their adaptation, including virulence genes for higher

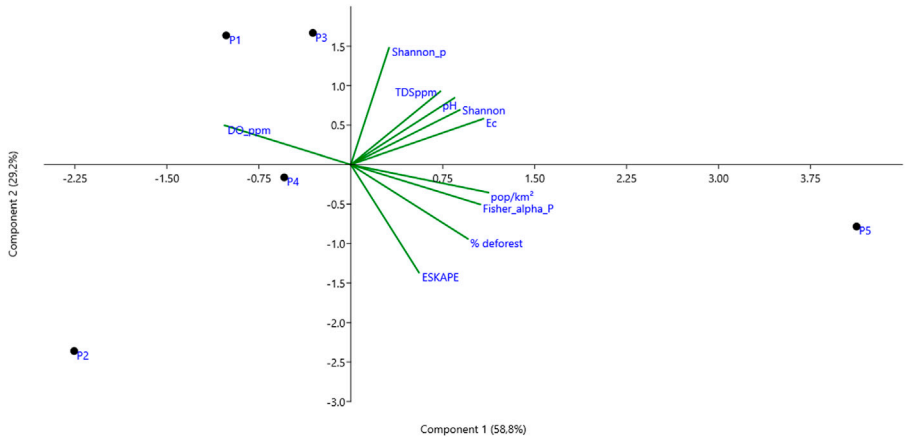

FIGURE 8
PCA analysis of the different relevant variables in this study for each sampling point in the Uraim River in the city of Paragominas/Brazil. DO ppm: Dissolved Oxygen, Shannon_p: Shannon alpha diversity index of pathogenic bacteria, TDS ppm: Total Dissolved Solids, Ec: Electrical Conductivity, pop/Km^2: Number of inhabitants per Km^2, deforestation percentage.

organisms (Godoy et al., 2020). Among the identified components, DO is inversely associated with the diversity of virulence genes and the presence of certain pathogens. This association could be attributed to anthropogenic activities, with human presence notably increasing the likelihood of greater contact with these types of organisms.

4 Conclusion

The metagenomic investigation of the Uraim River, utilizing samples extracted from its surface water, underscores the discernible influence of anthropogenic endeavors on both the diversity and prevalence of pathogenic bacterial strains and their corresponding virulence genes at various sampling locations along the riverine course. Notable among the bacterial taxa are the Enterobacteria and members of the ESKAPE group, with a clear linkage observed to deforestation activities and the density of human habitation in the vicinity of the Uraim River. Similarly, there is an observed trend of increased virulence gene diversity in sites influenced by anthropogenic activities.

However, the limitations identified in the development of this work were the number of points, which could be increased to be more precise regarding the causes of the observed impacts; carrying out studies in different periods (rainy and dry) and several times in each period, to compare the effect in the region, mainly due to agricultural activities that can generate bioaccumulation of chemical products that can later be carried to the river in the period of begin of rainy.

Studies investigating the presence of microorganisms in the water and their impact on the health of human populations and animals consuming river water are necessary to assess potential impacts and guide public policies aimed at minimizing/mitigating anthropogenic impact and its effects in a One Health approach. In this context, it is noteworthy that in 2022, the municipality of Paragominas established an institutional program called “Renascer Uraim” (“Rebirth Uraim”), aimed at implementing preservation actions for the river. These actions range from environmental education to river cleaning and restoration of native vegetation along its banks, which could positively impact the occurrence of pathogenic microorganisms observed due to anthropogenic activities.

Data availability statement

The data presented in the study was deposited in the National Center for Biotechnology Information NCBI database (https://www.ncbi.nlm.nih.gov/), accession number ID SUB14513086 and BioProject ID PRJNA1122411.

Author contributions

OC-A: Conceptualization, Formal Analysis, Writing–original draft, Writing–review and editing, VF: Software, Writing–original draft, WN: Data curation, Writing–review and editing. DM: Methodology, Writing–review and editing. AM: Software, Writing–review and editing, PM: Methodology, Writing–review and editing. RL: Methodology, Writing–review and editing. SA: Validation, Writing–review and editing, AL: Resources, Writing–review and editing, RG: Validation, Writing–review and editing. EF: Resources, Validation, Writing–review and editing, VA: Investigation, Resources, Writing–review and editing, RR: Conceptualization, Funding acquisition, Supervision, Writing–original draft, Writing–review and editing.

Funding

The author(s) declare that financial support was received for the research, authorship, and/or publication of this article. This work was supported by Dean’s Office for Research and Graduate Studies/Federal University of Pará–PROPESP/UFPA (PAPQ), UFPA

(Universidade Federal do Pará), CAPES (Coordenação de Aperfeiçoamento de Pessoal de Nível Superior), UFPA (Universidade Federal do Pará), CNPQ (Conselho Nacional de Desenvolvimento Científico e Tecnológico) project #312316/2022-4, and, SECTET (Secretaria de Estado de Ciência, Tecnologia e Educação Superior, Profissional e Tecnológica).

Acknowledgments

We thank the PROPESP/UFPA (Pró-Reitoria de Pesquisa e Pós-Graduação/Universidade Federal do Pará for the financial support on this paper.

Conflict of interest

The authors declare that the research was conducted in the absence of any commercial or financial relationships that could be construed as a potential conflict of interest.

The author(s) declared that they were an editorial board member of Frontiers, at the time of submission. This had no impact on the peer review process and the final decision.

Publisher's note

All claims expressed in this article are solely those of the authors and do not necessarily represent those of their affiliated organizations, or those of the publisher, the editors and the reviewers. Any product that may be evaluated in this article, or claim that may be made by its manufacturer, is not guaranteed or endorsed by the publisher.

Supplementary material

The Supplementary Material for this article can be found online at: https://www.frontiersin.org/articles/10.3389/fenvs.2024.1404230/full#supplementary-material

References

Acharya, K., Blackburn, A., Mohammed, J., Tamiru Haile, A., Mekpnnen Hiruy, A., and Werner, D. (2022). Metagenomic water quality monitoring with a portable laboratory. *Water Res.* 184, 116112. doi:10.1016/j.watres.2020.116112

Agência Nacional de Águas, (ANA) (2020). Corpos Hídricos Superficiais e Dominialidade. *Sist. Nac. Inf. Sobre Recur. Hídricos*. Available at: https://www.snirh.gov.br/(Accessed June 3, 2024).

Aguilar-Salazar, A., Martínez-Vázquez, A. V., Aguilera-Arreola, G., De Jesus De Luna-Santillana, E., Cruz-Hernández, M. A., Escobedo-Bonilla, C. M., et al. (2023). Prevalence of ESKAPE bacteria in surface water and wastewater sources: multidrug resistance and molecular characterization, an updated review. *Water* 15, 3200. doi:10.3390/w15183200

Alio, I., Moll, R., Hoffmann, T., Mamat, U., Schaible, U. E., Pappenfort, K., et al. (2023). *Stenotrophomonas maltophilia* affects the gene expression profiles of the major pathogens *Pseudomonas aeruginosa* and *Staphylococcus aureus* in an *in vitro* multispecies biofilm model. *Microbiol. Spectr.* 11, e0085923. doi:10.1128/spectrum.00859-23

Aono, R., Emi, S., Okabe-Watanabe, K., Nariya, H., Matsunaga, N., Hitsumoto, Y., et al. (2023). Autolysin as a fibronectin receptor on the cell surface of Clostridium perfringens. *Anaerobe* 83, 102769. doi:10.1016/j.anaerobe.2023.102769

Bartlett, A., Padfield, D., Lear, L., Bendall, R., and Vos, M. (2022). A comprehensive list of bacterial pathogens infecting humans. *Microbiology* 168, 001269. doi:10.1099/mic.0.001269

Bolger, A. M., Lohse, M., and Usadel, B. (2014). Trimmomatic: a flexible trimmer for Illumina sequence data. *Bioinformatics* 30, 2114–2120. doi:10.1093/bioinformatics/btu170

Cavalcante, R., Fleischmann, A., and Pontes, P. R. (2023). Looking upstream: analyzing the protection of the drainage area of Amazon rivers. doi:10.31223/X51M4F

Chong, J., Liu, P., Zhou, G., and Xia, J. (2020). Using MicrobiomeAnalyst for comprehensive statistical, functional, and meta-analysis of microbiome data. *Nat. Protoc.* 15, 799–821. doi:10.1038/s41596-019-0264-1

Chopyk, J., Nasko, D. J., Allard, S., Bui, A., Pop, M., Mongodin, E. F., et al. (2020). Seasonal dynamics in taxonomy and function within bacterial and viral metagenomic assemblages recovered from a freshwater agricultural pond. *Environ. Microbiome* 15, 18. doi:10.1186/s40793-020-00365-8

Correa, D. L. (2017). *Análise da Susceptibilidade a Inundações na Bacia Hidrográfica do Rio Uraim, Paragominas-PA*. Belém PA: Universidade Federal do Pará.

Da Silva, A. C. de S., Pereira Junior, A., and Farias, N. (2020). Diatomáceas como indicadoras da qualidade da água em rios urbanos/diatoms as indicators of water quality in urban rivers. *Braz. J. Dev.* 6, 34616–34643. doi:10.34117/bjdv6n6-125

De Araujo, R. da C. (2010). *Efeitos do desmatamento sobre o ciclo hidrológico: uma comparação entre a Bacia do Rio Curua-Una e a Bacia do Rio Uraim*. Belem, PA: Universidade Federal do Pará.

Demsar, J., Curk, T., Erjavec, A., Demsar, J., Curk, T., Erjave, A., et al. (2013). Orange: data mining toolbox in Python. *J. Mach. Learn. Res.* 8, 2349–2353. Available at: https://www.jmlr.org/papers/volume14/demsar13a/demsar13a.pdf

Denissen, J., Reyneke, B., Waso-Reyneke, M., Havenga, B., Barnard, T., Khan, S., et al. (2022). Prevalence of ESKAPE pathogens in the environment: antibiotic resistance status, community-acquired infection and risk to human health. *Int. J. Hyg. Environ. Health* 244, 114006. doi:10.1016/j.ijheh.2022.114006

Giuliatti, N. M., Rodrigues, A. B. M., Brito, V. L., Silva, I. A. V. D., and Pereira Junior, A. (2017). "Demanda bioquímica e química de oxigênio no rio uraim e o processo de urbanização no município de paragominas-pa." in *Blucher engineering proceedings* (Belo Horizonte, Brasil: Editora Blucher), 938–948. doi:10.5151/xveneeamb-094

Godoy, R. G., Marcondes, M. A., Pessôa, R., Nascimento, A., Victor, J. R., Duarte, A. J. D. S., et al. (2020). Bacterial community composition and potential pathogens along the Pinheiros River in the southeast of Brazil. *Sci. Rep.* 10, 9331. doi:10.1038/s41598-020-66386-y

Gomes, I. B., Maillard, J.-Y., Simões, L. C., and Simões, M. (2020). Emerging contaminants affect the microbiome of water systems—strategies for their mitigation. *Npj Clean. Water* 3, 39. doi:10.1038/s41545-020-00086-y

Green, E. R., and Mecsas, J. (2016). Bacterial secretion systems: an overview. *Microbiol. Spectr.* 4 (1), 13. doi:10.1128/microbiolspec.VMBF-0012-2015

Hammer, O., Harper, D. A. T., and Ryan, P. D. (2001). PAST: paleontological statistics software package for education and data analysis. *Palentologica Electron* 4 1, 1–9. Available at: http://palaeo-electronica.org.

Hamner, S., Brown, B., Hasan, N., Franklin, M., Doyle, J., Eggers, M., et al. (2019). Metagenomic profiling of microbial pathogens in the little bighorn river, Montana. *Int. J. Environ. Res. Public. Health* 16, 1097. doi:10.3390/ijerph16071097

He, C., Liu, Z., Wu, J., Pan, X., Fang, Z., Li, J., et al. (2021). Future global urban water scarcity and potential solutions. *Nat. Commun.* 12, 4667. doi:10.1038/s41467-021-25026-3

Ko, K. K. K., Chng, K. R., and Nagarajan, N. (2022). Metagenomics-enabled microbial surveillance. *Nat. Microbiol.* 7, 486–496. doi:10.1038/s41564-022-01089-w

Langmead, B., and Salzberg, S. L. (2012). Fast gapped-read alignment with Bowtie 2. *Nat. Methods* 9, 357–359. doi:10.1038/nmeth.1923

Li, K., Hu, J., Li, T., Liu, F., Tao, J., Liu, J., et al. (2021). Microbial abundance and diversity investigations along rivers: current knowledge and future directions. *WIREs Water* 8, e1547. doi:10.1002/wat2.1547

Li, R., Zhu, L., Wang, Y., and Zhu, Y.-G. (2022). Metagenomic insights into environmental risk of field microplastics in an urban river. *Water Res.* 223, 119018. doi:10.1016/j.watres.2022.119018

Lin, L., Yang, H., and Xu, X. (2022). Effects of water pollution on human health and disease heterogeneity: a review. *Front. Environ. Sci.* 10, 880246. doi:10.3389/fenvs.2022.880246

Liu, B., Zheng, D., Zhou, S., Chen, L., and Yang, J. (2022). VFDB 2022: a general classification scheme for bacterial virulence factors. *Nucleic Acids Res.* 50, D912–D917. doi:10.1093/nar/gkab1107

Mizusawa, N., Reza, Md. S., Oikawa, C., Kuga, S., Iijima, M., Kobiyama, A., et al. (2021). Diversity and functions of bacterial communities in water and sediment from the watershed of the Tama River flowing a highly urbanized area. *Fish. Sci.* 87, 697–715. doi:10.1007/s12562-021-01543-4

Pandey, P. K., Kass, P. H., Soupir, Mi. L., Biswas, S., and Singh, V. (2014). Contamination of water resources by pathogenic bacteria. *Amb. Express* 4, 51. doi:10.1186/s13568-014-0051-x

Pereira Júnior, A., Morales, G. P., Beltrão, N. E. S., Barbosa, A. J. S. D. S., Gutierrez, L. A. C. L., Jesus, E. D. S., et al. (2023a). Geospatial analysis of deforestation, land use and impacts of water resources in paragominas, Pará. *DELOS Desarro. LOCAL Sosten.* 16, 3399–3433. doi:10.55905/rdelosv16.n48-026

Pereira Júnior, A., Morales, G. P., Beltrão, N. E. S., Silva, A. P. D. S., and Pereira, L. C. (2023b). Multitemporal analysis of land use and land cover in the Uraim river microbasin, Paragominas–Pará: Análise multitemporal do uso e cobertura da terra na microbacia do rio Uraim, Paragominas, Pará. *Concilium* 23, 383–404. doi:10.53660/CLM-1093-23D20A

Philippot, L., Griffiths, B. S., and Langenheder, S. (2021). Microbial community resilience across ecosystems and multiple disturbances. *Microbiol. Mol. Biol. Rev.* 85, e00026-20. doi:10.1128/MMBR.00026-20

Rout, A. K., Tripathy, P. S., Dixit, S., Behera, D. U., Behera, B., Das, B. K., et al. (2023). Unveiling the microbiome landscape: a metagenomic study of bacterial diversity, antibiotic resistance, and virulence factors in the sediments of the river ganga, India. *Antibiotics* 12, 1735. doi:10.3390/antibiotics12121735

Santos, E. M., and Picanço, O. A. S. (2008). *Recomposição do ecossistema florestal da nascente do rio uraim localizado no município de paragominas/pa*. Belem, PA: Universidade Federal do Pará.

Santos-Júnior, C. D., Sarmento, H., Pellon de Miranda, F., Henrique-Silva, F., and Logares, R. (2020). Uncovering the genomic potential of the Amazon River microbiome to degrade rainforest organic matter. *Microbiome* 8, 151. doi:10.1186/s40168-020-00930-w

Sardinha, A. S., and Ventura, K. S. (2022). "Análise preliminar dos riscos ambientais da Bacia do Rio Uraim, em um Município da Amazônia Oriental," in *Proceedings of* (Brazil: Universidade Estadual de Campinas), 61–64. doi:10.20396/iwisdw.n1.2022.4790

Schwarzenbach, R. P., Egli, T., Hofstetter, T. B., Von Gunten, U., and Wehrli, B. (2010). Global water pollution and human health. *Annu. Rev. Environ. Resour.* 35, 109–136. doi:10.1146/annurev-environ-100809-125342

Strokal, M., Bai, Z., Franssen, W., Hofstra, N., Koelmans, A. A., Ludwig, F., et al. (2021). Urbanization: an increasing source of multiple pollutants to rivers in the 21st century. *Npj Urban Sustain* 1, 24. doi:10.1038/s42949-021-00026-w

Tornevi, A., Bergstedt, O., and Forsberg, B. (2014). Precipitation effects on microbial pollution in a river: lag structures and seasonal effect modification. *PLoS ONE* 9, e98546. doi:10.1371/journal.pone.0098546

VanEvery, H., Franzosa, E. A., Nguyen, L. H., and Huttenhower, C. (2023). Microbiome epidemiology and association studies in human health. *Nat. Rev. Genet.* 24, 109–124. doi:10.1038/s41576-022-00529-x

Vinueza, D., Ochoa-Herrera, V., Maurice, L., Tamayo, E., Mejía, L., Tejera, E., et al. (2021). Determining the microbial and chemical contamination in Ecuador's main rivers. *Sci. Rep.* 11, 17640. doi:10.1038/s41598-021-96926-z

Wingett, S., and Andrew, S. (2018). FastQ Screen: a tool for multi-genome mapping and quality control. *F1000Research* 7, 1338. doi:10.12688/f1000research.15931.2

Wood, D. E., Lu, J., and Langmead, B. (2019). Improved metagenomic analysis with Kraken 2. *Genome Biol.* 20, 257. doi:10.1186/s13059-019-1891-0

Xu, Y., Ma, S., Huang, Z., Wang, L., Raza, S. H. A., and Wang, Z. (2023). Nitrogen metabolism in mycobacteria: the key genes and targeted antimicrobials. *Front. Microbiol.* 14, 1149041. doi:10.3389/fmicb.2023.1149041

frontiers | Frontiers in Environmental Science

TYPE Original Research
PUBLISHED 16 August 2024
DOI 10.3389/fenvs.2024.1440635

Check for updates

OPEN ACCESS

EDITED BY
Visva Bharati Barua,
University of North Carolina at Charlotte,
United States

REVIEWED BY
Connor Brown,
Virginia Tech, United States
Jannatul Ferdous,
University of North Carolina at Charlotte,
United States

*CORRESPONDENCE
Jiyoung Lee,
lee.3598@osu.edu

RECEIVED 03 June 2024
ACCEPTED 06 August 2024
PUBLISHED 16 August 2024

CITATION
Mills M, Wittum T and Lee J (2024) Dynamic microbiome and mobile resistome are revealed in river biofilms from a multi-use watershed through long-read sequencing.
Front. Environ. Sci. 12:1440635.
doi: 10.3389/fenvs.2024.1440635

COPYRIGHT
© 2024 Mills, Wittum and Lee. This is an open-access article distributed under the terms of the Creative Commons Attribution License (CC BY). The use, distribution or reproduction in other forums is permitted, provided the original author(s) and the copyright owner(s) are credited and that the original publication in this journal is cited, in accordance with accepted academic practice. No use, distribution or reproduction is permitted which does not comply with these terms.

Dynamic microbiome and mobile resistome are revealed in river biofilms from a multi-use watershed through long-read sequencing

Molly Mills[1], Thomas Wittum[2,3] and Jiyoung Lee[1,3,4]*

[1]Division of Environmental Health Sciences, College of Public Health, The Ohio State University, Columbus, OH, United States, [2]Department of Veterinary Preventive Medicine, The Ohio State University, Columbus, OH, United States, [3]Infectious Diseases Institute, The Ohio State University, Columbus, OH, United States, [4]Department of Food Science and Technology, The Ohio State University, Columbus, OH, United States

The dissemination of antibiotic resistance (AR) through various environments and the role of AR hotspots in public health crises are gaining increasing attention. Aquatic biofilms are speculated to play a significant role in AR spread due to their collection of diverse microorganisms and facilitation of horizontal gene transfer (HGT). However, few studies have characterized the AR genes (resistome) present in natural river biofilms. The goal of this study was to use MinION long-read sequencing to analyze the microbiome, resistome, and mobile genetic elements (MGEs) in periphyton (epilithic biofilms) (n = 56) from a multiuse watershed in Ohio, to elucidate the role of periphyton in clinically relevant AR. Key members of the periphyton microbiome included *Flavobacterium* and *Aeromonas*. Overall, periphyton microbial communities shifted with season and location. Specifically, species of *Porphyrobacter* and *Cyanobacteria* were more abundant in biofilms during the summer season. Potentially pathogenic bacteria, including the family *Enterobacteriaceae*, the fish pathogen *Pseudomonas koreensis*, and the human pathogen *Shigella flexneri*, were more abundant in sites downstream of the large city, Columbus, OH, than upstream. The periphyton resistome carried diverse AR genes for a variety of classes, but had minimal clinical relevance. *Escherichia*, *Escherichia coli*, and *Muvirus* were common hosts of AR genes (ARGs) and MGEs. *Pseudomonas* and Cyanobacteria were frequently MGE hosts, but not AR genes, indicating the potentially important role of these taxa in HGT within and around biofilms. While the sequencing depth in this study was relatively shallow, these findings highlight the mobility potential for the transmission of ARGs in river biofilms.

KEYWORDS

One Health, mobile genetic elements, antibiotic resistance genes, MinION sequencing, metagenomics, freshwater, periphyton

1 Introduction

Antibiotic resistance (AR) is a longstanding and widespread health concern, and its modern escalation is attributed to human activities (Finley et al., 2013). Specifically, the historical overuse, misuse, and regular use of antibiotics in medicine and agriculture have promoted the spread and selection of antibiotic resistance genes (ARGs), which enable

bacteria to evade the therapeutic effects of antibiotics (Davies and Davies, 2010). This selective pressure encourages the transfer of ARGs among bacteria through horizontal gene transfer (HGT), facilitated by mobile genetic elements (MGEs) (Frost et al., 2005). In this way, ARGs are unique biological contaminants because they do not necessarily dissipate with distance from the pollution source, and they can propagate in the environment and spread between bacteria (Abe et al., 2020). Fecal contamination from sources like wastewater treatment plant (WWTP) effluent discharge and agricultural runoff is a major source of ARGs, AR bacteria (ARB), and antibiotics to the environment (Larsson and Flach, 2021; Yin et al., 2023). While the environment is increasingly recognized as a potential source of ARG evolution and transmission, its role in clinical AR remains poorly understood (Larsson and Flach, 2021).

Biofilms are hotspots of AR transmission and acquisition in the environment due to their high levels of HGT, unique structure, and ability to accumulate pollutants, such as antibiotics (Balcázar et al., 2015; Abe et al., 2020; Sentenac et al., 2021). The focus of this study, periphyton, which encompass various types of freshwater biofilms, are complex communities of microorganisms, including bacteria, algae, fungi, protozoa, and viruses surrounded by in extracellular polymeric substances (EPS) (Fernandes et al., 2020; Zhao et al., 2022). Periphyton attached to stones or other stationary surfaces are known as epilithic biofilms (Fernandes et al., 2020; Sentenac et al., 2021; Zhao et al., 2022). Compared to other aquatic matrices, including water and sediments, environmental biofilms have been found to harbor higher levels of ARGs (Reichart et al., 2021; Mills et al., 2022). Periphyton play a crucial role in freshwater ecosystems, as they significantly contribute to primary production and oxygen levels, are a key player in nitrogen and phosphorous cycling, and serve as a vital food source for aquatic animals, such as crayfish and fish (Zhao et al., 2022). Their role in nutrient cycling, particularly the removal of nitrogen and phosphorous from water, can mitigate eutrophication and combat some of the adverse effects of climate change (Zhao et al., 2022). Finally, because of periphyton's strong responses to environmental changes and its abundance in freshwater, they are a valuable indicator of environmental quality (Zhao et al., 2022) and impact. Analyzing epilithic biofilms provides the ability to assess contamination over a longer time frame compared to more traditional monitoring matrices, like surface water, because biofilms have greater stability over time (Fernandes et al., 2020; Sentenac et al., 2021). Studying the microorganisms and ARGs in aquatic biofilms provides the opportunity to elucidate the role of these unique microbial communities in AR.

This study aimed to characterize the microbiome and resistome (collection of ARGs) of periphyton collected from various sites over a one-year period from a mixed-use river watershed in central Ohio (OH), United States. The objective was to classify the ARGs and MGEs in periphyton, as well as their microbial hosts, using long-read sequencing technology, which has not frequently been used in environmental microbiome or resistome studies. Ultimately, the purpose of this study was to use the resistome and MGE data to evaluate the clinical relevance and transmissibility of ARGs in aquatic biofilms. Previous studies analyzing the microbiome of natural river biofilms have typically used 16S rRNA gene sequencing (Zeglin, 2015; Guo et al., 2021; Tamminen et al., 2022; Bagra et al., 2023). One meta-analysis previously compiled and analyzed shotgun sequencing data to annotate the freshwater biofilm resistome, including biofilms from rivers (Yao et al., 2022). This study used publicly available metagenomic data to catalog ARGs in freshwater biofilms on a large scale. They found that the sampling location and relative human footprint (human pressure) influenced the freshwater biofilm resistome. They annotated ARGs and ARG hosts, like our study, but the scale was much larger, encompassing four countries, and they used all short read data (Yao et al., 2022). To our knowledge, the present study is the first example of metagenomic MinION long-read sequencing of freshwater periphyton communities. Our primary focus was to elucidate the potential role of periphyton in clinical AR. Our previous analysis of these samples using droplet digital PCR revealed high concentrations of clinically relevant carbapenem resistance genes (bla_{KPC}, bla_{NDM}, bla_{OXA-48}) in periphyton compared to river water, sediment, and detritus (Mills et al., 2022). This subsequent study provides a comprehensive profile of the entire microbiome and resistome of periphyton from a microbial ecology perspective, examining spatial and temporal differences in this matrix.

2 Materials and methods

2.1 Sample collection

Periphyton samples were collected from 26 sites along the Scioto River watershed in OH United States, including the Scioto River, Olentangy River, and Big Darby Creek (Supplementary Figure S1). The collection methods and study sites are previously described in Mills et al. (2022). Briefly, the Scioto River watershed drains 6,513 square miles, with the northern part of the watershed being composed of mostly agricultural lands, and the large urban center, Columbus, OH, which is the largest city in the state (Ohio Environmental Protection Agency (EPA), 2014). The southern half of the watershed is mostly forests with some agricultural land (Ohio Environmental Protection Agency (EPA), 2014). Therefore, these rivers flow through many different sources of contamination. Periphyton samples were collected between October 2017 and August 2018 in four visits/seasons. The "Autumn" samples were collected between October and December 2017, "Winter" between February and March 2018, "Spring" between April and May 2018, and "Summer" between July and August 2018. Periphyton samples were collected by brushing the surface of large, submerged sediments or stones onto a tray. The detached periphyton were rinsed into an opaque plastic jar (Kautza and Sullivan, 2016). Samples were collected from near the right bank, left bank, and middle of the river for each site. Samples were transported to the lab on ice and stored at 4°C prior to DNA extraction.

2.2 DNA extraction and long-read sequencing

Periphyton DNA was extracted from 0.25 g of wet weight per sample with the DNeasy PowerSoil Kit (Qiagen, Valencia, California (CA), United States). DNA concentration was measured with the Qubit 3 Fluorometer (ThermoFisher Scientific, Waltham, Massachusetts (MA), United States). DNA quality was measured

with the NanoDrop™ 2000 Spectrophotometer (ThermoFisher Scientific). Periphyton DNA samples that were low in concentration, or outside the desired range of quality scores ($OD_{260/280}$ = 1.8–2.0; $OD_{260/230}$ = 2.0–2.2) were cleaned and concentrated with a basic ethanol precipitation protocol. The protocol is presented in Mills et al. (2023). In total, 56 periphyton samples were adequate quality and concentration for long-read metagenomic sequencing.

DNA samples were sequenced on Oxford Nanopore Technology's (ONT) long-read MinION sequencer (ONT, Oxford, England) using Flongle flow cells (FLO-FLG001 R9.4.1). DNA libraries were prepared and barcoded with the Rapid Barcoding Kit (SQK-RBK004, ONT), following the ONT instructions for the kit, which are available on the ONT website (https://community.nanoporetech.com/). This library prep kit with the Flongle flow cells allows multiplexing of up to 12 samples with inputs of 200 ng of DNA per sample. While the input for sequencing is low, the combination of these methods allowed for low-cost analysis of many samples. This was selected for this study, given the goals of analyzing many samples at a shallower sequencing depth, and these methods and workflow had been used successfully in prior study of fecal samples to achieve similar goals (Mills et al., 2023). Sequencing was run for 24 h or until the number of reads plateaued.

2.3 Long-read sequencing bioinformatics

Raw data were basecalled and demultiplexed using Guppy (v 3.2.4). Taxonomy were annotated with What's In My Pot (WIMP) on the EPI2ME platform (2020.05.19). TaxonKit was used to pair National Center for Biotechnology Information (NCBI) taxonomy IDs with the full taxonomy (Shen and Ren, 2021). Microbiome compositions are presented as relative abundances (RA), specifically, the number of reads annotated as a specific taxonomy divided by the total number of microbially, taxonomically annotated reads. ARGs, MGEs, and hosts were annotated with NanoARG (Arango-Argoty et al., 2019). ARG and MGE abundance are reported as read counts (gene hits) and normalized ARG abundance, based on the library size of each sample, reported in average gene counts/gigabase pair (gbp) (Ma et al., 2016). NanoARG also denotes which ARG hosts are putative pathogens, based on sequence similarity to the World Health Organization's list of pathogens of concern for ARGs and the ESKAPE database of pathogens with multidrug resistance (Arango-Argoty et al., 2019). These annotations are reported as "potential" pathogenic hosts, given the metagenomic nature of this analysis, since higher resolution methods would be required to confirm the definite presence of pathogens (Arango-Argoty et al., 2019). Sequencing depth and library size (taxonomic annotated reads) can be found in the Supplementary Material (Supplementary Table S1). Sequencing data and metadata can be found at the NCBI Sequence Read Archive (SRA) under the accession number PRJNA1116137 (http://www.ncbi.nlm.nih.gov/bioproject/1116137).

2.4 Statistical analyses

Statistical analyses were completed in R (v 3.6.2). Periphyton microbiome data were filtered and normalized before diversity and differential abundance analyses. Only taxa classified to at least a Superkingdom level were retained in the microbiome data, and non-microbial eukaryotic reads were removed. Following this filtering, samples with libraries <100 reads were removed from the dataset prior to normalizing, which resulted in a total of 47 periphyton samples for diversity analysis (Supplementary Table S1). Prior to normalizing, the average library size from the Flongle flow cells was 609 classified, taxonomic reads, with a minimum of 120 reads and a maximum of 3,345 in a single sample. Microbiome data were normalized by scaling each sample to the median library size. Due to the wide variety in library sizes and overall shallow sequencing depth, this method was selected to preserve as much of the dataset as possible (McMurdie and Holmes, 2013; Weiss et al., 2017). This resulted in a total of 3,117 unique taxa and a library size of 385 reads/sample. Resistome and MGE data were analyzed as normalized ARG abundance (ARG counts/gbp). There were no significant Spearman or Pearson correlations between sequencing depth (bp) and Shannon index ($p > 0.05$), indicating that although library sizes were small, differences in the microbiome were not attributed to sequencing depth. A community-style analysis was not included for the periphyton resistome or mobilome (MGE) data, given the limited annotations of functional genes at this sequencing depth (Supplementary Table S1). Furthermore, ARG abundance was dependent on sequencing depth, even with normalization ($p < 0.05$), limiting the statistical reliability of the analysis.

The overall goals of the statistical testing were to identify differences in the periphyton microbiome or resistome with season or location of sample collection. Alpha and beta diversity of the microbiome were calculated using the phyloseq (McMurdie and Holmes, 2013) and vegan (Oksanen et al., 2020) packages. Shannon index was calculated for alpha diversity. Normality was tested for Shannon index with Q-Q plots and Shapiro-Wilk tests. The Levene test was used to assess homogeneity of variance. Shannon index was normally distributed with equal variance between groups. Therefore, because these data fit the assumptions of the test, differences in Shannon index were tested with a one-way ANOVA by season and location. For season, only winter, spring, and summer samples were included in statistical testing because of the small number of samples collected from autumn (n = 2). Furthermore, for location in the watershed (way upstream, upstream, downstream, way downstream), samples from Canoe Livery/Trapper John's were excluded since these samples (n = 2) were the only taken from Big Darby Creek (Supplementary Table S1; Supplementary Figure S1). We also found that in our prior analysis (Mills et al., 2022), this site was heavily contaminated with carbapenem ARGs, likely due to its role in recreation as a canoe livery. These samples were treated as outliers and were thus removed from the statistical testing by location. In order to test microbiome alpha diversity by both location and season, a two-way ANOVA was run.

Community composition and structure were calculated with the beta diversity dissimilarity matrix, Bray Curtis, and plotted with Non-Metric Multidimensional Scaling (NMDS), which produces ordination plots that present the differences between each sample's microbial communities by distance. Differences beta diversity were tested with Permutational Multivariate Analysis of Variance (PERMANOVA) (adonis2) tests from the vegan package (Oksanen et al., 2020), followed with pairwise adonis, to

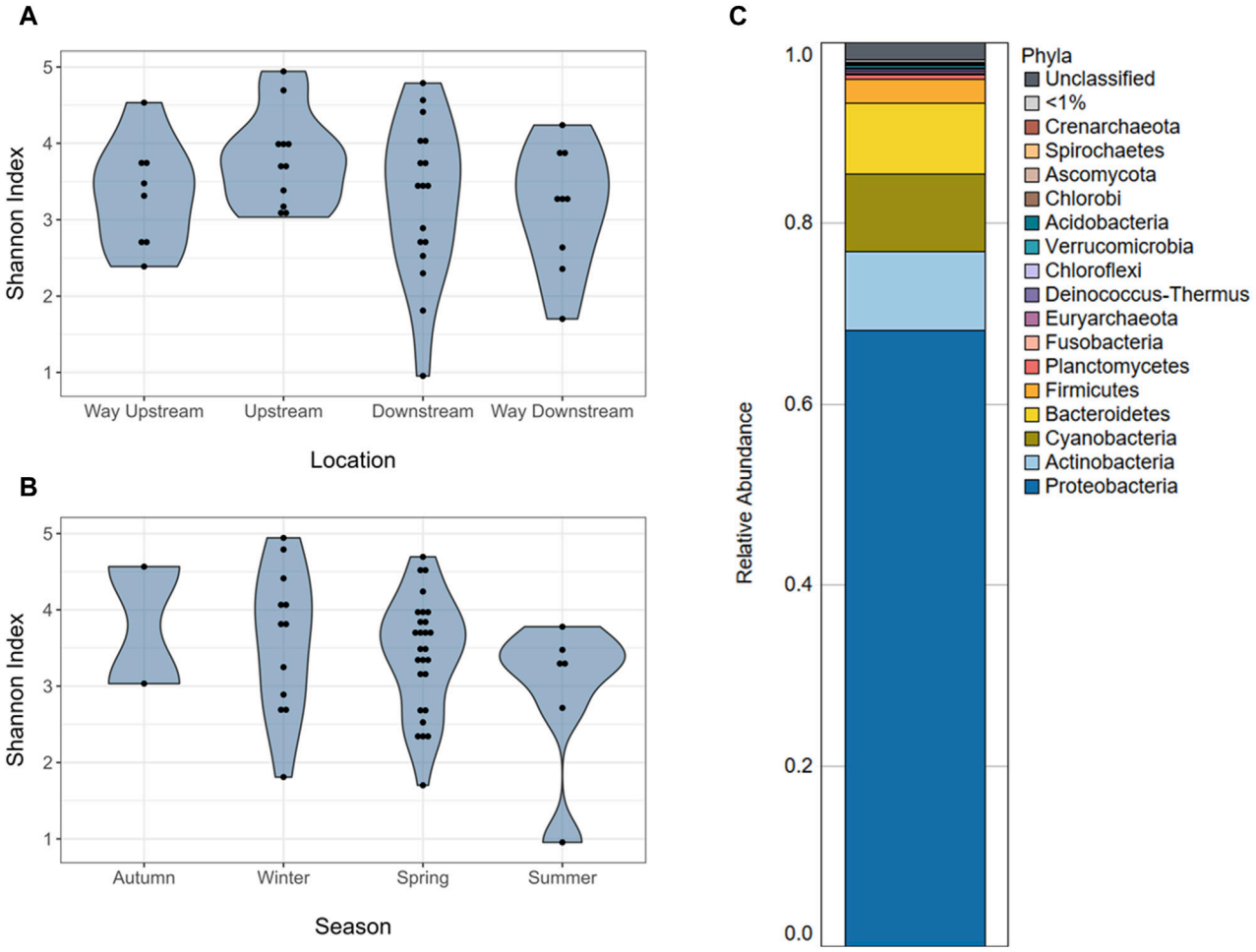

FIGURE 1
Microbiome alpha diversity and composition of periphyton samples. **(A)** Alpha diversity (Shannon index) of the microbiomes of periphyton samples by location in the watershed. **(B)** Alpha diversity (Shannon index) of the microbiomes of periphyton samples by season. **(C)** Average composition of periphyton microbiomes shown as a relative abundance at a phyla level.

determine if microbial communities significantly differ in composition/structure by season or location. Both season and location were tested individually, then a single model was created to test both season and location simultaneously. Similar to alpha diversity statistical testing, samples collected in Autumn and from Canoe Livery/Trapper John's were removed from comparisons made between season and location, respectively. Significance was assessed at $p < 0.05$ for alpha and beta diversity statistical tests.

Differences in periphyton microbiome composition (RA) were tested via Microbiome Multivariable Associations with Linear Models 2 (MaAsLin2) (Mallick et al., 2021) at a phyla, family, and species level of taxonomy to determine microorganisms that were increased in abundance in the periphyton microbiome with season or location. Models were created with both location and season as fixed effects. Only the samples included in the beta diversity testing were included in differential abundance testing. Taxa were included with a minimum RA of 0.001 and prevalence of 0.2. Chord diagrams for the functional gene host results were created in R, using the circlize package (Gu et al., 2014).

3 Results

3.1 Aquatic biofilm microbiome diversity and composition

Long-read sequencing generated an average of 4,432 reads/sample, with a minimum of 239 reads and a maximum of 20,428 reads in a single sample (Supplementary Table S1). The average sequencing depth was 2,503,173 basepairs (bp)/sample, with the smallest sample containing 1,372 bp and the largest containing 16,566,315 bp. A total of 3,116 unique taxa were identified in the 56 periphyton microbiomes in this study. This included Viruses, Fungi, Bacteria, and Archaea. At a phyla level, an average of 68.2% of the periphyton microbial community was Proteobacteria, followed by 8.70% Actinobacteria, 8.59% Cyanobacteria, 7.83% Bacteroidetes, and 2.61% Firmicutes (Figure 1C; Supplementary Figure S2). All other phyla were less than 1% of the microbiome. The ten genera with the highest RA (average) in all periphyton microbiomes were *Flavobacterium* (2.95%), *Aeromonas* (2.06%), *Chondrocystis* (1.89%), *Escherichia* (1.87%), *Acinetobacter* (1.25%), *Burkholderia*

TABLE 1 The top ten most abundant genera in the microbiome, hosting antibiotic resistance genes, and hosting mobile genetic elements in periphyton. Genera in the microbiome are shown as a relative abundance (RA) and gene hosts are shown as the total number of hits (annotations) in all samples.

	Periphyton microbiome			ARG hosts			MGE hosts		
	Genus	Phylum	RA	Genus	Phylum	Hits	Genus	Phylum	Hits
1	*Flavobacterium*	Bacteroidetes	0.030	*Escherichia*	Proteobacteria	17	*Escherichia*	Proteobacteria	106
2	*Aeromonas*	Proteobacteria	0.021	*Muviris*	Uroviricota	13	*Muviris*	Uroviricota	72
3	*Chondrocystis*	Cyanobacteria	0.019	*Janthinobacterium*	Proteobacteria	9	*Flavobacterium*	Bacteroidetes	29
4	*Escherichia*	Proteobacteria	0.019	*Pseudomonas*	Proteobacteria	9	*Nostoc*	Cyanobacteria	18
5	*Acinetobacter*	Proteobacteria	0.013	*Flavobacterium*	Bacteroidetes	5	*Stanieria*	Cyanobacteria	16
6	*Burkholderia*	Proteobacteria	0.007	*Acinetobacter*	Proteobacteria	3	*Chroococcidiopsis*	Cyanobacteria	12
7	*Bradyrhizobium*	Proteobacteria	0.006	*Brevundimonas*	Proteobacteria	3	*Oscillatoria*	Cyanobacteria	12
8	*Brevundimonas*	Proteobacteria	0.006	*Porphyrobacter*	Proteobacteria	3	*Pseudomonas*	Proteobacteria	12
9	*Acidovorax*	Proteobacteria	0.005	*Sphingobium*	Proteobacteria	3	*Acinetobacter*	Proteobacteria	10
10	*Arcobacter*	Proteobacteria	0.005	*Bradyrhizobium*	Proteobacteria	2	*Pleurocapsa*	Cyanobacteria	7

(0.68%), *Bradyrhizobium* (0.63%), *Brevundimonas* (0.56%), *Acidovorax* (0.53%), and *Arcobacter* (0.45%) (Table 1).

There were no differences in alpha diversity (Shannon index) of periphyton microbiome by season (winter, spring, summer) or sampling location (way upstream, upstream, downstream, way downstream) ($p > 0.05$; Figures 1A, B). Differences were tested by both season and location separately in one-way ANOVA analyses and together in a two-way ANOVA, and neither revealed significant differences ($p > 0.05$). However, there were differences in beta diversity of periphyton microbiomes with season and location. There were differences with season when tested via PERMANOVA alone ($p = 0.037$; Figure 2A), but there were no differences in location when tested alone ($p = 0.156$; Figure 2B). However, when both season and location were tested together via PERMANOVA, both were significant in structuring the biofilm microbiome. Specifically, when controlling for season ($p = 0.040$), location was also significant ($p = 0.021$). The interaction term of Season*Location was included in a PERMANOVA model, but it was not significant ($p > 0.05$). Pairwise tests (adonis2) revealed a significant difference between winter and summer microbiomes ($p = 0.01$), but there were no other significant pairwise comparisons ($p > 0.05$). No pairwise comparisons by location were significant ($p > 0.05$), however the smallest p-values were between way upstream and downstream ($p = 0.075$) as well as way upstream and upstream ($p = 0.089$).

Because both season and location were significant factors structuring the periphyton microbiome, differences in taxonomy were tested by these factors. There were no differentially abundant phyla by season or location in the periphyton microbiomes, as tested by MaAsLin2. By season, the family *Phyllobacteriaceae* was more abundant in winter than spring and summer (Supplementary Table S3). *Cellulomonadaceae* and *Nocardiodaceae* were more abundant in winter than summer. At a species level, *Mesorhizobium loti* was more abundant in winter than summer (Supplementary Table S5). *Porphyrobacter* sp. *LM 6* and *Leptolyngbya boryana* were more abundant in summer than winter or spring. *Porphyrobacter* sp. *YT40* and *Porphyrobacter neustonensis* were more abundant in summer than spring. Finally, *Aeromonas salmonicida* was more abundant in spring than winter.

By location, the families *Rhizobiaceae* and *Sphingomonadaceae* were more abundant in the way upstream and upstream sites than way downstream sites (Supplementary Table S4). *Enterobacteriaceae* was more abundant in the downstream compared to the way upstream sites. At a species level, *Polaromonas* sp. *Pch P* was more abundant in upstream sites than any other sites (Supplementary Table S6). *Citromicrobium* sp. *JL477* was more abundant in upstream than downstream sites, and *Tabrizicola piscis* was more abundant in upstream sites than way downstream sites. *Shigella flexneri* was more abundant in the downstream sites than the way upstream sites. Finally, *Pseudomonas koreensis* was more abundant in the way downstream sites than the upstream or downstream sites.

3.2 Periphyton resistome, mobilome, and microbial hosts

In total, 88 unique ARGs were annotated in a total of 35 periphyton samples from 17 antibiotic classes. Two hundred sixteen ARGs were annotated in all biofilm samples, with an average of 6 ARGs/sample. Twenty-one samples had zero ARGs annotated, and the most ARGs annotated in a single sample was 39 (sample P43; Supplementary Table S1). Most of the ARGs identified in periphyton samples were for multidrug resistance, which are ARGs offering resistance to multiple classes of antibiotics (39.8%), followed by glycopeptides (10.6%), bacitracins (7.41%), beta-lactams (7.41%), tetracyclines (6.48%), macrolides, lincosamides, and streptogramines (MLS) (5.56%), and aminoglycosides (5.09%) (Supplementary Figure S3). The five most frequently annotated ARGs were *ompR* (9.26%), *vanR* (6.02%), *bcrA* (5.56%), *rpoB2* (5.56%), truncated putative response regulator *ArlR* (5.09%), and *mtrA* (3.70%) (Supplementary Table S7).

For the 216 reads with an ARG annotated, 62.9% also had a microbial host annotated. ARG hosts were identified from the phyla

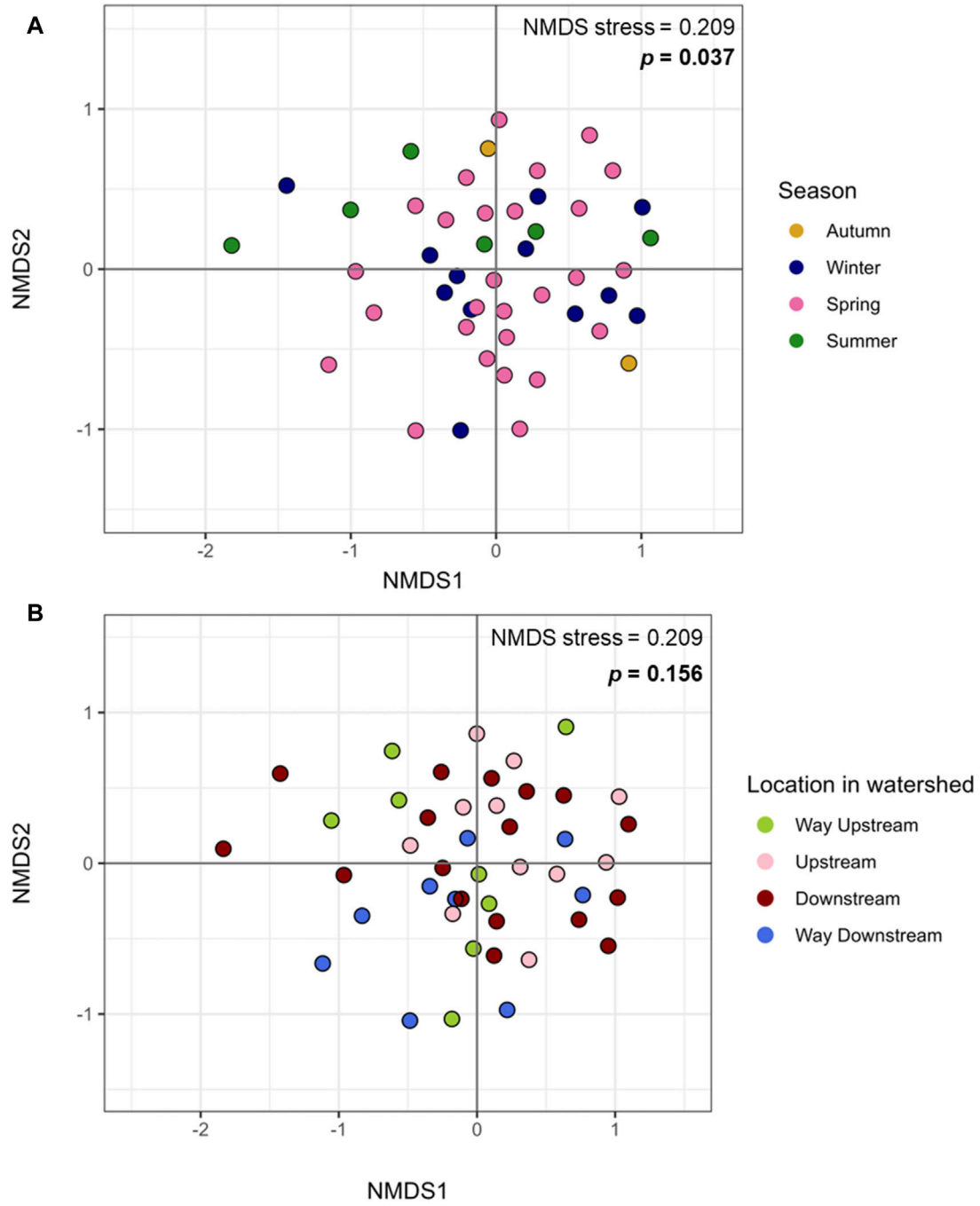

FIGURE 2
Microbiome beta diversity of periphyton samples. **(A)** Beta diversity of periphyton microbiomes by season, plotted with Bray Curtis dissimilarity and Non-Metric Multidimensional Sealing (NMDS).**(B)** Beta diversity of periphyton microbiomes by location in the watershed, plotted with Bray Curtis dissimilarity and NMDS.

Proteobacteria (64.7%), Urovirocota (9.56%), Bacteroidetes (8.82%), Actinobacteria (7.35%), Cyanobacteria (5.88%), Firmicutes (2.94%), and Euryarchaeota (0.74%) (Figure 3A). At a genus level, the most abundant ARG hosts were *Escherichia* (17.6%), *Muvirus* (9.56%), *Janthinobacterium* (6.62%), and *Pseudomonas* (6.62%) (Table 1). The remaining genera were all less than 5% of the ARGs annotated. Some ARG host taxa were classified to a species or even strain level, which included *Escherichia coli* (17.6%) as the most abundant ARG host (Table 2). One ARG host species was classified as potentially pathogenic, *Acinetobacter baumannii*, which hosted the multidrug resistant gene, *ompR*.

In total, 790 unique MGEs were annotated in the 46 periphyton samples, with an average 21 MGEs/sample. The majority of the MGEs were transposases (74.3%), followed in much lower abundance by integrases (12.7%), recombinases (12.2%), transposons (0.62%), and integrons (0.21%) (Supplementary

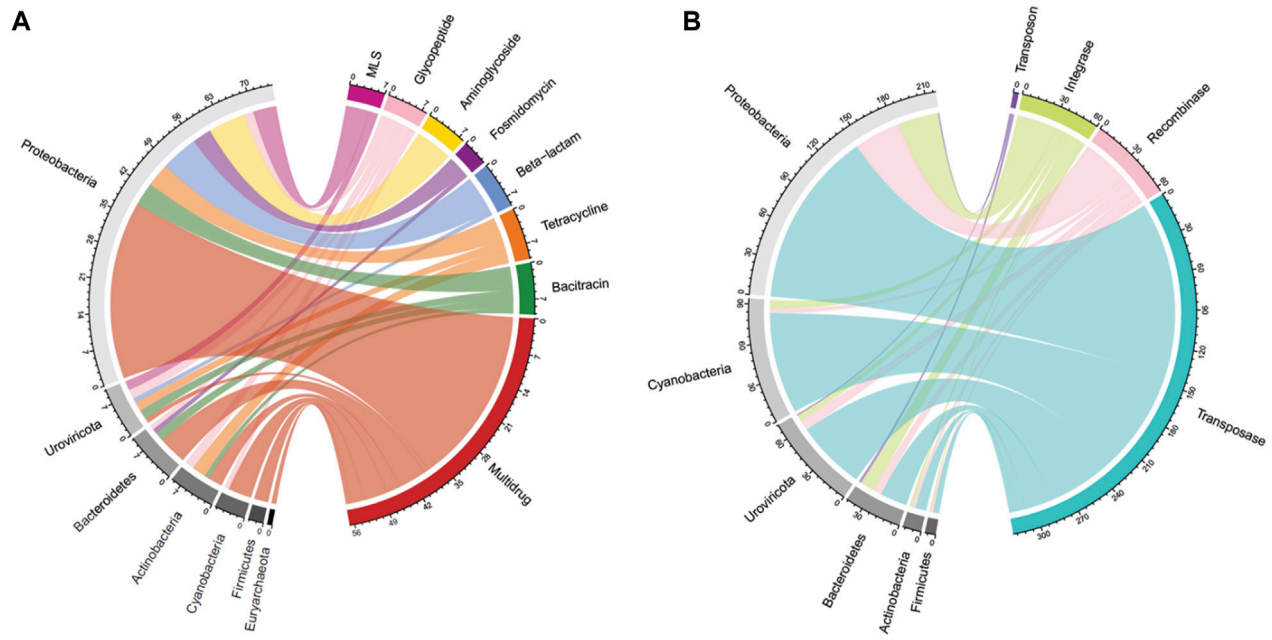

FIGURE 3
Periphyton antibiotic resistance gene and mobile genetic element host phyla. **(A)** A chord diagram of the top seven most abundant antibiotic resistance gene classes and their corresponding host phyla, shown as total antibiotic resistance gene hits. **(B)** A chord diagram of the types of mobile genetic elements and their corresponding top six host phyla, shown as total mobile genetic element gene hits.

TABLE 2 The top ten most abundant species hosting antibiotic resistance genes in periphyton samples, shown as total gene hits in all samples.

	Species	Phylum	ARG hits
1	*Escherichia coli*	Proteobacteria	24
2	*Janthinobacterium* sp. 1_2014MBL_MicDiv	Actinobacteria	8
3	*Escherichia virus Mu*	Uroviricota	7
4	*Enterobacteria phage SfMu*	Uroviricota	6
5	*Flavobacterium* sp. PK15	Bacteroidetes	4
6	*Pseudomonas fluorescens*	Proteobacteria	3
7	*Brevundimonas subvibrioides*	Proteobacteria	2
8	*Dyella jiangningensis*	Proteobacteria	2
9	*Pedobacter heparinus*	Bacteroidetes	2
10	*Porphyrobacter neustonensis*	Proteobacteria	2

TABLE 3 The top ten most abundant species hosting mobile genetic elements in periphyton samples, shown as total gene hits in all samples.

	Species	Phylum	MGE hits
1	*Escherichia coli*	Proteobacteria	106
2	*Escherichia virus Mu*	Uroviricota	43
3	*Enterobacteria phage SfMu*	Uroviricota	29
4	*Stanieria cyanosphaera*	Cyanobacteria	16
5	*Chroococcidiopsis thermalis*	Cyanobacteria	12
6	*Oscillatoria nigro-viridis*	Cyanobacteria	11
7	*Flavobacterium* sp. LPB0076	Bacteroidetes	10
8	*Flavobacterium psychrophilum*	Bacteroidetes	7
8	*Pleurocapsa minor*	Cyanobacteria	7

Figure S3). Out of the MGEs annotated, 47.4% were associated with a host. Among these microbial hosts, the top six most abundant phyla were Proteobacteria (48.0%), Cyanobacteria (20.6%), Uroviricota (15.8%), Bacteroidetes (9.43%), Actinobacteria (3.07%), and Firmicutes (1.75%) (Figure 3B). At a genus level, the most abundant MGE hosts were *Escherichia* (23.2%), *Muvirus* (15.8%), and *Flavobacterium* (6.36%) (Table 1). The remaining genera hosting MGEs were less common, comprising less than 5% of all the MGE hosts. The most abundant species hosting MGEs was *E. coli* (Table 3). Three species hosting MGEs were identified as potentially pathogenic, all of which contained transposases (IS630 family transposase, IS481 family transposase, IS5/IS1182 family transposase). These species were *Enterococcus faecium*, *Klebsiella pneumoniae*, and *Pseudomonas aeruginosa*, respectively.

Five reads within three different periphyton samples had both ARGs and MGEs annotated (Supplementary Table S8). The first read, identified as *Pseudomonas syringae*, contained the aminoglycoside ARG, *PvrR*, and an IS4 family transposase. The ARG *PBP-1A* for beta-lactam resistance was found on the same read as a transposase and was identified as *Janthinobacterium* sp. *1_2014MBL_MicDiv*. The ARG *vanS* for glycopeptide resistance was found on the same read as three MGEs, all transposases, in an undefined host. A read carrying *vanB*, another glycopeptide ARG,

carried a site-specific integrase for *Cyanothece sp. PCC 7822* in undefined species. Finally, one read identified as a synthetic construct, which is a classification in NCBI for DNA fragments like oligonucleotides and primers, but for this study we would consider an unclassified host, contained both the multidrug ARG, *smeS*, and a transposase MGE (IS4/IS5 family transposase).

4 Discussion

4.1 Long-read sequencing limitations

Long-read sequencing, such as ONT's MinION sequencing, holds much promise for the future of microbiome and resistome analysis (Boolchandani et al., 2019). While short read shotgun metagenomic sequencing requires algorithms for assembly to form longer reads for annotation, long-read sequencing does not. This limits some of the bias introduced from assembly algorithms, and it can result in obtaining results more quickly because assembly steps can be simplified (Boolchandani et al., 2019; Kamathewatta et al., 2019). Longer reads also give genetic context for the other functional genes, such as MGEs, and potential host information (Kamathewatta et al., 2019), which is extremely beneficial in studies of ARGs. A concern with long-read sequencing has been the higher error rates than short read sequencing, such as Illumina sequencing, however improvements in basecalling algorithms have improved sequencing accuracy (Logsdon et al., 2020).

In this analysis, we used small flow cells with low DNA inputs ("Flongle"), which others have referred to as "miniature" flow cells that can attain shallow sequencing depth (Mock et al., 2023; Viehweger et al., 2023). While the goal was to sequence many samples at a lower depth, our study revealed limitations with multiplexing ONT's MinION sequencing on a Flongle flow cell, particularly when using environmental samples. Specifically, we removed nine samples from the microbiome diversity analysis due to limited annotated reads. Although normalization showed no association between diversity and sequencing depth, the library size of samples following normalization (385 reads/sample) was low. More serious limitations were present in the resistome analysis, as the shallow sequencing depth limited ARG annotations (Supplementary Table S1), meaning that a community-style ARG diversity or abundance analysis could not be completed.

Our prior study utilizing these methods of multiplexing on Flongle flow cells used fecal DNA samples (Mills et al., 2023). Using these methods to sequence fecal samples resulted in a greater proportion of reads having classified taxonomy, with an average of 1,018/3,078 reads/sample (33.1%), compared to the average of 609/4,433 reads/sample (13.7%) with annotated taxonomy from the biofilm samples. Environmental DNA sequencing can have considerable challenges because of the variable and often low biomass of environmental DNA (Harper et al., 2019) and limitations in databases for reference data to many environmental microbial taxa (Perry et al., 2022). While the current study provides a snapshot of biofilm samples from a mixed-use watershed with a relatively shallow sequencing depth, future studies should use sequencing strategies with greater depth per sample, particularly when analyzing complex environmental samples. Specifically, we advise that individuals interested in annotating functional genes should not multiplex on ONT Flongle flow cells. These "mini" flow cells are ideal for quality testing before a larger experiment, as has recently been updated as the recommendation on ONT's website (https://nanoporetech.com/products/sequence/flongle). Other researchers have found success in using Flongle flow cells for adaptive sequencing (Viehweger et al., 2023; Wrenn and Drown, 2023), which is a targeted sequencing approach where nanopores only sequence regions of interest (Martin et al., 2022). This may be a beneficial use for Flongle flow cells in future to achieve sequencing of targeted regions, such as ARGs, while taking advantage of these flow cell's low cost.

4.2 Periphyton microbiome shifts with location and season

Although prior studies of natural, freshwater periphyton microbiomes used 16S rRNA gene sequencing, the major phyla identified via long-read sequencing were similar, including Proteobacteria, Bacteroidetes, Actinobacteria, Firmicutes, and Cyanobacteria (Zeglin, 2015; Guo et al., 2021; Tamminen et al., 2022; Bagra et al., 2023) (Figure 1C; Supplementary Figure S2). Most prior studies do not report the microbial community composition deeper than the phyla level of taxonomy (Zeglin, 2015; Guo et al., 2021; Tamminen et al., 2022). However, one prior study reported the composition of the natural biofilms from two rivers in Saxony, Germany, at a genus level (Bagra et al., 2023). Similar to the present study, one of the most abundant genera was *Flavobacterium*, which composed ~3% of both the periphyton microbiomes from Germany and the Ohio biofilms analyzed in the present study (Bagra et al., 2023) (Table 1). *Flavobacterium* are known biofilm formers (Jo et al., 2016). Furthermore, the species *F. psychrophilum*, *F. columnare*, and *F. branchiophilum*, are also known fish pathogens (Wahli and Madsen, 2018). These three species were identified in the periphyton microbiomes at various abundances. *Aeromonas* was the second most abundant genus in the periphyton microbiome (Table 1), and in addition to being known biofilm-formers (Talagrand-Reboul et al., 2017), these bacteria are often associated with fish infections, wastewater pollution, and urban sewage (Popovic et al., 2015). The abundance of *Flavobacterium* and *Aeromonas* in these biofilms highlights the potential One Health role of biofilms, particularly their potential relationship to animal health and wastewater. Analyzing the role of freshwater biofilm microbial communities, wastewater discharge, and fish health should be considered in future studies.

Our prior study, which analyzed a subset of these periphyton samples from the urban sites via 16S rRNA gene sequencing, showed similar major taxa as presented in this study, but at somewhat different abundances (Mills et al., 2022). This is likely due to the difference in methods and selection of different samples within the dataset, specifically the samples in this study were from the entire watershed. The biofilm microbiome composition from this larger dataset had about half the RA of Cyanobacteria (7.83% v. 13.0%) and Bacteroidetes (7.83% v. 16.0%) compared the urban subset (Mills et al., 2022) (Figure 1C). While this may be a reflection of the different sequencing methods, Cyanobacteria are known to favor water bodies with greater anthropogenic nutrient loading (Volk and Lee, 2023), which may explain the greater RA of Cyanobacteria in

the urban biofilms. Furthermore, while Bacteroidetes are common inhabitants of freshwater, they are known colonizers of animal guts, and often are the majority of the bacteria that make up the human gut microbiome (Thomas et al., 2011). The higher RA of Bacteroidetes in the prior periphyton subset may be due to the increased urbanization. Both *Pseudomonadaceae* and *Flavobacteriaceae* were in the top five families in the urban, 16S rRNA gene sequencing dataset and the full watershed, long-read dataset (Mills et al., 2022) (Supplementary Table S2). Finally, *Flavobacterium* and *Acinetobacter* were both in the top five genera for both study datasets (Table 1). While *Pseudomonas* was the second most abundant genus in the urban, 16S rRNA sequencing microbiome data, it was not in the top ten most abundant genera in the long-read sequencing microbiome data (Mills et al., 2022). From this comparison, it is possible to deduce that while *Flavobacterium* and *Acinetobacter* may be core taxa of these river biofilms, *Pseudomonas* may only be a key taxon in urban areas. However, it may also reflect a bias in the differences in sequencing methods.

Microbiomes within epilithic biofilms are known to shift temporally more frequently than with location (Zeglin, 2015), so differences in periphyton microbiome diversity and composition with season were expected (Figure 3). Our prior study showed a significant difference in alpha diversity of periphyton microbiomes with season, not location (Mills et al., 2022). It was surprising that the same result was not found here (Figures 1A, B), however this may be due to limitations in diversity analysis at this sequencing depth. For beta diversity, our prior study identified significant differences with season, not location (Mills et al., 2022). Similarly, in this long- read analysis, when testing beta diversity separately, season was also significant but location was not (Figure 2), verifying that season is a stronger driver of microbial community structure and composition than the location in the watershed (Zeglin, 2015).

Among the taxa that had different abundances between seasons, several species stood out, with three distinctive species of *Porphyrobacter* exhibiting higher abundance in summer biofilm samples compared to spring (Supplementary Table S5). *Porphyrobacter* have typically been isolated from water habitats (hot spring, seawater, lake), and thrive in warm temperatures, with an optimal growth between 30°C and 35°C (Xu et al., 2018), which may explain their abundance in the summer biofilms, when temperatures in this region are the highest. The Cyanobacteria *L. boryana* was also more abundant in the summer than in the winter and spring, which is also likely due to Cyanobacteria thriving in warmer temperatures (Volk and Lee, 2023). *A. salmonicida* was the only species that was more abundant in the spring than other seasons. This is potentially because this species is mesophilic and prefers an intermediary temperature, which is found during the spring season (Charette, 2021). *A. salmonicida* has a genome that is known to carry many MGEs, including plasmids that carry multidrug resistant ARGs and virulence factors; this is important because this species is mainly regarded as an opportunistic fish pathogen (Charette, 2021). While no ARGs were annotated on *A. salmonicada* hosts in this long-read analysis, two transposase MGEs were annotated on a single read from sample P33. *A. salmonicada* may play an important, yet understudied role in the biofilm resistome and environmental AR, particularly considering the One Health component of this species as a fish pathogen.

When controlling for season, there were significant differences with sampling location, which confirms changes in biofilm microbial communities longitudinally, along a watershed gradient. Factors that are known to change spatially, such as land use, hydrology, metal contamination, and nutrient concentrations, have a significant impact on freshwater microbiomes (Zeglin, 2015). Specifically, the largest difference in community structure by location in the watershed was found between the sites in and around Columbus, OH ("upstream" and "downstream"), and the way upstream site. This reflects the impact of urbanization on biofilm microbiomes. Specifically of interest in the differential abundance results by location were those taxa that increased downstream the urban center of Columbus, OH. The known fecal-associated family, *Enterobacteriaceae*, which has incredible medical, public health, and veterinary significance (Janda and Abbott, 2021), was more abundant in the downstream sites than way upstream (Supplementary Table S4). This is likely due to the numerous sources of fecal pollution entering waterways in Columbus, such as urban wastewater and stormwater (Lee et al., 2020). Furthermore, there could be a cumulative effect of agricultural nonpoint source fecal pollution that entered the watershed upstream of Columbus that contributed to the overall increased abundance of *Enterobacteriaceae*. It is also clear in the relative abundance of this family, that while only the comparison of downstream v. way upstream was significantly different, the way upstream relative abundance was the lowest (0.0619), followed by the upstream location (0.0983). The downstream location RA of *Enterobacteriaceae* was the highest (0.1651), but the way downstream RA, was still higher than the way upstream and upstream locations (0.1164). This finding shows the accumulation of *Enterobacteriaceae* in freshwater biofilms from upstream to downstream in a watershed with increased anthropogenic pressure. Downstream Columbus, there was also increased RA of the fish pathogen, *P. koreensis* (Lau et al., 2024), and one of the causative agents of shigellosis (bacillary dysentery), *S. flexneri* (Nisa et al., 2020) (Supplementary Table S6). None of the species that were more abundant in upstream sites are known pathogens (Willems, 2014; Zheng et al., 2016; Han et al., 2020). Prior studies have shown the impact of polluted river water from an urban area on periphyton microbial communities (Washington et al., 2013; Liao et al., 2019).

4.3 Periphyton carries a diverse and mobile resistome

It is uncommon to find prior metagenomic studies of the river biofilm resistome. Most studies target a panel of ARGs with quantitative PCR (Proia et al., 2016; Roberto et al., 2019; Li and Zhang, 2020; Reichart et al., 2021), which limits the conclusions that can be made, since only the pre-selected panel of genes are compared. One prior study that compiled sequence data of freshwater biofilms from several different locations identified the most abundant ARG classes as bacitracin, multidrug, MLS, aminoglycoside, beta-lactam, chloramphenicol, sulfonamide, and tetracycline (Yao et al., 2022). These Ohio biofilms had a similar resistome composition, with six of the same top eight ARG classes

(multidrug, bacitracin, MLS, tetracycline, beta-lactam, and aminoglycoside; Supplementary Figure S3).

An abundant ARG class in the periphyton resistome that was not expected was glycopeptide resistance. Glycopeptide antibiotics are reserved for human use against life-threatening Gram-positive bacterial infections (Yushchuk et al., 2020). The glycopeptide resistance genes were all for vancomycin resistance. However, none of these genes were identified in pathogenic bacterial hosts. Specifically, we did not find any vancomycin-resistant *Enterococcus* (VRE) or vancomycin-resistant *Staphylococcus aureus* (VRSA) (Yushchuk et al., 2020). It is most likely the vancomycin resistance in these biofilms are from naturally occurring environmental bacteria, as most of the genes identified in this study are from the biosynthetic gene clusters of environmental bacteria that naturally produce vancomycin, which are largely found on chromosomes (Yushchuk et al., 2020). Furthermore, two bacterial hosts of the *vanR* gene in this study were from families of bacteria known to produce vancomycin (*Micromonosporaceae* and *Streptosporangiaceae*) (Yushchuk et al., 2020). The large proportion of glycopeptide ARGs is likely due to a large presence of natural, not clinically relevant AR, so is not a major public health threat.

The most abundant MGE class in periphyton was transposase enzymes (Supplementary Figure S3), which catalyze the movement of DNA, including ARGs, between bacteria via phage or plasmids (Frost et al., 2005; Siguier et al., 2014). Transposases can also facilitate the movement of the MGEs integrons and transposons, which package mobile DNA (Frost et al., 2005; Gillings, 2014). Although this study did not analyze the proportion of the annotated functional genes that were hosted in plasmids versus chromosomes, transposases play a crucial role in plasmid gene transfer and acquisition (Frost et al., 2005). Furthermore, conjugation via plasmids is thought to be the main route of HGT in microbial communities (Abe et al., 2020), so this may explain the high abundance of transposase genes in periphyton communities.

Recombinase was the next most abundant MGE class, and these genes encode enzymes that catalyze gene movement within cells, not between cells (Frost et al., 2005). They facilitate gene acquisition by assisting in integrating DNA into the host genome, such as from phage (Wang et al., 2010). Integrase was the final major category of MGEs, and these enzymes are also important in ARG acquisition, as they catalyze integron recombination (Souque et al., 2021). Integrons carry and collect exogenous DNA on gene cassettes, which can include ARGs (Gillings, 2014). Integrons were identified in these biofilm samples, but at a much lower abundance than integrase or transposase (Supplementary Figure S2). Similarly, transposons were identified in the periphyton samples at a much lower abundance than other MGE categories. The transposon genes identified in periphyton samples exclusively encoded conjugative transposon proteins, which have great significance for AR due to their combination of transposons and transmissible plasmid traits (Clark and Padzernik, 2013). Conjugative transposons are capable of transferring genes between different species or genera as efficiently as within the same species (Scott and Churchward, 1995). This implies that in a diverse microbial population, such as an environmental biofilm, conjugative transposons greatly enhance the capacity for ARG transmission. These MGE results underscore the potential for gene mobility within biofilms. However, to fully understand the implications for ARG transmission and clinical relevance, it is essential to pair the MGE results with ARGs and their respective microbial hosts.

4.4 Periphyton have minimal clinically relevant ARG hosts

The use of long-read sequencing for the periphyton samples allowed for annotation of hosts from sequences containing ARGs without assembly or binning, which is unique compared to shotgun metagenomics (Kamathewatta et al., 2019). This study is crucial in documenting the ARG and MGE hosts within natural biofilms found in a river ecosystem. Shotgun metagenomic sequencing from freshwater biofilms identified ARG hosts via assembly methods and found that Proteobacteria were the most abundant hosts (Yao et al., 2022). Overall, 4/8 of the same phyla hosting ARGs as this study, including Proteobacteria, Bacteroidetes, Cyanobacteria, and Actinobacteria (Yao et al., 2022) (Figure 3A).

Although it might be expected that the most abundant ARG hosts are the most abundant bacteria in the microbiome, this is not the case (Table 1). Some bacteria are more common hosts than others. One study compared the abundance of horizontally transferred genes per genome and HGT hotspots between 80 different bacteria; HGT hotspots were defined as areas where horizontally transferred genes cluster in bacterial genomes (Oliveira et al., 2017). Several of the most abundant ARG and MGE hosts in this analysis had a relatively high abundance of horizontally transferred genes and hotspots, such as *E. coli* (Oliveira et al., 2017). *Escherichia* was the most abundant ARG and MGE host at a genus level (Table 1), and *E. coli* was the most abundant ARG and MGE host at a species level (Tables 2, 3). *E. coli* is known to be a common agent of HGT, transmitting and acquiring ARGs with relative ease (Hasegawa et al., 2018). Therefore, *E. coli* is an abundant host in periphyton because of the mobility potential in its genome, not necessarily its abundance in the microbial community. *Pseudomonas* was also a common ARG and MGE host, but it was not in the ten most abundant genera in the overall microbiome (Table 1). *Pseudomonas* may more frequently participate in HGT than other more abundant genera in the microbiome. This was demonstrated in Oliveira et al., as four different *Pseudomonas* species had relatively high horizontally transferred genes/genome and hotspots (2017). One species in Oliveira et al., *Pseudomonas fluoroscencs*, was identified several times in these periphyton samples, hosting transposase, recombinase, and integrase MGEs, as well as multidrug and phenicol ARGs (2017).

The high abundance of Cyanobacteria as hosts, specifically of MGEs is notable (Figure 3). Cyanobacteria may play a not yet fully known, but they play a critical role in the water resistome (Dias et al., 2019; Volk and Lee, 2023). Unlike other prokaryotes, Cyanobacteria form blooms and can produce hazardous toxins for human health (Cheung et al., 2012). Both factors may be important in the freshwater resistome. HGT may be increased while Cyanobacteria participate in blooms, due to the close contact and cell density during this phenomenon (Wang et al., 2020a). It has been shown

that bloom-forming Cyanobacteria host a greater abundance of insertion sequence MGEs than non-bloom-forming Cyanobacteria (Lin et al., 2010). Cyanobacterial toxins, such as microcystin, also promote HGT (Xu et al., 2020). Finally, ARG abundance has been shown to increase in water during Cyanobacteria blooms compared to non-bloom periods (Wang et al., 2020a).

Another unique host of ARGs and MGEs in these periphyton samples were viruses, specifically phage (Figure 3). While previous research has called into question the nature of viruses hosting ARGs in metagenomic studies, we interpret our findings cautiously, emphasizing that these results indicate ARGs being associated with phage in these biofilm samples (Enault et al., 2017). Phage have previously been identified as a significant carrier of AR genes in the environment (Lekunberri et al., 2017; Abe et al., 2020). At a phyla level, Uroviricota viruses were the second most abundant ARG hosts and the third most abundant MGE hosts in periphyton. Phage can act as MGEs (Frost et al., 2005), and many studies demonstrate ARG transfer via phage (Abe et al., 2020). The viruses identified as hosts in this study were all from the genus Muvirus (Table 2), also known as bacteriophage Mu. They are a hybrid of both viruses and transposons, so these phage can transpose into a host genome without the use of transposons (Clark and Padzernik, 2013). Mu viruses, including the *Escherichia virus mu* and *Enterobacteria phage SfMu*, which were the two phage associated with ARGs in these biofilm samples, are common inhabitants of diverse environments, including host-associated, aquatic, and terrestrial microbial communities (Zhang et al., 2023). The phage hosts of ARG and MGEs in this study demonstrate the high HGT potential from periphyton samples.

Overall, our analysis did not identify potential pathogens hosting ARGs in periphyton. A future study with greater sequencing depth may uncover more clinically relevant ARGs and their hosts, but the primary finding from this this study is that periphyton microbial communities are not important reservoirs of clinically relevant ARGs in pathogenic bacterial hosts. Therefore, we conclude that there is not a direct threat of transmission of AR bacteria from periphyton to humans or animals with exposure in similar settings. A future goal should be to identify if aquatic biofilms harbor more dangerous AR bacteria in different settings, such as low- and middle-income countries (LMICs) with more limited water, sanitation, and hygiene (WASH) regulations. While the exact role of environmental microorganisms in the global spread and persistence of ARGs is not yet fully known, it is acknowledged that the environment is a reservoir of gene evolution and transfer (Larsson and Flach, 2021). This study reveals that periphyton samples exhibit significant potential for transmitting mobile ARGs between bacteria, due to their high microbial diversity, abundant MGEs, and varied ARGs. AR is a global public health crisis, and environmental reservoirs must be considered in a One Health approach in combatting this issue. The abundance and diversity of ARGs in biofilms contribute to the overall environmental burden of AR, thereby perpetuating the public health crisis and potentially facilitating the emergence of novel ARGs.

Data availability statement

The datasets presented in this study can be found in online repositories. Sequencing data and metadata can be found at the NCBI Sequence Read Archive (SRA) under the accession number PRJNA1116137 (http://www.ncbi.nlm.nih.gov/bioproject/1116137).

Author contributions

MM: Formal Analysis, Funding acquisition, Investigation, Methodology, Visualization, Writing–original draft. TW: Funding acquisition, Project administration, Resources, Supervision, Writing–review and editing. JL: Conceptualization, Funding acquisition, Methodology, Resources, Supervision, Writing–review and editing.

Funding

The author(s) declare that financial support was received for the research, authorship, and/or publication of this article. This study was funded by the Centers for Disease Control and Prevention and SEED from the College of Food, Agricultural and Environmental Sciences, Ohio State University.

Acknowledgments

The authors thank the assistance from Drs. Dixie Mollenkopf and Seungjun Lee in sample handling and processing, and Dr. Mažeika Patricio Sullivan and his lab for field sampling.

Conflict of interest

The authors declare that the research was conducted in the absence of any commercial or financial relationships that could be construed as a potential conflict of interest.

Publisher's note

All claims expressed in this article are solely those of the authors and do not necessarily represent those of their affiliated organizations, or those of the publisher, the editors and the reviewers. Any product that may be evaluated in this article, or claim that may be made by its manufacturer, is not guaranteed or endorsed by the publisher.

Supplementary material

The Supplementary Material for this article can be found online at: https://www.frontiersin.org/articles/10.3389/fenvs.2024.1440635/full#supplementary-material

References

Abe, K., Nomura, N., and Suzuki, S. (2020). Biofilms: hot spots of horizontal gene transfer (HGT) in aquatic environments, with a focus on a new HGT mechanism. *FEMS Microbiol. Ecol.* 96 (5), fiaa031. doi:10.1093/femsec/fiaa031

Arango-Argoty, G. A., Dai, D., Pruden, A., Vikesland, P., Heath, L. S., and Zhang, L. (2019). NanoARG: a web service for detecting and contextualizing antimicrobial resistance genes from nanopore-derived metagenomes. *Microbiome* 7, 88. doi:10.1186/s40168-019-0703-9

Bagra, K., Bellanger, X., Merlin, C., Singh, G., Berendonk, T. U., and Klümper, U. (2023). Environmental stress increases the invasion success of antimicrobial resistant bacteria in river microbial communities. *Sci. total Environ.* 904, 166661. doi:10.1016/j.scitotenv.2023.166661

Balcázar, J. L., Subirats, J., and Borrego, C. M. (2015). The role of biofilms as environmental reservoirs of antibiotic resistance. *Front. Microbiol.* 6, 1216. doi:10.3389/fmicb.2015.01216

Boolchandani, M., D'Souza, A. W., and Dantas, G. (2019). Sequencing-based methods and resources to study antimicrobial resistance. *Nat. Rev. Genet.* 20, 356–370. doi:10.1038/s41576-019-0108-4

Charette, S. J. (2021). Microbe Profile: Aeromonas salmonicida: an opportunistic pathogen with multiple personalities. *Microbiology* 167, 5. doi:10.1099/mic.0.001052

Cheung, M. Y., Liang, S., and Lee, J. (2012). Toxin-producing Cyanobacteria in freshwater: a review of the problems, impact on drinking water safety, and efforts for protecting public health. *J. Microbiol.* 51 (1), 1–10. doi:10.1007/s12275-013-2549-3

Clark, D. P., and Pazdernik, N. J. (2013). "Chapter e22- Mobile DNA," in *Molecular biology*. Second Edn (Amsterdam, Netherlands: Elsevier), e553–e558.

Davies, J., and Davies, D. (2010). Origins and evolution of antibiotic resistance. *Microbiol. Mol. Biol. Rev.* 74 (3), 417–433. doi:10.1128/MMBR.00016-10

Dias, E., Oliveira, M., Manageiro, V., Vasconcelos, V., and Caniça, M. (2019). Deciphering the role of Cyanobacteria in water resistome: hypothesis justifying the antibiotic resistance (phenotype and genotype) in *Planktothrix* genus. *Sci. total Environ.* 652, 447–454. doi:10.1016/j.scitotenv.2018.10.167

Enault, F., Briet, A., Bouteille, L., Roux, S., Sullivan, M. B., and Petit, M.-A. (2017). Phages rarely encode antibiotic resistance genes: a cautionary tale for virome analyses. *ISME J.* 11, 237–247. doi:10.1038/ismej.2016.90

Fernandes, G., Bastos, M. C., de Vargas, J. P. R., Le Guet, T., Clasen, B., and Dos Santos, D. R. (2020). The use of epilithic biofilms as bioaccumulators of pesticides and pharmaceuticals in aquatic environments. *Ecotoxicology* 29 (9), 1293–1305. doi:10.1007/s10646-020-02259-4

Finley, R. L., Colignon, P., Larsson, D. G. J., McEwen, S. A., Li, X.-Z., Gaze, W. H., et al. (2013). The scourge of antibiotic resistance: the important role of the environment. *Clin. Infect. Dis.* 57 (5), 704–710. doi:10.1093/cid/cit355

Frost, L. S., Leplae, R., Summers, A. O., and Toussaint, A. (2005). Mobile genetic elements: the agents of open source evolution. *Nat. Rev. Microbiol.* 3 (9), 722–732. doi:10.1038/nrmicro1235

Gillings, M. R. (2014). Integrons: past, present, and future. *Microbiol. Mol. Biol. Rev.* 78 (2), 257–277. doi:10.1128/MMBR.00056-13

Gu, Z., Gu, L., Eils, R., Schlesner, M., and Brors, B. (2014). Circlize Implements and enhances circular visualization in R. *Bioinformatics* 30 (19), 2811–2812. doi:10.1093/bioinformatics/btu393

Guo, K., Wu, N., Li, W., Baattrup-Pedersen, A., and Riis, T. (2021). Microbial biofilm community dynamics in five lowland streams. *Sci. total Environ.* 798, 149169. doi:10.1016/j.scitotenv.2021.149169

Han, J. E., Kang, W., Lee, J.-Y., Sung, H., Hyun, D.-W., Kim, H. S., et al. (2020). Tabrizicola piscis sp. nov., isolated from the intestinal tract of a Korean indigenous freshwater fish, *Acheilognathus koreensis*. *Int. J. Syst. Evol. Microbiol.* 70 (4), 2305–2311. doi:10.1099/ijsem.0.004034

Harper, L. R., Buxton, A. S., Rees, H. C., Bruce, K., Brys, R., Halfmaerten, D., et al. (2019). Prospects and challenges of environmental DNA (eDNA) monitoring in freshwater ponds. *Hydrobiologia* 826, 25–41. doi:10.1007/s10750-018-3750-5

Hasegawa, H., Suzuki, E., and Maeda, S. (2018). Horizontal plasmid transfer by transformation in *Escherichia coli*: environmental factors and possible mechanisms. *Front. Microbiol.* 9, 2365. doi:10.3389/fmicb.2018.02365

Janda, J. M., and Abbott, S. L. (2021). The changing face of the family *Enterobacteriaceae* (order: "enterobacterales"): new members, taxonomic issues, geographic expansion, and new diseases and Disease syndromes. *Clin. Microbiol. Rev.* 34 (2), e00174-20. doi:10.1128/CMR.00174-20

Jo, S. J., Kwon, H., Jeong, S.-Y., Lee, C.-H., and Kim, T. G. (2016). Comparison of microbial communities of activated sludge and membrane biofilm in 10 full-scale membrane bioreactors. *Water Res.* 101, 214–225. doi:10.1016/j.watres.2016.05.042

Kamathewatta, K. I., Bushell, R. N., Young, N. D., Stevenson, M. A., Billman-Jacobe, H., Browning, G. F., et al. (2019). Exploration of antibiotic resistance risks in a veterinary teaching hospital with Oxford Nanopore long read sequencing. *PloS ONE* 14 (5), e0217600. doi:10.1371/journal.pone.0217600

Kautza, A., and Sullivan, S. (2016). Anthropogenic and natural determinants of fish food-chain length in a midsize river system. *Freshw. Sci.* 35 (3), 895–908. doi:10.1086/685932

Larsson, D. G. J., and Flach, C.-F. (2021). Antibiotic resistance in the environment. *Nat. Rev. Microbiol.* 20, 257–269. doi:10.1038/s41579-021-00649-x

Lau, M. M. L., Kho, C. J. Y., Chung, H. H., and Zulkharnain, A. (2024). Isolation, identification and characterisation of Pseudomonas koreensis CM-01 isolated from diseased Malaysian mahseer (*Tor tambroides*). *Fish and Shellfish Immunol.* 148, 109518. doi:10.1016/j.fsi.2024.109518

Lee, S., Suits, M., Wituszynski, D., Winston, R., Martin, J., and Lee, J. (2020). Residential urban stormwater runoff: a comprehensive profile of microbiome and antibiotic resistance. *Sci. total Environ.* 723, 138033. doi:10.1016/j.scitotenv.2020.138033

Lekunberri, I., Subirats, J., Borrego, C. M., and Balcázar, J. L. (2017). Exploring the contribution of bacteriophages to antibiotic resistance. *Environ. Pollut.* 220, 981–984. doi:10.1016/j.envpol.2016.11.059

Li, Q., and Zhang, Q. (2020). Prevalence and pollution characteristics of antibiotic resistant genes in one high anthropogenically-impacted river. *PLoS one* 15, e0231128. doi:10.1371/journal.pone.0231128

Liao, K., Bai, Y., Huo, Y., Jian, Z., Hu, W., Zhao, C., et al. (2019). Use of convertible flow cells to simulate the impacts of anthropogenic activities on river biofilm bacterial communities. *Sci. total Environ.* 653, 148–156. doi:10.1016/j.scitotenv.2018.10.363

Lin, S., Haas, S., Zemojtel, T., Xiao, P., Vingron, M., and Li, R. (2010). Genome-wide comparison of cyanobacterial transposable elements, potential genetic diversity indicators. *Gene* 473, 139–149. doi:10.1016/j.gene.2010.11.011

Logsdon, G. A., Vollger, M. R., and Eichler, E. E. (2020). Long-read human genome sequencing and its applications. *Nat. Rev. Genet.* 21, 597–614. doi:10.1038/s41576-020-0236-x

Ma, L., Xia, Y., Li, B., Yang, Y., Li, L.-G., Tiedje, J. M., et al. (2016). Metagenomic assembly reveals hosts of antibiotic resistance genes and the shared resistome in pig, chicken, and human feces. *Environ. Sci. and Technol.* 50 (1), 420–427. doi:10.1021/acs.est.5b03522

Mallick, H., Rahnavard, A., McIver, L. J., Zhang, Y., Nguyen, L. H., Tickle, T. L., et al. (2021). Multivariable association discovery in population-scale meta-omics studies. *PLoS Comput. Biol.* 17 (11), e1009442. doi:10.1371/journal.pcbi.1009442

Martin, S., Heavens, D., Lan, Y., Horsfield, S., Clark, M. D., and Leggett, R. M. (2022). Nanopore adaptive sampling: a tool for enrichment of low abundance species in metagenomic samples. *Genome Biol.* 23, 11. doi:10.1186/s13059-021-02582-x

McMurdie, P. J., and Holmes, S. (2013). phyloseq: an R package for reproducible interactive analysis and graphics of microbiome census data. *PLoS ONE* 8 (4), e61217. doi:10.1371/journal.pone.0061217

Mills, M., Lee, S., Mollenkopf, D., Wittum, T., Sullivan, S. M. P., and Lee, J. (2022). Comparison of environmental microbiomes in an antibiotic resistance-polluted urban river highlights periphyton and fish gut communities as reservoirs of concern. *Sci. total Environ.* 851, 158042. doi:10.1016/j.scitotenv.2022.158042

Mills, M. C., Lee, S., Piperata, B. A., Garabed, R., Choi, B., and Lee, J. (2023). Household environment and animal fecal contamination are critical modifiers of the gut microbiome and resistome in young children from rural Nicaragua. *Microbiome* 11, 207. doi:10.1186/s40168-023-01636-5

Mock, A., Braun, M., Scholl, C., Fröhling, S., and Erkut, C. (2023). Transcriptome profiling for precision cancer medicine using shallow nanopore cDNA sequencing. *Sci. Rep.* 13, 2378. doi:10.1038/s41598-023-29550-8

Nisa, I., Qasim, M., Yasin, N., Ullah, R., and Ali, A. (2020). *Shigella flexneri*: an emerging pathogen. *Folia Microbiol.* 65, 275–291. doi:10.1007/s12223-020-00773-w

Ohio Environmental Protection Agency (EPA) (2014). Scioto River watershed. Available at: https://epa.ohio.gov/dsw/tmdl/SciotoRiver.aspx (Accessed July 3, 2014).

Oksanen, J., Blanchet, F. G., Friendly, M., Kindt, R., Legendre, P., McGlinn, D., et al. (2020). Vegan: community ecology package. *R. package version* 2, 5–7. doi:10.32614/CRAN.package.vegan

Oliveira, P. H., Touchon, M., Cury, J., and Rocha, E. P. C. (2017). The chromosomal organization of horizontal gene transfer in bacteria. *Nat. Commun.* 8, 841. doi:10.1038/s41467-017-00808-w

Perry, I., Jâms, I. B., Casas-Mulet, R., Hamutoko, J., Marchbank, A., Lendelvo, S., et al. (2022). Challenges to implementing environmental-DNA monitoring in Namibia. *Front. Environ. Sci.* 9. doi:10.3389/fenvs.2021.773991

Popovic, N. T., Kazazic, S. P., Strunjak-Perovic, I., Barisic, J., Klobucar, R. S., Kepec, S., et al. (2015). Detection and diversity of aeromonads from treated wastewater and fish inhabiting effluent and downstream waters. *Ecotoxicol. Environ. Saf.* 120, 235–242. doi:10.1016/j.ecoenv.2015.06.011

Proia, L., von Schiller, D., Sànchez-Mesió, A., Sabater, S., Borrego, C. M., Rodríguez-Mozaz, S., et al. (2016). Occurrence and persistence of antibiotic resistance genes in river biofilms after wastewater inputs in small rivers. *Environ. Pollut.* 210, 121–128. doi:10.1016/j.envpol.2015.11.035

Reichart, G., Hilgert, S., Alexander, J., de Azevedo, J. C. R., Morck, T., Fuchs, S., et al. (2021). Determination of antibiotic resistance genes in a WWTP-impacted river in surface water, sediment, and biofilm: influence of seasonality and water quality. *Sci. total Environ.* 768, 144526. doi:10.1016/j.scitotenv.2020.144526

Roberto, A. A., Van Gray, J. B., Engohang-Ndong, J., and Leff, L. G. (2019). Distribution and co-occurrence of antibiotic and metal resistance genes in biofilms of an anthropogenically impacted stream. *Sci. total Environ.* 688, 437–449. doi:10.1016/j.scitotenv.2019.06.053

Scott, J. R., and Churchward, G. G. (1995). Conjugative transposition. *Annu. Rev. Microbiol.* 49, 367–397. doi:10.1146/annurev.mi.49.100195.002055

Sentenac, H., Loyau, A., Leflaive, J., and Schmeller, D. S. (2021). The significance of biofilms to human, animal, plant and ecosystem health. *Funct. Ecol.* 36 (2), 294–313. doi:10.1111/1365-2435.13947

Shen, W., and Ren, H. (2021). TaxonKit: a practical and efficient NCBI taxonomy toolkit. *J. Genet. genomics* 48 (9), 844–850. doi:10.1016/j.jgg.2021.03.006

Siguier, P., Gourbeyre, E., and Chandler, M. (2014). Bacterial insertion sequences: their genomic impact and diversity. *FEMS Microbiol. Rev.* 38 (5), 865–891. doi:10.1111/1574-6976.12067

Souque, C., Escudero, J. A., and MacLean, R. C. (2021). Integron activity accelerates the evolution of antibiotic resistance. *eLife* 10, e62474. doi:10.7554/eLife.62474

Talagrand-Reboul, E., Jumas-Bilak, E., and Lamy, B. (2017). The social life of Aeromonas through biofilm and *quorum* sensing systems. *Front. Microbiol.* 8, 37. doi:10.3389/fmicb.2017.00037

Tamminen, M., Spaak, J., Tlili, A., Eggen, R., Tamm, C., and Räsänen, K. (2022). Wastewater constituents impact biofilm microbial community in receiving streams. *Sci. total Environ.* 807, 151080. doi:10.1016/j.scitotenv.2021.151080

Thomas, F., Hehemann, J.-H., Rebuffet, E., Czjzek, M., and Michel, G. (2011). Environmental and gut Bacteroidetes: the food connection. *Front. Microbiol.* 2, 93. doi:10.3389/fmicb.2011.00093

Viehweger, A., Marquet, M., Hölzer, M., Dietze, N., Pletz, M. W., and Brandt, C. (2023). Nanopore-based enrichment of antimicrobial resistance genes – a case-based study. *GigaByte* 2023, 1–15. doi:10.46471/gigabyte.75

Volk, A., and Lee, J. (2023). Cyanobacterial blooms: a player in the freshwater environmental resistome with public health relevance? *Environ. Res.* 216 (2), 114612. doi:10.1016/j.envres.2022.114612

Wahli, T., and Madsen, L. (2018). Flavobacteria, a never ending threat for fish: a review. *Bacteriology* 5, 26–37. doi:10.1007/s40588-018-0086-x

Wang, Y., Yau, Y.-Y., Perkins-Balding, D., and Thomson, J. G. (2010). Recombinase technology: applications and possibilities. *Plant cell Rep.* 30, 267–285. doi:10.1007/s00299-010-0938-1

Wang, Z., Chen, Q., Zhang, J., Guan, T., Chen, Y., and Shi, W. (2020a). Critical roles of cyanobacteria as reservoir and source for antibiotic resistance genes. *Environ. Int.* 144, 106034. doi:10.1016/j.envint.2020.106034

Washington, V. J., Lear, G., Neale, M. W., and Lewis, G. D. (2013). Environmental effects on biofilm bacterial communities: a comparison of natural and anthropogenic factors in New Zealand streams. *Freshw. Biol.* 58 (11), 2277–2286. doi:10.1111/fwb.12208

Weiss, S., Xu, Z. Z., Peddada, S., Amir, A., Bittinger, K., Gonzalez, A., et al. (2017). Normalization and microbial differential abundance strategies depend upon data characteristics. *Microbiome* 5 (1), 27. doi:10.1186/s40168-017-0237-y

Willems, A. (2014). "The family comamonadaceae," in *The prokaryotes*. Editors E. Rosenberg, E. F. DeLong, S. Lory, E. Stackebrandt, and F. Thompson (Berlin, Heidelberg: Springer), 777–851.

Wrenn, D. C., and Drown, D. M. (2023). Nanopore adaptive sampling enriches for antimicrobial resistance genes in microbial communities. *GigaByte* 2023, 1–14. doi:10.46471/gigabyte.103

Xu, L., Wu, Y.-H., Zhou, P., Cheng, H., Liu, Q., and Xu, X.-W. (2018). Investigation of the thermophilic mechanism in the genus *Porphyrobacter* by comparative genomic analysis. *BMC genomics* 19, 385. doi:10.1186/s12864-018-4789-4

Xu, L., Zhou, Z., Zhu, L., Han, Y., Lin, Z., Feng, W., et al. (2020). Antibiotic resistance genes and microcystins in a drinking water treatment plant. *Environ. Pollut.* 258, 113718. doi:10.1016/j.envpol.2019.113718

Yao, Y., Liu, Z., Yip, K. K., Pu, Y., Cheng, W., Li, M., et al. (2022). Cross-regional scale pollution of freshwater biofilms unveiled by antibiotic resistance genes. *Sci. total Environ.* 818, 151835. doi:10.1016/j.scitotenv.2021.151835

Yin, X., Li, L., Chen, X., Liu, Y.-Y., Lam, T.T.-Y., Topp, E., et al. (2023). Global environmental resistome: distinction and connectivity across diverse habitats benchmarked by metagenomic analyses. *Water Res.* 235, 119875. doi:10.1016/j.watres.2023.119875

Yushchuk, O., Binda, E., and Marinelli, F. (2020). Glycopeptide antibiotic resistance genes: distribution and function in the producer *Actinomycetes*. *Front. Microbiol.* 11, 1173. doi:10.3389/fmicb.2020.01173

Zeglin, L. H. (2015). Stream microbial diversity in response to environmental changes: review and synthesis of existing research. *Front. Microbiol.* 6, 454. doi:10.3389/fmicb.2015.00454

Zhang, M., Hao, Y., Yi, Y., Liu, S., Sun, Q., Tan, X., et al. (2023). Unexplored diversity and ecological functions of transposable phages. *ISME J.* 17, 1015–1028. doi:10.1038/s41396-023-01414-z

Zhao, Y., Zhang, Y., Guo, J., Wang, J., and Li, Y. (2022). Shifts in periphyton research themes over the past three decades. *Environ. Sci. Pollut. Res.* 30, 5281–5295. doi:10.1007/s11356-022-24251-7

Zheng, Q., Liu, Y., Jeanthon, C., Zhang, R., Lin, W., Yao, J., et al. (2016). Geographic impact on genomic divergence as revealed by comparison of nine *citromicrobial* genomes. *Appl. Environ. Microbiol.* 82, 7205–7216. doi:10.1128/AEM.02495-16

frontiers | Frontiers in Environmental Science

TYPE Original Research
PUBLISHED 09 September 2024
DOI 10.3389/fenvs.2024.1439174

Check for updates

OPEN ACCESS

EDITED BY
Visva Bharati Barua,
University of North Carolina at Charlotte, United States

REVIEWED BY
Raju Sekar,
Xi'an Jiaotong-Liverpool University, China
Chandan Pal,
Zespri International Ltd., New Zealand

*CORRESPONDENCE
Yoshihiro Suzuki,
ysuzuki@cc.miyazaki-u.ac.jp

RECEIVED 27 May 2024
ACCEPTED 19 August 2024
PUBLISHED 09 September 2024

CITATION
Nishimura E, Xie H, Tamai S, Nishiyama M, Nukazawa K, Hoshiko Y, Ogura Y and Suzuki Y (2024) Year-round monitoring of antibiotic-resistant bacteria in pristine uppermost stream and estimation of pollution sources. *Front. Environ. Sci.* 12:1439174. doi: 10.3389/fenvs.2024.1439174

COPYRIGHT
© 2024 Nishimura, Xie, Tamai, Nishiyama, Nukazawa, Hoshiko, Ogura and Suzuki. This is an open-access article distributed under the terms of the Creative Commons Attribution License (CC BY). The use, distribution or reproduction in other forums is permitted, provided the original author(s) and the copyright owner(s) are credited and that the original publication in this journal is cited, in accordance with accepted academic practice. No use, distribution or reproduction is permitted which does not comply with these terms.

Year-round monitoring of antibiotic-resistant bacteria in pristine uppermost stream and estimation of pollution sources

Emi Nishimura[1,2], Hui Xie[1], Soichiro Tamai[1], Masateru Nishiyama[3], Kei Nukazawa[4], Yuki Hoshiko[5], Yoshitoshi Ogura[6] and Yoshihiro Suzuki[4]*

[1]Department of Environment and Resource Sciences, Interdisciplinary Graduate School of Agriculture and Engineering, University of Miyazaki, Miyazaki, Japan, [2]Division of Environmental Chemistry, IDEA Consultants, Inc., Tokyo, Japan, [3]Department of Food, Life and Environmental Science, Faculty of Agriculture, Yamagata University, Yamagata, Japan, [4]Department of Civil and Environmental Engineering, Faculty of Engineering, University of Miyazaki, Miyazaki, Japan, [5]Department of Health Science, School of Allied Health Sciences, Kitasato University, Kanagawa, Japan, [6]Division of Microbiology, Department of Infectious Medicine, Kurume University School of Medicine, Fukuoka, Japan

Studies on the conditions and pollution routes of antibiotic-resistant bacteria (ARB) in rivers can help provide countermeasures against the spread of ARB. This study focused on the pristine uppermost stream of a river, where *Escherichia coli* (*E. coli*) and enterococci were detected, although the stream flows through a pristine forest catchment. Antibiotic resistance of *E. coli* and enterococci isolated from the river water, riverbed sediment, and feces of waterside animals, such as birds and Mustelidae, were investigated throughout the year in the pristine uppermost sites. Antibiotic resistance was present in 1.4% (7/494) of the *E. coli* strains and 3.0% (24/812) of the enterococcal strains, and was low throughout the year. Although antibiotic resistance of bacteria isolated from feces was not detected in this watershed, the prevalence of multidrug-resistant *E. coli* was 0.4% (1/246) and 0.6% (1/172) in river water and riverbed sediment samples, respectively were observed. The presence of extended-spectrum β-lactamase (ESBL)-producing *E. coli* was confirmed in river water samples, and genomic analysis revealed that the samples possessed the *CTX-M-15* group. Multidrug-resistant strains and ESBL-producing strains were classified as phylogroups B1 and A, respectively, which are *E. coli* phenotypes isolated from wild animals. Pulsed-field gel electrophoresis revealed analysis targeting enterococci that strains isolated from river water and bird feces were in the same cluster with 100% similarity. Therefore, bird feces are a source of enterococci in the uppermost stream of the river. Because multidrug-resistant bacteria and ESBL-producing bacteria were present in the pristine uppermost stream of the pristine river, urgent elucidation of the spreading routes of ARB is important.

KEYWORDS

***Escherichia coli*, enterococci, antibiotic resistance, antibiotic-resistant bacteria, multidrug-resistant bacteria, extended-spectrum β-lactamase, genomic analysis, pristine uppermost stream**

1 Introduction

The emergence of antibiotic-resistant bacteria (ARB) is one of the most serious problems globally (O'Neill, 2014; Willyard, 2017; Antimicrobial Resistance Collaborators, 2022). The Group of Seven (G7) is promoting global efforts to address this important issue (G7 Health Ministers' Communiqué, 2022; World Health Organization, 2022b) and Centers for Disease Control and Prevention (CDC) annually update and publish information on ARB (World Health Organization, 2022a; Centers for Disease, 2019), warning of the seriousness of the problem. Currently, a wide variety of ARB have been detected, and the main sources of ARB include clinical institutions, livestock farms, and fish farms, where antibacterial drugs are frequently used. ARB are ubiquitous in other environments, such as the water environment (Zhang et al., 2015; Daniel et al., 2017; Osińska et al., 2020; Grenni, 2022). Strains resistant to clinically important antibiotics, such as cephalosporins, carbapenems, and vancomycin, have been detected in the water environments (Diwan et al., 2018; Givens et al., 2023). In recent years, ARB, and antibiotic resistance genes (ARGs) have been detected in natural environments and wild animals that are not directly affected by humans. Of the six Enterobacterales isolated from pristine freshwater (rivers) in Brazil, 52%–77% were antibiotic resistance (Lima-Bittencourt et al., 2007). ARGs ($1.7 \pm 1.0 \times 10^6$ copies/mL), predominantly those resistant to β-lactam and tetracycline, were detected in the ocean near Antarctica (Jang et al., 2022). In Uganda, 17% of the *Escherichia coli* (*E. coli*) strains isolated from wild gorillas were antibiotic resistant. Of these, 4.2% were resistant to antibiotics used for treating lung inflammation in livestock, such as ceftiofur (Rwego et al., 2008). According to a wildlife review, many Enterobacterales isolated from wild animals possessed plasmids encoding ARGs related to β-lactam antibiotics and colistin, causing concerns about the spread of antibiotic resistance in wild animals and the risk to public health (Dolejska and Papagiannitsis, 2018). Therefore, the global spread of ARB cannot be denied.

Information on rivers that transport and spread ARB over a wide area is crucial, but information on ARB in pristine rivers that are not directly affected by human areas remains scarce. Furthermore, it is difficult to identify the appearance of ARB in pristine environments and the specific source and route of contamination. Although limited information is available, 18% of *E. coli* detected in a pristine upstream site of the Kaeda River in Miyazaki, Japan, where the catchment area was forest, were ARB, including multidrug-resistant strains (Nishimura et al., 2021). In addition, headwaters are surrounded by forests, which have a rich ecosystem and are home to many wild animals. Studies from other countries suggest that the source of ARB load in headwater areas is likely to be wild animals (birds, mammals, etc.) that use waterside areas (Bonnedahl and Järhult, 2014; Rogers et al., 2018; García et al., 2020; Yuan et al., 2021). However, there is a lack of information on whether the development of antibiotic resistance in headwaters is human-introduced or naturally occurring. When focusing on wild animals as a source, direct contact with wild animals to perform study is difficult and risky. Thus, monitoring ARB in headwaters surrounded by forests and identification of contamination routes using scientific methods can be important countermeasures against the spread of ARB. In addition, pristine environments are ideal environments for understanding the mechanisms and interactions of the early stages of evolution, acquisition, and transmission of drug resistance, and can accumulate new information related to drug resistance (Hwengwere et al., 2022).

Elucidating the actual presence and diffusion routes of ARB in pristine rivers is crucial for controlling the transport and diffusion of ARB. The purpose of this study is to determine the prevalence of ARB in pristine river. Then, the presence of clinically important ARB will be confirmed, and the pollution source will be estimated by genomic analysis. The survey focused on the pristine uppermost stream of the Kaeda River (Figure 1) to determine the prevalence of antibiotic-resistant *E. coli* (AR-*E. coli*) and antibiotic-resistant enterococci (AR-ENT) in the river water, riverbed sediment, and feces of waterside animals every 2 months for 1 year. Then, information on the detected ARB was organized, and their characteristics and presence of antibiotic-resistant strains, which are important in clinical institutions, were ascertained. Strains from river water, riverbed sediment, and waterside bird feces were analyzed by genomic analysis and pulsed-field gel electrophoresis (PFGE) to trace the source of ARB.

In our previous study (Nishimura et al., 2021), we confirmed the presence of ARB in the upstream stream of the Kaeda River, and its prevalence was comparable between the upstream and downstream streams. However, we have not been able to elucidate the source of ARB in upstream streams, where deep in the forest and unaffected by humans. Therefore, this study was designed to focus on the uppermost reaches of the Kaeda River in the forest and the animals that use their banks. As the target bacteria, we focused on *E. coli* and enterococci. These bacteria, whose hosts are warm-blooded animals, including humans, livestock, and wild animals, are ubiquitous in aquatic environments (Farnleitner et al., 2010). They are also classified as fecal indicator bacteria and are important for the protection of public health (World Health Organization, 2022a; Ishii and Sadowsky, 2008). In addition, some important bacteria are resistant to antibiotics, and information is accumulated in the aquatic environment (Alonso et al., 2001; Baquero et al., 2008).

2 Materials and methods

2.1 Sampling sites and sample collection

Figure 1; Supplementary Table S1 show the sampling site map as land use data around the Kaeda River and the number of samples, respectively. The Kaeda River (channel length, 17.5 km; basin area, 53.8 km^2) originates from headwaters dominated by forests in their catchment areas, flows through a deep valley with land with various uses, and drains into the Hyuganada (Pacific Ocean). In this study, two sites were selected as pristine uppermost streams not directly affected by human activities: 1) a headwaters site (S1: width, 0.3 m; depth, 0.2 m; flow rate, 2 m^3/s) and 2) approximately 400 m below the headwaters site (S2: width, 4 m; depth, 0.4 m; flow rate, 13 m^3/s). The catchments of S1 and S2 were exclusively forested and consisted of natural and planted forests, respectively. There is no anthropogenic impact from human activity in this study area. Sampling was conducted every 2 months for 1 year (31 August 2017–30 August 2018).

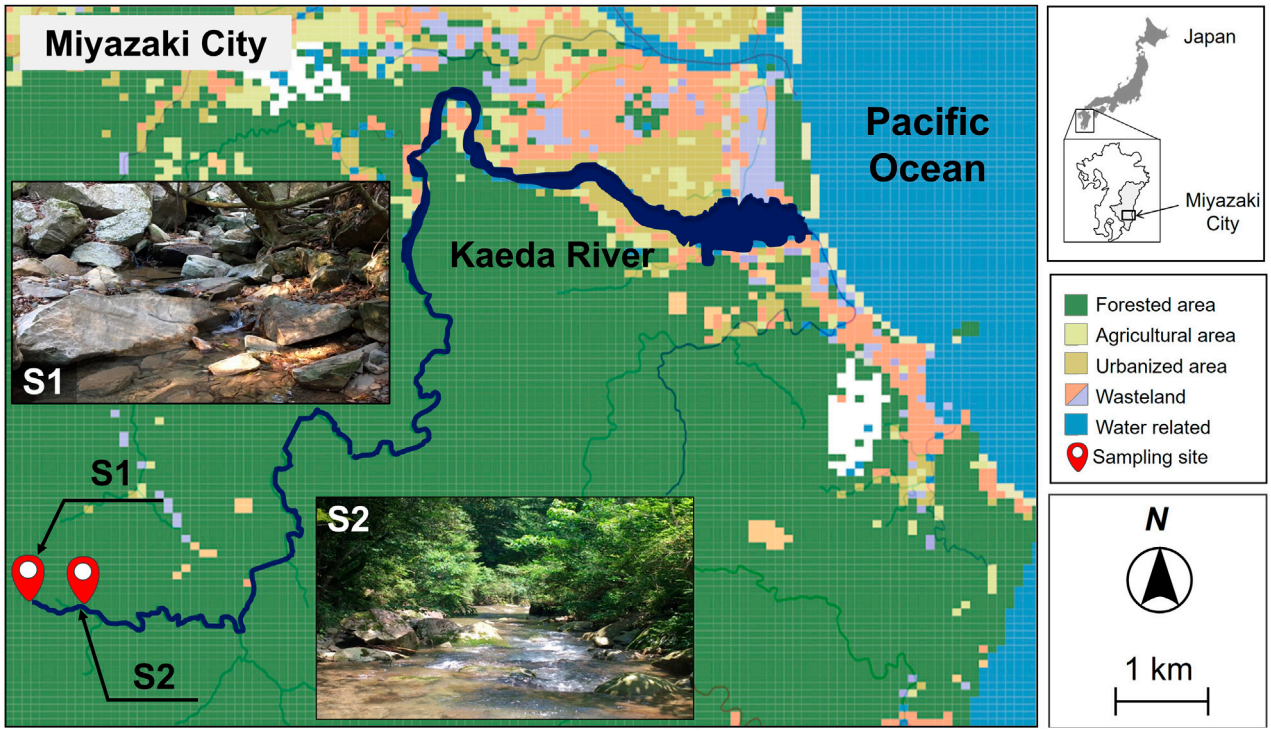

FIGURE 1
Sampling sites and major land use categories of pristine uppermost stream at the Kaeda River in southern Japan. S1, site1, river source; S2, site2, upstream.

River water, riverbed sediment, and feces from wild animals that use the waterside were collected. River water samples were stored in sterile 5-L polyethylene bottles for each site. Riverbed sediments were collected by shoveling 2–5 cm of the surface layer from 3 m radius of the water sample points. The feces of wild animals (birds and Mustelidae) on waterside rocks situated within a 10 m radius of the water sample points were collected with a sterile cotton swab and placed into 15 mL sterilized polyethylene tubes.

Water temperature and dissolved oxygen (DO) were determined using a fluorescent-type dissolved oxygen meter (HQ40d, Hach Company, COL., Tokyo, Japan) at the sampling site. A benchtop pH/water quality analyzer (LAQUA, HORIBA, Ltd., Kyoto, Japan) was used to measure pH and electrical conductivity. Turbidity was determined using a turbidity meter (SEP-PT-706D, Mitsubishi Chemical Co., Tokyo, Japan). All samples were transported back to the laboratory and used for experiments within 4 h of collection (Japanese Standard Association, 2016).

2.2 Counting and isolation of fecal indicator bacteria

The number of *E. coli* and enterococci, as well as other coliforms, was counted in each sample by the membrane filter method. Five liters of river water was collected from each sampling site. Bacterial counts varied greatly depending on the survey period, so the amount of passing water sample was set at three levels (10, 100, and 1,000 mL) for each survey and filtered through a 0.45 μm pore membrane filter (47 mm in diameter, mixed cellulose ester; Advantec, Tokyo, Japan). Membranes were placed on CHROMagar ECC agar plates (CHROMagar, Paris, France), and incubated at 37°C for 24 h. Subsequently, filters with appropriate flow volume for bacterial counting and isolation were selected and analyzed. On the filter, blue colonies were considered presumptive *E. coli* and mauve colonies were considered other presumptive coliform. Enterococci were counted using membrane-enterococci indoxyl-β-D-glucoside (mEI) agar plate (United States Environmental Protection Agency, 2014). The samples (10, 100, and 500 mL) were filtered through a membrane filter. Membranes were incubated on mEI agar plates at 41°C for 24 h. On the filter, blue colonies were considered presumptive enterococci. The number of bacteria in each sample was counted in three replicates and the mean was calculated as colony forming unit (CFU) per 100 mL. The detection limit of this method was 0.3 CFU/100 mL. Riverbed sediment samples (5 g) were mixed with 40 mL of sterilized physiological saline solution or phosphate-buffered saline (Boehm et al., 2009) and allowed to settle for 1 min. Supernatant liquid was filtered through a membrane filter. Then bacteria were isolated in a manner identical to that of water sample analysis. The detection limit of riverbed sediment samples was 7 CFU/100 g. Samples of wild animal feces (1 g) were mixed with 9 mL of sterilized physiological saline solution or phosphate-buffered saline and allowed to settle for 1 min. Then, 0.1–0.001 mL of the supernatant was filtered through a membrane filter. Bacterial counts of feces were not measured, only strains were isolated. Thirty single colonies were randomly isolated from CHROMagar ECC and mEI agar plates for each sample at

S1 and S2. The plates were streaked twice on Brain Heart Infusion agar (BD, New Jersey, United States) or Todd–Hewitt agar (Becton, Dickinson, NJ, United States) to isolate *E. coli* and enterococci, respectively. When less than 30 isolates were available, all single colonies were isolated. The plates were incubated for 24 h at 37°C. For *E. coli*-positive strains and enterococci-positive strains, max 30 strains were isolated from each sample at S1 and S2. Supplementary Tables S2, S3 show the number of *E. coli*-positive strains or enterococci-positive strains isolated from each sample at S1 and S2.

2.3 Identification of *E. coli* and enterococci by MALDI-TOF MS

For *E. coli*-positive (n = 567) and enterococci-positive (n = 839) strains isolated from all the samples, the identification of bacterial species was performed using MALDI-TOF MS (Fenselau and Demirev, 2001; Christner et al., 2014; Suzuki et al., 2018). All samples were analyzed using an Autoflex III TOF/TOF mass spectrometer (Bruker Daltonics, Billerica, MA, United States). Measurements were performed using flexControl 3.0 software (Bruker Daltonics, Billerica, MA, United States) for database construction and validation. The software settings were based on Suzuki et al. (2018). The instrument was calibrated using a Bruker bacterial test standard (part no. 8255343, Bruker Daltonics, Billerica, MA, United States). Recorded mass spectra were processed with the MALDI Biotyper Compass microbial identification system (Bruker Daltonics, Billerica, MA, United States) using standard settings. The MALDI Biotyper output score had a range of 0.00–3.00, and *E. coli* and enterococci identification scores were ≥ 2.00.

2.4 Antibiotic susceptibility testing

Antibiotic susceptibility testing was performed on strains identified as *E. coli* (n = 494) and enterococci (n = 813). The minimum inhibitory concentration (MIC) of each antibiotic was determined using the agar dilution method, according to the guidelines of Clinical Laboratory Standards Institute (CLSI) (Clinical Laboratory Standards Institute, 2017). Twelve antibiotics that are important in the resistance of *E. coli* and enterococci were used. The preculture, dissolution and dilution of antibiotics, and test procedure were based on Nishimura et al. (2021) for *E. coli* and Nishiyama et al. (2017) for enterococci. According to the recommendations of CLSI, 12 antibiotics were tested using plates containing 2-fold dilutions of antibiotics with five graded concentrations. MIC breakpoints for resistance were based on CLSI (CLSI, 2012) criteria. Quality control was used for *E. coli* ATCC 25922 (*E. coli*) and enterococci ATCC 29212 (*Enterococcus faecalis*).

2.5 Genomic analysis

Genomic analysis was performed on strains determined as ESBL-producing *E. coli* (n = 1) and multidrug-resistant *E. coli* (n = 1). In advance, the double-disk synergy test was performed for the ESBL-producing *E. coli* strain (Clinical Laboratory Standards Institute M100-S26). Genomic DNA was purified from 1 mL overnight culture of *E. coli* strains using DNeasy Blood and Tissue Kit (Qiagen). Libraries were prepared using Lotus DNA Library Prep Kit (Integrated DNA Technologies, Coralville, IA, United States) and NEBNext Multiplex Oligos for Illumina (96 Unique Dual Index Primer Pairs) (New England BioLabs Japan, Tokyo, Japan) and sequenced on an Illumina HiseqX Ten platform (Illumina, San Diego, CA, United States) to generate 151-bp paired-end reads. Genome assembly was performed using Platanus_b v1. 3.2 (Kajitani et al., 2020) with default parameters. Assembly quality was assessed using CheckM v1. 2.0 (Parks et al., 2015). Phylogroup and sequence type were determined by ClermonTyping v20.06 (Beghain et al., 2018) and srst2 v2.0 (Inouye et al., 2014), respectively. ARGs were identified by ABRicate v0.9.8 (https://github.com/tseemann/abricate) using the ARG-ANNOT database (Gupta et al., 2014) with default parameters. Mutations for quinolone resistance and colistin resistance were analyzed using AMRFinderPlus 3.11.14 (Feldgarden et al., 2021) with default settings.

2.6 Analysis of PFGE typing for *E. coli* and enterococci

In total, *E. coli* (n = 30) and enterococci (n = 29) strains were randomly selected from river water, riverbed sediment, and bird feces from the October 2017 (autumn) survey for genotyping using PFGE. Traces of wild animals at the study site were considered important for examining the bacterial load in the surface waters. Therefore, the analysis focused on October 2017, when the highest number of bird fecal samples were collected at the study site. For *E. coli* genotyping, PFGE was performed according to the standardized PulseNet protocol for PFGE provided by CDC (Centers for Disease Control, 2017). For enterococci genotyping, PFGE was performed using CHEF Bacterial Genomic DNA Plug Kit (Bio-Rad, Hercules, California, United States), according to the manufacturer's protocol, with slight modifications. A lambda DNA ladder (range 48.5–873 kb; Lonza, Rockland, ME, United States) was used as a size marker. The details of analysis are shown in Supplementary Text S1.

Band-based PFGE patterns were clustered using Gene Profiler software (Scanalytics, Buckinghamshire, United Kingdom). Levels of similarity between fingerprints were expressed as Dice coefficient. PFGE patterns were clustered using the unweighted pair group method with arithmetic mean. PFGE patterns with 100% similarity were considered identical genotypes.

3 Results and discussion

3.1 Water quality of the pristine uppermost stream in the Kaeda River

Supplementary Table S4 shows the water quality of the pristine uppermost stream in the Kaeda River. Water temperatures at S1 (22.8°C) and S2 (24.7°C) were highest in August (summer) and ranged from 6.6°C to 20.4°C in other surveys (spring, autumn, and

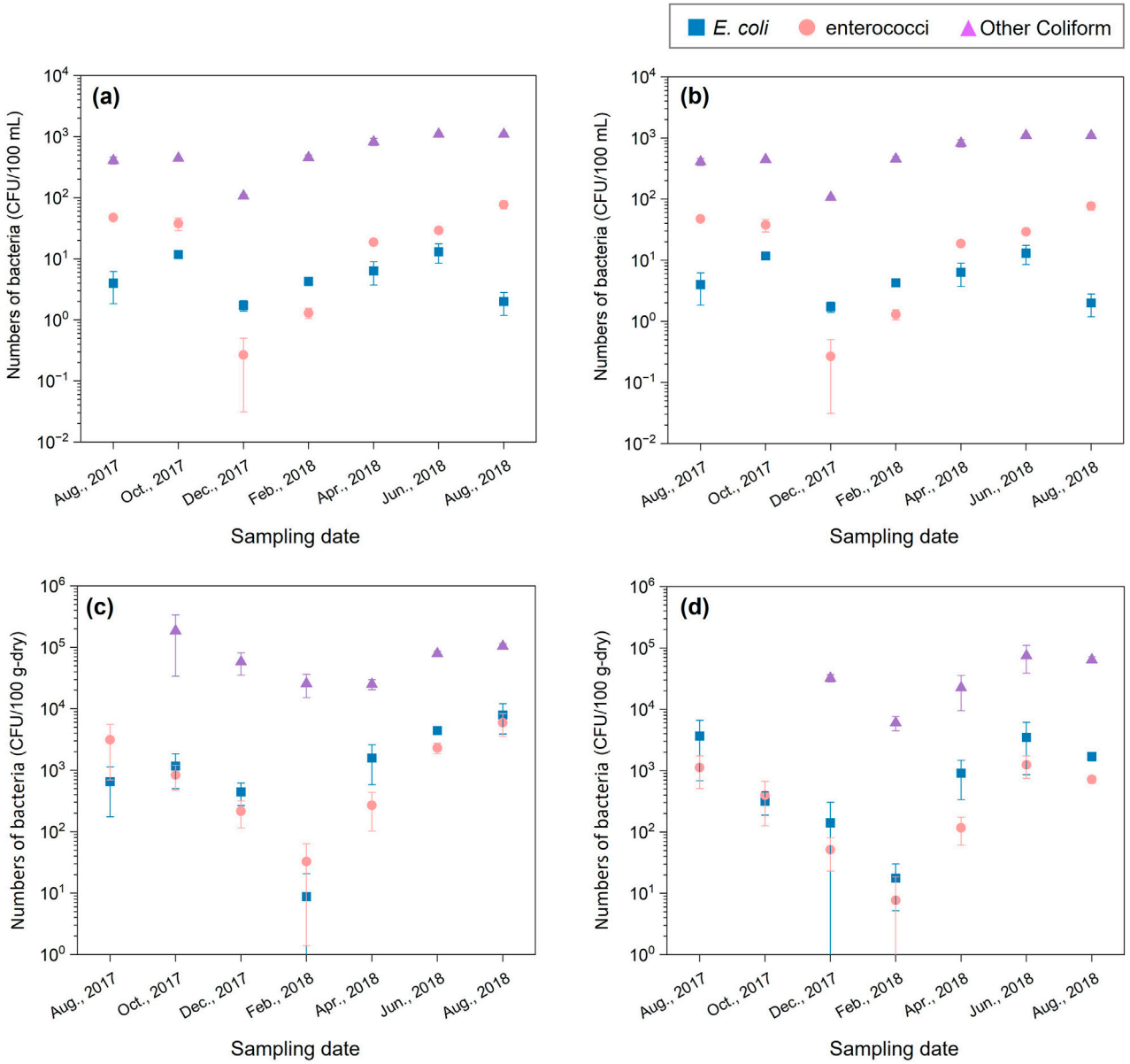

FIGURE 2
Changes in the numbers of *Escherichia coli* (*E. coli*) and enterococci at the S1 and S2 over a 1-year period. Bacteria counts of river water at S1 **(A)**, at S2 **(B)**. Bacteria counts of riverbed sediment at S1 **(C)**, at S2 **(D)**.

winter). The difference in water temperature between S1 and S2 was 1°C–2°C. DO was the highest in winter (10.9 mg/L, near the saturation concentration) and decreased in summer. pH ranged from 6.0 to 6.9, slightly lower than neutral. Electrical conductivity differed between S1 and S2 (47.9 and 58.9 μS/cm, respectively), presumably due to increased mineral components due to the flow processes. Turbidity was extremely low across all surveys, with mean values of 0.3 turbidity units at both sites, and the sample water was extremely clear. Analysis of DO, pH, and turbidity, the water quality parameters of river water, showed no significant differences in water quality between S1 and S2 ($p > 0.05$), resulting in the water quality in both stations being similar. It is unlikely that the process of flow downstream in these two points would directly affect bacterial inactivation.

3.2 Bacteria counts of in river water and riverbed sediment

Figure 2 shows changes in the numbers of *E. coli*, enterococci, and other coliforms at S1 and S2 in 1 year. In river water at S1 and S2, *E. coli* count was low throughout the year (range: 1.7 ± 0.3–20.0 ± 3.3 CFU/100 mL). In summer (August 2017 and 2018), enterococci count was higher than *E. coli* count, ranging from 47.3 ± 2.6 to 101.3 ± 14.6 CFU/100 mL. In winter (February 2018), enterococci count decreased to <0.3 CFU/100 mL and increased again in summer. Thus, seasonal variation in *E. coli* and enterococci count differed. Other coliform count showed seasonal variation similar to enterococci count, ranging from $9.2 \times 10^1 \pm 20.8$ to $1.9 \times 10^4 \pm 24.9$ CFU/100 mL. By contrast, the seasonal variation of *E. coli*

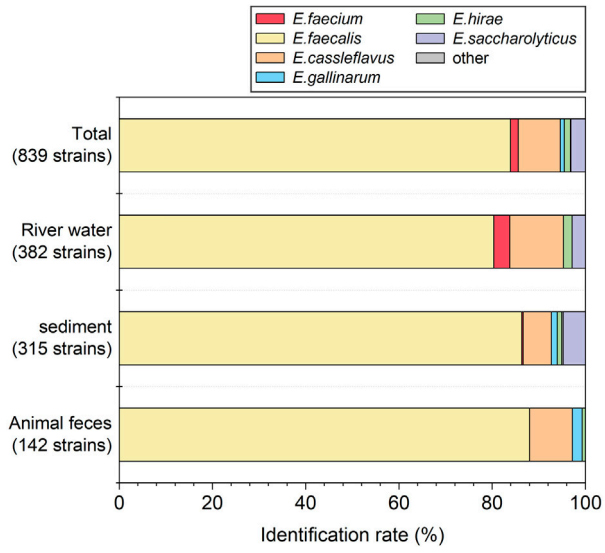

FIGURE 3
Identification rate of enterococci isolates collected from each sample by MALDI-TOF MS based on the MALDI biotyper software database.

and enterococci counts in the riverbed sediment from both S1 and S2 were similar. The numbers of *E. coli* and enterococci were high in summer ($6.5 \times 10^2 \pm 4.7 \times 10^2$–$7.9 \times 10^3 \pm 4.0 \times 10^3$ CFU/100 g) and decreased in winter (7.7 ± 10.9 to $7.9 \times 10^3 \pm 4.0 \times 10^3$ CFU/100 g). However, bacterial counts were not significantly different between summer and winter (*E. coli*: $p > 0.05$, enterococci: $p > 0.05$).

Escherichia coli and enterococci were detected throughout the year, although the stream flows through a pristine forest catchment. The sampling site are not a human living area. Seasonal variations in bacterial counts in river water and riverbed sediment are associated with the activity of wild animals. Some species of wild animals are more active in summer, leading to a potentially higher impact of fecal coliform bacteria in the water due to waste deposition. Therefore, bacteria in the river may have been loaded by wild animals (Hansen et al., 2020; Afolabi et al., 2023). In addition to wild animals, other environmental factors, such as rainfall, water temperature, and decomposition of organic matter also significantly influence bacterial counts.

3.3 Identification rate of each positive strain

In total, 567 strains were isolated as *E. coli*-positive strains from all samples, and 494 (87.1%) were identified as *E. coli* after MALDI-TOF MS. The identification rate of *E. coli* was 88.4% (252/285) in river water, 88.8% (175/197) in riverbed sediment, and 78.8% (67/85) in wild animal feces. The major bacterial species of the pseudo-positive strains detected in this study were *Escherichia marmotae*, *Citrobacter freundii*, and *Serratia fonticola*.

In total, 839 strains were isolated as enterococci-positive strains from all samples, and 813 (96.9%) were identified as enterococci (Figure 3). Of the 813 strains identified as enterococci, 83.9% (704/839) were *E. faecalis*, 9.1% (76/839) were *E. cassleflavus*, 1.7% (14/839) were *E. faecium*, 1.3% (11/839) were *E. hirae*, 0.8% (7/839) were *E. gallinarum*, and 0.1% (1/839) were *E. saccharolyticus*. The identification rate of enterococci for river water, riverbed sediment, and wild animal feces was 97.1% (371/382), 95.2% (300/315), and 100.0% (142/142) strains, respectively. *E. faecalis* was predominant in all samples (80.4%–88.0%). *E. faecium* was slightly detected (0.3%–3.4%). *E. faecalis* and *E. faecium* were frequently isolated in the clinical institutions as the major caUnited Statestive species of nosocomial infection (*E. faecalis*: 80%–90%, *E. faecium*: 5%–15%) (Ruoff et al., 1990; Gordon et al., 1992). The detection of *E. faecalis* and *E. faecium* in the pristine uppermost sites of the Kaeda River is a serious threat to public health, and it is important to investigate their antibiotic resistance.

3.4 Detection and seasonal variation of ARB in the pristine uppermost stream

The MIC values of the identified strains of *E. coli* (n = 494) and enterococci (n = 813) were tested for 8 and 9 antibiotics, respectively. One strain of enterococci was excluded because it did not grow. The antibiotic resistance rates of *E. coli* and enterococci strains isolated from all samples were 1.4% (7/494) and 3.0% (24/812), which were very low throughout the year (Figure 4). In river water, *E. coli* was highest in spring 4.8% (1/21) and enterococci was highest in winter 4.8%–9.6% (December 2017–February 2018). The riverbed sediment samples had a similar trend of antibiotic resistance as river water samples. Figure 4 shows the prevalence of ARB was very low throughout the year. The resistance rate of river water and riverbed sediment was slightly higher in spring than in summer and did not significantly correlate with the results of bacterial count ($p > 0.05$). In addition, ARB were not detected in the feces of wild animals.

In our previous survey, the antibiotic resistance rate of *E. coli* in the Kaeda River was 46% in the summer (July 2016) at S2 (Nishimura et al., 2021). By contrast, this value was significantly lower in this study. Although abrupt changes in the value can only be discussed by assumption, comparing this study with our previously reported study (Nishimura et al., 2021), the surrounding environment at the same site was altered. Parts of the artificial forest and riparian forest were cleared, and the number of trees covering the river was reduced. Although quantitative data are not available, the amount of light incident on the river increased. Therefore, the possibility that ecological changes or other factors affected the water cannot be excluded. By contrast, the resistance rate of AR-*E. coli* was 0.0%–2.5% upstream of the Tama River, which flows through Tokyo, Japan (Terada et al., 2012). We found that ARB were dispersed at a low rate in the pristine uppermost stream in Japan.

ARB were not detected in wild animal feces. This result contrasts with other study reporting detection of ARB in feces of wildlife (Ardiles-Villegas et al., 2011; Khare et al., 2020; Agga et al., 2021). Moreover, there are a few studies that indicate wildlife can also have an impact on ARB by spreading antibiotic resistance (Dolejska and Literak, 2019; Ramey and ahistrom, 2020; Laborda et al., 2022). In addition, several patterns of ARB occurrence in pristine environments have been considered in addition to the effects of wild animals. For example, plants are primary producers in pristine environments, and plants possess a diverse resistome (Berendonk et al., 2015; Chen et al., 2019; Obermeier et al., 2021). These

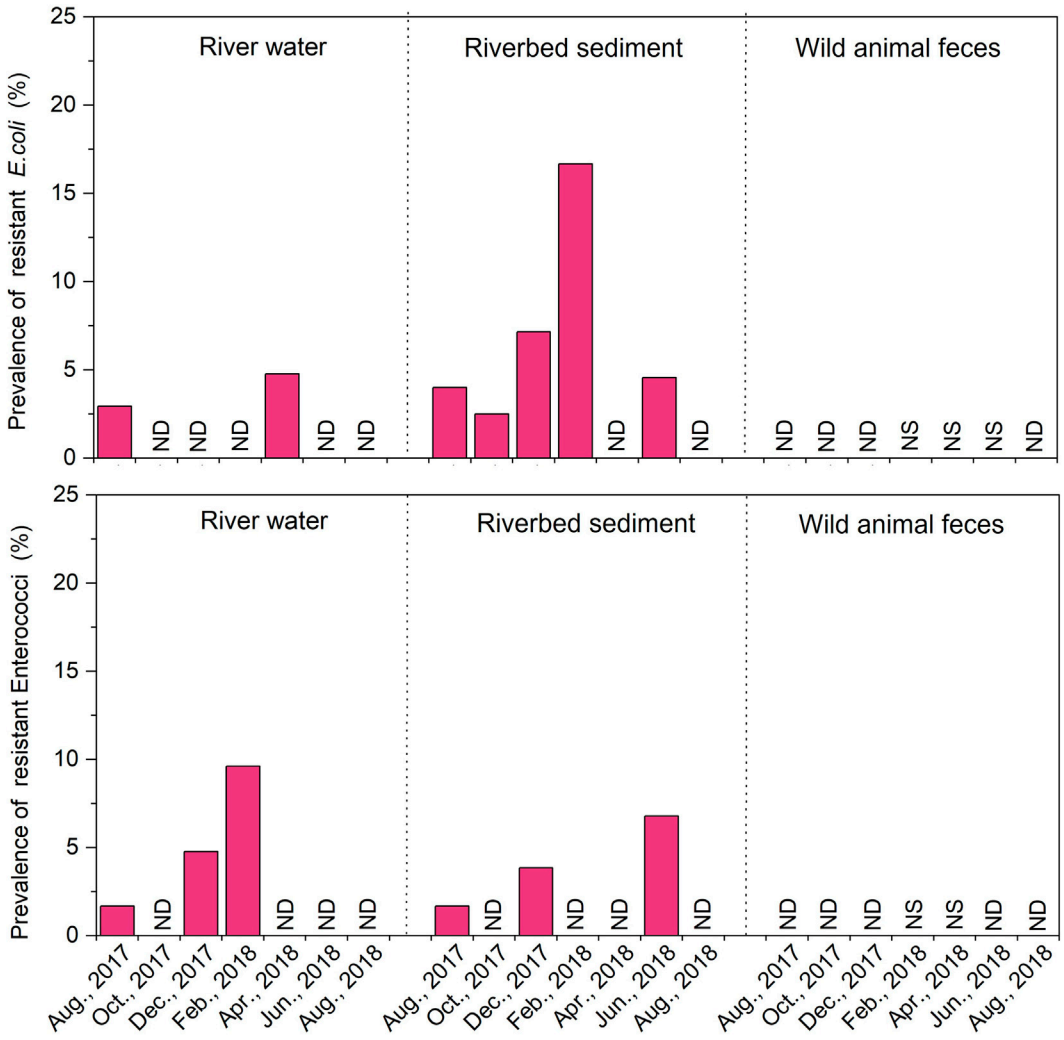

FIGURE 4
Changes in the prevalence of antibiotic resistant to one or more agents for *Escherichia coli* (*E. coli*) and enterococci strains isolated from the river water, riverbed sediment and wild animal feces samples over a 1-year period. No Date (ND), No Sample (NS).

resistomes may contribute to the antibiotic resistance of the bacteria in pristine environments. Thus, the occurrence of ARB in pristine rivers may need to consider both warm-blooded animal loading and natural occurrence (Allen et al., 2010; Hwengwere et al., 2022). Notably, ARB were detected in the uppermost pristine stream. When conducting surveys in such niche fields, it is important and prospects of this research to consider the occurrence of antibiotic resistance from multiple perspectives.

3.5 Characteristics of ARB

3.5.1 Resistance to various classes of antibiotics

Supplementary Table S5 shows the antibiotic resistance rates of *E. coli* isolated from all samples. Ampicillin (ABPC)-resistant strains (0.4%–1.7%), cefazolin (CEZ)-resistant strains (0.8%–1.7%), and oxytetracycline (OTC)-resistant strains (0.4%–1.2%) were detected in river water and riverbed sediment. The antibiotic resistance rates were similar between the two sample types. Additionally, ciprofloxacin (CPFX)-resistant strains were detected in riverbed sediment.

Supplementary Table S6 shows the antibiotic resistance rates of enterococci isolated from all samples. CPFX-resistant strains (1.9%; 7/371) were detected in river water. OTC-resistant (2.0%; 6/300) and minocycline-resistant (2.0%; 6/300) strains were detected in riverbed sediment. Among the AR-ENT detected, antibiotic-resistant *E. faecium*, an important enterococci species in clinical institutions, was not observed.

Notably, *E. coli* and enterococci resistant to semisynthetic or synthetic antibiotics were detected in each sample. Bacteria resistant to semisynthetic or synthetic antibiotics have been detected in pristine environments (Lenart-Boroń et al., 2022; Sajjad et al., 2023). This result confirms similar trends to previous studies.

3.5.2 Comparison of antibiotic-resistant profiles

Tables 1, 2 show the antibiotic resistance profiles of AR-*E. coli* and AR-ENT. In this study, strains resistant to ≥3 antibiotics were defined as multidrug-resistant strains. The resistance combinations

TABLE 1 Profiles of antibiotic-resistant *Escherichia coli* (AR-*E. coli*).

Antibiotic resistance profiles	Number of AR-*E. coli*		
	River water (n = 246)	Riverbed sediment (n = 172)	Animal feces (n = 67)
ABPC-CEZ-CTX-OTC	1 (0.4%)	—	—
ABPC-CPFX-OTC	—	1 (0.6%)	—
ABPC-CEZ	—	2 (1.2%)	—
CEZ	1 (0.4%)	1 (0.6%)	—
OTC	—	1 (0.6%)	—

(ABPC), Ampicillin; (CEZ), Cefazolin; (CTX), Cefotaxime; (CPFX), Ciprofloxacin; (OTC), Oxytetracycline.

TABLE 2 Profiles of antibiotic-resistant enterococci (AR-ENT).

Antibiotic resistance profiles	Number of AR-ENT		
	River water (n = 370)	Riverbed sediment (n = 300)	Animal feces (n = 142)
OTC-MINO	—	6 (2.0%)	—
CPFX	7 (1.9%)	—	—

(OTC), Oxytetracycline; (MINO), Minocycline; (CPFX), Ciprofloxacin.

of the 494 *E. coli* strains were profiled and compared between sample types (Table 1), revealing 2 and 4 patterns in river water and riverbed sediment, respectively. The major resistance patterns of river water strains were ABPC-CEZ-CTX-OTC (0.4%, 1/246) and CEZ (0.4%, 1/246), and the presence of multidrug-resistant *E. coli* was confirmed. In addition, the presence of multidrug-resistant *E. coli* was confirmed in riverbed sediment (profile: ABPC-CPFX-OTC; 0.6%, 1/172). Multidrug-resistant strains of enterococci were not identified (Table 2). Notably, multidrug-resistant *E. coli* (profile: ABPC-CEZ-CTX-OTC) detected in river water may be an important ESBL-producing strain in clinical institutions. In recent years, the rate of dissemination of ESBL-producing bacteria has been accelerating worldwide, making the control of their spread a significant challenge (Kawamura et al., 2017; Husna et al., 2023). The presence of ESBL-producing genes encoded on Enterobacteriaceae plasmids deserves is an issue of particular concern (Pana and Zaoutis, 2018). These genes can spread and disseminate across bacterial species, raising concerns about transmission (Stadler et al., 2018). Globally, the presence of ESBL-producing bacteria and associated genes has been confirmed in pristine environments (Hernandez et al., 2012), raising concerns about their dissemination. The presence of ESBL-producing bacteria in the pristine headwaters of rivers is highly significant information, and the spread and transportation of ARB in river water or downstream processes must be avoided. Therefore, our future challenge is to elucidate the mechanisms of antibiotic resistance in bacteria isolated pristine environment and to accumulate information on the horizontal transmission of antibiotic resistance.

3.5.3 Genomic analysis of multidrug-resistant *E. coli* and ESBL-producing *E. coli*

Genomic analysis of ESBL-producing *E. coli* (1 strain) and multidrug-resistant *E. coli* (1 strain) isolated from the Kaeda River was used to estimate the possession of ARGs and hosts. Table 3 shows the results of genomic analysis of ESBL-producing *E. coli* (ID:KS_R23, profile: ABPC-CEZ-CTX-OTC) isolated from river water and multidrug-resistant *E. coli* (ID: KS_S24, profile: ABPC-CPFX-OTC) isolated from riverbed sediment.

KS_R23 harbored CTX-M-15 and tetA. KS_S24 harbored TEM-214 and tetB, mutations in perC (A56T, S80I) and gyrA (D87N, S83L). CTX-M can break down a wide range of beta-lactam antibiotics, including penicillins and cephalosporins (Canton et al., 2012). The gene tet provides resistance to tetracycline antibiotics by encoding the efflux pumps that discharges the antibiotics out of the bacterial cell (Li and Nikaido, 2009). These were resistant genes and mutations that could explain the results of susceptibility testing. ARGs associated with antibiotic resistance to macrolide antibiotics (*mph*B) and polypeptide antibiotics [*pmr*B (Y358N)], which were not tested in this study, were detected from KS_R23. This strain may exhibit resistance to these two antibiotics. ARGs associated with antibiotic resistance to aminoglycoside antibiotics [*aph*(3")-Ib, *aph*(3')-La, *aph*(6)-Id, *str*A, *str*B]; macrolide antibiotics [*pmr*B (Y358N)]; and sulfonamide antibiotics (*sul*2) were detected from KS_S24. This strain may exhibit resistance to these three antibiotics. Among the detected genes, the difference between the resistance genes that could explain the results of susceptibility testing and other genes was considered to be ARGs originally possessed by the bacteria and ARGs acquired through horizontal spread via mobile genetic factors such as plasmids. KS_R23 and KS_S24 were classified into phylogroups B1 and A, respectively. *E. coli* isolated from wild animals was mainly classified into phylogroups A and B1 (Johnson et al., 2017; Cristovao et al., 2017; Haenni et al., 2020). Therefore, ESBL-producing *E. coli* and multidrug-resistant *E. coli* may be derived from wild animals. However, ARB were not detected in the feces of wild animals in this study. The only wild animals targeted in this study were bird and Mustelidae that excrete fecal matter on riverbanks. It is possible that other wild animals may have loaded ESBL-producing bacteria. It is

TABLE 3 The results of genomic analysis of ESBL-producing *Escherichia coli* (ID:KS_R23) isolated from the river water and multidrug-resistant *Escherichia coli* (ID:KS_S24) isolated from riverbed sediment.

Sample ID		KS_R23	KS_S24
Antibiotic resistance profiles		ABPC-CEZ-CTX-OTC	ABPC-CPFX-OTC
Antibiotic resistant gene	Aminoglycoside	—	*aph(3″)-Ib, aph(3′)-Ia, aph(6)-Id*, StrA, StrB
	B-lactam	CTX-M-15	TEM-214
	Fluoroquinolone	*qnrS1*	*parC* (A56T, S80I), *gyrA* (D87N, S83 L)
	Macrolide	*mphB*	*mphB*
	Polymyxin	*pmrB*(Y358 N)	—
	Sulfonamide		*sul2*
	Tetracycline	*tetA*	*tetB*
Serotype		-:H37	O89:H10
phylogroup		B1	A
ST		58	744

(ABPC), Ampicillin; (CEZ), Cefazolin; (CTX), Cefotaxime; (CPFX), Ciprofloxacin; (OTC), Oxytetracycline.
The names of bacterial species and genes.

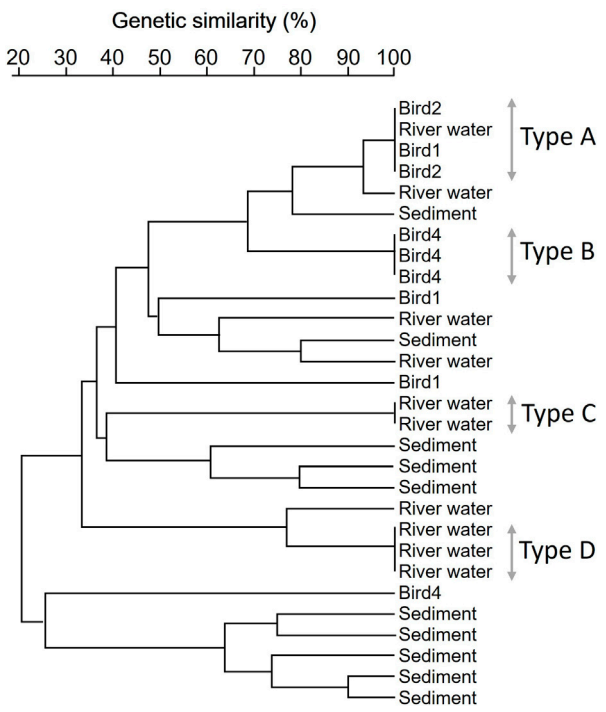

FIGURE 5
Dendrogram analysis based on the similarity of enterococci PFGE types. Enterococci strains isolated from the river water, riverbed sediment and of bird feces at S2 site. Bird 1, 2, 4: Enterococci strains isolated from bird 1, 2, 4.

possible that fecal matters from wild boars and deer live in the catchment may have been input into the river as surface water via forest surface soils with rainfall. Therefore, future items to be considered are feces of other major wild animals and surface water flows into the river.

3.6 Comparison of genotypic similarities between strains isolated from river water and bird feces by PFGE analysis

Based on genomic analysis, there was a high commonality of antibiotic resistance between strains obtained from river sample and bird feces. Therefore, PFGE analysis was used to compare genotypic similarities between strains isolated from river samples and bird feces. In a survey conducted on 27 October 2017, *E. coli* strains (n = 30) were randomly selected from river water, riverbed sediment, and bird feces collected at S2. A dendrogram based on the similarity of PFGE types of each *E. coli* strain is shown in Supplementary Figure S1. When the clusters were classified into groups with 100% similarity, PFGE types of *E. coli* were highly diverse, and no information on the source of the *E. coli* pollution. The 29 randomly selected enterococci strains from each sample were analyzed for the similarity of PFGE types for each strain (Figure 5). Three strains isolated from bird feces were excluded because PFGE band patterns could not be identified. When the clusters were classified into groups with 100% similarity, 4 clusters (A, B, C and D types) were identified, consisting of 2–4 strains each. Type A consisted of one strain isolated from river water and three strains isolated from bird feces strains. Thus, an identical enterococci clone was present in both the river water and bird feces. The results of enterococcal PFGE analysis suggest that bird feces is one of the sources of enterococci contamination of the pristine uppermost stream of the Kaeda River. In addition, the number of target strains needs to be increased to increase the significance of the PFGE analysis. This is an issue to be addressed in the future.

4 Conclusion

AR-*E. coli* and AR-ENT were investigated in river water, riverbed sediment, and feces of waterside animals, such as birds and Mustelidae, at pristine uppermost sites throughout the year. The resistance rates of *E. coli* and enterococci fluctuated at low levels (*E. coli*: 2.9%–17%, enterococci: 1.7%–9.6%). ESBL-producing *E. coli* (0.4%) with multidrug resistance (0.6%) were detected among the AR-*E. coli* detected in the river. Notably, multidrug-resistant bacteria and clinically important ESBL-producing bacteria were found in the pristine environment. This shows that rapid elucidation of the routes of ARB dissemination is important. Although we could not determine the sources of the detected ARB in this study, birds were one of the sources of bacterial contamination of the pristine uppermost stream of the Kaeda River. To elucidate the sources of ARB in pristine natural environments, conducting investigations from a multifaceted perspective (e.g., large wild animals, production by plants, climate change) and not limited to the influence of birds is necessary (Torres et al., 2020; Caliz et al., 2022).

Data availability statement

The original contributions presented in the study are included in the article/Supplementary Material, further inquiries can be directed to the corresponding author.

Author contributions

EN: Data curation, Investigation, Writing–original draft, Writing–review and editing. HX: Validation, Writing–original draft. ST: Validation, Writing–original draft. MN: Investigation, Writing–original draft. KN: Validation, Writing–original draft. YH: Investigation, Writing–original draft. YO: Investigation, Writing–original draft. YS: Conceptualization, Investigation, Methodology, Project administration, Supervision, Validation, Writing–original draft, Writing–review and editing.

Funding

The author(s) declare that no financial support was received for the research, authorship, and/or publication of this article.

Acknowledgments

The authors would like to thank laboratory member for technical cooperate with the experiments. Finally, we are grateful to the referees for useful comments.

Conflict of interest

Author EN was employed by IDEA Consultants, Inc.

The remaining authors declare that the research was conducted in the absence of any commercial or financial relationships that could be construed as a potential conflict of interest.

Publisher's note

All claims expressed in this article are solely those of the authors and do not necessarily represent those of their affiliated organizations, or those of the publisher, the editors and the reviewers. Any product that may be evaluated in this article, or claim that may be made by its manufacturer, is not guaranteed or endorsed by the publisher.

Supplementary material

The Supplementary Material for this article can be found online at: https://www.frontiersin.org/articles/10.3389/fenvs.2024.1439174/full#supplementary-material

References

Afolabi, E. O., Quilliam, R. S., and Oliver, D. M. (2023). Persistence of *E. coli* in streambed sediment contaminated with faeces from dairy cows, geese, and deer: legacy risks to environment and health. *Int. J. Environ. Res. Public Health* 20 (7), 5375. doi:10.3390/ijerph20075375

Agga, G. E., Silva, P. J., and Martin, R. S. (2021). Third-generation cephalosporin- and tetracycline-resistant *Escherichia coli* and antimicrobial resistance genes from metagenomes of mink feces and feed. *Foodborne Pathog. Dis.* 18 (3), 169–178. doi:10.1089/fpd.2020.2851

Allen, H. K., Donato, J., Wang, H. H., Cloud-Hansen, K. A., Davies, J., and Handelsman, J. (2010). Call of the wild: antibiotic resistance genes in natural environments. *Nat. Rev. Microbiol.* 8 (4), 251–259. doi:10.1038/nrmicro2312

Alonso, A., Sánchez, P., and Martínez, J. L. (2001). Environmental selection of antibiotic resistance genes. *Environ. Microbiol.* 3 (1), 1–9. doi:10.1046/j.1462-2920.2001.00161.x00161.x

Antimicrobial Resistance Collaborators,Ikuta, K. S., Sharara, F., Swetschinski, L., Robles Aguilar, G., Gray, A., et al. (2022). Global burden of bacterial antimicrobial resistance in 2019: a systematic analysis. *Lance* 399 (10325), 629–655. doi:10.1016/S0140-6736(21)02724-0

Ardiles-Villegas, K., González-Acuña, D., Waldenström, J., Olsen, B., and Hernández, J. (2011). Antibiotic resistance patterns in fecal bacteria isolated from Christmas shearwater (Puffinus nativitatis) and masked booby (*Sula dactylatra*) at remote Easter Island. *Avian Dis.* 55 (3), 486–489. doi:10.1637/9619-122010-ResNote.1

Baquero, F., Martínez, J. L., and Cantón, R. (2008). Antibiotics and antibiotic resistance in water environments. *Curr. Opin. Biotechnol.* 19 (3), 260–265. doi:10.1016/j.copbio.2008.05.006

Beghain, J., Bridier-Nahmias, A., Le Nagard, H., Denamur, E., and Clermont, O. (2018). ClermonTyping: an easy-to-use and accurate *in silico* method for Escherichia genus strain phylotyping. *Microb. Genom.* 4 (7), e000192. doi:10.1099/mgen.0.000192

Berendonk, T. U., Manaia, C. M., Merlin, C., Fatta-Kassinos, D., Cytryn, E., Walsh, F., et al. (2015). Tackling antibiotic resistance: the environmental framework. *Nat. Rev. Microbiol.* 13 (5), 310–317. doi:10.1038/nrmicro3439

Boehm, A. B., Griffith, J., McGee, C., Edge, T. A., Solo-Gabriele, H. M., Whitman, R., et al. (2009). Faecal indicator bacteria enumeration in beach sand: a comparison study of extraction methods in medium to coarse sands. *J. Appl. Microbiol.* 107 (5), 1740–1750. doi:10.1111/j.13652672.2009.0444-0.x

Bonnedahl, J., and Järhult, J. D. (2014). Antibiotic resistance in wild birds. *Ups. J. Med. Sci.* 119 (2), 113–116. doi:10.3109/03009734.2014.905663

Caliz, J., Subirats, J., Triadó-Margarit, X., Borrego, C. M., and Casamayor, E. O. (2022). Global dispersal and potential sources of antibiotic resistance genes in atmospheric remote depositions. *Environ. Int.* 160, 107077. doi:10.1016/j.envint.2022.107077

Canton, R., González-Alba, J. M., and Galán, J. C. (2012). CTX-M enzymes: origin and diffusion. *Front. Microbiol.* 3, 110. doi:10.3389/fmicb.2012.00110

Centers for Disease (2019). *Antibiotic resistance threats in the United States 2019*, 1–148. Atlanta, GA, UNITED STATES: U.S. Department of Health and Human Services. Available at: https://www.cdc.gov/drugresistance/pdf/threats-report/2019-ar-threats-report-508.pdf (accessed on May 7, 2024).

Centers for Disease Control (2017). Standard operating procedure for PulseNet PFGE of *Escherichia coli* O157: H7, *Escherichia coli* non-O157 (STEC), Salmonella serotypes, Shigella sonnei and Shigella flexneri. PNL05 last updated. Available at: https://www.cdc.gov/pulsenet/pdf/ecoli-shigella-salmonella-pfge-protocol-508c.pdf (accessed on May 7, 2024).

Chen, Q. L., Cui, H. L., Su, J. Q., Penuelas, J., and Zhu, Y. G. (2019). Antibiotic resistomes in plant microbiomes. *Trends. Plant Sci.* 24 (6), 530–541. doi:10.1016/j.tplants.2019.02.010

Christner, M., Trusch, M., Rohde, H., Kwiatkowski, M., Schlüter, H., Wolters, M., et al. (2014). Rapid MALDI-TOF mass spectrometry strain typing during a large outbreak of Shiga-Toxigenic *Escherichia coli*. *PLoS One* 9 (7), e101924. doi:10.1371/journal.pone.0101924

CLSI (2012). *M100-S22 performance standards for antimicrobial susceptibility testing; twenty-second informational supplement*. Wayne, Pennsylvania, America: Clinical and Laboratory Standards Institute, 1–184.

CLSI (2017). *M100 performance standards for antimicrobial susceptibility testing*. 27th Edition. Wayne, Pennsylvania, America: Clinical and Laboratory Standards Institute, 1–249. Replaces M100-S26.

Cristovao, F., Alonso, C. A., Igrejas, G., SoUnited States, M., Silva, V., Pereira, J. E., et al. (2017). Clonal diversity of extended-spectrum beta-lactamase producing *Escherichia coli* isolates in fecal samples of wild animals. *FEMS Microbiol/Lett.*, 364(5), doi:10.1093/femsle/fnx039

Daniel, D. S., Lee, S. M., Gan, H. M., Dykes, G. A., and Rahman, S. (2017). Genetic diversity of *Enterococcus faecalis* isolated from environmental, animal and clinical sources in Malaysia. *J. Infect. Public Health* 10 (5), 617–623. doi:10.1016/j.jiph.2017.02.006

Diwan, V., Hanna, N., Purohit, M., Chandran, S., Riggi, E., Parashar, V., et al. (2018). Seasonal variations in water-quality, antibiotic residues, resistant bacteria and antibiotic resistance genes of *Escherichia coli* isolates from water and sediments of the Kshipra river in central India. *Int. J. Environ. Res. Public Health* 15 (6), 1281. doi:10.3390/ijerph15061281

Dolejska, M., and Literak, I. (2019). Wildlife is overlooked in the epidemiology of medically important antibiotic-resistant bacteria. *Antimicrob. Agents Chemother.* 63 (8), 011677-19–e1219. doi:10.1128/AAC.01167-19

Dolejska, M., and Papagiannitsis, C. C. (2018). Plasmid-mediated resistance is going wild. *Plasmid* 99, 99–111. doi:10.1016/j.plasmid.2018.09.010

Farnleitner, A. H., Ryzinska-Paier, G., Reischer, G. H., Burtscher, M. M., Knetsch, S., Kirschner, A., et al. (2010). *Escherichia coli* and enterococci are sensitive and reliable indicators for human, livestock and wildlife faecal pollution in alpine mountainous water resources. *J. Appl. Microbiol.* 109 (5), 1599–1608. doi:10.1111/j.1365-2672.2010.04788.x04788.x

Feldgarden, M., Brover, V., Gonzalez-Escalona, N., Frye, J. G., Haendiges, J., Haft, D. H., et al. (2021). AMRFinderPlus and the Reference Gene Catalog facilitate examination of the genomic links among antimicrobial resistance, stress response, and virulence. *Sci. Rep.* 11 (1), 12728. doi:10.1038/s41598-021-91456-0

Fenselau, C., and Demirev, P. A. (2001). Characterization of intact microorganisms by MALDI mass spectrometry. *Mass Spectrom. Rev.* 20 (4), 157–171. doi:10.1002/mas.10004

G7 Health Ministers' Communiqué (2022). *Overview of the G7 documents: G7 health Ministers' Communiqué 20 may 2022, Berlin. Berlin, Germany*, 1–12. Available at: https://www.g7germany.de/g7-en/g7-documents (accessed on May 7, 2024).

García, L. A., Torres, C., López, A. R., Rodríguez, C. O., Espinosa, J. O., and Valencia, C. S. (2020). Staphylococcus Spp. from wild mammals in Aragón (Spain): antibiotic resistance status. *J. Vet. Res.* 64 (3), 373–379. doi:10.2478/jvetres-2020-0057

Givens, C. E., Kolpin, D. W., Hubbard, L. E., Meppelink, S. M., Cwiertny, D. M., Thompson, D. A., et al. (2023). Simultaneous stream assessment of antibiotics, bacteria, antibiotic resistant bacteria, and antibiotic resistance genes in an agricultural region of the United States. *Sci. Total Environ.* 904, 166753. doi:10.1016/j.scitotenv.2023.166753

Gordon, S., Swenson, J. M., Hill, B. C., Pigott, N. E., Facklam, R. R., Cooksey, R. C., et al. (1992). Antimicrobial susceptibility patterns of common and unusual species of enterococci causing infections in the United States. Enterococcal Study Group. *J. Clin. Microbiol.* 30 (9), 2373–2378. doi:10.1128/jcm.30.9.2373-2378.1992

Grenni, P. (2022). Antimicrobial resistance in rivers: a review of the genes detected and new challenges. *Environ. Toxicol. Chem.* 41 (3), 687–714. doi:10.1002/etc.5289

Gupta, S. K., Padmanabhan, B. R., Diene, S. M., Lopez-Rojas, R., Kempf, M., Landraud, L., et al. (2014). ARG-ANNOT, a new bioinformatic tool to discover antibiotic resistance genes in bacterial genomes. *Antimicrob. Agents Chemother.* 58 (1), 212–220. doi:10.1128/AAC.01310-13

Haenni, M., Métayer, V., Jarry, R., Drapeau, A., Puech, M. P., Madec, J. Y., et al. (2020). Wide spread of blaCTX-M-9/mcr-9 IncHI2/ST1 plasmids and CTX-M-9-producing *Escherichia coli* and enterobacter cloacae in rescued wild animals. *Front. Microbiol.* 11, 601317. doi:10.3389/fmicb.2020.601317

Hansen, S., Messer, T., Mittelstet, A., Berry, E. D., Bartelt-Hunt, S., and Abimbola, O. (2020). *Escherichia coli* concentrations in waters of a reservoir system impacted by cattle and migratory waterfowl. *Sci. Total Environ.* 705, 135607. doi:10.1016/j.scitotenv.2019.135607

Hernandez, J., Stedt, J., Bonnedahl, J., Molin, Y., Drobni, M., Calisto-Ulloa, N., et al. (2012). Human-associated extended-spectrum β-lactamase in the antarctic. *Appl. Environ. Microbiol.* 78 (6), 2056–2058. doi:10.1128/AEM.07320-11

Husna, A., Rahman, M. M., Badruzzaman, A. T. M., Sikder, M. H., Islam, M. R., Rahman, M. T., et al. (2023). Extended-spectrum β-lactamases (ESBL): challenges and opportunities. *Biomedicines* 11 (11), 2937. doi:10.3390/biomedicines11112937

Hwengwere, K., Paramel Nair, H., Hughes, K. A., Peck, L. S., Clark, M. S., and Walker, C. A. (2022). Antimicrobial resistance in Antarctica: is it still a pristine environment? *Microbiome* 10 (1), 71. doi:10.1186/s40168-022-01250-x

Inouye, M., Dashnow, H., Raven, L. A., Schultz, M. B., Pope, B. J., Tomita, T., et al. (2014). SRST2: rapid genomic surveillance for public health and hospital microbiology labs. *Genome Med.* 6 (11), 90. doi:10.1186/s13073-014-0090-6

Ishii, S., and Sadowsky, M. J. (2008). *Escherichia coli* in the environment: implications for water quality and human health. *Microbes. Environ.* 23 (2), 101–108. doi:10.1264/jsme2.23.101

Jang, J., Park, J., Hwang, C. Y., Choi, J., Shin, J., Kim, Y. M., et al. (2022). Abundance and diversity of antibiotic resistance genes and bacterial communities in the western Pacific and Southern Oceans. *Sci. Total Environ.* 822, 153360. doi:10.1016/j.scitotenv.2022.153360-2022.153360

Japanese Standard Association (2016). *Testing methods for industrial wastewate*, K 0102: 2016. Tokyo, Japan: Japanese Standard Association, 1–370. Available at: https://webdesk.jsa.or.jp/preview/pre-_jis_k_00102_000_000_2016_e_ed10_i4.pdf (accessed on May 7, 2024).

Johnson, J. R., Johnston, B. D., Delavari, P., Thuras, P., Clabots, C., and Sadowsky, M. J. (2017). Phylogenetic backgrounds and virulence-associated traits of *Escherichia coli* isolates from surface waters and diverse animals in Minnesota and Wisconsin. *Appl. Environ. Microbiol.* 83 (24), 013299-17–e1417. doi:10.1128/AEM.01329-17

Kajitani, R., Yoshimura, D., Ogura, Y., Gotoh, Y., Hayashi, T., and Itoh, T. (2020). Platanus_B: an accurate *de novo* assembler for bacterial genomes using an iterative error-removal process. *DNA Res.* 27 (3), dsaa014. doi:10.1093/dnares/dsaa014

Kawamura, K., Nagano, N., Suzuki, M., Wachino, J. I., Kimura, K., and Arakawa, Y. (2017). ESBL-Producing *Escherichia coli* and its rapid rise among healthy people. *Food Saf. . (Tokyo)* 5 (4), 122–150. doi:10.14252/foodsafetyfscj.2017011

Khare, N., Kaushik, M., Martin, J. P., Mohanty, A., and Gulati, P. (2020). Genotypic diversity in multi-drug-resistant *E. coli* isolated from animal feces and Yamuna River water, India, using rep-PCR fingerprinting. *Environ. Monit. Assess.* 192 (11), 681. doi:10.1007/s10661-020-08635-1

Laborda, P., Sanz-García, F., Ochoa-Sánchez, L. E., Gil-Gil, T., Hernando-Amado, S., and Martínez, J. L. (2022). Wildlife and antibiotic resistance. *Front. Cell. Infect. Microbiol.* 12, 873989. doi:10.3389/fcimb.2022.873989

Lenart-Boroń, A., Prajsnar, J., Guzik, M., Boroń, P., Grad, B., and Żelazny, M. (2022). Antibiotics in groundwater and river water of białka—a pristine mountain river. *Appl. Sci.* 12 (24), 12743. doi:10.3390/app122412743

Li, X. Z., and Nikaido, H. (2009). Efflux-mediated drug resistance in bacteria: an update. *Drugs* 69 (12), 1555–1623. doi:10.2165/11317030-000000000-00000

Lima-Bittencourt, C. I., Cursino, L., Gonçalves-Dornelas, H., Pontes, D. S., Nardi, R. M., Callisto, M., et al. (2007). Multiple antimicrobial resistance in Enterobacteriaceae isolates from pristine freshwater. *Genet. Mol. Res.* 6 (3), 510–521. Available at: https://pubmed.ncbi.nlm.nih.gov/17985304/.

Nishimura, E., Nishiyama, M., Nukazawa, K., and Suzuki, Y. (2021). Comparison of antibiotic resistance profile of *Escherichia coli* between pristine and human-impacted sites in a river. *Antibiot. (Basel)* 10 (5), 575. doi:10.3390/antibiotics10050575

Nishiyama, M., Ogura, Y., Hayashi, T., and Suzuki, Y. (2017). Antibiotic resistance profiling and genotyping of vancomycin-resistant enterococci collected from an urban river basin in the provincial city of Miyazaki, Japan. *Water* 9 (2), 79. doi:10.3390/w9020079

Obermeier, M. M., Wicaksono, W. A., Taffner, J., Bergna, A., Poehlein, A., Cernava, T., et al. (2021). Plant resistome profiling in evolutionary old bog vegetation provides new clues to understand emergence of multi-resistance. *ISME J.* 15 (3), 921–937. doi:10.1038/s41396-020-00822-9

O'Neill, J. (2014). *Review on antimicrobial resistance: antimicrobial resistance: tackling a crisis for the health and wealth of nations*. London, United Kingdom: The UK Department of Health, 1–20. Available at: https://wellcomecollection.org/works/rdpck35v (accessed on May 7, 2024).

Osińska, A., Korzeniewska, E., Harnisz, M., Felis, E., Bajkacz, S., Jachimowicz, P., et al. (2020). Small-scale wastewater treatment plants as a source of the dissemination of antibiotic resistance genes in the aquatic environment. *J. Hazard. Mat.* 381, 121221. doi:10.1016/j.jhazmat.2019.121221

Pana, Z. D., and Zaoutis, T. (2018). Treatment of extended-spectrum β-lactamase-producing Enterobacteriaceae (ESBLs) infections: what have we learned until now? *F1000Res* 7, 1347. F1000 Faculty Rev-1347. doi:10.12688/f1000research.14822.1

Parks, D. H., Imelfort, M., Skennerton, C. T., Hugenholtz, P., and Tyson, G. W. (2015). CheckM: assessing the quality of microbial genomes recovered from isolates, single cells, and metagenomes. *Genome Res.* 25 (7), 1043–1055. doi:10.1101/gr.186072.114

Ramey, A. M., and Ahlstrom, C. A. (2020). Antibiotic resistant bacteria in wildlife: perspectives on trends, acquisition and dissemination, data gaps, and future directions. *J. Wildl. Dis.* 56, 1–15. doi:10.7589/2019-04-099

Rogers, S. W., Shaffer, C. E., Langen, T. A., Jahne, M., and Welsh, R. (2018). Antibiotic-resistant genes and pathogens shed by wild deer correlate with land application of residuals. *Ecohealth* 15 (2), 409–425. doi:10.1007/s10393-018-1316-7

Ruoff, K. L., de la Maza, L., Murtagh, M. J., Spargo, J. D., and Ferraro, M. J. (1990). Species identities of enterococci isolated from clinical specimens. *J. Clin. Microbiol.* 28 (3), 435–437. doi:10.1128/-jcm.28.3.435-437.1990

Rwego, I. B., Isabirye-Basuta, G., Gillespie, T. R., and Goldberg, T. L. (2008). Gastrointestinal bacterial transmission among humans, mountain gorillas, and livestock in Bwindi Impenetrable National Park, Uganda. *Conserv. Biol.* 22 (6), 1600–1607. doi:10.1111/j.1523-1739.2008.01018.x01018.x

Sajjad, W., Ali, B., Niu, H., Ilahi, N., Rafiq, M., Bahadur, A., et al. (2023). High prevalence of antibiotic-resistant and metal-tolerant cultivable bacteria in remote glacier environment. *Environ. Res.* 239 (2), 117444. doi:10.1016/j.envres.2023.117444

Stadler, T., Meinel, D., Aguilar-Bultet, L., Huisman, J. S., Schindler, R., Egli, A., et al. (2018). Transmission of ESBL-producing Enterobacteriaceae and their mobile genetic elements-identification of sources by whole genome sequencing: study protocol for an observational study in Switzerland. *BMJ open* 8 (2), e021823. doi:10.1136/bmjopen-2018-021823

Suzuki, Y., Niina, K., Matsuwaki, T., Nukazawa, K., and Iguchi, A. (2018). Bacterial flora analysis of coliforms in sewage, river water, and ground water using MALDI-TOF mass spectrometry. *J. Environ. Sci. Health A Tox. Hazard. Subst. Environ. Eng.* 53 (2), 160–173. doi:10.1080/10934529.2017.13831-28

Terada, S., Miyake, H., and Urase, T. (2012). Profile of antibiotic resistance of *Escherichia coli* isolated from different water environments. *JSWE* 35, 73–80. doi:10.2965/jswe.35.73

Torres, R. T., Fernandes, J., Carvalho, J., Cunha, M. V., Caetano, T., Mendo, S., et al. (2020). Wild boar as a reservoir of antimicrobial resistance. *Sci. Total Environ.* 717, 135001. doi:10.1016/j.scitotenv.2019.135001

United States Environmental Protection Agency (2014). *Method 1600: enterococci in water by membrane filtration using membrane-Enterococcus indoxyl-β-D-glucoside agar (mEI)*. Washington, D.C., America: United States Environmental Protection Agency. Available at: https://www.epa.gov/sites/-default/files/2018-06/documents/method_1600_sept-2014.pdf (accessed on May 7, 2024).

Willyard, C. (2017). The drug-resistant bacteria that pose the greatest health threats. *Nature* 543 (7643), 15. doi:10.1038/nature.2017.21550

World Health Organization (2022b). *Guidelines for drinking-water quality: fourth edition incorporating the first and second addenda*. China: Licence: CC BY-NC-SA 3.0 IGO.

World Health Organization (2022a). *WHO and ECDC report: antimicrobial resistance surveillance in Europe 2022–2020*. Sweden: European Centre for Disease Prevention and Control: Stockholm County, 1–164. Available at: https://www.ecdc.europa.eu/sites/default/files/documents/Joint-WHO-ECDC-AMR-report-2022.pdf (accessed on May 7, 2024).

Yuan, Y., Liang, B., Jiang, B. W., Zhu, L. W., Wang, T. C., Li, Y. G., et al. (2021). Migratory wild birds carrying multidrug-resistant *Escherichia coli* as potential transmitters of antimicrobial resistance in China. *PLoS One* 16 (12), e0261444. doi:10.1371/journal.pone.0261444

Zhang, S. H., Lv, X., Han, B., Gu, X., Wang, P. F., Wang, C., et al. (2015). Prevalence of antibiotic resistance genes in antibiotic-resistant *Escherichia coli* isolates in surface water of Taihu Lake Basin, China. *Environ. Sci. Pollut. Res. Int.* 22 (15), 11412–11421. doi:10.1007/s11356-015-4371-4

frontiers | Frontiers in Environmental Science

TYPE Original Research
PUBLISHED 30 September 2024
DOI 10.3389/fenvs.2024.1450485

Check for updates

OPEN ACCESS

EDITED BY
Divya Pal,
Stockholm University, Sweden

REVIEWED BY
Krishna Yadav,
Iowa State University, United States
Anuradha Goswami,
University of Alabama at Birmingham, United States

*CORRESPONDENCE
Ahmed Barhoum,
ahmed.barhoum@science.helwan.edu.eg

RECEIVED 17 June 2024
ACCEPTED 10 September 2024
PUBLISHED 30 September 2024

CITATION
Hemmami H, Zeghoud S, Ben Amor I, Alnazza Alhamad A, Tliba A, Alsalme A, Cornu D, Bechelany M and Barhoum A (2024) Green synthesis of CaO nanoparticles from chicken eggshells: antibacterial, antifungal, and heavy metal (Pb^{2+}, Cr^{2+}, Cd^{2+} and Hg^{2+}) adsorption properties.
Front. Environ. Sci. 12:1450485.
doi: 10.3389/fenvs.2024.1450485

COPYRIGHT
© 2024 Hemmami, Zeghoud, Ben Amor, Alnazza Alhamad, Tliba, Alsalme, Cornu, Bechelany and Barhoum. This is an open-access article distributed under the terms of the Creative Commons Attribution License (CC BY). The use, distribution or reproduction in other forums is permitted, provided the original author(s) and the copyright owner(s) are credited and that the original publication in this journal is cited, in accordance with accepted academic practice. No use, distribution or reproduction is permitted which does not comply with these terms.

Green synthesis of CaO nanoparticles from chicken eggshells: antibacterial, antifungal, and heavy metal (Pb^{2+}, Cr^{2+}, Cd^{2+} and Hg^{2+}) adsorption properties

Hadia Hemmami[1,2], Soumeia Zeghoud[1,2], Ilham Ben Amor[1,2], Ali Alnazza Alhamad[3,4], Ali Tliba[5], Ali Alsalme[6], David Cornu[7], Mikhael Bechelany[7,8] and Ahmed Barhoum[9]*

[1]Department of Process Engineering and Petrochemical, Faculty of Technology, University of El Oued, El Oued, Algeria, [2]Renewable Energy Development unit in Arid Zones (UDERZA), University of El Oued, El Oued, Algeria, [3]Department of Chemistry, Faculty of Science, University of Aleppo, Aleppo, Syria, [4]Department of Technology of organic synthesis, Ural Federal University, Yekaterinburg, Russia, [5]Laboratory Valorisation and Technology of Saharan Resources (VTRS), University of El Oued, El Oued, Algeria, [6]Department of Chemistry, College of Science, King Saud University, Riyadh, Saudi Arabia, [7]Institut Européen des Membranes (IEM), UMR 5635, University of Montpellier, ENSCM, CNRS, Montpellier, France, [8]Functional Materials Group, Gulf University for Science and Technology (GUST), Mubarak Al-Abdullah, Kuwait, [9]NanoStruc Research Group, Chemistry Department, Faculty of Science, Helwan University, Cairo, Egypt

Background: Chicken eggshells, a common poultry byproduct, are rich in calcium and provide a sustainable source for producing calcium oxide nanoparticles (CaO NPs). Their use in eco-friendly synthesis aligns with the growing emphasis on sustainable materials for environmental and biomedical applications. Objectives: This study develops an eco-friendly method for synthesizing CaO NPs from chicken eggshells, characterizes their physicochemical properties, and evaluates their antibacterial and antifungal activities. It also tests their effectiveness in removing heavy metal ions (Pb^{2+}, Cr^{2+}, Cd^{2+}, and Hg^{2+}) from aqueous solutions.

Methods: CaO NPs were synthesized by calcining chicken eggshells at 700°C for 7 h. Comprehensive characterization included analysis of crystalline structure, morphology, optical properties, bandgap energy, chemical composition, and thermal stability. Antibacterial and antifungal activities were tested using the well-agar diffusion method. Batch adsorption experiments evaluated heavy metal ion removal under varying conditions of pH, temperature, stirring time, and adsorbent concentration

Results: The synthesis produced spherical, single-crystal CaO NPs with diameters ranging from 5 to 30 nm and a crystalline size of approximately 20 nm. The nanoparticles had a bandgap energy of about 4.7 eV. Significant antibacterial activity was observed against *Staphylococcus aureus*, *Klebsiella pneumoniae*, and *Escherichia coli*, with increasing inhibition zones correlating with nanoparticle concentration. The CaO NPs also effectively inhibited *Candida albicans*. For efficient metal ion removal, the optimal conditions were found to be 30 min at pH 6 with 40 mg of CaO NPs at 25°C, achieving recovery rates of 98% for Pb^{2+}, 97% for Cd^{2+}, 97% for Cr^{2+}, and 97% for Hg^{2+}. For near-complete removal,

extending the process to 70 min at pH 6 with 40 mg of CaO NPs at 45°C achieved the highest recovery rates: 99% for Pb^{2+}, 98% for Cd^{2+}, 99% for Cr^{2+}, and 99% for Hg^{2+}, though this approach involves higher energy and cost.

Conclusion: CaO NPs derived from chicken eggshells are effective antibacterial agents and adsorbents for heavy metal removal. These findings highlight their potential for sustainable applications in environmental and biomedical fields.

KEYWORDS

biowaste utilization, eco-friendly materials, environmental remediation, wastewater treatment, heavy metal removal, nano-adsorbents, antibacterial agents

Highlights

- Green synthesis of CaO NPs from chicken eggshells by thermal annealing at 700°C.
- Significant antibacterial and antifungal activity against various pathogens demonstrated.
- Heavy metal removal of 99% achieved in solutions under optimized conditions.
- Characterization revealed high-quality, spherical CaO NPs synthesized.

1 Introduction

The increasing volume of solid waste poses a significant challenge to sustainability worldwide and its improper management exacerbates public health and environmental issues. Vast quantities of solid waste, including municipal, industrial and hazardous waste, are generated worldwide (Ferdoush et al., 2024). Food waste is a primary contributor to environmental degradation, and it is expected to increase by 44% from 2005 to 2025 (Zhang et al., 2018). Industrialization and population growth drive this surge in waste production (Aditya et al., 2021). Eggshells, sourced predominantly from households, restaurants, and bakeries, represent a significant waste item. Despite their potential for transformation into valuable products, eggshells are typically disposed of in landfills, leading to environmental problems, such as malodorous emissions and pest attraction. Eggshell recycling is a promising solution to environmental concerns and landfill overuse. Transforming eggshell waste into useful products, such as CaO nanoparticles (NPs), can contribute to sustainable waste management practices. This approach mitigates their

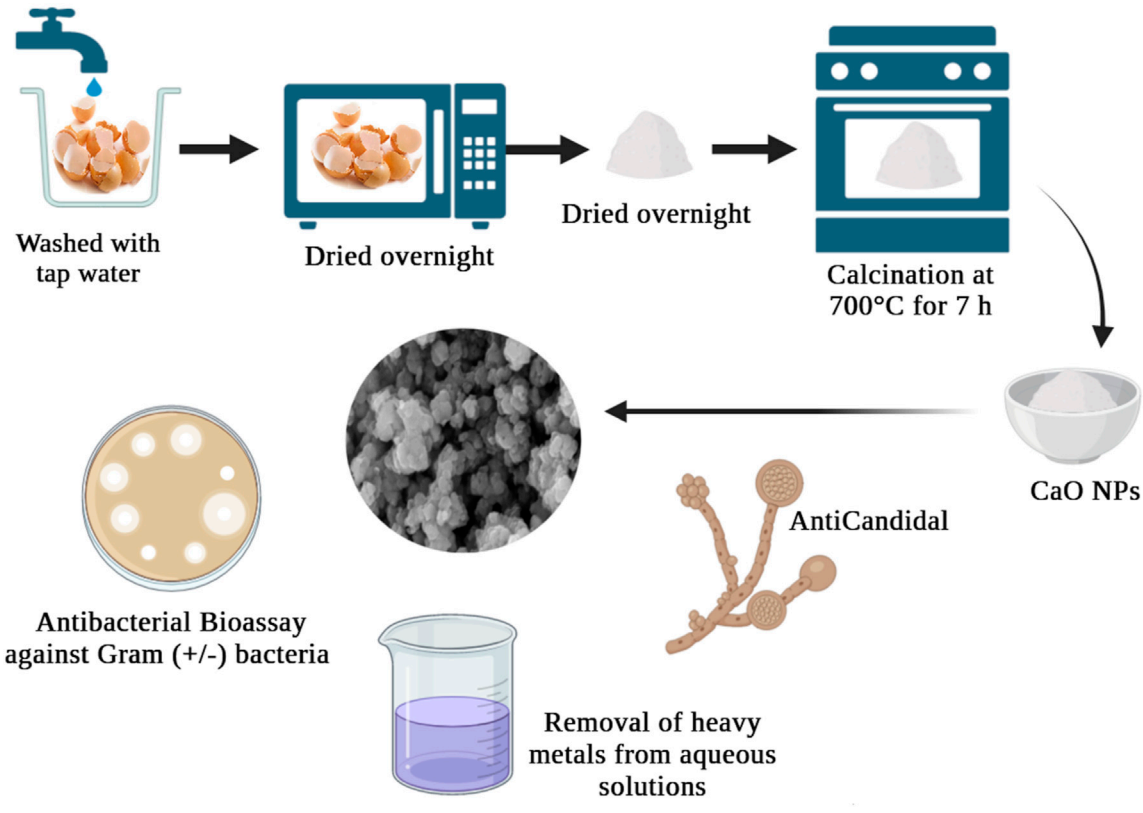

GRAPHICAL ABSTRACT

environmental impact and also supports the circular economy by converting waste into valuable resources. Recycling eggshells into CaO NPs highlights the importance of innovative recycling methods for achieving sustainability goals (Perkumienė et al., 2023; Varjani et al., 2021).

Calcium oxide (CaO), commonly known as quicklime or burnt lime, is essential across various industries including petroleum refining, biodiesel production, and water purification. Typically produced by heating $CaCO_3$ such as limestone or seashells above 825°C, CaO is a key component in many applications (Boey et al., 2011). Recent advancements have focused on CaO NPs, which are synthesised from eggshells an abundant source of $CaCO_3$ and have shown exceptional antibacterial properties against various microorganisms (Abuzeid et al., 2023). These nanoparticles are promising in medical and environmental fields, especially in combating antimicrobial resistance and biofilm-related infections (Kumari et al., 2023; Roy et al., 2013). In addition to their antimicrobial potential, CaO's versatility extends to wastewater treatment. Approximately half of the CaO produced is converted to $Ca(OH)_2$, or hydrated lime, used for disinfection and purification in wastewater management (Xiong et al., 2017). When added to wastewater, CaO raises the pH to 10.5–11.00, which helps to eliminate bacteria, viruses, and heavy metals. CaO is also crucial in drinking water treatment, where it aids in impurity removal through coagulation, precipitation, and pH adjustment, effectively neutralizing acidic waters and disinfecting by destroying pathogens (Chen et al., 2009; Kataki et al., 2021; Silva, 2023). This wide array of applications underscores CaO's critical role in ensuring clean water and advancing antimicrobial solutions.

Various chemical methods are employed to synthesize CaO NPs, each with unique advantages and challenges. Hydrothermal synthesis involves dissolving $Ca(NO_3)_2$ in deionized water, adjusting the pH with NaOH, and heating the solution in a Teflon-lined autoclave at 120°C–200°C for 6–24 h (Naz et al., 2023). This method provides precise control over nanoparticle characteristics but requires expensive equipment and extended processing times. The sol-gel method starts with dissolving a calcium precursor, such as $Ca(NO_3)_2$ or $Ca(CH_3COO)_2$, in a solvent (ethanol or water) with chelating agents to stabilize the solution. Gelation occurs by adjusting the pH with NH_4OH, resulting in a sol that ages into a gel, which is then dried and calcined at high temperatures (500°C–900°C) to form CaO NPs. Similarly, the precipitation method dissolves calcium salts like $CaCl_2$ in water and induces precipitation by adding a strong base like NaOH. The precipitate is filtered, washed, and calcined to yield CaO NPs, though this process may require extensive purification steps to remove residual chemicals. Another approach, the solvothermal method, uses organic solvents at high temperatures and pressures to control nanoparticle morphology but also demands sophisticated equipment (Andarini et al., 2021). While these methods offer versatility in tailoring particle size and crystallinity, they often involve expensive reagents, longer reaction times, and complex setups (Alobaidi et al., 2022). In contrast, thermal decomposition of a $CaCO_3$-rich source, such as eggshells, offers a more cost-effective and sustainable approach (Naz et al., 2023).

This study introduces a novel, eco-friendly method for synthesizing CaO NPs from chicken eggshells, emphasizing its sustainability and cost-effectiveness. By recycling eggshell waste, this approach not only produces valuable nanomaterials but also does so with minimal environmental impact. The synthesis method is both cost-effective and sustainable, avoiding harmful chemicals and complex procedures, and operates at a relatively low temperature sufficient to achieve the desired CaO NPs properties. This low-temperature process reduces energy consumption compared to traditional methods and involves minimal equipment and shorter processing times, making it economically viable for large-scale production. Comprehensive characterization included analysis of crystalline structure, morphology, optical properties, bandgap energy, chemical composition, and thermal stability. The study uniquely evaluates the antimicrobial properties of the CaO NPs against Gram-negative and Gram-positive bacteria, as well as *Candida* albicans, and assesses their effectiveness in removing heavy metal ions (Pb^{2+}, Cr^{2+}, Cd^{2+}, and Hg^{2+}) from aqueous solutions. Key factors influencing adsorption, such as temperature, contact time, pH, and CaO NPs dosage, were systematically explored. This research contributes to green nanotechnology by providing a sustainable solution to environmental and health challenges through the innovative use of waste materials.

2 Experimental

2.1 Materials and reagent

Chicken eggshells, discarded as waste, were collected from various sources in El Oued, Algeria (6°52′03″E, 33°22′06″N), including local restaurants, bakeries, and poultry farms. These eggshells served as the precursor for CaO NPs synthesis. Dimethyl sulfoxide (DMSO; 99%), hydrochloric acid (HCl; 99%), and sodium hydroxide (NaOH; 97%) were obtained from Biochem Chemopharma. DMSO was used as a solvent for the preparation of nanoparticle suspensions in biological assays. HCl and NaOH were employed for adjusting the pH of solutions during metal adsorption experiments. Mueller-Hinton agar, sourced from Bioscan Industrie, Algeria, was used as the growth medium for bacterial cultures during antibacterial testing. Bacterial strains, including *Pseudomonas aeruginosa* (ATCC 27853), *Klebsiella pneumoniae* (ATCC 13883), *Escherichia coli* (ATCC 25922), and *Staphylococcus aureus* (ATCC 25923), were obtained from the Algerian Culture Centre of Microorganisms and used to evaluate the antibacterial efficacy of the CaO nanoparticles. Stock solutions of heavy metal ions were prepared for adsorption studies, using chromium (II) from $CrCl_2$ (95%), mercury (II) from $HgCl_2$ (99%), cadmium (II) from $CdCl_2$ (99.9%), and lead (II) from $Pb(NO_3)_2$ (99.9%) sourced from Sigma-Aldrich. Ciprofloxacin (CIP-5), obtained from Humeau Laboratories, France, was used as a reference antibiotic for antibacterial comparison during bioassays.

2.2 CaO NP synthesis

The synthesis of CaO NPs from chicken eggshells (Figure 1) started by thoroughly washing the collected eggshells in distilled water, followed by air drying for 48 h to ensure complete moisture removal. Then, the dried eggshells were finely ground into a powder using mortar and pestle to achieve a uniform consistency. This

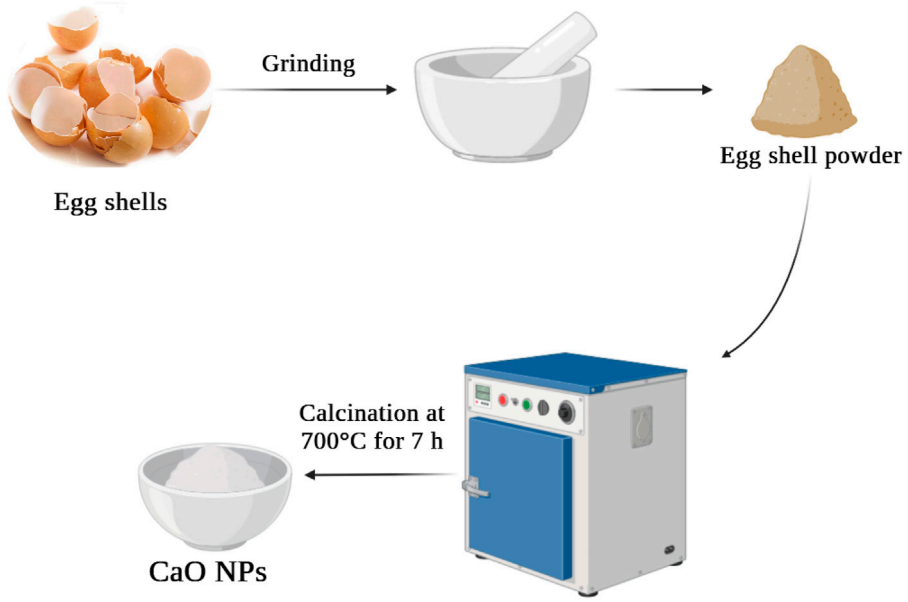

FIGURE 1
Schematic presentation showing the CaO NP synthesis starting from chicken eggshells.

powder was calcined in a furnace at 700°C in open air atmosphere for 7 h, allowing the complete decomposition of $CaCO_3$ and organic matters present in the eggshells. Throughout this process, gaseous H_2O and CO_2 were efficiently evaporated, resulting in the formation of pure CaO NPs.

2.3 CaO NP characterization

The crystalline structure of the CaO NPs was assessed by XRD using a Rigaku Miniflex 600 instrument. The scan speed was set at 0.02° per step for higher resolution of the diffraction peaks, and the angle range was expanded to 10°–90° 2θ to obtain comprehensive data on the crystalline phases. UV-vis spectra were obtained with a Jasco V160 UV-vis spectrophotometer, after dissolving 0.1 mg of CaO NPs in 2 mL of distilled water, to determine the optical properties. The bandgap energy (E.g.,) was computed using the Tauc equation with n fixed at 2, and the UV-vis parameters were adjusted to extend the wavelength range to 200–800 nm, ensuring better detection of absorption edges. FTIR spectra were acquired using a Nicolet iS50 FTIR spectrometer and the KBr technique, with optimized sample-to-KBr ratio (1:100) to enhance signal clarity. The elemental composition, shape, and size of the CaO NPs were analyzed using Field Emission Scanning Electron Microscopy (FE-SEM, Leo Supra 55-Zeiss Inc., Germany), with magnification increased up to ×100,000 for detailed imaging. To assess thermal stability, the CaO NPs were subjected to thermogravimetric analysis using a Mettler-Toledo AG instrument, with heating from room temperature to 900°C at a controlled rate of 10 C/min, and the system was maintained at 900°C for 2 h to ensure complete $CaCO_3$ decomposition. Cooling was performed at 10 C/min to stabilize the material properties.

2.4 Antibacterial assays

The antibacterial activity of eggshells and CaO NPs was evaluated using the well-agar diffusion method. Four bacterial strains were used: *P. aeruginosa* (ATCC 27853), *K. pneumoniae* (ATCC 13883), *E. coli* (ATCC 25922), and *S. aureus* (ATCC 25923). Sample solutions were prepared at concentrations of 0.5, 1, 2, and 3 mg mL^{-1} in DMSO and Mueller-Hinton agar served as growth medium. Bacterial strains were cultured on agar plates at 37°C for 24 h. Then, 6-mm wells were created in the agar and 50 µL of the compound solutions (at different concentrations) was added to each well. The antibacterial activity was compared to that of CIP-5, used as reference. After incubation at 37°C for 24 h, the zones of inhibition were measured. To ensure reliability and consistency, experiments were carried out in triplicate.

2.5 Anticandidal activity

Candida albicans (ATCC 14053) was obtained from the Pasteur Institute of Algiers, Algeria, and cultured on Sabouraud dextrose agar (SDA) plates at 37°C for 48 h. The suspension turbidity was adjusted to the desired cell density (0.5 McFarland standard) using the DensiChek Densitometer from Biomérieux®. To assess the antifungal activities of the samples, *C. albicans* (ATCC 14053) was prepared in SDA using the same method employed for the antibacterial activity evaluation, using the well diffusion technique (Abadi & Abdul-Hussein Mejbel, 2020; Nabila and Putra, 2020; Singh et al., 2020). To calculate the percentage of inhibition of *Candida albicans* (ATCC 14053) using the well diffusion technique, you can use the following formula Equation 1:

$$\text{Percentage of Inhibition} = \left(\frac{\text{D control} - \text{D sample}}{\text{D control}}\right) \times 100 \quad (1)$$

Where: D control is the diameter of the zone of inhibition for the control (no antifungal agent) and D sample is the diameter of the zone of inhibition for the sample (with antifungal agent).

2.6 Heavy metal removal by adsorption

The influence of the following experimental parameters on heavy metal removal was investigated: stirring time (from 0 to 70 min), pH (2-11), CaO NPs amount (from 5 to 40 mg per 100 mL), and temperature (25°C, 35°C, and 45°C). The desired pH values were obtained by NaOH and HCl solutions. For each test, a 50 mL solution containing metal ions (Pd^{2+}, Cr^{2+}, Cd^{2+}, Hg^{2+}) and a known quantity of CaO NPs (the adsorbent) was placed in a 100 mL beaker. The mixture was stirred with a continuous stream of air bubbles (as CO_2 source) at 250 rpm for a specific time to achieve the adsorption equilibrium and facilitate $CaCO_3$ formation at room temperature. At specific time points, the solutions were separated from the CaO NPs by filtration using Whatman filter papers. The removal efficiency (%) and adsorption capacity (mg/L) of the different metal ions was calculated using the following Equations 2, 3:

$$\text{Removal efficiency } (\%) = \left(\frac{(C_0 - C_e)}{C_0}\right) \times 100 \quad (2)$$

$$\text{Adsorption capacity } (\text{mg/L}) = \left(\frac{(C_0 - C_e) \times V}{m}\right) \quad (3)$$

where: C_0 is the initial concentration (ppm) of various metal ions, C_e represents the residual concentration (ppm) and V (L) is the solution volume of heavy metal ions, m (g) is the mass of the CaO NPs.

3 Results and discussion

3.1 Morphological and elemental composition

CaO NPs were synthesized from chicken eggshells (Figure 1) by thermal calcination at 700°C for 7 h to obtain the complete decomposition of $CaCO_3$ and organic matters present in the eggshells (Kumari et al., 2023). High-resolution SEM imaging provides crucial insights into the morphology and size distribution of the CaO NPs, allowing for an assessment of the uniformity and quality of the synthesis process. FE-SEM analysis of the CaO NPs revealed a consistently spherical morphology with diameters ranging from 5 to 30 nm (Figure 2). These observations are consistent with findings from (Khine et al., 2022; Kamran et al., 2023), who also reported spherical CaO NPs within similar size ranges. The uniform spherical shape indicates a well-controlled synthesis process and supports the reproducibility of the nanoparticle formation technique used.

SEM-EDX enhances SEM by providing elemental analysis, confirming the presence and relative abundance of key elements in the CaO NPs. EDX identified oxygen (O) and calcium (Ca) in CaO (Figure 2C), with atomic percentages of 47.75% for O and 52.25% for Ca, which correspond to weight percentages of approximately 26.73% for O and 73.27% for Ca. These values are close to the theoretical 1:1 atomic ratio for CaO. No other elements were detected beyond Ca and *O. Minor* carbon contamination, likely due to CaO's hygroscopic nature, which allows it to absorb water and CO_2 from the air, may affect the EDX analysis. Together, SEM and EDX analyses confirm the successful synthesis and appropriate composition of the CaO NPs, validating their potential effectiveness for various applications (Khine et al., 2022).

3.2 Crystalline structure

XRD diffraction patterns provides crucial insights into the polymorph and size distribution of the CaO NPs. XRD spectra (Figure 3) demonstrated the distinctive characteristics of CaO NPs. Prominent peaks were observed at 18.12°, 28.86°, 34.29°, 47.44°, 51.04°, 54.09°, 62.85°, 64.35°, 67.51°, and 71.92°, indicative of the presence of CaO NPs (JCPDS Card No. 00-037-1497). The Miller indices corresponding to these peaks are as follows: (111) for 18.12°, (200) for 28.86°, (211) for 34.29°, (220) for 47.44°, (310) for 51.04°, (222) for 54.09°, (400) for 62.85°, (331) for 64.35°, (420) for 67.51°, and (422) for 71.92°. These findings are in agreement with previous studies by Bharathiraja et al. (2018), Ramli et al. (2019), and Yazıcılar et al. (2021). The Debye–Scherrer equation, $D = k\lambda/\beta\cos\theta$, was used to estimate the average particle size, where D is the particle size (nm), λ is the wavelength of X-ray radiation (1.5406 Å), k is a constant (0.94), β is the full width at half maximum of the diffraction peak (FWHM), and θ is the Bragg's angle. The average particle size of the CaO NPs was estimated to be approximately 20 nm. This measurement of crystallite size supports the nanostructured nature of the material. Notably, this size is in good agreement with the particle diameters observed via FE-SEM, which ranged from 5 to 30 nm. The close match between the XRD-derived crystallite size and the SEM particle size suggests that the CaO NPs are likely single crystals or possess single-crystal characteristics. These findings highlight the successful production of high-quality CaO NPs, which is crucial for ensuring their effectiveness in various applications.

3.3 UV-vis spectra and bandgap

UV-Vis spectra were recorded for both grinded eggshells and CaO nanoparticles (CaO NPs) dispersed in water, spanning a wavelength range of 200–800 nm. Figure 4A shows the spectra before calcination (grinded eggshells) and after calcination (CaO NPs). The pre-combustion spectra of eggshells exhibit a peak from 250 nm extending to 200 nm, indicative of $CaCO_3$ and related to the electronic transitions and vibrational modes of carbonate ions (CO_3^{2-}). After calcination, the UV-Vis spectrum of CaO NPs in water shifts to start from 240 nm and extends to 200 nm, likely due to the formation of $Ca(OH)_2$. While bulk CaO has a large band gap and shows minimal UV-Vis absorption, dissolved $Ca(OH)_2$ can

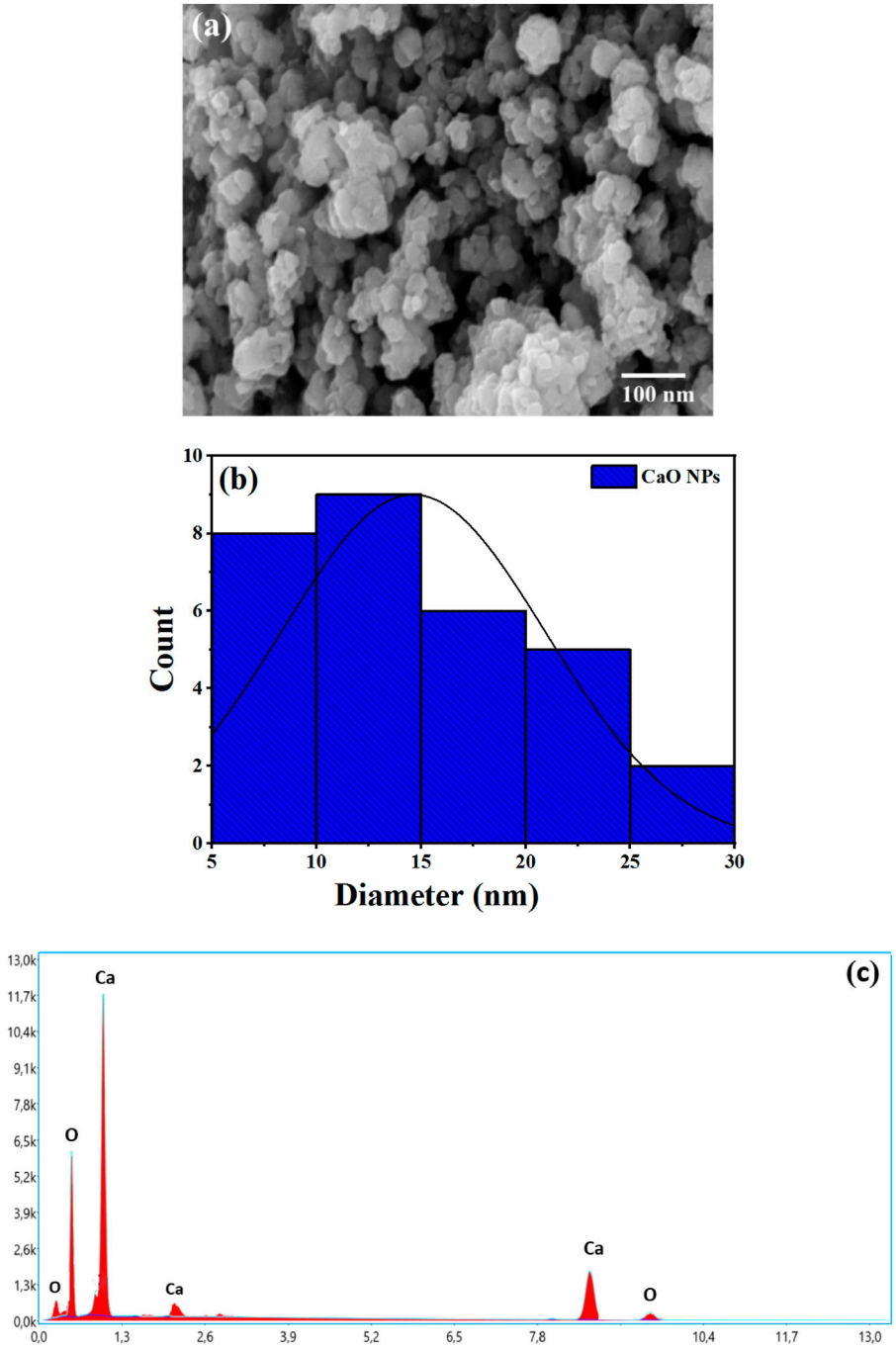

FIGURE 2
FE-SEM analysis of the CaO NPs synthesised from Eggshells: **(A)** SEM images; **(B)** particle size distribution estimated using ImageJ Software and **(C)** EDX analyses.

display weak absorption peaks around 200–240 nm. These observations align with studies by Ikram et al. (2022) and Butt et al. (2015). The bandgap energy of the synthesized CaO NPs (suspension in water) was calculated to be 4.7 eV, determined using the Tauc equation from the plot of $(hv)^2$ versus energy (eV), as shown in Figure 4B. This value is in agreement with previous studies, which report the photonic bandgap of CaO NPs ($CaO/Ca(OH)_4$ in water suspension) to be between 3.5 and 4.9 eV (Lalou and Kadari, 2019).

3.4 Chemical composition and bonding structure

The FTIR spectra before (eggshells) and after calcination (CaO NPs) (Figure 5A) showed that the eggshell sample exhibited a prominent peak at 1395 cm^{-1}, indicative of the high density of eggshell particles and a strong association with carbonate minerals (Carvalho et al., 2011). Additional peaks at ~705 and 874 cm^{-1} further confirmed the presence of $CaCO_3$, corresponding to the in-

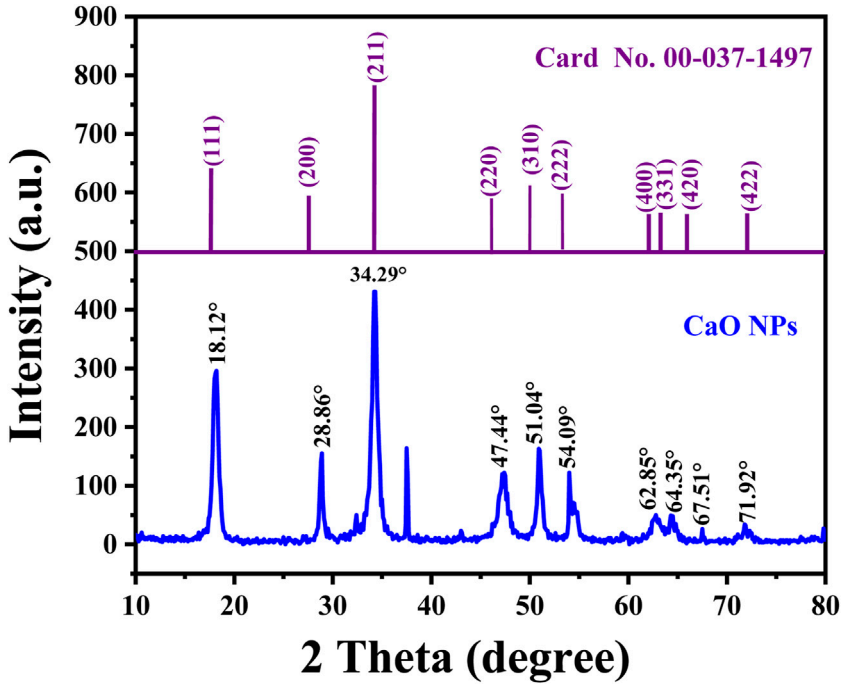

FIGURE 3
XRD patterns of CaO NPs synthesised from Egg shells.

plane and out-of-plane deformation modes (Carvalho et al., 2011). The presence of amines and amides in the eggshell membranes was highlighted by the significant peaks ranging from 3,051 to 3,552 cm^{-1}, 1661 cm^{-1}, and 1395 cm^{-1}, respectively (Carvalho et al., 2011). For CaO NPs, the peak detected at 3,637 cm^{-1} was attributed to the O–H free hydroxyl bond, likely resulting from residual hydroxide or moisture content in the sample (Amor et al., 2023). The sharpness of this peak suggests the formation of particles consisting of a single phase. The additional absorbance bands at ~1600 cm^{-1} and ~800 cm^{-1} confirmed the presence of residual OH groups (Maringgal et al., 2020). The formation of C-O bonds, attributed to CaO NP carbonation, was confirmed by the strong, wide band observed at 1480 cm^{-1} and a peak at 871 cm^{-1} (Atchudan et al., 2022). During calcination, CaO NPs react with air, leading to the generation of CO_2 and H_2O, which are subsequently absorbed onto the CaO surface as free–OH and carbonate species. This indicates the reactivity of surface–OH and lattice oxygen of CaO NPs due to the NP high surface area. Additionally, the minor dips observed in the spectra at 1733 cm^{-1} and 2,533 cm^{-1} were attributed to C–O stretch and CO_2 stretching, respectively (Cavia et al., 2002). The characteristic peak observed at 547 cm^{-1} indicated the Ca–O bond stretch, confirming the presence of chemical residues associated with CaO NP synthesis. Hence, the FTIR analysis provided valuable insights into the chemical composition and structural characteristics of eggshells and CaO NPs.

TGA was employed to analyze mass changes in CaO NPs as a function of temperature under controlled conditions (Figure 5B). A minimal weight reduction of 4.8% was observed in the temperature range of 356°C–385 °C. This weight loss is attributed to the hygroscopic nature of CaO, which absorbs moisture from the atmosphere, rather than the decomposition of residual $CaCO_3$ from the thermal treatment process. The decomposition of $CaCO_3$ typically occurs at temperatures above 550 °C (Barhoum et al., 2015). Since no additional weight loss was detected between 550°C and 700°C, it suggests that the carbonates present in the eggshells had already decomposed during calcination at 700 °C. This minimal mass change confirms the complete transformation of Ca-based materials in the eggshells into CaO, demonstrating the purity, thermal stability, and reliability of the synthesized CaO NPs for various applications.

3.5 Antibacterial activities

Figure 6 and Table 1 show the inhibition zones in the presence of eggshells or the synthesized CaO NPs. When eggshells were used, the inhibition zones against Gram-negative bacteria (*P. aeruginosa*, *K. pneumoniae*, and *E. coli*) increased with the eggshell concentration. For instance, at a concentration of 3 mg mL^{-1}, the inhibition zones ranged from 16 ± 0.2 mm to 17 ± 0.2 mm. Similarly, the inhibition zones against Gram-positive bacteria (*S. aureus*) increased with the eggshell concentration, ranging from 12 ± 0.1 mm to 15 ± 0.1 mm. In the presence of the synthesized CaO NPs, the inhibition zones generally were larger compared with eggshells. At a concentration of 3 mg mL^{-1}, the inhibition zones against Gram-negative bacteria ranged from 18 ± 0.2 mm to 20 ± 0.1 mm and those against Gram-positive bacteria ranged from 16 ± 0.1 mm to 19 ± 0.1 mm. These results indicate an enhancement of the antibacterial activity following the formation of CaO NPs. Comparison with the inhibitory effects of CIP-5 (50 µg) showed that the synthesized CaO NPs exhibited comparable or superior antibacterial activity. Significant differences ($p < 0.05$) were detected

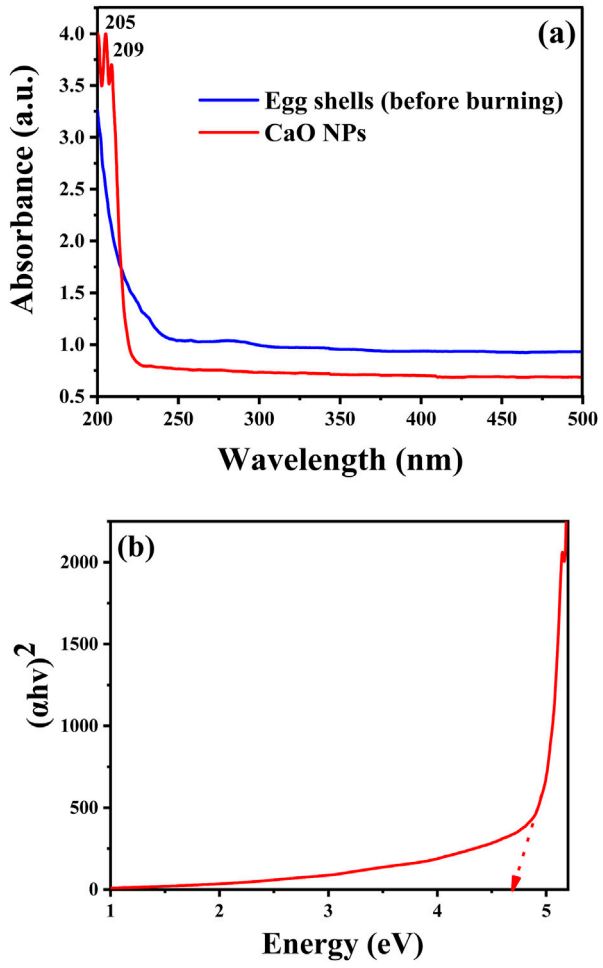

FIGURE 4
Optical properties of eggshells before calcination and the synthesised CaO NPs: **(A)** UV-vis spectra and **(B)** Optical energy bandgap of CaO NPs.

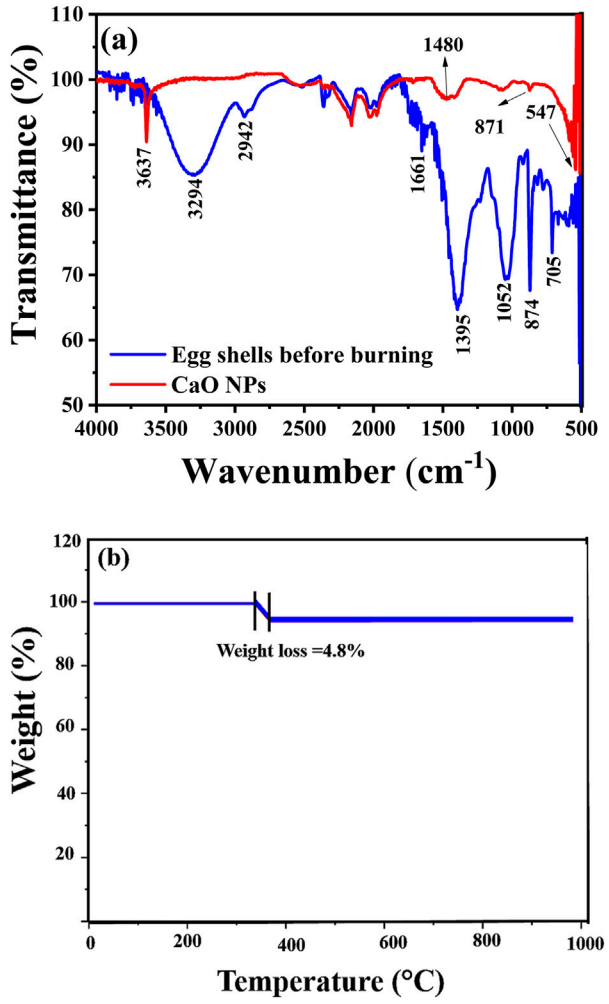

FIGURE 5
Composition of eggshells before calcination and the synthesised CaO NPs: **(A)** FTIR spectra and **(B)** TGA curve of CaO NPs.

between the inhibition zones of different bacterial strains at varying concentrations of CaO NPs. The antibacterial efficacy of the synthesized CaO NPs was statistically superior to that of the raw eggshells across all tested bacterial strains, confirming the enhanced antimicrobial properties of the CaO NPs. For instance, against *P. aeruginosa*, the inhibition zones of CaO NPs (3 mg mL^{-1}) and CIP-5 were 18 ± 0.2 mm and 20 ± 0.1 mm, respectively. These findings are in line with those of previous studies (Alobaidi et al., 2022; Anantharaman et al., 2016; Zaater et al., 2024).

Mina et al. (Carvalho et al., 2011) previously reported an inhibition zone of 15.24 mm for CaO NPs against *E. coli*. Similarly, Alobaidi et al. (2022) observed a positive correlation between CaO NP concentration and inhibition zone diameters, with the largest diameter occurring at 560 µg/mL of CaO NPs against both *S. aureus* and *E. coli*. In various studies, the antimicrobial effectiveness of different materials was assessed against multiple bacterial strains. Chicken eggshells demonstrated a zone of inhibition of 12 mm against *E. coli* (Ismael et al., 2024), and 26.33 mm against *P. aeruginosa* and 33 mm against *E. coli* in another study (Alsohaimi et al., 2020). Carica fruit showed broad-spectrum activity with inhibition zones ranging from 11 to 28 mm across five bacterial species ((Khan et al., 2023). $CaCl_2{\cdot}H_2O$ demonstrated a 28 mm inhibition zone against *E. coli* (Kumar et al., 2021). Shrimp shells and $CaCO_3$ both inhibited *S. aureus* and *E. coli* with inhibition zones of 17–19 mm (Gedda et al., 2015).

In the present study, the antibacterial effectiveness of eggshells and CaO NPs against bacterial strains was compared with that of CaO NPs synthesized using different materials (Table 2).

The enhanced antibacterial activity of CaO NPs compared with eggshells can be attributed to several factors. First, CaO NP synthesis involves the transformation of $CaCO_3$ (present in eggshells) into CaO, resulting in NPs with increased surface area and reactivity. The increased surface area-to-volume ratio of CaO NPs promotes their interaction with bacterial membranes, facilitating their disruption and compromising their integrity, ultimately leading to bacterial cell death. Additionally, upon contact with bacterial cells, CaO NPs can generate reactive oxygen species (ROS) that induce oxidative stress and cause damage to essential biomolecules, further contributing to their antibacterial activity. The alkaline pH environment created by CaO NPs upon dissolution in water disrupts the bacterial homeostasis and metabolic processes, inhibiting bacterial growth

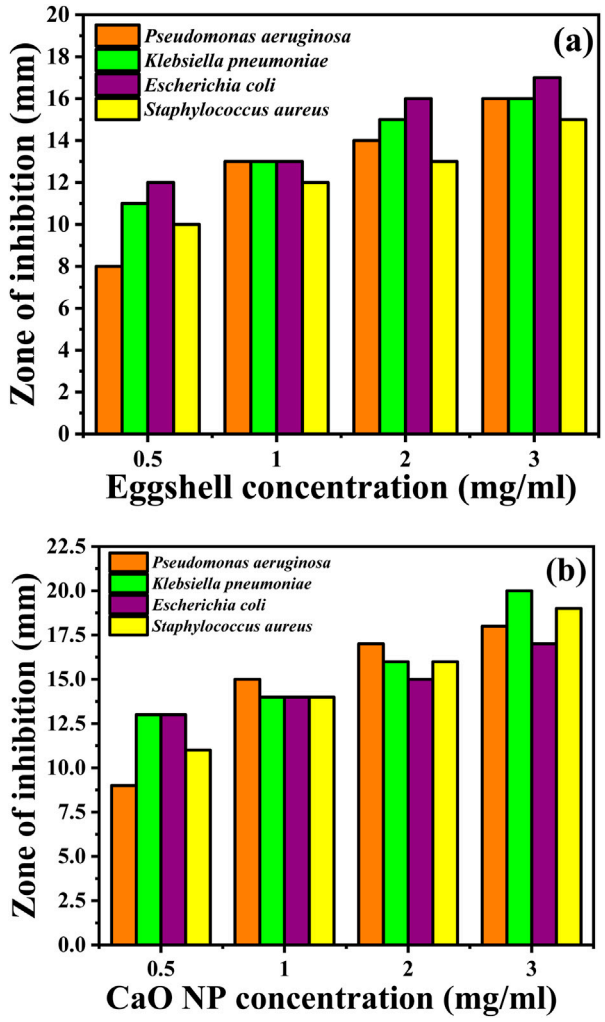

FIGURE 6
Antibacterial activity against the indicated bacteria of **(A)** Eggshells before calcination and **(B)** synthesised CaO NPs.

and survival. Overall, the transformation of eggshells into CaO NPs resulted in NPs with superior antibacterial properties due to their enhanced surface area, reactivity, and ability to generate ROS, making them more effective against a wide range of pathogens.

3.6 Antifungal activity

Percentages of inhibition of *C. albicans* are calculated by comparing the diameter of the inhibition zone (mm) for the control and the sample (mm) using the Agar well diffusion method. Both eggshells and CaO NPs exhibited significant inhibitory effect on *C. albicans* growth after 8 days of incubation (Figures 7A, B; Table 2). Eggshells showed inhibition percentages ranging from 10% to 33% at various concentrations and time points. Higher concentrations led to higher inhibition over time. CaO NPs displayed dose-dependent and time-dependent inhibition of *C. albicans* growth, with inhibition percentages ranging from 15% to 86% across different concentrations and time intervals. CaO NP antifungal activity was higher than that of eggshells, particularly at higher concentrations and longer incubation periods.

The mechanism of *C. albicans* growth inhibition by eggshells and CaO NPs involves several factors (Garcia-Rubio et al., 2020; Han et al., 2023). Eggshells contain $CaCO_3$ that has alkaline properties. The alkaline environment resulting from $CaCO_3$ dissolution disrupts the fungal cell membrane, inhibiting *C. albicans* growth. Additionally, eggshells contain chitinase enzymes that can degrade chitin, a crucial component of fungal cell walls, further compromising *C. albicans* cell integrity. CaO NPs exert antifungal effects through multiple mechanisms. First, CaO NPs have a high surface area-to-volume ratio that facilitates the interaction with the fungal cell membranes, leading to disruption of the lipid bilayer structure and membrane integrity. This is followed by leakage of essential cellular components, leading to fungal cell lysis and death. Second, CaO NPs can generate ROS, such as superoxide radicals (O2•-) and hydroxyl radicals (•OH), upon contact with fungal cells, inducing oxidative stress that damages proteins, DNA, and other essential biomolecules for *C. albicans* survival (Abdal Dayem et al., 2017). Therefore, oxidative stress contributes to inhibiting fungal growth and proliferation.

4 Heavy metal adsorption

Eggshells, primarily composed of $CaCO_3$, have been explored as potential adsorbents for heavy metal removal. However, their effectiveness is limited by several factors. The natural structure of eggshells necessitates extensive grinding to increase surface area and enhance adsorption capacity. Even with such processing, eggshells generally exhibit lower efficiency as adsorbents compared to like CaO NPs. Additionally, the use of eggshells carries the risk of introducing contaminants, such as proteins and other organic waste residues, into the water, which can further complicate the treatment process. The synthesized CaO NPs are highly effective in removing heavy metals such as Pb^{2+}, Cr^{2+}, Cd^{2+}, and Hg^{2+} from water sources due to various adsorption mechanisms including surface complexation, ion exchange, physical adsorption, and precipitation (Alibrahimi and Toamah, 2019; Eddy et al., 2024; Kasirajan et al., 2022). These mechanisms involve distinct chemical interactions and surface properties, which contribute to the efficiency of the adsorption process (see Figure 8).

(1) *Surface Complexation*: Surface complexation occurs when heavy metal ions interact with reactive sites on the CaO NPs surface, such as hydroxyl groups (-OH) or oxygen atoms (-O-). This mechanism can be divided into inner-sphere and outer-sphere complexation. Inner-sphere complexation involves the direct coordination of metal ions to surface groups, forming strong chemical bonds. For example, lead ions (Pb^{2+}) can form inner-sphere complexes with hydroxyl groups on the CaO surface, resulting in the formation of lead (II) hydroxide ($Pb(OH)_2$), which precipitates out of the solution. This reaction is characterized by a high stability constant (log K ~ 6) for the formation of these complexes, indicating strong binding. Outer-sphere complexation, on the other hand, involves weaker electrostatic interactions where water molecules

TABLE 1 Inhibition zones in the presence of eggshells or CaO NPs; the inhibition zone value is the mean value obtained from three separate experiments conducted independently.

Sample	Conc	Zone of inhibition (mm)			
		Gram-negative			Gram-positive
		Pseudomonas aeruginosa	*Klebsiella pneumoniae*	*Escherichia coli*	*Staphylococcus aureus*
Eggshells before burning[a]	0.5 mg mL^{-1}	8 ± 0.2	11 ± 0.1	12 ± 0.1	10 ± 0.1
	1 mg mL^{-1}	13 ± 0.1	13 ± 0.2	13 ± 0.1	12 ± 0.1
	2 mg mL^{-1}	14 ± 0.1	15 ± 0.15	16 ± 0.2	13 ± 0.1
	3 mg mL^{-1}	16 ± 0.2	16 ± 0.1	17 ± 0.2	15 ± 0.1
Eggshells after burning (CaO NPs)[a]	0.5 mg mL^{-1}	9 ± 0.2	13 ± 0.1	13 ± 0.1	11 ± 0.1
	1 mg mL^{-1}	15 ± 0.1	14 ± 0.2	14 ± 0.1	14 ± 0.1
	2 mg mL^{-1}	17 ± 0.1	16 ± 0.2	15 ± 0.2	16 ± 0.1
	3 mg mL^{-1}	18 ± 0.2	20 ± 0.1	17 ± 0.2	19 ± 0.1
Ciprofloxacin	50 µg	20 ± 0.1	22 ± 0.2	19 ± 0.2	21 ± 0.2

[a]DMSO, had no effect on the inhibition zone or antibacterial activity of eggshells and CaO NPs.

TABLE 2 Percentage of *Candida albicans* growth inhibition after incubation with eggshells, CaO NPs at different concentrations, compared to the control (100% growth), for up to 8 days, calculated using the well diffusion technique.

Sample concentration		72 h	96 h	120 h	144 h	168 h	192 h
Eggshells	1 wt%	10	13	18	24	28	33
	5 wt%	19	24	31	37	40	45
	10 wt%	33	54	65	73	76	80
CaO NPs	1 wt%	15	18	23	27	33	42
	5 wt%	23	29	35	39	49	51
	10 wt%	41	60	68	75	81	86

remain between the metal ion and the surface, resulting in less stable adsorption. The small particle size, and high density of reactive sites on CaO NPs enhance these interactions.

(2) Ion Exchange: In ion exchange, metal ions in the aqueous solution replace Ca^{2+} ions on the CaO nanoparticle surface. Heavy metal ions such as Pb^{2+}, Cr^{2+}, Cd^{2+}, and Hg^{2+} can exchange with Ca^{2+} due to their similar ionic radii and charge densities. For instance, Cd^{2+} can effectively replace Ca^{2+} ions on the CaO surface due to their comparable size (Cd^{2+} radius ~0.95 Å vs. Ca^{2+} radius ~1.00 Å) and charge density. The ion exchange process is characterized by a high selectivity for metal ions, with values of selectivity coefficients indicating how favorably different metal ions are exchanged. This mechanism can be particularly effective in removing toxic heavy metals from aqueous solutions, with exchange capacities varying from 1.5 to 3.0 mmol/g depending on the metal ion and CaO surface properties.

(3) Physical Adsorption: Physical adsorption involves the adherence of heavy metal ions to the CaO NP surface through weak van der Waals forces and electrostatic interactions. The small particle size and high surface area of CaO NPs enhance this process by providing more active sites for adsorption. For instance, Pb^{2+}, Cr^{2+}, Cd^{2+}, and Hg^{2+} adhere to the surface of CaO through non-specific interactions. The process is typically reversible due to the weak nature of van der Waals forces, with the adsorption capacity being sensitive to temperature changes.

(4) Precipitation: During precipitation, CaO NPs react with metal ions in the solution to form insoluble metal hydroxides or carbonates. For example, metal ions such as Pb^{2+}, Cr^{2+}, Cd^{2+}, and Hg^{2+} can react with hydroxide ions (OH^-) in the solution to form metal hydroxides like $Pb(OH)_2$, chromium (III) $Cr(OH)_3$, $Cd(OH)_2$, and $Hg(OH)_2$, which precipitate out of the water. Additionally, metal ions can react with carbonate ions (CO_3^{2-}), if present, to form metal carbonates such as $PbCO_3$, $Cr_2(CO_3)$, $CdCO_3$, and $HgCO_3$, which also precipitate and remove the metals from the solution (Kasirajan et al., 2022). The formation of these precipitates is driven by the low solubility products (Ksp) of these compounds. For instance, the solubility product of $Pb(OH)_2$is very low (Ksp ~1.2×10^{-15}), leading to significant precipitation and removal of Pd^{2+} ions from the solution. Similarly, $CdCO_3$ has a low solubility

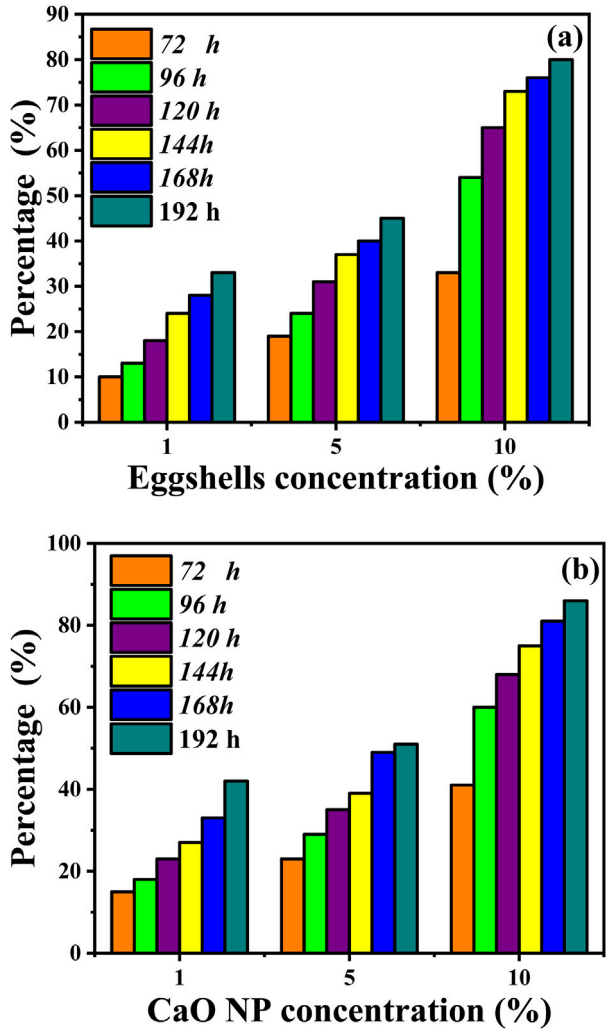

FIGURE 7
Percentage of *Candida albicans* growth inhibition after incubation with eggshells (before calcination) and synthesized CaO NPs, compared to the control (100% growth). Inhibition was measured using the well diffusion technique based on the diameter of the inhibition zone (mm).

product (Ksp ~8.3 × 10^{-12}), facilitating effective removal of Cd^{2+} ions.

After removal of heavy metals, techniques such as sedimentation, filtration, and centrifugation are employed to separate and remove the metal precipitates from the solution (Banković–Ilić et al., 2017). The residual metal hydroxides and carbonates can be repurposed in industrial applications, such as the production of construction materials. For CaO NPs, regeneration methods like acid washing or thermal regeneration are used to restore the nanoparticles for reuse. Acid washing removes adsorbed metals, while thermal regeneration involves heating the nanoparticles to release the metals. Residual substances, such as metal hydroxides and carbonates, can be incorporated into other processes, thus enhancing sustainability and minimizing environmental impact (Velempini et al., 2023).

4.1 Effect of pH on heavy metal adsorption

Figure 9 illustrates the strong dependence of metal ion adsorption by CaO NPs on the pH of the solution, which affects both the adsorbent's surface properties and the metal ion distribution (Supplementary Tables S1, S2 in Supplementary Material). In the experiment, 30 mg of CaO NPs were exposed to 10 ppm solutions of Pb^{2+}, Cr^{2+}, Cd^{2+}, or Hg^{2+} across a pH range from 2 to 11, with the solutions stirred for 30 min to ensure effective interaction between the adsorbent and the metal ions. The results show that the highest removal efficiency and adsorption capacity were achieved at pH 6 or higher. Specifically, at pH 6, the adsorption capacities were 14.5 mg/L for Cd^{2+}, 13.83 mg/L for Pb^{2+}, 14.5 mg/L for Cr^{2+}, and 13.83 mg/L for Hg^{2+}, with removal efficiencies of 94% for Cd^{2+}, 91% for Pb^{2+}, 89% for Cr^{2+}, and 83% for Hg^{2+}. Conversely, at pH levels below 6, there was a noticeable decline in both removal efficiency and adsorption capacity. For instance, at pH 2, the removal efficiencies were significantly lower: 6.83% for Cd^{2+}, 6.5% for Pb^{2+}, 6.83% for Cr^{2+}, and just 2.33% for Hg^{2+}, with adsorption capacities of 8.67 mg/L for Cd^{2+}, 6.5 mg/L for Pb^{2+}, 6.5 mg/L for Cr^{2+}, and 2.33 mg/L for Hg^{2+}.

The observed differences in metal ion removal efficiency can be attributed to the varying chemical properties of the metal ions and their interactions with the sorbent surface. Mercury (Hg^{2+}) shows lower removal efficiency compared to other ions due to its relatively low electronegativity and larger atomic size, which result in weaker interactions with the sorbent. In contrast, Cr^{2+}, Pb^{2+}, and Cd^{2+}, with their higher electronegativity and smaller atomic sizes, exhibit stronger interactions and thus higher removal efficiencies. Additionally, the speciation and complexation behavior of these ions in aqueous solutions influence their adsorption. For example, Cr and Pb form stable complexes with ligands, enhancing their adsorption, while Cd ions form hydroxyl complexes at higher pH, improving their removal efficiency relative to Hg^{2+}. The removal efficiency decreases in very acidic environments due to increased H^+ ion concentration, which makes the sorbent surface more positively charged and weakens the attraction between the sorbent and metal ions. As pH increases, especially in the range of 6–11, the concentration of H_3O^+ ions decreases, making the CaO NPs surface more negatively charged and available for metal ion binding. At pH values above 8, the removal efficiency remains relatively constant, indicating that pH 6 is optimal for maximizing metal ion uptake. (Cruz-Lopes et al., 2021; Mnasri-Ghnimi and Frini-Srasra, 2019).

4.2 Effect of reaction time on heavy metal adsorption

Figure 10 illustrates the effect of reaction time on the removal of Pb^{2+}, Cd^{2+}, Cr^{2+}, and Hg^{2+} by CaO NPs, showing both recovery

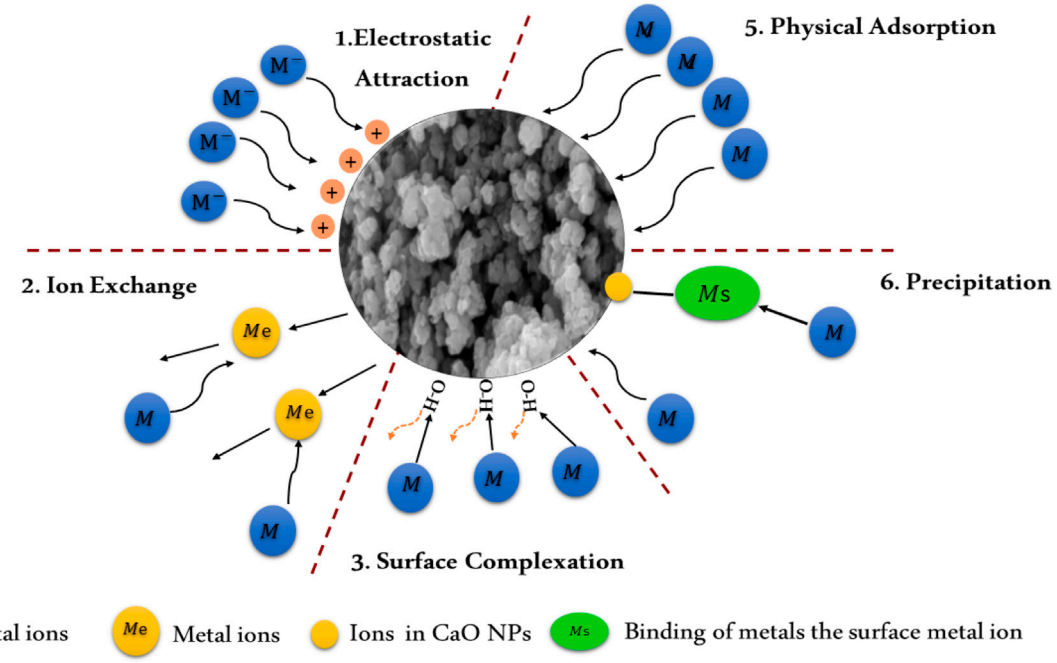

FIGURE 8
Mechanisms of interaction of metal ions with CaO NPs, including surface complexation, ion exchange, physical adsorption, and precipitation, illustrating the removal of heavy metals from aqueous solutions.

percentages and adsorption capacities over various intervals (Supplementary Tables S1, S2 in Supplementary Material). At time zero, no metal ion recovery was observed. After 5 min, the adsorption capacities were 9.17 mg/L for Pb^{2+} and 9 mg/L for Cd^{2+}, while Cr^{2+} and Hg^{2+} had lower capacities of 8 mg/L and 6.33 mg/L, respectively. At 30 min, recoveries had improved significantly, with Pb^{2+} and Cd^{2+} showing adsorption capacities of 16.17 mg/L and 15.67 mg/L, while Cr^{2+} and Hg^{2+} were 15.67 mg/L and 15.17 mg/L. Recovery rates continued to increase, reaching 98% for Pb^{2+} and 97% for Cd^{2+} at 50 min, with adsorption capacities of 16.33 mg/L and 15.83 mg/L, respectively. By 70 min, the maximum recoveries were achieved: 99% for Pb^{2+} and Cr^{2+}, 98% for Cd^{2+}, and 99% for Hg^{2+}, corresponding to the highest adsorption capacities of 16.5 mg/L for Pb^{2+}, 16 mg/L for Cd^{2+}, 16.5 mg/L for Cr^{2+}, and 16.5 mg/L for Hg^{2+}.

These results indicate that extending the reaction time enhances the adsorption efficiency of CaO NPs, allowing for near-complete removal of heavy metal ions. Pb^{2+} and Cr^{2+} achieve higher removal percentages more quickly than Cd^{2+} and Hg^{2+}, reflecting their stronger affinity for the CaO NPs. This rapid saturation is attributed to their smaller ionic radii and higher charge densities, which increase their interactions with the CaO NPs surface. Consequently, Pb^{2+} and Cr^{2+} form more effective bonds, leading to faster binding and higher removal rates. In contrast, Hg^{2+}, although capable of reaching high removal percentages over extended periods, consistently exhibits lower adsorption capacities due to its larger atomic size and lower charge density. This results in weaker interactions with the CaO NPs, requiring more time for Hg^{2+} to approach its maximum removal capacity. These differences highlight how variations in ionic size and charge density influence the rate and effectiveness of metal ion removal (Raji et al., 2023).

4.3 Effect of the adsorbent concentration on heavy metal adsorption

Figure 11 illustrates the impact of CaO NPs concentration on the removal of various metal ions using CaO NPs (Supplementary Tables S1, S2 in Supplementary Material). As the CaO NPs concentration increases, removal efficiency percentages for Pb^{2+}, Cd^{2+}, Cr^{2+}, and Hg^{2+} also rise. At an adsorbent concentration of 5 mg, the removal percentages were 74% for Pb^{2+}, 71% for Cd^{2+}, 70% for Cr^{2+}, and 64% for Hg^{2+}, with corresponding adsorption capacities of 6.83 mg/L for Pb^{2+}, 8.67 mg/L for Cd^{2+}, 6.5 mg/L for Cr^{2+}, and 2.33 mg/L for Hg^{2+}. Increasing the CaO NPs concentration to 30 mg resulted in notable improvements, with removal efficiencies reaching 98% for Pb^{2+} (adsorption capacity of 16.33 mg/L) and Cd^{2+} (16.5 mg/L), and 97% for Cr^{2+} (16.5 mg/L) and Hg^{2+} (16.5 mg/L). However, further increasing the CaO NPs concentration to 40 mg did not significantly enhance the removal efficiency, as the percentages plateaued at 98% for all metal ions. This plateau suggests that, beyond a certain concentration, additional CaO NPs does not lead to significant improvements in removal efficiency, likely due to the saturation of available adsorption sites on the CaO NPs (Hashem et al., 2024).

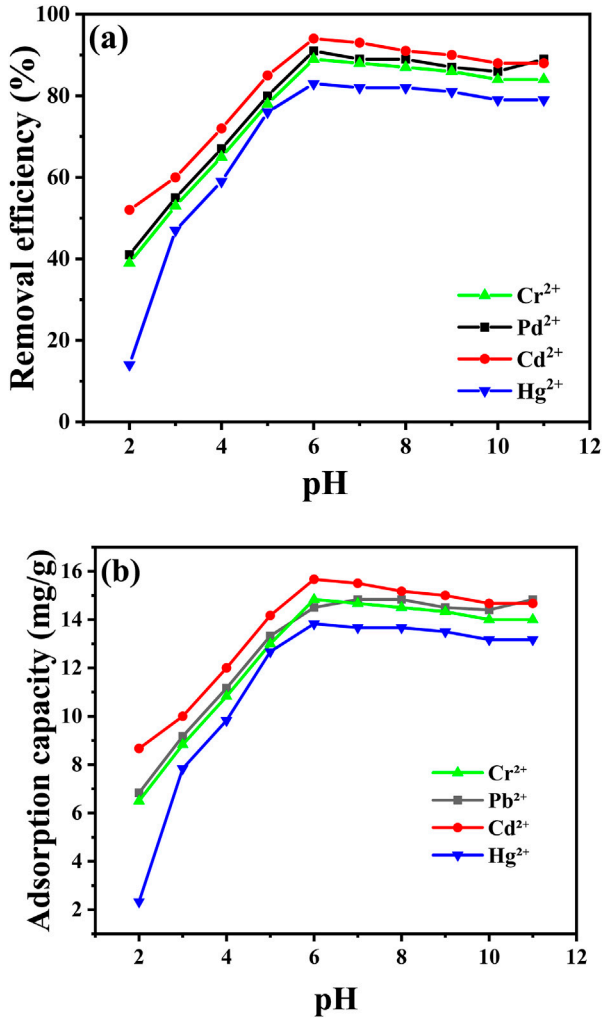

FIGURE 9
Impact of pH (2-11) on removal efficiency **(A)** and adsorption capacity **(B)** of the indicated metal ions at the adjusted conditions (30 min, 25°C, 10 ppm metal ions, 50 mL volume).

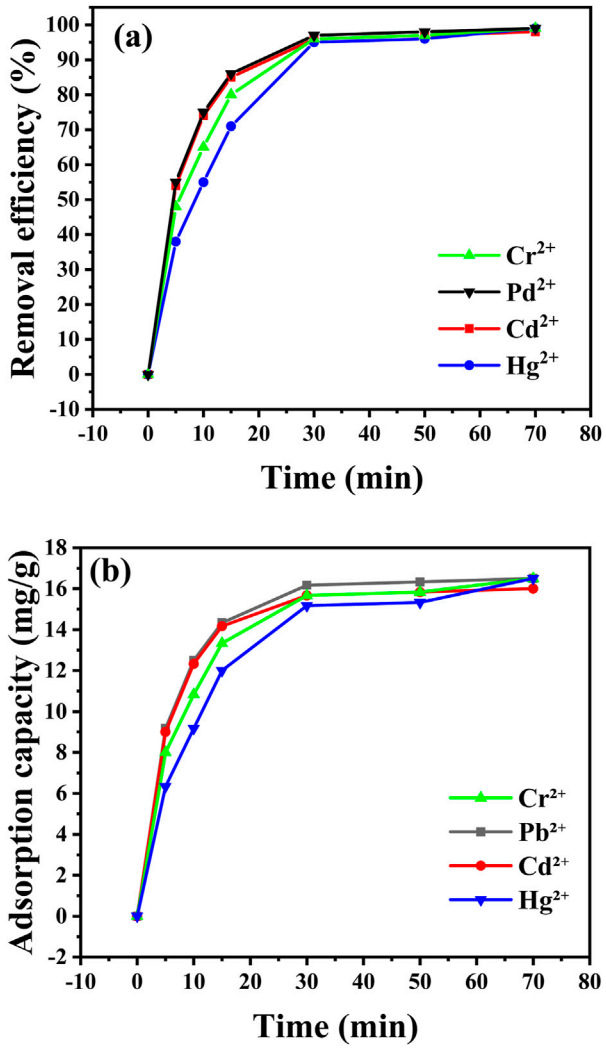

FIGURE 10
Impact of stirring time (from 0 to 70 min) on removal efficiency **(A)** and adsorption capacity **(B)** of the indicated metal ions at conditions (30 mg CaO NPs, pH = 6, 25°C, 10 ppm metal ions, 50 mL volume).

4.4 Effect of temperature on heavy metal adsorption

Effect of temperature on heavy metal adsorption is a critical factor influencing the efficiency of metal ion removal by adsorbents such as CaO NPs. As shown in Figure 12, the removal percentages of Pb^{2+}, Cd^{2+}, Cr^{2+}, and Hg^{2+} by CaO NPs increase with temperature, reaching their maximum values at 45°C (Supplementary Tables S1, S2 in Supplementary Material). At 25°C, the removal rates are 98% for Pb^{2+}, 96% for Cd^{2+}, 97% for Cr^{2+}, and 95% for Hg^{2+}, corresponding to adsorption capacities of approximately 7.8 mg/g, 7.6 mg/g, 7.7 mg/g, and 7.5 mg/g, respectively. The highest removal rates are observed at 45°C, with Pb^{2+}, Cd^{2+}, Cr^{2+}, and Hg^{2+} achieving 99.8%, 99.7%, 99.8%, and 99.5%, respectively, leading to slightly increased adsorption capacities of around 7.9 mg/g for Pb^{2+} and Cr^{2+}, and 7.8 mg/g for Cd^{2+} and Hg^{2+}. The increase in removal efficiency with temperature can be explained by the enhanced kinetics of adsorption and increased mobility of metal ions at higher temperatures. Elevated temperatures typically increase the diffusion rate of metal ions towards the adsorbent surface and can also strengthen the interaction between metal ions and the adsorbent by providing the energy necessary to overcome activation barriers (Kubilay et al., 2007). However, excessively high temperatures might lead to potential desorption of adsorbed metal ions or damage to the adsorbent structure, as noted in various studies (Raji et al., 2023).

The results of these experiments indicate that the conditions for optimal removal of Pb^{2+}, Cr^{2+}, Cd^{2+}, and Hg^{2+}, as summarized in Supplementary Table S1 (supplementary), provide a clear balance between efficiency and practicality. For effective recovery with practical efficiency, 30 min at pH 6 with 40 mg of CaO NPs at 25°C offers a highly effective solution. Under these conditions, the removal rates are 98% for Pb^{2+}, 97% for Cd^{2+}, 97% for Cr^{2+}, and 97% for Hg^{2+}, with corresponding adsorption capacities of approximately 7.84 mg/g for Pb^{2+}, 7.76 mg/g for Cd^{2+}, 7.78 mg/g for Cr^{2+}, and 7.75 mg/g for Hg^{2+}. This approach balances practical

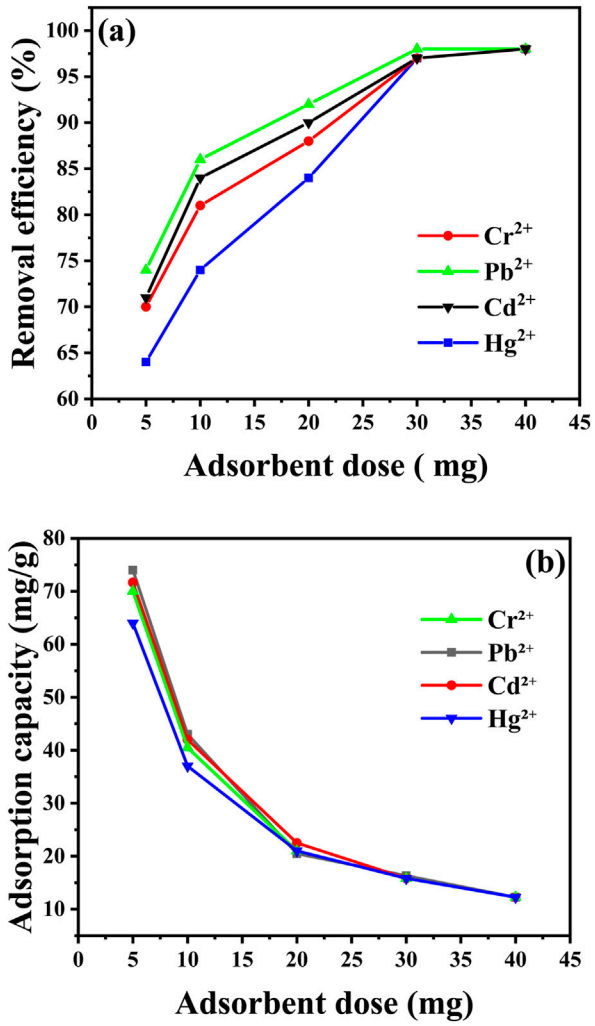

FIGURE 11
Impact of the adsorbent dose (from 5 to 40 mg) on removal efficiency **(A)** and adsorption capacity **(B)** of various metal ions at adjusted conditions (30 min, pH = 6, 25°C, 10 ppm metal ions, 50 mL volume).

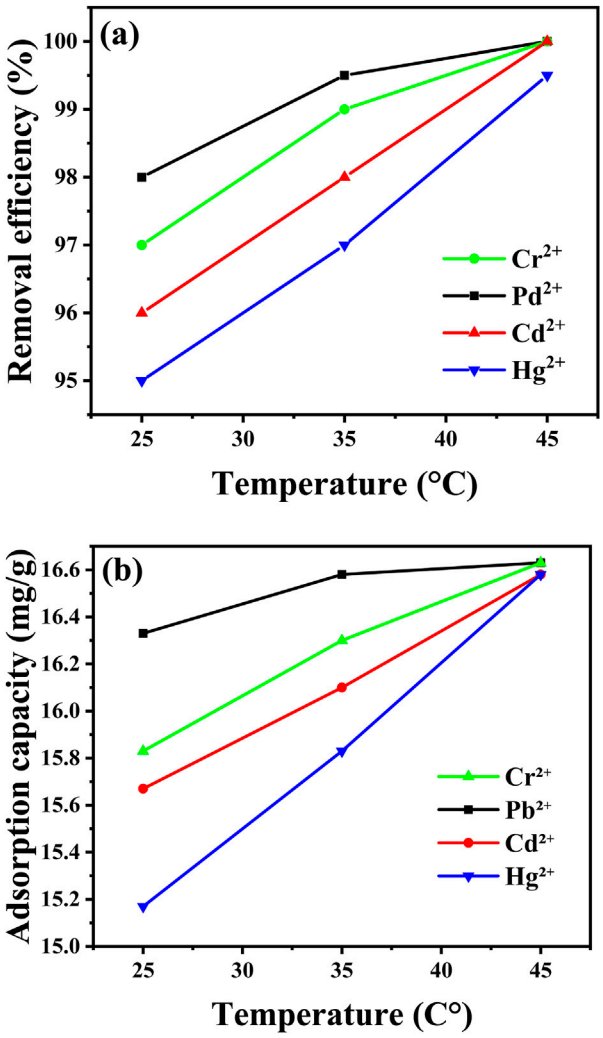

FIGURE 12
Effect of temperature (25°C, 35°C, and 45°C) on removal efficiency **(A)** and adsorption capacity **(B)** of the indicated metal ions at conditions (pH = 6, 10 ppm metal ions, 30 mg of CaO NPs).

considerations of time and cost while delivering substantial metal ion removal. Conversely, if near-complete removal is critical and time or cost is less of a concern, extending the process to 70 min at pH 6 with 40 mg of CaO NPs at 45°C yields the highest removal rates: 99% for Pb^{2+}, 98% for Cd^{2+}, 99% for Cr^{2+}, and 99% for Hg^{2+}, with slightly higher adsorption capacities of around 7.88 mg/g for Pb^{2+}, 7.80 mg/g for Cd^{2+}, 7.82 mg/g for Cr^{2+}, and 7.79 mg/g for Hg^{2+}. While this extended condition achieves nearly complete removal, it involves increased energy consumption and operational costs.

Comparison of the efficacy of CaO NPs derived from different sources (eggshells, $CaCl_2$, and periwinkle shells) for removing various heavy metal ions from aqueous solutions (Table 3) showed that the obtained CaO NPs displayed unique characteristics in terms of size and shape. For instance, CaO NPs derived from eggshells had a crystalline size of 24.34 nm and a spongy appearance, while those from $CaCl_2$ had irregular shapes with a size <100 nm. Similarly, the absorption conditions (pH, stirring time, temperature, and adsorbent dosage) varied among studies. The results show high removal efficiencies of different heavy metal ions (e.g., cadmium, lead, cobalt, and mercury) in specific conditions. The high removal rate (99% using the optimal conditions) obtained with CaO NPs derived from eggshells highlighted their effectiveness in mild conditions. These findings provide valuable insights for the development of efficient and environmentally friendly methods for heavy metal ion removal from aqueous solutions.

5 Conclusion

This study highlights the potential of utilizing chicken eggshells, a common and sustainable waste product, for the eco-friendly synthesis of calcium oxide nanoparticles (CaO NPs). By calcining eggshells at 700°C, we successfully produced spherical, single-crystal CaO NPs with diameters ranging from 5 to 30 nm and a bandgap energy of approximately 4.7 eV. These nanoparticles were thoroughly

TABLE 3 Comparative analysis of metal ion removal using CaO NPs obtained using different CaO sources.

CaO source	CaO NP size and shape	Adsorption conditions	Heavy metal removal	References
Eggshells	24.34 nm	Heavy metal (35, 55 and 75 ppm CdII), volume of 100 mL, (0.25, 0.5, 0.75 and 1.25 g) adsorbent dose, pH (3-9), and time 30 min	99.1% removal achieved at initial 55 ppm Cd (II), pH 7, time of 50 min, 0.75 g adsorbent	Muleta et al. (2024)
$CaCl_2$	Irregular shapes with a size <100 nm	Heavy metal of 10 ppm (Hg2+,Cr2+), volume of 100 mL, 30 g adsorbent dose, pH (2-10), temperature of (64.85, 44.85, 24.85°C and 9.85°C), and time of 5–50 min	100% of Hg^{2+} and Cr^{2+} removal was achieved at an initial 30 mg adsorbent, 30 min stirring, ≈338°C, and pH 7	Toamah and Fadhil (2019)
Eggshells	Crystalline size of 24.34 nm, with a spongy and foamy appearance	Heavy metal of 60–120 ppm Pb-II, volume of xx mL, (0.5, 0.75 and 1 g) adsorbent dose, pH (3-9), and time of 45, 75, and 105 min	99.07% Pd removal was achieved at the initial concentration of 75.46 ppm Pd (II), pH 6.94, 0.838 g adsorbent, and time of 101.97 min	Kasirajan et al. (2022)
$CaCl_2$	Particle size <100 nm	Heavy metal 50–350 ppm Co(II), volume of 100 mL, 0.05 mg adsorbent dose, pH 2-10, temperature of 5, 25, 45°C and 65°C, and time 30 min	99% Co(II) removal was achieved at 50 ppm Co(II), 0.05 mg adsorbent, 30 min, pH 7, and 25°C	Alibrahimi and Toamah (2019)
Periwinkle shells	Crystallite size 18 nm	Heavy metal of 250 ppm Pb2+, volume of 100mL, 0.5 g adsorbent dose, temperature of 45°C, and time of 75 min	80% Pb^{2+} removal achieved at 250 ppm, 0.5 g adsorbent, 75 min and 45°C	Eddy et al. (2024)
Eggshells	Size = 20 nm and spherical morphology	Heavy metal of 60–120 ppm ($Pb2^+$, $Cr2^+$, $Cd2^+$, and $Hg2^+$), volume of 100 mL, (5–40 mg per 100 mL) adsorbent dose, pH (2–11), temperature of 25°C, 35°C and 45°C, and time of 0–70 min	99% for Pb^{2+}, 98% for Cd^{2+}, 99% for Cr^{2+}, and 99% for Hg^{2+} removal achieved at 40 mg adsorbent, 70 min, pH = 6, and 45°C	This study

characterized, demonstrating significant antibacterial activity against *S. aureus*, *K. pneumoniae*, and *E. coli*, as well as effective inhibition of *Candida* albicans. The CaO NPs also exhibited considerable promise in environmental applications, particularly for the removal of heavy metal ions from aqueous solutions. The optimization of key variables—pH, contact time, adsorbent dose, and temperature—revealed that the optimal conditions for metal ion removal were at pH 6, with a contact time of 30 min, 40 mg of CaO NPs, and 25°C. This configuration achieved recovery rates of 98% for Pb^{2+}, 97% for Cd^{2+}, 97% for Cr^{2+}, and 97% for Hg^{2+}, with corresponding adsorption capacities of 16.17 mg/L for Pb^{2+}, 15.67 mg/L for Cd^{2+}, 15.67 mg/L for Cr^{2+}, and 15.17 mg/L for Hg^{2+}. For near-complete removal, extending the process to 70 min at pH 6°C and 45°C resulted in the highest recovery rates: 99% for Pb^{2+}, 98% for Cd^{2+}, 99% for Cr^{2+}, and 99% for Hg^{2+}, with enhanced adsorption capacities of 16.5 mg/L for Pb^{2+}, 16.0 mg/L for Cd^{2+}, 16.5 mg/L for Cr^{2+}, and 16.5 mg/L for Hg^{2+}. However, this enhanced efficiency comes with increased energy consumption and operational costs. Finally, we can conclude that this study offers a sustainable and cost-effective solution for environmental and biomedical challenges, promoting the recycling of waste materials and supporting green nanotechnology.

Data availability statement

The raw data supporting the conclusions of this article will be made available by the authors, without undue reservation.

Author contributions

HH: Writing–original draft, Visualization, Validation, Software, Resources, Methodology, Investigation, Formal Analysis, Data curation, Conceptualization. SZ: Conceptualization, Data curation, Formal Analysis, Investigation, Methodology, Resources, Software, Validation, Visualization, Writing–original draft. IB: Writing–original draft, Visualization, Validation, Software, Resources, Methodology, Investigation, Formal Analysis, Data curation, Conceptualization. AAn: Writing–original draft, Validation, Software, Resources, Methodology, Investigation, Formal Analysis, Data curation, Conceptualization. AT: Writing–original draft, Validation, Software, Methodology, Investigation, Formal Analysis, Data curation, Conceptualization. AAs: Funding acquisition, Project administration, Resources, Validation, Visualization, Writing–review and editing. DC: Writing–review and editing, Visualization, Validation, Resources, Project administration. MB: Visualization, Writing–review and editing, Validation, Supervision, Resources, Project administration, Funding acquisition, Formal Analysis. AB: Writing–review and editing, Writing–original draft, Visualization, Validation, Supervision, Software, Resources, Project administration, Methodology, Investigation, Funding acquisition, Formal Analysis, Data curation, Conceptualization.

Funding

The author(s) declare that financial support was received for the research, authorship, and/or publication of this article. The authors declare that financial support was received for this article's research, authorship, and/or publication. Consortium Author AB and AAl were financially supported by the Science, Technology and Innovation Funding Authority (Project ID 42811) and Researchers Supporting Project number (RSP-2024R78), King Saud University, Riyadh, Saudi Arabia.

Conflict of interest

The authors declare that the research was conducted in the absence of any commercial or financial relationships that could be construed as a potential conflict of interest.

Publisher's note

All claims expressed in this article are solely those of the authors and do not necessarily represent those of their affiliated organizations, or those of the publisher, the editors and the reviewers. Any product that may be evaluated in this article, or claim that may be made by its manufacturer, is not guaranteed or endorsed by the publisher.

Supplementary material

The Supplementary Material for this article can be found online at: https://www.frontiersin.org/articles/10.3389/fenvs.2024.1450485/full#supplementary-material

References

Abadi, A. K., and Abdul-Hussein Mejbel, F. (2020). Study of the effect of antifungal on candida albicans isolated from different cases. *Plant Arch. (09725210)* 20 (1).

Abdal Dayem, A., Hossain, M. K., Lee, S. B., Kim, K., Saha, S. K., Yang, G.-M., et al. (2017). The role of reactive oxygen species (ROS) in the biological activities of metallic nanoparticles. *Int. J. Mol. Sci.* 18 (1), 120. doi:10.3390/ijms18010120

Abuzeid, H. M., Julien, C. M., Zhu, L., and Hashem, A. M. (2023). Green synthesis of nanoparticles and their energy storage, environmental, and biomedical applications. *Crystals* 13 (11), 1576. doi:10.3390/cryst13111576

Aditya, S., Stephen, J., and Radhakrishnan, M. (2021). Utilization of eggshell waste in calcium-fortified foods and other industrial applications: a review. *Trends Food Sci. & Technol.* 115, 422–432. doi:10.1016/j.tifs.2021.06.047

Alibrahimi, A. A., and Toamah, W. (2019). Removing metal ions of cobalt (II) from aqueous solutions by CaO nanoparticle. *J. Phys. Conf. Ser.* 1279, 012023. doi:10.1088/1742-6596/1279/1/012023

Alobaidi, Y. M., Ali, M. M., and Mohammed, A. M. (2022). Synthesis of calcium oxide nanoparticles from waste eggshell by thermal decomposition and their applications. *Jordan J. Biol. Sci.* 15 (2). doi:10.54319/jjbs/150215

Alsohaimi, I. H., Nassar, A. M., Elnasr, T. A. S., and amar Cheba, B. (2020). A novel composite silver nanoparticles loaded calcium oxide stemming from egg shell recycling: a potent photocatalytic and antibacterial activities. *J. Clean. Prod.* 248, 119274. doi:10.1016/j.jclepro.2019.119274

Amor, I. B., Hemmami, H., Laouini, S. E., Temam, H. B., Zaoui, H., and Barhoum, A. (2023). Biosynthesis MgO and ZnO nanoparticles using chitosan extracted from Pimelia Payraudi Latreille for antibacterial applications. *World J. Microbiol. Biotechnol.* 39 (1), 19. doi:10.1007/s11274-022-03464-5

Anantharaman, A., Ramalakshmi, S., and George, M. (2016). Green synthesis of calcium oxide nanoparticles and its applications. *Int. J. Eng. Res. Appl.* 6 (10), 27–31.

Andarini, N., Farida, R. S., and Haryati, T. (2021). The effect of different precursor concentration on the synthesis of CaO nanoparticles with coprecipitation methods for palm oil transesterification catalysis. *Reaktor* 21 (2), 45–51. doi:10.14710/reaktor.21.2.45-51

Atchudan, R., Perumal, S., Joo, J., and Lee, Y. R. (2022). Synthesis and characterization of monodispersed spherical calcium oxide and calcium carbonate nanoparticles via simple pyrolysis. *Nanomaterials* 12 (14), 2424. doi:10.3390/nano12142424

Boey, P.-L., Maniam, G. P., and Abd Hamid, S. (2011). Performance of calcium oxide as a heterogeneous catalyst in biodiesel production: A review. *Chem. Enginee. J.* 168 (1), 15–22. doi:10.1016/j.cej.2011.01.009

Banković–Ilić, I. B., Miladinović, M. R., Stamenković, O. S., and Veljković, V. B. (2017). Application of nano CaO–based catalysts in biodiesel synthesis. *Renew. Sustain. Energy Rev.* 72, 746–760. doi:10.1016/j.rser.2017.01.076

Barhoum, A., Van Assche, G., Makhlouf, A. S. H., Terryn, H., Baert, K., Delplancke, M.-P., et al. (2015). A green, simple chemical route for the synthesis of pure nanocalcite crystals. *Cryst. Growth & Des.* 15 (2), 573–580. doi:10.1021/cg501121t

Bharathiraja, B., Sutha, M., Sowndarya, K., Chandran, M., Yuvaraj, D., and Praveen Kumar, R. (2018). Calcium oxide nanoparticles as an effective filtration aid for purification of vehicle gas exhaust. *Adv. Intern. Combust. Engine Res.*, 181–192. doi:10.1007/978-981-10-7575-9_9

Butt, A., Ejaz, S., Baron, J., Ikram, M., and Ali, S. (2015). CaO nanoparticles as a potential drug delivery agent for biomedical applications. *Dig. J. Nanomater. & Biostructures (DJNB)* 10 (3).

Chen, Q., Luo, Z., Hills, C., Xue, G., and Tyrer, M. (2009). Precipitation of heavy metals from wastewater using simulated flue gas: sequent additions of fly ash, lime and carbon dioxide. *Water Resea.* 43 (10), 2605–2614. doi:10.1016/j.watres.2009.03.007

Carvalho, J., Araújo, J., and Castro, F. (2011). Alternative low-cost adsorbent for water and wastewater decontamination derived from eggshell waste: an overview. *Waste Biomass Valorization* 2, 157–167. doi:10.1007/s12649-010-9058-y

Cavia, M., Fernandez-Muino, M., Gömez-Alonso, E., Montes-Pérez, M., Huidobro, J., and Sancho, M. (2002). Evolution of fructose and glucose in honey over one year: influence of induced granulation. *Food Chem.* 78 (2), 157–161. doi:10.1016/s0308-8146(01)00393-4

Cruz-Lopes, L. P., Macena, M., Esteves, B., and Guiné, R. P. (2021). Ideal pH for the adsorption of metal ions Cr6+, Ni2+, Pb2+ in aqueous solution with different adsorbent materials. *Open Agric.* 6 (1), 115–123. doi:10.1515/opag-2021-0225

Eddy, N. O., Garg, R., Ukpe, R. A., Ameh, P. O., Garg, R., Runde, M., et al. (2024). Application of periwinkle shell for the synthesis of calcium oxide nanoparticles and in the remediation of Pb2+-contaminated water. *Biomass Convers. Biorefinery*, 1–19. doi:10.1007/s13399-024-05285-y

Ferdoush, M. R., Al Aziz, R., Karmaker, C. L., Debnath, B., Limon, M. H., and Bari, A. M. (2024). Unraveling the challenges of waste-to-energy transition in emerging economies: implications for sustainability. *Innovation Green Dev.* 3 (2), 100121. doi:10.1016/j.igd.2023.100121

Garcia-Rubio, R., de Oliveira, H. C., Rivera, J., and Trevijano-Contador, N. (2020). The fungal cell wall: Candida, Cryptococcus, and Aspergillus species. *Front. Microbiol.* 10, 2993. doi:10.3389/fmicb.2019.02993

Gedda, G., Pandey, S., Lin, Y.-C., and Wu, H.-F. (2015). Antibacterial effect of calcium oxide nano-plates fabricated from shrimp shells. *Green Chem.* 17 (6), 3276–3280. doi:10.1039/c5gc00615e

Han, C., Chen, Y., Shi, L., Chen, H., Li, L., Ning, Z., et al. (2023). Advances in eggshell membrane separation and solubilization technologies. *Front. Veterinary Sci.* 10, 1116126. doi:10.3389/fvets.2023.1116126

Hashem, A., Aniagor, C. O., Farag, S., Fikry, M., Aly, A., and Amr, A. (2024). Evaluation of the adsorption capacity of surfactant-modified biomass in an aqueous acid blue 193 system. *Waste Manag. Bull.* 2 (1), 172–183. doi:10.1016/j.wmb.2024.01.004

Ikram, M., Muhammad Khan, A., Haider, A., Haider, J., Naz, S., Ul-Hamid, A., et al. (2022). Facile synthesis of La-and chitosan-doped CaO nanoparticles and their evaluation for catalytic and antimicrobial potential with molecular docking studies. *ACS omega* 7 (32), 28459–28470. doi:10.1021/acsomega.2c02790

Ismael, E., Fahim, K. M., Ghorab, S. M., Hamouda, R. H., Rady, A. M., Zaki, M. M., et al. (2024) Sustainable recycling of poultry eggshell waste for the synthesis of calcium oxide nanoparticles and evaluating its antibacterial potency against food-borne pathogens.

Kataki, S., Chatterjee, S., Vairale, M. G., Sharma, S., and Dwivedi, S. K. (2021). Concerns and strategies for wastewater treatment during COVID-19 pandemic to stop plausible transmission. *Resources, Conservation and Recycling.* 164, 105156. doi:10.1016/j.resconrec.2020.105156

Kamran, U., Jamal, H., Siddiqui, M. I. H., and Park, S.-J. (2023). Surfactant-capped silver-doped calcium oxide nanocomposite: efficient sorbents for rapid lithium uptake and recovery from aqueous media. *Water* 15 (19), 3368. doi:10.3390/w15193368

Kasirajan, R., Bekele, A., and Girma, E. (2022). Adsorption of lead (Pb-II) using CaO-NPs synthesized by solgel process from hen eggshell: response surface methodology for modeling, optimization and kinetic studies. *South Afr. J. Chem. Eng.* 40 (1), 209–229. doi:10.1016/j.sajce.2022.03.008

Khan, A. U., Hussain, T., Abdullah, Khan, M. A., Almostafa, M. M., Younis, N. S., et al. (2023). Antibacterial and antibiofilm activity of Ficus carica-mediated calcium oxide (CaONPs) phyto-nanoparticles. *Molecules* 28 (14), 5553. doi:10.3390/molecules28145553

Khine, E. E., Koncz-Horvath, D., Kristaly, F., Ferenczi, T., Karacs, G., Baumli, P., et al. (2022). Synthesis and characterization of calcium oxide nanoparticles for CO2 capture. *J. Nanoparticle Res.* 24 (7), 139. doi:10.1007/s11051-022-05518-z

Kubilay, Ş., Gürkan, R., Savran, A., and Şahan, T. (2007). Removal of Cu (II), Zn (II) and Co (II) ions from aqueous solutions by adsorption onto natural bentonite. *Adsorption* 13, 41–51. doi:10.1007/s10450-007-9003-y

Kumar, S., Sharma, V., Pradhan, J. K., Sharma, S. K., Singh, P., and Sharma, J. K. (2021). Structural, optical and antibacterial response of CaO nanoparticles synthesized via direct precipitation technique. *Nano Biomed. & Eng.* 13 (2). doi:10.5101/nbe.v13i2.p172-178

Kumari, S., Raturi, S., Kulshrestha, S., Chauhan, K., Dhingra, S., András, K., et al. (2023). A comprehensive review on various techniques used for synthesizing nanoparticles. *J. Mater. Res. Technol.* 27, 1739–1763. doi:10.1016/j.jmrt.2023.09.291

Lalou, N., and Kadari, A. (2019). Influence of Li 2+ doping on the structural and optical properties of CaO synthesized by sol–gel process. *J. Mol. Eng. Mater.* 7 (01n02), 1950002. doi:10.1142/s2251237319500023

Maringgal, B., Hashim, N., Tawakkal, I. S. M. A., Hamzah, M. H., and Mohamed, M. T. M. (2020). Biosynthesis of CaO nanoparticles using Trigona sp. Honey: physicochemical characterization, antifungal activity, and cytotoxicity properties. *J. Mater. Res. Technol.* 9 (5), 11756–11768. doi:10.1016/j.jmrt.2020.08.054

Mnasri-Ghnimi, S., and Frini-Srasra, N. (2019). Removal of heavy metals from aqueous solutions by adsorption using single and mixed pillared clays. *Appl. Clay Sci.* 179, 105151. doi:10.1016/j.clay.2019.105151

Muleta, W. S., Denboba, S. M., and Bayu, A. B. (2024). Corncob-supported calcium oxide nanoparticles from hen eggshells for cadmium (Cd-II) removal from aqueous solutions; Synthesis and characterization. *Heliyon* 10 (6), e27767. doi:10.1016/j.heliyon.2024.e27767

Nabila, V. K., and Putra, I. B. (2020). The effect of Aloe vera ethanol extract on the growth inhibition of Candida albicans. *Med. Glas. (Zenica)* 17 (2), 485–489. doi:10.17392/1098-20

Naz, S., Gul, A., Zia, M., and Javed, R. (2023). Synthesis, biomedical applications, and toxicity of CuO nanoparticles. *Appl. Microbiol. Biotechnol.* 107 (4), 1039–1061. doi:10.1007/s00253-023-12364-z

Perkumienė, D., Atalay, A., Safaa, L., and Grigienė, J. (2023). Sustainable waste management for clean and safe environments in the recreation and tourism sector: a case study of Lithuania, Turkey and Morocco. *Recycling* 8 (4), 56. doi:10.3390/recycling8040056

Raji, Z., Karim, A., Karam, A., and Khalloufi, S. (2023). *Adsorption of heavy metals: mechanisms, kinetics, and applications of various adsorbents in wastewater remediation—a review,* Waste. MDPI. Available at: https://www.mdpi.com/2813-0391/1/3/46.

Ramli, M., Rossani, R. B., Nadia, Y., Darmawan, T. B., Febriani, S., and Ismail, Y. S. (2019) "Nanoparticle fabrication of calcium oxide (CaO) mediated by the extract of red dragon fruit peels (Hylocereus Polyrhizus) and its application as inorganic–anti-microorganism materials," in *IOP conference series: materials science and engineering*. IOP Publishing. Available at: https://iopscience.iop.org/article/10.1088/1757-899X/509/1/012090.

Roy, A., Gauri, S. S., Bhattacharya, M., and Bhattacharya, J. (2013). Antimicrobial activity of CaO nanoparticles. *J. Biomedi. Nanotec.* 9 (9), 1570–1578. doi:10.1166/jbn.2013.1681

Silva, J. A. (2023). Wastewater treatment and reuse for sustainable water resources management: a systematic literature review. *Sustainability* 15 (14), 10940. doi:10.3390/su151410940

Singh, S., Srivastava, B., Gupta, K., Gupta, N., Singh, R., and Singh, S. (2020). Comparative evaluation of antifungal efficacy of five root canal sealers against clinical isolates of candida albicans: a microbiological study. *Int. J. Clin. Pediatr. Dent.* 13 (2), 119–123. doi:10.5005/jp-journals-10005-1718

Toamah, W. O., and Fadhil, A. K. (2019) "Preparation of nanoparticles from CaO and use it for removal of chromium (II), and mercury (II) from aqueous solutions," in *Journal of physics: conference series*. IOP Publishing. Available at: https://iopscience.iop.org/.

Varjani, S., Shah, A. V., Vyas, S., and Srivastava, V. K. (2021). Processes and prospects on valorizing solid waste for the production of valuable products employing bio-routes: a systematic review. *Chemosphere* 282, 130954. doi:10.1016/j.chemosphere.2021.130954

Velempini, T., Ahamed, M., and Pillay, K. (2023). Heavy-metal spent adsorbents reuse in catalytic, energy and forensic applications-a new approach in reducing secondary pollution associated with adsorption. *Results Chem.* 5, 100901. doi:10.1016/j.rechem.2023.100901

Xiong, S., Bozaghian, M., Lestander, T. A., Samuelsson, R., Hellqvist, S., and Öhman, M. (2017). Calcium oxide as an additive for both conservation and improvement of the combustion properties of energy grass: a preliminary study. *Biomass and Bioenergy.* 99, 1–10. doi:10.1016/j.biombioe.2017.02.010

Yazıcılar, B., Böke, F., Alaylı, A., Nadaroglu, H., Gedikli, S., and Bezirganoglu, I. (2021). *In vitro* effects of CaO nanoparticles on Triticale callus exposed to short and long-term salt stress. *Plant Cell Rep.* 40, 29–42. doi:10.1007/s00299-020-02613-0

Zaater, A., Serhoud, M. O., Ben Amor, I., Zeghoud, S., Hemmami, A., Rebiai, A., et al. (2024). Exploring the potential of a Ephedra alata leaf extract: phytochemical analysis, antioxidant activity, antibacterial properties, and green synthesis of ZnO nanoparticles for photocatalytic degradation of methylene blue. *Front. Chem.* 12, 1367552. doi:10.3389/fchem.2024.1367552

Zhang, M., Gao, M., Yue, S., Zheng, T., Gao, Z., Ma, X., et al. (2018). Global trends and future prospects of food waste research: a bibliometric analysis. *Environ. Sci. Pollut. Res.* 25, 24600–24610. doi:10.1007/s11356-018-2598-6

frontiers | Frontiers in Public Health

TYPE Systematic Review
PUBLISHED 03 December 2024
DOI 10.3389/fpubh.2024.1440908

Check for updates

OPEN ACCESS

EDITED BY
Visva Bharati Barua,
University of North Carolina at Charlotte, United States

REVIEWED BY
Piyush Baindara,
University of Missouri, United States
Yabing Li,
Michigan State University, United States
Tista Prasai Joshi,
Nepal Academy of Science and Technology (NAST), Nepal

*CORRESPONDENCE
Belay Desye
belaydesye.2001@gmail.com

RECEIVED 30 May 2024
ACCEPTED 19 November 2024
PUBLISHED 03 December 2024

CITATION
Desye B, Woldetsadik Mawugatie T, Asmare L, Tsega Y, Melak D, Endawkie A and Daba C (2024) Antimicrobial resistance profile of *Escherichia coli* in drinking water from one health perspective in low and middle income countries.
Front. Public Health 12:1440908.
doi: 10.3389/fpubh.2024.1440908

COPYRIGHT
© 2024 Desye, Woldetsadik Mawugatie, Asmare, Tsega, Melak, Endawkie and Daba. This is an open-access article distributed under the terms of the Creative Commons Attribution License (CC BY). The use, distribution or reproduction in other forums is permitted, provided the original author(s) and the copyright owner(s) are credited and that the original publication in this journal is cited, in accordance with accepted academic practice. No use, distribution or reproduction is permitted which does not comply with these terms.

Antimicrobial resistance profile of *Escherichia coli* in drinking water from one health perspective in low and middle income countries

Belay Desye[1]*, Temeselew Woldetsadik Mawugatie[2], Lakew Asmare[3], Yawkal Tsega[4], Dagnachew Melak[5], Abel Endawkie[5] and Chala Daba[1,6]

[1]Department of Environmental Health College of Medicine and Health Sciences, Wollo University, Dessie, Ethiopia, [2]Department of Economic, College of Management and Economics, Wollo University, Dessie, Ethiopia, [3]Department of Epidemiology and Biostatistics, Institute of Public Health, College of Medicine and Health Sciences, University of Gondar, Gondar, Ethiopia, [4]Department of Health System and Management, School of Public Health, College of Medicine and Health Sciences, Wollo University, Dessie, Ethiopia, [5]National Center for Epidemiology and Population Health, The Australia National University, Dessie, Ethiopia, [6]National Center for Epidemiology and Population Health, The Australia National University, Canberra, ACT, Australia

Introduction: Antimicrobial resistance is a major global public health concern, especially in low-resource settings. In low- and middle-income countries, the existing evidence about antimicrobial resistance in drinking water is inconsistence and not comprehensive. Therefore, this study aimed to estimate the pooled prevalence of antimicrobial resistance profiles of *Escherichia coli* from drinking water in low- and middle-income countries.

Methods: This study was conducted using comprehensive literature searches using various databases such as PubMed, Scientific Direct, HINARI, and Google Scholar. Data extraction was performed using Microsoft Excel and exported to STATA 14/SE software for analysis. We used the Joanna Briggs Institute's quality appraisal tool to ensure the quality of the included studies. A random effects model was employed to estimate the pooled prevalence. Publication bias was evaluated using funnel plots and Egger's regression test. Subgroup and sensitivity analysis were also conducted in this study.

Results: The study found that the pooled prevalence of *Escherichia coli* isolates in drinking water was 37.94% (95% CI: 26.73–49.13). The prevalence of multidrug resistance was 43.65% (95% CI: 31.15–56.15). Regarding specific antimicrobials, the pooled resistance levels of *Escherichia coli* were 54.65% (95% CI: 41.35–67.96) against contrimoxazole, followed by 48.64% (95% CI: −3.6–101) against amoxicillin and 48% (95% CI: −18.1–114.2) against cefuroxime.

Conclusion: The findings indicated a significant prevalence of antimicrobial resistance of *Escherichia coli* isolated from drinking water and its multidrug resistance. To address this issue, it recommends focusing on improving basic hygiene and sanitation practices and enhancing water and wastewater treatment systems.

Systematic review registration: Identifier CRD42024533592.

KEYWORDS

antimicrobial resistance, *Escherichia coli*, drinking water, one health, low and middle income countries

1 Introduction

Antimicrobial Resistance (AMR) occurs when microorganisms such as bacteria, viruses, fungi, and parasites no longer respond to antimicrobials, making infections difficult to treat (1). AMR occurs through genetic changes that occur naturally. This resistance can occur in humans, animals, and the environment (air, water, and soil). The drivers of AMR include misuse and overuse of antimicrobials, lack of access to clean Water, Sanitation and Hygiene (WASH), poor Infection Prevention and Control (IPC) practices, etc. (2, 3).

In our interconnected world, AMR has gained global attention as a significant public health challenge (4). The World Health Organization (WHO) has recognized AMR as one of the top ten global health threats (5). Additionally, AMR has been identified as a significant hurdle and one of the foremost challenges in attaining the Sustainable Development Goals (SDGs) (6–8). Consequently, addressing the escalating threat of AMR necessitates the implementation of a One-Health initiatives (9). One Health is a comprehensive and integrated approach that recognizes the interconnected nature and mutual dependence of the health of humans, animals, and the environment (10, 11).

In 2019, global reports indicated that 1.23 million deaths were attributed directly to AMR, and in addition, 4.95 million deaths were indirectly attributed to AMR (6). Disturbingly, projections suggest that by the year 2050, AMR could potentially lead to up to 10 million deaths per year worldwide (12). The impact of AMR is more severe in Low- and Middle-Income Countries (LMICs) where limited resources and inadequate implementation of WASH measures prevail. Insufficient sanitation facilities in these regions can contribute to water contamination and facilitate the transmission and spread of AMR (2, 13).

As per the United Nations, access to safe water and sanitation is recognized as a basic human right (14). However, AMR has emerged as a concerning contaminant in drinking water. Water plays a main role in the dissemination of AMR within the environment (15). Therefore, it is vital to establish a clean water supply system while improving the use of disinfectant chemicals or exploring effective options. This approach is important for improving water quality at the point of use and reducing the possible transmission of resistance bacteria through water sources (16).

Current treatment technologies used in water and wastewater treatment plants primarily focus on reducing physical and chemical contaminants, but they often provide limited removal of biological contaminants such as AMR (17). Moreover, there is often insufficient monitoring and assessment of AMR following water treatment (18). The water distribution system is recognized as a complex system, posing challenges for the inactivation and treatment of AMR. Despite the availability of advanced water treatment technologies like membrane filtration, activated carbon filtration, and advanced oxidation, these methods may not effectively treat AMR (19, 20). Enteric bacterial pathogens, particularly *Escherichia coli* (*E. coli*) isolates originating from drinking water, are a significant public health concern for humans (21, 22). The WHO has identified *E. coli* as a top priority pathogen and a main contributor to the AMR burden (23).

The identification of *E. coli* in drinking water samples in LMICs has gained increasing importance due to its potential risks to public health. Mahmud et al. (24) in Bangladesh reported that drinking water samples are sources of pathogenic *E.coli*. Many studies have revealed the occurrence of *E. coli* in drinking water samples in LMICs, with isolation rates ranging from 5.3% in Egypt (25) to 79.6% in Ghana (26). *E. coli* isolates from drinking water have shown resistance to antimicrobial agents such as cotrimoxazole, amoxicillin, ampicillin, and tetracycline (27–30). Multidrug resistance (MDR) has been observed among *E. coli* isolates from drinking water, with prevalence ranging from 19.7% in Peru (27) to 80% in Ethiopia (31).

The emergence and widespread prevalence of AMR present a significant challenge, especially in LMICs (32, 33). Although various countries worldwide have implemented antimicrobial stewardship programs to tackle the issue of AMR (17), and the WHO has launched a global AMR surveillance system (34). There are multiple studies conducted about AMR in health care settings, but there is limited evidence about the general environment, like drinking water, particularly in LMICs (35). Despite limited and inconsistent evidence, to the best of our literature search, no systematic review and meta-analysis has been conducted from a One Health perspective to examine the AMR profiles of *E. coli* isolates from drinking water in LMICs.

Therefore, the aim of this study is to estimate the overall prevalence of *E.coli* isolated from drinking water in LMICs. Through this review, the study aims to generate comprehensive evidence regarding the AMR profiles of *E. coli* isolates from drinking water in LMICs. This research will contribute to the One Health approach and support the attainment of the SDGs. Additionally, the findings of this study can inform decision-making processes and increase awareness among stakeholders and policymakers. Ultimately, the study has the potential to drive action and facilitate necessary interventions to tackle AMR in drinking water systems.

2 Methods

2.1 Study setting and protocol of registration

The guidelines for updated Preferred Reporting Items for Systematic Reviews and Meta-Analysis (PRISMA) were used for this study (36) (Figure 1). The review protocol for this study was registered in the International Prospective Register of Systematic Reviews (PROSPERO) with the record id CRD42024533592. This study was conducted in LMICs, following the list of World Bank data (37).

2.2 Sources of information and search strategies

A systematic literature search was undertaken using a database of PubMed, Scientific Direct, HINARI, and Google Scholar. For example, for the PubMed search, key terms were used in combination with the Boolean operators "AND" and "OR." Apart from conducting an electronic database search, additional articles were obtained by searching the gray literature through direct Google searches and by examining the bibliographies of the included articles.

2.3 Eligibility criteria

Inclusion criteria: this review included studies that fulfilled the following criteria.

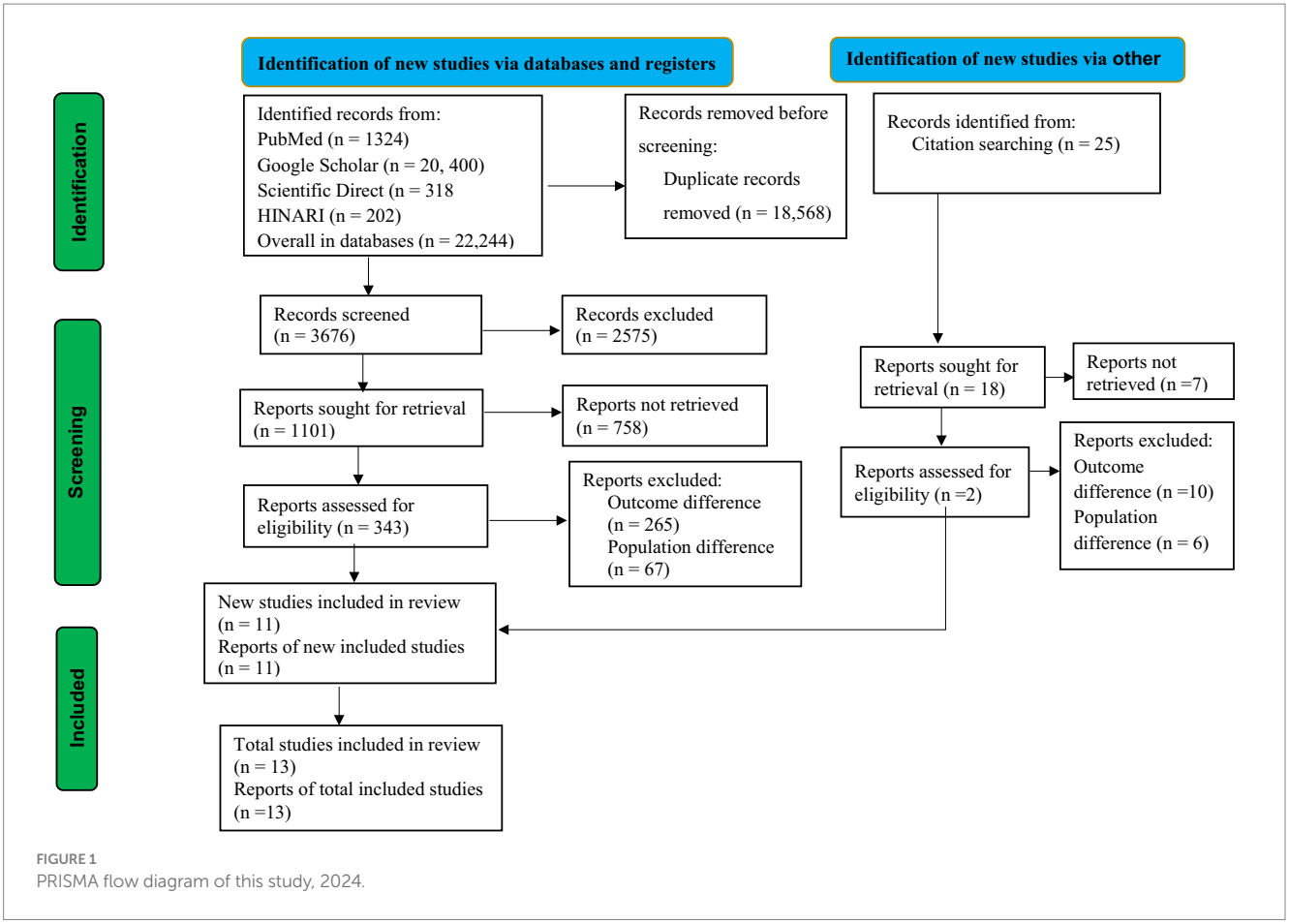

FIGURE 1
PRISMA flow diagram of this study, 2024.

a Population: articles conducted specifically on drinking water.
b Outcomes: articles reported the quantitative outcome of *E.coli* isolates (%), selected antimicrobial agents (%), and MDR of *E.coli* (%) in samples of drinking water.
c Study design: any observational studies (cross-sectional, case control, and cohort).
d Study setting: studies conducted in LMICs.
e Time frame: all studies reported from January, 02, 2000 to April, 30, 2024.
f Language of published studies: articles written in English.
g Publication issue: both published and unpublished studies.

***Exclusion criteria*:** studies that were not fully accessible despite three personal email contacts with the primary and corresponding authors, and studies that did not clearly show us the outcome interest of the study were excluded. Furthermore, certain types of research articles, including letters to editors, qualitative studies, systematic reviews, short communications, and commentaries, were not considered.

2.4 Study selection

Two investigators, BD and YT, conducted independent screenings of articles based on their titles, abstracts, and full texts to identify eligible articles. They followed pre-established criteria during this process. The screened studies were then combined by the two investigators, and any disagreements that arise during data abstraction and selection were resolved by discussions and the involvement of a third investigator (CD).

2.5 Data extraction and management

The format of data extraction for this study included author name, year of publication, country of the study, number of samples, number of *E.coli* isolates, % of *E.coli* isolates, % MDR of *E.coli* isolates, and risk of bias, these details were organized in a table format (Table 1). To collect articles and remove duplicate studies, Zotero Reference Manager was used. Additionally, the updated PRISMA checklist was employed to effectively summarize the study conditions (36) (Supplementary file 1).

2.6 Quality assessment of the studies

The quality appraisal tools of Joanna Briggs Institute (JBI) for analytical cross-sectional studies were used to assess the quality of the included studies (38). The quality of the articles was independently assessed by the two reviewers (BD and YT). Eight criteria were used to assess the quality of each article. The assessment options were categorized as yes, no, unclear, or not applicable. The risk of bias was classified as low (total score between 6 to 8), moderate (total score between 3 to 5), and high (total score

between 0 to 2). Finally, articles scored more than 50% were considered in this study (39, 40), detailed assessment in Supplementary file 2.

2.7 Outcome of interest

This study has three main outcomes:

- The pooled prevalence of *E.coli* isolates in drinking water in LMICs, expressed as (%).
- The pooled prevalence of selected antimicrobial agents against *E.coli* in drinking water in LMICs, expressed as (%).
- The pooled prevalence of MDR of *E.coli* isolates in drinking water in LMICs, expressed as (%)

2.8 Statistical methods and data analysis

Microsoft Excel was used to extract data and transported to STATA version-14 for analysis. Index of heterogeneity (I2 statistics) was used to assess heterogeneity among the included articles, where values of 25–50%, 50–75%, and > 75% indicated low, moderate, and high heterogeneity, respectively (41). The metaprop command in STATA was used to estimate the pooled prevalence. Subgroup analysis to explore potential variations in the pooled prevalence in this study was conducted using study countries, sample size, and study year. In this study, the effect of each study on the estimated pooled results was assessed using sensitivity analysis. A funnel plot test and Egger's regression test with a significance level of $p < 0.05$ as the cut point were used to ensure the presence of publication bias. To identify a possible heterogeneity source, a univariate meta-regression was employed. Finally, the findings of this study were presented using tables, figures, a forest plot, and descriptive text.

3 Results

3.1 Overview of search process

Using a database and other methods of search, a total of 22,244 studies were identified. After duplicate records were removed, 3,676 records were screened for this review. According to the records, only 1,101 reports were sought for retrieval. After being identified for retrieval, 343 reports were evaluated for eligibility. Following eligibility, a total of 332 studies were excluded due to differences in outcome interest and population differences. Ultimately, a total of 11 studies were included in this review from database sources. In addition to the database sources, 2 studies were included in this review from other sources. Finally, a total of 13 articles were included in this study, as presented in the PRISMA flowchart (Figure 1).

3.2 Characteristics of the eligible studies

All the included articles were cross-sectional studies. In this review, a total of 2,662 drinking water samples were included. Most of the studies were conducted in Ethiopia ($n = 4$) and Ghana ($n = 3$). The included studies were conducted between 2012 and 2023. In this study, the number of *E.coli* isolates was ($n = 874$), and the number of MDR of *E.coli* isolates was ($n = 243.33$). The *E.coli* isolates in this review ranged from 5.3% in Egypt (25) to 79.6% in Ghana (26), and the MDR of *E.coli* was found between 19.7% in Peru (27) and 80% in Ethiopia (31). All the included articles were categorized under moderate levels of risk of bias (Table 1).

TABLE 1 Summary of the included articles in AMR profiles of *Escherichia coli* isolates from drinking water in LMICs, 2024.

Author, publication year	Study country	No. of samples	No. of *Escherichia coli* isolates	*Escherichia coli* isolates (%)	Resistance of *Escherichia coli*	MDR of *Escherichia coli* (%)	Quality score (%)
Abera et al. (59)	Ethiopia	140	25	17.9	16.68	66.7	62.5
Ahmed et al. (28)	Ghana	524	115	21.9	67	58.2	75
Bonso et al. (60)	Ethiopia	100	68	68	23	33.8	75
Chen et al. (61)	China	404	200	49.5	49	24.5	75
Dhengesu et al. (29)	Ethiopia	75	20	26.7	-	-	75
Fakhr et al. (25)	Egypt	300	16	5.3	10	62.5	75
Hartinger et al. (62)	Peru	69	41	59.4	10.25	25	75
Kichana et al. (26)	Ghana	49	39	79.6	18.8	48.2	75
Larson et al. (27)	Peru	314	117	37.3	23	19.7	62.5
Odonkor et al. (30)	Ghana	110	23	20.9	6.4	27.8	75
Sahoo et al. (63)	India	417	151	36.2	-	-	75
Shakoor et al. (64)	Pakistan	100	35	35	-	-	62.5
Yenew et al. (31)	Ethiopia	60	24	40	19.2	80	62.5

-, not reported; *E.coli*, *Escherichia coli*; No., number, MDR, multidrug resistance which means resistance of antibiotics to three and more than three antibiotics.

3.3 The pooled prevalence of *Escherichia coli* isolates from drinking water in LMICs

The pooled prevalence of *E.coli* isolates using a random-effect model was estimated at 37.94% (95% CI: 26.75–49.13), with high heterogeneity (I^2 = 98%, *p*-value < 0.001) (Figure 2). A sub-group analysis based on study countries, year of publication, and sample size was performed to assess the heterogeneity sources, which were presented in Table 2. The highest pooled prevalence of 49.5% (95% CI: 44.63–54.38) was observed in China, and the lowest pooled prevalence was estimated at 5.33% (95% CI: 2.79–7.88) in Egypt. Heterogeneity was highest among studies conducted in Ghana (I2 = 97.9%), followed by Ethiopia (I^2 = 96.3%). Based on the year of publication, a study conducted in above 2018 was estimated at 43.87% (95% CI: 30–57.75) with (I^2 = 96.4%, p-value < 0.001) and 28.72% (95% CI: 9.50–47.94) with (I^2 = 98.8%, *p*-value < 0.001) for a study conducted in 2018 and below. In addition, a study conducted with a sample size of ≤ 200 found 43.22% (95% CI: 27.12–59.32) with (I^2 = 95.9%, *p*-value < 0.001) and sample size of >200 found 29.97% (95% CI: 13.42–46.53) with (I^2 = 98.9%, *p*-value < 0.001).

Furthermore, univariate meta-regression was conducted using study country, sample size, and study year as factors to identify the source of heterogeneity. However, neither of them was found to be statistically significant as sources of heterogeneity (Supplementary file 3). A sensitivity analysis was also conducted to evaluate a single study effect. It was found that 37.94% (95%CI: 23.72–52.46) indicates a slightly broader confidence interval from the pooled prevalence of *E.coli* isolates, there is no a strong evidence for the effect of a single study (Supplementary file 4). In addition, the funnel plot showed that there was no evidence for publication bias, the included articles were symmetrically distributed (Figure 3). In addition to the funnel plot, the Egger-regression test confirmed that there is no publication bias for this study (*p*-value = 0.110).

3.4 Pooled prevalence resistance pattern of *Escherichia coli* isolates from drinking water in LMICs

Eleven antimicrobial agents were used to assess the resistance pattern of *E. coli*. The finding revealed a high pooled resistance level of *E.coli* was 54.65% (95% CI: 41.35–67.96) against contrimoxazole, 48.64% (95% CI: −3.6-101) against amoxicillin and 48% (95% CI: −18.1-114.2) against cefuroxime. However, a low pooled resistance level of *E.coli* was found at 15% (95% CI: 4.95–25.1) against for gentamicin and 15.73% (95% CI: 7.8–23.7) against ciprofloxacin (Table 3).

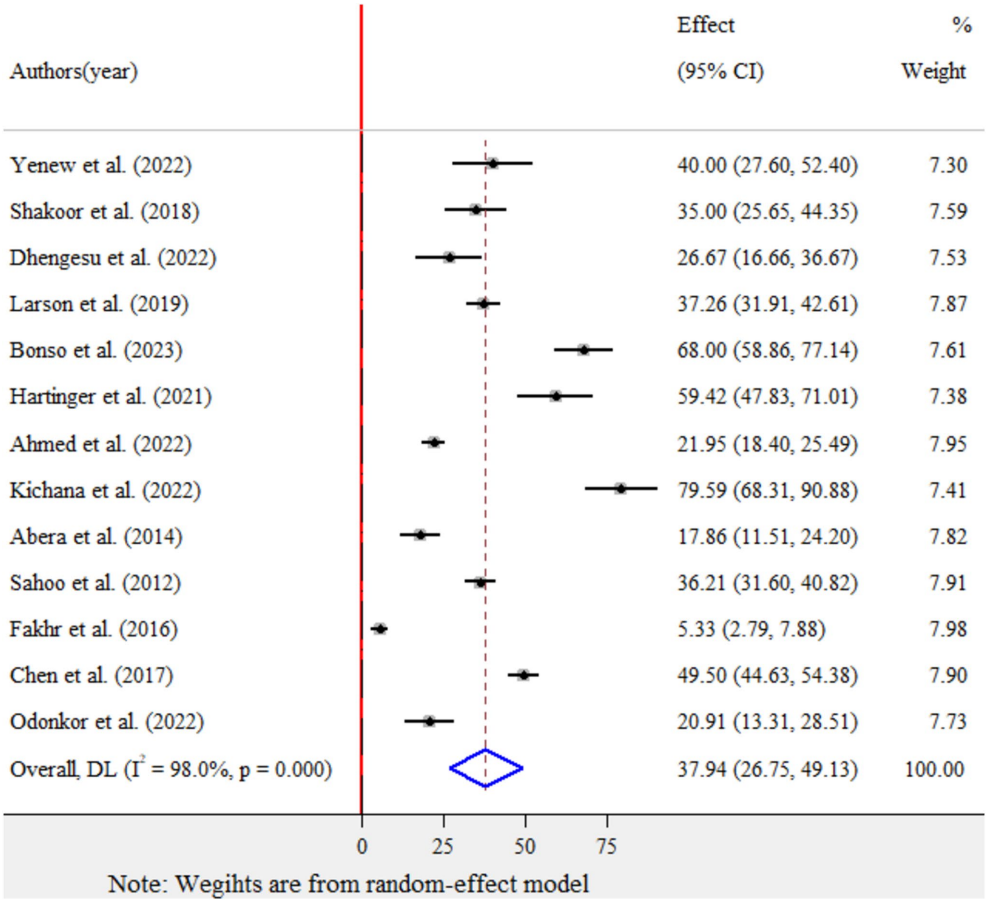

FIGURE 2
Forest plot for the pooled prevalence of *Escherichia coli* isolates from drinking water in LMICs, 2024.

TABLE 2 Subgroup analysis of the pooled prevalence of *Escherichia coli* isolates from drinking water in LMICs, 2024.

Subgrouping criteria	Number of studies	Pooled prevalence (95% CI)	Heterogeneity	
			I^2	*p*-value
Study country				
Ethiopia	4	38.04% (95% CI: 14.40–61.68)	96.3	<0.001
Pakistan	1	35% (95% CI: 25.65–43.25)	0.0	<0.001
Peru	2	47.72% (95% CI: 26.04–69.40)	91.4	0.001
Ghana	3	40.31% (95% CI: 12.60–68.01)	97.9	<0.001
India	1	36.21% (95% CI: 31.6–40.82)	0.0	<0.001
Egypt	1	5.33% (95% CI: 2.79–7.88)	0.0	<0.001
China	1	49.5% (95% CI: 44.63–54.38)	0.0	<0.001
Year of publication				
Above 2018	8	43.87% (95% CI: 30–56.75)	96.4	<0.001
2018 and below	5	28.72.% (95% CI: 9.50–47.94)	98.8	<0.001
Sample size				
≤200	8	43.22% (95% CI: 27.12–59.32)	95.9	<0.001
>200	5	29.97% (95% CI: 13.42–46.53)	98.9	<0.001

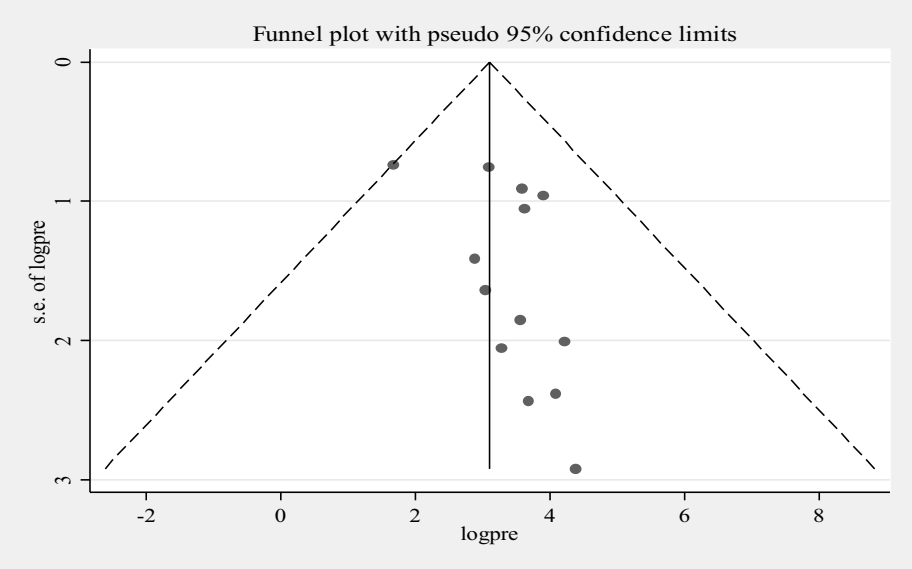

FIGURE 3
Funnel plot for *Escherichia coli* isolates from drinking water in LMICs, 2024.

3.5 The pooled prevalence of MDR for *Escherichia coli* isolates from drinking water in LMICs

The pooled prevalence of MDR for *E.coli* isolates using a random-effects model was estimated at 43.65% (95% CI: 31.15–56.15), with high heterogeneity (I^2 = 91.6%, *p-value* < 0.001) (Figure 4). A sub-group analysis based on study countries, year of publication, and sample size was performed to assess the heterogeneity sources, which were depicted in Table 4. The highest pooled prevalence of 62.50% (95% CI: 38.78–86.22) was observed in Egypt, and the lowest pooled prevalence was estimated 20.88% (95% CI: 14.55–27.20) in Peru. Heterogeneity was highest among studies conducted in Ethiopia (I^2 = 91.7%, *p*-value = <0.001), followed by Ghana (I^2 = 77.1%, *p*-value = 0.013). Based on the year of publication, a study conducted in above 2018 was estimated at 41.58% (95% CI: 25.58–57.78) with (I^2 = 92.3%, *p*-value < 0.001) and 50.06% (95% CI: 17.81–82.30) with (I^2 = 92.2%, *p*-value < 0.001) for a study conducted in 2018 and below. In addition, a study conducted with a sample size of ≤ 100 found

TABLE 3 Pooled prevalence of AMR patterns of *Escherichia coli* isolates from drinking water in LMIC, 2024.

Antimicrobial agents	Number of studies	Number of isolates	Number of resistance	Pooled prevalence of AMR (95% CI)	I^2 (%)	*p*-value
Ceftriaxone	4	185	114	33.9% (−13.4–81.2)	98.5	<0.001
Amoxicillin	3	255	85	48.64% (−3.6–101)	99.3	<0.001
Ciprofloxacin	9	532	96	15.73% (7.8–23.7)	87.8	
Trimethoprim-sulfamethoxazole	5	481	155	29.1% (11.7–46.5)	94.6	<0.001
Ampicillin	7	558	194	41.2% (19.1–63.3)	97.2	<0.001
Chloramphenicol	6	528	114	23.1%1 (14.8–31.4)	79.8	<0.001
Cefuroxime	3	255	118	48% (−18.1–114.2)	99.7	<0.001
Tetracycline	8	603	259	43.6% (32.5–54.8)	86.5	<0.001
Nalidixic acid	3	296	99	27.5% (−4.44–59.4)	97.7	<0.001
Gentamicin	5	204	28	15% (4.95–25.1)	78.2	<0.001
Cotrimoxazole	4	229	117	54.65% (41.4–68)	67.8	0.025

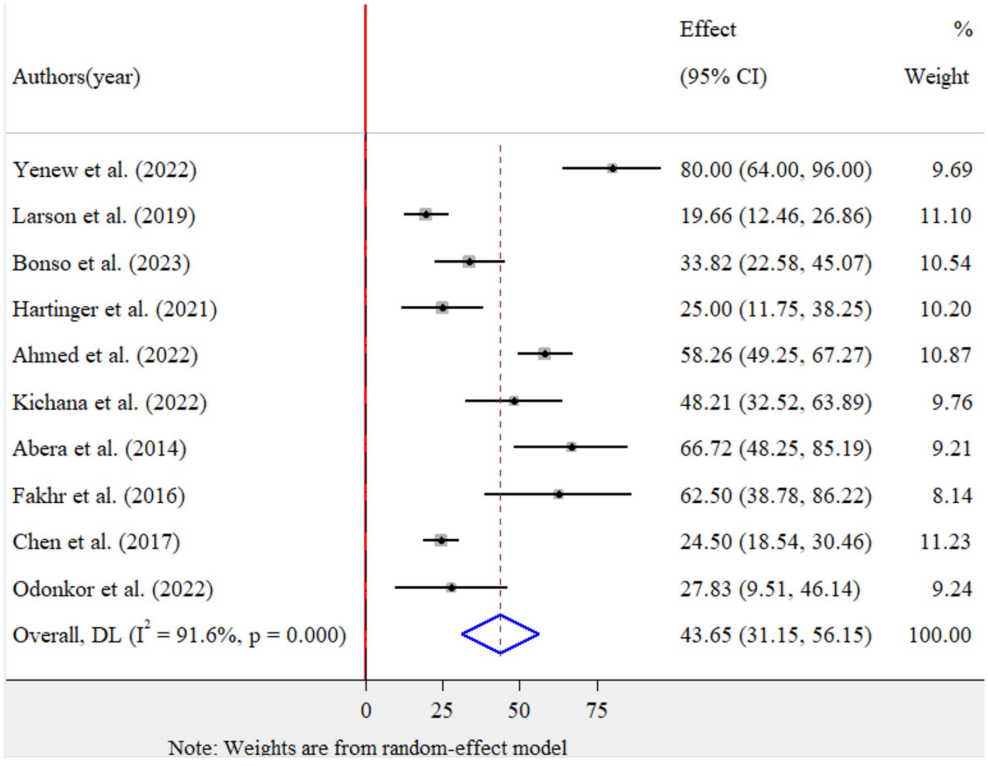

FIGURE 4
Forest plot for the pooled prevalence of MDR of *Escherichia coli* isolates from drinking water in LMICs, 2024.

48.53% (95% CI: 32.66–64.40) with (I^2 = 85.7%, *p*-value < 0.001) and a studies conducted with sample size of >100 found 33.92% (95% CI: 13.10–54.74) with (I^2 = 95.6%, *p*-value < 0.001). Furthermore, univariate meta-regression was conducted using study country, sample size, and study year to identify the sources of factor for heterogeneity. However, neither of them was found to be statistically significant for sources of heterogeneity (Supplementary file 5). The findings of the sensitivity analysis indicated that it was 43.65% (95%CI: 28–60.69), only slightly broader in confidence interval from the pooled prevalence, that cannot assured the presence of the effect of a single study (Supplementary file 6). In addition, the funnel plot revealed that there was no evidence of publication bias, the included articles were symmetrically distributed (Figure 5). Moreover, the

TABLE 4 Subgroup analysis of the pooled prevalence of MDR of *Escherichia coli* isolates from drinking water in LMICs, 2024.

Subgroup criteria	Number of studies	Pooled prevalence (95% CI)	Heterogeneity	
			I^2 (%)	*p*-value
Study country				
Ethiopia	3	59.69% (95% CI: 29.47–89.90)	91.7	<0.001
Peru	2	20.88% (95% CI: 14.55–27.20)	0.0	0.488
Ghana	3	46.21% (95% CI: 29.19–63.22)	77.1	0.013
Egypt	1	62.50% (95% CI: 38.78–86.22)	0.0	<0.001
China	1	24.5% (95% CI: 18.54–30.46)	0.0	<0.001
Year of publication				
Above 2018	7	41.58% (95% CI: 25.58–57.58)	92.3	<0.001
2018 and below	3	50.06.% (95% CI: 17.81–82.30)	92.2	<0.001
Sample size				
≤100	7	48.53% (95% CI: 32.66–64.40)	85.7	<0.001
>100	3	33.92% (95% CI: 13.10–56.74)	95.9	<0.001

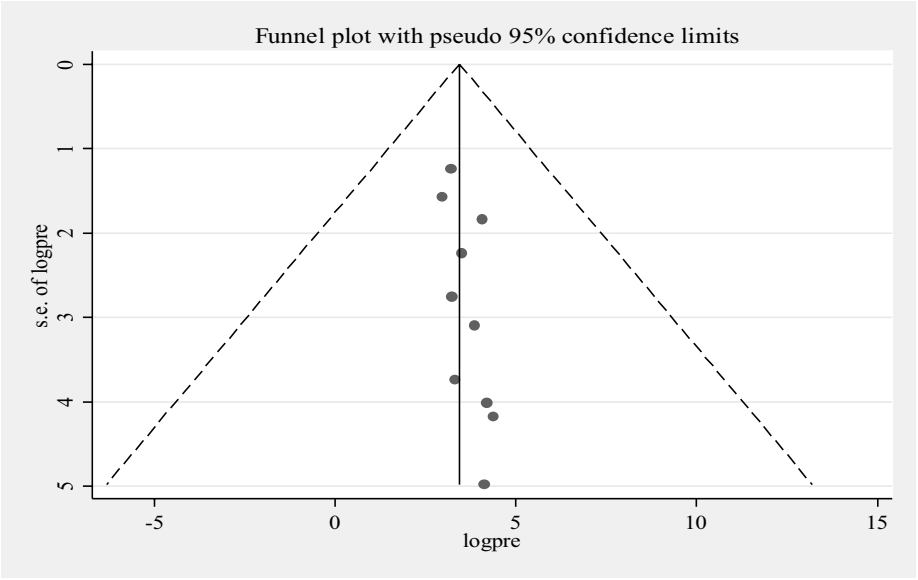

FIGURE 5
Funnel plot of MDR for *Escherichia coli* isolates from drinking water in LMICs, 2024.

Egger- regression test confirmed that there is no publication bias for this study (*p*-value = 0.070).

4 Discussion

AMR has emerged as a significant worldwide public health problem in the 21st century. It causes high rates of illness and death, particularly in LMICs (42). The presence of AMR exacerbates the high burden of bacterial infections in such areas, where access to adequate diagnostic tools is limited, antimicrobials are often misused or overused, and environmental conditions are poor (43, 44). The presence of AMR in drinking water increases the risk to human health. In this study, we estimate the prevalence and AMR patterns of *E.coli* isolates from drinking water in LMICs.

In this study, the pooled prevalence estimate of *E.coli* isolates from drinking water in LMICs was found to be 37.94% (95% CI: 26.75–49.13). This prevalence is lower than the 61.9% reported in a study of systematic reviews and meta-analysis conducted in Africa (45). The differences in prevalence could be attributed to variations in sample characteristics and the effectiveness of water treatment systems in place. The present findings might be explained by the lack of adequate water treatment and poor hygiene and sanitation conditions in those resource-constrained settings (44). However, WHO recommends

drinking water be free from *E.coli* (46). Therefore, it is crucial to strengthen AMR stewardship efforts and improve hygiene and sanitation conditions to address this issue effectively.

In this study, *E. coli* demonstrated a high level of resistance to several antimicrobials. The highest resistance rates were observed for cotrimoxazole (54.65%), amoxicillin (48.64%), cefuroxime (48%), tetracycline (43.6%), and ampicillin (41.2%). On the other hand, the lowest resistance rates were found for gentamicin (15%), ciprofloxacin (15.73%), and chloramphenicol (23.1%). The current result is supported by many studies showing that *E.coli* is resistant to many antimicrobials. For example, studies have shown *E.coli* resistance rates of 69.4 and 77% for ampicillin (45, 47). Another study documented the resistance of *E. coli* to amoxicillin (24.5%), ampicillin (23.5%), chloramphenicol (12.3%), and trimethoprim-sulfamethoxazole (22.5%) (42). In addition, studies reported lower resistance rates for *E.coli* rates for ciprofloxacin, ranging from 3 to 13.1% (45, 47). The observed variations in the reported resistance rates could be due to geographical locations and the nature of the study samples. Different countries may have varying levels of antimicrobial use, healthcare practices, surveillance, and sanitation systems, which can influence the resistance level of *E.coli* to each antimicrobial. Additionally, the condition of the samples analyzed, the source of the sample, and the setting conditions can also contribute to the differences in resistance rates (45, 47).

Overuse of these antibiotics and a lack of safe disposal may lead to resistance by promoting resistance development (48). For instance, cefuroxime is one of the major resistances against *E.coli* in this study, it is effective against Entrobacteriaceae bacteria, and it is a second-generation cephalosporin antibiotic (49). It is also used for the treatment of urinary tract infections (50). Therefore, the results of the resistance of *E.coli* in this study may be due to inappropriate treatment of human and animal wastes and their disposal in the environment. Hence, these untreated water sources contribute to AMR dissemination (28).

In this study, the pooled prevalence of MDR in *E. coli* was found to be 43.65%. This prevalence is lower than the 50.7% reported in a study conducted on water samples in Africa (45). The present finding is supported by earlier studies, which have highlighted the continued significance of *E. coli* resistance (42, 51). Additionally, in humans, animals and the environment, there have been reports for a high prevalence of AMR (47, 52, 53). Mostly, the present water treatment methods are unable to treat AMR adequately (48). Thus, improving basic hygiene and sanitation and advancing the treatment system will reduce the spread of resistant organisms (44).

LMICs are disproportionally affected by AMR due to the high infectious disease burden and poor antimicrobial use control and regulation (54). The sources of resistance can be environmental sources like sewerage systems, abattoirs, and waste from healthcare facilities that cannot be treated adequately and can contaminate drinking water sources (55). Although treatment systems for water and wastewater have been effective in reducing antimicrobial levels, findings revealed that antimicrobials are still present in drinking water (56, 57). This is a matter of concern because the existence of antibiotics in the environment can exert a strong selective pressure, promoting the acquisition and spread of resistance mechanisms among bacteria (58). Given these implications, it is highly recommended to advance and improve treatment systems to safeguard against the development and dissemination of AMR. By implementing more advanced treatment processes, it can minimize the existence of antimicrobials in sources of water.

4.1 Limitation of the study

This study was limited to publications in the English language and did not consider studies in other languages. In addition, this study focused exclusively on *E.coli* isolates and their resistance, neglecting the importance of multiple other enteric pathogens that have significant implications for public health. Moreover, the study did not identify the factors associated with *E.coli* resistance in drinking water.

5 Conclusion

AMR has emerged as a critical worldwide public health issue, particularly in LMICs. This study highlights *E.coli* isolates and their resistance to drinking water in LMICs were prevalent. The study revealed that *E. coli* resistance to various antimicrobial agents, with high resistance observed for contrimoxazole, amoxicillin, cefuroxime, and tetracycline. To tackle this concerning issue, it is essential to improve basic hygiene and sanitation practices. Additionally, advancing and upgrading water and wastewater treatment systems is essential to minimize the spread of resistant organisms. Taking a One-Health approach, it is recommended that concerned bodies and international organizations collaborate to mitigate health risks and minimize the environmental impact of AMR. For future researchers, it is advisable to conduct comprehensive investigations of other enteric pathogens in drinking water. Furthermore, identifying the drivers or factors contributing to AMR in drinking water would provide valuable insights for developing targeted interventions and strategies. By taking these actions, researchers and policymakers can work together to tackle the critical challenge of AMR in drinking water, particularly in LMICs where the burden is most severe.

Data availability statement

The raw data supporting the conclusions of this article will be made available by the authors, without undue reservation.

Author contributions

BD: Conceptualization, Investigation, Methodology, Software, Writing – original draft, Writing – review & editing. TW: Data curation, Investigation, Methodology, Supervision, Writing – review & editing. LA: Formal analysis, Methodology, Software, Supervision, Writing – review & editing. YT: Methodology, Supervision, Validation, Visualization, Writing – review & editing. DM: Data curation, Formal analysis, Methodology, Software, Writing – review & editing. AE: Methodology, Software, Supervision, Validation, Writing – review & editing. CD: Conceptualization, Investigation, Validation, Writing – original draft.

Funding

The author(s) declare that no financial support was received for the research, authorship, and/or publication of this article.

Conflict of interest

The authors declare that the research was conducted in the absence of any commercial or financial relationships that could be construed as a potential conflict of interest.

Publisher's note

All claims expressed in this article are solely those of the authors and do not necessarily represent those of their affiliated organizations, or those of the publisher, the editors and the reviewers. Any product that may be evaluated in this article, or claim that may be made by its manufacturer, is not guaranteed or endorsed by the publisher.

Supplementary material

The Supplementary material for this article can be found online at: https://www.frontiersin.org/articles/10.3389/fpubh.2024.1440908/full#supplementary-material

References

1. United Nations Environment (2023). Bracing for superbugs: strengthening environmental action in the one health response to antimicrobial resistance. UNEP - UN Environment Programme. (2023). Available at: http://www.unep.org/resources/superbugs/environmental-action (Accessed April 4, 2024).

2. Graham DW, Bergeron G, Bourassa MW, Dickson J, Gomes F, Howe A, et al. Complexities in understanding antimicrobial resistance across domesticated animal, human, and environmental systems. *Ann N Y Acad Sci*. (2019) 1441:17–30. doi: 10.1111/nyas.14036

3. Larsson DGJ, Flach C-F. Antibiotic resistance in the environment. *Nat Rev Microbiol*. (2022) 20:257–69. doi: 10.1038/s41579-021-00649-x

4. Kalungia AC, Mwambula H, Munkombwe D, Marshall S, Schellack N, May C, et al. Antimicrobial stewardship knowledge and perception among physicians and pharmacists at leading tertiary teaching hospitals in Zambia: implications for future policy and practice. *J Chemother*. (2019) 31:378–87. doi: 10.1080/1120009X.2019.1622293

5. World Health Organization (2021). Antimicrobial resistance: key facts, 17 November. Available at: https://www.who.int/news-room/fact-sheets/detail/antimicrobial-resistance (Accessed April 4, 2024).

6. Murray CJL, Ikuta KS, Sharara F, Swetschinski L, Aguilar GR, Gray A, et al. Global burden of bacterial antimicrobial resistance in 2019: a systematic analysis. *Lancet*. (2022) 399:629–55.

7. WHO. The fight against antimicrobial resistance is closely linked to the sustainable development goals. Available at: https://www.who.int/europe/publications/i/item/WHO-EURO-2020-1634-41385-56394. (Accessed April 8, 2024).

8. Tang KL, Caffrey NP, Nóbrega DB, Cork SC, Ronksley PE, Barkema HW, et al. Restricting the use of antibiotics in food-producing animals and its associations with antibiotic resistance in food-producing animals and human beings: a systematic review and meta-analysis. *Lancet Planet Health*. (2017) 1:e316–27. doi: 10.1016/S2542-5196(17)30141-9

9. Panel (OHHLEP) OHH-LE, Adisasmito WB, Almuhairi S, Behravesh CB, Bilivogui P, Bukachi SA, et al. One health: a new definition for a sustainable and healthy future. PLoS Pathog. (2022) 18:e1010537. doi: 10.1371/journal.ppat.1010537,

10. Brack W, Barcelo Culleres D, Boxall ABA, Budzinski H, Castiglioni S, Covaci A, et al. One planet: one health. A call to support the initiative on a global science–policy body on chemicals and waste. Environmental sciences. *Europe*. (2022) 34:21. doi: 10.1186/s12302-022-00602-6

11. Hernando-Amado S, Coque TM, Baquero F, Martínez JL. Defining and combating antibiotic resistance from one health and Global Health perspectives. *Nat Microbiol*. (2019) 4:1432–42. doi: 10.1038/s41564-019-0503-9

12. O'Neill J. Tackling drug-resistant infections globally: final report and recommendations Available at: https://apo.org.au/node/63983 (Accessed August 2, 2022).

13. Nadimpalli ML, Marks SJ, Montealegre MC, Gilman RH, Pajuelo MJ, Saito M, et al. Urban informal settlements as hotspots of antimicrobial resistance and the need to curb environmental transmission. *Nat Microbiol*. (2020) 5:787–795. doi: 10.1038/s41564-020-0722-0

14. United Nation. Human rights to water and sanitation. UN-Water. Available at: https://www.unwater.org/water-facts/human-rights-water-and-sanitation (Accessed April 9, 2024).

15. Walker GT, Quan J, Higgins SG, Toraskar N, Chang W, Saeed A, et al. Predicting antibiotic resistance in gram-negative Bacilli from resistance genes. *Antimicrob Agents Chemother*. (2019) 63:e02462–18. doi: 10.1128/AAC.02462-18

16. Bürgmann H, Frigon D, H Gaze W, M Manaia C, Pruden A, Singer AC, et al. Water and sanitation: an essential battlefront in the war on antimicrobial resistance. *FEMS Microbiol Ecol*. (2018) 94:94. doi: 10.1093/femsec/fiy101

17. Khan S. Antimicrobial resistance in environment and antimicrobial stewardship IntechOpen (2023). doi: 10.5772/intechopen.113224

18. Tan Q, Li W, Zhang J, Zhou W, Chen J, Li Y, et al. Presence, dissemination and removal of antibiotic resistant bacteria and antibiotic resistance genes in urban drinking water system: a review. *Front Environ Sci Eng*. (2019) 13:36. doi: 10.1007/s11783-019-1120-9

19. Zheng J, Chen T, Chen H. Antibiotic resistome promotion in drinking water during biological activated carbon treatment: is it influenced by quorum sensing? *Sci Total Environ*. (2018) 612:1–8. doi: 10.1016/j.scitotenv.2017.08.072

20. Xu L, Ouyang W, Qian Y, Su C, Su J, Chen H. High-throughput profiling of antibiotic resistance genes in drinking water treatment plants and distribution systems. *Environ Pollut*. (2016) 213:119–26. doi: 10.1016/j.envpol.2016.02.013

21. Abo-State M, Mahdy H, Ezzat S, Shakour E, Elbahnasawy M. Antimicrobial resistance profiles of Enterobacteriaceae isolated from Rosetta branch of River Nile. *Egypt World Appl Sci J*. (2012) 19:1234–43. doi: 10.5829/idosi.wasj.2012.19.09.2785

22. Leslie E, Hinds J, Hai FI. Causes, factors, and control measures of opportunistic premise plumbing pathogens—a critical review. *Appl Sci*. (2021) 11:4474. doi: 10.3390/app11104474

23. WHO publishes list of bacteria for which new antibiotics are urgently needed. Available at: https://www.who.int/news/item/27-02-2017-who-publishes-list-of-bacteria-for-which-new-antibiotics-are-urgently-needed (Accessed April 22, 2024).

24. Mahmud ZH, Kabir MH, Ali S, Moniruzzaman M, Imran KM, Nafiz TN, et al. Extended-Spectrum Beta-lactamase-producing *Escherichia coli* in drinking water samples from a forcibly displaced, densely populated community setting in Bangladesh. *Front Public Health*. (2020) 8:228. doi: 10.3389/fpubh.2020.00228

25. Fakhr AE, Gohar MK, Atta AH. Impact of some ecological factors on fecal contamination of drinking water by Diarrheagenic antibiotic-resistant *Escherichia coli* in Zagazig City. *Egypt Int J Microbiol*. (2016) 2016:6240703. doi: 10.1155/2016/6240703

26. Kichana E, Opare-Boafoa MS, Bekoe EMO. Prevalence of multidrug-resistant *Escherichia coli* in household drinking water in rural Ghana. *J Water Sanit Hygiene Dev*. (2022) 12:862–8. doi: 10.2166/washdev.2022.082

27. Larson A, Hartinger SM, Riveros M, Salmon-Mulanovich G, Hattendorf J, Verastegui H, et al. Antibiotic-resistant *Escherichia coli* in drinking water samples from rural Andean households in Cajamarca. *Peru Am J Trop Med Hyg*. (2019) 100:1363–8. doi: 10.4269/ajtmh.18-0776

28. Ahmed H, Zolfo M, Williams A, Ashubwe-Jalemba J, Tweya H, Adeapena W, et al. Antibiotic-resistant Bacteria in drinking water from the Greater Accra region, Ghana: a cross-sectional study, December 2021–march 2022. *Int J Environ Res Public Health*. (2022) 19:12300. doi: 10.3390/ijerph191912300

29. Dhengesu D, Lemma H, Asefa L, Tilahun D. Antimicrobial resistance profile of Enterobacteriaceae and drinking water quality among households in Bule Hora town. *South Ethiopia Risk Manag Healthc Policy*. (2022) 15:1569–80. doi: 10.2147/RMHP.S370149

30. Odonkor ST, Simpson SV, Morales Medina WR, Fahrenfeld NL. Antibiotic-resistant Bacteria and resistance genes in isolates from Ghanaian drinking water sources. *J Environ Public Health*. (2022) 2022:2850165. doi: 10.1155/2022/2850165

31. Yenew C, Kebede M, Mulat M. Drinking water antimicrobial resistance enteric bacterial load and public health risk in northwest, Ethiopia |. *Ethiop Med J*. (2022)

32. Augustin J-C, Carlier V. Lessons from the organization of a proficiency testing program in food microbiology by interlaboratory comparison: analytical methods in use, impact of methods on bacterial counts and measurement uncertainty of bacterial counts. *Food Microbiol*. (2006) 3:1–38. doi: 10.1016/j.fm.2005.01.010

33. Founou RC, Founou LL, Essack SY. Clinical and economic impact of antibiotic resistance in developing countries: a systematic review and meta-analysis. *PLoS One*. (2017) 12:e0189621. doi: 10.1371/journal.pone.0189621

34. WHo. Global action plan on antimicrobial resistance. 2016. Available at: https://www.who.int/publications-detail-redirect/9789241509763. Accessed April 22, 2024.

35. Sanganyado E, Gwenzi W. Antibiotic resistance in drinking water systems: occurrence, removal, and human health risks. *Sci Total Environ*. (2019) 669:785–797. doi: 10.1016/j.scitotenv.2019.03.162

36. Page MJ, McKenzie JE, Bossuyt PM, Boutron I, Hoffmann TC, Mulrow CD, et al. The PRISMA 2020 statement: an updated guideline for reporting systematic reviews. *Syst Rev*. (2021) 10:89. doi: 10.1186/s13643-021-01626-4

37. World Bank Open Data. Available at: https://data.worldbank.org (Accessed April 16, 2024).

38. Moola S, Munn Z, Tufanaru C, Aromataris E, Sears K, Sfetcu R, et al (2017). Chapter 7: Systematic reviews of etiology and risk. In: eds. E. Aromataris and Z. Munn *Joanna Briggs Institute Reviewer's Manual*. The Joanna Briggs Institute, Available at: https://reviewersmanual.joannabriggs.org/

39. Aromataris E, Lockwood C, Porritt K, Pilla B, Jordan Z. JBI Manual for Evidence Synthesis. JBI. (2024). Available at: https://synthesismanual.jbi.global.

40. Munn Z, Moola S, Lisy K, Riitano D, Tufanaru C. Methodological guidance for systematic reviews of observational epidemiological studies reporting prevalence and cumulative incidence data. *Int J Evid Based Healthc*. (2015) 13:147–53. doi: 10.1097/XEB.0000000000000054

41. Higgins JPT, Thompson SG. Quantifying heterogeneity in a meta-analysis. *Stat Med*. (2002) 21:1539–58. doi: 10.1002/sim.1186

42. WHO. Antimicrobial resistance in the WHO African region: a systematic literature review. WHO | regional Office for Africa. (2024). Available at: https://www.afro.who.int/publications/antimicrobial-resistance-who-african-region-systematic-literature-review. Accessed April 21, 2024.

43. Irek EO, Amupitan AAObadare TO, Aboderin AO. A systematic review of healthcare-associated infections in Africa: an antimicrobial resistance perspective. *Afr J Lab Med*. (2018) 7:796. doi: 10.4102/ajlm.v7i2.796

44. Ayukekbong JA, Ntemgwa M, Atabe AN. The threat of antimicrobial resistance in developing countries: causes and control strategies. *Antimicrob Resist Infect Control*. (2017) 6:47. doi: 10.1186/s13756-017-0208-x

45. Ramatla T, Ramaili T, Lekota KE, Ndou R, Mphuti N, Bezuidenhout C, et al. A systematic review and meta-analysis on prevalence and antimicrobial resistance profile of *Escherichia coli* isolated from water in africa (2000–2021). *Heliyon*. (2023) 9:e16123. doi: 10.1016/j.heliyon.2023.e16123

46. WHO. Drinking-water. WHO fact sheet on water: key facts, access to water, water and health. 2023. Available at: https://www.who.int/news-room/fact-sheets/detail/drinking-water (Accessed April 24, 2024).

47. Gemeda BA, Assefa A, Jaleta MB, Amenu K, Wieland B. Antimicrobial resistance in Ethiopia: a systematic review and meta-analysis of prevalence in foods, food handlers, animals, and the environment. *One Health*. (2021) 13:100286. doi: 10.1016/j.onehlt.2021.100286

48. Duarte AC, Rodrigues S, Afonso A, Nogueira A, Coutinho P. Antibiotic resistance in the drinking water: old and new strategies to remove antibiotics, resistant Bacteria, and resistance genes. *Pharmaceuticals*. (2022) 15:393. doi: 10.3390/ph15040393

49. Chang U-I, Kim HW, Wie S-H. Use of cefuroxime for women with community-onset acute pyelonephritis caused by cefuroxime-susceptible or -resistant *Escherichia coli*. *Korean J Intern Med*. (2016) 31:145–55. doi: 10.3904/kjim.2016.31.1.145

50. Venkatesh S, Chauhan L, Gadpayle A, Jain T, Wattal C, Aneja S, et al. National Treatment Guidelines for antimicrobial use in infectious diseases. (2016).

51. GBD. Antimicrobial resistance collaborators. Global mortality associated with 33 bacterial pathogens in 2019: a systematic analysis for the global burden of disease study 2019. *Lancet*. (2019) 2022:2221–48. doi: 10.1016/S0140-6736(21)02724-0

52. Fujita AW, Werner K, Jacob JT, Tschopp R, Mamo G, Mihret A, et al. Antimicrobial resistance through the Lens of one health in Ethiopia: a review of the literature among humans, animals, and the environment. *Int J Infect Dis*. (2022) 119:120–9. doi: 10.1016/j.ijid.2022.03.041

53. Sonola VS, Katakweba AS, Misinzo G, Matee MIN. Occurrence of multi-drug-resistant *Escherichia coli* in chickens, humans, rodents and household soil in Karatu, northern Tanzania. *Antibiotics*. (2021) 10:1137. doi: 10.3390/antibiotics10091137

54. Kariuki S, Kering K, Wairimu C, Onsare R, Mbae C. Antimicrobial resistance rates and surveillance in sub-Saharan Africa: where are we now? *Infect Drug Resist*. (2022) 15:3589–609. doi: 10.2147/IDR.S342753

55. Hu Y, Gao GF, Zhu B. The antibiotic resistome: gene flow in environments, animals and human beings. *Front Med*. (2017) 11:161–8. doi: 10.1007/s11684-017-0531-x

56. Xu L, Zhang H, Xiong P, Zhu Q, Liao C, Jiang G. Occurrence, fate, and risk assessment of typical tetracycline antibiotics in the aquatic environment: a review. *Sci Total Environ*. (2021) 753:141975. doi: 10.1016/j.scitotenv.2020.141975

57. Ben Y, Hu M, Zhang X, Wu S, Wong MH, Wang M, et al. Efficient detection and assessment of human exposure to trace antibiotic residues in drinking water. *Water Res*. (2020) 175:115699. doi: 10.1016/j.watres.2020.115699

58. Karkman A, Do TT, Walsh F, Virta MPJ. Antibiotic-resistance genes in waste water. *Trends Microbiol*. (2018) 26:220–8. doi: 10.1016/j.tim.2017.09.005

59. Abera B, Kibret M, Goshu G, Melaku M. Bacterial quality of drinking water sources and antimicrobial resistance profile of Enterobacteriaceae in Bahir Dar city, Ethiopia. *J Water Sanitation Hygiene Dev*. (2014) 4:384–90. doi: 10.2166/washdev.2014.105

60. Bonso M, Bedada D, Dires S. Bacterial contamination and antimicrobial resistance in drinking water from food and drinking establishments in Shashemane town. *Ethiopia Environ Health Insights*. (2023) 17:11786302231216864. doi: 10.1177/11786302231216864

61. Chen Z, Yu D, He S, Ye H, Zhang L, Wen Y, et al. Prevalence of antibiotic-resistant *Escherichia coli* in drinking water sources in Hangzhou City. *Front Microbiol*. (2017) 8:8. doi: 10.3389/fmicb.2017.01133

62. Hartinger SM, Medina-Pizzali ML, Salmon-Mulanovich G, Larson AJ, Pinedo-Bardales M, Verastegui H, et al. Antimicrobial resistance in humans, animals, water and household environs in rural Andean Peru: exploring dissemination pathways through the one health Lens. *Int J Environ Res Public Health*. (2021) 18:4604. doi: 10.3390/ijerph18094604

63. Sahoo KC, Tamhankar AJ, Sahoo S, Sahu PS, Klintz SR, Lundborg CS. Geographical variation in antibiotic-resistant *Escherichia coli* isolates from stool, cow-dung and drinking water. *Int J Environ Res Public Health*. (2012) 9:746–59. doi: 10.3390/ijerph9030746

64. Shakoor S, Ahmed I, Mukhtiar S, Ahmed I, Hirani F, Sultana S, et al. High heterotrophic counts in potable water and antimicrobial resistance among indicator organisms in two peri-urban communities of Karachi. *Pakistan BMC Res Notes*. (2018) 11:350. doi: 10.1186/s13104-018-3461-z

frontiers | Frontiers in Environmental Science

TYPE Original Research
PUBLISHED 11 December 2024
DOI 10.3389/fenvs.2024.1498893

Check for updates

OPEN ACCESS

EDITED BY
Maria Elisa Magri,
Federal University of Santa Catarina, Brazil

REVIEWED BY
Mahmuda Yasmin,
University of Dhaka, Bangladesh
Hongxia Ming,
National Marine Environmental Monitoring Center, China

*CORRESPONDENCE
Leonard Kachienga,
leokachienga@gmail.com

RECEIVED 19 September 2024
ACCEPTED 26 November 2024
PUBLISHED 11 December 2024

CITATION
Kachienga L, Rikhotso MC, Traore AN and Potgieter N (2024) Surveillance of *Vibrio cholerae* serogroups (O1 and O139) from surface and ground water sources in the Vhembe district, Limpopo province, South Africa.
Front. Environ. Sci. 12:1498893.
doi: 10.3389/fenvs.2024.1498893

COPYRIGHT
© 2024 Kachienga, Rikhotso, Traore and Potgieter. This is an open-access article distributed under the terms of the Creative Commons Attribution License (CC BY). The use, distribution or reproduction in other forums is permitted, provided the original author(s) and the copyright owner(s) are credited and that the original publication in this journal is cited, in accordance with accepted academic practice. No use, distribution or reproduction is permitted which does not comply with these terms.

Surveillance of *Vibrio cholerae* serogroups (O1 and O139) from surface and ground water sources in the Vhembe district, Limpopo province, South Africa

Leonard Kachienga*, Mpumelelo Casper Rikhotso, Afsatou Ndama Traore and Natasha Potgieter

Department of Biochemistry and Microbiology, Faculty of Sciences, Engineering and Agriculture, University of Venda, Thohoyandou, South Africa

Introduction: *Vibrio cholera* is increasingly emerging as a significant public health concern in developing countries. Choleragenic *Vibrio cholerae* O1 and O139 has reported to cause devastating disease and economic burdens in developing countries. In rural areas of the Vhembe district, most rivers and several communal boreholes are polluted as a result of sanitation issues around these water sources. The aim of this study was to determine the presence of choleragenic *V. cholerae* O1 and O139 in rivers and communal boreholes.

Methods: The analysis of physicochemical parameters and molecular techniques was used to establish the adaptation and detect the serogroups of *V. cholerae* in the water samples.

Results and Discussion: The results reported that electrical conductivities (EC) ranged between 18.78 and 154 µS/cm, with rivers such as Madandze and Mvudi recording >80 µS/cm, and those of the communal boreholes were ranged between 23.4 and 295 µS/cm, which were above the acceptable South African water quality guidelines of 0–70 µS/cm for rivers and communal boreholes. The results further revealed that most of the rivers detected positive for *V. cholerae*, except for the Mukhase river; the downstream points of Livuvhu and Nwedi rivers and the upstream point of the Nzhelele river; and several of the communal boreholes (Mak B1, B2, Kwe B3, 4, and 6) also tested positive for the presence of V. cholerae. The toxigenic *Vibrios* was also reported in Mutshundudi, Tshinane rivers, the upstream of Dzindi, Madanzhe, Nwedi, and the downstream of Sambandou rivers, as well as Mak B1, B2, and Kwe3 of communal boreholes. The serogroup O1 was detected on the Mutshundudi and Tshinane rivers, while serogroup O139 was detected upstream of the Dzindi, Madanzhe, Mutshundudi, and Tshinane rivers. There was also detection of the O1 serogroup in the communal boreholes (Mak B1 and Kwe B3), while O139 was only detected in one communal borehole (Mak B2). The development of robust policies,

including an integrated water and sanitation safety surveillance web tool for monitoring water resources and public health protection, is required to make sure that drinking water in rural communities is safe for consumption.

KEYWORDS

serotype group, *Vibrio cholerae* O1, surface water, communal borehole, water quality, waterborne transmission

1 Introduction

Access to safe, clean water and sanitation is a core human right, and it will also drive the achievement of sustainable development goals (SDGs), particularly Agendas 3 and 6 (Sikder et al., 2023; United Nations, 2024). According to the World Health Organisation (WHO), the common definition of safe drinking water and improved sanitation is access to piped water, protected wells, springs, rainwater, packaged water, boreholes, and sanitation facilities capable of effectively managing human excreta and urine (Bain et al., 2018).

The bacteria that cause cholera disease is known as *V. cholerae,* and it's transmitted either by food or water that is contaminated by this microorganism (Harris et al., 2012). *V. cholerae* has continued to ravage millions across the globe, especially in underdeveloped and developing countries such as South Africa and other Sub-Saharan, Asian, and Caribbean countries. This is because they have lagged in terms of inadequate access to safe, clean water and inadequate sanitation facilities, while these have been reduced or eradicated in developed countries (USA, United Kingdom, Canada, among other countries) with the development of an adequate safe water and sanitation infrastructure (Ali et al., 2015). Ozochi et al. (2024) further opined that the resent cholera cases around the world suggested that the outbreaks are due to *ctx*-positive *V. cholerae* O1. Currently, most of the pandemics or cases are not known, even with the World Health Organisation (WHO), which maintains a repository of cases or mortality through their weekly database, and they record less than 10% of cases due to inadequate reporting, especially in poor countries (WHO, 2014). According to Masuet et al. (2011) and Griffith et al. (2006), inadequate reporting of *V. cholerae* across the globe is a result of economic challenges, lack of political and social goodwill, inadequate capacity of both laboratories and epidemiological surveillance systems, and poor patient records. The outbreaks also arise from floods, conflicts, or extreme weather conditions that have triggered faecal contamination of water sources (Almagro-Moreno and Taylor, 2013).

There are approximately 200 serogroups of *Vibrio cholera* that are known, of which O1 and O139 are known for pathogenic symptoms and serious diarrhoea in humans (Almagro-Moreno and Taylor, 2013; Sharma et al., 2021). According to WHO (2005), choleragenic *V. cholerae* O1 and O139 are the only causative agents of cholera, a waterborne and foodborne disease with epidemic and pandemic potential. The most significant symptoms are watery diarrhoea, discomfort of the abdomen, and anorexia, which cause mild to severe gastrointestinal illness, dehydration, and death (WHO, 2005). The two serogroups are known for producing cholera toxins (CT) and toxin-coregulated pilus (TCP). There are also two non-O1 and non-O139 serogroups that are also associated with mild gastroenteritis and bloody diarrhoea to some extent and do not cause cholera (Yadava, Jain, and Goel, 2013; Bhandari, 2023). The two toxins (CT and TCP) produced by choleragenic serogroups are major triggers of watery diarrhoea and colonisation factors in humans (Arteaga et al., 2020).

Kaper, Morris, and Levine (1995) further stated that the O1 serogroup is further divided into three serotypes, mainly Inaba, Ogawa, and Hikojima, which are further divided into two biotypes, which are classical and El Tor. According to Marin et al. (2013), the O1 serogroup is widespread across the globe, while O139 is only restricted to the Asian continent. Mondiale de la Santé and the World Health Organisation (WHO) (2017) also reported that El Tor survives longer in environments that are linked to mild cases, which are shredded in high numbers in the faeces.

Most of the rivers and communal boreholes in rural areas such as the Vhembe district of South Africa and other developing countries are the immediate sources of water for domestic, agricultural, and other activities due to inadequate access to clean water and sanitation, which are not or are partially treated by dysfunctional treatment facilities (Potgieter et al., 2020). The irony is that most of the surface and ground water sources are highly polluted, triggering contamination and cases of *V. cholerae* in these areas. Potgieter et al. (2020) further stated that to reverse pollution challenges, there is a need for effective, robust, and continuous surveillance of bacterial, microbiological, and physiochemical parameters to establish any possible risks that are associated with pollution of a given water source for the rural populace, leading to *V. cholerae* cases or epidemics. Given the extent of potential pathogenic cases of the O1 and O139 serogroups in rural areas of Vhembe district, there is a need for continuous surveillance, rapid detection, and identification because the devastation can be catastrophic, as reported by Keddy et al. (2013). This will not only revert the community's ill-health issues but also assist in developing mitigation measures in terms of an integrated water sanitation and hygiene system (Keddy et al., 2013; Tasnia, 2023). Therefore, the main aim of this study was to establish the presence of choleragenic serogroups O1 and O139 in rivers and communal boreholes in the Vhembe district of Limpopo Province.

2 Methods and materials

2.1 Study area description

This District Municipality of Vhembe (Figure 1) is found in the province of Limpopo, further north of South Africa, and occupies a landmass of approximately twenty thousand square kilometres, according to Vhembe (2013). This area is blessed with fertile soil, and agricultural activities are taking place across the region. According to Kachienga et al. (2024), this area has both seasonal

and permanent rivers. There are a few existing communal boreholes that are still found in some villages that lack access to municipal water supply. Permanent rivers (n = 11) and communal boreholes (n = 12) that were sampled for this study are indicated by the red dots in Figure 1.

2.2 Collection of water samples

Water samples were collected between the months of April and July 2024 in 2-L sterile plastic bottles using aseptic techniques from rivers at specific sites as described by Kachienga et al. (2024) and communal boreholes. The collection was done once off, and the samples were in duplicates from both river (down and downstream) and communal boreholes. The samples were transported to the laboratory at the University of Venda in a cooler box containing ice and analysed upon arrival (Rice et al., 2012).

2.3 Physicochemical analysis of river and communal borehole samples

Various parameters, such as total dissolved solids (TDS), temperature, electrical conductivity (EC), and pH, were determined on site using a pH probe (Hach Intellical™ PHC101). The dissolved oxygen (DO) was analysed using a DO probe (Hach LDO® Model 2). In addition, a Lovibond TB 211 turbidimeter (Lovibond. IR, Germany) was used to analyse turbidity on site.

2.4 Culturing/enrichment of isolated *Vibrio cholerae* colonies

The filtration of the samples was done according to the protocol of the National Center for Infectious Diseases, 1994; Momtaz et al. (2013), where a 47 mm cellulose acetate filter with a 0.45 µm pore size was used to filter the samples. The enrichment of filtrate that was trapped in the filter paper after sample filtration was done in 100 mL of sterile alkaline peptone water (NutriSelect® Plus, Sigma Aldrich, SA); thereafter, the incubation was done at 37°C for one full day.

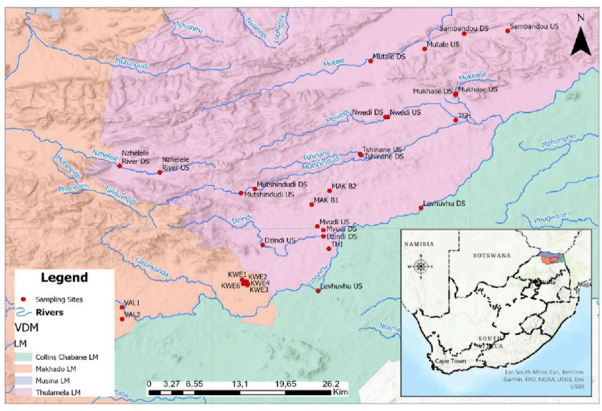

FIGURE 1
Map showing names of the rivers and communal boreholes (red dots) that were sampled in Vhembe District (developed by the department of environmental science, University of Venda).

The enriched samples (10 µL) were transferred into the sterile thiosulphate citrate bile salt (TCBS) (Mass Group Ltd. Reinfeld, Germany) agar plates and then incubated for 24 h at 37°C. The analysis was done in triplicate for each sample. The presumptive positive *V. cholerae* and their colonies forming units were determined according to Kachienga et al. (2024). The preservation of the presumptive *Vibrio* colonies was done according to Huq et al. (2012), and we further tested using biochemical tests for the confirmation of presumptive positive *V. cholerae.* The presumptive *Vibrio* colonies obtained were further used to extract the genomic DNA, which was used for molecular analysis for confirmation of toxigenic and serogroups of choleragenic *V. cholerae*.

2.5 API 20E technique (biochemical test) for analysing of the isolates

The presumptive colonies were tested with the API 20E system, and the interpretation of the isolates was based on the API 20E analytical profile index (Version 5, Biomerieux Industries, France). This technique was used to identify the presumptive positive *V. cholerae* obtained from other closely related Vibrionaceae species that might be present.

2.6 DNA extraction and PCR conditions

DNA extraction from samples was carried out using the ZymoBIOMICSTM DNA Miniprep Kit (Zymo Research, CA, USA) per the protocol of the manufacturer from the purified preserved presumptive *Vibrio* colonies. The NanoDropTM 2000 spectrophotometer (Thermo Scientific, Johannesburg, South Africa) was used to quantify the extracted DNA. The PCR reactions were performed in a total volume of 25 µL, as previously reported (Kachienga et al., 2024). The PCR technique was necessary to confirm the presence of *V. cholerae*, toxigenic *V. cholerae,* and serogroups of choleragenic *V. cholerae* in the samples using specific primers reported in Table 1. Amplification reactions were done in the following order: heat denaturation at 94°C for 2 min, followed by 35 cycles of heat denaturation at 94°C for 1 min, annealing at 58°C for 1 min, and DNA extension at 72°C for 1 min (Momtaz et al., 2013) using a qPCR Eppendorf Master Cycler 5330 (Eppendorf-Nethel-Hinz GmbH, Hamburg, Germany). The specific primers used included *OmpW, ctxA,* and *O1rfb/O139rfb* for detecting *V. cholerae*, toxigenic *V. cholerae,* and serogroups of choleragenic *V. cholerae* (Nandi et al., 2000; Huang et al., 2009; Mehrabadi et al., 2012) (Table 1).

2.7 Statistical analysis

The correlation of physiochemical parameters based on different sampling sites (upstream and downstream rivers, communal boreholes) through principal component analysis (PCoA) was

TABLE 1 List of primers used for the detection of *Vibrio cholerae*.

Primer	Nucleotide sequences 5′-3′	Length (bp)	References
OmpW	F-CACCAAGAAGGTGACTTTATTGTG R-GAACTTATAACCACCCGCG	588	Nandi et al. (2000)
ctxA	F-GGTCTTATGCCAGAGGACAG R-GTTGGGTGCAGTGGCTATAAC	219	Mehrabadi et al. (2012)
O1rfb	F- CCAGATTGTAAAGCAGGATGGA R- GGTCATCTGTAAGTACAAC	203	Huang et al. (2009)
O139rfb	F- CATACCAACGCCCTTATCCATT R- GCATGACTGGCATCCCAAAAT	160	Huang et al. (2009)

done using ClustVis (Metsalu and Vilo, 2015). The clustring together of these parameters visa vis their sampling sites based on the geographical areas and the surrounding activities.

3 Results and discussion

3.1 Activities around the rivers of study

The activities observed around these water sampling points were agricultural (subsistence and commercial farming), brickmaking, laundry, car washing, and open defecation by community members, amongst others. Various activities taking place around the water sources and occasional flooding trigger the presence of pathogenic microbes through runoff into the water sources. Yeung and Thorsen (2016) further reported that most of the urinal infections are also spread during recreational activities in and around rivers and communal boreholes.

3.2 Physicochemical parameters of the rivers

Polluted water is associated with a heavy burden on the population's overall health, and this has negatively impacted the life expectancy in developing countries such as South Africa (WHO, 2002). Cases of *V. cholera* have become a burden in poorer communities, especially in sub-Saharan countries where there is inadequate safe, clean water and sanitation infrastructure (Khouadja et al., 2014). According to Huq et al. (2012), assessment of vital parameters (temperature, turbidity, TDS, pH, DO, and EC) is necessary to establish the survival and adaptation of pathogenic and serogroups O1 and 139 and non-O1/O139. The results of the above parameters are captured in Table 2.

The pH counts of the rivers ranged from 7.03 to 8.21 for rivers and 6.88 to 8.21 for communal boreholes. They were both within the acceptable South African water quality guidelines of 6.5–8.5 for aquatic environments (rivers) and 6.0–9.0 for domestic usage (communal bore holes) (Department of Water Affairs and Forestry, 1996a). A pH between 7.5 and 9.0 normally influences the survival or adaptability of microorganisms; moreover, a pH > 8.5 is optimal for their survival in water (Grandjean et al., 2005). *V. cholerae,* especially serogroup O1, is extremely sensitive to acidic environments, and normachlorohydric people are not easily susceptible to cholera. This type of *vibrio* is also sensitive to desiccation and heat (ICMSF, 1996).

The average electrical conductivities (EC) for rivers and communal boreholes ranged between 18.78 and 154 µS/cm and 23.4 and 295 µS/cm (Table 2), which were above the acceptable South African water quality guidelines of 0–70 µS/cm for rivers and domestic use (Department of Water Affairs and Forestry, 1996a). The higher conductivity value recorded is directly proportional to an increase in ions and organic compounds that can conduct electric current (Holmes, 1996; Ferreira, 2011). Atekwana et al. (2004) further reported that the high levels of conductivity and TDS in water and the environment are due to the biodegradation of organic compounds by natural microorganisms. The presence of chitinase that is produced by *V. cholera* also assists them in adapting and surviving in extreme conditions such as saline and acidic environments, as reported by Huq et al. (2012).

The overall range for the TDS for the rivers in this study ranged between 10 and 90 mg/L, while for communal boreholes, it ranged between 70 and 320 mg/L. These data revealed that both rivers and communal boreholes were still within the acceptable South African water quality guidelines of 0–450 mg/L (Department of Water Affairs and Forestry, 1996a; Department of Water Affairs and Forestry, 1996b).

The average temperature obtained ranged between 18.05°C and 30.60°C for both rivers and communal boreholes. According to Franco et al. (1997), temperature is vital in triggering the formation of environmental biofilms and sediments that are supporting the survival of *V. cholera,* which will increase their counts and human illness. Huq et al. (2012) also state that a wider range of temperatures is critical for the heterogeneous nature of *V. cholera.* Temperature and other parameters, such as salinity, are the main drivers of the adaptability and survival of *V. cholerae in* any given environment, including contaminated water (Takahashi et al., 2023).

Most of the rivers ranged between 1.01 and 14.85 NTU, while the turbidity of communal boreholes ranged between 0.71 and 13.23 NTU. Despite all, most of the rivers were found to be within the acceptable set standards limit of <25 NTU for river water containing sediments and untreated aquatic water (Department of Water Affairs and Forestry, 1996a). However, only some communal boreholes (Val B1, Kwe B1, B3, and B4) were reported to be within the acceptable South African water quality guidelines of 0–1 NTU for domestic use (Department of Water Affairs and Forestry, 1996b). Turbidity is influenced by the formation of biofilms, sediments, and eutrophication by the presence of nitrates and phosphates because of the agricultural,

10.3389/fenvs.2024.1498893

TABLE 2 Physicochemical parameters of the river and communal borehole samples.

Sample origin	Sample ID	pH	Temp (°C)	EC (µS/cm)	TDS (mg/L)	Turbidity (NTU)	DO (ppm)
Mvudi River	Upstream	7.85	22.90	83.65	53.45	9.613	16.8
	Downstream	7.71	22.65	81.10	66.55	9.525	15.0
Livuvhu River	Upstream	8.09	24.45	63.40	40.45	4.615	16.6
	Downstream	7.81	25.35	80.05	50.70	2.890	22.1
Dzindi River	Upstream	7.94	18.95	34.80	22.30	9.910	8.56
	Downstream	8.21	23.70	65.00	41.60	14.85	19.1
Nzhelele River	Upstream	7.98	19.65	23.05	14.78	3.085	9.23
	Downstream	7.69	18.00	30.90	19.84	4.210	9.91
Mutshundudi River (Phiphidi)	Upstream	8.20	18.90	18.78	12.02	2.240	8.61
	Downstream	8.09	19.30	19.38	12.42	2.870	8.37
Mutale River	Upstream	7.03	21.9	27.00	11.33	5.28	8.55
	Downstream	7.12	24.4	27.00	17.25	5.87	8.75
Sambandou River	Upstream	8.52	23.6	21.35	13.58	1.01	14.6
	Downstream	7.03	21.85	24.65	15.79	1.96	9.43
Nwedi River	Upstream	7.73	24.90	35.2	22.55	3.94	8.15
	Downstream	7.19	25.00	35.6	23.15	5.50	8.51
Tshinane River	Upstream	8.07	26.1	43.3	27.7	8.31	10.7
	Downstream	7.87	24.4	43.4	27.8	8.26	11.4
Mukhase River	Upstream	7.72	22.1	21.15	13.56	1.47	8.47
	Downstream	7.44	23.50	21.10	13.57	1.40	9.85
Madandze River	Upstream	8.70	20.00	150.5	51.9	12.70	2.09
	Downstream	8.05	20.25	153.55	88.45	11.55	1.97
South Africa water quality guidelines by Department of Water and Sanitation		6.5–8.5	NA	0–70	0–450	0–5 <25 for rivers	6.5–8.0
Communal boreholes							
Mak B1	Common tap	7.14	17.9	188.8	121.55	1.165	9.34
Mak B2	Common tap	7.79	18.05	23.35	15.25	1.740	9.10
Thi B1	Common tap	7.29	26.7	364	233	1.205	18.6
Val B1	Common tap	7.09	22.4	112.60	72.20	0.81	8.64
Val B2	Common tap	6.88	27.3	114	73.1	2.44	10.2
Kwe B1	Common tap	7.00	26.2	173.4	110.7	0.86	9.38
Kwe B2	Common tap	7.35	25.55	497	318	3.23	2.77
Kwe B3	Common tap	7.54	28.6	257	261	0.95	5.83
Kwe B4	Common tap	7.07	29.0	282.5	181	0.71	1.65
Kwe B5	Common tap	8.21	30.6	376	240	1.18	4.01
Kwe B6	Common tap	7.26	30.2	285	180	2.31	1.35
Tsh B1	Common tap	7.46	28.3	295	189.15	1.06	8.71
South Africa water quality guidelines by Department of Water and Sanitation		6.0–9.0	NA	0–70	0–450	0–1	NA

NA, no standards given by DWA.

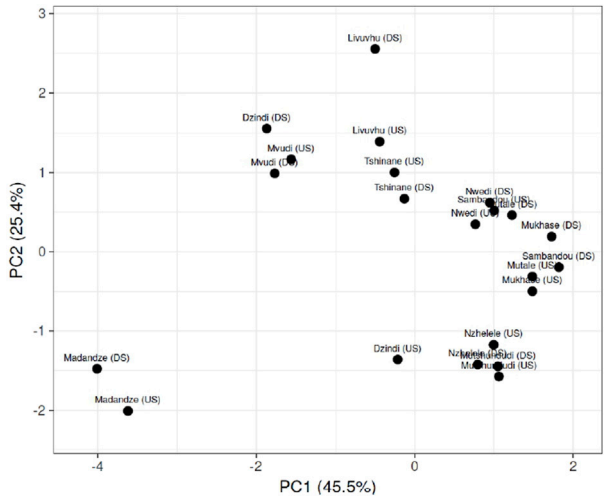

FIGURE 2
PCoA showing the correlation of physiochemical parameters on the difference between upstream and downstream rivers sampled.

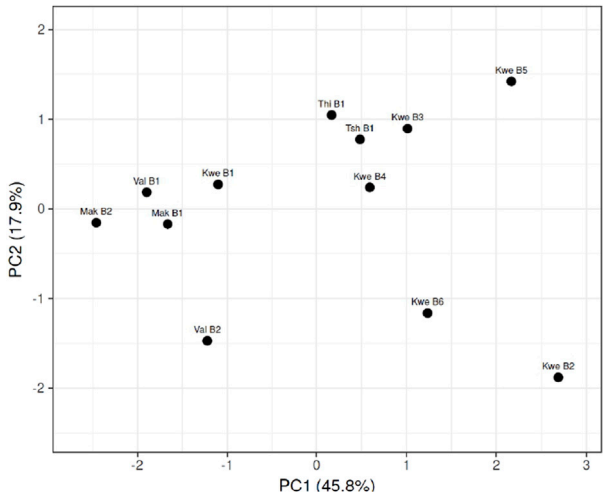

FIGURE 3
PCoA showing the correlation of physiochemical parameters on different communal boreholes sampled.

bathing, laundry, and brick-making activities inside and along the water sources (Fong et al., 2010). Ntema et al. (2014) also stated that the presence of debris and biotic surfaces in the rivers also facilitates *V. cholera* attachment and mobility.

Based on the availability of DO, the study revealed that most of the rivers were above the acceptable South African water quality guidelines of 6.5–8.0 ppm, except for Madanzhe River, whose DO counts were below the acceptable water quality guidelines. This is driven by the high-water runoff, higher flow rates of waters within these rivers, and pollution of rivers.

The principal component analysis (PCoA) correlation of different physicochemical parameters also revealed that most of the rivers and boreholes are clustered based on the geographical areas and the surrounding activities. The rivers such as Mvudi, Livuvhu, Tshinane, and Nwedi have clustered together based on PCoA in terms of high levels of variance in physicochemical parameters because farming and laundry activities around these water catchments, while Madandze, Mutshundudi, Nzhelele, and Mukhase rivers were also clustering together due to anthropogenic activities such as brickmaking and farming around them (Figure 2). These activities play a role in the physicochemical parameters obtained from the samples from these river sources.

Figure 3 reported that the Mak B1, B2, and Val B1 boreholes were clustered due to high levels of variance in physicochemical parameters. This was also due to the similarity of geographical location and poor sanitation around these boreholes that influenced their physicochemical parameters. The Kwe B3, Kwe B4, Thi B1, and Tsh B1 boreholes highly clustered together, while the Kwe B2, B5, and B6 boreholes least clustered together based on the variance of parameters. Most of these boreholes that were highly clustered were also influenced by agricultural activities and salty water that was associated with them. The boreholes that were least clustered, such as Kwe B2, B5, and B6, were difficult to identify because they were from similar geographical settings yet they least clustered.

3.3 The biochemical test results using analytical profile index (API)

The API test is one of the biochemical tests that is used to identify various families of microorganisms, such as Enterobacteriaceae and *V. cholerae*. Most of these rivers reported presumptive *Vibrio flavialis, Erwina* spp., *Raoutella planticolla or terrigena, Aeromonas* spp., *Klebsiella* spp., and *Serrati* spp., except for Madanzhe, Sambandou, and Nzhelele, which also had presumptive *V. cholerae* after being identified on the downstream site by the API test (Biomerieux Industries, South Africa) (Table 3). There were no microorganisms identified in the Makhase River. In communal boreholes, most of them reported presumptive *V. flavialis* and/or *Aeromonas* spp., *Erwina* spp., and *Raoutella planticolla or terrigena,* and communal boreholes such as Mak B1, B2 and Val B1, B2 reported none of the microorganisms (Table 3). These *Erwina* spp. bacteria are known to be well adapted to growth on vegetables because they are capable of fermenting many of the sugars and alcohols that exist in certain vegetables, unlike other common bacteria (Warriner et al., 2003; Gustaw et al., 2021). They might find their way into rivers and boreholes because of runoff from the surrounding farms or backyards from floods or rainfall. *Raoutella planticolla or terrigena, Aeromonas* spp., *Klebsiella* spp., and *Serrati* spp. are some of the microorganisms that are Gram-positive and sugar fermenters that lead to yellow colonies (Abbott, 2011; Yeung and Thorsen, 2016). They also cause urinary tract infections.

3.4 Molecular detection of serogroups of the toxigenic *V. Cholera* O1 and O139 from various rivers and communal boreholes using qPCR analysis

Most of the rivers detected positive for *V. cholerae* using the *OmpW* primer, except for the Mukhase river, the downstream

10.3389/fenvs.2024.1498893

TABLE 3 The biochemical test: API results for the identification of *Vibrio cholerae* in rivers and communal borehole samples.

River	Sample site	Biochemical test: API identification
Mvudi River	Upstream	presumptive *V. flavialis, Erwina spp*
	Downstream	presumptive *V. flavialis*, *Erwina spp*
Livuvhu River	Upstream	N/A
	Downstream	*Erwina spp*
Dzindi River	Upstream	*Erwina spp, Raoutella planticolla or terrigena*
	Downstream	*Erwina* spp, *Raoutella terrigena*
Madanzhe River	Upstream	presumptive *V. flavialis*, *Erwina* spp, *Raoutella planticolla*
	Downstream	presumptive *V. cholerae and V. flavialis, Erwina* spp, *Raoutella planticolla or terrigena*
Nzhelele River	Upstream	presumptive *V. cholerae, Serratia* spp
	Downstream	presumptive *V. flavialis, Serratia* spp
Mutshundudi River (Phiphidi)	Upstream	presumptive *V. flavialis, Erwina spp*
	Downstream	presumptive *V. flavialis, Klebsiella* spp., *Erwina spp*
Mutale River	Upstream	presumptive *V. flavialis, Erwina spp*
	Downstream	presumptive *V. flavialis, Erwina spp*
Sambandou River	Upstream	*Raoutella planticolla*, *Erwina spp*
	Downstream	presumptive *V. cholerae*
Nwedi River	Upstream	*Erwina spp, Serratia* spp
	Downstream	*Aeromonas* spp, *Serratia* spp., *Raoutella planticolla*
Mukhase River	Upstream	N/A
	Downstream	N/A
Tshinane River	Upstream	*Erwina* spp
	Downstream	*Raoutella planticolla*, *Serratia* spp., *Proteus vulgaris group*
Communal boreholes		
Mak B1	Common tap	N/A
Mak B2	Common tap	N/A
Thi B1	Common tap	presumptive *V. flavialis, Erwina spp*, *Raoutella planticolla or terrigena*
Val B1	Common tap	N/A
Val B2	Common tap	N/A
Kwe B1	Common tap	presumptive *V. flavialis* and/or *Aeromonas spp*
Kwe B2	Common tap	presumptive *V. flavialis, Erwina spp*, *Raoutella planticolla or terrigena*
Kwe B3	Common tap	presumptive *V. flavialis, Erwina spp*
Kwe B4	Common tap	presumptive *V. flavialis, Erwina spp*
Kwe B5	Common tap	presumptive *V. flavialis, Erwina spp*
Kwe B6	Common tap	*Erwina spp*
Tsh B1	Common tap	*Erwina spp*

N/A-there were no yellow colonies analyzed using biochemical test due to no growth.

Livuvhu and Nwedi rivers, and the upstream Nzhelele river point (Table 4). Only Mak B1, B2, Kwe B3, 4 and 6 boreholes tested positive for *V. cholerae,* using the *OmpW* primer (Table 4), which specifically targets the outer membrane of *V. cholerae,* and according to Fu et al. (2018), this gene acts as a passage of iron and other organic molecules that are pumped across and regulate survival in extreme environments. The detection of *V. cholerae* was also directly connected to the higher

10.3389/fenvs.2024.1498893

TABLE 4 qPCR results for the detection of toxigenic *Vibrio* from river samples.

River	Sample site	Molecular test (qPCR) using the *OmpW* primer/probes	qPCR analysis for toxigenic *V. cholera* using *CtxA* primer	qPCR analysis for serogroups of the toxigenic *V. cholera* detected using O1 *rfb* and O139 *rfb* primers	
				O1rfb	*O139rfb*
Mvudi River	Upstream	+	—	—	—
	Downstream	+	—	—	—
Livuvhu River	Upstream	+	—	—	—
	Downstream	—	—	—	—
Dzindi River	Upstream	+	+	—	+
	Downstream	+	—	—	—
Madanzhe River	Upstream	+	+	—	+
	Downstream	+	—	—	—
Nzhelele River	Upstream	—	—	—	—
	Downstream	+	—	—	—
Mutshundudi River (Phiphidi)	Upstream	+	+	+	+
	Downstream	+	+	+	—
Mutale River	Upstream	+	—	—	—
	Downstream	+	—	—	—
Sambandou River	Upstream	—	—	—	—
	Downstream	+	+	—	—
Nwedi River	Upstream	+	+	—	—
	Downstream	—	—	—	—
Mukhase River	Upstream	—	—	—	—
	Downstream	—	—	—	—
Tshinane River	Upstream	+	+	+	+
	Downstream	+	+	+	+
Communal boreholes					
Mak B1	Common tap	+	+	+	+
Mak B2	Common tap	+	+	-	+
Thi B1	Common tap	—	—	—	—
Val B1	Common tap	—	—	—	—
Val B2	Common tap	—	—	—	—
Kwe B1	Common tap	—	—	—	—
Kwe B2	Common tap	—	—	—	—
Kwe B3	Common tap	+	+	+	+
Kwe B4	Common tap	+	—	—	—
Kwe B5	Common tap	—	—	—	—
Kwe B6	Common tap	+	—	—	—
Tsh B1	Common tap	—	—	—	—

physicochemical parameters such as EC, TDS, and turbidity that were reported in both river and communal boreholes. The higher values obtained trigger the survival and distribution of *V. cholerae* in these water sources.

From the rivers that tested positive for *V. cholerae,* the pathogenicity of these *Vibrio* isolates was assessed using the *ctxA* primer and Mutshundudi, Tshinane rivers, the upstream of Dzindi, Madanzhe, and Nwedi samples, and the downstream of Sambandou rivers reported positive for toxigenic *V. cholerae* (Table 4). Only Mak B1, B2, and Kwe 3 communal boreholes were found to have toxigenic *V. cholerae* (Table 4). Bina et al. (2003) reported that toxigenic *V. cholerae* produces a toxin-regulated pilus that facilitates colonisation of the intestine walls and is the main regulator of the *ctx*A gene, and this gene was targeted by *the ctxA* primer. According to Liang et al. (2007), colonisation results in the activation of the G protein, which stimulates the adenylate cyclase. This process leads to the loss of electrolytes from the cell membrane, resulting in vomiting and watery, loose stools into the large intestines (World Health Organization, 2017). It is imperative to understand that any mutation or mismatch in the *ctx*A gene sequence leads to either a positive ctxA or a non-toxin-producing strain (Hoshino et al., 1998; Takahashi et al., 2023). The presence of toxigenic *V. cholerae* in these water sources was driven by the conditions and activities around them, as shown in S1-3, where some of the water sources were closer to sewer lines, toilets, and backyard farming. For the contamination or pollution of communal boreholes, Barcelona et al. (1988) stipulated different routes such as infiltration, direct migration, inter-aquifer exchange, and recharge from surface water that are the major drivers. In the clinical context, pathogenic *V. cholerae* differs from the non-pathogenic ones based on toxin-co-regulated pilus (TCP) and cholera toxin (CTX), which allow colonisation of the gut encoded by the phage CTXφ, which uses the TCP to attach to the bacterium (Waldor and Mekalanos, 1996; Ja'afar et al., 2021). Toxigenic *V. cholerae* also utilises the commensal association, leading to the formation of biofilm with copepods on their chitinous surfaces, which further leads to the formation of algal (de Magny et al., 2011; Rita and Colwell, 2009).

Once the pathogenicity had been analysed using PCR, the serogroups of the detected toxigenic were determined using the *O1 rfb* and *O139 rfb primers.* Serogroup O1 was detected on the Mutshundudi and Tshinane rivers, while serogroup O139 was detected on the upstream of the Dzindi, Madanzhe, Mutshundudi, and Tshinane rivers (Table 4). There was detection of both the O1 and O139 serogroups in the communal boreholes Mak B1 and Kwe B3, while serogroup O139 was only detected in the communal borehole Mak B2 (Table 4). In a study done by Phetla (2021), there was a higher percentage of serogroup O1 from sewage sludge and the riverbed from the Limpopo region, and therefore, there was a potential for O1 circulation in water sources leading to sporadic cholera outbreaks. The study of Phetla (2021) also reported that the O139 *V. cholerae* serotype was not found, and it was similar to a study done by Ansaruzzaman et al. (2007), who reported that this serotype was not endemic to the African continent but more endemic to India, Bangladesh, and other parts of the Asian continent. However, in this study, serogroup O139 was identified in both rivers and communal boreholes. This might be due to cross-border migration from cholera-prone countries/areas into South Africa through seeking medical treatment, tourism, traders, relatives, and refugees from neighbouring cholera-endemic countries or communities with ongoing epidemics like Haiti, Malawi, or Mozambique and Asian countries (Chin et al., 2011; Zarocostas, 2017). The serogroups detected from rivers and communal boreholes in the study were also due to the discharge of raw sewage, especially on the upstream side of the Madanzhe River, and the discharge of partially or untreated wastewater effluents into the rivers. The communal boreholes were also closer to the septic pit, leaking sewer line, and latrine, as depicted in S1-3.

Keddy et al. (2013) and Alaoui et al. (2021) stated that non-O1 or non-O139 strains of *V. cholerae* have been identified in birds, which might act as carriers/hosts into the environment. Therefore, continuous surveillance of rivers and communal boreholes, an integrated approach, and robust policies are needed to monitor these cases in a timely and reliable manner to prevent further discharge of raw sewage into rivers and closer to communal boreholes.

S1-3 depict images of rivers (upstream and downstream) and communal boreholes where serogroups (O1 and O139) were discovered. The majority of the rivers were contaminated, and the communal boreholes were closer to the pit latrine while the sewer line also discharged dirty effluent directly into the river catchment.

3.5 Limitation of this study

The study involved analysing water samples from rivers and communal boreholes, which could also be reservoirs for other organisms such as fish, snails, and others that are involved in commensal association with *V. cholerae,* including feeding, but were not considered in this study (You et al., 2019; Cho et al., 2021). Further studies using appropriate techniques targeting ecosystems that were not covered by this study should be conducted to provide more informed and reliable information on the presence of choleragenic *V. cholerae* in both surface water sources and communal boreholes. This study was conducted for a period of 4 months only, and a longer study might be needed to establish the prevalence and distribution of *V. cholerae O1* or *O139* and the potential health risk to vulnerable communities in Vhembe district, which is predominantly in rural areas.

4 Conclusion

The findings of this investigation indicate that pathogenic serotypes (O1 and O139) of *V. cholerae* were found in rivers and several communal boreholes. The presence of all *V. cholerae* serotypes in these contaminated water sources should be closely monitored at all times because the communities that rely on them are at risk. As a result, continual surveillance of rivers and communal boreholes, an integrated approach, and strong policies are required to monitor these cases in a timely and consistent

manner. This will also help to improve cleanliness around these sources of water. Further research is also needed to identify the ecology, virulence characteristics, and antibiotic sensitivity of the various serogroups (O1 and O139) found in this location.

Data availability statement

The original contributions presented in the study are included in the article/Supplementary Material, further inquiries can be directed to the corresponding author.

Author contributions

LK: Conceptualization, Data curation, Formal Analysis, Investigation, Methodology, Project administration, Resources, Software, Supervision, Validation, Visualization, Writing–original draft, Writing–review and editing. MR: Formal Analysis, Investigation, Methodology, Software, Writing–review and editing. AT: Investigation, Methodology, Supervision, Writing–review and editing. NP: Conceptualization, Data curation, Formal Analysis, Funding acquisition, Investigation, Methodology, Project administration, Resources, Software, Supervision, Validation, Visualization, Writing–review and editing.

Funding

The author(s) declare that no financial support was received for the research, authorship, and/or publication of this article.

Acknowledgments

The authors would like to thank Damien Jacobs and Miss Mafunise for dedicating their time during sampling period and always available to assist throughout the study. We also like to thank Farai from the department of Environmental Science for developing the map of the study sites.

Conflict of interest

The authors declare that the research was conducted in the absence of any commercial or financial relationships that could be construed as a potential conflict of interest.

Publisher's note

All claims expressed in this article are solely those of the authors and do not necessarily represent those of their affiliated organizations, or those of the publisher, the editors and the reviewers. Any product that may be evaluated in this article, or claim that may be made by its manufacturer, is not guaranteed or endorsed by the publisher.

Supplementary material

The Supplementary Material for this article can be found online at: https://www.frontiersin.org/articles/10.3389/fenvs.2024.1498893/full#supplementary-material

References

Abbott, S. L. (2011). *Klebsiella, enterobacter, citrobacter, serratia, plesiomonas*, and other Enterobacteriaceae. *Man. Clin. Microbiol.*, 639–657. doi:10.1128/9781555816728.ch37

Alaoui, H. L., Oufdou, K., and Mezrioui, N. E. (2021). *Prevalence, antimicrobial resistance and pathogenicity of non-O1* Vibrio cholerae *in suburban and rural groundwater supplies of marrakesh area (Morocco)*. IntechOpen: Infections and Sepsis Development.

Ali, M., Nelson, A. R., Lopez, A. L., and Sack, D. A. (2015). Updated global burden of cholera in endemic countries. *PLoS neglected Trop. Dis.* 9 (6), e0003832. doi:10.1371/journal.pntd.0003832

Almagro-Moreno, S., and Taylor, R. K. (2013). Cholera: environmental reservoirs and impact on disease transmission. *Microbiol. Spectr.* 1 (2), 10–1128. doi:10.1128/microbiolspec.oh-0003-2012

Ansaruzzaman, M., Bhuiyan, N. A., Safa, A., Sultana, M., Mcuamule, A., Mondlane, C., et al. (2007). Genetic diversity of El Tor strains of *Vibrio cholerae O1* with hybrid traits isolated from Bangladesh and Mozambique. *Int. J. Med. Microbiol.* 297 (6), 443–449. doi:10.1016/j.ijmm.2007.01.009

Arteaga, M., Velasco, J., Rodriguez, S., Vidal, M., Arellano, C., Silva, F., et al. (2020). Genomic characterization of the non-O1/non-O139 *Vibrio cholerae* strain that caused a gastroenteritis outbreak in Santiago, Chile, 2018. *Microb. genomics* 6 (3), e000340. doi:10.1099/mgen.0.000340

Atekwana, E. A., Atekwana, E. A., Rowe, R. S., Werkema, D. D., and Legall, F. D. (2004). The relationship of total dissolved solids measurements to bulk electrical conductivity in an aquifer contaminated with hydrocarbon. *J. Appl. Geophys.* 56 (4), 281–294. doi:10.1016/s0926-9851(04)00057-6

Bain, R., Johnston, R., Mitis, F., Chatterley, C., and Slaymaker, T. (2018). Establishing sustainable development goal baselines for household drinking water, sanitation and hygiene services. *Water* 10, 1711. doi:10.3390/w10121711

Barcelona, M., Keely, J. F., Pettyjohn, W. A., and Wehrmann, A. (1988) "Handbook of groundwater protection," in *Science information centre*. Washington DC, USA: Hemisphere Publishing Corporation.

Bhandari, M. (2023). *Genomic and virulence studies of* Vibrio cholerae *O1 and non-O1, non-O139 in queensland Australia*. Queensland, Australia: Queensland University of Technology.

Bina, J., Zhu, J., Dziejman, M., Faruque, S., Calderwood, S. J., and Mekalanos, J. (2003). ToxR regulon of *Vibrio cholerae* and its expression in *Vibrios* shed by cholera patients. *Proc. Natl. Acad. Sci. U. S. A.* 100 (5), 2801–2806. doi:10.1073/pnas.2628026100

Chin, C. S., Sorenson, J., Harris, J. B., Robins, W. P., Charles, R. C., Jean-Charles, R. R., et al. (2011). The origin of the Haitian cholera outbreak strain. *N. Engl. J. Med.* 364 (1), 33–42. doi:10.1056/nejmoa1012928

Cho, J. Y., Liu, R., Macbeth, J. C., and Hsiao, A. (2021). The interface of *Vibrio cholerae* and the gut microbiome. *Gut Microbes* 13 (1), 1937015. doi:10.1080/19490976.2021.1937015

de Magny, G. C., Mozumder, P. K., Grim, C. J., Hasan, N. A., Naser, M. N., Alam, M., et al. (2011). Role of zooplankton diversity in *Vibrio cholerae* population dynamics and in the incidence of cholera in the Bangladesh Sundarbans. *Appl. Environ. Microbiol.* 77 (17), 6125–6132. doi:10.1128/aem.01472-10

Department of Water Affairs and Forestry (DWAF) (1996a). "South African water quality guidelines,", 7. Pretoria, South Africa: Aquatic Ecosystems.

Department of Water Affairs and Forestry (DWAF) (1996b). "South African water quality guidelines,", 1. Pretoria, South Africa: Domestic Use.

Ferreira, S. L. (2011). *Microbial and physico-chemical quality of groundwater in the North-West Province, South Africa*. North-West University (South Africa)).

Fong, J. C., Syed, K. A., Klose, K. E., and Yildiz, F. H. (2010). Role of Vibrio Polysaccharide (vps) genes in VPS production, biofilm formation and *Vibrio cholerae* pathogenesis. *Microbiology* 156, 2757–2769. doi:10.1099/mic.0.040196-0

Franco, A. A., Fix, A. D., Prada, A., Paredes, E., Palomino, J. C., Wright, A. C., et al. (1997). Cholera in Lima, Peru, correlates with prior isolation of *Vibrio cholerae* from the environment. *Am. J. Epidemiol.* 146 (12), 1067–1075. doi:10.1093/oxfordjournals.aje.a009235

Fu, X., Zhang, J., Li, T., Zhang, M., Li, J., and Kan, B. (2018). The outer membrane protein OmpW enhanced *V. cholerae* growth in hypersaline conditions by transporting carnitine. *Front. Microbiol.* 8, 2703. doi:10.3389/fmicb.2017.02703

Grandjean, D., Fass, S., Tozza, D., Cavard, J., Lahoussine, V., Saby, S., et al. (2005). Coliform culturability in over-versus undersaturated drinking waters. *Water Res.* 39, 1878–1886. doi:10.1016/j.watres.2005.03.012

Griffith, D. C., Kelly-Hope, L. A., and Miller, M. A. (2006). Review of reported cholera outbreaks worldwide, 1995–2005. *Am. J. Trop. Med. Hyg.* 75, 973–977. PMID: 17123999. doi:10.4269/ajtmh.2006.75.973

Gustaw, K., Niedźwiedź, I., Rachwał, K., and Polak-Berecka, M. (2021). New insight into bacterial interaction with the matrix of plant-based fermented foods. *Foods* 10 (7), 1603. doi:10.3390/foods10071603

Harris, J. F., Ryan, E. T., Calderwood, S. B., and Calderwood, S. B. (2012). Cholera. *Lancet* 379, 2466–2476. doi:10.1016/S0140-6736(12)60436-X

Holmes, S. (1996). South African water quality guidelines. *Aquat. Ecosyst.* 7.

Hoshino, K., Yamasaki, S., Mukhopadhyay, A. K., Chakraborty, S., Basu, A., Bhattacharya, S. K., et al. (1998). Development and evaluation of a multiplex PCR assay for rapid detection of toxigenic *Vibrio cholerae* O1 and O139. *FEMS Immunol. Med. Microbiol.* 20 (3), 201–207. doi:10.1016/s0928-8244(98)00014-5

Huang, J., Zhu, Y., Wen, H., Zhang, J., Niu, J., and Li, Q. (2009). Quadruplex real-time PCR assay for detection and identification of *Vibrio cholerae* O1 and O139 strains and determination of their toxigenic potential. *Appl. Environ. Microbio.* 75 (22), 6981–6985. doi:10.1128/AEM.00517-09

Huq, A., Haley, B. J., Taviani, E., Chen, A., Hasan, N. A., and Colwell, R. R. (2012). Detection, isolation, and identification of *Vibrio cholerae* from the environment. *Curr. Protoc. Microbiol.* 26 (1), Unit6A.5–65. doi:10.1002/9780471729259.mc06a05s26

ICMSF (International Commission for Microbiological Specifications for Foods) (1996). "*Vibrio cholerae*," in *Microorganisms in foods: 5. Characteristics of microbial pathogens* (London, United Kingdom: Blackie Academic and Professional), 414–425.

Ja'afar, A. Z., Nillian, E., Bilung, L. M., Bebey, G., Zakaria, D., and Benjamin, P. G. (2021). Detection of cholera toxin (ctxA and ctxAB) genes in *Vibrio cholerae* isolated from clinical and environmental samples in Limbang Sarawak by multiplex polymerase chain reaction (PCR). *Malays. J. Microbiol.* 17 (1).

Kachienga, L., Prosperit, M., Traore, A. N., and Potgieter, N. (2024). Assessment of the presence of *Vibrio cholera* and detection of toxigenic *Vibrio cholerae* in river sources within the Vhembe District Municipality Limpopo province of South Africa. *J. Water Health* 2024062. doi:10.2166/wh.2024.062

Kaper, J. B., Morris, J. G., Jr., and Levine, M. M. (1995). Cholera. *Clin. Microbiol. Rev.* 8, 48–86. doi:10.1128/cmr.8.1.48-86.1995

Keddy, K. H., Sooka, A., Parsons, M. B., Njanpop-Lafourcade, B. M., Fitchet, K., and Smith, A. M. (2013). Diagnosis of *Vibrio cholerae* O1 infection in Africa. *J. Infect. Dis.* 208 (Suppl. l_1), S23–S31. doi:10.1093/infdis/jit196

Khouadja, S., Suffredini, E., Baccouche, B., Croci, L., and Bakhrouf, A. (2014). Occurrence of virulence genes among *Vibrio cholerae* and Vibrio parahaemolyticus strains from treated wastewaters. *Environ. Monit. Assess.* 186, 6935–6945. doi:10.1007/s10661-014-3900-9

Liang, W., Pascual-Montano, A., Silva, A. J., and Benitez, J. A. (2007). The cyclic AMP receptor protein modulates *quorum* sensing, motility and multiple genes that affect intestinal colonization in *Vibrio cholerae*. *Microbiology* 153 (9), 2964–2975. doi:10.1099/mic.0.2007/006668-0

Marin, M. A., Thompson, C. C., Freitas, F. S., Fonseca, E. L., Aboderin, A. O., Zailani, S. B., et al. (2013). Cholera outbreaks in Nigeria are associated with multidrug resistant atypical El Tor and non-O1/non-O139 *Vibrio cholerae*. *PLoS Neglected Trop. Dis.* 7 (2), 2049. doi:10.1371/journal.pntd.0002049

Masuet, A., umatell, C., Ramon Torrell, J. M., and Zuckerman, J. N. (2011). Review of oral cholera vaccines: efficacy in young children. *Infect. drug Resist.* 4, 155–160. doi:10.2147/idr.s10339

Mehrabadi, J. F., Morsali, P., Nejad, H. R., and Fooladi, A. A. I. (2012). Detection of toxigenic *Vibrio cholerae* with new multiplex PCR. *J. Infect. Pub. Health.* 5 (3), 263–267. doi:10.1016/j.jiph.2012.02.004

Metsalu, T., and Vilo, J. (2015). ClustVis: a web tool for visualizing clustering of multivariate data using Principal Component Analysis and heatmap. *Nucleic acids Res.* 43 (W1), W566–W570. doi:10.1093/nar/gkv468

Momtaz, H., Dehkordi, F. S., Rahimi, E., and Asgarifar, A. (2013). Detection of *Escherichia coli*, Salmonella species, and *Vibrio cholerae* in tap water and bottled drinking water in Isfahan, Iran. *BMC Public Health* 13, 556–557. doi:10.1186/1471-2458-13-556

Nandi, B., Nandy, R. K., Mukhophyay, S., Nair, G. B., Shimada, T., and Ghose, A. C. (2000). Rapid method for species-specific identification of *Vibrio cholerae* using primers targeted to the gene of outer membrane protein OmpW. *J. Clin. Microbio* 38, 4145–4151. doi:10.1128/jcm.38.11.4145-4151.2000

World Health Organization (WHO) (2017). 2017 Cholera vaccines: WHO position paper–August 2017–Vaccins anticholériques. *Wkly. Epidemiol. Rec. Relevé épidémiologique Hebd.* 92 (34), 477–498.

National Center for Infectious Diseases (US) (1994). *1994 laboratory methods for the diagnosis of* Vibrio cholerae. New York, USA: CDC/NCID.

Ntema, V. M., Potgieter, N., Van Blerk, G., and Barnard, T. G. (2014). Investigating the occurrence and survival of *Vibrio cholerae* in selected surface water sources in the KwaZulu-natal province of South Africa: *Report to the water research commission. Water Res. Comm.*

Ozochi, C. A., Okonkwo, C. C., Adukwu, E. C., Ujor, V. C., Enebe, M. C., and Chigor, V. N. (2024). Detection and quantitative microbial risk assessment of pathogenic *Vibrio cholerae* in a river used for drinking, domestic, fresh produce irrigation and recreational purposes. *Discov. Water* 4 (1), 7. doi:10.1007/s43832-024-00059-z

Phetla, V. (2021). Assessment of *Vibrio cholerae* and its biotypes associated with wastewater, sludge, river water and riverbed sediment: a case study in Limpopo province. *J. Environ. Microbiol.* 1 (1).

Potgieter, N., Karambwe, S., Mudau, L. S., Barnard, T., and Traore, A. (2020). Human enteric pathogens in eight rivers used as rural household drinking water sources in the northern region of South Africa. *Int. J. Environ. Res. public health* 17 (6), 2079. doi:10.3390/ijerph17062079

Rita, R., and Colwell, R. R. (2009). Cholera and climate: a demonstrated relationship. *Trans. Am. Clin. Climatol. Assoc.* 120, 119–128.

Sharma, A., Dutta, B. S., Rabha, D., Rasul, E. S., and Hazarika, N. K. (2021). Molecular characterization of *Vibrio cholerae* O1 strains circulating in Assam: a northeastern state of India. *Iran. J. Microbiol.* 13 (5), 583–591. doi:10.18502/ijm.v13i5.7420

Sikder, M., Deshpande, A., Hegde, S. T., Malembaka, E. B., Gallandat, K., Reiner, R. C., et al. (2023). Water, sanitation, and cholera in sub-saharan Africa. *Environ. Sci. and Technol.* 57 (28), 10185–10192. doi:10.1021/acs.est.3c01317

Takahashi, E., Kitahara, K., Miyoshi, S. I., Chowdhury, G., Mukhopadhyay, A. K., Dutta, S., et al. (2023). Environmental water in Kolkata is suitable for the survival of *Vibrio cholerae* O1. *Environ. Res.* 222, 115374. doi:10.1016/j.envres.2023.115374

Tasnia, R. (2023). *Production of polyclonal antisera of vibrio cholerae O1 and O139 to detect pathogenic vibrio cholerae*. Dhaka, Bangladesh: Brac University.

United Nations (2024). OHCHR, UN-habitat, WHO. The right to water, fact sheet No. 35 2010. Available at: https://www.ohchr.org/en/publications/fact-sheets/fact-sheet-no-35-right-water (Accessed July 10, 2024).

Vhembe, D. (2013). "Vhembe district municipality profile," in *Cooperative governance and traditional Affairs*. Pretoria.

Waldor, M. K., and Mekalanos, J. J. (1996). Lysogenic conversion by a filamentous phage encoding cholera toxin. *Science* 272 (5270), 1910–1914. doi:10.1126/science.272.5270.1910

Warriner, K., Ibrahim, F., Dickinson, M., Wright, C., and Waites, W. M. (2003). Internalization of human pathogens within growing salad vegetables. *Biotechnol. Genet. Eng. Rev.* 20 (1), 117–136. doi:10.1080/02648725.2003.10648040

WHO. 2002. Cholera, 2001. Weekly epidemiological record 77, 257–268.

WHO (2014). *Cholera surveillance and number of cases*. Geneva: World Health Organization.

WHO (World Health Organization) (2005). *Risk assessment of choleragenic* Vibrio cholerae *01 and 0139 in warm water shrimp for international trade: interpretative summary and technical report*. Geneva, Switzerland: World Health Organization.

Yadava, J. P., Jain, M., and Goel, A. K. (2013). Detection and confirmation of toxigenic *Vibrio cholerae* O1 in environmental and clinical samples by a direct cell multiplex PCR. *Water sa.* 39 (5), 611–614. doi:10.4314/wsa.v39i5.4

Yeung, M., and Thorsen, T. (2016). Development of a more sensitive and specific chromogenic agar medium for the detection of *vibrio parahaemolyticus* and other vibrio species. *J. Vis. Exp.* 117, 54493. doi:10.3791/54493

You, J. S., Yong, J. H., Kim, G. H., Moon, S., Nam, K. T., Ryu, J. H., et al. (2019). Commensal-derived metabolites govern *Vibrio cholerae* pathogenesis in host intestine. *Microbiome* 7, 1–18. doi:10.1186/s40168-019-0746-y

Zarocostas, J. (2017). Cholera outbreak in Haiti—from 2010 to today. *Lancet* 389 (10086), 2274–2275. doi:10.1016/s0140-6736(17)31581-7

frontiers | Frontiers in Environmental Science

TYPE Original Research
PUBLISHED 23 January 2025
DOI 10.3389/fenvs.2024.1458153

Check for updates

OPEN ACCESS

EDITED BY
Vivek Pulikkal,
Civil and Environmental Consultants, Inc., Charlotte, United States

REVIEWED BY
Joseph Delesantro,
The Pennsylvania State University (PSU), United States
Abhisek Manikonda,
Carollo Engineers, United States

*CORRESPONDENCE
Joshua A. Steele,
joshuas@sccwrp.org
John F. Griffith,
johng@sccwrp.org

†PRESENT ADDRESS
Darcy Ebentier McCargar,
Rick Engineering, San Diego, CA, United States
Sierra Wallace,
Rick Engineering, San Diego, CA, United States

RECEIVED 02 July 2024
ACCEPTED 10 December 2024
PUBLISHED 23 January 2025

CITATION
Steele JA, González-Fernández A, Griffith JF, Ebentier McCargar D, Wallace S and Schiff KC (2025) Extrapolating empirical measurements of wastewater exfiltration from sanitary sewers to estimate watershed-scale fecal pollution loading in urban stormwater runoff. *Front. Environ. Sci.* 12:1458153. doi: 10.3389/fenvs.2024.1458153

COPYRIGHT
© 2025 Steele, González-Fernández, Griffith, Ebentier McCargar, Wallace and Schiff. This is an open-access article distributed under the terms of the Creative Commons Attribution License (CC BY). The use, distribution or reproduction in other forums is permitted, provided the original author(s) and the copyright owner(s) are credited and that the original publication in this journal is cited, in accordance with accepted academic practice. No use, distribution or reproduction is permitted which does not comply with these terms.

Extrapolating empirical measurements of wastewater exfiltration from sanitary sewers to estimate watershed-scale fecal pollution loading in urban stormwater runoff

Joshua A. Steele[1]*, Adriana González-Fernández[1], John F. Griffith[1]*, Darcy Ebentier McCargar[2†], Sierra Wallace[2†] and Kenneth C. Schiff[1]

[1]Southern California Coastal Water Research Project, Costa Mesa, CA, United States, [2]WSP, San Diego, CA, United States

Inflow and infiltration are well-known issues for sanitary sewer collection systems, but exfiltration is understudied and rarely empirically quantified. The goal of this study is to estimate the potential human fecal contribution from wastewater exfiltration from sanitary sewers to stormwater in an urban watershed with separate sanitary sewer and storm sewer systems. This study uses newly developed techniques to empirically measure sanitary sewage exfiltration, then compares these exfiltration rates to human fecal pollutant loading in stormwater runoff from multiple urban catchments without other sources of human inputs (i.e., no septic systems, no homeless encampments, no reported sanitary sewer overflows) to estimate the amount of exfiltrated sewage that reaches stormwater. The human-specific genetic marker HF183, which is highly concentrated in raw sewage, was used as a surrogate for human fecal pollution and was measured in nearly every stormwater sample collected. We extrapolated measured exfiltration to the entire 419 km^2 watershed and estimated up to 4.25×10^6 L exfiltrate each day. This is 0.6% of the average daily volume of sewage treated in this sewer collection system and is similar in scale to exfiltration allowed by design standards. Based on ratios of exfiltration loading predictions vs. stormwater loading measurements, the proportion of exfiltrated human fecal load that is estimated to be transported via subsurface pathways (i.e., the subsurface transfer coefficient, STC) to stormwater in the studied catchments is 8.27×10^{-5} (95% CI: 6.30×10^{-5} to 1.37×10^{-4}). Human fecal pollution loads from exfiltration via subsurface transfer during a storm event were calculated to be 1.5×10^{13} (95% CI: 1.79×10^{12} to 3.59×10^{13}) HF183 gene copies per storm. This estimate is similar in scale to the measured mass loading estimates in stormwater for the studied watershed and comparable to independently-measured tracers of sewage. Future work is needed to better understand subsurface transport mechanisms of exfiltrated sewage and to test this approach, and the assumptions used, in other watersheds and sewer systems.

KEYWORDS

sewer exfiltration, municipal separate storm sewer systems, sewer pipes, HF183, decay rates, flow-weighted loading

Introduction

Urban sanitary sewer collection systems have well-characterized issues with inflow and infiltration, particularly during wet weather (Beheshti et al., 2015; Crawford et al., 1999). Infiltration has been estimated to increase wastewater collection system flows by as much as 35% (Staufer et al., 2012; Karpf et al., 2011). Because of the large costs associated with treating non-sewage flows, management programs to upgrade sewer collection systems and private laterals to prevent infiltration and inflow are seen worldwide. In contrast, exfiltration, which typically has smaller volumes, has received less attention.

If urban stormwater can infiltrate urban sanitary sewer collection systems, then a reasonable question would be whether raw sewage could exfiltrate urban collection systems, especially when it is not raining and water tables are low. Researchers have demonstrated that exfiltration occurs regularly in sewer systems throughout the world using a variety of approaches to attempt to quantify exfiltration rates (see Rutsch et al., 2008; Nguyen et al., 2021 for reviews) and the subsequent impacts on shallow groundwater or nearby surface waters (Ellis et al., 2004; Lee et al., 2015, Roehrdanz et al., 2017). For example, Sercu et al. (2009), (2011) demonstrated the occurrence of sewage exfiltration, and that the subsequent inflow to nearby storm drains impacted microbial water quality of nearby creeks and beaches. Delesantro et al. (2022) identified urban sanitary sewer exfiltration as the likely cause of increased nutrient loading to streams. Nguyen and Venohr (2021) used modeled nutrient pollution in urban surface waters and estimated that sewage exfiltration could account for a substantial proportion of nitrate and phosphate loads. Delesantro et al. (2024) showed subsurface storm flows and baseflows mobilized multiple sources of nutrient loading to streams areas of moderate development intensity.

Exfiltration and subsequent transport to surface waters requires multiple steps and is dependent on a variety of factors. First, sewage volume and any associated contaminants must exit the subsurface pipe. The factors that control this exfiltration include the frequency and magnitude of pipe defects, size of the pipe, pipe material of construction including joint materials, quality of construction including backfill material, soil type, in-pipe flow rates, and groundwater height (Selvakumar et al., 2010). Second is subsurface transport of the exfiltrated sewage and associated pollutants, which is controlled by shallow groundwater movement, soil type, and proximity to storm drainage systems or surface waters (Selvakumar et al., 2010, Roehrdanz et al., 2017).

In spite of numerous advancements, researchers continue to encounter challenges bridging the gap between small-scale pipe measurements of exfiltration and extrapolation to watershed (or larger) scale (e.g., Nguyen et al., 2021). Small scale pipe measurements are most frequently made *ex situ* in the laboratory with the advantage of full control over the variables that could affect exfiltration (e.g., Vollertson and Hvitved-Jacobsen, 2003; Nguyen et al., 2021; Nguyen and Venohr, 2021). Subsequently, many researchers have relied on modeling techniques to scale up these small scale measurements to watershed or larger scales, even extending to national levels (Karpf and Krebs, 2005; Held et al., 2006). However, as demonstrated by Wolf et al. (2006), discrepancies in exfiltration rates arise between small scale estimates, large scale models, and empirical data, presenting a persistent challenge in accurately extrapolating exfiltration dynamics. At the watershed scale, researchers mapping buried streams and sewer infrastructure using a high spatial resolution GIS model found sewer stream interactions were common and up to 70% of streams within a city were at risk of sewer leakage, but did not directly measure exfiltration (Hopkins and Bain, 2018). Researchers recently have made progress bridging these gaps between modeling efforts and *in situ* groundwater measurements using a GIS based model to predict areas of sewage exfiltration across a city and then demonstrating that this was a source of microbial and chemical pollution to the shallow groundwater (Lee et al., 2015, Roehrdanz et al., 2017).

Within a watershed, if sewage exfiltrates from a given pipe, this phenomenon could potentially act as a mechanism for surface water pollution in semi-arid urban systems where groundwater tables are low and sanitary sewer and storm drainage systems are typically separate. Sanitary sewer exfiltration could allow for the build-up of sewage in areas outside of the sewer pipe, which would then be mobilized in subsequent storm events and transported to storm drainage systems or other surface waters. This is illustrated in the diagram showing the multiple points of exfiltration that can build up to be mobilized when subsurface flow increases during rainstorms (Figure 1). Selvakumar et al. (2010) identified that the southwestern United States could be especially prone to this scenario where most urban sanitary sewer systems are above groundwater tables. This would be consistent with the widespread presence of human fecal markers in arid urban watersheds (Noble et al., 2003) regardless of land use or storm characteristics (Tiefenthaler et al., 2011).

The goal of this study is to estimate the potential human fecal contribution from wastewater exfiltration from sanitary sewers to stormwater in a semi-arid urban watershed with separate sanitary sewer and storm sewer systems. Our objective is to extrapolate localized *in situ* measurements of wastewater exfiltration to the watershed scale and to place it in the context of estimates of total fecal pollution mass loading in the watershed, specifically on its contribution to stormwater contamination. We utilize the human-specific genetic marker *Bacteroides* HF183 as a surrogate for human fecal pollution (Boehm et al., 2013). We focus on wet weather, as previous studies have consistently shown widespread prevalence of human fecal markers during such periods (Steele et al., 2018, Sauer et al., 2011).

Methods

General approach

This project had four integrated study design elements to link exfiltration from sanitary sewers to watershed-scale estimates of human fecal loading in stormwater runoff: (1) empirically measure exfiltration *in situ* to quantify volume loss, (2) estimate the HF183 mass loading from exfiltration volume loss, (3) empirically measure HF183 in stormwater runoff from small urban catchments to estimate subsurface transfer rates, (4)

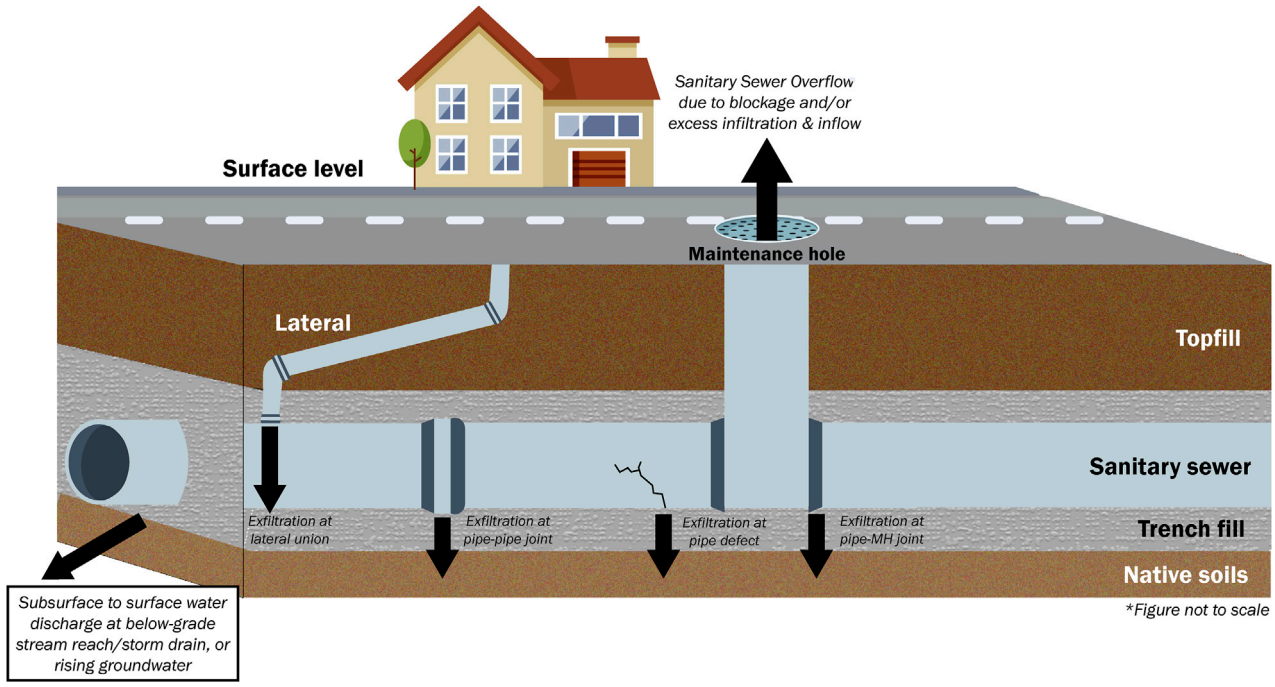

FIGURE 1
Diagram showing the basic concept of sewage exfiltration in this study. There are multiple examples of locations in sewer lines where sewage can exfiltrate. The exfiltrated sewage would accumulate in the soils prior to being transported to surface waters or storm drains by subsurface flow during rain or due to rising groundwater. See Nguyen et al., 2021 or Delesantro et al., 2024 for diagrams showing potential transport pathways to groundwater, storm drains, rivers, or creeks.

extrapolate human fecal pollutant loads from predicted exfiltration and subsurface transfer rates to the entire watershed.

Study watershed

This study was conducted in the 419 km^2 lower San Diego River Watershed (SDR) (Figure 2). Roughly 72% of the lower watershed is urbanized with the major land use being single family or multi-family residential. This waterbody is subject to a Total Maximum Daily Load (TMDL) based on exceedances of fecal indicator bacteria water quality standards (RWQCB 2010).

There are 1736 km of public sanitary sewer gravity lines servicing this watershed and conveys an average of 665 million liters of sewage per day. The most common sewer line diameter (70.4%) is 203.2 mm (i.e. 8 inches) with 90.9% between 152.8 and 304.8 mm (6–12inches; SanDAG Regional Data Warehouse). Approximately 138,510 developed parcels of which 94.2% are connected to the public sanitary sewer system via (mostly private) laterals. The remaining 5.8% of parcels utilize onsite wastewater treatment systems (OWTS or septic systems) and are isolated in the upper reaches of the watershed. There is no recycled water distribution system in this watershed.

Thirty year average annual rainfall in the watershed ranges from 26.2 cm near the coast to 27.7 cm inland. Most of this rainfall occurs between October and April, with the greatest precipitation occurring in February and March. Flows at the USGS (United States Geological Survey) gaging station at Fashion Valley (station 11023000, https://waterdata.usgs.gov/monitoring-location/11023000)– the most downstream on the SDR (river km 10) - can increase from <0.03 m^{3}s^{-1} to >300 m^{3}s^{-1} in less than a day when storms occur. There are no major dams in this section of the SDR.

Empirically measure sanitary sewer exfiltration

The empirical measurements of exfiltration are described in Griffith et al. (2024). Briefly, this method simulates typical in-pipe flows for collector pipes roughly 8- to 10-inches inside diameter. After isolating a section of sewer pipe utilizing inflatable or mechanical plugs and employing a sewer diversion, potable water is introduced at a constant flow rate in the upstream maintenance hole until the pipe is approximately one-third full and then the volume is recovered at the downstream maintenance hole using vacuum pumps. Sodium hypochlorite solution is added during the priming run and then the water is dechlorinated utilizing sodium thiosulfate prior to test runs. The volume is measured prior to starting the experiment and then measured at the end of experiment. Volume loss is the difference between the volume at the beginning and end of the experiment. Flow meters are used to ensure the pipe is never surcharged or pressurized, and video cameras or fluorescent dye is used to ensure the plugs do not leak. This experiment is repeated six times at each site achieving a measurement sensitivity of approximately 1 L (0.25 gallons) volume loss. Typically, 4,200 L (ca. 1,100 gallons) are used during each experimental run, which takes 0.75–1 h. Pipes of various materials (e.g., clay, polyvinyl chloride (PVC), lined pipe,

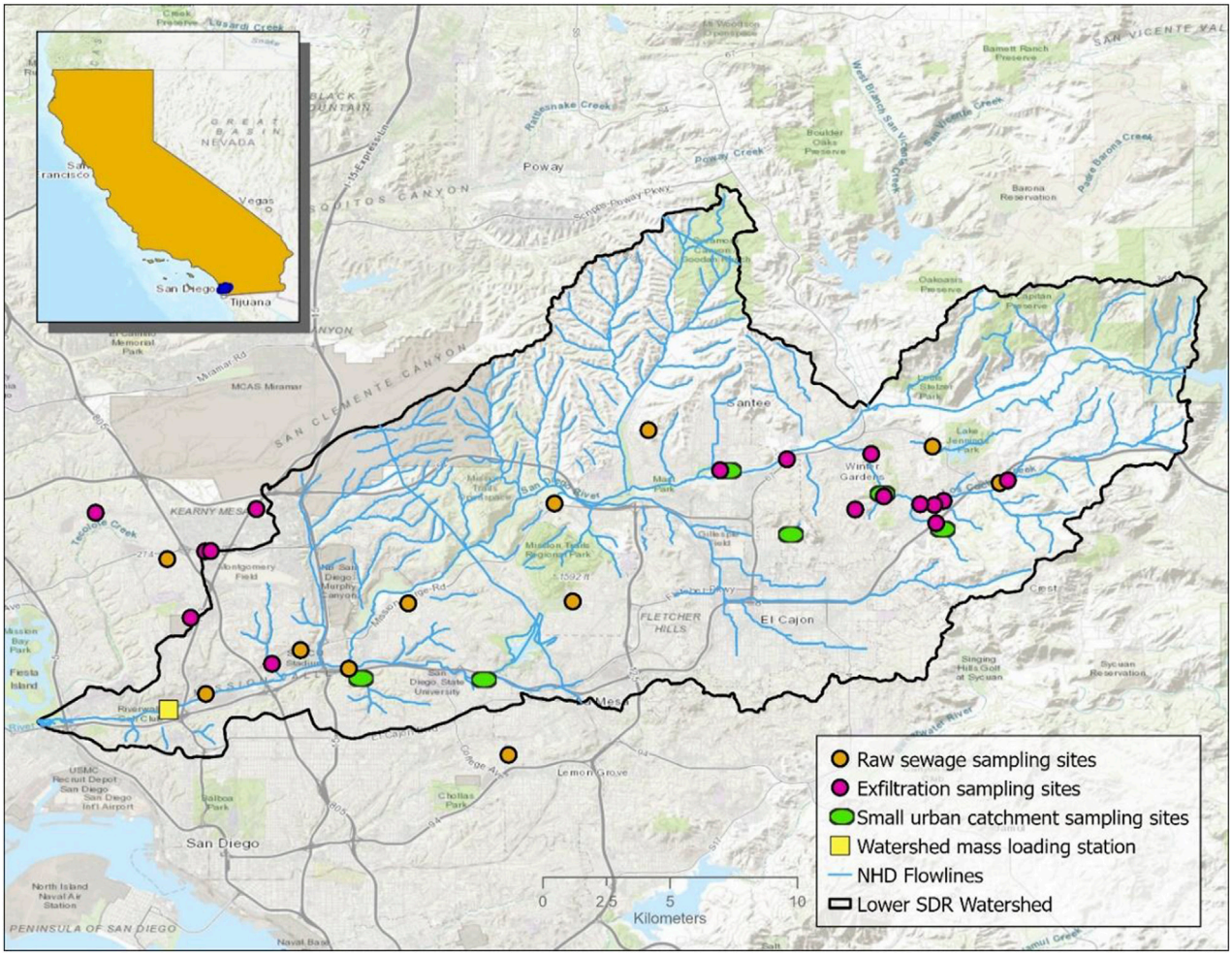

FIGURE 2
Map of the San Diego River watershed, including locations of raw sewage, exfiltration, and small urban catchment sampling.

i.e., cured in place pipe (CIPP) and RIBLOC) and ages (<1 year to 75 years) were tested.

Empirically measure HF183 in stormwater runoff from small catchments

There were six small urban catchments sampled for this portion of the study (Figure 1, See Supplementary Material for catchment characteristics and sampling inventory). Catchment areas were approximated using a combination of desktop delineation based on previous drainage area delineations, desktop delineations, and field verification. Some small catchments are co-located or upstream of major MS4 outfalls with existing drainage area delineations. Where existing delineations were available, these were leveraged (SanDAG regional data warehouse). Counts of parcels were approximated by superimposing catchment area over parcel maps. Where partial parcels overlapped with the catchment boundaries, they were included if more than 50% of the parcel was inside the boundary.

Each catchment consisted of almost entirely single- or multi-family residential land uses and had no other known sources of human fecal contamination present other than sanitary sewer exfiltration or private lateral exfiltration (Supplementary Tables SI1, SI2 Each catchment was between 3.6 and 31.2 ha (9 and 77 acres) with between 23 and 324 property parcels. The age of homes ranged from 20 to 70 years old and public sanitary sewer pipes were made of vitreous clay (VC) or PVC or plastic. Land use within the catchments was primarily low to medium intensity developed land with except for SDR-203A which was primarily scrubland (Supplementary Table SI2). Each catchment was sampled between 2 and 4 storm events totaling 19 site-events over the two-year sampling campaign.

Sampling consisted of locations where flow could be rated and measured using a combination of weirs, flumes, pressure transducers and/or area-velocity meters. Flow was measured using stage-discharge relationships, stage-velocity measurements, or both. Stage measurements were made using either a Sigma 950 Submerged AV sensor bubbler (Hach, Loveland, CO) or Onset HOBO level logger pressure transducer (Onset Computer

Co., Bourne, MA). Velocity measurements were made using a Hach acoustic Doppler sensor (Hach, Loveland, CO). To provide calibration checks for continuous flow estimates, instantaneous flow estimates were collected manually at multiple points throughout storm events, to the extent feasible. Instantaneous flow was estimated using the area velocity method; stage was estimated using visual observations and/or staff gauge measurements, and velocity measurements were collected using a handheld Marsh McBirney meter. Field sampling consisted of 10 L flow-weighted samples collected from 15 min subsamples for 6 h or until flow ceased. 6 h conforms with holding time criteria for fecal indicator bacteria analysis. If storm flows lasted longer than 6 h, then a second six-hour flow-weighted composite was collected. Samples were collected using Teflon tubing connected to a peristaltic pump. All parts that touched the sample were pre-cleaned prior to field deployment and equipment blanks were collected. Field blanks were collected during every storm. Additionally, precipitation data were collected at 1-min intervals from the County of San Diego ALERT gauge network (https://www.sdcfcd.org/content/sdc/sdcfcd/data.html) during each monitored storm event.

Measurement of HF183 in sewage

Raw sewage was collected in sanitary sewer pipes at 30 sites in the City of San Diego and the County of San Diego as described in Schiff et al. (2024) (2024, Appendix D) and Steele et al., in review. Briefly, pipes were accessed via sewer maintenance holes, sterilized PVC plastic tubing (Nalgene, United States) attached to a support pole and connected to a peristaltic pump (Masterflex I/P, Avantor, United States) was used to collect the sewage into sterile, rinsed polypropylene bottles, stored on ice in the dark, and transported to the laboratory for processing.

Laboratory analysis

All samples collected during small catchment sampling and sewage sampling were analyzed for HF183 and biofilm microbial communities. Once delivered to the laboratory, 100 mL portions of the well-mixed water samples were filtered through 0.4-micron polycarbonate membranes to collect bacteria, then flash frozen in liquid nitrogen and stored at −80°C prior to DNA extraction.

Frozen filters were processed in batches using commercially available DNA extraction kits (PowerSoil Pro Kit, Qiagen, MD, United States). DNA extraction followed the methods developed by Cao et al. (2017), Steele et al. (2018) and Steele et al., in review. Briefly, frozen filters were placed into sterile 2 mL plastic tubes preloaded with glass beads. A lysis buffer was added and the tubes were placed on an Omni BeadRuptor 24 (Omni International, GA, United States) at maximum speed for 2 min. The extraction then proceeded according to the manufacturer's instructions. DNA was eluted from the spin column in 100 µL of elution buffer. Aliquots of eluted sample DNA were stored at −80°C until they were analyzed by droplet digital PCR.

Negative extraction controls (NECs) containing only a lysis buffer in addition to a lysis buffer and control DNA (e.g., halophile or salmon testes DNA) were processed for every extraction in the same manner as the samples. These served to check for contamination from the laboratory or from other samples during the extraction of bacterial DNA from stormwater filters.

Human-associated *Bacteroidales* (HF183) were measured via the use of a droplet digital PCR assay following previously published protocols (Cao et al., 2017; Steele et al., 2018). Samples were measured in replicate, using at least 20,000 droplets for an absolute quantification of HF183. Field and equipment blanks were 100% nondetectable for HF183. Filtration controls were also 100% nondetectable.

Data analysis

Theory and calculations of HF183 mass load exfiltrating from sewer pipes

This study employs a set of calculations to extrapolate measured exfiltration rates from sewer pipes to a watershed-wide estimate of human fecal contamination from sewage exfiltration from an urban sewer system. Through empirical measurements of volume loss from the sanitary sewer pipe and HF183 concentrations measured in raw sewage across the watershed from a previous study (Steele et al., in review), we determined the mass of HF183 exiting the pipe alongside volume loss, as described in Equations 1, 2.

Volume loss per day was calculated according to Equation 1:

$$V_d = V_l \times L \times F_p \times t_d \quad (1)$$

where:

V_d = Daily volume loss from exfiltration measured *in situ* (L/day)

V_l = Volume loss from exfiltration measured *in situ* (L/km-sec)

L = Length of pipe (km)

F_p = Proportion of the sewer system that is able to exfiltrate (estimated at 0.75)

t_d = Duration of time the sewer pipe is flowing each day (sec/day)

Note that F_p is an estimate based on expert judgement.

HF183 mass loading from exfiltration was calculated according to Equation 2:

$$M_E = V_d \times D_s \times C_{tot} \quad (2)$$

where:

M_E = Estimated mass of HF183 from sanitary sewer exfiltration (gene copies)

V_d = Volume loss from exfiltration measured *in situ* (L/day)

D_s = Days of accumulation prior to storm event

C_{tot} = Concentration of HF183 at time t (gene copies/L)

Acknowledging the continuous flow of sewage and limited survival HF183 outside the gut, we refined our loading estimates by integrating accumulation and die-off dynamics until reaching equilibrium. Informed by die-off rates identified through a literature review, we augmented the exponential decay model (first-order decay equation after Zimmer-Faust et al., 2017 who measured the decay of HF183 in sediments and soils, Equation 3), to accommodate concentration increase over time based on the decay rate constant over the specified period. The decay rate (k) was 0.6983 per day (with a reported range of 0.96 to 0.5 per day).

First-order decay equation:

$$C_t = C_0 \times e^{(-k \times t)} \quad (3)$$

where:

C_t = Concentration of HF183 at time t (gene copies per L)
C_0 = Initial concentration of HF183 in sewage (gene copies per L)
k = Decay constant (per day)
t = Time point (days)

Implementation of this model was facilitated using R, allowing for iterative computation of the HF183 concentration for each day within a loop. Each iteration considers the previous day's concentration and the accumulation rate determined by the decay rate constant according to Equation 4. HF183 concentration in exfiltrated sewage, considering both the decay rate in soils and accumulation over time was calculated according to Equation 4:

$$C_{tot} = C_0 + \sum_{t=1}^{n} C_t \quad (4)$$

where:

C_t = Concentration of HF183 at time t (gene copies per L) Equation 3
C_0 = Initial concentration of HF183 in sewage (gene copies per L)
k = Decay constant (per day)
t = Time point (days) from 1 to n (n = 6)

Sampling small urban catchments enabled the derivation of a subsurface transfer coefficient to estimate the fraction of exfiltrated HF183 mobilized into stormwater. This estimation relied on comparing HF183 loads from storm events to those from exfiltration. The formulas detailing these calculations are provided below in Equations 5, 6.

Average HF183 mass loading from small urban catchments was calculated according to Equation 5:

$$M_R = 1 \Big/ N \sum_{i=1}^{N} \left(F_w^i \times V_s^i\right) \quad (5)$$

where:

M_R = Flow—weighted, per storm mean mass of HF183 from small catchments (gene copies)
F_w = Flow-weighted mean HF183 concentration in stormwater (gene copies per L)
V_s = Storm volume (L)
N = Number of storms

Calculation of the subsurface transfer coefficient estimating the fraction of the exfiltrated HF183 load from pipes within the small catchments (Equation 2) that is mobilized into stormwater during storm events at small catchments (Equation 4) was calculated according to Equation 6:

$$STC = M_R / M_E \quad (6)$$

Note that the STC is unitless as it is a ratio of HF183 mass estimated to reach the stormwater in the small catchments over the total HF183 mass calculated to be exfiltrated in the small catchments.

Combining these variables allowed us to extrapolate human fecal loading to the entire watershed, as outlined in Equation 7. This extrapolation enabled us to extend our findings beyond the sampled locations, providing a broader understanding of fecal contamination distribution and dynamics throughout the watershed.

Human fecal pollutant loads were extrapolated to the entire watershed utilizing Equation 7:

$$M_w = V_l \times L \times F_p \times t_d \times (C_{tot} \times D_s) \times STC \quad (7)$$

M_w = Mass of HF183 in watershed streams and rivers per storm (gene copies)
V_l = Volume loss from exfiltration measured *in situ* (L/km-sec)
L = Length of pipe section (km)
F_p = Proportion of the sewer system exfiltrating
t_d = Duration of time the sewer pipe is flowing each day (sec/day)
C_{tot} = Concentration of HF183 considering accumulation and decay over time (gene copies/L)
D_s = Days of accumulation prior to storm event (days)
STC = Subsurface transfer coefficient

The 95% CI for the human fecal pollutant load (M_w) was calculated using a pooled standard deviation taking the square root of the sum of the variance weighted by the sample size for each variable.

Sensitivity analysis methodology for assessing mass loading estimate

A sensitivity analysis was performed to gauge the influence of input variables on the mass loading estimate. Initially, a dataset was generated comprising randomly sampled combinations of input variables falling within predetermined ranges (Supplementary Table SI3). Subsequently, Spearman rank correlation coefficients were used to examine the relationships between the change in the HF183 mass loading estimate and the change in each input variable. A tornado diagram provided a visual representation of the mass loading estimate's sensitivity to variations in each input variable. Furthermore, multiple linear regression analysis was conducted to ascertain the proportion of variance explained by each input variable.

Results

Empirically measured sanitary sewer exfiltration

Volume loss measured *in situ* from sanitary sewer pipes in the SDR watershed in a prior study (Griffith et al., 2024) was used for the loading calculations. Volume loss ranged from 9.18×10^{-3} to 1.25×10^{-1} L per second per kilometer pipe length across 20 different pipe segments (Figure 3). There was no significant difference in volume loss between pipe materials or pipe age based on two-way ANOVA ($p = 0.31$ and $p = 0.50$, respectively). Therefore, we used an average volume loss across all 20 pipe segments of 3.78×10^{-2} (SD = 2.70×10^{-2}) L per second per kilometer for estimating exfiltration (V_l, Equation 1). Assuming all 1736 km of sewer pipe in the SDR watershed were exfiltrating every minute of every day, which is an obvious over-estimation, we estimate approximately 2.5×10^3 L of volume loss per km per day (4.25×10^6 L total when multiplied

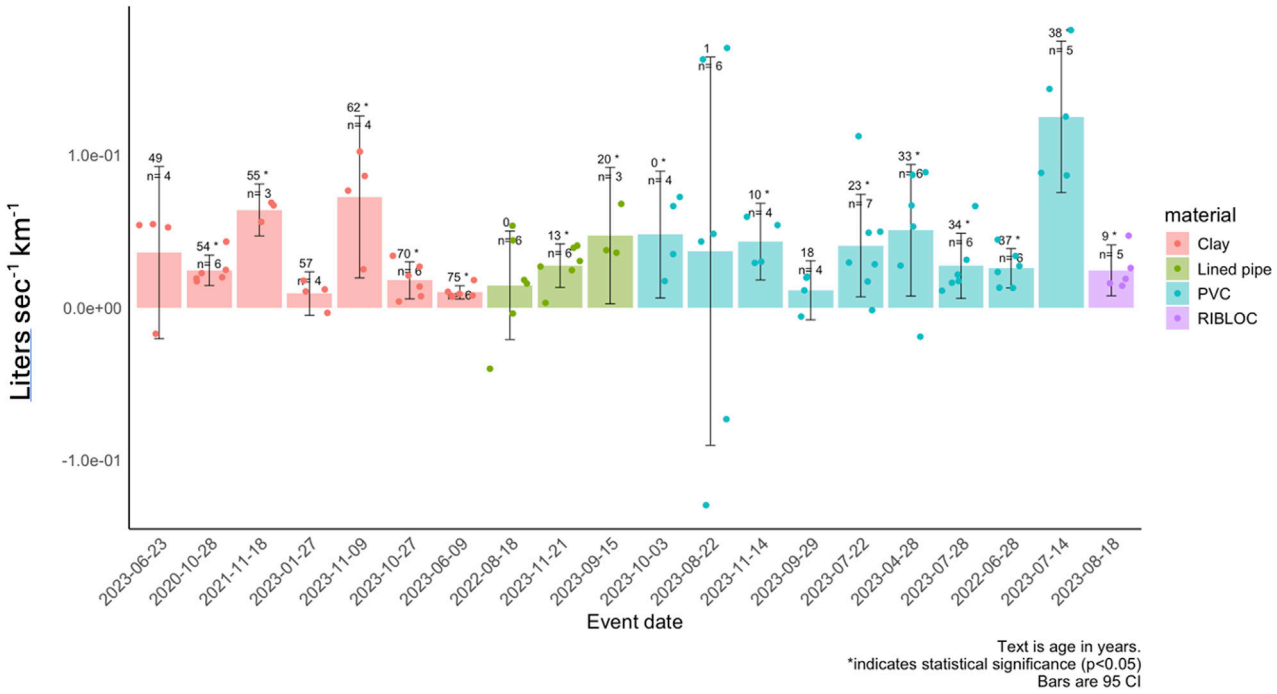

FIGURE 3
Measurements of volume loss per second per kilometer of sewer pipe in 20 different pipe segments of different pipe materials (lined pipe or cured in place pipe, RIBLOC or spiral wound lining, clay, or polyvinyl chloride or PVC). Bars represent average volume loss, dot symbols represent individual replicate measurements per segment, n = number of replicate measurements per pipe segment, number above bar is the age of the pipe segment in years since installation. Error bars are 95% confidence intervals. * indicates volume loss is significantly different from zero. Data from Griffith et al. (2024).

across all sewer pipes) from exfiltration in this watershed. We assume, based on expert opinion from sewer operators, that only a proportion (ca.75%) of the system would be able to exfiltrate because there is no flow in the pipe due to daily fluctuations in sewer use or because of infiltration (V_d, Equation 1).

Estimate of HF183 mass loading from exfiltration

The HF183 concentrations in raw sewage ranged from 1.31×10^6–3.25×10^8 HF183 gene copies per 100 mL across the 30 sites sampled in the SDR watershed (Figure 4). This range of concentration includes multiple seasons, multiple years (2019–2021), multiple pipe materials (clay, PVC, and lined pipe), and multiple pipe ages (0.02–75 years). The geometric mean HF183 concentration in raw sewage used for calculating the mass of HF813 exfiltrating was 5.05×10^7 (95% CI: 3.25×10^7 to 7.85×10^7) HF183 gene copies per 100 mL (C_0, Equation 3).

An estimated 2.86×10^{15} (SD = 1.08×10^7) HF183 gene copies exfiltrate from the sanitary sewers in the SDR every day based on volume loss and raw sewage concentrations. Accounting for the proportion (ca. 25%) of the sewer system that is not able to exfiltrate, and decay of HF183 after 7 days of exfiltration, an estimated 1.80×10^{17} (SD = 2.56×10^6) HF183 gene copies are available for sub-surface mobilization when rainstorms occur in the region ($V_l \times L \times F_p \times t_d \times (C_{tot} \times D_s)$, Equation 7). The number of gene copies cannot go beyond this estimate because decay becomes a dominant factor.

Empirically measure HF183 in stormwater runoff from small catchments

The geometric mean of flow-weighted mean HF183 concentrations ranged from 1.06×10^2 to 1.05×10^6 gene copies per liter across the six small urban catchments (Figure 5A). Results indicated this range of concentrations were not correlated to rainfall depth, intensity, or antecedent rainfall (data not shown). Site 0951 had the greatest flow-weighted mean concentration and site 1085 had the lowest flow-weighted mean concentration. At five site events (24%), HF183 concentrations were below the limit of quantification (estimated at 50 gene copies/100 mL). These low HF183 concentrations were not consistently found at one site, but occurred at four different catchments. Like HF183 concentrations, the geometric mean HF183 loading per storm event was variable among sites and storms in the small urban catchments (Figures 5B, C). The HF183 loading among catchments ranged from 9.01×10^7 to 2.06×10^{11} gene copies per storm event, with additional variability due to differences in flow and total runoff volume. The geometric mean HF183 loading across all catchments was 1.49×10^9 gene copies per storm event (95%CI: 5.95×10^8 to 2.29×10^9).

The geometric mean of the subsurface transfer coefficient (STC, Equation 6) across all six catchments was 8.27×10^{-5} (95% CI: 3.3 ×

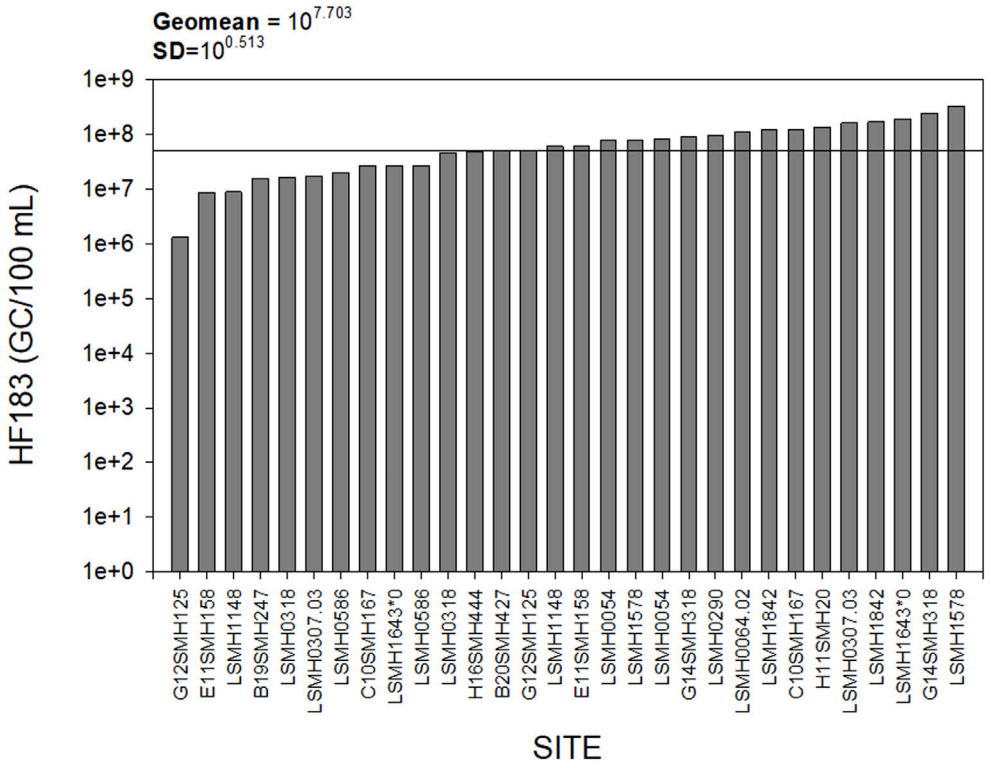

FIGURE 4
Concentration of HF183 gene copies/100 mL in raw sewage samples from the San Diego River watershed collected between 2019 and 2021. Data from Steele et al. (in review).

10^{-5} to 1.27×10^{-4}) (Figure 5D). This key metric was comparable among four of the six catchments ranging from 4.08×10^{-6} to 7.90×10^{-5} per storm event. Two catchments (951 and 098B) had greater subsurface transfer coefficients at 4.98×10^{-3} and 1.26×10^{-4}, respectively. The catchment above site 0951 had substantially greater HF183 concentrations, HF183 loading, and HF183 loading per km sewer pipe. We note that this catchment had the greatest number of parcels, was one of the older developments measured, and had a reported sewage spill within the last 10 years. The catchment above site 098B had the third highest number of parcels and had no reported sewage spills. These two catchments had the second most and third most km of sewer pipe (Supplementary Table SI1).

Extrapolation to watershed

Based on the measured sanitary sewer exfiltration volume loss, the concentration of HF183 in raw sewage, the decay rate of HF183 in soils, and the subsurface transfer coefficient, we estimate 1.49×10^{13} gene copies per storm event (95% CI: 1.79×10^{12} to 3.59×10^{13} gene copies per storm event) are discharged from the entire watershed. With an average of 10 storms annually, we estimate 10^{14} gene copies are discharged each wet season.

Sensitivity analysis indicated the most important factors controlling our estimates of human fecal loading from exfiltration was empirical measurements of volume loss and the subsurface transfer coefficient (Figure 6). These each accounted for the greatest proportion of the variation in the HF183 loading estimate: subsurface transfer coefficient accounted for 32% and volume loss accounted for 31% of the variance in the sensitivity analysis. After the subsurface transfer coefficient and volume loss variables, the next most important variable was the estimate of the proportion of sewer pipe miles that was not exfiltrating (i.e., were infiltrating or had no flow). The least sensitive variables were the HF183 concentration in raw sewage and the HF183 decay rate, which each accounted for <1% of the variability in our sensitivity analysis.

The estimate of 10^{13} HF183 gene copies per storm event aligns well with the estimate of HF183 mass loading at the end of the watershed. The mass loading at the end of the watershed was measured to be 10^{12}–10^{15} HF183 gene copies per storm event across 25 site-events of various sizes, durations, and antecedent dry periods (Schiff et al., 2024).

Discussion

This study successfully used empirical exfiltration rates and extrapolated the subsurface transport of exfiltrated sewage to stormwater runoff in a municipal separate storm sewer system at a watershed scale. The result was that exfiltration could possibly account for a substantial proportion of the human fecal pollution–as measured by the human genetic marker HF183 – in the San Diego River watershed during wet weather (Schiff et al., 2024). These results are substantiated by the presence of microbial community

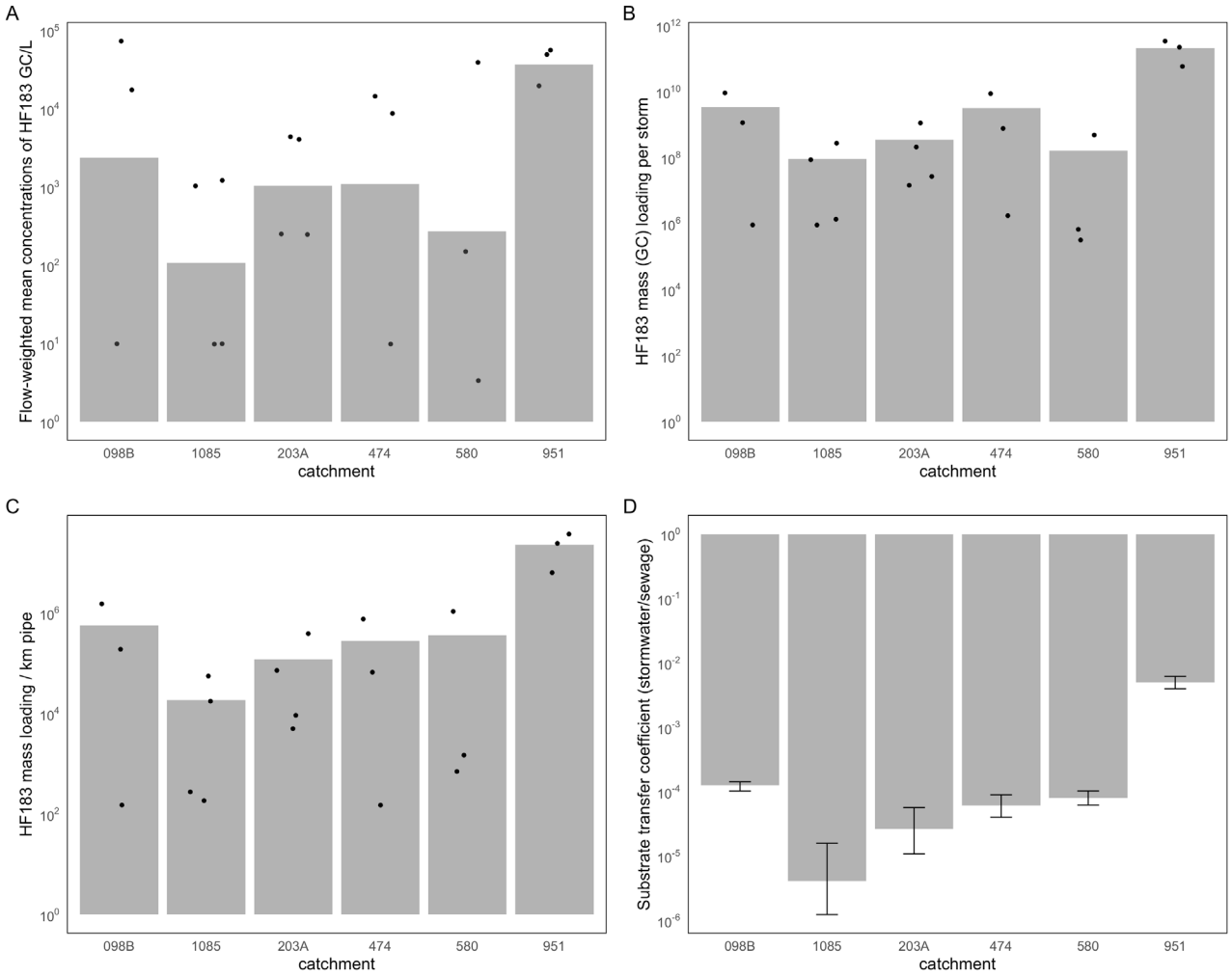

FIGURE 5
Results from small urban catchment site samples for **(A)** flow-weighted mean concentration per storm event, **(B)** HF183 mass loading per storm event, **(C)** HF183 mass loading per storm event normalized by the length of sewer pipe in each catchment, and **(D)** the calculated subsurface transfer coefficient per storm event. The subsurface transfer coefficients are calculated as the ratio of measured stormwater HF183 load per storm event to predicted HF183 load per storm event from sanitary sewer exfiltration within the catchment.

analysis of sanitary sewer biofilms (Steele et al. in review) which revealed a persistent but dilute sewer community signature in stormwater and chemical markers of sewage such as caffeine/sucralose ratios which were found to increase during storm events (Pinongcos et al., 2022).

Our estimates of HF183 mass loading from the SDR due to sanitary sewer exfiltration and subsurface transport were within the range of estimated mass loading in stormwater at the bottom of the watershed. However, sanitary sewer exfiltration is one of multiple potential sources of HF183 during wet weather. A comparable level of HF183 loading during wet weather is estimated from sanitary sewer overflows (Zimmer-Faust et al., 2021). The sanitary sewer overflow data are based on reported overflows that purportedly reached receiving waters (https://www.waterboards.ca.gov/water_issues/programs/sso/sso_map/sso_priv.html https://www.waterboards.ca.gov/water_issues/programs/sso/sso_map/sso_pub.html). Delesantro et al. (2024) also found that in highly developed areas there was substantial contribution of wastewater derived nitrogen from both surface and subsurface flows. Another potential source of human fecal pollution in the SDR is people experiencing homelessness, a widespread phenomenon along the river corridor. However, studies of HF183 loading during storm events from defecation by people experiencing homelessness are estimated to be at least one to two orders of magnitude lower than what is estimated via exfiltration (Hinds et al., 2024).

There are many potential sources of error in the estimation of human fecal loading from exfiltration. Our sensitivity analysis examined the influence of uncertainty in the measured exfiltration rate. Sources of uncertainty included the exfiltration volume loss, concentration of HF183 in raw sewage, the decay rate of HF183 after exiting the sewer pipe in the subsurface zone, the subsurface transport coefficient, and the proportion of the sewer system (a that is exfiltrating. Of these, exfiltration volume loss had the greatest impact on HF183 loading. Intuitively, even small changes in volume loss when extrapolated to hundreds of miles of sewer collection system will greatly influence mass loading

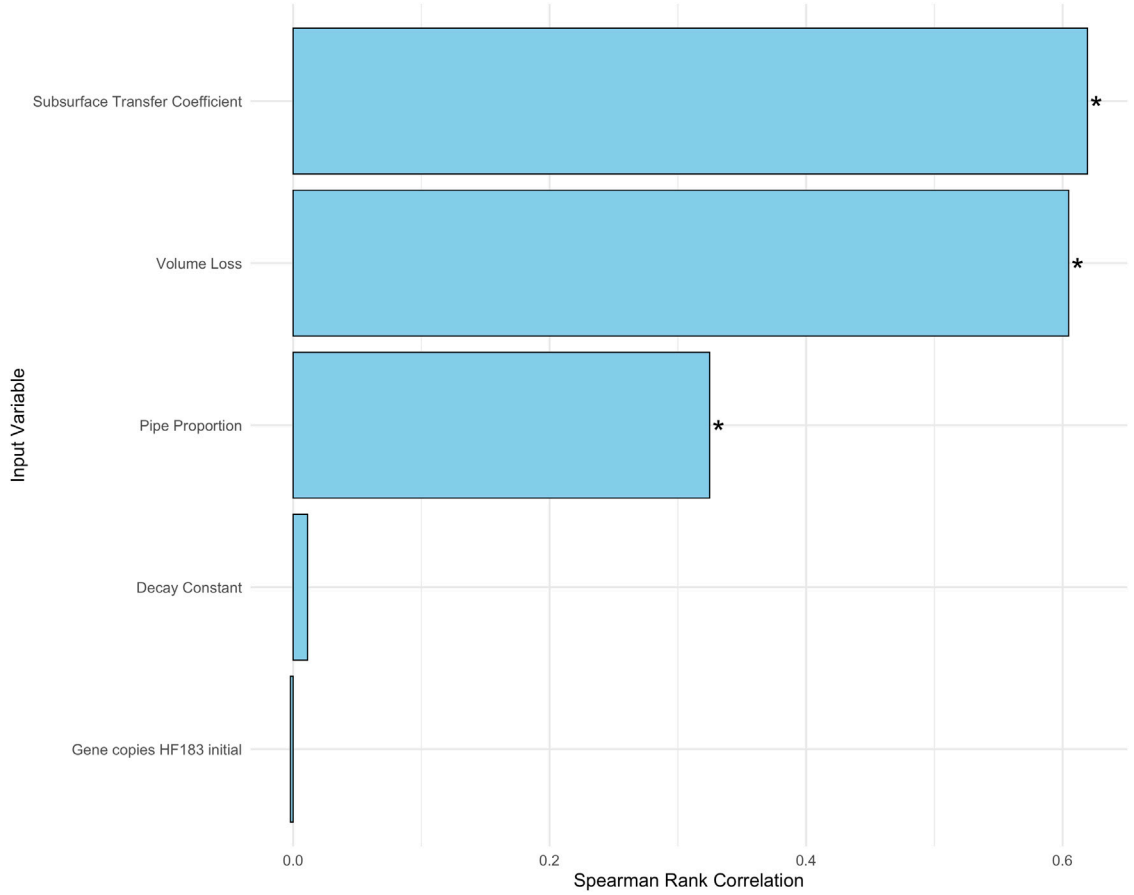

FIGURE 6
Tornado plot indicating the relative influence of the different variables used to estimate end of the watershed HF183 loading from sanitary sewer exfiltration. The greater the correlation, the greater the influence on the loading estimate. Asterisks denote that Spearman rank correlations are significant.

calculations. As noted in Griffith et al. (2024) the use of potable water, may have resulted in an increased measured rate of exfiltration compared to what may have been observed using sewage. However, the presence of sewage material and colmation layer in pipes for the *in situ* empirical measurements of exfiltration likely attenuated this difference. The accuracy of exfiltration rates should be refined as this new measurement technology is implemented more broadly (Griffith et al., 2024), but the exfiltration rates measured during this study (3.78×10^{-2} L per s-km) were within the range of exfiltration rates empirically measured by other researchers and estimated from modeled leakage rates (10^{-9}–10 L per s-km) (Nguyen et al., 2021). This rate also corresponds to a rate of 2.5×10^{3} L of volume loss per km per day, similar to the ASTM standard for hydrostatic testing of vitrified clay pipes 3.76×10^{3} L volume loss per km per day (for 203.2 mm diameter pipes; ASTM C1901-03a, 2022). Application of this approach to estimating watershed-wide exfiltration outside of the original study area will necessarily be subject to the uncertainties inherent to the location and the method for measuring or estimating exfiltration.

The proportion of pipe exfiltrating had the third greatest impact on the sensitivity analysis. This is notable because it was a value that was primarily based on expert opinion of the sewer treatment plant operators. It was assumed that a substantial portion of the sewer pipes would not be flowing for 6 h a day or were not able to exfiltrate due to external circumstances. There is also support for 75% of the system being able to exfiltrate in the literature (e.g., Ellis et al., 2004). Detailed flow measurements or modeling in the collection system could refine this number to ground-truth this assumption.

A noteworthy case study from the exfiltration measurements is that CIPP lining of pipes with known defects can reduce or stop exfiltration. Our study measured statistically significant volume loss in a 54-year old clay pipe. This section of pipe was subsequently lined using CIPP technology. Re-testing of the newly lined pipe resulted in no statistically significant volume loss. We assume but are not certain that the volume loss we did measure in other CIPP lined pipes, which were between 13–20 years old, resulted from either improper installation, subsequent defects, material deterioration with age, or perhaps losses in the non-lined portions of the test segment (i.e., at the pipe maintenance hole junctions).

Exfiltration in other studies indicate that subsurface contributions from the sanitary sewer system regularly occur. Ellis et al. (2004) estimated that 75% of the sanitary sewer system in small Prague catchments experienced exfiltration. Roehrdanz

et al. (2017) found increased levels of the artificial sweetener acesulfame, tryptophan-like fluorescent dissolved organic matter, nitrate, and a stable isotope of water ($\delta^{18}O$) – which are all indicators of raw sewage–in shallow groundwater from a small urban community in California. Delesantro et al. (2022) demonstrated that the hydrogeomorphic position of sewer pipes was a primary contributor to catchment wastewater derived nitrogen loading and that nitrogen loading was more sensitive to flow when pipes were in wet areas of the landscape, suggesting that subsurface flow paths and groundwater table depth drives loading from pipes to streams. Moreover, the strength of the association between exfiltration probability and indicators of wastewater increased when multiple pipe attributes, distance weighting, and groundwater flow direction were considered. Rieckermann et al. (2005) used multiple tracers and estimated as much as 10% of the sewage volume exfiltrated into shallow groundwater in a study from Switzerland. This study estimated as much as 0.6% of the daily average sewage volume exfiltrating where it could be mobilized by shallow groundwater. This low percentage is partly due to the high volume of sewage that is conveyed though this system. Differences in infrastructure, geology, topography, and hydrologic conditions between the San Diego River watershed and studies performed in other locations (e.g., the east coast of the United States or Europe) likely also account for the differences between our exfiltration rates and previous studies.

While the empirical evidence points to exfiltration as a potentially large source of human fecal pollution in the SDR, the exact mechanisms of subsurface transport are not known. In the SDR watershed, 76% of sewer pipe segments are within 100 m of a storm drain or waterbody and 36% are within 7 m of a storm drain or waterbody (Supplementary Figure S1). Ellis et al. (2004) notes that exfiltration is a function of hydrostatic head and backfill material, and that the rate of exfiltration can change over time. Vollertson and Hvitved-Jacobsen (2003) indicated that exfiltration rates can be initially high but reach steady state within an hour. Our study utilized multiple runs to measure exfiltration cumulatively lasting up to 6 h of flow. Rutsch et al. (2008) discusses the importance of the colmation layer (a layer of organic rich particles), sediment, and biofilm that can clog cracks and joint separations, to accurately model exfiltration. Since we utilized *in situ* pipes for empirical measurements of exfiltration, much of the sediment, biofilm, and colmation layer were likely present. But exactly how exfiltrated sewage can accumulate in the subsurface, and then get mobilized either by rising groundwater, transported downgradient until reaching surface waters, or infiltrating storm drains remains an area of future research for the San Diego River watershed (Figure 1).

This project did not address public health risk of exfiltrated sewage, but other projects have demonstrated an increase in public health risk during wet weather. Arnold et al. (2017) conducted an epidemiology study in San Diego and found an increased risk of highly credible gastrointestinal illness in those entering the ocean during or immediately following a rainstorm compared to those not entering the ocean. Soller et al. (2017) confirmed these findings using a quantitative microbial risk assessment (QMRA) based on the work of Steele et al. (2018) who measured human specific genetic markers as well as human pathogens in wet weather runoff from the San Diego River.

While we estimated human fecal loading from exfiltration during wet weather, dry weather does not appear to be a substantial source of fecal loading in the San Diego River. Schiff et al. (2023) conducted multiple surveys of the San Diego River during dry weather, including immediately after a storm and again at the end of the wet season, and HF183 was infrequently quantified. Where HF183 was quantified, surface and not subsurface contributions were identified as the likely source.

Summary and conclusion

In this study we extrapolated empirical measurements of sewage exfiltration to a 419 km^2 watershed and estimated a daily rate of 2.5×10^3 L per kilometer per day. A human fecal pollution load of 1.5×10^{13} (95% CI: 1.79×10^{12} to 3.59×10^{13}) HF183 gene copies per storm was calculated from the exfiltration rate, the proportion of sewer pipes that were exfiltrating, the decay rate of HF183, and the proportion of exfiltrated sewage that reaches storm drains, streams, and rivers. This human fecal pollution load was similar in scale to the measured human fecal pollution mass loading estimates in stormwater for this watershed and comparable to independently-measured tracers of sewage. We note that this is the first application based on this empirical measurement of exfiltration and recommend additional testing in other systems and geographies to help refine the estimates used in the calculations. Refinements to the measurements, including improved understanding of sewage flow and empirical measurements with artificial sewage would help improve the estimates. We also recommend future studies on refining the understanding of subsurface transport mechanisms of exfiltrated sewage.

Data availability statement

The datasets presented in this study can be found in online repositories. The names of the repository/repositories and accession number(s) can be found in the article/Supplementary Material.

Author contributions

JS: Conceptualization, Data curation, Formal Analysis, Investigation, Methodology, Supervision, Validation, Visualization, Writing–original draft, Writing–review and editing. AG-F: Data curation, Formal Analysis, Investigation, Methodology, Validation, Visualization, Writing–review and editing. JG: Conceptualization, Investigation, Methodology, Project administration, Resources, Supervision, Writing–review and editing. DE: Data curation, Investigation, Methodology, Writing–review and editing. SW: Data curation, Investigation, Methodology, Writing–review and editing. KS: Conceptualization, Formal Analysis, Funding acquisition, Investigation, Methodology, Project administration, Resources, Supervision, Visualization, Writing–original draft, Writing–review and editing.

Funding

The author(s) declare that financial support was received for the research, authorship, and/or publication of this article. This project was partially funded by the City of San Diego, County of San Diego, Padre Dam Municipal Water District, City of El Cajon and City of La Mesa under County of San Diego Contract 563356.

Acknowledgments

The authors are grateful for the guidance of the project Technical Review Committee; Martha Tremblay, Patricia Holden, Sandra McLellan, John Izbicki, Mia Mattioli, Jennifer Wolch. The authors are grateful for the partnership and collaboration with the collection system professionals at the City of San Diego, County of San Diego, Padre Dam Municipal Water District, and City of La Mesa including Daniel Carter, Jeff Van Every, Margaret Llagas, Terrell Powell, Bradley Burns, Sean Willis, Gary Harris, Ted Kautzman, Jimmy Vargas, and Daniel Lockhart. The authors appreciate discussions and suggestions provided by Steve Jepsen. The authors are grateful for the project Steering Committee.

Conflict of interest

Authors DE and SW were employed by WSP.

The remaining authors declare that the research was conducted in the absence of any commercial or financial relationships that could be construed as a potential conflict of interest.

Publisher's note

All claims expressed in this article are solely those of the authors and do not necessarily represent those of their affiliated organizations, or those of the publisher, the editors and the reviewers. Any product that may be evaluated in this article, or claim that may be made by its manufacturer, is not guaranteed or endorsed by the publisher.

Supplementary material

The Supplementary Material for this article can be found online at: https://www.frontiersin.org/articles/10.3389/fenvs.2024.1458153/full#supplementary-material

References

Arnold, B. F., Schiff, K. C., Ercumen, A., Benjamin-Chung, J., Steele, J. A., Griffith, J. F., et al. (2017). Acute illness among surfers after exposure to seawater in dry-and wet-weather conditions. *Am. J. Epidemiol.* 186 (7), 866–875. doi:10.1093/aje/kwx019

ASTM Standard C1091-03a (2022). *Standard test method for hydrostatic infiltration testing of vitrified clay pipe lines*. West Conshohocken, PA: ASTM International.

Beheshti, M., Sægrov, S., and Ugarelli, R. (2015). Infiltration/inflow assessment and detection in urban sewer system. *Vann* 01, 24–34. Available at: https://vannforeningen.no/wp-content/uploads/2015/01/Beheshti.pdf.

Boehm, A. B., Van De Werfhorst, L. C., Griffith, J. F., Holden, P. A., Jay, J. A., Shanks, O. C., et al. (2013). Performance of forty-one microbial source tracking methods: a twenty-seven lab evaluation study. *Water Res.* 47 (18), 6812–6828. doi:10.1016/j.watres.2012.12.046

Cao, Y., Anderson, G. L., Boehm, A. B., Holden, P. A., Jay, J. A., and Griffith, J. F. (2017) "Determination of DNA-based fecal marker aging characteristics for use in quantitative microbial source tracking," in *Technical report 978. Southern California coastal water research project*. Available at: http://ftp.sccwrp.org/pub/download/DOCUMENTS/TechnicalReports/978_DNA_FecalMarkerAgingQuantMicrobialSourceTracking.pdf.

Crawford, D., Eckley, P. L., and Pier, E. (1999). Methods for estimating inflow and infiltration into sanitary sewers. *J. Water Manag. Model.*, R204–R217. doi:10.14796/JWMM.R204-17

Delesantro, J. M., Duncan, J. M., Riveros-Iregui, D., Blaszczak, J. R., Bernhardt, E. S., Urban, D. L., et al. (2022). The nonpoint sources and transport of baseflow nitrogen loading across a developed rural-urban gradient. *Water Resour. Res.* 58 (7), e2021WR031533. doi:10.1029/2021wr031533

Delesantro, J. M., Duncan, J. M., Riveros-Iregui, D., Whitmore, K. M., and Band, L. E. (2024). High frequency monitoring and nitrate sourcing reveals baseflow and stormflow controls on total dissolved nitrogen and carbon export along a rural-urban gradient. *Water Resour. Res.* 60. doi:10.1029/2023wr036750

Ellis, J. B., Revitt, D. M., Blackwood, D. J., and Gilmour, D. J. (2004). "Leaky sewers: assessing the hydrology and impact of exfiltration in urban sewers," in *Hydrology: science and practice for the 21st century* (London, England: British Hydrological Society) 2, 266–271.

Griffith, J. F., Steele, J. A., Gonzalez-Fernández, A., and Schiff, K. C. (2024). Towards quantifying exfiltration from in situ sanitary sewer pipes. *Front. Environ. Sci.* doi:10.3389/fenvs.2024.1458146

Held, I., Wolf, L., Eiswirth, M., and Hötzl, H. (2006). "Impacts of sewer leakage on urban groundwater: review of a case study in Germany," in *Urban groundwater management and sustainability* (Netherlands: Springer), 189–204.

Hinds, J. B., Garg, T., Hutmacher, S., Nguyen, A., Zheng, Z., Griffith, J., et al. (2024). Assessing the defecation practices of unsheltered individuals and their contributions to microbial water quality in an arid, urban watershed. *Sci. Total Environ.* 920, 170708. doi:10.1016/j.scitotenv.2024.170708

Hopkins, K. G., and Bain, D. J. (2018). Research Note: mapping spatial patterns in sewer age, material, and proximity to surface waterways to infer sewer leakage hotspots. *Landsc. Urban Plan.* 170, 320–324. doi:10.1016/j.landurbplan.2017.04.011

Karpf, C., Hoeft, S., Scheffer, C., Fuchs, L., and Krebs, P. (2011). Groundwater infiltration, surface water inflow and sewerage exfiltration considering hydrodynamic conditions in sewer systems. *Water Sci. Technol.* 63 (9), 1841–1848. doi:10.2166/wst.2011.388

Karpf, K., and Krebs, P. (2005). Application of a leakage model to assess exfiltration from sewers. *Water Sci. and Technol.* 52 (5), 225–231. doi:10.2166/wst.2005.0137

Lee, D. G., Roehrdanz, P. R., Feraud, M., Ervin, J., Anumol, T., Jia, A., et al. (2015). Wastewater compounds in urban shallow groundwater wells correspond to exfiltration probabilities of nearby sewers. *Water Res.* 85, 467–475. doi:10.1016/j.watres.2015.08.048

Nguyen, H. H., Peche, A., and Venohr, M. (2021). Modelling of sewer exfiltration to groundwater in urban wastewater systems: a critical review. *J. Hydrology* 596, 126130. doi:10.1016/j.jhydrol.2021.126130

Nguyen, H. H., and Venohr, M. (2021). Harmonized assessment of nutrient pollution from urban systems including losses from sewer exfiltration: a case study in Germany. *Environ. Sci. Pollut. Res.* 28, 63878–63893. doi:10.1007/s11356-021-12440-9

Noble, R. T., Weisberg, S. B., Leecaster, M. K., McGee, C. D., Dorsey, J. H., Vainik, P., et al. (2003). Storm effects on regional beach water quality along the southern California shoreline. *J. Water Health* 1 (1), 23–31. doi:10.2166/wh.2003.0004

Pinongcos, F., Mladenov, N., Calderon, J., Verbyla, M. E., Kinoshita, A. M., Gersberg, R., et al. (2022). Chemical and microbial markers for discriminating sanitary sewer contamination in coastal, urban streams. *ACS ES&T Water* 2, 1747–1759. doi:10.1021/acsestwater.2c00265

Rutsch, M., Rieckermann, J., Cullmann, J., Ellis, J. B., Vollertsen, J., and Krebs, P. (2008). Towards a better understanding of sewer exfiltration. *Water Res.* 42 (10-11), 2385–2394. doi:10.1016/j.watres.2008.01.019

Rieckermann, J., Borsuk, M., Reichert, P., and Gujer, W. (2005). A novel tracer method for estimating sewer exfiltration. *Water. Resour.* 41. doi:10.1029/2004wr003699

Roehrdanz, P. R., Feraud, M., Lee, D. G., Means, J. C., Snyder, S. A., and Holden, P. A. (2017). Spatial models of sewer pipe leakage predict the occurrence of wastewater indicators in shallow urban groundwater. *Environ. Sci. Technol.* 451, 1213–1223. doi:10.1021/acs.est.6b05015

Sauer, E. P., VandeWalle, J. L., Bootsma, M. J., and McLellan, S. L. (2011). Detection of the human specific Bacteroides genetic marker provides evidence of widespread sewage contamination of stormwater in the urban environment. *Water. Res.* 45, 4081–4091. doi:10.1016/j.watres.2011.04.049

Schiff, K. C., Griffith, J. F., Steele, J. A., and Gonzalez-Fernandez, A. (2024) "Summary of technical research: quantifying sources of human fecal pollution in the lower San

Diego River Watershed," in *Technical report 1380. Southern California coastal water research project*. Costa Mesa, CA.

Schiff, K. C., Griffith, J. F., Steele, J. A., and Zimmer-Faust, A. G. (2023). Dry and wet weather survey for human fecal sources in the San Diego River Watershed. *Water* 15, 2239. doi:10.3390/w15122239

Selvakumar, A., Field, R., Burgess, E., and Amick, R. (2010). Exfiltration in sanitary sewer systems in the US. *Urban Water J.* 1 (3), 227–234. doi:10.1080/15730620410001732017

Sercu, B., Van De Werfhorst, L. C., Murray, J. L., and Holden, P. A. (2011). Sewage exfiltration as a source of storm drain contamination during dry weather in urban watersheds. *Environ. Sci. and Technol.* 45 (17), 7151–7157. doi:10.1021/es200981k

Sercu, B., Werfhorst, L. C. V. D., Murray, J., and Holden, P. A. (2009). Storm drains are sources of human fecal pollution during dry weather in three urban southern California watersheds. *Environ. Sci. Technol.* 43, 293–298. doi:10.1021/es801505p

Soller, J. A., Schoen, M., Steele, J. A., Griffith, J. F., and Schiff, K. C. (2017). Incidence of gastrointestinal illness following wet weather recreational exposures: harmonization of quantitative microbial risk assessment with an epidemiologic investigation of surfers. *Water Res.* 121, 280–289. doi:10.1016/j.watres.2017.05.017

Staufer, P., Scheidegger, A., and Rieckermann, J. (2012). Assessing the performance of sewer rehabilitation on the reduction of infiltration and inflow. *Water Res.* 46 (16), 5185–5196. doi:10.1016/j.watres.2012.07.001

Steele, J. A., Blackwood, A. D., Griffith, J. F., Noble, R. T., and Schiff, K. C. (2018). Quantification of pathogens and markers of fecal contamination during storm events along popular surfing beaches in San Diego, California. *Water Res.* 136, 137–149. doi:10.1016/j.watres.2018.01.056

Steele, J. A., McCargar, D. E., Wallace, S., Zimmer-Faust, A. G., Langlois, K., Griffith, M. L., et al. In review. Application of a microbial community sequencing approach to identify contamination from sewers in an urban watershed. *Environ. Pollut.*

Tiefenthaler, L. L., Stein, E. D., and Schiff, K. C. (2011). Levels and patterns of fecal indicator bacteria in stormwater runoff from homogenous land use sites and urban watersheds. *J. Water Health* 9, 279–290. doi:10.2166/wh.2010.056

Vollertson, J., and Hvitved-Jacobsen, T. (2003). Exfiltration from gravity sewer: a pilot scale study. *Water Sci. Technol.* 47 (4), 66–76. doi:10.2166/wst.2003.0223

Wolf, L., Eiswirth, M., and Hötzl, H. (2006). Assessing sewer–groundwater interaction at the city scale based on individual sewer defects and marker species distributions. *Environ. Geol.* 49, 849–857. doi:10.1007/s00254-006-0180-x

Zimmer-Faust, A., Schiff, K., and Nguyen, D. (2021). Quantify sources of human fecal contamination loading to the San Diego river, technical memorandum, task 8A: compiling and analyzing existing data for sanitary sewer overflow events. *Rep. Prep. San Diego River Investigative Order Steer. Comm. South. Calif. Coast. Water Res. Proj. Costa Mesa, CA*, 28.

Zimmer-Faust, A. G., Thulsiraj, V., Marambio-Jones, C., Cao, Y., Griffith, J. F., Holden, P. A., et al. (2017). Effect of freshwater sediment characteristics on the persistence of fecal indicator bacteria and genetic markers within a Southern California watershed. *Water Res.* 119, 1–11. doi:10.1016/j.watres.2017.04.028

frontiers | Frontiers in Environmental Science

TYPE Original Research
PUBLISHED 23 January 2025
DOI 10.3389/fenvs.2024.1458146

Check for updates

OPEN ACCESS

EDITED BY
Vivek Pulikkal,
Civil & Environmental Consultants, Inc.,
United States

REVIEWED BY
Joseph Delesantro,
The Pennsylvania State University (PSU),
United States
Abhisek Manikonda,
Carollo Engineers, United States

*CORRESPONDENCE
John F. Griffith,
johng@sccwrp.org
Joshua A. Steele,
joshuas@sccwrp.org

RECEIVED 02 July 2024
ACCEPTED 15 November 2024
PUBLISHED 23 January 2025

CITATION
Griffith JF, Steele JA, Gonzalez-Fernández A and Schiff KC (2025) Towards quantifying exfiltration from *in situ* sanitary sewer pipes. *Front. Environ. Sci.* 12:1458146. doi: 10.3389/fenvs.2024.1458146

COPYRIGHT
© 2025 Griffith, Steele, Gonzalez-Fernández and Schiff. This is an open-access article distributed under the terms of the Creative Commons Attribution License (CC BY). The use, distribution or reproduction in other forums is permitted, provided the original author(s) and the copyright owner(s) are credited and that the original publication in this journal is cited, in accordance with accepted academic practice. No use, distribution or reproduction is permitted which does not comply with these terms.

Towards quantifying exfiltration from *in situ* sanitary sewer pipes

John F. Griffith*, Joshua A. Steele*, Adriana Gonzalez-Fernández and Kenneth C. Schiff

Southern California Coastal Water Research Project, Costa Mesa, CA, United States

Exfiltration from sanitary sewers has been researched for many years because of its potential impact on shallow groundwater or surface water, but measurements of exfiltration *in situ* are rare. Most previous measurements of sanitary sewer exfiltration have been done in the laboratory, in the field using natural, chemical or pharmaceutical tracers or modeled. Relatively few studies have employed physical measurements of volume loss in field settings. Here, we design, test, and apply at a watershed scale, a new methodology for measuring volume loss from sanitary sewer pipes that are currently in use and under typical operating conditions (i.e., not pressurized). The measurement system works by: (1) isolating a section of sanitary sewer between maintenance holes using a sewer bypass or equivalent, (2) introducing roughly 4,200 L of water at a controlled rate into the upstream inspection hole so that pipes remain one-third to one-half full, (3) using vacuum pumps to recover the introduced water at the downstream inspection hole, then (4) measuring differences in the volume from what was pumped into the inspection hole to what was recovered. This process is repeated up to six times to achieve a sensitivity of 0.95 L per experimental pipe segment. This technique was applied to 23 pipe segments of various ages and materials of construction that were selected to be a representative sample of the pipes throughout San Diego. Collectively, these pipes averaged averaged 3.78×10^{-2} L/s-km exfiltration rates (95%CI: 4.96×10^{-2}, 2.60×10^{-2}). Two of the pipe segments were infiltrating groundwater. Six pipe segments were not statistically different from zero (i.e., no exfiltration). There was no statistical difference between pipe segments of differing ages ($p = 0.5$) or materials of construction ($p = 0.3$). This study represents an initial effort at measuring exfiltration from *in situ* sanitary pipes. Future applications of this methodology should focus on method optimization, measurements at additional locations, and expanding measurements to collect data from additional types of pipe to better understand the geographic portability of the method and the relationship between exfiltration rates, pipe material, and pipe age.

KEYWORDS

sewer exfiltration, municipal separate storm sewer systems, sewer pipe material, sewer pipe age, sewage flow

Introduction

Exfiltration from the sanitary sewer has been the subject of research for more than 60 years (Amick and Burgess, 2000; Ducci et al., 2022; Ramseier, 1972; Rutsch et al., 2008; Selvakumar et al., 2004; Vazquez-Sune et al., 1990; Yang et al., 1999). The concern from watershed managers is the potential for exfiltrated sewage to impact shallow groundwater

(Lee et al., 2015; Roehrdanz et al., 2017) or nearby surface waters (Delesantro et al., 2022; Sercu et al., 2011; Sercu et al., 2009) with a variety of potential contaminants including bacteria, nutrients, and emerging contaminants (Delesantro et al., 2022; Sercu et al., 2011; Sercu et al., 2009).

While exfiltration from the sanitary sewer has been identified as a potential environmental problem, it is a particularly challenging problem to quantify. Previous studies have employed a wide variety of methodologies to measure exfiltration rates, including *ex situ* testing in the laboratory (Ellis et al., 2009; Sercu et al., 2003; Vollertsen and Hvitved-Jacobsen, 2003), inferred leakage rates using chemical or naturally occurring tracers *in situ* (Barrett et al., 1999; Kobayashi et al., 2021; Prigiobbe and Giulianelli, 2011; Rieckermann et al., 2005; Rivers et al., 1996; Wolf et al., 2006), or by modelling (Karpf et al., 2009; Karpf and Krebs, 2011; Sercu et al., 2005; Nguyen et al., 2021; Selvakumar et al., 2004). Each of these techniques has advantages and disadvantages, but few previous studies (Amick and Burgess, 2000) have attempted to measure exfiltration from publicly operated sanitary sewer pipes *in situ*.

One watershed where exfiltration is a concern is the lower San Diego River (SDR) watershed in San Diego, California, United States. San Diego is the fifth most populous county in the United States (United States Census Bureau, 2024) and, as with most cities in semiarid climates, San Diego has separate sanitary and storm sewer systems. Yet, the SDR and its tributaries have a long history of exceeding water quality objectives for fecal indicator bacteria during wet weather throughout the watershed (Schiff et al., 2023). In addition to fecal indicator bacteria, wet weather is associated with concomitantly elevated levels of the HF183 human fecal marker (Steele et al., 2018) and human specific pathogens (Soller et al., 2017), demonstrating that some portion of fecal indicator bacteria in the separate stormwater system are derived from human sources of fecal contamination (Steele et al., 2018).

There are multiple potential sources of human fecal contamination in the SDR watershed during wet weather. These potential sources include unhoused persons (Hinds et al., 2024), illegal discharges and illicit dumping (Schiff et al., 2023), sanitary sewer overflows (Zimmer-Faust et al., 2021) and onsite wastewater treatment systems. However, measurement of human fecal pollutant inputs due to exfiltration does not exist.

Here we describe a study designed to measure volume loss through exfiltration from gravity pipelines of publicly operated sanitary sewer systems. The study describes the new technique used to measure exfiltration *in situ*, the operating parameters of the new methodology such as sensitivity, and application of the new technique in sanitary sewer pipes of various ages and materials of construction across San Diego.

Methods

We used a volumetric approach to measure exfiltration *in situ*, whereby a discreet volume of water could be passed through a section of underground pipe and recovered under controlled conditions, with the difference in measured volume attributed to exfiltration. In order to simulate typical water flows in underground test pipes, a system consisting of three 1,250 L holding tanks, a 757 L measuring tank with stilling well, a pump, a set of flow meters, and multiple valves was devised. Water moved through the system via hard piping constructed of laboratory-grade schedule 80 grey PVC and braided polypropylene tubing. Pipes were either glued together, per the manufacturer's instructions or plumbed using threaded fittings and PTFE pipe sealant. Connections from hard pipe to braided polypropylene tubing were secured with crimped stainless steel band clamps. A schematic of the system is shown in Figure 1.

Briefly, the pipe section being tested was first isolated using inflatable plugs. Water contained in the holding and measuring tanks was then pumped at a metered rate to exhaustion through the underground test pipe via the upstream maintenance hole and subsequently captured at the downstream maintenance hole using a vacuum truck. During the test, an above ground flow meter, two in-pipe flow meters, and two water level loggers were employed to monitor flow rate and to maintain the water level in the pipe between one-third and one-half full. The captured water in the vacuum truck was then returned to the test and measurement tanks by the vacuum truck and any volume loss (or gain) recorded. This procedure was repeated up to 6 times at each site. A detailed description of the system, its components, and standard operating procedure is provided in Supplementary Material.

Validating the system and power analysis

A test of the holding tanks and measurement methods was performed by filling the tanks, connecting the tanks to a PVC manifold, and suctioning the water into a vacuum truck (Ledwell Classic, Texarkana, TX). After approximately 4,200 L of water were transferred to the tank of the vacuum truck, the truck tank was then elevated 12–15° and pressurized, and the entire volume of water transferred back to the original tanks. An initial transfer prior to measurement was performed to prime the system and fill in any voids that would sequester water, resulting in a false loss measurement. To measure loss or gain of water from the tanks, level measurements were taken from the stilling well, which had a fixed scale measured in millimeters. The test was repeated 4 times.

To calibrate the measurement tank, known volumes of water (0.945, 3.78, and 37.85 L) were removed from the tank and the level of water in the stilling well was measured. This was repeated ten times at each volume and the mean and standard deviation were calculated. This test was performed both with the holding tanks connected to the measuring tank and with the measuring tank isolated.

To confirm the ability to detect a loss in volume during field tests, and to confirm the sensitivity of the measurement tank, known volumes ranging from 1.97 to 18.93 L were removed during the runs via a valve installed for this purpose on the PVC manifold. The volume removed during field tests was measured using a graduated cylinder and compared to the level loss measured in the stilling well.

Preliminary tests were also used to perform a power analysis to determine the number of repetitions needed to detect a small loss. A test of 6 runs which produced a standard deviation of 1.32 L was used to calculate the statistical power. The analysis was performed in R version 4.3.1 using the power.t.test function with a significance level of 0.05 and a power of 0.8.

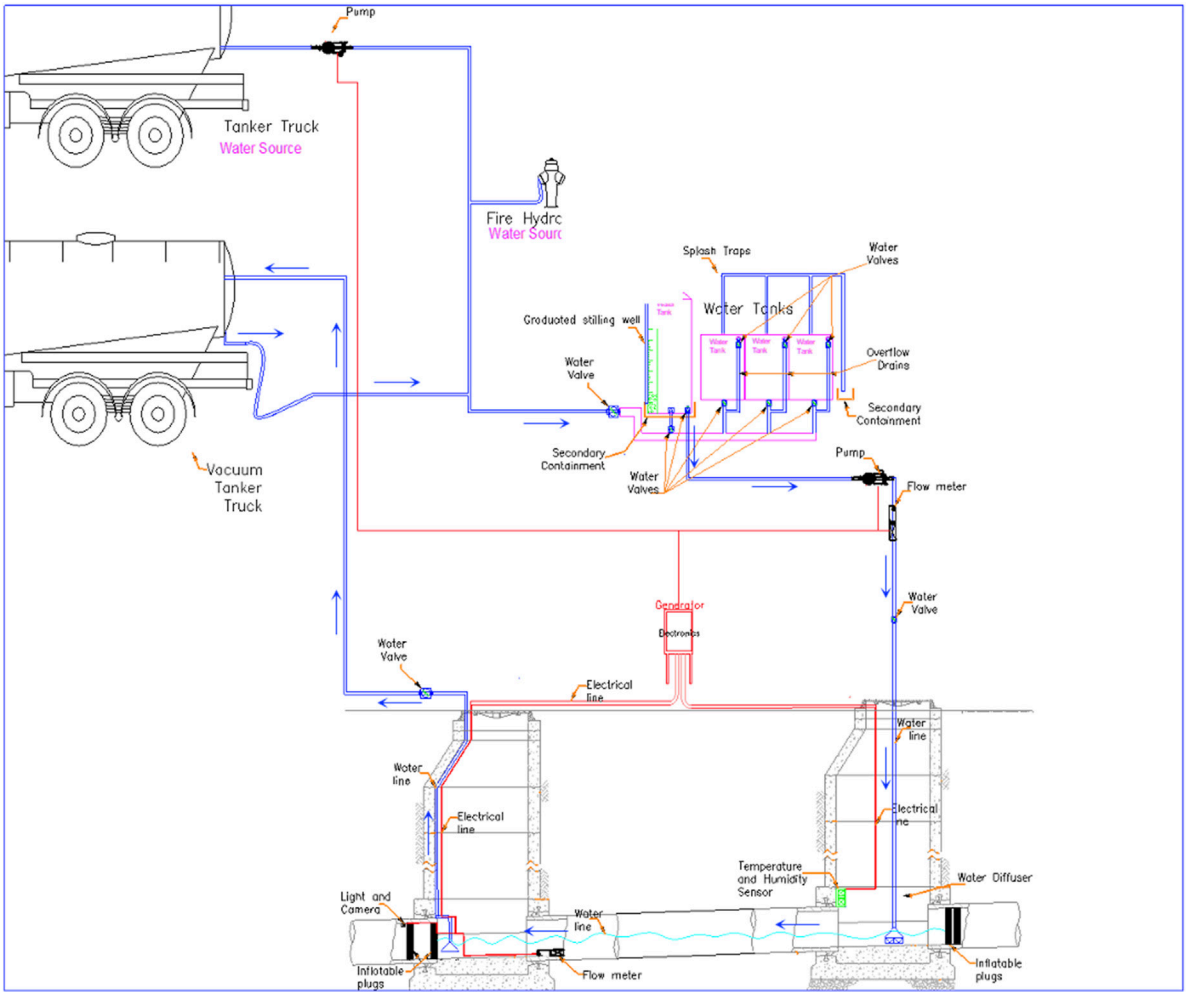

FIGURE 1
Schematic of *in situ* measurement system for quantifying exfiltration. Blue arrows indicate direction of water flow. See Supplemental Information for a detailed description of the measurement system and standard operating procedure.

Site selection

All sites were located on the coastal plain and foothills of southern San Diego County, CA. More than two-thirds of the soil in this region falls into Hydrogroup D: Soils with very low infiltration rates, typically made of finer particles such as silty or clay loams. Another 10% are classified as having low infiltration rates (Hydrogroup C), with only 17% classified as having moderate to high infiltration rates (Hydrogroups A & B) (SANDAG, 2024). The climate is semi-arid, with average rainfall of 9.79″ per year.

Sites were selected based on a defined set of criteria. The first criterion was that, due to the volume limitations of our equipment, the inner diameter of test pipes could be no larger than 10 inches. The second criterion was that there were no lateral connections coming into test pipes between maintenance holes. The third was the capability to either stop, capture with a vacuum truck, or bypass sewage flows around the test pipe segments. The fourth criterion was that there was ample room to locate and operate the equipment near the maintenance holes. The final and most important consideration was that, since these pipes were predominantly under roadways, traffic could be diverted and testing performed safely.

The materials with which sewers are constructed has changed over time. The first municipal sewers in San Diego date back to 1888 and were constructed of vitrified clay. Since that time, a range of additional materials has been used. These include vitrified clay, but also iron, concrete, PVC, and most recently, lined pipe, which includes cured-in-place pipe (CIPP) and to a lesser degree, Rib-Loc (a spiral-wound PVC liner), which is installed within existing pipes to rehabilitate older sewer lines without the need to dig them up. All segments available for testing included multiple pipe sections, joints, and the troughs of two maintenance holes. Our intention was to test the a representative cross section of the types of sewer construction materials and age classes of the existing pipes found in the watershed (Table 2). To facilitate this, GIS layers from the entire lower San Diego River watershed were utilized to determine the prevalence of each type of pipe material present. This data was then stratified by age into bins of <15 years, 15–30 years, 30–60 years, and >60 years, which is consistent with trends in construction practices.

Isolating the pipe being tested

Sewer pipes were tested by passing approximately 4,200 L of water through them under typical conditions (one-third to one-half full), which required isolating the test pipe from the rest of the collection system (Figure 1). To accomplish this, sewage in test pipes was diverted or interrupted by using maintenance holes up and downstream to pump sewage around the test pipe, capturing upstream flow with a vacuum truck, or shutting down access and water to buildings upstream of the test pipe. With sewage flow interrupted, three commercially-available inflatable plugs designed for this purpose were used to isolate each test pipe section; two in the pipe section just upstream and one plug in the pipe section just downstream of the pipe section to be tested. Prior to installing the downstream plug, a GoPro camera and light package was installed into the pipe, facing upstream, in order to capture video of any water leakage around the plug. Once all three plugs were in place, Signature® Bubbler flowmeter systems equipped with TIENet® Area Velocity sensors (Teledyne ISCO, Lincoln NE) were installed on spring rings into both the upstream and downstream ends of the test pipe.

With the test pipe plugged and meters in place, the next step was to fill the system tanks with water. The outlets of the three trailer mounted holding tanks were closed and the holding tanks filled from the top until the water rose just above the lower edge of the top bulkhead in each tank. Water was then added to the 757 L exterior measurement tank until it was about ¾ full. To ensure that the inflatable plugs were not leaking and the line to be tested was properly sealed, a static test was performed. Briefly, about 189 L of water was released from the 757 L exterior measurement tank and allowed to collect in the downstream inspection hole so that it just covered the plug at the downstream inspection hole. After waiting 15 min for the water level to stabilize, water depth was measured using a measuring stick devised for underground tanks which had been coated with Gasoila® water-finding paste (FedPro, OH, United States) which turns from brown to pink when wet. After another 15-min interval, water in the downstream maintenance hole was remeasured. If the water level was stable, then the plug was properly sealed and the test would proceed. If the water level had dropped, the plug was checked for air leaks or other damage and either reinserted or replaced, and the static test repeated. Only when the static test revealed no leakage could testing begin.

Priming the measurement system

With the static test complete, the measurement system was "primed" by running the entire volume of water tanks through the system to fill any low spots (sags) in the pipe and fill any voids in the vacuum truck or system piping. To begin the priming procedure the vacuum truck, which had been cleaned and emptied prior to arriving, was stationed at the downstream maintenance hole and its hose positioned to capture the water in the trough in the bottom of the vault with vacuum engaged. 22.68 L of 10% sodium hypochlorite solution were added to the water prior to the priming run. All valves on the water holding tanks were opened and water pumped into the upstream inspection hole at a metered rate, typically 50–70 L/min, to produce a one-third to one-half full pipe condition. Water was captured by the vacuum truck at the downstream maintenance hole. Once all water had been emptied from the holding tanks, the pump was halted, valves were closed, and the vacuum truck continued to operate for at least 15 min until no flow was observed in the vault at the downstream end of the test pipe.

The vacuum truck then returned the water to the holding and measuring tanks. To reduce variability, a box was drawn with spray paint or chalk on the ground around both rear wheels so that the truck would return to the same position after each test run reducing measurement variability introduced by the position of the truck from test run to test run. The discharge port on the truck was then connected to the inlet valve on the holding tank system. Valves at the top of the holding tanks were closed, as was the outlet valve to the measuring tank, while the holding tanks filled from the bottom through the PVC manifold. Each holding tank valve was closed individually when its level reached a predetermined point just above the outlet of the upper bulkhead valves.

With the holding tanks full, the upper bulkhead valves and outlet to the measuring tank were opened, allowing water to flow through the upper bulkhead valves to the measuring tank. After 15 min, upper bulkhead valves were closed, sequestering the majority of water in the holding tanks. With the outlet valve to the exterior tank still open and the vacuum hose still connected, the tank on the vacuum truck was elevated to 12–15° and pressurized to ~5 psi, forcing the remainder of the water into the measuring tank. When large bubbles were observed, the inlet valve to the system was closed. The hose was then depressurized and carefully disconnected from the truck, making sure to capture any water still in the hose. Air was removed from the system through a valve installed for this purpose, ensuring any water that might accidentally escape was captured. All water captured during this process was added to the measuring tank. An initial measurement of water volume was taken by visually recording the level in the stilling well using the mm scale permanently affixed to the stilling well tube. Sodium thiosulfate was added to neutralize the residual chlorine. The measurement of water volume was taken again following the addition.

With the measurement system primed, a measurement of the water level that had collected at the downstream plug was recorded as described previously, effectively repeating the static leak test. This measurement was taken before each subsequent test run to ensure that there were no plug leaks that would allow volume loss or infiltration of groundwater into the test pipe between test runs. The vacuum truck was repositioned at the downstream inspection hole.

To initiate the test run, the vacuum truck at the downstream maintenance hole was activated to preclude the creation of a hydralic head, and all the water in the holding and measurement tanks was pumped into the test pipe at a controlled rate as described previously. When all water had left the holding and measurement tanks (0.75–1 h), the outlet valve was closed and the pump switched off. Once the flow at the downstream inspection hole ceased, which varied by location, the vacuum truck continued to operate at full power for a period of 15 min as described previously. Water was then returned to the tanks following the same procedure described above for priming the system. Once again, the water level in the exterior measuring tank was recorded using the stilling well. The difference between the starting height of the stilling well prior to pumping and the height of the stilling well after refilling the holding and measurement tanks at

the end of the test run was used to calculate the loss or gain of volume from the test pipe. This procedure was repeated 3 to six times based on the results of our power analysis and the observed variability of the measurements in the field.

Data analysis

Data analysis required a three-step process. First, experimental results were summarized as average experimental volume loss by pipe segment (liters/experiment). Second, outliers were removed and the remaining data were normalized by the length of pipe segment tested and the duration of the experiment for more appropriate comparisons (liters/s-km). Third, normalized experimental results were statistically tested for significant differences using a two-way ANOVA based on pipe material and age group factors (R v 4.3.1, R Core Team, 2023).

Results

System validation

Initial validation testing of the system to see if the volume could be recovered from the vacuum truck, was performed for four runs. Across these four initial validation runs an average difference of 0.91 L (standard deviation of 2.3 L) was measured. Note that the standard deviation included zero. This was followed by laboratory calibration testing of the measurement variability of the stilling well using calibrated volumes. Thirty laboratory calibration tests found the level measurement in the stilling well was ~0.2 cm (with the largest standard deviation of 0.075 cm) per liter of removed volume in the measurement tank (Table 1).

This sensitivity testing was repeated in the field with comparable results. Field sensitivity testing found an average level change in the stilling well of 0.76 cm (n = 10, standard deviation 0.09 cm) per 3.785 L or 0.2 cm per liter of removed volume. These measurements had increased variability compared to the laboratory calibration tests but were not statistically different from the laboratory calibration tests. The laboratory calibration measurement number was used to calculate volume loss *in situ* due to its greater precision. Power analysis performed on preliminary tests found 6 runs to be sufficient to detect a difference (i.e., effect size) of 2.3 L and 3 runs to be sufficient to detect a difference of 4.2 L (Figure 2).

TABLE 1 Results of the calibration and sensitivity experiments.

Volume removed (L)	Average level change (cm) in stilling well +/− standard deviation
0.945	0.215+/−0.047
3.785	0.815+/−0.075
37.85	8.155+/−0.037

In situ measurements of exfiltration

A total of 23 individual segments of public sanitary sewer pipe were tested during the study. Sites were located throughout the San Diego area (Figure 3; Table 2). Most sites were in the City of San Diego, while others were in surrounding communities including Lakeview, La Mesa or in unincorporated areas of San Diego County. Note that the isolated test segments include multiple pipe sections, joints, and the troughs of the maintenance holes. The pipes tested consisted of 3 different materials and all were 8″ or 10″ inner diameter. Pipe materials consisted of vitreous clay (n = 11), PVC (n = 8), and lined (CIPP and Rib-Loc, n = 4). No concrete or cast iron pipes were available for testing based on the site selection criteria; both materials were rare in this watershed. Pipes ranged in age from newly installed CIPP to 75-year-old vitreous clay. CIPP ranged in age from <1 to 20 years, PVC pipe ranged in age from <1 to 38 years, and vitreous clay pipe from 49 to 75 years, since installation. Pipe test sections ranged from 80 to 394 feet (Supplementary Table S1).

All but two of the pipes lost volume during testing (Figure 4). Average volume lost ranged from zero to more than 76 L. Of the 21 pipes that lost volume, measurements from 15 were statistically different from zero. Two pipes gained volume during testing due to infiltration: One test pipe segment near an embayment gained volume with the rising tide, and another gained volume due to an obvious irrigation leak. A third pipe lost four times as much volume as the next highest volume loss pipe. All three of these pipes were removed from the data set for purposes of estimating average volume loss due to exfiltration (Figure 5).

After normalizing the test system results by the time and length of pipe during testing, the average volume loss varied by pipe material with lined pipe losing the least and PVC the most (Table 2; Figure 6A). There was no trend toward greater loss associated with pipe age; volume loss across all age groupings fell within a similar range (Figure 6B). Despite differences in mean volume loss between pipe materials and ages, the results of two-way ANOVA indicated no statistical difference in volume loss (Supplementary Table S2).

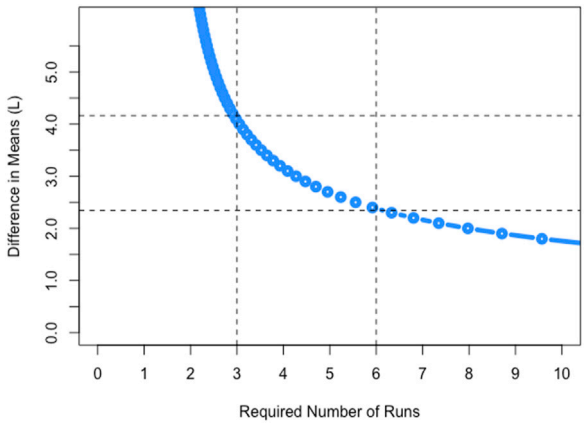

FIGURE 2
Power analysis curve showing the increase in measurement sensitivity based on increased number of test runs at a single site. Vertical lines show where the curve crosses at 3 and 6 runs, horizontal lines show where the power curve crosses at 2.3 L and 4.2 L.

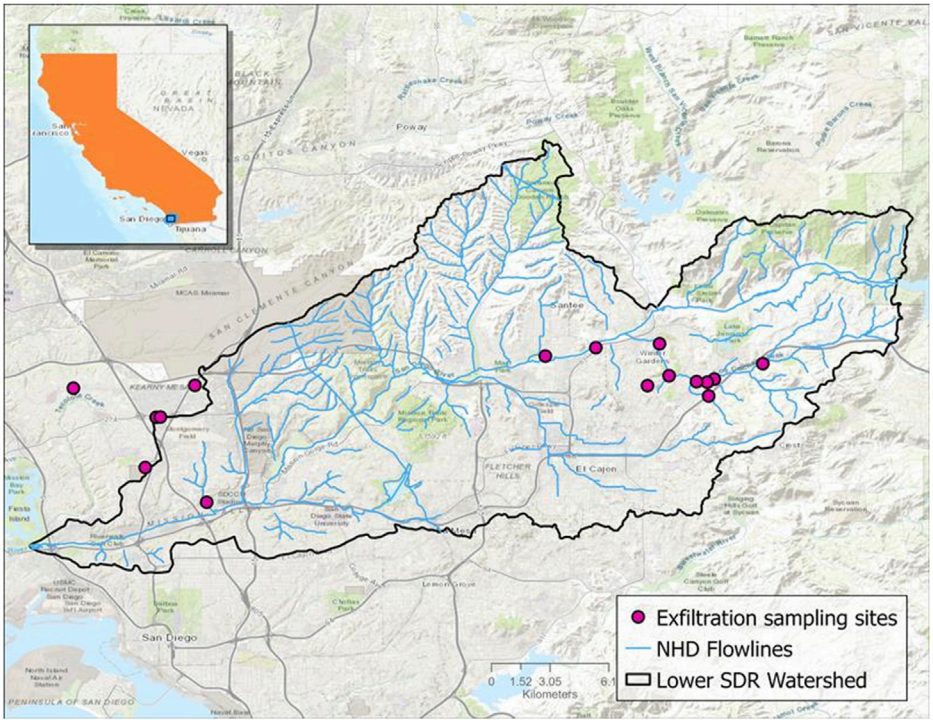

FIGURE 3
Map of sampling sites showing the flowlines and boundaries of the lower San Diego River watershed.

TABLE 2 Sewer pipe characteristics and *in situ* measured mean volume loss. The pipe characteristics are grouped by pipe material and age. Each material and age group is also expressed as a percent of total sewer pipe in the San Diego River watershed. *In situ* measured mean volume loss is shown in liters per second per kliometer, 95% confidence intervals, and number of pipes (N) in each category.

Material	Age group	% of pipe	Volume loss					
			l per sec per km	95% CI	N	l per sec per km	95% CI	N
Clay	<15	0.1	--	--	0	6.23×10^{-2}	$(1.68 \times 10^{-3}, 1.23 \times 10^{-1})$	8
	15–30	0.9	--	--	0			
	30–60	32.6	7.97×10^{-2}	$(-2.86 \times 10^{-2}, 1.88 \times 10^{-1})$	5			
	60+	24.3	3.32×10^{-2}	$(-5.05 \times 10^{-2}, 1.17 \times 10^{-1})$	3			
PVC	<15	6.2	3.84×10^{-2}	$(-2.78 \times 10^{-2}, 4.90 \times 10^{-2})$	3	2.01×10^{-2}	$(-1.14 \times 10^{-2}, 6.16 \times 10^{-2})$	11
	15–30	10.2	-3.23×10^{-2}	$(-1.412 \times 10^{-1}, 7.67 \times 10^{-2})$	4			
	30–60	10.8	5.88×10^{-2}	$(-1.33 \times 10^{-2}, 1.31 \times 10^{-1})$	4			
	60+	2.2	--	--	0			
Lined Pipe	<15	1.4	2.21×10^{-2}	$(5.45 \times 10^{-3}, 3.89 \times 10^{-2})$	4	2.84×10^{-2}	$(6.66 \times 10^{-3}, 5.01 \times 10^{-2})$	4

Discussion

The methodology developed for this study was able to empirically measure volume loss *in situ* from public sanitary sewer pipes under simulated normal operating conditions and without pressure. Previous *in situ* studies of exfiltration at the pipe level incorporated pressure tests (Dohmann et al., 1999; Ullmann, 1994), which by their nature are likely to overestimate leakage, or employed a water balance approach that relied on in-pipe measurements of flow (Amick and Burgess, 2000). The main advantage of the volumetric loss methodology employed in this study is that it dispenses with the many assumptions and correction factors necessary to carry out sewer exfiltration modeling and replaces estimates with empirical results. Most previous studies of sewer exfiltration rates have relied on either data driven or physically-based models (see Nguyen et al., 2021 for a review).

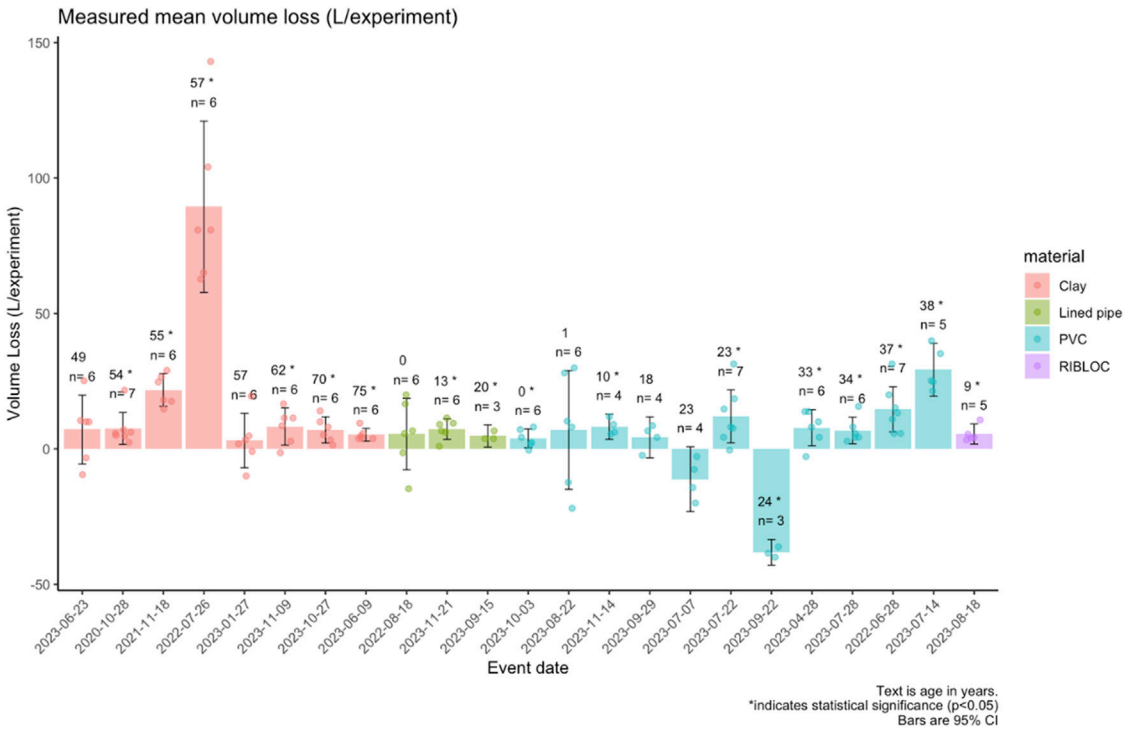

FIGURE 4
Mean volume loss (liters per experiment) from the 23 test pipe segments across San Diego, CA United States between 2021–2023.

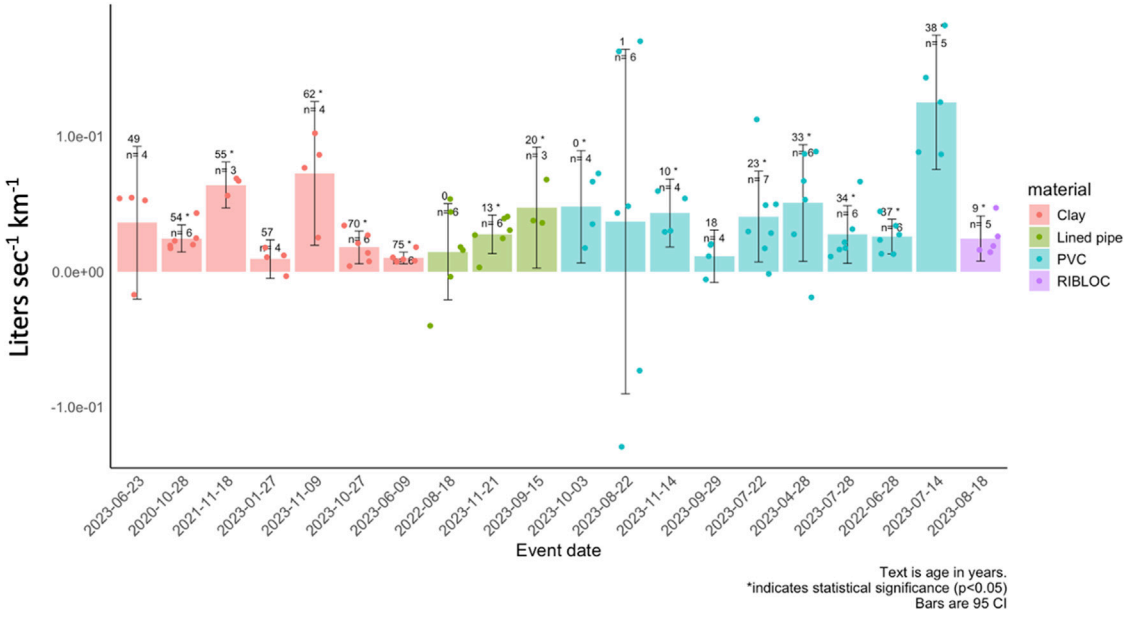

FIGURE 5
Mean volume loss (liters per second per km) from the 20 test pipe segments across San Diego, CA United States between 2021–2023 after removing outliers and normalizing across sites by the length of pipe and duration of testing.

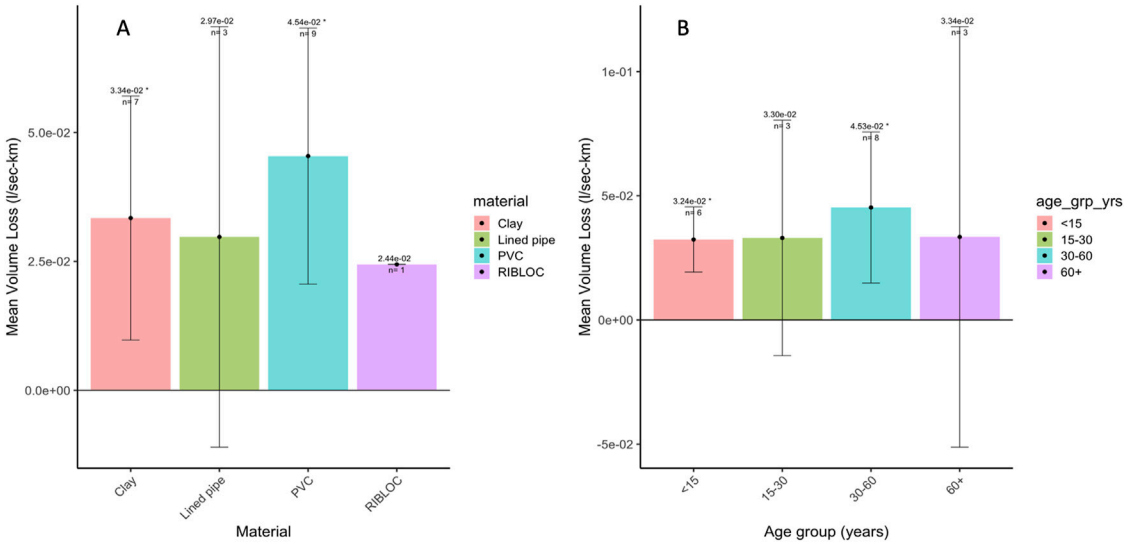

FIGURE 6
Mean volume loss by categories of **(A)** pipe material and **(B)** pipe age since installation. Error bars are 95% confidence intervals. Note that RIBLOC has no confidence interval, as it had a single pipe in the category.

TABLE 3 Compilation of sewer exfiltration rate per pipe length in modeling studies (from Nguyen et al., 2021) compared to *in situ* measurements from this study.

Scale of study	Exfiltration rate (L/s-km)	Reference
Pipe scale	0.1 – 0.2	Blackwood et al. (2005)
Pipe scale	1.7×10^{-2} – 0.45	Trauth et al. (1995)
Multiple pipe segments across a watershed	*3.78×10^{-2}*	*This study*
Pipe network of a city	1.2×10^{-2}	Hoffman and Lerner (1992)
Catchment area of a city	1.4×10^{-2}	Yang et al. (1999)
Catchment area of a city	1.4×10^{-9} – 0.179	Chisala and Lerner (2008)
District area of a city	3.0×10^{-2} – 7.5×10^{-2}	Morris et al. (2006)
Multiple scales of the country	1.0–2.0	Amick and Burgess (2000)
Single pipe to catchment scales	6.2×10^{-2} – 17.9×10^{-2}	Reynolds and Barrett (2003)
Review of various scale studies	1.7×10^{-9} – 0.179	Ellis et al. (2009)

Data driven models include a variety of statistical model types (e.g., Baur and Herz, 2002; DeSilva et al., 2005; Roehrdanz et al., 2017), as well as artificial intelligence and machine learning models (e.g., Khan et al., 2010; Sousa et al., 2014; Hernández et al., 2018), while physically-based models rely on groundwater recharge estimates (Yang et al., 1999; Lerner, 2002; Wolf et al., 2012), water balance principles based on consumption, precipitation and discharge rates (e.g., Karpf and Krebs, 2005; Nakayama et al., 2006), sewer pipe models (e.g., DeSilva et al., 2005; Peche et al., 2017), and exfiltration estimates based on measurements of various sewage constituents and their concentration in subsurface ground water (e.g., Rieckermann et al., 2005; Roehrdanz et al., 2017; Kobayashi et al., 2021; Delesantro et al., 2022). These models, reviewed in Nguyen et al. (2021), have produced a wide range of estimated sewage exfiltration rates, from 2 to 1.4×10^{-9} of L/s-km with a median exfiltration rate of 7.5×10^{-2} L/s-km (25th percentile: 1.7×10^{-2}; 75th percentile: 1.8×10^{-1}). Our overall sewer exfiltration rate estimate of 3.78×10^{-2} L/s-km, derived from empirical measurements, falls within a similar range as the majority of results reported by previous studies (Table 3).

Although our sewer exfiltration rates are within the same range as multiple other studies (Table 3), they are orders of magnitude higher than lowest rates reported by some (e.g., Chisala and Lerner, 2008). One possible reason for this disparity has to do with model assumptions surrounding the colmation layer that forms on the inside of sewer pipes. Many models of sewer exfiltration factor in the clogging nature of the colmation layer which has been observed in experimental settings to reduce flow through pipe defects over time

(Vollertsen and Hvitved-Jacobsen, 2003). We employed paired in-pipe flow meters and water level sensors, and took great care to ensure that in-pipe flow did not exceed typical operating conditions so as not to scour the colmation layer. However, we still observed a greater volume loss than would be predicted by these models, which may suggest the colmation layer *in situ* may not behave similarly to laboratory conditions or that the less particle dense water used in our tests may have led to additional incremental volume loss.

Based on *ex situ* experiments, Vollertsen and Hvitved-Jacobsen (2003) suggest that sewer flushing and subsequent loss of the colmation layer may temporarily increase exfiltration rates through pipe defects. In our study, there were three occasions when the test pipe had to be flushed before testing could proceed (due to large non-sewage debris interfering with our ability to carry out measurements). However, our exfiltration measurements from these pipes were not dramatically different than for pipes that had not been flushed. Interestingly, the largest volume loss was observed on July 26, 2022, for a pipe which had been taken out of service years prior to the study (Figure 2). One hypothesis in that this pipe, which had been dry for many years prior to the study, had lost its colmation layer. Regardless, for data analysis, we eliminated the anomalous site tested on July 26, 2022, but retained the three sites that had been flushed of non-sewage debris.

One factor that may have influenced our measured *in situ* exfiltration rates is that we used potable water mixed with the residual solids in our test pipe segments from the priming runs. Thus, our test system utilized volumes with sewage particles, but possibly at concentrations of solids lower than what may be found in raw sewage from the tested segments. Further, the high chlorine content in the water in the priming run (~500 ppt), although subsequently neutralized to <2 ppm, may have also disrupted the colmation layer. We employed flow meters, one at the pump discharge and two in-pipe, to ensure flow rates during testing mimicked typical operating conditions so as to prevent scouring of the pipe surface. Nonetheless, if solids content is an important factor limiting exfiltration *in situ*, then our system may be biasing exfiltration rates high. *In situ* studies using raw or synthetic sewage would be helpful in informing these results.

A second factor that may have influenced our measured *in situ* exfiltration rates is that we only tested public sewer pipe segments without lateral connections to private laterals. This was intentional since our test procedure could not account for additions of unknown volumes of water from private laterals and we could not intercept or stop water usage from private connections. Because defects at lateral connections have been identified as a location that can lead to exfiltration (Decker, 1994), it is possible that our methodology may actually underestimate exfiltration–or that private lateral exfiltration may be as large or larger than public sewer exfiltration–because some of these defects would have been missed by our methodology. A separate study in San Diego that employed static testing of leakage from private laterals estimated a mean rate of 0.33 L (sd = 0.55 L) per hour (Schiff et al., 2024). However, these measurements also excluded the connection between the private laterals and sanitary sewers and thus did not capture potential losses at these connections.

A variable which we were unable to control was the type of soil surrounding our test pipes. Laboratory experiments conducted using different soil types have shown that the composition of the soil surrounding a pipe may influence exfiltration rates (Karpf et al., 2009). Our test sites were primarily located on the large alluvial plain below San Diego's coastal mountains, where the soil characteristics are primarily low infiltration throughout with only 17% of soils from high infiltration hydrogroups. However, because we made empirical measurements and had no way to examine the soil or the pipe bedding material surrounding our test pipes, we cannot know what, if any, influence soil type may have on exfiltration rates in this study. Because this method was tested exclusively at sites in San Diego, CA, its results are subject to the uncertainties associated with its application under the specific geographic, environmental and physical conditions present at the time of the study. For example, methodological limitations and logistical concerns excluded pipes more that 10″ in diameter, which excluded large trunk lines. Further, no concrete pipes, which may be more common in other locales have been largely replaced in this watershed and were therefore unavailable for testing. Thus, any application of this measurement technique outside the original study area will be subject to the set of uncertainties inherent to that location and should be assessed accordingly.

Our measurements were conducted during periods of dry weather over a two-year time span across all four seasons. It is possible that groundwater levels could have influenced our results since water saturation levels in soil have been shown to reduce exfiltration rates in experimental settings (Karpf et al., 2009). In fact, our test system quantified seawater infiltration at a coastal site due to the rising tide through both continual increases in volume and increasing conductivity of the test water. The test system also measured infiltration of subsurface groundwater at a non-coastal site. Further investigation identified a constant leak in a water main less than 10 m from our test pipe segment.

The methodology developed during this study has broad implications for managing exfiltration from sewer pipes (Steele et al. in review). Local sewer agencies typically use video inspections to monitor the condition of their collection systems. This standard practice works well for finding major defects and assessing capital improvement plans. However, many of the pipes we tested had minor or no defects identified by their most recent video inspection. Nonetheless, some of these pipe segments lost volume under test conditions. Wolf et al. (2006) identified that video inspections were not good predictors of public sewer exfiltration because video resolution is not sufficient to detect small cracks or joint separations that are still large enough for water to pass through. As such, future research should focus on new more sensitive technologies that could be used in routine inspections of collection systems.

Obtaining empirical measurements from *in situ* sanitary pipes is by its nature a challenging endeavor and would have been impossible without an extraordinary degree of cooperation between the research team and the sanitary collection system owners. The first hurdle was simply to identify pipes of the desired age, material, diameter and depth that had no lateral connections between manholes, an acceptable slope, and where the normal flow of wastewater could theoretically be halted, bypassed around the study site, or collected using vacuum trucks. This was followed by field visits to determine if sites were logistically suitable in terms of equipment placement and could be made safe for workers, who were often operating in roadways where they were exposed to vehicular traffic. Finally, it required weeks of planning for each sampling event to notify residents, control parking, set up traffic control and schedule the equipment and operators to be on-site from early morning until well into the

early morning hours of the next day. Throughout the process, wastewater utilities supplied their equipment, personnel and operational and engineering expertise to make this study possible. Simply put, it literally could not have been done without them.

Despite the challenges associated with *in situ* exfiltration measurements, this new methodology has its place amongst the other tools used to estimate exfiltration and produced results that were very similar to the median value calculated from previous studies regardless of disparities between methods (Nguyen et al., 2021). Similar exfiltration rates were measured or modeled at the pipe scale (e.g., Trauth et al., 1995), the catchment scale (e.g., Yang et al., 1999; Reynolds and Barrett, 2003), or city scale (e.g., Morris et al., 2006; Chisala and Lerner, 2008). Each method has its own set of assumptions and bias, but together, the weight of evidence from *in situ* measurements, *ex situ* measurements, and modeling may help collection system managers understand exfiltration in their systems.

Data availability statement

The datasets presented in this study can be found in online repositories. The names of the repository/repositories and accession number(s) can be found in the article/Supplementary Material.

Author contributions

JG: Conceptualization, Investigation, Methodology, Project administration, Resources, Supervision, Validation, Writing–original draft, Writing–review and editing. JS: Conceptualization, Data curation, Formal Analysis, Investigation, Methodology, Project administration, Supervision, Validation, Writing–original draft, Writing–review and editing. AG-F: Data curation, Formal Analysis, Investigation, Methodology, Writing–review and editing. KS: Conceptualization, Investigation, Project administration, Resources, Visualization, Writing–review and editing.

Funding

The author(s) declare that financial support was received for the research, authorship, and/or publication of this article. This project was partially funded by the City of San Diego, County of San Diego, Padre Dam Municipal Water District, City of El Cajon and City of La Mesa under County of San Diego Contract 563356.

Acknowledgments

The authors are grateful for the guidance of the project Technical Review Committee: Martha Tremblay, Patricia Holden, Sandra McLellan, John Izbicki, Mia Mattioli, Jennifer Wolch. The authors wish to acknowledge the partnership and collaboration with the collection system professionals at the City of San Diego, County of San Diego, Padre Dam Municipal Water District, and the City of La Mesa including Daniel Carter, Jeff Van Every, Margaret Llagas, Terrell Powell, Bradley Burns, Sean Willis, Gary Harris, Ted Kautzman, Jimmy Vargas, and Daniel Lockhart. The authors appreciate discussions and suggestions provided by Steve Jepsen. The authors are grateful for the project Steering Committee. This project was partially funded by the City of San Diego, County of San Diego, Padre Dam Municipal Water District, City of El Cajon and City of La Mesa.

Conflict of interest

The authors declare that the research was conducted in the absence of any commercial or financial relationships that could be construed as a potential conflict of interest.

Publisher's note

All claims expressed in this article are solely those of the authors and do not necessarily represent those of their affiliated organizations, or those of the publisher, the editors and the reviewers. Any product that may be evaluated in this article, or claim that may be made by its manufacturer, is not guaranteed or endorsed by the publisher.

Supplementary material

The Supplementary Material for this article can be found online at: https://www.frontiersin.org/articles/10.3389/fenvs.2024.1458146/full#supplementary-material

References

Amick, R. S., and Burgess, E. H. (2000). *Exfiltration in sewer systems*. Cincinnati OH: US EPA, Office of Research and Development.

Barrett, M. H., Hiscock, K. M., Pedley, S., Lerner, D. N., Tellam, J. H., and French, M. J. (1999). Marker species for identifying urban groundwater recharge sources: a review and case study in Nottingham, UK. *UK. Water Res.* 33, 3083–3097. doi:10.1016/s0043-1354(99)00021-4

Baur, R., and Herz, R. (2002). Selective inspection planning with ageing forecast for sewer types. *Water Sci. Technol.* 46, 389–396. doi:10.2166/wst.2002.0704

Blackwood, D. J., Ellis, J. B., Revitt, D. M., and Gilmour, D. J. (2005). Factors influencing exfiltration processes in sewers. *Water Sci. Technol.* 51, 147–154. doi:10.2166/wst.2005.0042

Chisala, B. N., and Lerner, D. N. (2008). Distribution of sewer exfiltration to urban groundwater. *Proc. Institution Civ. Eng. - Water Manag.* 161, 333–341. doi:10.1680/wama.2008.161.6.333

Decker, J. (1994). "Pollution load of subsoil, groundwater and surface water by leaky sewers," in *Proceedings from hydrotop* (Marseille, France).

Delesantro, J. M., Duncan, J. M., Riveros-Iregui, D., Blaszczak, J. R., Bernhardt, E. S., Urban, D. L., et al. (2022). The nonpoint sources and transport of baseflow nitrogen loading across a developed rural-urban gradient. *Water Resour. Res.* 58. doi:10.1029/2021wr031533

DeSilva, D., Burn, S., Tjandraatmadja, G., Moglia, M., Davis, P., Wolf, L., et al. (2005). Sustainable management of leakage from wastewater pipelines. *Water Sci. Technol.* 52, 189–198. doi:10.2166/wst.2005.0459

Dohmann, M., Decker, J., and Menzenbach, B. (1999). *Water contamination due to sewer leakage*. Berlin, Heidelberg: Springer.

Ducci, L., Rizzo, P., Pinardi, R., Solfrini, A., Maggiali, A., Pizzati, M., et al. (2022). What is the impact of leaky sewers on groundwater contamination in urban semi-

confined aquifers? A test study related to fecal matter and personal care products (PCPs). *Hydrology* 10, 3. doi:10.3390/hydrology10010003

Ellis, J. B., Revitt, D. M., Lister, P., Willgress, C., and Buckley, A. (2003). Experimental studies of sewer exfiltration. *Water Sci. Technol.* 47, 61–67. doi:10.2166/wst.2003.0221

Ellis, J. B., Revitt, D. M., Vollertsen, J., and Blackwood, D. J. (2009). Sewer exfiltration and the colmation layer. *Water Sci. Technol.* 59, 2273–2280. doi:10.2166/wst.2009.271

Hernández, N., Caradot, N., Sonnenberg, H., Rouault, P., and Torres, A. (2018). Support tools to predict the critical structural condition of uninspected pipes for case studies of Germany and Colombia. *Water Pr. Technol.* 13, 794–802. doi:10.2166/wpt.2018.085

Hinds, J. B., Garg, T., Hutmacher, S., Nguyen, A., Zheng, Z., Griffith, J., et al. (2024). Assessing the defecation practices of unsheltered individuals and their contributions to microbial water quality in an arid, urban watershed. *Sci. Total Environ.* 920, 170708. doi:10.1016/j.scitotenv.2024.170708

Hoffman, J. M., and Lerner, D. N. (1992). Leak free sewers – who needs them? *Water Waste Treat.* 35 (8), 18–19.

Karpf, C., and Krebs, P. (2011). A new sewage exfiltration model – parameters and calibration. *Water Sci. Technol.* 63, 2294–2299. doi:10.2166/wst.2011.167

Karpf, C., Traenckner, J., and Krebs, P. (2009). Hydraulic modelling of sewage exfiltration. *Water Sci. Technol.* 59, 1559–1565. doi:10.2166/wst.2009.172

Karpf, K., and Krebs, P. (2005). Application of a leakage model to assess exfiltration from sewers. *Water Sci. and Technol.* 52 (5), 225–231. doi:10.2166/wst.2005.0137

Khan, Z., Zayed, T., and Moselhi, O. (2010). Structural condition assessment of sewer pipelines. *J. Perform. Constr. Facil.* 24, 170–179. doi:10.1061/(asce)cf.1943-5509.0000081

Kobayashi, J., Kuroda, K., Miyamoto, C., Uchiyama, Y., Sankoda, K., and Nakajima, D. (2021). Evaluating sewer exfiltration in groundwater by pharmaceutical tracers after the 2016 Kumamoto earthquakes, Japan. *J. Hazard. Mater.* 411, 125183. doi:10.1016/j.jhazmat.2021.125183

Lee, D. G., Roehrdanz, P. R., Feraud, M., Ervin, J., Anumol, T., Jia, A., et al. (2015). Wastewater compounds in urban shallow groundwater wells correspond to exfiltration probabilities of nearby sewers. *Water Res.* 85, 467–475. doi:10.1016/j.watres.2015.08.048

Lerner, D. N. (2002). Identifying and quantifying urban recharge: a review. *Hydrogeol. J.* 10, 143–152. doi:10.1007/s10040-001-0177-1

Morris, B. L., Darling, W. G., Cronin, A. A., Rueedi, J., Whitehead, E. J., and Gooddy, D. C. (2006). Assessing the impact of modern recharge on a sandstone aquifer beneath a suburb of Doncaster, UK. *Hydrogeol. J.* 14, 979–997. doi:10.1007/s10040-006-0028-1

Nakayama, T., Watanabe, M., Tanji, K., and Morioka, T. (2006). Effect of underground urban structures on eutrophic coastal environment. *Sci. total Environ.* 373, 270–288. doi:10.1016/j.scitotenv.2006.11.033

Nguyen, H. H., Peche, A., and Venohr, M. (2021). Modelling of sewer exfiltration to groundwater in urban wastewater systems: a critical review. *J. Hydrol.* 596, 126130. doi:10.1016/j.jhydrol.2021.126130

Peche, A., Graf, T., Fuchs, L., and Neuweiler, I. (2017). A coupled approach for the three-dimensional simulation of pipe leakage in variably saturated soil. *J. Hydrol.* 555, 569–585. doi:10.1016/j.jhydrol.2017.10.050

Prigiobbe, V., and Giulianelli, M. (2011). Quantification of sewer leakage by a continuous tracer method. *Water Sci. Technol.* 64, 132–138. doi:10.2166/wst.2011.639

Ramseier, R. E. (1972). Testing new sewer pipe installations. *Water Pollut. Control Fed.* 44 (4), 557–564. Available at: http://www.jstor.org/stable/25037423.

R Core Team (2023). *R: a language and environment for statistical computing*. Vienna, Austria. Available at: https://www.R-project.org/.

Reynolds, J., and Barrett, M. (2003). A review of the effects of sewer leakage on groundwater quality. *Water Environ. J.* 1, 34–39. doi:10.1111/j.1747-6593.2003.tb00428.x

Rieckermann, J., Borsuk, M., Reichert, P., and Gujer, W. (2005). A novel tracer method for estimating sewer exfiltration. *Water Resour. Res.* 41. doi:10.1029/2004wr003699

Rivers, C. N., Barrett, M. H., Hiscock, K. M., Dennis, P. F., Feast, N. A., and Lerner, D. N. (1996). Use of nitrogen isotopes to identify nitrogen contamination of the sherwood sandstone aquifer beneath the city of nottingham, United Kingdom. *Hydrogeol. J.* 4, 90–102. doi:10.1007/s100400050099

Roehrdanz, P. R., Feraud, M., Lee, D. G., Means, J. C., Snyder, S. A., and Holden, P. A. (2017). Spatial models of sewer pipe leakage predict the occurrence of wastewater indicators in shallow urban groundwater. *Environ. Sci. Technol.* 51, 1213–1223. doi:10.1021/acs.est.6b05015

Rutsch, M., Rieckermann, J., Cullmann, J., Ellis, J. B., Vollertsen, J., and Krebs, P. (2008). Towards a better understanding of sewer exfiltration. *Water Res.* 42, 2385–2394. doi:10.1016/j.watres.2008.01.019

SANDAG (2024). San Diego association of governments regional data warehouse. Available at: https://geo.sandag.org/portal/apps/experiencebuilder/experience/?id=fad9e9c038c84f799b5378e4cc3ed068&page=Home#data_s=id%3AdataSource_1-0%3A204 (Accessed September 27, 2024).

Schiff, K., Griffith, J., Steele, J., and Zimmer-Faust, A. (2023). Dry and wet weather survey for human fecal sources in the San Diego River watershed. *Water* 15 (12), 2239. doi:10.3390/w15122239

Schiff, K. C., Griffith, J. F., Steele, J. A., and Gonzalez-Fernandez, A. (2024). *Summary of technical research: quantifying sources of human fecal pollution in the lower San Diego River watershed*. Technical Report 1380. Costa Mesa, CA: Southern California Coastal Water Research Project.

Selvakumar, A., Field, R., Burgess, E., and Amick, R. (2004). Exfiltration in sanitary sewer systems in the US. *Urban Water J.* 1, 227–234. doi:10.1080/15730620410001732017

Sercu, B., Werfhorst, L. C. V. D., Murray, J., and Holden, P. A. (2009). Storm drains are sources of human fecal pollution during dry weather in three urban southern California watersheds. *Environ. Sci. Technol.* 43, 293–298. doi:10.1021/es801505p

Sercu, B., Werfhorst, L. C. V. D., Murray, J. L. S., and Holden, P. A. (2011). Sewage exfiltration as a source of storm drain contamination during dry weather in urban watersheds. *Environ. Sci. Technol.* 45, 7151–7157. doi:10.1021/es200981k

Soller, J. A., Schoen, M., Steele, J. A., Griffith, J. F., and Schiff, K. C. (2017). Incidence of gastrointestinal illness following wet weather recreational exposures: harmonization of quantitative microbial risk assessment with an epidemiologic investigation of surfers. *Water Res.* 121, 280–289. doi:10.1016/j.watres.2017.05.017

Sousa, V., Matos, J. P., and Matias, N. (2014). Evaluation of artificial intelligence tool performance and uncertainty for predicting sewer structural condition. *Autom. Constr.* 44, 84–91. doi:10.1016/j.autcon.2014.04.004

Steele, J. A., Blackwood, A. D., Griffith, J. F., Noble, R. T., and Schiff, K. C. (2018). Quantification of pathogens and markers of fecal contamination during storm events along popular surfing beaches in San Diego, California. *Water Res.* 136, 137–149. doi:10.1016/j.watres.2018.01.056

Trauth, R., Hahn, H. H., and Xanthopoulos, C. (1995). *In-situ* method to determine water exchange between sewerage and groundwater. *Abwassertechnik* 4, 55–57.

Ullmann, F. (1994). *Umweltorientierte Bewertung der Abwasserexfiltrationen bei undichten Kanälen dargestellt am Beispiel einer Bundeswehrkaserne*. Dissertation. Aachen (Germany): Institut für Siedlungswasserwirtschaft.

United States Census Bureau (2024). County population totals and components of change: 2020-2023. Available at: https://www.census.gov/data/tables/time-series/demo/popest/2020s-counties-total.html (Accessed May 15, 2024).

Vazquez-Sune, E., Castillo, O., Sanchez-Vila, X., Alberich, C., and Carrera, J. (1990). "Use of natural and anthropogenic tracers to identify sources of groundwater recharge in urban areas on Barcelona," in *Tracers and modeling in hydrogeology, atmospheric environment. Part B. Urban atmosphere. Presented at the TraM'2000* (Liege, Belgium: IAHS), 7. doi:10.1016/0957-1272(90)90006-g

Vollertsen, J., and Hvitved-Jacobsen, T. (2003). Exfiltration from gravity sewers: a pilot scale study. *Water Sci. Technol.* 47, 69–76. doi:10.2166/wst.2003.0223

Wolf, L., Eiswirth, M., and Hötzl, H. (2006). Assessing sewer–groundwater interaction at the city scale based on individual sewer defects and marker species distributions. *Environ. Geol.* 49, 849–857. doi:10.1007/s00254-006-0180-x

Wolf, L., Zwiener, C., and Zemann, M. (2012). Tracking artificial sweeteners and pharmaceuticals introduced into urban groundwater by leaking sewer networks. *Sci. Total Environ.* 430, 8–19. doi:10.1016/j.scitotenv.2012.04.059

Yang, Y., Lerner, D. N., Barrett, M. H., and Tellam, J. H. (1999). Quantification of groundwater recharge in the city of Nottingham, UK. *Environ. Geol.* 38, 183–198. doi:10.1007/s002540050414

Zimmer-Faust, A., Schiff, K., and Nguyen, D. (2021). "Quantify sources of human fecal contamination loading to the San Diego river, technical memorandum, task 8A: compiling and analyzing existing data for sanitary sewer overflow events," in *Report prepared for the San Diego river investigative order steering committee* (Costa Mesa, CA: Southern California Coastal Water Research Project), 28.

Frontiers in Environmental Science

Explores the anthropogenic impact on our natural world

An innovative journal that advances knowledge of the natural world and its intersections with human society. It supports the formulation of policies that lead to a more inhabitable and sustainable world.

Discover the latest Research Topics

See more →

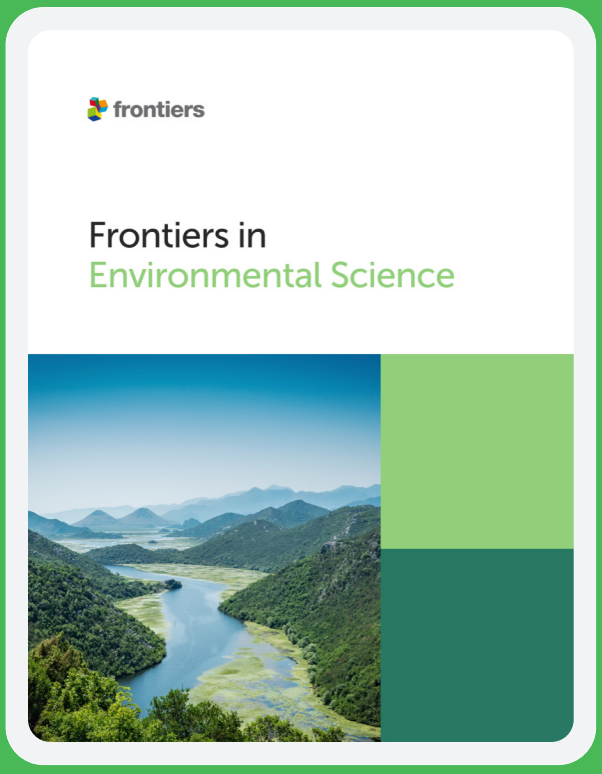

Frontiers

Avenue du Tribunal-Fédéral 34
1005 Lausanne, Switzerland
frontiersin.org

Contact us

+41 (0)21 510 17 00
frontiersin.org/about/contact